The Impact of Material Surface Characteristics on the Clinical Wetting Properties of Silicone Hydrogel Contact Lenses

Michael Leonard Read

Faculty of Life Sciences

The University of Manchester

A thesis submitted to the University of Manchester for the degree of Doctor of Philosophy in the Faculty of Life Sciences

2010

Contents

Total word count: 86,135 words

List of Figures

Abstract

This PhD project investigated the ramifications of air-cured and nitrogen-cured manufacturing processes during silicone hydrogel contact lens manufacture in terms of lens surface characterisation and clinical performance. A one-hour contralateral clinical study was conducted for ten subjects to compare the clinical performance of the two study lenses. The main clinical findings were reduced levels of subjective performance, reduced surface wettability and increased deposition. Contact angle analysis showed the air-cured lenses had consistently higher advancing and receding contact angle measurements, in comparison with the nitrogen-cured lens. Chemical analysis of the study lens surfaces in the dehydrated state, by x-ray photoelectron spectroscopy (XPS) and time-of-flight mass spectrometry (ToF-SIMS), showed no difference due to surface segregation of the silicone components. Analysis of frozen lenses limited surface segregation and showed a higher concentration of silicone polymer components and lower concentration of hydrophilic polymer components at the surface of the air-cured lens, in comparison with the nitrogen-cured lens. Scanning electron microscope (SEM) imaging showed the nitrogen-cured lens to have a surface typical of a hydrogel material, whereas the air-cured lens had regions of apparent phase separation. In addition, atomic force microscopy (AFM) showed the air-cured lens to have a rougher surface associated with greater adherence of contaminants (often observed in materials with reduced polymer cross-linking). In conclusion, clinical assessment of the study lenses confirmed the inferior performance of the air-cured lens. Surface analysis suggested that the non-wetting regions on the air-cured lenses were associated with elevated level of silicone components, reduced polymer cross-linking and polymer phase separation.

Declaration

The University of Manchester

PhD Candidate Declaration

Candidate Name: Michael Leonard Read

Faculty: Life Sciences

Thesis Title: The Impact of Material Surface Characteristics on the Clinical Wetting Properties of Silicone Hydrogel Contact Lenses

Declaration to be completed by the candidate:

I declare that no portion of this work referred to in this thesis has been submitted in support of an application for another degree or qualification of this or any other university or other institute of learning.

Signed:

Date: 14th February 2011

Copyright Statement

To my mother and father

Acknowledgements

The nature of this PhD study has meant that I have had the great pleasure of working with many people from a wide range of scientific backgrounds. I have constantly been surprised and warmed by their willingness to help and by the amount of time they have given me. It is fair to say that without their patient help and advice this thesis would never have been possible.

I would like to express my sincere gratitude to my supervisors, Dr Philip Morgan and Dr Carole Maldonado-Codina for initially seeking the funding and then allowing me the opportunity to study in Manchester. I have been fortunate to have had two quite brilliant supervisors, who have in different ways guided me through the last four years of study. I thank Phil for his sharp scientific mind, constant flow of ideas and sense of humour. I thank Carole for her expert advice on contact lens materials and manufacturing, her sharp eye for detail and for keeping me on track to complete the thesis. Their skills as supervisors have been complementary and they have both been immensely generous with their time, always willing to discuss problems and suggest solutions, and have always treated me kindly and with respect, and for that I am eternally grateful.

The members of the Eurolens Research group have contributed immensely to my personal and professional time at Manchester. The group has been a source of friendships as well as good advice and collaboration. I am especially grateful to Paul Chamberlain for his clinical advice and input into this PhD, Tracey Burgoyne for her unquestioning assistance especially when times were stressful and Andy Plowright for reviewing sections of this thesis and for providing frequent coffee breaks. Their support has helped me find my way through tricky problems and perhaps most importantly provided me with a happy and relaxed environment in which to carry out my studies and for that I am very grateful.

The surface analysis techniques discussed in this dissertation would not have been possible without support from a number of research groups within the University of Manchester. I would like to thank John Walton for his assistance with XPS analysis, especially his time spent customising the instrument to allow cryogenic sample handling and his ex-

pert advice on data analysis. The ToF-SIMS analysis was possible due to the generous assistance of the Surface Analysis Research Centre and in particular Alan Piowawar for finding the time to analyse the lens samples and in assisting me with the complex data analysis. I also wish to thank Nigel Hodson, based in the Bioimaging Facility, for many many hours of discussion during the troublesome AFM imaging and his 'never give in' attitude to the project. I would also like to thank Stephen Caldwell for his assistance with the ESEM imaging of the lens samples. In addition I also wish to extend my thanks to Jeremiah Kelly for his help and advice regarding the use of MATLAB for image analysis.

Furthermore, I am deeply indebted to CooperVision Inc. for not only supporting this work financially, but also for manufacturing the experimental lenses and assisting with some of the hydrated AFM analysis. I would especially like to thank Arthur Back, Nick Manesis, Charles Francis, Charlie Chen and Jonathan Walker for their extremely valuable support and providing an insight into commercial contact lens research and manufacturing. My thanks also to the Medical Research Council who jointly supported this PhD through a Doctoral Training Award.

I am also grateful to the ISCLR, the College of Optometrists and the American Academy of Optometry for travel grants which have allowed me to present my work at several international conferences.

My time at Manchester has been made enjoyable in large part due to the friends that have become a part of my life. I would like to show my gratitude to my fellow PhD students who I have spent many hours with. In particular, I have appreciated the camaraderie of Mera Haddad and Marco Miranda who ensured that there was never a dull moment and aided in lunch time escapism.

Lastly, I would like to thank my family for all their love and encouragement. For my parents who raised me with a love of science and supported me in all my pursuits, and most of all for my loving, supportive, encouraging, and eternally optimistic fiancée Ana whose faithful support and positive outlook on life has been a powerful source of inspiration and energy throughout my PhD studies. Thank you.

Nomenclature

ACLM	Association of contact lens manufacturers
AFM	Atomic force microscopy
ANOVA	Analysis of variance
AOE	2-allyloxy-ethanol
BVP	Back vertex power
CA	Contact angle
CB	Captive bubble
CCLRU	Cornea and contact lens research unit
CLAPC	Contact lens associated papillary conjunctivitis
COR	Coefficient of repeatability
COV	Coefficient of variation
Dk	Oxygen permeability
Dk/t	Oxygen transmissibility
DS	Dioptres spherical
DMA	N,N-dimethyl acrylamide
EDS	Energy-dispersive X-ray spectroscopy
EGDMA	Ethylene glycol dimethacrylate
ESCA	Electron spectroscopy for chemical analysis
ESEM	Environmental scanning electron microscopy
EWC	Equilibrium water content
FDA	US food and drug administration
GMA	Glyceryl methacrylate
GSED	Gaseous secondary electron detector
HEMA	Poly(2-hydroxyethyl methacrylate)
HPLC	High-performance liquid chromatography
HPMC	Hydroxypropyl methylcellulose
ISO	International organisation for standardisation
KS	Kolmogorov-Smirnov test
LED	Light emitting diode
LOM	Lens orientation markers

M3U	Principle silicone component in experimental lens polymer
MAA	Methacrylic acid
MALDI-MS	Matrix-assisted laser desorption ionisation mass spectrometry
MK	Microbial keratitis
MMA	Methyl methacrylate
NCVE	N-carboxyvinyl ester
NITBUT	Non-invasive tear film break-up time
NVP	N-vinyl pyrrolidine
PAOS	Polyalkylene oxide silicone
PBS	Phosphate buffered saline
PC	Papillary conjunctivitis
PDMS	Poly-dimethylsiloxane
PEG	Poly(ethylene glycol)
PEO	Polyethylene oxide
PLTF	Pre-lens tear film
PMMA	Polymethyl methacrylate
PoLTF	Post-lens tear film
PSI	Pounds per square inch
PVA	Polyvinyl alcohol
PVP	Polyvinyl pyrrolidone
R_a	Mean surface roughness
RF	Resonant frequency
RGP	Rigid gas permeable contact lens
RH	Relative humidity
R_{max}	Maximum roughness
RMS	Root mean square
RSF	Relative sensitivity factor
SD	Sessile droplet
SE	Secondary electrons
SEAL	Superior epithelial arcuate lesions
SEM	Scanning electron microscopy
SFG	Sum frequency generation vibrational spectroscopy
SIGMA	2- propenoic acid

SiH	Silicone hydrogel
SIMS	Secondary ion mass spectrometry
SMS	Short message service
STM	Scanning tunnelling microscopy
TEGDMA	Trimethylene glycol dimethacrylate
TDC	Time-to-digital converters
T_g	Glass transition temperature
ToF-SIMS	Time of flight secondary ion mass spectrometry
TPVC	Vinyl carbamate derivative of TRIS
TRIS	Trimethylsiloxysilane
UHV	Ultra hugh vacuum
USAN	United states adopted name
UV	Ultraviolet
VMA	N-vinyl-N-methyl acetamide
XPS	X-ray photoelectron spectroscopy
γ_{sv}	Interfacial free energy for solid-vapour interface
γ_{lv}	Interfacial free energy for liquid-vapour interface
γ_{sl}	Interfacial free energy for solid-liquid interface

Chapter 1

Introduction

1.1 Introduction to silicone hydrogel contact lenses

Silicone hydrogel contact lenses were first introduced in the late 1990s and have rapidly increased their share in the soft contact lens market, currently accounting for around a third of all new contact lens fits in the UK (Morgan *et al.*, 2008). They are manufactured from soft, water-swollen hydrogel materials and aim to combine the advantageous properties of silicone materials and hydrophilic hydrogel materials. The development of silicone hydrogel materials was driven by clinical complications observed with conventional hydrogel materials. These were primarily associated with hypoxic conditions at the ocular surface which included corneal oedema (Fatt & Chaston, 1982; Mandell & Polse, 1969; Mandell *et al.*, 1970), conjunctival hyperaemia (Papas, 1998) and neovascularisation of the peripheral cornea (Holden & Mertz, 1984). Attempts to reduce the level of corneal hypoxia experienced during contact lens wear by increasing the water content and reducing thickness of the lens material (and therefore increasing oxygen permeability) were only partially successful. Contact lens manufactures therefore sought to develop materials which possessed superior oxygen permeability.

Silicones have been used widely as biomaterials (Colas & Curtis, 2004) and are known to possess extremely high oxygen permeability (Hwang *et al.*, 1971). Silicones are synthetic polymers with a linear, repeating silicon-oxygen backbone and organic groups attached directly to the silicon atoms by carbon-silicon bonds (Figure 1.1). The first lenses which incorporated silicones were silicone elastomer lenses manufactured from polydimethylsiloxane (PDMS) and were launched in 1972 (Zekman & Sarnat, 1972). These silicone materials

have low intermolecular forces and relatively unhindered single bonds that link the silicon and oxygen backbone chain atoms together, resulting in a highly flexible polymer chain (Owen, 1993). The movement of these polymer chains results in high gas solubility, allowing rapid diffusion of gases through the material (Zhang, 2006). A potential negative consequence of the inclusion of silicone into contact lenses is the inherent hydrophobicity this imparts to the material (Kunzler, 1996), which occurs due to the abundance of hydrophobic methyl groups (-CH_3) at the surface of the material, due to the highly flexible silicon-oxygen backbone (Holly & Refojo, 1975). These hydrophobic materials are largely incompatible with the predominately aqueous tear film and clinically resulted in poor lens surface wetting.

Wettability can be defined as the tendency for a liquid to spread over a solid surface (Johnson & Dettre, 1993) and is particularly relevant to contact lenses. The lens surface needs to support a stable ocular tear film layer and failure to achieve this is likely to adversely affect visual performance (Thai *et al.*, 2002a), increase lens surface deposition (Jones *et al.*, 2003), and reduce comfort (Maldonado-Codina *et al.*, 2004b). A stable pre-lens tear film provides a lubricating effect, allowing comfortable lid movement over the front surface of the lens (French, 2005). Lenses with poor wettability have a tendency to become uncomfortable, as surface drying between blinks can result in hydrophobic areas which may irritate the lid as it moves over the lens surface (Jones *et al.*, 2006). In order to achieve optimum visual performance with contact lenses, a stable uniform tear film must be supported over the front surface of a contact lens. A lens that does not have good wetting characteristics will result in a rapid break-up of the tear film and consequently a reduction in visual performance (Rieger, 1992). Contact lens surface wetting can also influence tear film deposition, as lens surface dehydration in the inter-blink pe-

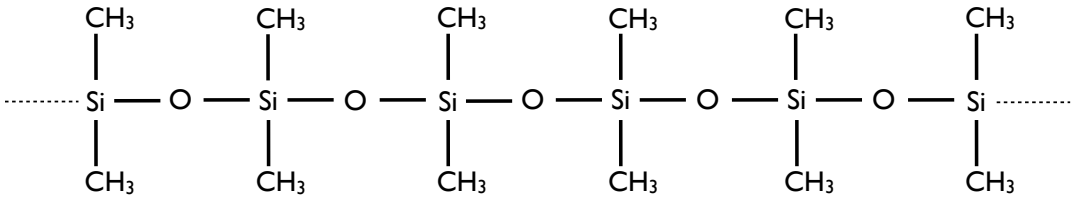

Figure 1.1: The structure of silicone rubber.

riod can produce non-wetting areas on the lens surface, which encourage the deposition of hydrophobic tear film components (Jones *et al.*, 2006). The deposition of tear film components onto a contact lens surface does not always have a negative affect on the wettability. An absorbed layer of mucous glycoproteins on a contact lens has been shown to allow for a continuous pre-lens tear film and good wettability (Cheng *et al.*, 2004). Early silicone elastomer contact lenses showed heavy deposition, poor comfort and reduced acuity due to their hydrophobic nature, which resulted in a destabilised tear film (Huth & Wagner, 1981; Zekman & Sarnat, 1972). Contact lens manufacturers spent many years developing silicone-containing materials to improve oxygen permeability whilst maintaining adequate surface wetting and lens movement. Modern silicone hydrogel materials use a range of fabrication techniques, including plasma surface treatments (Weikart *et al.*, 1999, 2001) and the inclusion of hydrophilic monomers (Iwata *et al.*, 2001) (Maiden *et al.*, 2002; McCabe *et al.*, 2004) to the bulk material, which serve to mask surface hydrophobicity and improve ocular biocompatibility (Kunzler, 1996; Tighe, 2004; Weikart *et al.*, 1999, 2001).

Clinical assessment of the lens surface and overlying tear film can be performed using a range of techniques (e.g. slit lamp, tearscope, keratometry). Given the apparently obvious relationship between subjective comfort and tear film stability, there is, however, little evidence suggesting such a link. This may be related to limitations in the sensitivity of the clinical techniques used to observe the tear film or with other factors such as subject lacrimation or a variation in blink rate during testing. Although there is little evidence in the literature of a direct link between tear film stability and subjective comfort, recent research has shown a link between subjective comfort and apparent mechanical irritation of the upper lid (Korb *et al.*, 2002; Yeniad *et al.*, 2010). As the tear film acts as a lubricating layer between the lens surface and the inner lid surface (Tighe, 2004), this suggests subtle differences in the lens surface wetting for symptomatic wearers, which we are currently unable to consistently detect clinically.

Given that the primary reason for contact lens discontinuation in the UK is contact lens-induced discomfort (Morgan, 2001; Young, 2004), it is perhaps surprising that this problem is not better understood. Many potential factors, such as lens design, material stiffness, surface wettability, surface friction and material dehydration have been identified, but no studies have shown definitively the aetiology of discomfort. Investigation of the

factors influencing contact lens-associated discomfort is often performed by comparing commercially-available contact lenses, but due to the numerous material and lens design differences, forming a definitive conclusion on which factors influence comfort is near impossible.

This PhD study sought to investigate the clinical performance of two experimental silicone hydrogel contact lenses, especially manufactured for this PhD work. These lenses were manufactured with a matching design and from identical material components. The only difference between the two lenses was a single step in the manufacturing process which provided a marked difference in the surface wettability of the lenses. By independently varying the surface characteristics it was possible to investigate the influence of lens surface wettability on their clinical performance. In addition, laboratory characterisation of the lens surfaces was performed in order to investigate how the surface chemistry, surface topography and surface wetting, differed between two lenses with such different clinical wetting characteristics.

1.2 Introduction to polymeric materials

All modern contact lens materials, since the introduction of polymethylmethacrylate (PMMA) have been based on polymer technology. In attempting to understand the clinical performance of contact lenses it is important to understand the properties these materials possess and how this is influenced by manufacturing conditions. A basic knowledge of polymer science is therefore necessary in order to allow an understanding of the bulk and surface characteristics of these materials.

1.2.1 Introduction to polymers

Polymers include groups such as plastics (thermo & thermosetting), elastomers (rubber), fibres and hydrogels. The unique properties that polymers possess arise from the ability of certain atoms to link together to form stable bonds. Carbon has the ability to link together with four other atoms, such as hydrogen, oxygen, nitrogen, sulphur, chlorine or itself. It is the ability of carbon to act in this way that forms the basis of organic chemistry. A polymer is formed when many smaller units, called monomers, link together to form a long chain. The conversion of monomer units to form polymer chains can be expressed by

the chemical reaction shown in Figure 1.2. The essential requirement of a small molecule to qualify as a monomer is the possession of two or more bonding sites, through which they can be linked together to form a polymer chain. The number of bonding sites is referred to as the functionality. Structural and functional groups (X and Y in Figure 1.2) are present along the polymer chain. It is the way these functional groups interact with each other and their surrounding environment that influences the interaction of polymer chains and the resultant polymer properties. Polymers are often very long in relation to their cross sectional diameter. This gives the material unique characteristics, such as toughness or elasticity. In addition these polymer chains are often randomly arranged and are entangled with other polymer chains. The degree of interaction and entanglement imparts distinctive properties on the polymer, which can cause a material to vary from that of a hard glassy material to that of an elastomeric material. A polymer can be given more elastomeric behaviour with the inclusion of plasticiser. A plasticiser is a liquid (usually organic) with a high boiling point, which acts as an internal lubricant allowing polymer chains to move more freely.

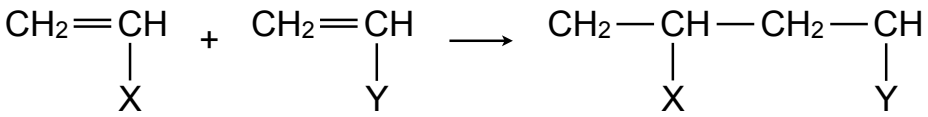

Figure 1.2: Schematic representation of monomer conversion to polymer (X and Y represent structural and/or functional groups)

1.2.2 Classification of polymers

A homopolymer is a type of polymer in which all the monomer units are chemically and stereochemically identical, with the exception of the terminal units. Homopolymers can be linear (all monomers arranged in a linear sequence) or branched (non-linear) (Figure 1.3). Although chemically similar, linear and branched homopolymers often have very different properties (e.g. high and low-density polyethylene). A copolymer is a type of polymer in which more than one type of monomer is present. For linear copolymers the monomers can be arranged in an alternating, block or random patterns, and can also form branched and graft structures (Figure 1.4). Complex three-dimensional structures can develop with a more extensive distribution of branched points, leading to highly ramified structures. Similar complex structures can form when linear chains are covalently linked together by

cross-linking agents, as shown in Figure 1.5. Cross-linking a polymer improves dimension stability, lowers creep rate, increases resistance to solvents and reduces tendency for heat distortion.

1.2.3 Principles of polymerisation

There are two main types of polymerisation reactions; step-growth (or condensation) and chain-growth (or addition) processes. Step-growth polymers are produced by the reaction of monomer units with each other, with the elimination of a small molecule such as water (Figure 1.6). Hydrogels are not typically formed through this method of polymerisation but through chain-growth polymerisation. Chain-growth polymers are formed by the reaction of monomer units with each other, without the elimination of by-product molecules. Each monomer typically has at least one double bond and is described as

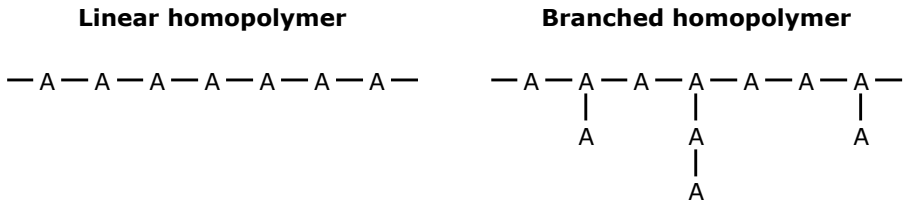

Figure 1.3: Schematic representation of linear and branched homopolymer.

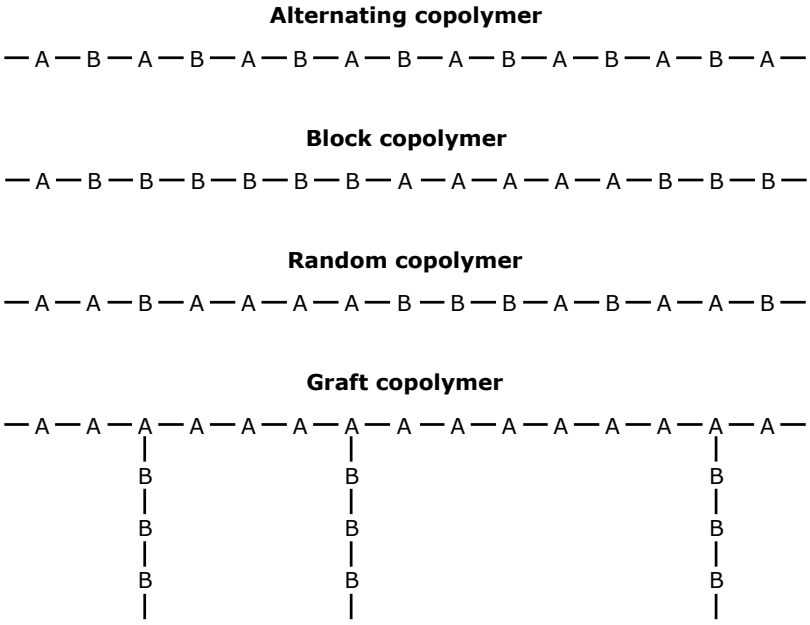

Figure 1.4: Schematic representation of alternating, block, random and graft copolymers.

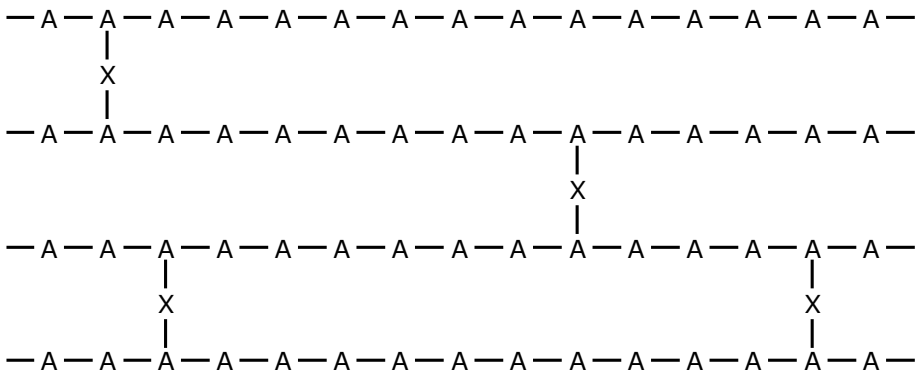

Figure 1.5: Schematic representation of a crosslinked polymeric system (X represents the cross-linking agent).

unsaturated. The polymerisation process is triggered with the production of free radicals (Figure 1.7(a)). These free radicals combine with the monomer, resulting in a free radical of the monomer (Figure 1.7(b)). The radical monomers combine with other monomers to form a radical compound (Figure 1.7(c)). Radical compounds can continue to propagate, resulting in a polymer chain thousands of monomers long. Polymerisation does not usually continue until all the monomers have been polymerised, as the highly reactive free radicals inevitably lose their reactivity. Termination usually occurs either by recombination (where two propagating polymer chains, each containing free radicals, meet and share the unpaired electron (Figure 1.7(d))) or disproportionation (when two radicals interact via hydrogen abstraction, leading to the formation of two reaction products, one of which is saturated and the other unsaturated (Figure 1.7(e))). Due to the reactivity of the free radicals other reactions can occur, including chain transfer and free radical combination with retarders or inhibitors (Maldonado-Codina & Efron, 2003).

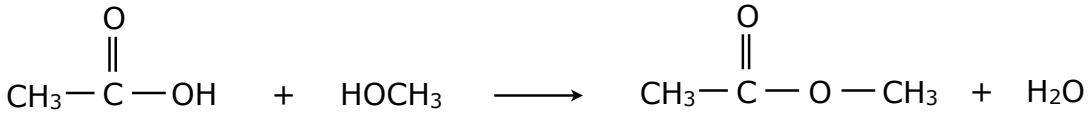

Figure 1.6: Schematic representation of a condensation reaction.

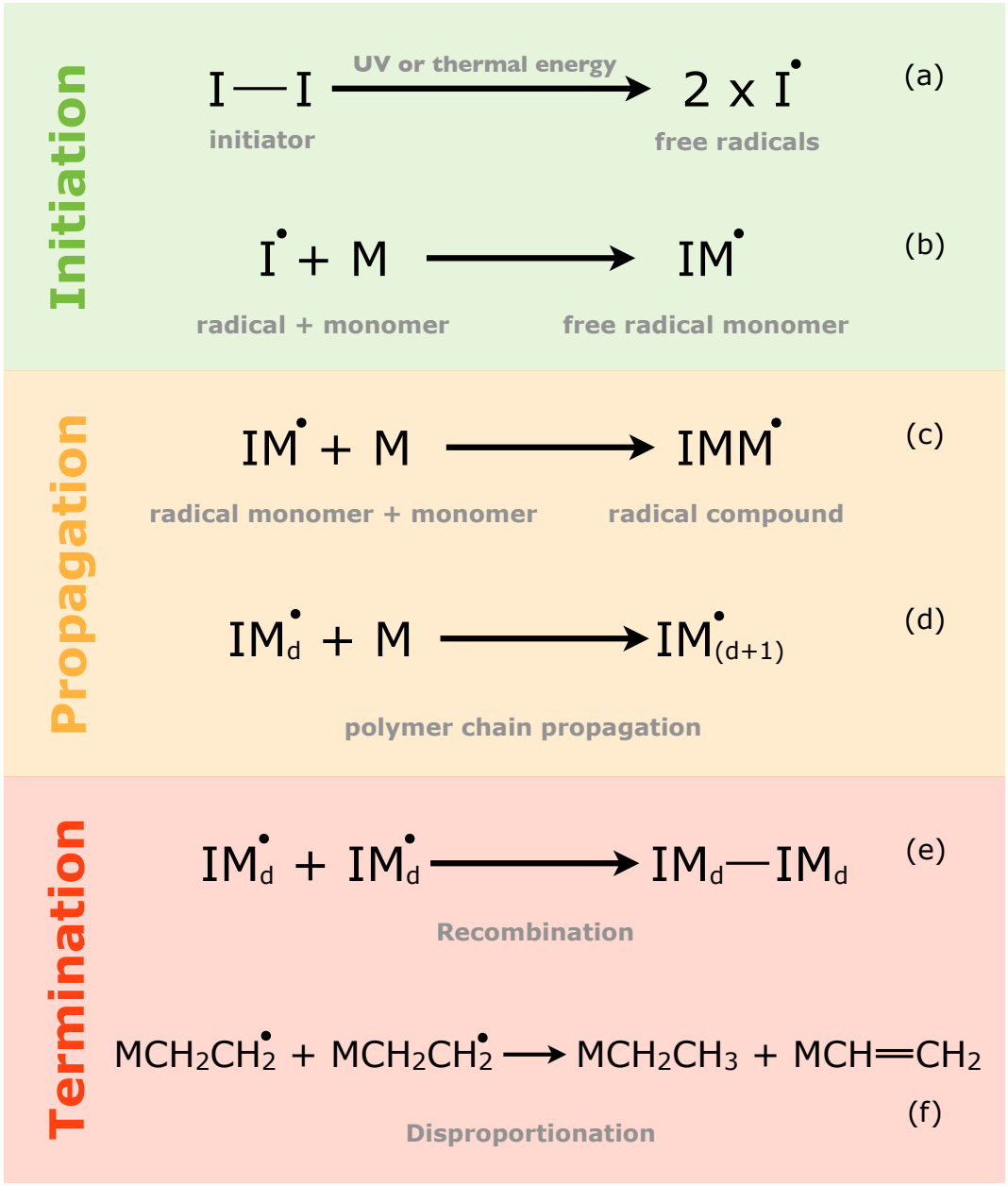

Figure 1.7: Schematic diagram of the initiation, propagation and termination stages of polymerisation (Based on diagram from Cowie (1991)).

1.3 Methods of soft contact lens manufacture

There are three main methods of soft contact lens manufacture: lathing, spin casting and cast moulding.

1.3.1 Lathed lens manufacture

In lathed manufacture, lenses are formed from solid buttons of dehydrated polymeric material. The buttons are mounted in a lathe where the back surface is cut using a diamond tool. This newly formed back surface is subsequently polished and a solvent then used to remove the polish. The back surface is attached to a chuck by means of melted wax and the front surface is then lathe cut and polished. Following lathing the lenses are hydrated and packaged in individual glass vials or blisters (disposable packaging). The lathing process is not well suited to mass production and is favoured for low-volume custom lenses.

1.3.2 Spin-cast lens manufacture

The spin-cast manufacturing method involves spinning a cast, at a computer-controlled speed, into which the mixture of monomers is injected. The shape of the mould controls the front surface of the lens and the back surface is dependant on gravity, centrifugal force, surface tension, the amount of liquid monomer in the cast and the rate of spin. The back vertex power (BVP) of the lens is essentially determined by the spin speed, and the centre thickness mainly by the dose of monomer. When polymerisation is complete the lenses are demoulded, hydrated and packaged in a similar way to lathed lenses.

1.3.3 Cast-moulded lens manufacture

Lens manufacture by cast-moulding involves the formation of a lens from the monomer mixture placed between two casts (Figure 1.8). The monomer is in liquid form and is introduced into a concave (female) mould, which defines the front shape of the lens. A male mould is then mated to the female mould which defines the back surface of the lens. The mould is then either irradiated with UV light or placed in an oven, which initiates polymerisation, resulting in the formation of a contact lens. The moulds are then disassembled and discarded and the lens is hydrated in saline, inspected, packaged and sterilised.

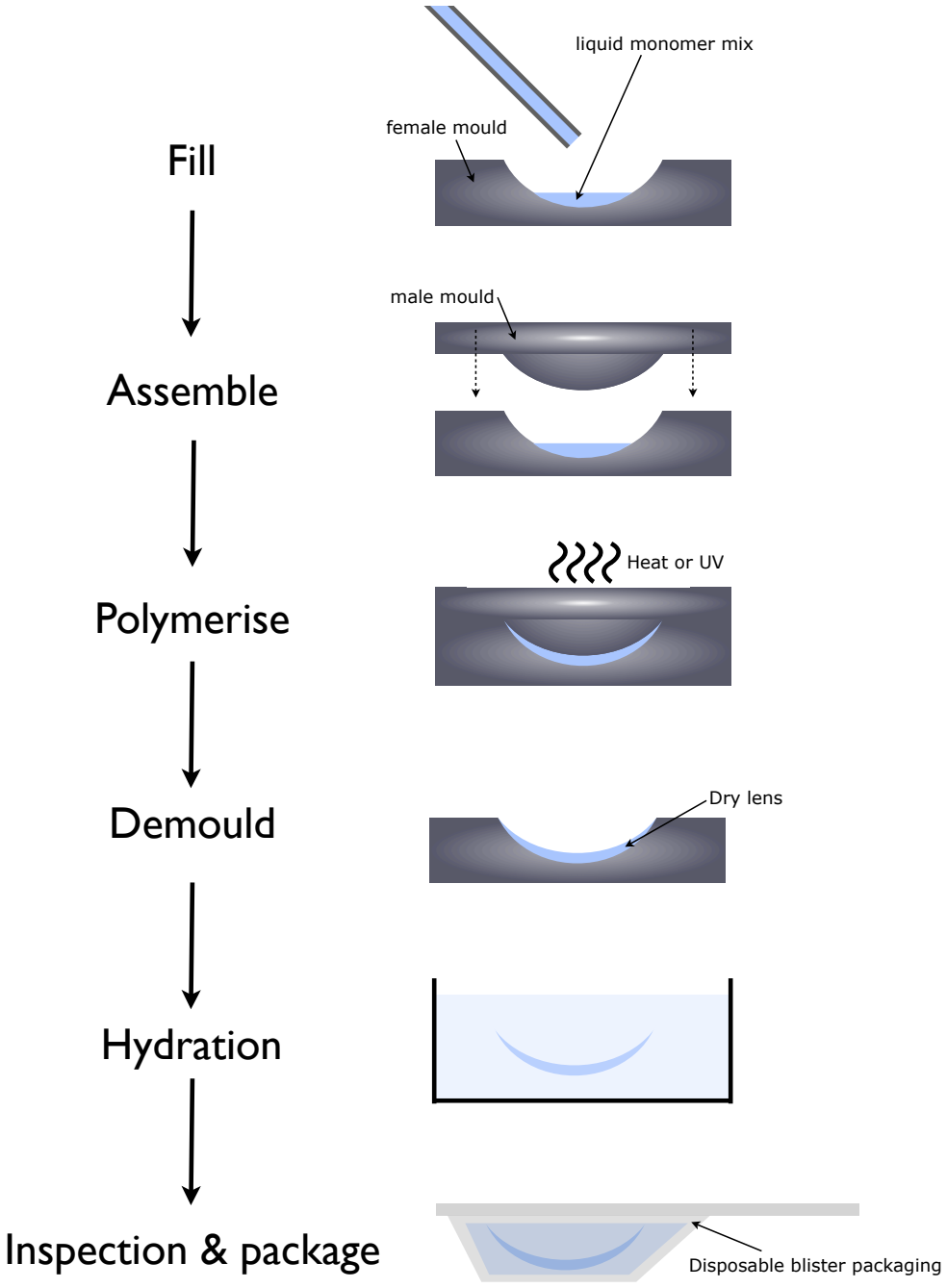

Figure 1.8: A schematic diagram of the manufacture of soft contact lenses by a cast-moulding process.

The method of lens manufacture affects the conditions under which polymerisation occurs. These differing conditions affect the physical and chemical properties of the lens (Grobe *et al.*, 1996) and its resulting clinical performance (Maldonado-Codina & Efron, 2003). Conventional hydrogel contact lenses have been manufactured by all three techniques, but the cast moulding method is favoured as it is the most economically viable for mass manufacture. Until recently, all silicone hydrogel contact lenses were manufactured using the cast moulding technique, however, several manufacturers have recently released lathe cut silicone hydrogel contact lenses, allowing a greater prescription and parameter range (Air Optix Individual by CibaVision and Ultrawave SiH by Ultravision).

1.4 Polymeric contact lens materials

To understand why current contact lens materials are used and to appreciate the advantageous properties they possess, it is logical to follow the evolution of polymer-based contact lens materials.

1.4.1 Poly(methyl methacrylate) (PMMA)

PMMA was the first polymer used in the manufacture of contact lenses, when it began replacing glass as the material of choice during the 1940s. PMMA is in many ways an excellent material for contact lens manufacture due to its toughness, dimensional stability, optical properties, ease of manufacture and physiological inactivity (Tighe, 2002). Unfortunately, the PMMA surface has relatively poor wetting properties and almost negligible permeability to oxygen, resulting in corneal hypoxia.

1.4.2 Poly(2-hydroxyethyl methacrylate) (HEMA)

A key development came in 1960 when Otto Wichterle and Drahoslav Lim based at Institute of Macromolecular Research in Czechoslovakia engineered a monomer similar to PMMA but with the addition of a hydroxyl group (Wichterle & Lim, 1960). Due to initial problems with the cast moulding method of manufacture, a spin-casting method of production was developed, with the first soft contact lens manufactured in 1961 (Wichterle & Lim, 1961). This new material was 2-hydroxyethyl methacrylate (HEMA). HEMA can be polymerised to make pHEMA due to its two double carbon bonds in much the same way as MMA is polymerised to make PMMA (Figure 1.9). As HEMA has this addition

hydroxyl group, in the presence of water, hydrogen bonding occurs between the hydroxyl group and water molecules. The material is therefore much more hydrophilic and causes water to be drawn into the polymer matrix.

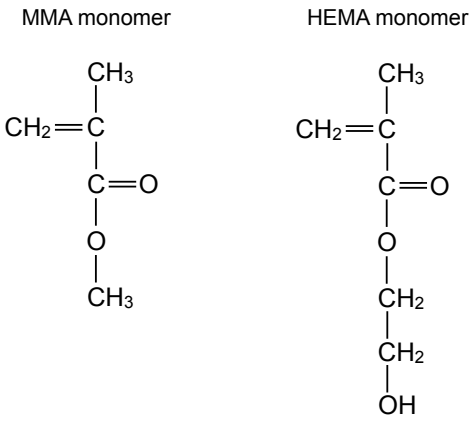

Figure 1.9: A schematic diagram of MMA and HEMA monomer.

1.4.2.1 Equilibrium water content

The ability a material has to bind water is known as the equilibrium water content (EWC). The EWC can be calculated using equation 1.1.

$$EWC\ (\%)\ =\ (weight\ of\ water\ /\ weight\ of\ hydrated\ gel)\ x\ 100\% \qquad (1.1)$$

The value of EWC can vary significantly and is dependant on temperature and the nature of the hydrating medium. In its fully hydrated state pHEMA has a water content of approximately 38%. Due to the ability of pHEMA to bind water, it is able to transport substantially more oxygen through the contact lens (compared to PMMA), as oxygen diffuses through the aqueous phase of the material. pHEMA contact lenses quickly became successful due to increased comfort, rapid adaptation time, ease of fitting and biocompatibility (Tighe, 2002). As the popularity of pHEMA contact lenses rapidly increased, it became apparent that this lens material was also not without problems. Many of these problems stemmed from the fact that the lenses caused corneal hypoxia. Early animal experiments indicated that the poor physiological response of the anterior eye during wear of the thick pHEMA lenses could be reduced by making soft lenses more permeable to oxygen

(McMahon & Zadnik, 2000). In addition, pHEMA lenses suffered from other problems relating to solution toxicity and lens spoliation (Maldonado-Codina & Efron, 2003).

1.4.2.2 Oxygen permeability

Materials have differing ability to transport oxygen. PMMA transports very little oxygen through the lens during wear (Tighe, 2002), whereas hydrated pHEMA is able to transport significant amounts of oxygen through the lens. The ability of the material to transport oxygen is known as the oxygen permeability (Dk), where D is the diffusivity of the material and k is solubility of the material. The units of Dk are barrers:

$$Dk \;=\; 10^{-11}\ (cm^2\ x\ mlO_2)\ /\ (sec\ x\ ml\ x\ mmHg) \tag{1.2}$$

The amount of oxygen diffusion through a contact lens is related not only to the oxygen permeability of the contact lens material, but also to the lens thickness (Novicky & Hill, 1981; Polse & Mandell, 1970). Oxygen transmissibility is defined as the oxygen permeability of the material divided by the lens thickness. Oxygen transmissibility has the units barrers/cm:

$$Dk/t \;=\; 10^{-9}\ (cm^2\ x\ mlO_2)\ /\ (sec\ x\ ml\ x\ mmHg) \tag{1.3}$$

With pHEMA contact lenses, the oxygen passes though the water, which is bound within the polymer matrix. The oxygen permeability of the lens material is linked directly with the EWC. The relationship between EWC and oxygen permeability has been shown to be (Morgan & Efron, 1998):

$$Dk \;=\; 1.67\ e^{0.0397EWC} \tag{1.4}$$

The challenge for the contact lens manufacturers was that they either had to increase the Dk or reduce the thickness of the material to allow increased oxygen transmission of the cornea. Manufacturers therefore developed thinner contact lenses to increase the oxygen transmission of the lens. The Hydrocurve thin lens (Soft Lenses Inc.) and O3 Series (Bausch & Lomb) were both significantly thinner (0.035-0.06mm) than the original Bausch & Lomb pHEMA lenses (Maldonado-Codina & Efron, 2003). Further reduction in lens thickness was shown to cause problems with dehydration of the lens surface, epithelial staining, corneal erosions and poor lens handling (Holden *et al.*, 1986; Mobilia *et al.*, 1980).

An increase in Dk was therefore required in an attempt to reduce the hypoxia-related complications associated with contact lens wear.

1.4.3 pHEMA monomer additives

In pHEMA-based materials, oxygen is transported through the lens material by diffusion through the water phase. Thus, by increasing the water content of the lens material, an associated increase in oxygen permeability is observed. Several monomer additives are used to increase the materials affinity for water and therefore increase the level of water binding. These monomer additives include:

1. **Methacrylic acid (MAA)** When MAA monomer is combined with pHEMA there is a significant increase in EWC (Figure 1.10). To bring about this increase in EWC the material first needs to be ionised, often by immersion in sodium bicarbonate. This converts the CO_2H group into a CO_2^- group by removal of the hydrogen atom and thus increasing the EWC by expanding the network due to repulsion between the negatively charged carboxylate ions (Maldonado-Codina & Efron, 2003). MAA is typically used in low quantities in contact lens manufacture, varying between 0.25% and 2.5% of the polymer composition.

2. **N-vinyl pyrrolidine (NVP)** The amide group (N-C=O) of NVP is very polar and two molecules of water can become bound to it (Figure 1.10). NVP can either be used as a graft copolymer or random copolymer. Hydrogels can be manufactured with up to 90% EWC using NVP.

3. **Glyceryl methacrylate (GMA)** Although similar in structure to HEMA, GMA has two hydroxyl groups (Figure 1.10). It is therefore able to bind water much more strongly than HEMA. GMA is non-ionic and inert and when combined with pHEMA a material with EWC of up to 70% can be obtained.

4. **Cross-linking monomers** Cross-linking chemical groups are also added usually at around 1% of the monomer mix (Tighe, 2002). These cross-linking monomers have two C=C double bonds and bond the polymer chain together to increase polymer stability. Cross-linking agents used in contact lens manufacture include ethylene glycol dimethacrylate (EGDMA shown in Figure 1.10) and divinyl benzene (Guillon, 1994; Maldonado-Codina & Efron, 2003).

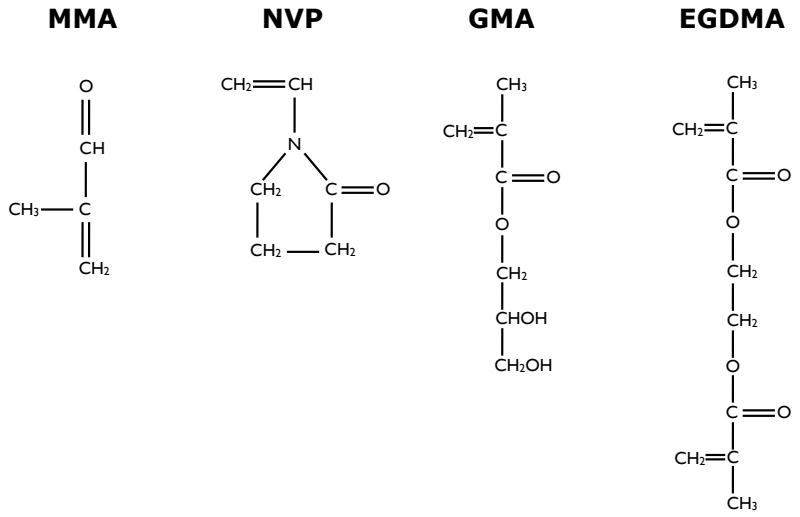

Figure 1.10: A schematic diagram of hydrogel monomers.

1.4.4 Extended wear of hydrogel contact lenses

Although the initial development of hydrogel lenses was intended for use on a daily wear basis, as both material and manufacturing technology developed, so arose the possibility of overnight wear with high EWC HEMA-based hydrogel lenses. This lead to contact lenses being fitted on an extended wear (up to seven nights of continuous lens wear) or continuous wear basis (up to 30 nights of continuous lens wear). Unfortunately, although these lenses were well accepted by the patients, it became apparent that the risk of serious ocular complications was substantially higher with this modality of wear. Poggio *et al.* (1989) and Schein *et al.* (1989) showed that the risk of microbial keratitis (MK) was 5x - 15x greater with extended wear. In a key paper, Holden & Mertz (1984) showed that even with an extremely high water content, conventional hydrogel lenses were still inducing corneal hypoxia. They concluded that the required oxygen transmissibility necessary to avoid hypoxia for daily wear was 24.1 barrers/cm and for overnight wear 87.0 barrers/cm. The development of HEMA-based contact lenses with improved oxygen transmission, had reached a limit, leaving little scope for further development. Even with the advances that had been made with the addition of more hydrophilic monomers and the associated increases in EWC and Dk, these materials were unable to supply sufficient oxygen to the cornea to avoid oedema. Even with a 90% EWC and a centre thickness of 0.1mm, the oxygen transmissibility would only be 60 barrers/cm (Maldonado-Codina & Efron, 2003), clearly well below the modified criterion of 125 barrers/cm (Harvitt & Bonanno, 1999)

necessary for overnight wear. Manufacturers therefore sought to develop other materials that offered superior oxygen transmissibility in an attempt to break the dependence on water for the transfer of oxygen through the lens.

1.5 Silicone hydrogel contact lens materials

1.5.1 Properties of silicon-containing polymers

Silicon is a chemical element that lies just below carbon in the periodic table. Siloxane is a class of organosilicon compounds with the empirical formula R_2SiO, where R is an organic group. Siloxane compounds have an inorganic backbone (Si-O-Si-O-) while having organic side chains. Polymerised siloxanes are commonly known as silicones, although strictly this is incorrect terminology as silicone should have a double bond between oxygen and silicon. In the field of contact lenses, silicone therefore describes an inorganic-organic polymer comprising a silicon-oxygen backbone. The most common siloxane is linear polydimethylsiloxane (PDMS) (Figure 1.11).

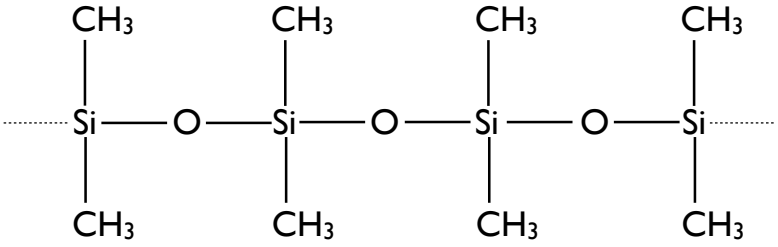

Figure 1.11: A schematic diagram of the structure of PDMS.

Silicones are noted for their high thermal stability, biocompatibility, hydrophobicity and releasing properties (Owen, 2000). The hydrophobic properties of these materials are a result of two phenomena: (i) the methyl groups provide hydrophobic characteristics to the polymer (Figure 1.12(i)); and (ii) the flexibility of the silicone polymer chain permits the rearrangement of the polymer backbone such that the methyl groups may orient themselves efficiently at an interface (Brook, 2000). The uniquely high chain flexibility arises from the very large bond angle of the Si-O-Si linkage (approximately 145^o) and the low bending force constant for this linkage (Figure 1.12(ii)). Rotation about the siloxane bond in PDMS is virtually free, the energy being almost zero, compared with 14mJ/mol for rotation about C-C bonds in polyethylene and 20kJ/mol for polytetrafluroethylene (Owen, 1993). The

glass transition temperature (T_g) of dimethylsilicone polymers, which reflect the ease of segmental motion along the chain, are very low, typically less than -120^{o}C (Brook, 2000). The flexibility of the polymer backbone explains the reorientation observed when the environment of the polymer changes. The surface reorientation of polymeric solids and its dependancy on different environments is a familiar phenomenon (Andrade *et al.*, 1985b) and is particularly prevalent in silicone because of the high backbone flexibility (Owen, 2000).

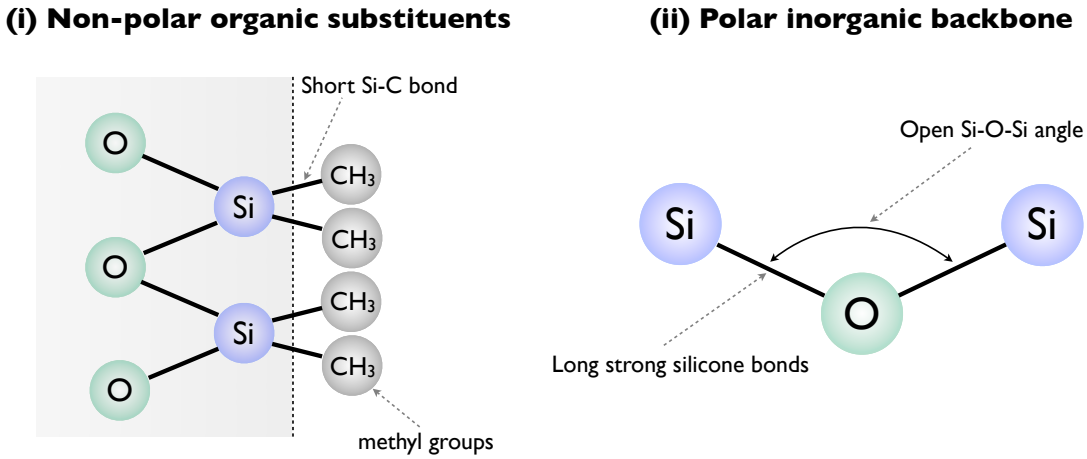

Figure 1.12: Properties of PDMS.

1.5.2 Silicone elastomer contact lenses

Silicone elastomer lenses seemed to go some way towards solving the problems associated with the limited oxygen transmission of contact lens materials. This material is known to have oxygen permeability several times greater than that of conventional pHEMA-based materials. Silicone elastomer though is hydrophobic which leads to poor clinical wettability and rapid tear film deposition (Huth & Wagner, 1981). In addition, these lenses are not permeable to ions leading to a thinning of the post-lens tear film and an associated reduction in lens movement, with a potential for the lens to bind to the ocular surface (Rae & Huff, 1991). Attempts were made at surface coating these lenses, but problems with durability were observed (Maldonado-Codina & Efron, 2004).

1.5.3 Combining the properties of hydrogels and silicone

HEMA-based contact lens materials therefore exhibited good clinical wettability, comfort and parameter stability but lacked sufficient oxygen permeability for both daily wear and extended wear (Morgan *et al.*, 2010). Silicone elastomer materials exhibit high oxygen permeability but possess a poorly wettable surface which is prone to tear film deposition. Manufacturers therefore attempted to combine the advantageous properties of pHEMA with the oxygen transmission properties of silicone. In conventional hydrogel materials oxygen diffuses through the aqueous phase of the material and therefore oxygen permeability is limited by the EWC. Silicone hydrogels behave in a similar way at higher EWC, but at lower EWC the silicone elements of the polymer allow much greater amounts of oxygen to be dissolved within the material, significantly increasing the material oxygen permeability. As EWC reduces, the proportion of polymer that contains silicone increases, resulting in raised oxygen permeability (Figure 1.13). The oxygen permeability of silicone hydrogel materials, when EWC is below 50%, is very dependant upon the composition of the non-aqueous group within the polymer. By varying the composition of the non-aqueous groups the Dk can be altered compared with that shown in Figure 1.13. The challenge was to combine the advantageous properties of these two materials. The rigid gas permeable (RGP) contact lens industry had already developed a material containing silicone, which possessed excellent oxygen permeability. Trimethylsiloxysilane (TRIS), a modified silicone elastomer type material, had been developed for the rigid contact lens industry in the early 1970's (Gaylord, 1974). The logical step was to combine the hydrophobic TRIS with a hydrogel material. However, in practice this resulted in impaired optical clarity due to a separation of the two material phases, known as phase separation. Thus, attempts were made to chemically modify TRIS to allow it to combine with a hydrogel, such as the Tanaka *et al.* (1979) patent. They proposed a solution to this problem by inserting hydrophilic groups into the TRIS material (Figure 1.14) and copolymerising it with a hydrophilic monomer and cross linking agent to produce a polymer suitable for soft contact lens manufacture. Although this material allowed the experimental production of low water content soft contact lenses with good comfort and excellent oxygen permeability (Tanaka *et al.*, 1979), there were still many problems with insufficient lens movement and lens binding to the ocular surface (Tighe, 2004).

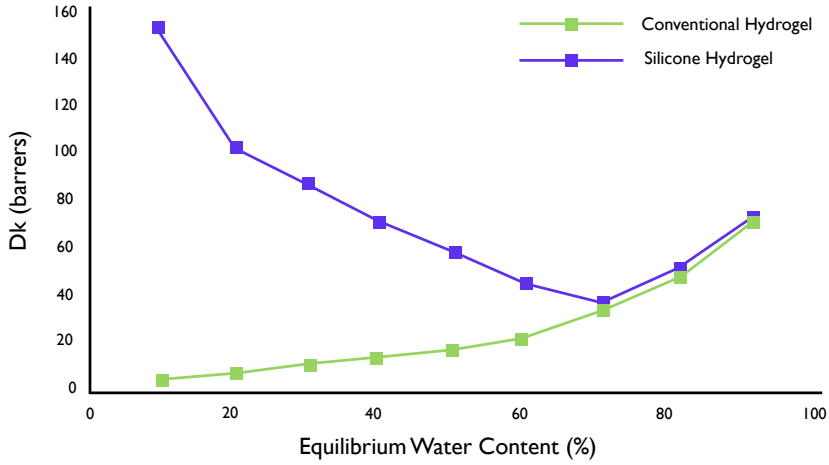

Figure 1.13: The relationship between water content (EWC) and oxygen permeability (Dk).

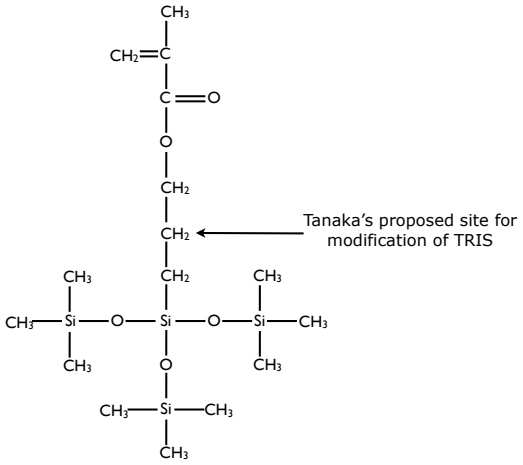

Figure 1.14: Site for modification of TRIS.

1.5.4 First generation silicone hydrogel lens materials

A breakthrough in the development of silicone hydrogels materials came with the realisation of the importance of hydraulic and ionic permeability for a contact lens material. Traditional hydrogel contact lens materials have the ability to transport water and dissolved ions through the lens material, whereas silicone elastomer materials possess very low hydraulic and ionic permeability. Nicholson *et al.* (1996) suggested that these material properties were critical in providing sufficient on eye lens movement for a contact lens. Future attempts at developing silicone hydrogel materials therefore looked to provide

high levels of oxygen permeability, sufficient to maintain corneal health, while providing adequate ion permeability to allow clinically acceptable lens movement. Contact lens manufacturers adopted different approaches in the development of materials which would offer these required characteristics. In the late 1990s the first two commercially-available silicone hydrogel contact lens materials were introduced into the market. These two lenses, often termed the first generation silicone hydrogel materials, were the Focus Night & Day lens (now marketed as the Air Optix Night & Day lens) manufactured by CibaVision and PureVision lens manufactured by Bausch & Lomb. Both of these contact lenses had a recommended wearing regime of up to 30 nights continuous wear.

1.5.4.1 Focus Night & Day material

CibaVision developed the use of macromer technology in an attempt to improve the oxygen permeability of contact lens materials. Macromers are large monomers formed by pre-assembly of structural units that are designed to bestow particular properties on the final polymer (Tighe, 2002). Robertson *et al.* (1991) described the macromer as being constituted from hydrophilic polyethylene oxide segments and oxygen-permeable polysiloxane units. The level of oxygen permeability for the lens material was proposed to be sufficient to maintain corneal health, while the ion permeability was designed to be sufficient to allow the lens to move on the eye. The manufacturing process results in a material that has a biphasic structure, with one oxygen permeable segment providing the oxygen pathway and one ion permeable pathway providing the ion transmission pathway, allowing both ions and oxygen to permeate freely thought the material in two co-continuous phases (Tighe, 2004). The oxygen permeable materials (60-85%) are monomers and macromers that are siloxane containing, fluorine containing or contain carbon-carbon triple bonds. The ion permeable materials (15-40%) are hydrophilic monomers and polyethylene glycol (PEG). The novel nature of this material is not in the component monomers it contains, but the technology associated with the morphology of the polymer. A biphasic polymer would normally lack transparency if the phase dimensions were greater than the wavelength of light. It is suggested that inter-phase regions allow the material to remain transparent (Tighe, 2004). Even with the presence of the hydrophilic components within the material, the surface is too hydrophobic and is required to undergo surface treatment to provide an acceptable level of clinical wetting. The lens surface is therefore treated using a gas plasma coating process in the presence of reactive nitrous precursors, which

are fed into the plasma (Maldonado-Codina *et al.*, 2004a). This gives a smooth uniform surface (Gonzalez-Meijome *et al.*, 2005), with a thickness of around 25nm (Weikart *et al.*, 2001). Atomic force microscopy (AFM) has revealed a gently undulating surface in the form of curved diffuse ridges, only a few nanometers in height, thought to be lathing marks transferred from the moulds during manufacture or associated with the coating process (González-Méijome *et al.*, 2006a). The Focus Night & Day material is based on a fluroether macromer copolymerised with TRIS monomer and N,N-dimethyl acrylamide (DMA) in the presence of a diluent (Tighe, 2004). The Focus Night & Day material has a water content of 24% and oxygen permeability of 140 barrer (Alvord *et al.*, 1998).

1.5.4.2 PureVision lens material

Bausch and Lomb focused their research on the insertion of more polar groups into the section of TRIS identified by Tanaka *et al.* (1979). Kunzler & Ozark (1994) showed their attempts to add a polar fluorinated side group having a hydrogen atom attached to a terminal difluro-substituted carbon atom. The aim of this was to increase the compatibility of silicone containing monomers with hydrophilic monomers to give material with a EWC of around 40%. Numerous further developments and patents led to the production of the PureVision material (Bambury & Seelye, 1991; Grobe & Kunzler, 1999). This is produced by modification of the TRIS monomer by replacing the CO-O group with a O-CO-NH link and with the methyl group replaced by a single hydrogen. This monomer is known as a vinyl carbamate derivative of TRIS (TPVC) (Figure 1.15).

The TPVC is copolymerised with NVP to form the PureVision material. The water content of the PureVision material suggests ion permeability lower than that measured for balafilcon, suggesting an element of phase separation (Lopez-Alemany *et al.*, 2002). The PureVision lens also requires a surface treatment to obtain acceptable clinical wetting by the tear film. A plasma oxidation process is used to convert the hydrophobic organic silicone to a relatively hydrophilic inorganic silicate (Tighe, 2004). AFM has shown the surface of balafilcon to have glassy silicate islands, which do not completely occlude the surface (González-Méijome *et al.*, 2006a). It has been suggested that these glassy islands might reduce oxygen permeability, but as the substrate is partially exposed at the surface, it appears to have little effect on the permeability of the material. This partial exposure of the hydrophobic substrate was thought potentially problematic, although these exposed

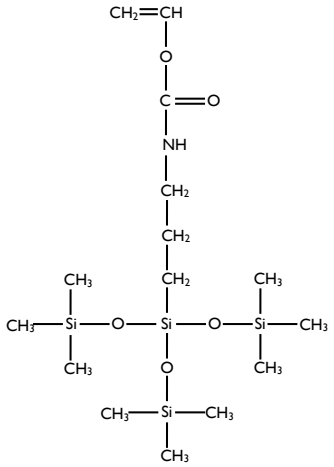

Figure 1.15: Vinyl carbamate derivative of TRIS.

Table 1.1: First generation silicone hydrogel lenses

	Focus Night & Day	**PureVision**
Water Content (%)	24	36
Oxygen permeability (Barrers)	140	99
Modulus (Mpa)	1.52	1.1
Surface treatment	Plasma coating	plasma oxidation
Principle monomers	DMA, TRIS, siloxane monomer[1]	NVP, TPVC, NCVE, PBVC[2]

regions may also have been influenced to some extent by the plasma and thus be less hydrophobic than the bulk material Tighe (2004). The glassy islands have a depth of between 10 and 50nm, and due to their isolated structure the surface is able to flex. The PureVision material has an EWC of 36% and a Dk of 99 barrers.

1.5.5 Second-generation silicone hydrogels

A second generation of silicone hydrogel contact lens materials were subsequently introduced, typically with a lower modulus and higher water content than the first generation materials. These materials tend to possess lower oxygen permeability than first generation materials and are primarily intended for daily wear.

[1]DMA: N, M-dimethylacrylamide; TRIS: tris-(trimethyl siloxysilyl).

[2]NVP: N-vinyl pyrrolidone; TPVC: tris-(trimethyl siloxysilyl); NCVE: N-carboxyvinyl ester; PBVC: poly(dimethysiloxy)di(silylbutanol)bis(vinyl carbamate).

1.5.5.1 Acuvue Advance & Acuvue Oasys lens materials

Johnson and Johnson released Acuvue Advance contact lenses in 2004, followed shortly afterwards by Acuvue Oasys in 2005. These materials differ in several key ways to the first generation silicone hydrogels. The design of both materials is based on the modified TRIS monomer (Tanaka *et al.*, 1979), but with a much improved method of synthesis. The monomer is polymerised in conjunction with a siloxy macromer, hydrophilic monomers (such as HEMA and N, N- dimethyl acrylamide (DMA)) and a small amount of cross-linking agent, in the presence of PVP and an organic diluent (Tighe, 2006). Acuvue Oasys has a water content of 38% and a Dk of 103 Barrers and is approved in the UK for daily wear and up to seven days of continuous wear, whilst Acuvue Advance has a higher water content and a lower Dk (Figure 1.2) and is approved only for daily wear (Tighe, 2006). Acuvue Advance and Oasys lenses differ to first generation silicone hydrogels in both surface and mechanical properties. They were the first silicone hydrogel lenses to be released without application of a surface treatment subsequent to fabrication of the lens. This has the advantage of avoiding possible patent infringement and reduces manufacturing costs. Both materials use a high molecular weight polyvinyl pyrrolidone (PVP) internal wetting agent, which is incorporated into the lens material at the fabrication stage and is designed to provide a hydrophilic layer at the surface of the material that shields the silicone at the material interface (Tighe, 2006). It has been suggested that partially attached PVP chains can extend out from a hydrogel surface and may form polymer brushes at the lens surface (Yañez *et al.*, 2008). The technique appears to be successful in terms of wettability, lubricity and clinical acceptability (Riley *et al.*, 2006). The second significant difference between these lenses and the first generation silicon hydrogel lenses is their lower modulus of elasticity. The modulus of a material describes its relative stiffness. It can be seen in Table 1.1 that the modulus of both the PureVision and Night & Day lenses is significantly higher than those of the second generation silicone hydrogel lenses. Material properties for second generation silicone hydrogel lenses are given in Table 1.2.

1.5.5.2 Air Optix lens material

The Air Optix contact lens manufactured by CibaVision was introduced in 2004. The material was developed in response to the clinical problems experienced by some patients with the higher modulus contact lens materials (Sweeney, 2004) and the increasing pop-

Table 1.2: Second generation silicone hydrogel lenses.

	Acuvue Advance	**Acuvue Oasys**	**Air Optix Aqua**
Water Content (%)	47	38	33
Oxygen permeability (Barrers)	60	103	110
Modulus (Mpa)	0.43	0.72	1.22
Surface treatment	None (internal wetting agent)	None (internal wetting agent)	Plasma coating
Principle monomers	mPDMS, HEMA, DMA, SiGMA, EGDMA, PVP[1]	mPDMS, HEMA, DMA, SiGMA, EGDMA, PVP	DMA, TRIS, fluorine-containing siloxane macromer

ularity of daily wear silicone hydrogels (Morgan *et al.*, 2008). The Air Optix material is essentially a lower modulus, lower oxygen permeability, higher water content version of Night & Day material (González-Méijome *et al.*, 2006a). The monomers used appear to be the same as those in Focus Night & Day material, but with a modification to the relative monomer concentration (Plesnarski, 2004). These changes in the polymer composition result in a higher water content and an associated lower modulus. The lenses are primarily intended for daily wear, although it also has a six night extended wear indication in the UK. Material properties are given in Table 1.2.

1.5.6 Third-generation silicone hydrogel materials

A third generation of silicone hydrogel contact lens materials have more recently become available which also show a trend for decrease modulus and higher water content, but break the traditional inverse relationship between oxygen permeability and water content (Figure 1.13) by having a higher oxygen permeability than water content would predict.

1.5.6.1 Biofinity lens material

The Biofinity contact lens manufactured by CooperVision was introduced in 2006. Biofinity has a Dk that lies well above that expected for a material with such a high EWC (Figure 1.16). This is related to the fact that it is solely macromer-based with no TRIS derivatives and allows a superior oxygen permeability/water content relationship to TRIS-based lens materials. Another interesting feature of Biofinity is the absence of either surface treatment or an internal wetting agent. The technology underpinning the material originates

[1] mPDMS: monofunctional methacryloxypropyl terminated polydimethylsiloxane; SIGMA: 2- propenoic acid; PVP: poly(vinyl pyrrolidone).

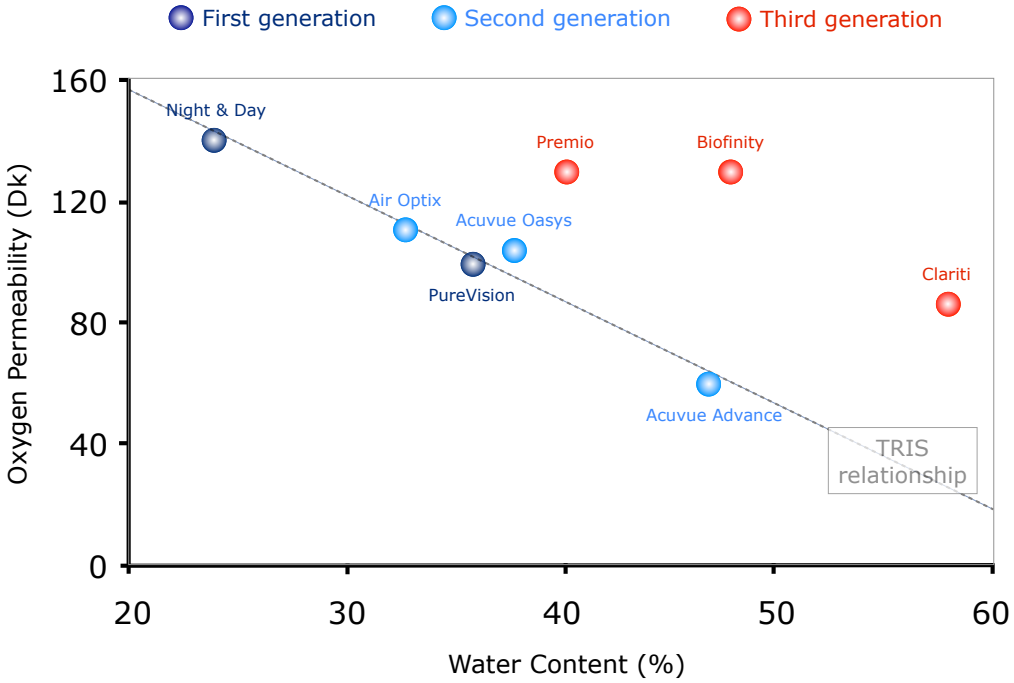

Figure 1.16: Relationship between EWC and Dk for silicone hydrogel materials.

in a Japanese patent filed in December 2000 by the Asahikasei Aime Co. (Iwata *et al.*, 2001). The patent claims that two siloxy macromers of different sizes, one of which is monofunctionalised (contains only one polymerisable double bond), when used together produce advantageously high oxygen permeabilities. The patent contains other subtleties, some relating to particular hydrophilic monomers, which enhance the compatibility of the silicone moieties with the hydrophilic domains. This explains the absence of internal wetting agents or surface treatment (Tighe, 2006). The ability to increase the EWC of a material while maintaining high Dk levels brings obvious advantages in terms of the mechanical properties of the material. This can also be seen as a potential disadvantage as increasing the EWC has been associated with an increased rate of material dehydration (Tighe, 2006). These lenses have been approved for up to 30 days continuous wear in the UK. Material properties for these lenses are given in Table 1.3.

1.5.6.2 PremiO lens material

The PremiO lens, manufactured by Menicon was introduced in 2007. It is a macromer-based material which is composed primarily of silicone methacrylates, silicone acrylates, N,N-dimethyl acrylamide (DMA) and pyrrolidone derivates (Baba & Watanabe, 2005).

The DMA and pyrrolidone derivates make up a significant part of the lens material (around 50% by weight) and are hydrophilic co-monomers. The siloxane co-monomers used to form the macromer in PremiO are TRIS and a repeating poly-dimethyl siloxane structure. The lens is cast moulded and is surface treated to improve hydrophilicity. The surface treatment is a plasma process in the presence of oxygen and other gases (Baba & Watanabe, 2005). A hydrophilic polymer film is coated on the lens material either by a plasma polymerisation method or a plasma graft polymerisation method (Parvin *et al.*, 2008), resulting in an apparently smooth, lubricious surface with favourable wetting properties (Baba & Watanabe, 2005). These lenses have been approved for up to six nights of extended wear in the UK. Properties for this material are given in Table 1.3.

1.5.6.3 Clariti lens material

The Clariti lens is manufactured by Sauflon and was introduced in 2008. The Clariti material is the reaction product of TRIS (at least 10%), a poly dimethyl siloxane (trimethylsilyl methacryloxypropyl) (10%), NVP (40-60%) and at least one other non-ionic hydrophilic monomer (HEMA and/or DMA) (2-10%) (Broad, 2009). The hydrophilic NVP is present in such an amount that the reaction product comprises a PVP homopolymer. The solvent (mixture of primary alcohol and a more hydrophobic solvent) improves monomer component compatibility and is effective at preventing phase separation of the hydrophilic and hydrophobic monomers. The addition of relatively small amounts of MAA reduces optical haze in the finished contact lens. The lens material is therefore composed of a silicon-containing copolymer and a PVP homopolymer in the form of an interpenetrating network, which is wettable and does not suffer from phase separation or significant haze (Broad, 2009). The lenses have been approved for daily wear. Properties for this material are given in Table 1.3.

1.5.7 New silicone hydrogel lens modalities

1.5.7.1 Acuvue Trueye

Acuvue Trueye was the first silicone hydrogel daily disposable when it was introduced in 2008 to the UK market. This lens comprises both hydrophobic silicone materials and hydrophilic materials. As with the Acuvue Oasys and Acuvue Advance products, it incorporates polyvinyl pyrrolidone (PVP) throughout the lens matrix, which acts as a mois-

Table 1.3: Third generation silicone hydrogel lenses.

	Biofinity	**PremiO**	**Clariti**
Water Content (%)	48	40	58
Oxygen permeability	128	129	60
Modulus (Mpa)	0.75	0.91	0.50
Surface treatment	None	Plasma oxidation and plasma coating	None
Principle monomers	M3U, FMM, TAIC, IBM, HOB, NMNVA, NVP[1]	Silicone methacrylates, silicone acrylates, DMA, pyrrolidone derivative	Alkyl methacrylates, silicone acrylates, siloxane monomers, NVP

turising and wetting agent. On introduction to the US market in 2010 changes to relative composition of the material have been made, which result in altered lens parameters, with a lower Dk and higher EWC.

1.5.7.2 Lathed silicone hydrogels

The Air Optix Individual lens was the first lathe cut silicone hydrogel contact lens when it arrived in the market in 2007. This allows the lens to be ordered in a very wide range of lens powers (+20DS to -20DS), lens diameters and curvatures. The difficulty in manufacturing a lathe-cut silicone hydrogel lens is that the material is very rubbery and does not lend itself well to being cut on a lathe. CibaVision altered the formulation of their material, in part by the addition of styrene, allowing it to be lathed (Subbaraman *et al.*, 2009). It then undergoes a plasma coating process to improve surface wetting and reduce tear film deposition.

1.5.8 CL Classification

The two main classification systems for soft contact lens materials are the US Food and Drug Administration (FDA) classification system and the International organisation for standardisation (ISO) system for contact lens material classification.

[1]M3U: ao-bis(methacryloyloxyethyliminocarboxyethyloxypropyl)-poly(dimethylsiloxane)-poly(tri fluoropropyl methylsiloxane)-poly(methoxy-poly(ethyleneglycol)propylmethyl-siloxane; FMM: a- meth acryloyloxyethyliminocarboxyethyloxypropyl -poly(dimethylsiloxy)-butyldimethylsilane; TAIC: 1,3,5-triallyl-1,3,5-triazine-2,4,6(1H,3H,5H)-trione; IBM: isobornyl methacrylate; HOB: 2-hydroxybutyl methacrylate; NMNVA: N-methyl-N-vinyl acetamide.

Table 1.4: FDA categorisation of hydrogels contact lens materials.

FDA Categorisation	**Group I**	**Group II**	**Group III**	**Group IV**
Water Content	Low	High	Low	High
Charge	Non-Ionic	Non-Ionic	Ionic	Ionic
Low = ≤ 50% water; High = > 50% water; Ionic = Charged; Non-Ionic = No charge				

Table 1.5: The ISO system of soft contact lens material classification.

Prefix	This is one of two parts of the code administered by USAN. Use of the prefix is optional outside of the USA. For example, Etafilcon A has the USAN code 'Eta'.
Stem	filcon for soft lenses (hydrogel-containing lenses having at least 10% water content by mass)
Series suffix	Also administered by USAN, a capital letter added to the stem to indicate the revision level of the chemical formula: A is the original (first) formulation, B the second and so on. Can be omitted if there is only one formulation.
Group sufix	
I	$<$ 50% water content, non-ionic
II	$\geqslant$ 50% water content, non-ionic
III	$<$ 50% water content, ionic
IV	$\geqslant$ 50% water content, ionic
Dk range	A numeric code which identifies the permeability in ranges which are considered significant in contact lens wear. 0:<1Dk, 1:1-15 Dk, 2:16-30 Dk, 3:31-60 Dk, 4:61-100 Dk, 5:101-150 Dk, 6:151-200 Dk.
Modification code	A lower case m, which denotes that the surface of the lens is modified, having different chemical characteristics from the bulk material.

1.5.8.1 FDA classification system

In the United States all contact lens materials are issued with a USAN (United States Adopted Name) identity by the FDA (e.g. etafilcon A) which is specific to the composition of the material. The material will also fall into one of the four groups for the USA Food and Drug Administration (FDA) classification scheme (Table 1.4), which offers a simple but effective subdivision of lens materials on the basis of water content and ionic character (Tighe, 2002). The main drawback of the FDA system is that materials composed of very different chemistry can be classified within the same material group.

1.5.8.2 ISO system of soft lens classification

European standards (BS EN ISO 18369: 2006) have set out the ISO system for contact lens material classification (Table 1.5). Each material is classified by a six-part code: (prefix)(stem)(series suffix)(group suffix)(Dk range)(surface modification code).

1.6 Clinical performance of silicone hydrogel contact lenses

Clinical studies have confirmed that many of the hypoxic-related clinical observations with extended-wear of conventional lenses were overcome with these highly oxygen permeable materials. Papas *et al.* (1997) showed that silicone hydrogel contact lenses produced significantly less limbal hyperaemia than conventional hydrogel lenses, with levels similar to no lens wear. Keay *et al.* (2000) reported that extended wear of silicone hydrogels did not cause a long term increase in microcyst numbers (tiny cystic vesicles in the corneal epithelium primarily associated with hypoxia), although a transient increase was observed when a patient was refitted from low Dk/t hydrogel lenses. Covey *et al.* (2001) compared continuous wear silicone hydrogel contact lens wearers to non-lens wearers. They found no hypoxia-associated effects but did find higher levels of tear film debris and conjunctival staining with the lens wearers. Fonn & Pritchard (2000) noted that in a clinical environment the majority of silicone hydrogel lenses wearers reported that their lenses felt less dry than their previous conventional hydrogel lenses, despite considerably longer wearing times. It has been suggested that the lower water content of silicone hydrogel contact lenses is related to reduced lens dehydration. Published work shows that silicone-hydrogel lens materials dehydrate at a slower rate and to a lesser extent than conventional hydrogel materials (Jones *et al.*, 2002b; Morgan & Efron, 2003) and may partially help to explain this reduction in the sensation of dryness. The material elasticity of silicone hydrogels is significantly less than that of silicone elastomer lenses (Jones *et al.*, 2006), but still significantly higher than conventional hydrogel lenses (2-6 times greater). This increased rigidity gives the lens enhanced patient handling properties and initially it was thought it may be of benefit in masking astigmatism, although a study by Edmondson & Edmondson (2003) showed that this was not the case. These mechanical properties though, can cause clinical problems as they are less able to conform to the shape of the eye and require careful fitting, as loose lenses typically exhibit poorer comfort (Dumbleton *et al.*, 2002). In addition, the rigidity of these materials may be implicated in a variety of mechanical complications seen

with silicone-hydrogel lenses, including papillary conjunctivitis (Skotnitsky *et al.*, 2002) and superior epithelial lesions (Jalbert *et al.*, 2001).

1.6.1 Modulus of elasticity and silicone hydrogel contact lenses

The incidence of superior epithelial arcuate lesions (SEAL) has been shown to be higher with first generation silicone hydrogel than convectional hydrogels contact lenses (Dumbleton, 2003; Dumbleton *et al.*, 2002; Holden *et al.*, 2001; Jalbert *et al.*, 2001; Long *et al.*, 2000). The aetiology of a SEAL is thought to be multifactorial, related both to patient characteristics (eyelid tautness, upper lid position, race, cornea steepness and sagittal height) and lens characteristics (modulus of elasticity, lens thickness, lens curvature, lens surface and lens age) (Sankaridurg *et al.*, 2004). Contact lens associated papillary conjunctivitis (CLAPC) is typically found in 2-3% of patients wearing disposable daily wear hydrogel contact lenses (Sankaridurg *et al.*, 2004) and more frequently in patients wearing lens on an extended wear basis (Levy *et al.*, 1997). Several studies have shown that silicone hydrogel lenses appear to induce an isolated CLAPC, rather than a diffuse CLAPC, suggesting a mechanical rather than immunological aetiology (Skotnitsky *et al.*, 2002). Another possible cause can be attributed to surface wettability (Dumbleton, 2003). First generation silicone hydrogel materials have an increased modulus, which is thought to increase lens movement. This along with potential marginal fitting characteristics of the lens can lead to the lens edge fluting or lifting. This raised lens edge can act as a mechanical irritant, simulating localised papillary conjunctivitis (Jones & Dumbleton, 2002). Second and third generation materials are typically of lower modulus than the first generation silicone hydrogel lenses, but they are still generally higher than tradition hydrogel materials (Steffen & Schnider, 2004). Contact lenses with higher modulus have been associated with a greater incidence of contact lens papillary conjunctivitis (Tighe, 2004), superior epithelial arcuate lesions (Holden *et al.*, 2001) and mucin balls (Tan *et al.*, 2003). These clinical observations are thought to be related to a mechanical interaction of the contact lens with ocular surface in part associated with these higher modulus materials. These clinical observation are not, though, solely associated with modulus, with factors such as lens design and surface characteristics also implicated as causative factors. This is demonstrated by fewer mechanical-related clinical complications and better subjective comfort as a result of a change in lens design following introduction of the 8.4 base curve Night & Day (lotrafilcon A) lens (Dumbleton *et al.*, 2002; Montero Iruzubieta *et al.*, 2001). With the reduction

in the modulus and improvement in lens design we have generally seen a reduction in the incidence of these gross mechanical ocular complications (Jones & French, 2009). Brennan *et al.* (2007) have recently suggested that modulus still remains an important factor which appears related to subjective comfort, with the low modulus materials generally showing better subjective comfort. This analysis, as with many other studies, was performed using commercially available contact lenses which differ in numerous parameters and material characteristics making controlled investigation difficult.

1.6.2 Post-lens debris

Several early studies with first generation silicone hydrogel contact lenses (Dumbleton *et al.*, 2000; Fonn & Pritchard, 2000) noted the presence of translucent spherical debris, 20-100μm in size, observed between the back surface of the contact lens and the cornea, which were described as mucin balls. Fonn & Pritchard (2000) reported that mucin balls increased in number and size following use of extended wear contact lenses. Morgan & Efron (2002) reported that the incidence of mucin balls peaked four weeks after commencing lens wear and began to decline thereafter, with more mucin balls noticed in subjects wearing Focus Night & Day (lotrafilcon A) lenses than with the PureVision (balafilcon A) lenses. Flemming *et al.* (1994) performed biochemical analysis of mucin balls which indicated that the deposits are composed mainly of mucin and tear proteins and have little lipid content. Mucin balls have been hypothesised to result from interactions between the lens surface and the corneal epithelium and can occur with both conventional and silicone hydrogel contact lenses (Tan *et al.*, 2003). The overnight wear of silicone hydrogel contact lenses results in a viscous mucin-rich layer between the lens and the epithelial surface due to depletion of the post lens tear film. Sheering forces caused by blinking during open eye conditions and rapid eye movements during sleep have the effect of rolling the mucin-rich post lens layer into spheres, which are observed as mucin balls. Dumbleton *et al.* (2000) proposed that reducing lens motion, by more closely aligning lens shape to that of the ocular surface, would be a possible means of cutting down mucin ball numbers. Other studies have observed that altering the composition of a surface treatment can affect the number of mucin balls observed with a particular material substrate, suggesting that it is not the modulus of the lens material alone that accounts for the interaction with the lens and anterior ocular surface (Sweeney *et al.*, 2004). As second and third generation silicone hydrogel contact lenses typically have a lower modulus, lack of surface treatment and are

worn on a daily wear basis, the incidence and severity of mucin balls would be expected to have reduced.

1.6.3 Lens deposition on silicone hydrogel lenses

Deposition of tear film components onto the lens surface can result in reduced vision (Gellatly *et al.*, 1988), reduced comfort (Pritchard *et al.*, 1996) and increased inflammatory responses (Mondino *et al.*, 1982). Due to the ability of silicone components to migrate towards the surface, silicone hydrogel contact lenses have a tendency to become hydrophobic, potentially resulting in marked lipid deposition (Huth & Wagner, 1981). The type and extent of tear film deposition is dependant on the water content of the material, the surface charge, length of wear, degree of hydophilicity and tear film composition (Jones *et al.*, 2003). Silicone hydrogel materials have been shown to deposit lower levels of proteins than ionic conventional hydrogel materials (McKenney & Becker, 1998; Senchyna *et al.*, 2004; Subbaraman *et al.*, 2006), although substantially more protein appears denatured on the silicone hydrogel materials (Jones *et al.*, 2003). Lipid deposition, in contrast, is substantially greater on the surface of silicone hydrogel materials, compared with the ionic conventional hydrogel materials (Jones *et al.*, 2003). The higher level of lipid deposition observed on silicone hydrogel lenses is likely due to (i) hydrophobic-to-hydrophobic interactions with the lens surface, and (ii) due to the presence of N-vinyl pyrrolidone (NVP) in some silicone hydrogel lenses (PureVision (balafilcon A), Biofinity (comfilcon A) and Clariti), which enhances lipid deposition (Jones *et al.*, 2000; Maissa *et al.*, 1998). Cheung *et al.* (2007b) and Nichols (2006) have observed a build-up of lipid on the lens surface, especially during 30 nights continuous wear which can become an clinical issue for some patients. The presence of the lipid is also thought to provide benefits to the patient as they have lubricious properties and have been shown to improve the *in vitro* wettability for some contact lens materials (Lorentz *et al.*, 2007).

1.6.4 Microbial inflammation/infection with silicone hydrogel lenses

A major driving force behind the development of silicone hydrogel was the thought that contact lens related hypoxia was a causative factor in the development of ocular surface inflammation and infection. Unfortunately, recent epidemiological studies investigating the risk of corneal infections have found that there has been no reduction in the risk of infection with silicone hydrogel lenses, with overnight wear of contact lenses appearing

to be a major risk factor for both lens types (Dart *et al.*, 2008). Indeed in some studies the risk of infiltrative keratitis was shown to be greater for the silicone hydrogel lens type in daily wear (Stapleton *et al.*, 2008), although this may be partially associated with factors such as longer wearing times and more contact lens wearing days with the silicone hydrogel lenses. Morgan *et al.* (2005) found that the severity of infection and the risk of vision loss appeared related to oxygen permeability, but the actual risk of infection did not differ between the lens types. The literature is therefore clear that silicone hydrogels do not reduce the risk of inflammatory events or infection and therefore further material developments and an improved understanding of the predisposing risks factors are needed in order to reduce the future risk of infection/inflammation for contact lens wearers.

1.6.5 Bacterial binding to silicone hydrogel lenses

The level of bacterial binding to silicone hydrogel contact lens is disputed in the literature. Some studies suggest silicone hydrogel materials exhibit significantly higher bacterial adhesion than conventional hydrogel lenses (Giraldez *et al.*, 2010; Henriques *et al.*, 2005; Kodjikian *et al.*, 2008), possibly due to greater hydrophobicity and/or higher oxygen transmissibility. In contrast, Keay *et al.* (2001) showed little difference in adhesion between silicone hydrogel and conventional lenses and other studies suggest that silicone hydrogel materials adhere less bacteria than conventional hydrogel materials (Santos *et al.*, 2008). Such differences are likely explained by the different methodologies and bacterial strains used in these investigations. Differences in bacterial adhesion between silicone hydrogel lens types appear small and lenses appear generally less prone to bacterial adhesion following wear (Santos *et al.*, 2008; Vermeltfoort *et al.*, 2006).

1.6.6 Solution toxicity with silicone hydrogel contact lenses

Silicone hydrogel materials were originally brought to market primarily as a continuous wear product, but they have become equally, if not more, successfully worn on a daily wear basis (Morgan *et al.*, 2008). This has required the use of contact lens care solutions to clean and store the lens. Several studies have reported significant levels of corneal staining with certain silicone hydrogel lenses and contact lens care and storage solutions (Epstein, 2002; Garofalo *et al.*, 2005; Jones *et al.*, 2002a). It often appears as diffuse punctate staining either across the whole cornea or in a ring around the peripheral cornea and is most marked 2 to 4 hours after lens insertion (Garofalo *et al.*, 2005). Studies have looked at the dif-

ferent lens/solution combinations to quantify the levels of staining observed, finding very low levels with hydrogen peroxide solution compared to the multipurpose solution which varied for both solution and lens type (Andrasko & Ryen, 2008; Garofalo *et al.*, 2005). In these studies PureVision (balafilcon A) exhibited relatively high levels of staining, whereas Acuvue Advance (galyfilcon A) lenses produced very low levels with the same solutions, suggesting a strong material as well as solution dependancy. There appears to be no obvious cause for this material dependancy, although the PureVision lens has been shown to be effective as a drug delivery device (Hui *et al.*, 2008) and it may be that its highly porous nature (Lopez-Alemany *et al.*, 2002) is extending the period of corneal exposure to the contact lens solution components, resulting in the observed corneal staining. The relevance of this type of corneal staining is disputed in the literature with some suggesting it is asymptomatic (Garofalo *et al.*, 2005; Jones *et al.*, 2002a), whereas others have suggested it can influence comfort (Andrasko & Ryen, 2008, 2007). Carnt *et al.* (2007) suggested that eyes that experience solution toxicity are more likely to experience a corneal inflammatory event, although there is absolutely no evidence to suggest that solution-induced corneal staining predisposes a patient to more serious events, such as microbial keratitis (Sweeney & Naduvilath, 2007; Ward, 2008). Recent work has suggested that a rub and rinse stage prior to lens storage and lens insertion significantly reduces solution induced staining, suggesting the lens surface may also play a role in these observations (Peterson, 2010).

1.6.7 Comfort and silicone hydrogel lenses

It has been reported that the primary reason for discontinuation of contact lens wear in the UK is contact lens-induced discomfort (Morgan, 2001; Young, 2004). Both conventional hydrogel and silicone hydrogel lens wearers show a reduction in comfort at the end of the daily wearing period (Dumbleton *et al.*, 2010, 2008; Fonn, 2007; Fonn *et al.*, 1999; Pritchard & Fonn, 1995a) as shown in Figure 1.17. Comfort has been shown to be reduced at the end of a silicone hydrogels wear cycle (2 weeks or 1 month) and also reduced for both the beginning and at the end of lens wearing cycle if the lenses were not replaced as scheduled (Dumbleton *et al.*, 2010).

Several studies have suggested that better comfort is obtained with silicone hydrogel lenses compared with conventional hydrogel lenses (Brennan *et al.*, 2002; Dumbleton *et al.*, 2006;

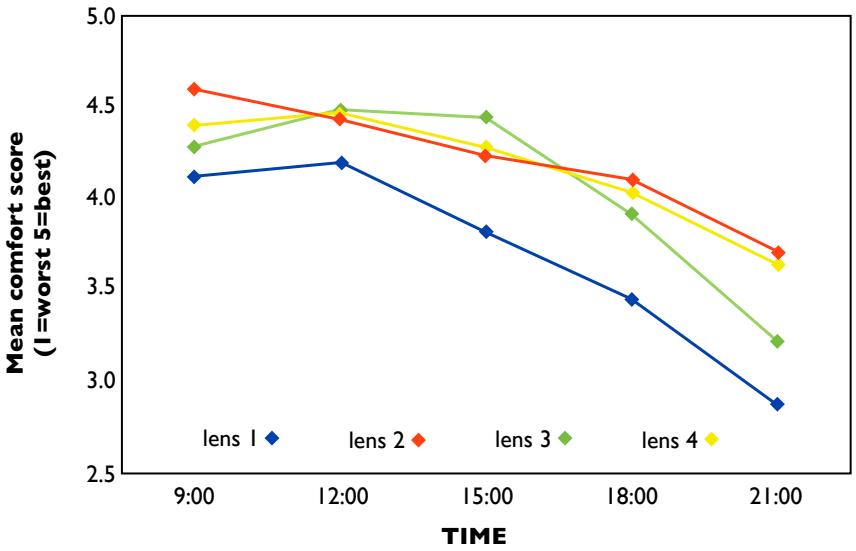

Figure 1.17: Change in subjective comfort through the day for four contact lens types, using SMS messaging responses (Plowright *et al.*, 2008).

Fonn & Pritchard, 2000; Sweeney *et al.*, 2004), although other studies have shown little difference from conventional hydrogels (Coles-Brennan *et al.*, 2006; Fonn & Dumbleton, 2003). Where present, these differences in comfort may be due to a variation in tear film deposition between materials (Senchyna *et al.*, 2004), or due to differences in the water content of the lens materials (which might in turn influence factors such as surface dehydration (Jones *et al.*, 2002b; Morgan & Efron, 2003), although the link between dehydration and comfort is somewhat debated (Brennan, 1988; Hall *et al.*, 1999; Young *et al.*, 1997)). The influence higher oxygen permeability has on lens comfort is debated with some suggesting comfort is related to the oxygen permeability (Dillehay, 2007), whereas others have suggested that there is no conclusive link between Dk and comfort (Brennan & Morgan, 2009). Indeed it has been suggest that comfort might be higher with a low Dk lens as hypoxia has been shown to induce cornel hypoesthesia (Millodot & O'Leary, 1980). Clinical studies comparing the levels of comfort provided by silicone hydrogel lenses have differed in their findings, with some reporting differences in comfort between silicone hydrogel lens types (Brennan *et al.*, 2006; Dillehay, 2007; Dumbleton *et al.*, 2002; Fonn & Dumbleton, 2003; Young *et al.*, 2007), whilst others have found little difference in comfort (Dumbleton *et al.*, 2008). Brennan & Morgan (2009) have suggested that potentially critical factors such as material modulus, lens design and surface properties differ between

silicone hydrogel contact lenses and therefore we are likely to see differences in comfort between silicone hydrogel lenses, as observed when comparing conventional lenses (Brennan, 1988; Fonn *et al.*, 1999; Young *et al.*, 1997).

Contact lens comfort is clearly influenced by multiple factors, which can be sub-divided into lens-related factors (lens material, lens design, lens age), patient related factors (ocular sensitivity, tear film chemistry, blink pattern) and environmental factors (temperature, humidity, environmental contaminants, air flow). It is likely a complex interaction of these factors dictates the lens comfort. Lens-related factors are difficult to investigate independently. When a comparison of commercial products is made, there are often numerous differences in lens characteristics, resulting in difficulty attributing differences in comfort to a specific lens factor. By applying complex statistical techniques it is possible to draw general conclusions about the more critical clinical variables. Brennan (2009) applied a statistical technique to a large data set obtained from a range of clinical studies and suggested that modulus and surface friction appear to be the key material determinants of subjective lens comfort.

1.7 Lens surface wettability

In addition to understanding the material from which a contact lens is manufactured, it is also important to understand the biological system in which the contact lens is worn and the factors influencing how the tear film is able to be spread across the lens surface.

1.7.1 The structure and function of the tear film

Due to the intimate contact between the contact lens, the tear film and the ocular surface during wear, it is important to understand the structure and function of each. The functions of the tear film are (i) to form an smooth optical surface, (ii) to lubricate the movement of the eyelids, (iii) remove debris from the eye, (iv) an antimicrobial affect, (v) maintaining epithelial hydration and (vi) nourishment of the corneal epithelium (oxygen and other nutrients). The tear film consists of three layers, the superficial lipid layer which makes up about 4% of the total thickness; the middle aqueous layer, which represents around 90% of the tear film; and the mucus layer which typically comprises around 6% of the tear film (Figure 1.18). The total thickness of the tear film is believed to be

less than 10 microns (Holly, 1981), with more recent optical coherence tomography data (Wang *et al.*, 2003) suggesting around 3 - 4 microns. The inner most mucin layer contributes to the epithelial cell surface structure and anchors the overlying aqueous gel. The mucins which span the membranes are produced by the corneal and conjunctival epithelial cells, whereas the gel-forming mucins are derived from the goblet cels of the conjunctiva (Lemp, 2003). These gel forming mucins help to cleanse the surface by removal of debris from the ocular surface, act to stabilise the tear film and interact with the outmost lipid layer. The lipid layer is produced by the meibomian glands of the eyelids. Its function is to reduce evaporative losses from the tear film and, with the gel-forming mucins, to lubricate the movement of the lid over the ocular/contact lens surface. The aqueous component of the tears is produced by the lacrimal glands and contains all of the water-soluble elements of the tear film (proteins, peptides and electrolytes). In addition to the relatively stable proteins such as lysozyme, albumin and lactoferrin, there are numerous cytokines, growth factors and other factors that are often present in low levels or completely absent under normal condition, but can increase in response to injury, disease or environmental stress (Lemp, 2003). This responsive system is controlled by the central nervous system via sensory feedback and influences glandular secretion, in response to disease, injury or environmental stress.

1.8 *In vivo* assessment of lens wettability

A range of techniques have been developed to assess the stability of the tear film. Table 1.6 shows several methods of evaluating the tear film stability along with a brief description of each. These techniques can be separated into two groups. Some use a dark background and project a light grid onto the tear film while others use a light background and allow direct observation of the tear film and its structure. Hirji *et al.* (1989) suggested that dark background instruments are measuring tear film instability, whereas light background instruments are measuring the tear break up time. This may explain why the results do not correlate, although more recent literature dispute these findings (Cho *et al.*, 2004). The field of assessment also varies with the types of assessment (Table 1.6). Bruce *et al.* (2001) showed that the most likely region for the pre-lens tear film to first destabilise is in the parameniscal zones, although the paper suggested significant variability with differing lens materials. It is therefore advantageous to use an instrument with a field of

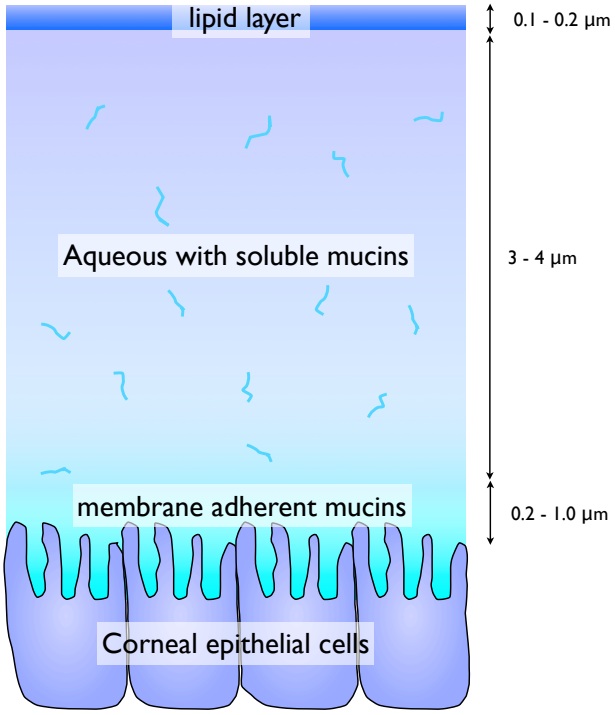

Figure 1.18: Schematic diagram of the tear film structure.

assessment that covers all of the visible tear film. In clinical trials, the two main methods used to study the *in vivo* wettability of contact lenses are slit-lamp examination and the tear scope.

1.8.1 Slitlamp examination of lens wettability

Clinically, the anterior eye and tear film are usually viewed using a slitlamp biomicroscope. This can be used to assess several aspects of the tear film. The thickness of the tear film can be assessed using specular reflection and diffuse illumination. The tear film produces a red/green interference fringe pattern when thin, which is not produced when the film is thicker (Guillon, 1994). Slitlamp biomicroscopy can also be used to assess the *in vivo* wetting of the contact lens surface by studying tear film break-up. The time taken from completion of a blink to the appearance of interference patterns/tear film break-up can be measured (Guillon, 1994). Further observations can be made of the rate of drying of the lens surface by watching the spreading area of tear break-up across the lens (Shiobara *et al.*, 1989). The percentage of the lens covered by the tear film is observed during normal blinking. Incomplete coverage of the contact lens by the tear film can indicate problems

Table 1.6: Methods previously reported for clinical evaluation of tear-film stability during contact lens wear. (French, 2005)

Technique	**Comment**	**Field**	**Background**
Slitlamp biomicroscope	Direct observation of tear film structure and time taken for distortion to develop following blinking.	Narrow	Dark
Handheld keratoscope	Bright grid projected onto the tear film. Observation of time taken for deformation of grid.	Narrow	Dark
Hir-Cal modified keratometer	Modified enlarged keratometer.	Narrow	Dark
Tear scope	External monocular illuminator used in conjunction with tear film. Observation of tear film structure and thinning.	Wide	Light
Modified bowl perimeter	Modified lighting system allowing bright grid to project onto tear film. Observation of time taken for deformation of the grid.	Wide	Dark
Videokeratography	Automated system (eg topographic modelling system projecting bright grid onto tear film. Observation of time taken for deformation of grid.	Wide	Dark
External illuminator	External bilateral illuminator used in conjunction with slit lamp biomicroscope allowing direct observation of tear film structure and thinning.	Wide	Light

with the surface due to manufacturing residue, tear film deposits or surface contamination due to lens care regime (Shiobara *et al.*, 1989).

1.8.2 Lens wettability grading scales

Lens wettability grading scales are a subjective assessment of lens wetting made following slit-lamp observations. Lens wettability is assessed from a combination of the pattern; size and speed of tear break-up, stability of the tear film and the lipid layer appearance. There are several different scales based on these factors that are used to grade lens wettability. Examples of wettability grading scales include the Eurolens Research, CibaVision and CCLRU grading scales (Table 1.7).

Table 1.7: CCLRU wettability grading scale

Grade	Description
0	Totally hydrophobic (non-wetting)
1	Non-wetting patches immediately after blinking
2	Appearance equivalent to HEMA lens surface
3	More wettable than HEMA lens surface
4	Appearance approaching that of normal healthy cornea
5	Appearance equivalent to normal healthy cornea

1.8.3 Tearscope-Plus

In addition to slitlamp-based tear film assessment the other commonly used clinical instrument is the Tearscope Plus (Keeler, UK). The Tearscope Plus is a handheld instrument that is used in conjunction with a slitlamp biomicroscope. It is a wide field instrument allowing observation of the tear film over the entire cornea, giving direct observation of the tear film structure and thinning. The instrument consists of a diffuse hemispherical cold cathode light source (to minimise drying of the tear film) with a central hole to allow viewing. It is used in conjunction with the slitlamp biomicroscope to allow increased magnification. Interference fringes result from the reflected light at the air/lipid interface and the lipid/aqueous interface. Interpretation of these interference patterns can give information about the thickness and quality of the pre-lens tear film. The interference

pattern can be described using a six-category classification (Guillon, 1994). Assessment of the aqueous layer in the contact lens tear film is possible when the lipid layer is very thin. Aqueous layer thickness is estimated by counting the fringes that form (Guillon, 1994).

1.8.4 The influence of contact lens wear on the tear film

The application of a contact lens onto the ocular surface is effectively a foreign body placed into the preocular tear environment. Contact lenses have been shown to influence the ocular surface by inducing hypoxia, increasing corneal temperature, causing corneal micro-trauma, reducing metabolic rate, decreasing epithelial mitotic rate, increasing epithelial fragility, compromising junctional integrity and increasing corneal lactate (Lemp, 2003). Even with these changes, most patients with a healthy tear film and ocular surface can achieve comfortable wear with contact lenses for prolonged periods. The presence of a contact lens disrupts the tear film, resulting in its thinning and increasing evaporative loss. In patients with an adequate tear film volume, the contact lens presents an acceptable stress on the tear film, but for patients with a low tear volume the contact lens can induce a dry eye state. This appears to influence around 20-30% of soft contact lens wearers and around 80% of rigid contact lens wearers (Tomlinson, 2006). The presence of a contact lens on the ocular surface separates the tear film into two layers, where the pre-lens tear film (PLTF) probably contains the superficial lipid layer and aqueous layer and the post-lens tear film (PoLTF) consists primarily of aqueous and mucin (Nichols & Sinnott, 2006). Increased evaporation associated with lens wear likely results in a thinning of the PLTF and subsequent thinning of the PoLTF film due to pervaporation (Fonn, 2007). This pervaporation process has been shown to result in significant corneal staining (Guillon *et al.*, 1992; Orsborn & Zantos, 1988), although this does not necessarily lead to subjective dryness or discomfort, possibly due to a shielding effect of the lens over the corneal surface (Fonn, 2007). Other factors associated with contact lens induced discomfort and dryness include inflammation, evaporation, decreased osmolarity (Stahl *et al.*, 2009; Tomlinson *et al.*, 2006), decreased tear production linked to hypoesthesia and instability of the PLTF with reduced tear film break-up time. It is therefore evident that the cause of contact lens discomfort/dryness is complex and likely to be multifactorial.

1.8.5 The tear film and lens wettability

The ability of a contact lens surface to wet is determined by the tear film deposition, break-up and recovery on the lens surface. The presence of a contact lens disrupts the typical three-layer structure of the tear film (Dilly, 1994). In the PLTF the air and the tear film compete to reside adjacent to the solid surface. It is the interaction between the lens surface and the components of the tear film that dictate the wettability of the contact lens surface during wear (Cheng *et al.*, 2004). During eyelid opening, a tear film is generated across the lens/ocular surface by the tear meniscus, through a hydrodynamic coating mechanism (Wong *et al.*, 1996). As the eyelid reaches its fully open position, so begins the inter-blink period. During this period the PLTF begins to evaporate and may rupture leading to the formation of dry patches on the lens surface. As the lid begins to close, the tear meniscus on the edge of the lid advances across the dry spots on the lens and thus rewets the surface. It is thought that the more hydrophobic the lens material is, the more difficult it is for the tear film to wet the dry spots (Cheng *et al.*, 2004). Cheng *et al.* (2004) suggested that a contact lens surface must allow the formation of a stable PLTF and resist tear film break-up in the inter-blink period.

1.8.6 Wettability of conventional hydrogel contact lenses

Although a conventional hydrogel (pHEMA) material is generally seen as a hydrophilic, the surface can become susceptible to wetting problems under certain circumstances. The wettability of a hydrogel material varies depending on its surface water content. It rises rapidly up to 30% water content and then more slowly above this level (French, 2005). In their fully hydrated state, all hydrogels can be expected to have adequate wettability. Following a period of wear of the contact lenses, progressive dehydration and a dynamic response by the hydrophilic pendant groups to air or lipid deposition, can result in a lens surface with reduced wettability. Depending on the severity of these changes, this can cause irreversible deposition of the tear film components, resulting in a potential reduction in patient comfort and physiological response.

1.8.7 Wettability of silicone hydrogel contact lenses

A potential disadvantage of silicone hydrogel contact lenses is the hydrophobic tendency of silicone-containing materials. Silicone polymers are therefore combined with hydrogel

forming polymers, in an attempt to improve surface wettability. Even with the addition of these hydrophilic components, the highly flexible silicone polymer can structurally reorganise at the contact lens surface, potentially leading to hydrophobic surfaces (Maldonado-Codina & Morgan, 2007). Laboratory analysis of surface wettability has shown silicone hydrogels to be less wettable than conventional hydrogel contact lenses (Maldonado-Codina & Morgan, 2007), with chemical analysis showing the presence of silicon on the surface of these lenses (Karlgard *et al.*, 2004). It is generally thought that lenses with poor clinical wettability have a tendency to become uncomfortable, as surface drying between blinks results in hydrophobic areas that irritate the lid as it moves over the lens surface (Jones *et al.*, 2006). Numerous studies have therefore investigated the clinical surface wetting of silicone hydrogel materials. Sweeney *et al.* (2004) studied the clinical wetting of conventional and first generation silicone hydrogel contact lenses and found similar wetting performance. Similar wetting characteristics have also been observed for second and third generation contact lens materials. Steffen & Schnider (2004) compared the clinical wettability of Acuvue Oasys and Advance to conventional hydrogel materials and showed little difference between them. This highlights the ability of the internal wetting agent, PVP, to enrich the lens surface and mask the hydrophobic nature of the silicone components. Other clinical studies comparing tear film stability on silicone hydrogel and conventional hydrogel materials have given contradictory findings with some suggesting greater tear film stability on silicone hydrogel materials (Guillon & Maissa, 2007), while others showed similar (Cheung *et al.*, 2007a; Morris *et al.*, 1998) or greater stability on conventional hydrogels (Maldonado-Codina *et al.*, 2004b), indicating this may be highly dependant on both the lens materials being investigated and the method of assessment and highlighting a possible lack of sensitivity in the current methods of tear film assessment. Dumbleton *et al.* (2008) suggested that there are relatively small differences in the clinical wetting characteristics of the silicone hydrogel materials. They observed that where significant differences in the clinical wetting properties were present, there appears to be no link with subjective comfort (Dumbleton *et al.*, 2008), although Guillon & Maissa (2007) have reported an apparent association between comfort and surface wetting for certain silicone hydrogel materials. This complex wetting relationship between the silicone hydrogel contact lens and the tear film is likely to be associated with the interaction of tear film components with the lens surface, which improves lens surface wettability, masking the differences between material type.

1.8.8 The effect of tear film components on the wettability of contact lenses

Holly & Refojo (1976) showed that surface-active components, such as dissolved proteins and glycoproteins, present within the tear film may affect the surface characteristics of the contact lens. Cheng *et al.* (2004) investigated the individual and additional effect of two important tear film components (lyzozyme and mucin) when measuring the contact angle using captive bubble technique. They found that the addition of mucin and/or lyzozyme (at levels typically found in the tear film) improved surface wettability for all lens types (silicone hydrogel and conventional lenses). This suggests that molecular adsorption of tear protein components impart hydrophilicity to the lens surface. In addition *ex vivo* studies have shown improved laboratory wetting performance for lens materials over the first few hours of wear, with differences in initial wetting performance between materials rapidly reducing with wear. This results in contact lenses with very similar wetting characteristics following wear (Read *et al.*, 2010a; Tonge *et al.*, 2001). Clinical studies have shown changes in *in vivo* wettability with some studies suggesting tear film stability can improve with lens wear (Guillon & Maissa, 2007) while other studies have suggested a reduction in tear film stability with prolonged wear. These differences in tear film stability with wear are likely to be both patient and material dependant and appear to relate to the type of deposition occurring on the lens surface and possibly the clinical method of tear film stability assessment. A recent *in vivo* study assessed surface wettability for a range of silicone hydrogel materials by placing a droplet of water onto the contact lens surface during lens wear (Haddad, 2010). They found only very small differences between the lens types when comparing wetting properties after both 30 minutes and 6 hours of lens wear. In addition, the surface of all the study lenses showed excellent wettability, when compared with laboratory measurements for these materials. This suggests that a bioconversion of the lens surface does occur with wear and that this process seems to occur rapidly following application of the contact lens. An interesting addition finding of this study was a correlation between the rate of spread of the droplet and subjective comfort, suggesting that this bioconversion process (tear film adhesion to the contact lens surface) is critical to the clinical performance of the contact lens.

1.8.9 Factors that influence *in vivo* contact lens wettability

1. **Material**

   The material a contact lens is manufactured from has been shown to influence *in vivo* wettability. The tear film wetting of silicone elastomer lenses, for example, is known to be very poor (Guillon & Maissa, 2007); whereas a material such as pHEMA is known to have comparatively good *in vivo* wettability. The water content of the material is also thought to influence the thickness of lipid layer in the pre-lens tear film (Guillon *et al.*, 1992; Young & Efron, 1991), which potentially could influence tear film stability.

2. **Patient-dependant characteristics** The quality and quantity of the tear film varies significantly between patients (Ozdemir & Temizdemir, 2010; Wang *et al.*, 2006). There are numerous subject-dependant variables, such as tear film thickness, tear volume, tear secretion rate, tear film outflow rate, blink rate, tear meniscus height/volume, tear film stability, abnormal underlying morphology, lipid chemistry/polarity, mucin chemistry, protein chemistry, tear osmolarity and tear film composition. The individual tear film characteristics of the lens wearer are therefore likely to heavily influence the *in vivo* lens performance (French, 2005).

3. **Wetting agents**

   Increasingly contact lens manufacturers are adding wetting agents or viscosity agents to the blister packaging solution. Surfactants and humectants, such as polyvinyl alcohol (PVA), hydroxypropyl methylcellulose (HPMC) or block copolymers, have been added to packaging solutions in an effort to deliver increased wettability, improved comfort and decreased surface tension on the lens upon removal from the blister pack (Sindt, 2010). CibaVision have recently introduced the Night & Day Aqua (lotrafilcon A) and the Air Optix Aqua (lotrafilcon B). These products contain a hydrophilic moisturising agent in the packaging saline (1% copolymer 845 (PEG and PVP)), which is said to bind to the lens surface and claimed to enhance comfort on insertion (Jones & French, 2009). Johnson & Johnson include 0.005% methyl ether cellulose in the saline packaging solution for the Acuvue Oasys (senofilcon A) and Acuvue Advance (galyfilcon A) lenses. Methyl cellulose is a thickening and coating agent, which is commonly used as an ophthalmic protectant in artificial tears and contact lens solutions (Troy, 2005). Menzies & Jones (2010) clearly

demonstrated the presence of these blister packaging additives in silicone hydrogel lens blister solutions, with reduced surface tension measurements and increased viscosity measurements. These blister packaging solution additives have been shown to influence laboratory wetting measurements (Maldonado-Codina & Morgan, 2007; Menzies & Jones, 2010), but their influence on clinical performance is less clear. Typically silicone hydrogel lenses are replaced either on a fortnightly or monthly basis and thus the packaging solution is only likely to influence performance on the first day of wear. Increasingly though contact lens care solutions are also including wetting additives and lubricants (Dalton *et al.*, 2008), allowing this potentially positive effect to be extended thought the life of the lens. Indeed several studies have shown improvements in the surface wetting and comfort for lens care solutions including these additives (Simmons *et al.*, 2001; Subbaraman *et al.*, 2006; Thai *et al.*, 2002b), although other studies have shown little difference (Ramamoorthy *et al.*, 2008; Santodomingo-Rubido *et al.*, 2008). The modality which could benefit most from any advantageous effect of these blister solution additives are daily disposable contact lenses, as they are replaced on a daily basis and on insertion are directly from the blister packaging. Focus Dailies All Day Comfort lenses are made from a PVA-based material. A small quantity of PVA within the material is unbound and therefore these PVA strands are eluted during wear in a blink-activated process. PVA is commonly used in artificial tears and contact lens rewetting drops, where it lowers the surface tension (improving surface wetting) and reduces the coefficient of friction. Nick *et al.* (2005) showed that Focus Dailies All Day Comfort offered a significant improvement in both overall and end of day comfort, when compared with original Focus Dailies. Another daily contact lens material which uses a different approach is the 1 Day Acuvue Moist. This material is manufactured from a conventional hydrogel material, with the addition of PVP. The PVP is bound within the lens and is not released during wear. These lenses are packaged in saline that includes up to 0.05% PVP. As with PVA, PVP is also used in artificial tears and rewetting drops and shares similar properties. Due to the recent release of two silicone hydrogel daily disposable contact lenses (Sauflon Clariti 1-Day and Johnson Johnson Trueye), these type of additives and their relative effect on contact lens performance are likely to become of increasing interest. Wetting agents present in both blister packaging solutions and contact lens care solution are thought to form a

molecular monolayer across the contact lens surface, with non-polar heads adhering to the contact lens surface and polar tails exposed. These polar tails then form a surface on which water or an aqueous solution such as the tear fluid can spread more readily (Fatt, 1984). Lubricants and surfactants when included in a contact lens blister solutions have been shown to improve lens wettability and enhance subjective comfort (Simmons *et al.*, 2001; Thai *et al.*, 2002b).

1.9 Experimental study contact lens material

The experimental study lens material is based on enfilcon A. This material is composed of silicone-based macromers and several non-silicone based monomers. These components are combined with a non-reactive silicone-based material prior to polymerisation to improve monomer compatibility. Following polymerisation, this non-reactive silicone-based material is removed by an extraction process and therefore does not form part of the lens material. This allows the study contact lens material to be manufactured in non-polar polypropylene moulds, which are easy to work with and relatively inexpensive to manufacture.

1.9.0.1 Silicone macromer

The reactive silicone macromer present in the lens material is known as M3U. The macromer is characterised as a siloxane tri-block polymer, being made up of three different siloxane polymer blocks or segments, with a reactive acryloyl group at both ends of the linear macromer, making it homobifunctional (Figure 1.19). This silicone macromer is comprised of the following three blocks of repeated units which can be arranged in any order.

1. Copolymer block possess the repeated unit, -[$Si(CH_3)_2O$]-, shown in Figure 1.19 (a) and is repeated between 50 and 200 times.

2. Copolymer block comprises a silicone atom having a fluorine-containing substituent, shown in Figure 1.19 (b) and is repeated between 2 and 50 times. Fluorine is often included in silicone hydrogel materials as it can improve compatibility with hydrophilic copolymers (Kunzler & Seelye, 2007) and also has the advantage of reducing lipophilicity and deposit formation on the hydrated polymer (Kunzler & Ozark, 1994; Ozark & Kunzler, 1995).

3. Copolymer block comprising a silicone atom with a substituted alkyl group comprising a hydrophilic component (e.g. a short polyethylene glycol (PEG) chain, $(CH_2CH_2O)_p$), shown in Figure 1.19 (c) which is repeated between 1 and 15 times. These PEG chains have been shown to improve compatibility between siloxane-containing materials and hydrophilic monomers (Owen, 1993).

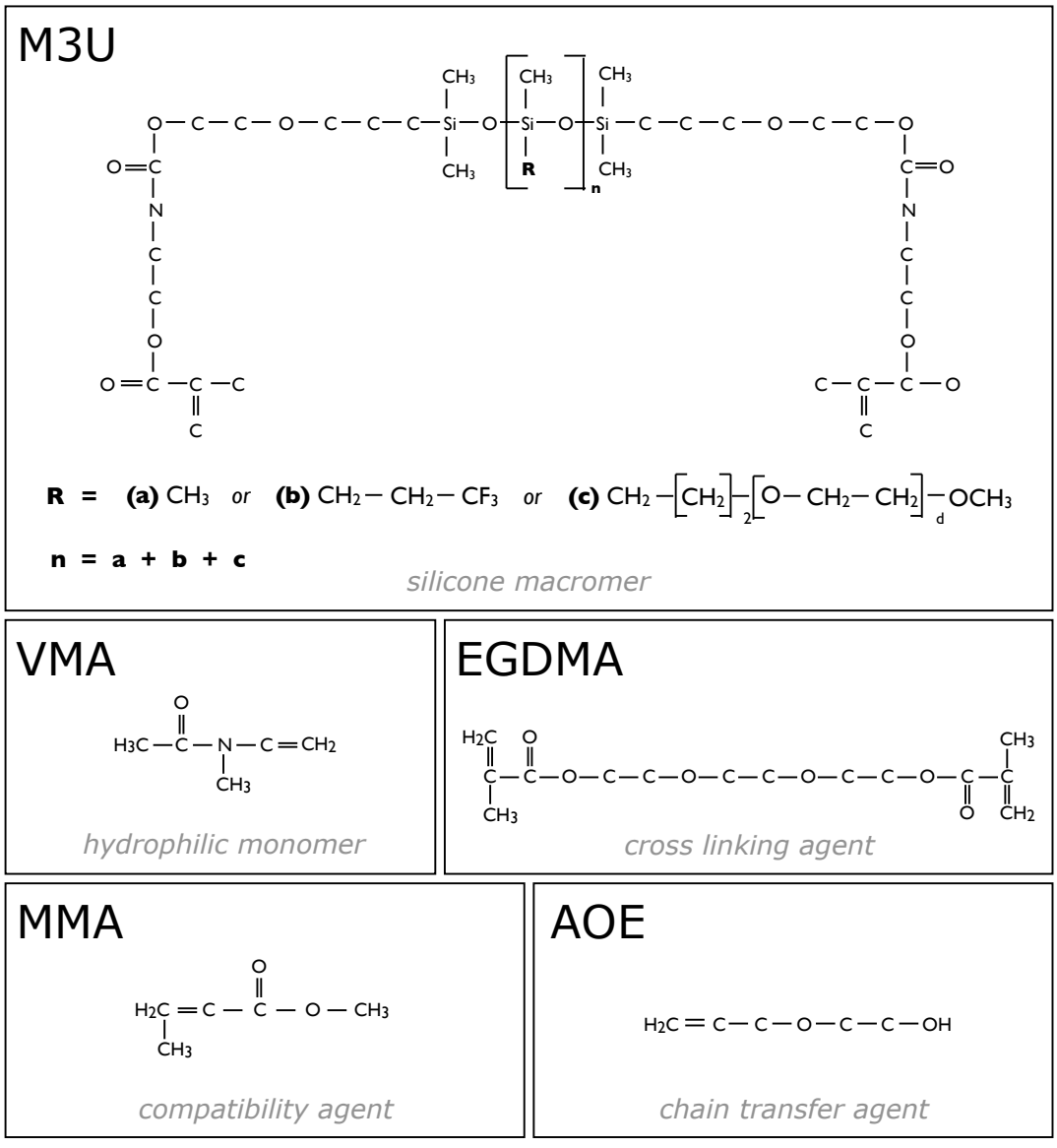

Figure 1.19: The structural formula of the component monomers used in manufacture of the experimental study contact lens material.

1.9.0.2 Silicone-free monomer composition

In addition to the silicone macromer, there are a number of silicone-free monomer components which comprise around 45% - 55% by weight of the monomer mixture. These monomers typically possess at least one polymerisable double bond and at least one hydrophilic functional group and include cross-linking agents. The enfilcon A material is comprised of the following non-silicone containing components:

1. A hydrophilic vinyl-containing (CH2=CH-) monomer, known as N-vinyl-N-methyl acetamide (VMA). This typically makes up at least 25-42% by weight of the monomer mixture.

2. An acrylic monomer known as methyl methacrylate (MMA). MMA possess relatively poor hydrophilicity and oxygen transmission properties, but it may serve here as a monomer additive to reduce the ionflux of the material, as a demolding agent and/or to aid compatibility of the polymer components.

3. An acrylate functionalised ethylene oxide -$(OCH_2CH_2)_n$ oligomer, known as trimethylene glycol dimethacrylate (TEGDMA). This is present in relatively small amounts in the precursor composition (0.075% to 5% by weight) and functions as a cross-linking agent.

4. A chain transfer agent 2-allyloxy-ethanol (AOE) which promotes the reaction between a radical species and a non-radical species. The addition of the chain transfer agent allows post-extracted and hydrated contact lenses to be manufactured with reduced variability in both dimensional and physical properties.

1.9.0.3 Non-reactive silicone removable component

The monomer mix includes a polyalkylene oxide silicone (PAOS) removable component, which possesses a PDMS backbone in which around 75% of methyl groups have been replaced by polyalkylene oxide groups (i.e. PDMS-co-PEG). The PAOS component makes up around 10% to 30% of the monomer mix by weight. POAS is unreactive with the other silicone hydrogel lens components and therefore the additive does not become a covalently bound part of the resulting polymerised lens product. Depending on their molecular weight and shape, most, if not all is removed during the extraction process along with other additives (e.g. unreacted monomers, oligomers, partially reacted monomers, or

other agents which have not become covalently attached or otherwise immobilised relative to the lens component).

1.9.1 Experimental study contact lens manufacture

The experimental study contact lenses were specifically manufactured for this PhD. They were manufactured using a cast-moulding technique, the process of which is highlighted in Figure 1.20. The monomer components of the silicone hydrogel contact lens were combined, mixed and filtered to remove particulates. The monomer mix was then placed into a female polypropylene lens mould and the male polypropylene lens mould brought into contact to form a contact lens shaped cavity occupied by the monomer mixture. The mould and monomer mix were then exposed to heat which triggered the initiator to begin the polymerisation process. After removal from the oven the lenses were demoulded, either mechanically or by soaking. The lenses then underwent a series of sequential extraction steps using an extraction medium (a mixture of ethanol and water) resulting in fully hydrated and extracted contact lenses (i.e. POAS and any unpolymerised components were removed from the lenses). The lenses were then sealed into individual blister packages with a volume of buffered saline and then heat sterilised by autoclaving. The ovens were enclosed allowing the environment to be carefully controlled during contact lens manufacture. The two experimental study lens types produced for this PhD were identical in their monomer composition and method of manufacture, differing only in the environment in which they were manufactured. One lens type was manufactured with the oven environment filled with atmospheric air and is known from here on as the 'air-cured' study contact lens type. The other lens type was manufactured in a nitrogen-purged environment in the same oven and is known from here on as the 'nitrogen-cured' study contact lens type. These study lenses were chosen as they are of identical design except for differences in the curing process. These differences likely result in the presence of oxygen at the mould/lens interface during manufacture of the air-cured lens, due to oxygen permeation through the polypropylene mould. In contrast, little or no oxygen is likely to be present at the interface for the nitrogen-cured lens during polymerisation. The presence of oxygen during lens manufacture is thought to result in termination of the polymerisation process, resulting in polymer chains with a lower molecular weight and which are less heavily cross-linked. This has previously been shown to result in a tackier lens surface with a greater hydrophobic tendency as the highly mobile hydrophobic polymer chains are more readily

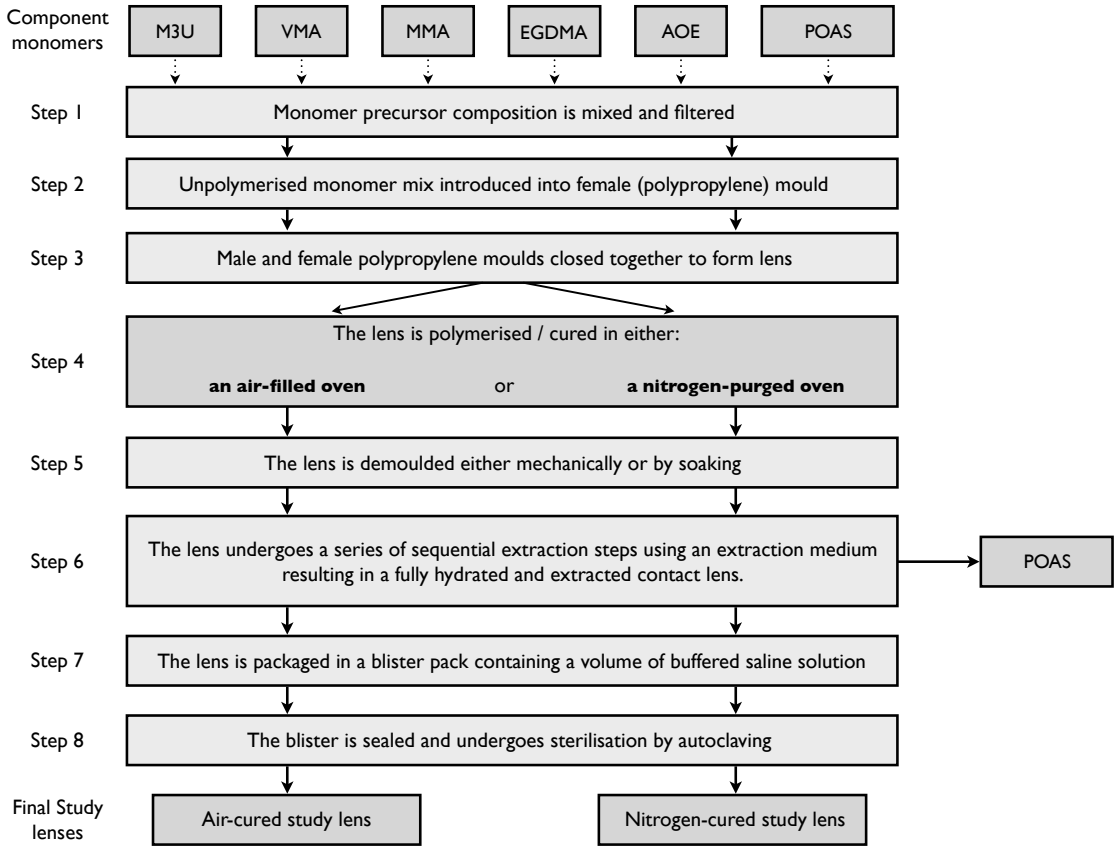

Figure 1.20: The manufacturing process for the study contact lenses.

expressed at the lens surface (Biswal & Hilt, 2009). This is in agreement with early clinical observations made by the sponsor company, which suggested poorer clinical performance for the air-cured lens, when compared with the nitrogen-cured lens.

1.9.2 Parameters of the experimental contact lens

A pilot study (Appendix F) showed no significant differences between the two study lens types in either base curve, lens diameter or centre thickness. Both contact lens types exhibited a base curve of around 8.3mm, a total diameter of around 14.2mm and a centre thickness of 75 microns. These values are typical of commercial silicone hydrogel contact lenses (Association of Contact Lens Manufacturers (ACLM) handbook, 2010), allowing findings from this PhD work to be compared with results from other studies, which have used commercial lens types. Given the observed similarity in the parameters of the two study contact lenses (Appendix F) it was apparent that any differences were likely to be related only to the surface of the contact lenses. Oxygen iunhibition at the polymer

interface is well-understood and known to predominately influence the surface region of the polymeric material, due to the reactive nature of the oxygen molecules diffusing into the polymer (Biswal & Hilt, 2009; Maldonado-Codina & Efron, 2004). These lenses were thus of interest as they had a matched design, differing in their clinical performance solely because of suspected differences in their surface properties. This work therefore focused on the surface characteristics of the study contact lenses and their influence on clinical performance.

1.10 Surface characteristics of polymers

The surface characteristics of a polymer are critically important when used for biomedical applications. In developing biomedical devices such as contact lenses, we are concerned with function, durability, and biocompatibility. In order to function, contact lenses must have appropriate bulk properties, such as mechanical strength, oxygen permeability, or material elasticity. Well-developed methods typically exist to measure these bulk properties, often with standardised procedures (e.g. ISO standards). In contrast, methodologies for the analysis of surface characteristics such as durability or biocompatibility are less well defined. The surface of a contact lens is the major influence on material biocompatibility and directly influences the biological system (proteins, cells and the organism) driving many of the biological reactions that occur in response to the biomaterial (protein adsorption, cell adhesion, cell growth, blood compatibility, etc.). This can result in clinical problems such as excessive deposition, non-wetting lenses or bacterial contamination and therefore it is critical to improve understanding of the surface structure of contact lenses. Investigation of the surface characteristics can be complicated by several factors:

1. The surface region of a material is known to be of unique reactivity, which can lead to surface oxidation and other surface chemical reactions.

2. The surface of a material is inevitably different from the bulk, due to the unbalanced forces acting on the surface material (Hoffman & Ratner, 2004).

3. The layer of material which makes up the surface is very thin and therefore of low total mass, requiring highly sensitive analysis/detection.

4. The surfaces readily become contaminated with components from the vapour phase (e.g. hydrocarbons and silicones) and although a vacuum environment can be used

to retard this, the conditions are different to those which the material is habitually exposed to.

5. The surface of the polymer material is often mobile and able to reorganise depending on the surrounding environment (Holly & Refojo, 1975).

The surface is generally thought to describe the zone where the structure and composition, influenced by the interface, differs from the average bulk composition and structure. This value often scales with the size of the molecules forming the surface. For a polymer, the unique surface zone may extend from 10 nm to 100 nm depending on the polymeric system and the chain molecular weight (Hoffman & Ratner, 2004). The surface of a material has several key properties that can be characterised:

- **Surface wetting** - Surface wetting is thought to be an important property of contact lens materials due to the need for the tear film to spread and maintain itself across the surface of the contact lens. Characterisation of surface wetting is normally performed by contact angle analysis which is detailed in Section 1.11.

- **Surface chemistry** - The surface chemistry of a contact lens influences not only the hydrophilicity of the surface, but also its resistance to bacterial and protein adsorption. Understanding contact lens surface chemistry is therefore critical in engineering contact lenses with optimal clinical performance. Several different techniques are available to investigate polymeric surfaces. In this thesis we focused on the use of X-ray Photoelectron Spectroscopy (XPS) (Section 1.12.1) and time of flight secondary ionisation mass spectroscopy (Section 1.12.3). These technique were chosen as they are highly surface sensitive, can be performed in a hydrated frozen state and are complementary in the information they provide, with XPS primarily providing elemental characterisation, whereas ToF-SIMS provides molecular characterisation of the polymer surface.

- **Surface topography** - This property describes the shape and features of the polymer surface. It is know to be a important property for contact lens materials, particularly with respect to optical quality, adhesion and biocompatibility. Surface topography can be characterised directly using an instrument such as an AFM (1.14.1) or indirect by imaging using an instrument such as a SEM (1.14.1).

- **Surface friction** - The frictional forces present between the contact lens, the eye lids and the ocular surface are thought to be important factors influencing subjective comfort. This thesis did not set out to investigate surface friction, focusing primarily on the topography, chemistry and wetting of the contact lens surface.

1.11 *In vitro* assessment of wettability

The term wettability is used to describe in a qualitative way the tendency for a fluid to spread over a solid surface (Fatt, 1984). Wettability is not a property of the surface, but rather a property of a liquid/solid interface. To understand wettability, it is necessary to understand the forces present when this wetting process occurs.

1.11.1 Cohesion and Adhesion

Cohesion is the force of attraction between individual molecules of the same substance. Adhesion is the force of attraction between individual molecules of two different substances. The wetting of a surface can be thought of as adhesion between the liquid molecules and the surface molecules. The relative influence of cohesion between individual liquid molecules and the adhesion between liquid and solid molecules, dictate the wetting of the surface.

1.11.2 Surface tension

A drop of liquid is formed due to the imbalance of the cohesive forces at the surface of a droplet (Figure 1.21). Molecules near the surface experience an inward attraction due to cohesion but no outward balancing force. These imbalanced forces create an excess amount of potential energy, known as surface-free energy or surface tension. Surface tension acts to resist any attempt to deform its surface (Adamson, 1976). Solids also possess similar surface-free energy, but the bonding within the solid is stronger and does not allow deformation of its shape. When a liquid wets a solid the surface-free energy due to the liquid cohesive forces are counteracted by the adhesive forces between the liquid and solid molecule (Figure 1.22). The resultant energy value is referred to as the interfacial tension. The lower the interfacial tension is the greater the liquid/solid adhesion and the greater the likelihood the liquid will spread over the surface.

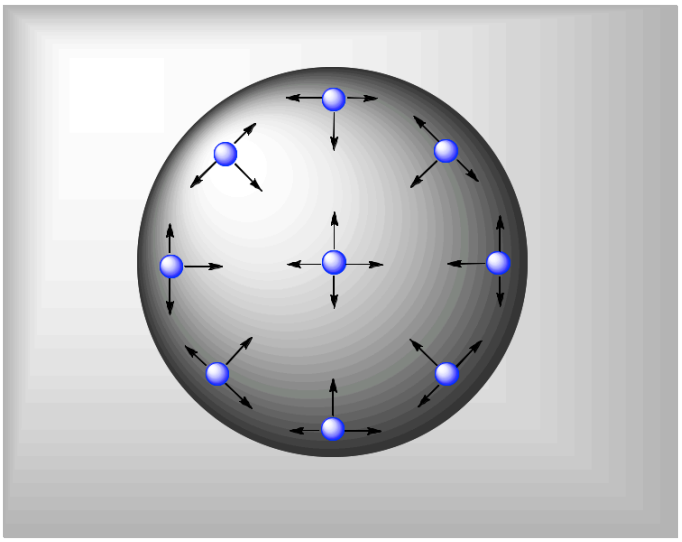

Figure 1.21: Surface tension of a liquid drop

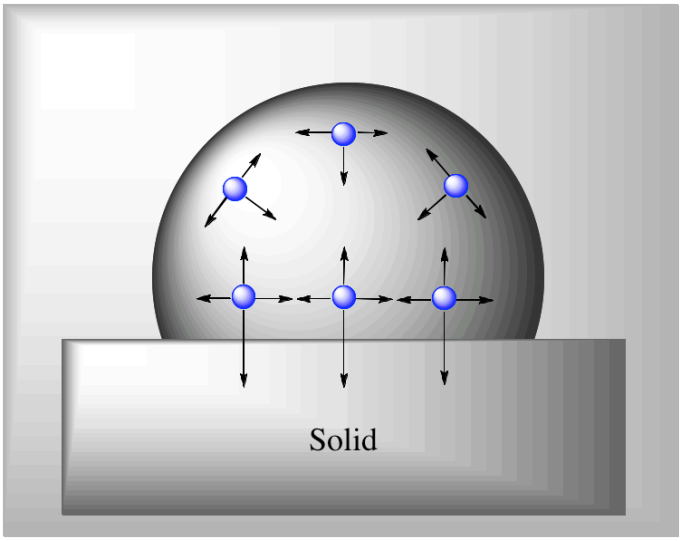

Figure 1.22: Interfacial tension between liquid and solid surface

1.11.3 Introduction to *in vitro* lens wettability

There are no generally accepted measures of lens wettability that can be used to assess the surface condition of a contact lens or the effectiveness of lens care solutions (Fatt, 1984). Contact angle and wettability are commonly used interchangeably but are not synonyms and the properties they describe may not be directly related. Contact angle is close to being, but is not quite, a standard physical measurement. Wettability, on the other hand, has no accepted methods for its measurement (Fatt, 1984). The physical processes in-

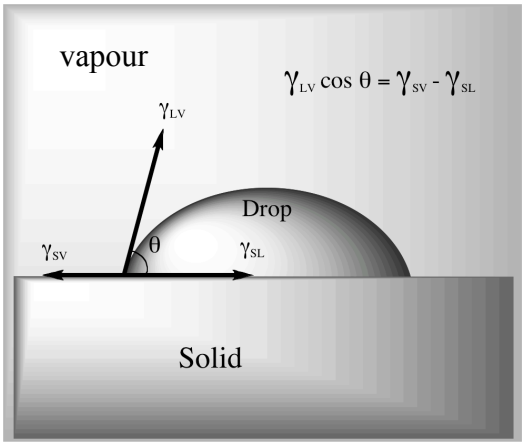

Figure 1.23: Schematic diagram of a liquid drop on a solid surface with energy vectors and contact angle (θ), as described by Youngs equation.

volved in the formation of a contact angle are debated. Young (1805) suggested that the shape of the edge of a drop of liquid on a flat plate of a solid material was governed by three forces acting along the line of intersection (Figure 1.23).[1]

If a liquid is unable to completely spread on a solid surface, a contact angle (θ) is formed. A contact angle is a quantitative measure of the wetting of a solid by a liquid. It is the angle formed by the liquid at the three-phase boundary where a liquid, gas (or a second immiscible liquid) and solid intersect. It is a direct measure of interactions taking place between the participating phases (gas/liquid/solid or liquid/liquid/solid). The contact angle is determined by drawing a tangent at the contact where the liquid and the solid intersect. The lower the contact angle the more completely the liquid wets the surface, with an angle of zero degrees implying that the surface is completely wettable. The shape of the drop and size of the contact angle are controlled by three interaction forces of interfacial tension of each participating phase (gas, liquid and solid). In an ideal situation the relation between these forces and the contact angle can be described by the Young's equation (Figure 1.23). However, often non-ideal conditions exists due to environmental, chemical and roughness heterogeneity effects, leading to deviation from this relationship (Marmur, 2003; Whyman *et al.*, 2008). Many other theoretical approaches based on the Young's equation have therefore been developed to account for these non-ideal contributions (Good, 1992).

[1] γ_{sv}: interfacial free energy for solid-vapour interface; γ_{lv} : interfacial free energy for liquid-vapour interface; γ_{sl} : interfacial free energy for solid-liquid interface.

A contact angle can vary for a given solid/fluid interface depending on whether the fluid is static or moving/has moved. Dynamic contact angle analysis refers to the fact that a contact angle can be advancing, receding or in equilibrium (Maldonado-Codina & Efron, 2006). An advancing contact angle is the angle a liquid makes as it slowly advances across an unwetted surface. This can be shown by increasing the amount of liquid on a fresh dry surface or by tilting the surface. The receding angle is the angle a liquid makes when it is withdrawn from a wetted surface, which it was previously in contact with. A receding angle is produced when the size of a liquid drop is reduced or the sample surface is tilted. The advancing contact angle is often larger than the receding angle, as the receding angle is a measure of the wettability of an already wet surface. The difference between the advancing and receding contact angle is known as the contact angle hysteresis. There are two classes of hysteresis, thermodynamic and kinetic (Maldonado-Codina & Efron, 2006). Classical thermodynamic hysteresis produces repeatable hysteresis loops using the Wilhelmy plate technique. Kinetic hysteresis shows change in the hysteresis loops as a function of measurement (Andrade *et al.*, 1985a). Classic thermodynamic hysteresis is due to surface roughness, surface heterogeneity (Penn & Miller, 1980) and possibly surface entropy and surface deformation (Maldonado-Codina & Efron, 2006). The type of hysteresis observed with contact lenses is likely to be kinetic in nature (Fatt, 1984). This kinetic hysteresis is thought to be due to swelling and penetration effects, surface mobility and reorientation and possibly surface deformation (Holly & Refojo, 1975; Morra *et al.*, 1990). Holly & Refojo (1975) suggested that the contact angle hysteresis that occurs with hydrogels is primarily related to reorientation of the polymer chains at the surface of the material. Most polymer chains have a level of mobility allowing them to rotate at the polymer surface. When a hydrophobic surface (such as air) is present at the polymer surface then it is suggested that the hydrophobic components, such as methyl groups (CH_3), rotate to sit close to the polymer surface while the hydrophilic components, such as hydroxyl groups (OH), move away from the surface. When a polymer surface is exposed to a hydrophobic environment the groups reverse with hydrophilic groups rotating towards the surface and hydrophilic groups rotating inwards. If water is made to advance across an air exposed polymer surface it encounters a relatively hydrophobic surface giving an increased contact angle. If the water is then receded it encounters a relatively hydrophilic surface giving a reduced contact angle (Figure 1.24). The reorientation at the polymer surface occurs as the system seeks the conformation with the lowest free energy. This results

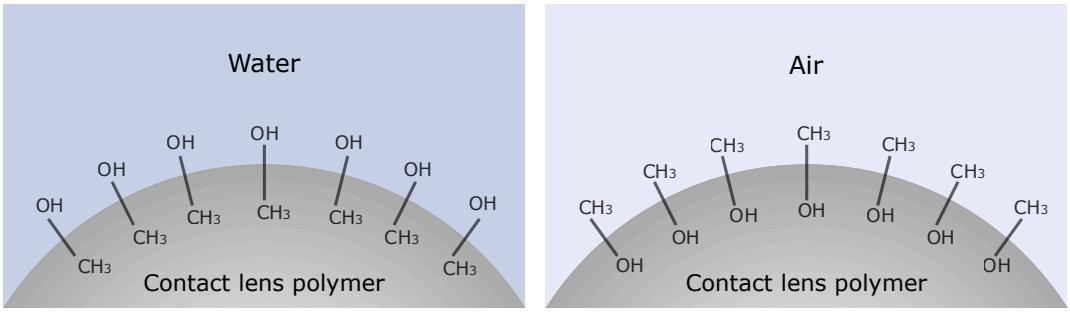

Figure 1.24: The affect of hysteresis on the wettability of a contact lens surface

in the measurement of contact angle varying depending on the hydrophilic/hydrophobic nature of surrounding environment.

1.11.4 Methods for contact angle measurement

Laboratory assessment of contact angle is typically performed in one of three ways:

1.11.4.1 Sessile drop technique

A drop of test fluid produced using a syringe, is placed onto the surface of the sample to be tested and the syringe withdrawn. The contact angle is observed with a telescopic observation system (goniometer). The contact angle formed by the water phase at the three-phase interface is measured by adjusting an eyepiece graticule so that it lies at a tangent to the surface of the liquid as it contacts the solid surface (Figure 1.25). In modern systems a computer often assists with the measurement of a contact angle. Small droplets (typically around 5μm) have been used in previous studies (Maldonado-Codina & Morgan, 2007) as the lens surface is not flat and as gravity is thought to have a more significant affect as drop size increases.

An obvious advantage of the sessile drop technique is that it allows direct optical analysis of the contact angle, as the light is in a continuous medium except where it is interrupted by the edge of the drop (Fatt, 1984). However, this technique presents several problems when applied to soft contact lenses. Surface dehydration of the contact lens surface and droplet can occur which influences the accuracy of the results. In addition, the surface also requires blotting to allow a drop to form stably on the lens surface (Maldonado-Codina & Efron, 2006), which is also likely to affect the measured contact angle.

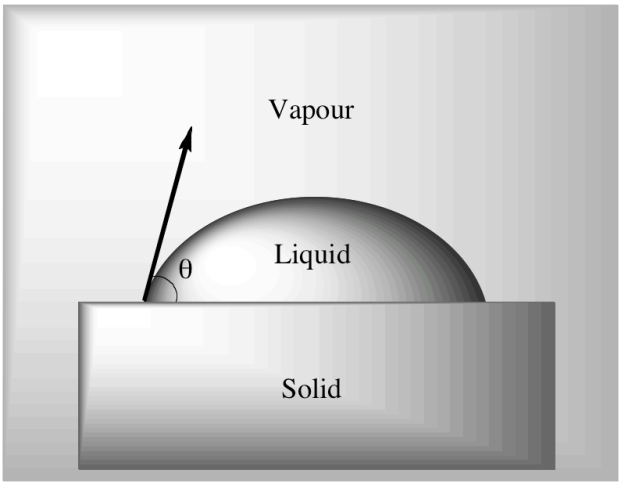

Figure 1.25: Schematic representation of the sessile droplet technique

1.11.4.2 Captive bubble technique

A bubble of air (or low density fluid) is introduced onto the lower surface of a sample material immersed in a higher density fluid (typically water). A observation system similar to that used for sessile drop analysis is used to observe the contact angle. The angle formed by the liquid at the three-phase interface is measured as the air bubble pushes water away from the material surface (Figure 1.26). This technique requires little preparation and is performed in a hydrated environment therefore minimising material dehydration. Dynamic measurement of both advancing and receding contact angles are possible, although it involves varying the bubble volume, which is difficult to perform (Maldonado-Codina & Efron, 2006). Contact angle measurements with the captive bubble technique are typically lower than that recorded by other methods, due primarily to hysteresis. Atomic force microscopy (AFM) results suggest that under most humidity conditions the surface of a contact lens is not fully hydrated even when the lens bulk is fully hydrated (Opdahl *et al.*, 2003). The captive bubble technique may therefore not give a representative contact angle compared to that of a contact lens under *in vivo* conditions, although these findings do not take into account the constant reformation of the tear film during blinking and therefore may be misleading.

1.11.4.3 Wilhelmy balance method

This method involves the introduction of a linear strip of sample material into a test liquid. The strip of sample material is held from above by a microbalance. The material is slowly

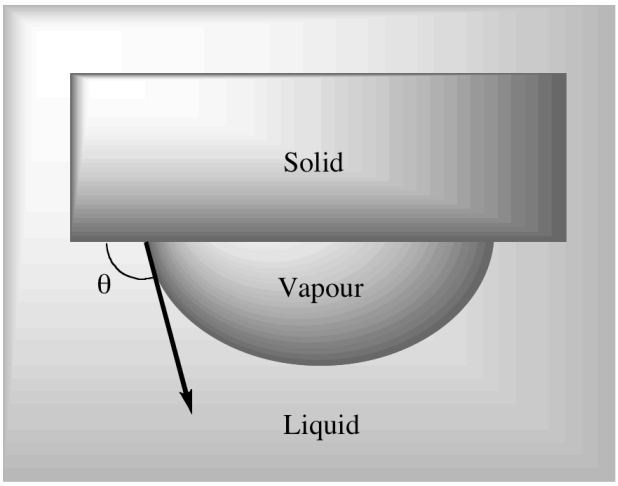

Figure 1.26: Schematic representation of the captive bubble technique

immersed into a test liquid and then slowly withdrawn. The advancing contact angle is the angle formed between the test sample and meniscus of the immersion fluid during sample immersion. The receding contact angle is the angle formed between the test sample and the meniscus of the immersion fluid when it is being withdrawn from the fluid. The contact angle is calculated from the measurements of force given by the microbalance (Tonge *et al.*, 2001). The principal problem with this technique when applied to hydrogel contact lenses is that the strip of material tends to float upon immersion into a probe fluid (Tonge *et al.*, 2001). A weighted hook is therefore used to pierce the hydrogel material at one end of the strip. Unfortunately, this technique requires the loss of the curved lens shape, the cutting of the lens material and stretching of the material with a hooked weight. Such processing of the lens material may induce contamination, stretching and tearing (Cheng *et al.*, 2004). Other potential problems involve exposure of the lens surface to uncontrolled drying when not immersed in the fluid (Cheng *et al.*, 2004) and the influence of sample movement rate on the contact angle measured (Cain *et al.*, 1983), with a slow movement of the sample tending to lead to excessive dehydration and a rapid movement leading to a loss of sensitivity (Cheng *et al.*, 2004). In addition, the measurement is not directly of the angle but calculated indirectly from the force measurements. The use of the weighted hook allows the study of hydrogel materials, but the analysing software needs to be customised, which can lead to further potential errors when calculating the contact angle. Other calculation problems can arise as the lens is typically a non-linear sample and calculation of the sample perimeter is based upon a linear sample. The main advantages with the

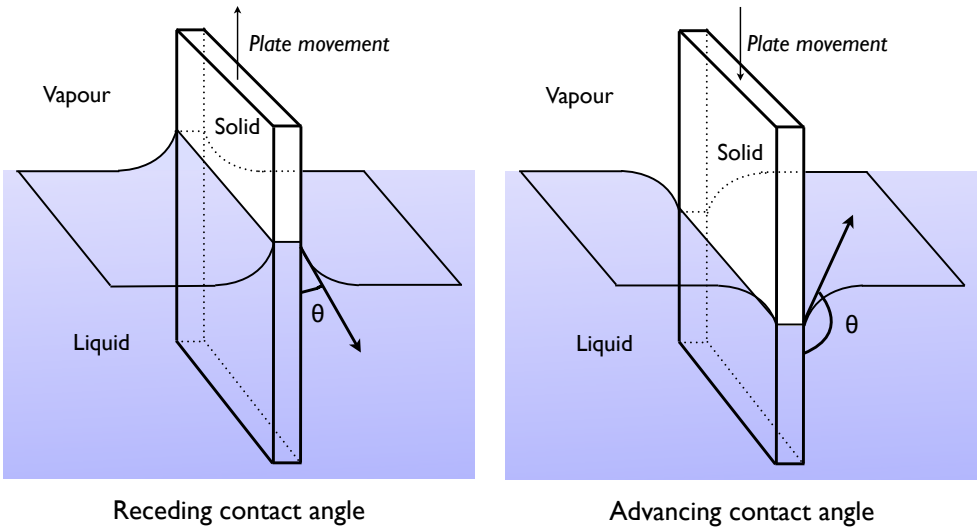

Figure 1.27: Schematic representation of the Wilhelmy balance technique showing advancing and receding contact angles

Wilhelmy balance method is that it is thought to be more objective than either sessile drop or captive bubble technique (Cheng *et al.*, 2004).

1.11.5 Contact angle measurement variables

1. **Test material**

   The surface properties of the test material are likely to affect the contact angle measurement. This occurs as the surface free energy of the material influences the attraction between the liquid and surface, and therefore the wetting of the surface. Typically when analysing contact lenses we intentionally alter the test material, while keeping all other variables stable. With polymeric materials, polymer chains have some mobility, allowing rotation of the functional groups. This chemical heterogeneity causes the contact angle to vary depending on the surrounding environment during testing.

2. **Testing methodology**

   Due to the difficulty in accurately measuring the contact angle on a contact lens surface, several different tests have been developed. These tests often measure different types of contact angle (sessile drop analogous to advancing angle; captive bubble analogous to receding angle). Contact angle values are therefore strongly dependant

on the measurement technique (Zhang & Herskowitz, 1992).

3. **Processing of surface**

   Sample preparation can affect the contact angle measured. Procedures such as surface cleaning, soaking in solutions, stretching, cutting, flattening or blotting are all likely to influence contact angle measurements.

4. **Test conditions**

   The conditions under which the testing is performed are likely to influence the contact angle. Environmental conditions such as humidity, temperature and airflow need to be careful controlled. These conditions are likely to vary depending on the technique used and laboratory conditions present.

5. **Test fluid**

   The liquid used to form the sessile droplet or used to immerse the lens is an important variable in the measurement of the contact angle (Cheng *et al.*, 2004). Typically this is either saline, blister solution or de-ionised water. The choice of liquid is likely to affect its surface tension and therefore alter the contact angle measured.

1.11.6 The clinical relevance of in vitro wettability

The stability of the pre-lens tear film is thought to affect the clinical performance of a contact lens (Jones *et al.*, 2006). It has been suggested that the stability of the tear film is related to the wettability and hydrophilicity of the lens surface (Maldonado-Codina & Efron, 2006). Tonge *et al.* (2001) suggested that the advancing contact angle is the most clinically relevant measure as it provides an indication of lens wettability when the surface is orientated such that the hydrophobic groups are exposed. Maldonado-Codina & Efron (2006) suggested that the receding angle also gives important information about the formation and development of dry spots on a dehydrating lens surface and should not be ignored. Although the link between the wettability of a contact lens and its clinical performance seems theoretically an obvious one, there is little literature to support this theory. Larke *et al.* (1973) showed that the contact angle for a rigid gas permeable contact lens should be less than 70^o to give successful in eye wettability. No similar hydrogel study has been performed, but it has been suggested that the contact angle would be similar (Maldonado-Codina & Efron, 2006), although this may also be related to insensitive clinical and laboratory tests for contact lens wetting.

The wettability of a contact lens surface is evidently a very important surface property and it has been shown that a poorly wetting lens is likely to result in various clinical complications (Zekman & Sarnat, 1972). The correlation between laboratory assessments of wettability and clinical wettability though is weak, suggesting that better understanding of this relationship is required in order to develop materials with enhanced *in vivo* wettability and biocompatibility.

1.12 Analysis of contact lens surface chemistry

1.12.1 X-ray Photoelectron Spectroscopy

X-ray Photoelectron Spectroscopy (XPS), also known as Electron Spectroscopy for Chemical Analysis (ESCA), is a widely used analytical tool to study primarily solid surfaces (Seah, 1980). It is an extremely surface sensitive technique allowing the identification and quantification of the chemical elements in the surface region of a solid and provides information on the binding states of these elements. During analysis the specimen is exposed to a source of monochromatic x-ray radiation (i.e. photons of fixed energy). The energy of the x-ray photons, as with all types of electromagnetic radiation, is given by the Einstein relationship (Equation 1.5), where h is the Planck constant (6.62 x 10^{-34} Js) and v is the frequency (Hz) of the radiation.

$$E = hv \tag{1.5}$$

When a photon is absorbed by an atom in a molecule, it leads to ionisation and the emission of a core (inner shell) electron, known as a photoelectron. The kinetic energy of the emitted photoelectron is related to the energy required to remove it from its initial level. As the monochromatic excitation (x-ray) energy is known, the binding energy is the difference between the excitation energy and the kinetic energy of the emitted electron (Figure 1.28). An XPS instrument measures the kinetic energy distribution of the emitted photoelectrons (i.e. the number of emitted photoelectrons as a function of their kinetic energy) using an electron energy analyser and a photoelectron spectrum can thus be recorded. For each element there is a characteristic binding energy associated with each core atomic orbital, giving rise to a characteristic set of peaks in the photoelectron spectrum at specific binding energies. The presence of peaks at particular energies therefore indicates the presence of a specific element in the sample and the intensity of the peak is related to the concentration

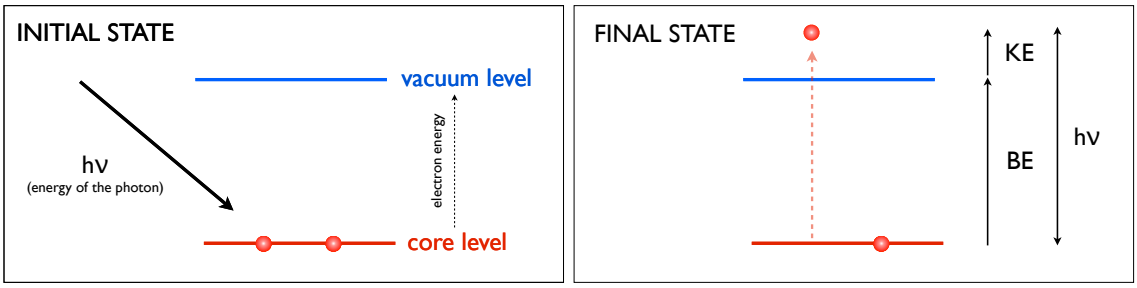

Figure 1.28: A schematic diagram of electron excitation and the relationship between kinetic energy (KE) and binding energy (BE).

of the element within the sample regions. As these photoelectrons have very short inelastic mean free paths in solids, the technique is highly surface sensitive. It is able to detect all elements with an atomic number (Z) between lithium (Z=3) and lawrencium (Z=103).

1.12.1.1 Components of an XPS system

The XPS instrument is composed of (i) a fixed-energy monochromatic x-ray radiation source, (ii) a high vacuum environment and (iii) an electron energy analyser (Figure 1.29). Following exposure of the sample to monochromatic x-rays, the photoelectrons emitted from the sample are then accelerated towards an lens system before passing into a hemispherical analyser, which sorts the electrons according to their kinetic energy. The top plate of the analyser is negatively charged and deflects the path of the electrons onto an electron multiplier. Many modern instruments contain a multi-channel analyser, which is able to detect all kinetic energies simultaneously. Ultra-high vacuum conditions are required to allow the accurate counting of electrons at each kinetic energy value. A XPS spectrum is a plot of the number of electrons detected (Y-axis) versus the binding energy of electrons detected (X-axis) (Figure 1.30a). Each element produces a characteristic set of XPS peaks at characteristic binding energy values that directly identify each element that exists on the surface of the material being analysed. The characteristic peaks correspond to the electron configuration of the electrons within the atoms (e.g. 1s, 2s, 2p, 3s, etc.). The number of detected electrons in each of the characteristic peaks is directly related to the amount of an element within the area irradiated. To generate atomic percentage values (the percentage of an element at the sample surface), each raw XPS signal must be corrected by dividing its signal intensity (no. of electrons detected) by a relative sensitivity factor (RSF) and normalised over all of the elements detected.

Investigation of the elemental peaks with high resolution XPS spectra also allows the evaluation of the chemical state and bonding of those elements. The high resolution spectrum obtained experimentally is then fitted with a number of generated curves typical of different bond types which are then optimised using software (Figure 1.30b). By using this XPS technique it is possible to provide chemical state information regarding the sample, in addition to the elemental percentage values present at the surface. XPS is a surface sensitive technique because only those photoelectrons generated near the surface can escape and become available for detection. The XPS instrument detects electrons from within the top 1-10 nm of the surface. Atoms from deeper layers in the material (1-5 μm) do release electrons but these are recaptured/trapped in various excited states within the material. Therefore, in most applications, it is in effect, a non-destructive technique that measures the surface chemistry of a material.

1.12.1.2 Uses of XPS

XPS can be used to determine the elemental composition of a surface, surface contamination, empirical formula of material (free of contamination), chemical state identification, binding energy of electron states and density of electron states. Advanced XPS systems are capable of line profiling (measure uniformity of elemental composition across the top of the surface), depth profiling (measure uniformity of elemental composition as a function of depth by ion beam etching) and angle resolved XPS (measure uniformity of elemental composition as a function of depth by tilting the sample).

1.12.2 Contact lens research using XPS

XPS can be used to analyse the surface chemistry of contact lenses. Karlgard *et al.* (2004) compared methods for drying contact lenses prior to XPS analysis. In addition, they analysed the surface composition of a selection of both silicone and conventional hydrogels. The study concluded that the preferred method for lens dehydration was by drying in nitrogen, which maintained optical clarity and minimised surface contamination. XPS analysis of the lens surface showed that this technique could be used to calculate surface chemical composition for a range of unworn soft contact lens materials and these findings were shown to correlate well to previous published data (Grobe *et al.*, 1996; McArthur *et al.*, 2001; Willis *et al.*, 2001). Willis *et al.* (2001) applied XPS analysis to assess coating

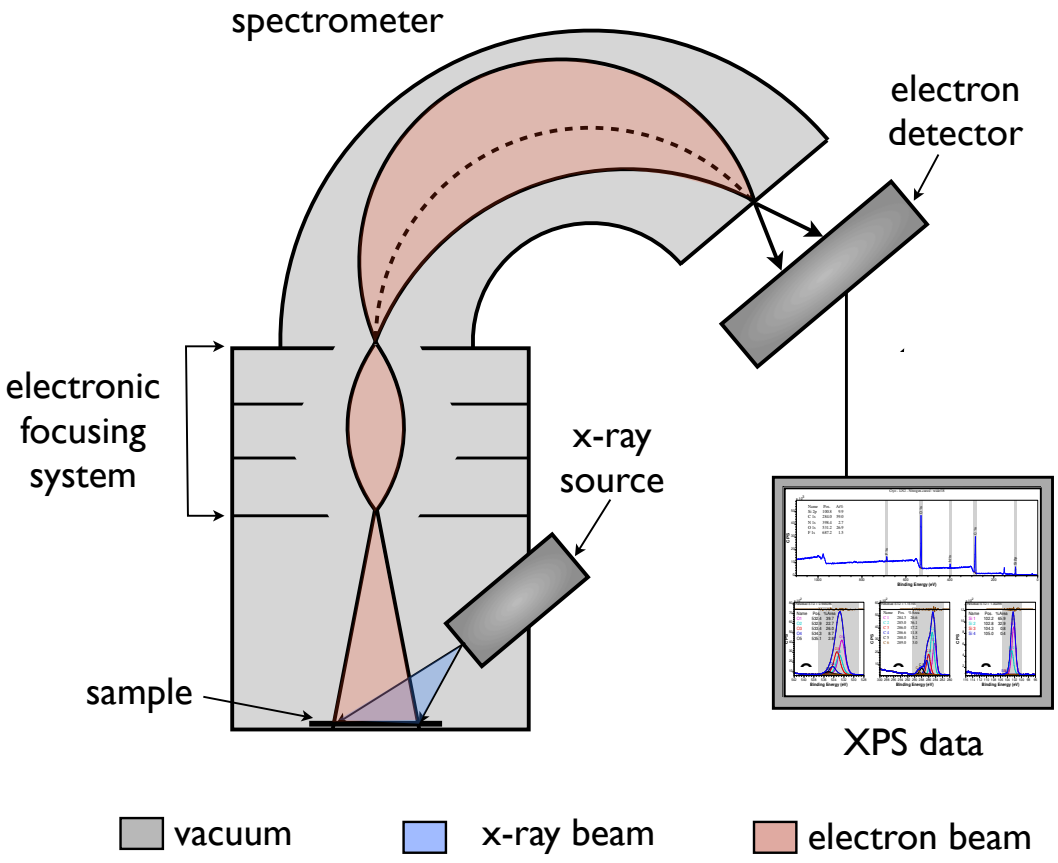

Figure 1.29: A schematic diagram of an XPS system.

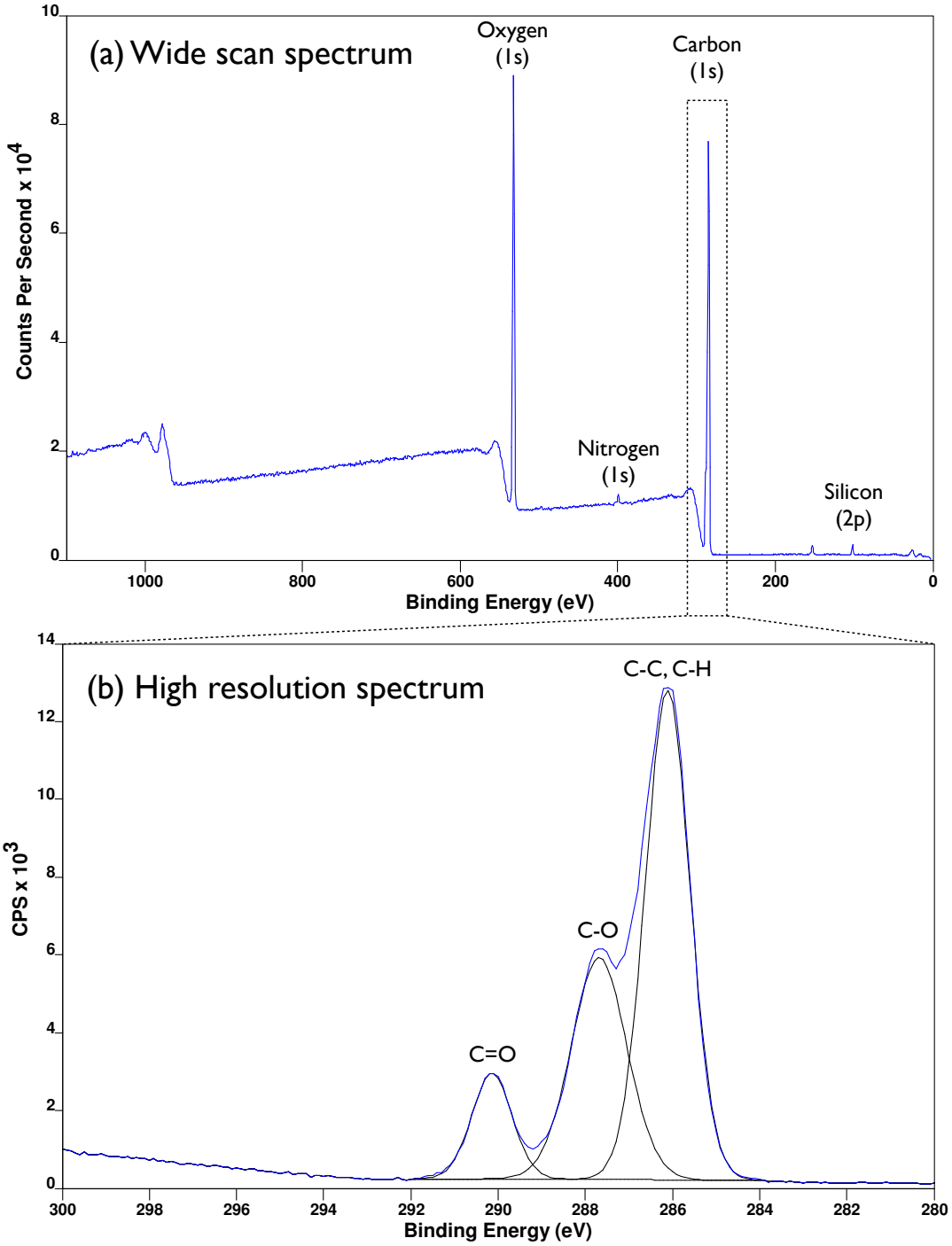

Figure 1.30: A typical (a) wide survey XPS scan and (b) high resolution XPS scan.

homogeneity. This was determined by studying the presence of phosphorylcholine on the surface of an unworn contact lens. XPS was also used to confirm the stability of the coating following disinfection of the lenses in an autoclave and cleaning with commercial contact lens solution. The results of XPS analysis were identical to those prior to lens cleaning,

suggesting the surface coating was stable following these processes. In addition to studying unworn contact lenses, XPS can also be used to analyse contact lens deposition. McArthur *et al.* (2001) used XPS to perform qualitative and quantitative analysis of contact lens deposition. They showed that all of the conventional hydrogel lenses tested in their study accumulated tear deposits within the first 10 minutes of wear. By monitoring the change in nitrogen levels, XPS analysis showed that sub-monolayer levels of protein were adsorbed onto the lens surface. In their study, matrix-assisted laser desorption ionisation mass spectrometry (MALDI-MS) also indicated the presence of adsorbed protein molecules after as little as 10 minutes of wear (McArthur *et al.*, 2001). The nature of the deposition was found to vary and was influenced by the lens chemistry. Etafilcon A and polymacon materials, when analysed with XPS, showed similar surface chemistry prior to wear (as MAA is present in etafilcon A only in small ($\sim$ 2%) quantities). The amount of nitrogen found on the etafilcon A after 10 minutes of wear was twice that found on the polymacon lens. This agreed with previous studies (Leahy *et al.*, 1990; Lin *et al.*, 1991; Tighe *et al.*, 1998) which found that etafilcon A lenses deposited large amounts of protein both onto the surface and into the matrix. The increased protein adsorption found with etafilcon A was thought to be linked to its charged nature (due to the negatively charge MAA), leading to the expected electrostatic attraction of the positively charge proteins such as lysozyme and lactoferrin. McArthur *et al.* (2001) used XPS analysis to show that the significant increases in the hydrocarbon component detected on vilifilcon A lenses was not evident on etafilcon A lenses. This agreed with previous studies suggesting that the presence of NVP in a polymer is linked to the increased adsorption of lipids both onto the lens surface and into the bulk (Jones *et al.*, 1997a; Maissa *et al.*, 1998; Tighe *et al.*, 1998). Using XPS and MALDI-MS analysis on worn contact lenses, McArthur *et al.* (2001) also showed that initial adsorption events are diverse. They analysed sub-monolayer levels of deposition and observed a predominance of low molecular weight proteins. This type of analysis is crucial in identifying which biomolecules influence interface conversion by settling onto the 'naked' polymer surface. XPS is clearly a useful tool in the analysis of the surface chemical composition of unworn conventional and silicone hydrogel lenses. It is also able to measure comparative rates of *in vitro* and *in vivo* fouling on contact lenses, discern variations in lipid, protein and mucin content of a contact lens deposit and quantify adsorbed protein at levels well below monolayer coverage.

1.12.3 Introduction to ToF-SIMS

1.12.3.1 Mass Spectrometry

The general principle of mass spectrometry involves ionising a chemical compound to generate charged molecules or molecular fragments and then measuring their mass-to-charge ratio. This allows the determination of the elemental composition and chemical structure of a sample material. There are many types of mass spectrometers and sample introduction techniques, which allow a wide range of analyses. One such method which is particularly suited to the analysis of surfaces is time of flight secondary ion mass spectrometry (ToF-SIMS).

1.12.3.2 ToF-SIMS analysis

ToF-SIMS is a highly sensitive surface analytical technique that has considerable utility in contact lens surface characterisation. It can be used to identify the molecular polymeric arrangement of a lens surface and provide detailed elemental information to a sampling depth of only one or two molecular layers (Maldonado-Codina *et al.*, 2004a). The instrument is composed of three main components: (1) the ion source, (2) the flight tube and (3) the detector (Figure 1.31).

If an atom loses or gains an electron it possesses an electrical charge (electron lost = positively charged; electron gained = negatively charged). This charged atom is known as an ion and the process is called ionisation. If an ion is in an electric field it will accelerate in the direction opposite to its polarity. Charged repeller plates and extraction grids can be used to control the movement of these ions. The ions can be produced by electron bombardment (causing the atom to lose or gain an electron), laser exposure (causing emission of electrons) or high voltage plasma formation.

Secondary Ion Mass Spectrometry (SIMS) is the mass spectrometry of ionised particles which are emitted from the surface when energetic primary particles bombard the surface. Pulsed primary ions are used to bombard the sample surface, causing secondary elemental or cluster ions to be emitted from the surface. The next stage in the process is the ion optics. The secondary ions initially pass through a grid, which accelerates the extracted ions to the required velocity for entry into the flight tube. The secondary ions are then

accelerated into a field-free flight tube where the ions with lower mass have higher flight velocity than ions with higher mass. The flight tube is usually a vacuum enclosure between the ion source and the detector, which does not normally interact with the ion packets. A vacuum is required to allow the ions to pass down the flight tube to the detector, without colliding with other molecules. The 'time-of-flight' of an ion is proportional to the square root of its mass, so that all the different masses are separated during the flight and can be detected individually. To improve instrument sensitivity an ion reflector can be used to increase the secondary ion flight time therefore allowing improved peak separation.

On the surface of the detector is the entry grid. Here the ions are accelerated to a collision with the top of the first micro-channel plate. This collision jars loose one or more electrons from the plate, which liberate further electrons and this electron avalanche continues all the way through the plate, meaning that over a million electrons exit the plate for each ion that strikes the detector. Time-to-digital converters (TDC) register the arrival of a single ion at discrete time bins and thresholding discriminates between noise and ion events. Summing a large number of single-ion detection events, each peak is in fact a histogram

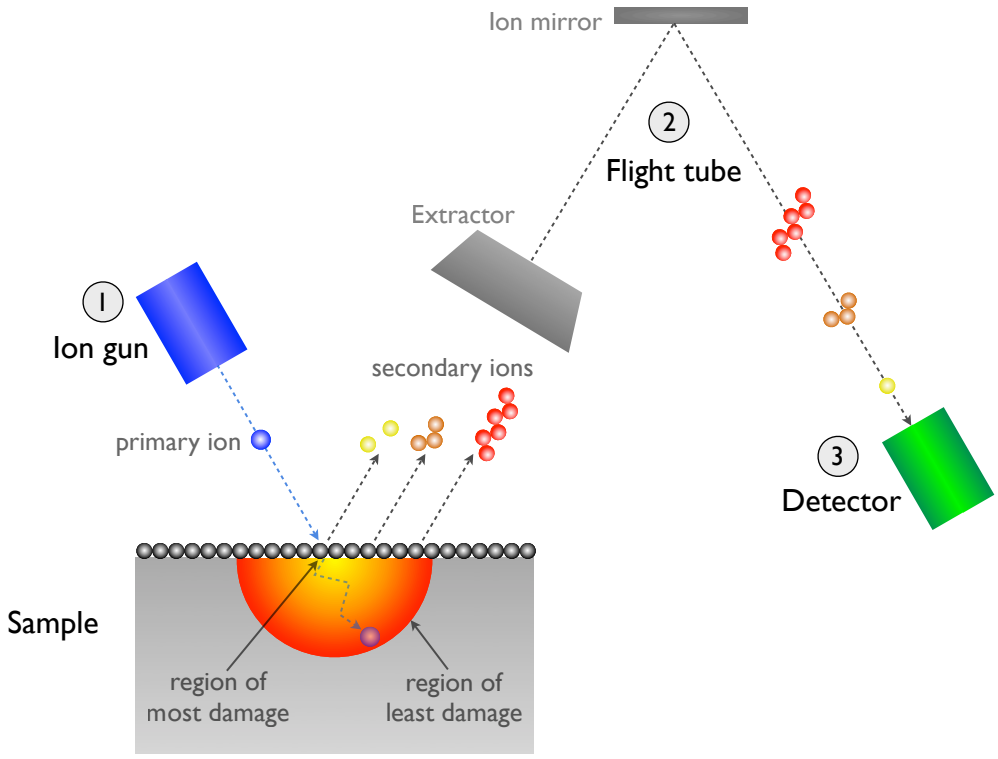

Figure 1.31: Schematic diagram of a ToF-SIMS system.

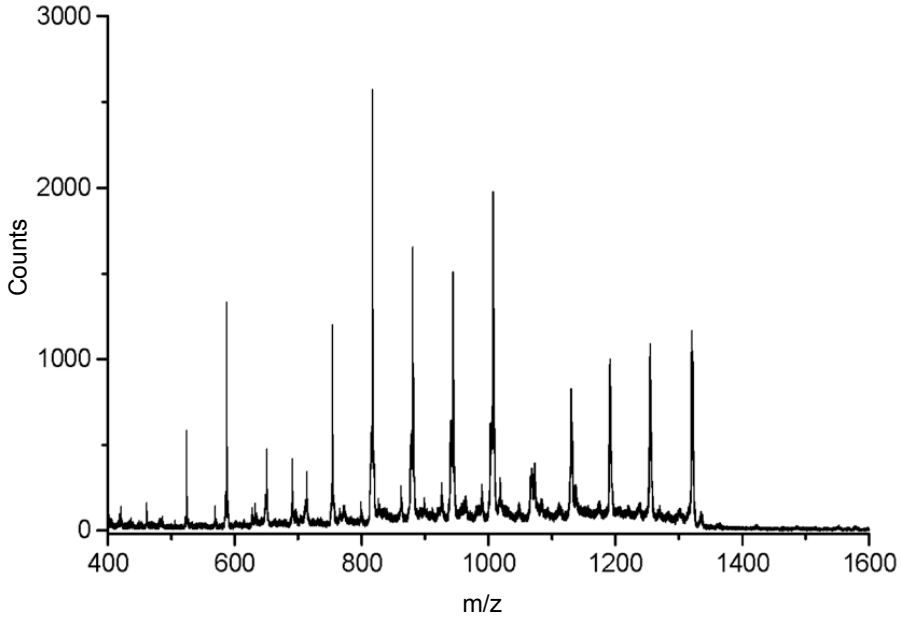

Figure 1.32: A typical ToF-SIMS spectrum (Maldonado-Codina *et al.*, 2004a).

obtained by adding up counts in each of individual bins. The TDC therefore functions as an ion counting detector. A mass spectrum can therefore be produced with number of ions detected (y-axis) versus the molecular weight of the secondary ions (x-axis) as shown in Figure 1.32.

1.12.3.3 Matrix-assisted laser desorption ionisation (MALDI)

MALDI mass spectrometry is a pulsed ionisation technique that is readily compatible with ToF-SIMS. MALDI is based on the bombardment of sample molecules with a laser to bring about sample ionisation. The sample is pre-mixed with a highly absorbing matrix compound, which transforms the laser energy into excitation energy for the sample, leading to sputtering of analyte and matrix ions from the surface of the mixture. In this way energy transfer is efficient and the analyte molecules are spared excessive direct energy that may otherwise cause decomposition. MALDI deals well with thermolabile, non-volatile organic compounds especially those of high molecular mass and is used successfully in biochemical areas for the analysis of proteins, peptides, glycoproteins, oligosaccharides, and oligonucleotides. In the context of contact lenses materials, this technique is particularly useful for the chemical characterisation of tear film deposits on the lens surface (St John *et al.*, 1997).

1.12.3.4 ToF-SIMS contact lens research

Maldonado-Codina *et al.* (2004a) used ToF-SIMS to characterise the dehydrated surface of unworn conventional hydrogel and silicone hydrogel contact lenses. This technique detected the presence of the bulk polymer pHEMA at the surface of all the conventional lenses, along with numerous contaminants. The author suggested that the likely source of these contaminants was from the manufacturing and packaging processes. pHEMA lenses manufactured by spin casting, cast moulding and lathe cutting were analysed by ToF-SIMS. The intensity of the pHEMA signal varied depending on the method of manufacture (strongest signal with spun-cast, then lathe cut and the weakest signal from cast-moulded lenses), with the authors suggesting that the spun-cast lens had a higher signal due to a lower level of surface contamination when compared with the other manufacturing techniques. ToF-SIMS surface analysis of balafilcon A identified the siloxane-related copolymer and the PVP hydrogel component of the polymer. Surprisingly, no silicate was detected on the surface as would have been expected following an oxidation reaction (surface plasma treatment). Other surface contaminants included sodium and chlorine likely from the saline solution and metallic signals likely associated with material splutter during coating. Analysis of the lotrafilcon A material showed low levels of surface silicone as might be expected given that the plasma coating tends to mask the underlying bulk material. A low level of fluorine was also detected on the lotrafilcon A surface likely arising from the fluro-ether component of the bulk polymer. Similar sodium, chlorine and metallic signals were found, as with the balafilcon A material. These ToF-SIMS findings indicated that the surface coating was an organo-nitrogen material, formed from the plasma deposition of reactive precursors CN^-, OCN^-, C_3N^-, C_3NO^- species. Maldonado-Codina *et al.* (2004a) showed varying levels of degradation and contamination on hydrogels lenses manufactured using differing techniques and on the surface of commercial silicone hydrogel contact lens, highlighting the ability of ToF-SIMS to chemically characterise the surface of both hydrogel and silicone hydrogel contact lenses.

Hook *et al.* (2006) used both ToF-SIMS and XPS to analyse the surface of conventional hydrogel contact lens materials and the reorganisation of amphiphillic PDMS graft copolymers with different concentrations and graft chain length. These materials were analysed in both hydrated (frozen) and dehydrated states. When a pure pHEMA lens was analysed with XPS in both a hydrated and dehydrated state the surface gave a composition

consistent with pHEMA, with no detectable contaminants. With quantitate XPS analysis the estimated water content was consistent with that of the bulk material. When this lens was analysed by ToF-SIMS in a hydrated state it gave similar findings, but in its dehydrated state PDMS was found in low levels on the lens surface (6-7% of a monolayer contamination). This was undetected by the XPS analysis. ToF-SIMS was also used to analyse a series of graft copolymers (containing allyl methacrylates and PDMS). This showed that the polymer surface reorganised upon water exposure, expressing a lower concentration of PDMS. When the surface was dehydrated, PDMS was detected by ToF-SIMS at concentrations above 15%, but with a hydrated surface it was only detectable at concentrations greater than 25%. This type of analysis is therefore able to determine the results of configurational changes on surfaces and show the preferential segregation of particular segment lengths. In addition, it demonstrates the ability of ToF-SIMS to detect trace concentrations on the lens surface and detect hydrocarbon species, which are not easily detected/distinguished by XPS analysis. Fakes *et al.* (1988) described the use of SIMS in the analysis of plasma coating applied to RGP contact lenses. They showed the progressive conversion of organosiloxane to an inorganic silica phase. Accompanying this surface chemistry change was a progressive increase in surface wettability. Although this study was performed on RGP lenses, it gives useful information regarding the conversion of a surface by plasma coating.

As can be seen from the literature, mass spectrometry is a useful tool in the analysis of contact lens surfaces. It can be used to analysis the lens surface in regard to surface composition, lens spoliation, care system efficacy and lens manufacture; and is highly sensitive and surface specific.

1.13 Introduction to contact lens surface topography

1.13.1 Surface Topography

Very few materials possess a surface which is atomically flat, with the majority of materials exhibiting surface features such as undulations, steep gradients, pores and imperfections. These features constitute the topography of the surface and can have a considerable impact on a material's performance (Assender *et al.*, 2002). Soft matter when relaxed will form surface undulations, known as capillary waves, as a result of the inherent entropy of the system balancing the increased energy of the greater surface area (Sferrazza *et al.*, 1997).

This effect is particularly important in soft hydrogel materials as they have a compliant nature and relatively low surface energy. For polymeric materials such as hydrogels the molecular size (Goldbeck-Wood *et al.*, 2002) and the presence of two or more phases at or near the polymer surface can also influence the topography of the surface (Assender *et al.*, 2002). Other factors such as material processing (e.g. the transfer of a defect from the mould to the surface profile of the moulded item) or rheological effects during manufacture (Tadmor & Gogos, 2006) can also influence surface topography. The surface topography of a biomaterial has been shown to influence several key factors:

1. **Adhesion**

   The adhesion between one surface and another depends on factors such as the degree of chemical interaction between the two components, the proximity and the area of contact. The last two factors are dependant on the topography of the two surfaces to be joined (Assender *et al.*, 2002).

2. **Optical finish**

   The optical finish of the contact lens is directly linked to its surface topography (Meeten, 1986).

3. **Biocompatibility**

   The surface topography has been shown to strongly influence its interaction with biological components (Curtis & Wilkinson, 1997).

In the context of contact lens materials, surface topography has been shown to influence factors such as optical performance (Bennett, 1992), bacterial adhesion (Vermeltfoort *et al.*, 2004) and tear film deposition (Baguet *et al.*, 1995a). Several types of instrumentation are available for analysis of surface topography. These can be split into contact and non-contact technqiues.

1.13.2 Topographical analysis involving direct surface contact

These instruments involve the use of a mechanical stylus, which is traversed across a surface. The vertical motion of the stylus is monitored via a pickup, amplified and then analysed by a computer. The stylus or surface is moved in a raster scan to give three dimensional data. This can be static analysis (the stylus is static during topographic measurement and then moves to the next defined position and stops for the next measurement), or it may be dynamic (the height measurement is analysed during the continuous

movement of the stylus). Dynamic scanning is typically quicker to perform, but can be limited by the dynamic characteristics of the stylus, where at high speeds it can induce stylus bounce. This type of topographic analysis can lead to surface damage and is limited by the size of the stylus (i.e. may smooth over steep surface pits).

1.13.3 Non-contact topographical analysis

1.13.3.1 Focus detection system

This system uses a convergent laser beam, which is projected onto the surface. The position of a focusing lens is adjusted by a focus error signal. The laser beam performs a raster scan across the surface and the focusing lens is adjusted to maintain focus of the laser on the surface (Stout & Dong, 1994). It is this movement of the focusing lens that represents the measured surface roughness, following analysis by a computer. Focus detection systems are limited to surfaces with a significant level of reflection (opaque surfaces cannot be measured). Other problems occur when analysing surfaces which are steeply sloped as the focus spot can struggle to maintain focus, bring about spurious spikes and sharp points which appear to be present on the surface.

1.13.3.2 Optical interference technique

This system works on the principle of interference of two beams of light where one is reflected off the surface of the specimen. During measurement of the surface, light reflected from the specimen surface interferes with light reflected from the internal reference and is recorded by a 3D image detector array. The interference fringe pattern is then analysed, with deviation in the interference fringe pattern related to height deviation on the specimen surface. The main drawback with the system is that it is limited to surfaces with reasonable reflectance (more so than for focus detection systems). Problems can also occur with rapid gradient changes in the surface and environmental vibrations need to be controlled to a high degree during testing. Giraldez *et al.* (2010) used this technique to observe differences in the surface of commercial conventional contact lenses and concluded that the larger area of analysis might be adequate to detect differences between lenses in terms of surface characteristics, which may not be so obvious if smaller areas are studied (Such as with AFM techniques (Section 1.14.1)).

1.13.3.3 Scanning tunnelling microscopy (STM)

A conducting probe with a tip consisting of nominally one atom is advanced to within nanometers of the specimen surface. A voltage of between 2mV and 2V is applied across the gap between tip and surface. The current increases exponentially as the gap reduces, allowing a vertical resolution of 0.01Å. A feedback loop keeps current constant by controlling the probe-surface distance via piezoelectric elements. This system allows lateral resolution of 1Å, a vertical range of around 5nm and a lateral range of 100 x 100 μm (Kuk & Silverman, 1989). One major limitation of the STM is that it is only possible to analyse a conductive surface, although STM has been demonstrated to work on thin layers of non-conducting material deposited onto conducting substrates (Rabke *et al.*, 1995).

1.13.3.4 Atomic force microscopy (AFM)

A tip positioned at the end of a spring leaf cantilever is brought either very close to (non-contact mode), or in contact with the surface (contact mode) depending on which mode of assessment is being used. AFM works by measuring the attractive and repulsive forces between the tip and the sample (Binning *et al.*, 1986). A laser beam is reflected from the top of the cantilever (Figure 1.33) and deflection of the cantilever brings about a doubling of the angular deflection of the laser beam. The reflected laser beam is directed towards a segmented photodiode which monitors its position. As the cantilever-to-detector distance is thousands of times larger than the length of the cantilever, the optical laser greatly magnifies the motion of the tip. Due to this magnification, noise level is massively reduced (Putman *et al.*, 1992). The probe or sample performs a raster scan, allowing a topographical image of the surface to be built up.

The ideal cantilever should have a high flexibility, exerting only low downward forces on the sample, therefore lowering the distortion and damage to the surface while scanning. It should also have a high resonant frequency allowing it to respond rapidly as it passes over features of the surface. Equation 1.6 shows the relationship between resonant frequency (RF) and flexibility (spring constant).

$$RF = \frac{1}{2\pi}\sqrt{\frac{spring\ \ constant}{Mass}} \tag{1.6}$$

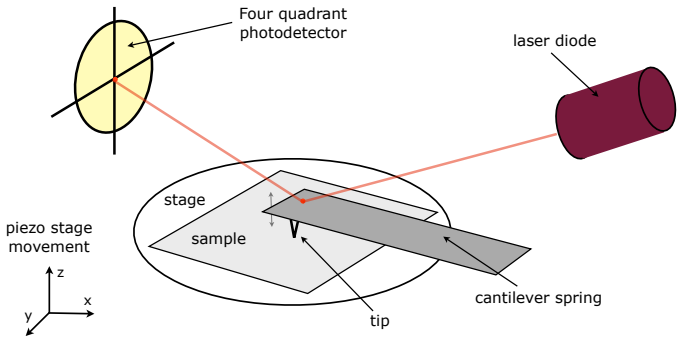

Figure 1.33: Schematic illustration of atomic force microscopy.

A cantilever of low mass is therefore required, allowing it to have both a low spring constant and high resonant frequency. The cantilever is typically made from silicone oxynitinide (with a thin coating of gold for reflectivity) and is manufactured using micro-lithographic techniques. The probe is often made with the cantilever. Most probe tips are rounded off at the point and they are therefore evaluated by a measurement of their end radius. Three common types of AFM probes are shown in Figure 1.34. The resolution of AFM is generally dictated by the end radius of the probe and probe-sample interactions.

Relative movement between the probe and the surface is required to perform the raster scan. Piezoceramics allow a 3D positioning device with arbitrarily high precision. These piezoceramics are usually in tubular form with four electrodes covering sections on the outer surfaces and one electrode covers the inner surface. By applying a voltage to the electrodes, the tube bends or stretches, moving the sample in three dimensions. This simple design gives high stability and a large scan range. The force feedback loop attempts

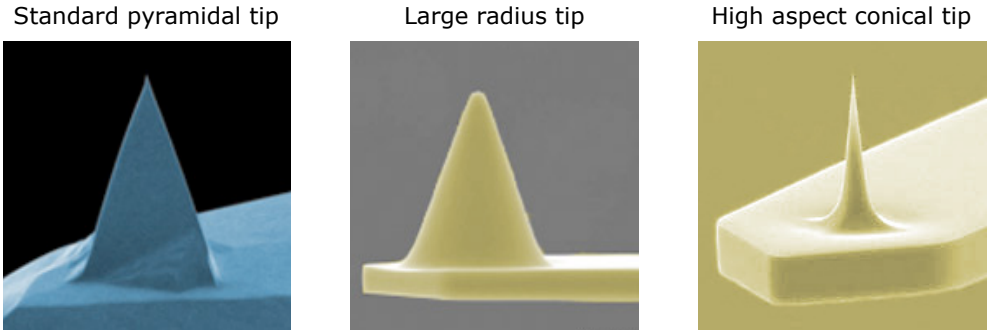

Figure 1.34: Three common types of AFM tip.

to keep the cantilever deflection constant by adjusting the voltage applied to the scanner. This allows the acquisition of images at very low force by both monitoring and regulating the force on the sample (Figure 1.35). If the force feedback loop is well adjusted (i.e. cantilever deflection is zero) then the specimen surface topography is given by the feedback output.

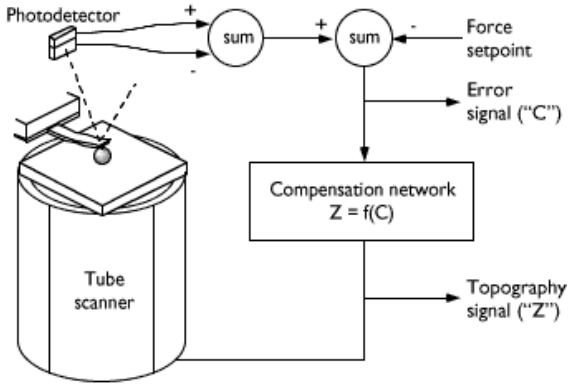

Figure 1.35: The AFM feedback loop. A compensation network monitors the cantilever deflection and keeps it constant by adjusting the height of the sample (or cantilever) (Baselt, 1993).

1.13.4 Alternative imaging modes for AFM

1.13.4.1 (i) Tapping mode AFM

Tapping mode imaging is performed by oscillating the cantilever at or near the cantilever's resonant frequency using a piezoelectric crystal, causing the cantilever to oscillate with a high amplitude (typically greater than 20nm) when the tip is not in contact with the surface. The oscillating tip is then moved toward the surface until it begins to lightly tap the surface, with the vertically oscillating tip alternately contacting the surface and lifting off, generally at a frequency of 50,000 to 500,000 cycles per second. Due to the intermittent contact with the surface the cantilever oscillation is reduced due to energy loss caused by the tip contacting the surface. The reduction in oscillation amplitude is used to identify and measure surface features. During tapping mode operation, the cantilever oscillation amplitude is maintained constant by a feedback loop. Due to the high frequency of the tip oscillations the surfaces is made stiff (viscoelastic) and the tip-sample adhesion forces are greatly reduced, minimising tip interaction and surface damage during scanning. Tapping mode AFM can be performed in both an air and liquid medium.

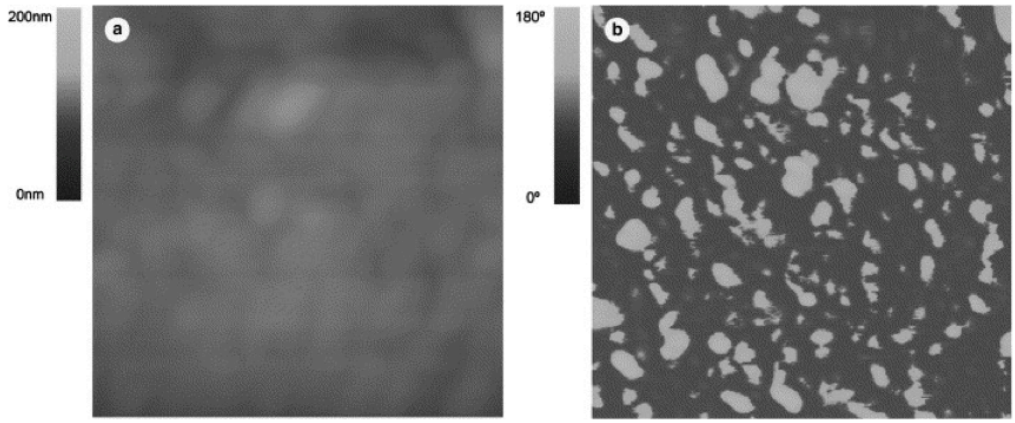

Figure 1.36: AFM height (a) and phase (b) imaging of polymer blend (Sanchez *et al.*, 2006).

1.13.4.2 (ii) AFM phase imaging

In contrast to the measurement of topographic variations of a sample (by measurement of the oscillation amplitude feedback signal), phase imaging is performed by monitoring the phase lag of the cantilever oscillation, relative to the signal sent to the cantilever's piezo driver during tapping mode AFM. The phase lag is very sensitive to variations in material properties such as adhesion and viscoelasticity. It can be performed during standard mode AFM with no negative impact on topographical imaging. Figure 1.36 shows the ability of phase imaging to distinguish between different material compsition on a surface.

1.13.4.3 (iii) Friction measurements with AFM

The friction between tip and sample can be detected by measuring the torsional deflection of the cantilever. A photo detector, position-sensitive in two dimensions, can distinguish the resulting left-and-right motion of the reflecting laser beam from the up-and-down motion caused by topographical variations (Meyer *et al.*, 2004) (Figure 1.37).

1.13.4.4 (iv) Sample elasticity measured with AFM

Sample elasticity can be measured by pressing the cantilever into the sample by a preset amount, the manipulation amplitude (usually 1-10nm). The cantilever deflects an amount related to the surface elasticity (softer = less deflection; harder = more deflection) (Figure 1.38).

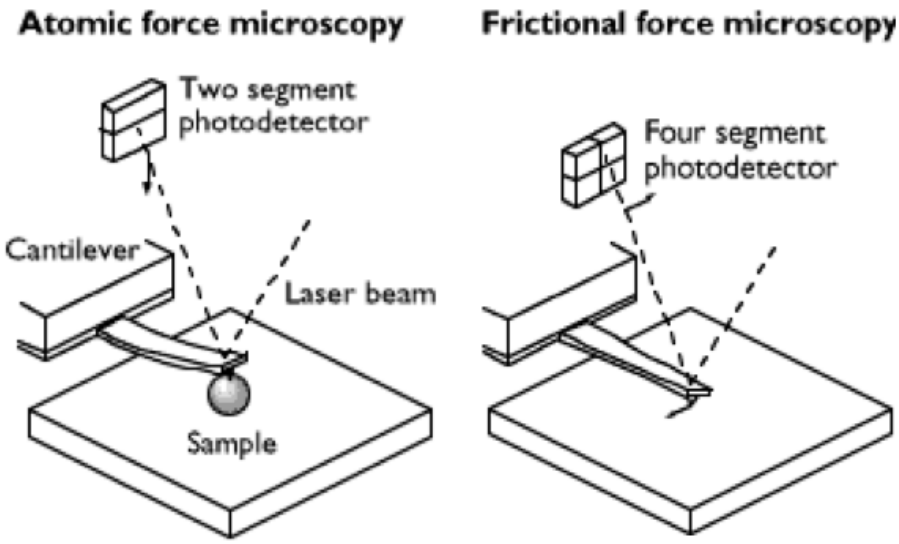

Figure 1.37: Friction measurements with AFM (Baselt, 1993).

1.13.4.5 (v) Meniscus force when imaging in air

When a surface sample is imaged in air a layer of water condensation and contaminants can form on the surface of the sample and probe tip. With the tip in contact with the surface there is a net repulsive force, which is counteracted by the force applied via the

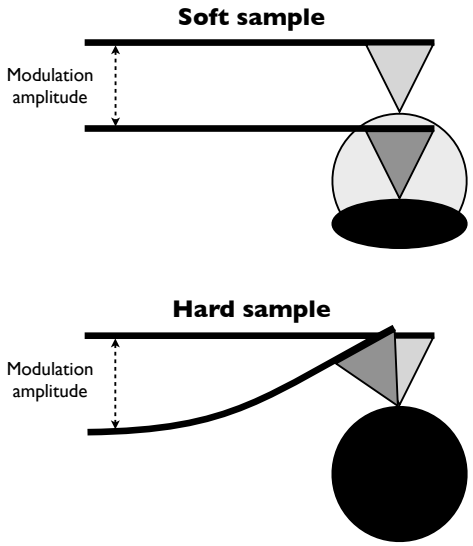

Figure 1.38: Surface elasticity measured with AFM (Redrawn from Baselt (1993)).

cantilever downwards. As the downward force cantilever is reduced the tip starts to come away from the sample surface. As the downward cantilever force reduces still further, the probe continues to move away until the force on the cantilever is upwards. When the upward cantilever force is sufficient, the tip will be pulled free from the meniscus. This upward force is equal to the attractive force of the meniscus (usually 10-100 nN). After this point only attractive forces influence the cantilever. The meniscus is the most important influence on tip-surface interaction. The meniscus effect can be eliminated by performing the surface analysis with complete immersion of both the tip and sample in water.

1.13.5 Atomic force microscopy on contact lens surfaces

When studying the surface of a contact lens, AFM has several key advantages over other analytical surface techniques. AFM allows the surface under examination to be in any state of hydration (from complete emersion in water to a completely dehydrated surface) (Gonzalez-Meijome *et al.*, 2005; Rabke *et al.*, 1995). The surface also requires no coating, no staining, no freezing and it need not be electrically conductive. This therefore allows the direct observation of contact lenses under a variety of ambient conditions (Baguet *et al.*, 1992). AFM is potentially non-destructive (Rabke *et al.*, 1995) and it has even been suggested that the lenses could be imaged at different wearing periods (Baguet *et al.*, 1995a).

1.13.6 AFM and surface topography

Baguet *et al.* (1992) were the first to image contact lenses with AFM. Their work demonstrated that direct observation of soft contact lens surfaces under near physiological conditions was possible. This study presented several images demonstrating that AFM was capable of imaging hydrogels surfaces at a level of vertical resolution superior to that observed with scanning electron microscopy.

1.13.7 The use of AFM in contact lens research

Grobe *et al.* (1996) showed that AFM is able to observe differences in surface morphology between contact lens types. This study contrasted the morphology of etafilcon A lenses produced by either lathing or cast-moulding the surface. They showed that the lathed lenses had a surface structure and RMS (root mean square) roughness consistent with that of a lathed surface (grooves/scratching from polishing), whereas the cast-moulded

surface had a relatively smooth surface and was relatively featureless. Rabke *et al.* (1995) not only studied the final lens product of the contact lens manufacturing process, but also each manufacturing step. They used AFM to examine the effect of varying the amount of polishing on the contact lens surface, in an attempt to increase productivity. This showed that decreasing the polishing time within a limited range, did not change the surface topography or roughness significantly. Rabke *et al.* (1995) also identified defects on the surface of cast-moulded contact lenses that could be traced back to defects arising from the polishing received by the tool used in the initial step of the moulding process.

Clinical contact lenses problems can often be better understood by analysis of the surface with AFM. Rabke *et al.* (1995) described a problematic contact lens where lens wettability was reduced following a particular step in the manufacturing process. AFM analysed pre-treated and post-treated lenses, in both a dehydrated and hydrated state. This showed that the manufacturing step caused cracking of the surface when the matrix was hydrated. This occurred, as the surface matrix was unable to expand sufficiently compared to the underlying primary matrix. The lens surface had wettability which was better than the primary matrix (pre-treated material), but worse than that expected from the secondary matrix (post-treated surface) and with a significant increase in surface roughness. Topographical analysis has also been performed on silicone hydrogel contact lenses. Gonzalez-Meijome *et al.* (2005) analysed the lens surface of three types of unworn silicone hydrogel contact lenses, balafilcon A, lotrafilcon A and galyfilcon A. They showed that balafilcon A lenses have raised silicate islands and macro pores with an estimated diameter of up to around 0.5μm, similar to that observed by scanning electron microscopy (SEM) (Lopez-Alemany *et al.*, 2002). The lens surface of galyfilcon A appeared as a uniformly distributed globular formation, differing from the uniformly smooth non-treated conventional hydrogel lens surfaces. The author suggests this globular formation may be due to polymer moieties. The surface topography of the lotrafilcon A material showed linear marks similar to those observed by Merindano *et al.* (1998) on conventional hydrogel materials. The cause of these marks was thought to be due to defects in the mould surfaces, which were then transferred to the lens material during polymerisation. Surface roughness is known to have important clinical implications. Bruinsma *et al.* (2002) showed that surface roughness was one of the major determinants of Pseudomonas aeruginosa adhesion to etafilcon A and RGP materials. Baguet *et al.* (1995a) has also shown that an increased surface roughness can bring about an increase in the bio-film deposited on a hydrogel

contact lens. This research suggests a link between surface roughness and bacterial/tear film component binding.

Surface roughness can be analysed in several different ways. Roughness parameters RMS (mean-square-roughness) and Ra (mean surface roughness) seem to be the most useful and reliable to characterise surface topography of siloxane hydrogel contact lenses. Rmax (maximum roughness) has been shown to be easily affected by local imperfections or sample contaminations leading to high values and therefore potentially unreliable (Gonzalez-Meijome *et al.*, 2005). AFM topographic research shows that when considering the clinical performance of a lens it is important to consider not only the bulk material, but also the surface properties of the completed product. The surface characteristics of a contact lens have been shown to be directly related to the steps involved in its manufacture.

1.13.8 Non-topographical AFM contact lens studies

Topographical studies alone cannot provide complete insight into the relationship between the surface properties of a contact lens and its clinical performance. Additional surface analysis techniques are needed to gain a fuller understanding of interfacial properties. In addition to topographical analysis, AFM is also able to perform adhesion, modulus and friction analysis. Several studies have used these techniques to extract further surface information for both hydrogel and silicone hydrogel contact lenses.

1.13.9 Bacterial adhesion and lens surface hydrophilicity

AFM has been used to identify differences in hydrophilicity and affinity for bacteria (physiochemical surface properties) (Vermeltfoort *et al.*, 2006). Vermeltfoort *et al.* (2006) showed that continuous wear of silicone hydrogel lenses did not substantially increase the risk of bacterial adhesion and more often reduces it. They also showed that changes in physiochemical surface properties were most apparent over the first week of wear, with an increase in wettability and a generally reduced susceptibility to bacterial binding with wear. In contrast, others have found the opposite findings (Borazjani *et al.*, 2004; Miller *et al.*, 1988; Schultz *et al.*, 2000), with lens wear increasing bacterial adhesion to contact lenses. These differences are likely caused by the use of differing solutions, lenses and bacterial strains.

1.13.10 Protein deposition analysed with AFM

Reduced surface hydrophobicity has been seen following wear of contact lenses (Read *et al.*, 2010a; Tonge *et al.*, 2001) and linked to hydrophilic tear film deposits (Leahy *et al.*, 1990). Baguet *et al.* (1992, 1995a) monitored the deposition of bio-films on soft contact lens surfaces. They showed that surface roughness increased as biofilms were deposited. Conventional hydrogel lenses have been shown to undergo major changes in surface roughness and elemental surface composition after wear (Bruinsma *et al.*, 2001, 2002; McArthur *et al.*, 2001). Silicone hydrogels, though, showed comparatively small changes when worn on a continuous wear basis (Vermeltfoort *et al.*, 2006), possibly due to the reduced levels of protein adhesion seen on silicone hydrogel materials (Senchyna *et al.*, 2004).

Lactoferrin is an important protein found in the tear film and has been implicated in contact lens fouling (Fowler & Allansmith, 1980; Franklin *et al.*, 1993). Meagher & Griesser (2002) used an AFM probe with a modified scanning tip (colloid particle attached to the tip) to investigate the interaction forces between lactoferrin layers adsorbed onto a hydrophobic substrate, as a function of electrolyte concentration, solution pH and protein concentration. AFM detected repulsive forces at larger separation distances consistent with that described by the Deraguin, Landau, Verwey and Overbeek (DLVO) theory. At a shorter range additional repulsive forces were detected due to compression of the adsorbed protein layer. The orientation of molecules within the adsorbed monolayer appeared to be fairly random, although the range of the interaction forces and the high compressibility of the adsorbed layers indicate that a significant number were present in an end-on orientation. Meagher & Griesser (2002) showed that adsorbed lactoferrin forms a steric repulsive barrier resisting the further deposition of lactoferrin, thus spontaneous multilayer adsorption appears unfavourable.

AFM also allows the study of lens care treatments and direct evaluation of cleaning solution efficacy. Rabke *et al.* (1995) compared contact lens surfaces following wear and disinfection with, thermal disinfection, multipurpose chemical solution treatment and peroxide solution treatment. Their results illustrated that the deposit condition of the lens was generally patient dependant but that there was a trend towards thermal disinfection lenses being more deposited than the lenses subjected to the multipurpose chemical or peroxide solution treatments.

1.13.11 Surface hydration and AFM

The hydration of a soft contact lens affects its surface stiffness, tribiology, protein and lipid deposition, oxygen transport to the cornea and dimensional stability (Koffas *et al.*, 2004). It has been observed that bulk water content affects both the oxygen permeability and the mechanical properties of the lens (Lai & Friends, 1997). It is also believed that a high surface water content and good surface hydrophilicity are desirable properties to increase the wettability of a contact lens by the tear film (Lopez-Alemany *et al.*, 2002). In hydrogels, water hydration is regulated at two regions: the lens/air interface and the lens/eye interface. This usually involves fluid entering the lens from the post lens tear film and leaving from the lens into the PLTF and evaporating (Little & Bruce, 1995). Bulk rehydration is therefore normally influenced by the evaporation occurring at the air interface. This can lead to a partially dehydrated surface, giving distinct mechanical properties of both regions (Koffas *et al.*, 2004). Although it is known that bulk and interfacial hydration has an effect on surface mechanics, the relationship is not well understood (Barbieri *et al.*, 1998; McConville & Pope, 2000).

Water content affects the mechanical properties of the contact lens, such as viscoelasticity and friction. When pHEMA is dry it is rigid and glassy, but when in a hydrated state it is soft and flexible. Contact lenses with high bulk water content tend to dehydrate when they are on the eye (Pritchard & Fonn, 1995a). If this is significant it can lead to reduced oxygen diffusion at the interface for conventional materials (Opdahl *et al.*, 2003), although in silicone hydrogel materials it has been suggested this might even increase oxygen permeability of the material (Morgan & Efron, 2003). Opdahl *et al.* (2003) presented a method for characterising the mechanical properties of bulk hydrated pHEMA contact lenses as a function of humidity, at the contact lens/air interface. The measurement of the surface mechanical properties can be related to the water content of the surface region. Water within the hydrogel matrix complicates the physical properties of a contact lens. The lens material responds as a solid to fast rates of deformation (elastically), but at slower rates of deformation the material responds as a liquid (viscoelastically) (Koffas *et al.*, 2004). This transition between elastic and viscoelastic mechanics depends on the probing rate, humidity and bulk water content of the system. When comparing the pHEMA and p(HEMA + MAA) materials, there is a difference in the onset of viscoelastic behaviour, surface stiffness and the work of adhesion. This therefore suggests a lower

interfacial water content for p(HEMA + MAA), with the pHEMA lens surface appearing softer and retaining more water even though the bulk contains less water. This indicates that water in the neutral hydrogel is bound more strongly at the surface than in ionic hydrogel materials, supporting the results of clinical trials which suggest that ionic hydrogel materials tend to dehydrate faster on eye than non-ionic hydrogels (Jones *et al.*, 2002b). These AFM studies agree with clinical studies (Kohler & Flanagan, 1985), which show that lenses with high bulk water content dehydrate more quickly and to a greater extent than those with lower bulk water content (Koffas *et al.*, 2004). The surface mechanical properties reported by Opdahl *et al.* (2003) suggest that the surface water content of pHEMA contact lenses are strongly dependent on the bulk dehydration state and on the relative humidity of the environment. They also suggested that air-exposed surfaces of pHEMA based contact lenses are likely to be quite dry and rigid, and stiffer than the bulk material.

1.13.12 AFM analysis of non-crosslinked pHEMA chains

Kim *et al.* (2001) have shown that AFM friction force analysis of a surface-dehydrated lens was able to detect surface species of low friction present on pHEMA soft contact lenses. These surface species were identified as non-crosslinked polymers by adhesive-force measurement. When the lens was surface dehydrated, the non-crosslinked pHEMA chains were anchored to the crosslinked pHEMA network by entanglement and were 2-4nm higher than the surrounding surface. In saline solution, large domains of non-crosslinked polymer chains were found at the lens surface extending tens of nanometers out of the surface. These non-crosslinked chains collapsed to the surface as the surface dehydrated, maintaining their low friction behaviour. They showed that in saline solution, surface friction and the adhesive force of the contact lens surface reduced, compared to that of the dehydrated contact lens surface (Kim *et al.*, 2001).

The results of these studies demonstrate the usefulness of the AFM as an ophthalmic research tool for analysis of the contact lens surface. AFM is able to investigate lens surface topography, lens deposition, lens surface hydration, disinfecting efficacy, surface elasticity and surface hardness. AFM therefore has the potential to bridge the gap between fundamental lens research and the clinical performance of contact lenses.

1.14 Scanning electron microscopy

1.14.1 Introduction

The basic function of a scanning electron microscope (SEM) is to produce an image of three-dimensional appearance derived from the action of an electron beam scanning across the surface of a specimen. The resolution can be better than 7nm, with a depth of focus at least 300 times greater than that of a light microscope at the limit of resolution. The range of magnification is a few times (typically x10) to several hundred thousand times and is limited by the microscopes resolution. The basic operating principle of a SEM is shown in Figure 1.39. It can be seen that the SEM consists of five main components:

1. **The electron gun** The electron gun is located at the top of the electron optical column and produces a large, high intensity electron beam with an effective source diameter of about 30 μm. The electrons are emitted from a heated tungsten wire (the filament) and are accelerated towards the specimen by an accelerating voltage.

2. **The column** The column consists of several electromagnetic lenses acting on the electron beam, which control the size and shape of the electron beam, focusing it onto the specimen.

3. **Scanning system** To allow an image to be produced, the scanning of the electron beam over the specimen and on the display tube must be in synchronism. The magnification of the displayed image is defined as in equation 1.7.

$$\text{Magnification} = \frac{\text{Linear dimension of scan on the display}}{\text{Linear dimension of scan on the sample}} \tag{1.7}$$

4. **Electron collection and display** When the specimen is struck by the electron beam several processes occur:

   (a) Some of the incident electron beam are reflected (high energy reflected electrons).

   (b) Some of the electrons are absorbed, flowing to ground through the specimen current contact.

   (c) The specimen will emit low energy secondary electrons.

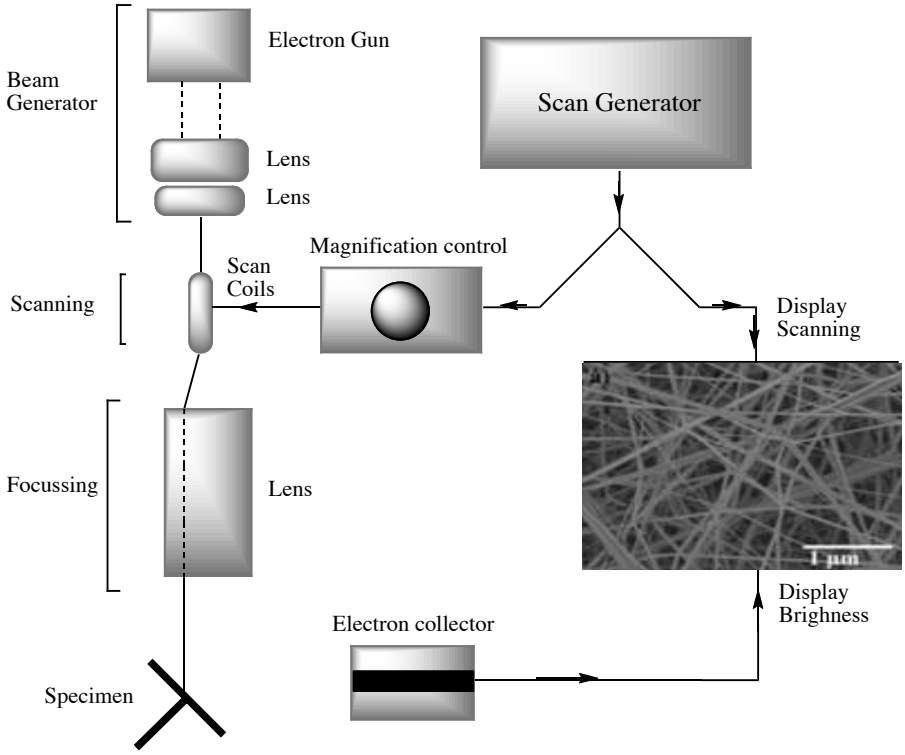

Figure 1.39: Schematic diagram of a scanning electron microscope.

(d) X-rays are emitted.

(e) Light is emitted.

A collector system for any of these can be used to provide information about the sample.

5. **The control electronics** This controls all of the circuitry necessary for an SEM to function.

1.14.2 Uses of SEM

The most common use of an SEM is in the study of surface topography, by detecting the low energy secondary electrons emitted from the specimen surface when hit by the electron beam. Other methods of analysis include detection of X-rays emitted when the electron beam strikes the specimen, which allows elemental analysis of the specimen as these x-rays are characteristic of the element from which they were emitted. Detection of the specimen current can also provide valuable information about what is occurring below

the surface of the sample. In addition detection of backscattered (reflected) electrons can be used to provide images of the variations of atomic number in the sample surface.

1.14.3 Sample preparation for SEM

The aim of sample preparation is to preserve the sample in its natural state, to dry the sample, to mount the sample and to coat the sample to maintain electrical connectivity and assist in the production of secondary electrons. The two main procedures to preserve the specimens are chemical fixation and freeze fixation. Chemical fixation uses chemicals such as gluteraldehyde or paraformaldehyde to form cross-links within the specimen to retain structure. Freeze fixation is performed by freezing the sample as quickly as possible (usually in liquid nitrogen ice) to avoid ice crystals forming, which may damage the sample surface. The specimen is then dehydrated either by air-drying (usually when no preservation was necessary), critical point drying or freeze drying. The dried samples are mounted on a stub to allow orientation of the sample in the microscope and to protect the sample from a build up of damaging negative charge from the electron beam. Most biological specimens are poor conductors of electrical charge and poor emitters of secondary electrons. The surface of the specimen is therefore coated in a thin layer of conducting metal. The coating is required to be thin enough not to obscure detail in the specimen, to be thick enough to conduct electrical charge and emit secondary electrons, to have a structure smaller than the resolution of the microscope and to avoid heat transfer to the sample. Gold is typically used for quality images but carbon is the coating of choice for X-ray microanalysis. The coating is applied using either a splutter method (gold) or evaporation (carbon).

1.14.4 Environmental SEM (ESEM)

An ESEM instrument is a type of SEM that is able to operate without requiring a vacuum in the specimen chamber and does not require the specimen to be conductive, therefore avoiding the need to desiccate or coat the specimen. ESEM imaging allows the characteristics of hydrated samples to be preserved during analysis. Due to its versatile analysis environment it was decided to use ESEM to image the surface of the contact lenses in this PhD study.

ESEM allows hydrated specimens to be imaged by cooling the specimens on a peltier

stage (to around 4°C) and by using high water vapour pressure to allow 100% humidity to be obtained at the sample surface avoiding sample dehydration (Stokes, 2003). The ESEM also requires the specimen chamber to be isolated from the vacuum column to allow water vapour to be used in the specimen chamber as an imaging gas (Figure 1.40). With ESEM the maximum water vapour pressure in the specimen chamber can reach around 10 Torr of water vapour (1/76 of an atmosphere). By closing off the main valve on the specimen chamber and pumping the upper portion of the chamber, the vacuum of the chamber is maintained by tiny pressure-limiting apertures which allow the passage of the electron beam, while restricting the flow into the column vacuum. The hole in the centre of the gaseous secondary electron detector (GSED) functions as the final aperture through which the primary electron beam passes. The GSED is given a positive bias (up to 600 Volts) to attract secondary electrons (Danilatos, 1988). The primary ion beam is very energetic and can penetrate the water vapour with minimal scatter while scanning the sample. Secondary electrons are released from the sample, but they encounter water molecules when they exit the surface. These water molecules produce secondary electrons, which in turn produce secondary electrons from adjacent water vapour molecules, thus the water vapour functions as a cascade amplifier (Danilatos, 1990). The amplified secondary electron signal is collected by the positively charged GSED and the intensity for the signal is converted into brighter or darker portions of the image at a given point on the sample as the electron beam moves across it. An ESEM instrument can also be operated in high vacuum mode or with cryogenically frozen samples using a stage cooled with liquid nitrogen.

1.14.5 SEM contact lens research

SEM has been used for many years to analyse the surface of contact lenses. Holden *et al.* (1974) used SEM to observe the micro structure of the surface of soft hydrophilic contact lenses. They found that the surfaces of lathed contact lenses were scratched with numerous polishing marks compared to the smooth surfaces found on lenses manufactured by cast moulding or spin casting. This increased surface roughness has been linked with increased tear film deposits (Baguet *et al.*, 1995a) and bacterial binding (Bruinsma *et al.*, 2002). Several studies have used SEM to analyse lens deposition. Tomlinson (1989) used SEM to analyse surface deposits on materials of differing type and water content. The amount of surface deposition was measured in terms of the area of the lens covered by

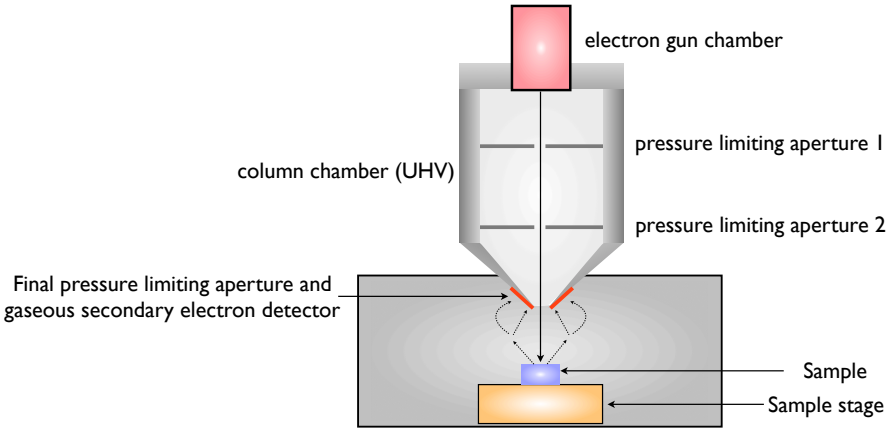

Figure 1.40: Schematic diagram of a environmental SEM.

deposit as visualised on a standard series of SEM photographs. Ilhan *et al.* (1998) used SEM to compare the level of surface deposition with frequent replacement lenses and conventional lenses, concluding that fewer deposits were present on frequent replacement lenses. Lopez-Alemany *et al.* (2002) used SEM to study the surface and bulk appearance of lotrafilcon A, balafilcon A and conventional hydrogel control lenses. The lens surface of lotrafilcon A had a wrinkled appearance, which the author felt was probably an artefact of the dehydration process of the specimens. Balafilcon A was shown to have a macro-porous surface structure, which the author suggested may influence the high gas permeability of the material and in the prevention of lens adhesion to the cornea. The conventional hydrogel lenses presented a smooth and homogeneous surface, with salt deposits visible due to dehydration of the material.

Gonzalez-Meijome *et al.* (2005) used Cryo-SEM to analyse the surface of three silicone hydrogel contact lenses. Cryo-SEM is where the specimen is kept at cryogenic temperature in an attempt to better preserve its structure during SEM imaging. This method of sample preparation allows the analysis of the hydrogel without dehydration, but can cause points of stress to develop within the surface of the material, resulting in areas of damage. This study used these areas of damage to observe the bulk material structure. Galyfilcon A had a solid polymeric bulk with an overlying thin granulated cover attached to each other by a characteristic formation of lamellae with small projections rounded at the end. Lotrafilcon A and balafilcon A were shown to have a loose network that attached

an outer surface membrane to the bulk of the polymeric network. The bulk ultra structure of lotrafilcon A displayed a morphological pattern of porosity where the pores are intercommunicated by a loose network of filamentous structures. The bulk ultra structure of balafilcon A showed a rounded appearance to the terminal ramifications of the structure.

Scanning electron microscopy has been shown to allow detailed analysis of the morphology of the surface of a contact lens. The main problem with conventional electron microscopy of a contact lens is that it is required to undergo several processing steps to allow imaging of the surface. These processing steps tend to alter the surface and introduce artefacts (Deg & Binder, 1986) and it is therefore difficult to know whether the surface being analysed is in its natural state. Cryo-SEM allows the observation of hydrated polymer samples, but the material can suffer serious damage, resulting in fracturing of the lens surface. This damage does allow analysis of the ultra structure of the bulk lens material, but as with SEM it is time consuming and the preparation processing can alter the specimen. Both SEM and Cryo-SEM require sample preparation prior to imaging which can modify the structure of the contact lens material. When interpreting the electron microscopy images it is therefore necessary to consider the effect of the sample preparation on the surface.

1.15 The importance of the contact lens surface

The surface properties of a hydrogel contact lens play a key role in determining its biocompatibility in the ocular environment (Maldonado-Codina *et al.*, 2004a). The surface of the lens comes into contact with the tear film and the ocular tissues, so understanding the structure and nature of the contact lens surface is likely to contribute significantly to an understanding of its clinical performance (Maldonado-Codina *et al.*, 2004a). Many of the key areas for future contact lens development are heavily associated with one or more of the these surface properties. In areas of lens performance such as subjective comfort, bacterial adhesion and tear film wetting, the lens surface characteristics are likely to be highly influential. Contact lens surface characteristics are influenced by factors such as the polymeric materials used in its manufacture (Cheng *et al.*, 2004; Ngai *et al.*, 2005), the type of lens manufacture (Grobe *et al.*, 1996; Maldonado-Codina & Efron, 2005), the manufacturing conditions (Grobe *et al.*, 1996; Maldonado-Codina & Efron, 2005) and the type of surface treatment (González-Méijome *et al.*, 2009; Karlgard *et al.*, 2004). This

means that when the clinical performance of commercial contact lenses is compared, it is difficult to know which of the numerous differences in bulk and surface characteristics is responsible. One advantage of the apparent differences in the surface properties of the two study lenses is that they have a matched design and bulk characteristics. This implies that any difference in clinical performance of the study lenses will be primarily associated with the differences in surface characteristics.

1.16 Study aims

By combining the clinical and laboratory findings for the study lenses, the aim is to better understand how these non-wetting regions are generated on the lens surface, how they influence clinical performance and which specific surface characteristics are responsible for these observations.The main aims for this PhD work are:

1. **To investigate the clinical performance of the two study contact lens types** (i.e. air-cured vs nitrogen-cured lenses). A short non-dispensing clinical study will be performed, which will primarily focus on surface wetting/deposition characteristics and subjective comfort.

2. **To characterise the in vitro surface wettability of the two study lens types**. Surface wettability will be undertaken using both static and dynamic contact angle analysis techniques.

3. **To characterise the in vitro surface chemistry of the two study lens types**. Surface chemical characterisation will be undertaken using the XPS and ToF-SIMS instruments. Use of these instruments will allow an understand of both the elemental and molecular composition of the contact lens surfaces both in a dehydrated state and a hydrated (cryo-frozen) state.

4. **To characterise the in vitro surface topography of the two study lens types**. Surface topography analysis with be performed using both an AFM and SEM instrument. This combination will allow information to be gather over a wide magnification range, in both a hydrated and dehydrated state and with an understanding of the mechanical chacryeristic of the lens material.

These findings were then compared to a range of commercially available contact lenses, which were known to have acceptable clinical performance.

Chapter 2

Clinical investigation of study contact lenses

2.1 Comparative clinical study

2.1.1 Introduction

The ability of the tear film to spread and maintain itself across the surface of a contact lens has been shown to influence subjective vision (Thai *et al.*, 2002a; Timberlake *et al.*, 1992; Tutt *et al.*, 2000), comfort (Guillon & Maissa, 2007) and tear film deposition (Nicholson & Vogt, 2001; Tighe, 2004). The development of contact lens materials which allow a stable tear film to reside on the lens surface is likely to be key in providing lenses with enhanced clinical performance. The incorporation of siloxane polymers into contact lenses has greatly enhanced the ability of hydrogel materials to transmit oxygen, but has also increased the hydrophobic tendency of the lens surface. Contact lens manufactures have looked to enhance the surface wetting characteristics of these materials in order to improve their clinical performance (Nicholson & Vogt, 2001; Tighe, 2004). During the development of a silicone hydrogel contact lens material, the PhD sponsoring company (CooperVision Inc.) observed that when an experimental polymer was cured in polypropylene moulds within an air-filled oven, the material tended to possess a relative hydrophobic surface. In contrast, when the same polymer was polymerised in the same polypropylene moulds within a nitrogen-purged oven, the surface was significantly more hydrophilic. In an attempt to better understand the clinical differences between these two contact lens types a clinical study was performed.

2.1.2 Purpose

To compare the initial clinical performance of the two experimental silicone hydrogel study contact lenses over a one hour wearing period.

2.1.3 Ethical approval

Ethical approval for this clinical work was granted by The Committee on the Ethics of Research on Human Beings at The University of Manchester (REF/06204) in April 2007.

2.1.4 Study design

This study was a prospective, double-masked, randomised, non-dispensing clinical study. Ten subjects were required to wear both lens types on a contralateral basis for a period of one hour. A one hour clinical assessment was chosen as (i) initial testing suggested large differences in clinical performance between the two lens types, (ii) a limited power range restricted dispensing and (iii) marked tear film deposition during wear reduced acuity significantly for one of the lens types. Recruitment was initially limited to 10 subjects due to the large apparent differences in clinical performance between the two lens type and due to limitations on the number of study lenses available.

2.1.5 Masking

To minimise bias in the clinical study both the subject and investigator were masked from the lens type. Both study lenses arrived from the manufacturer in plain white blister packaging, with labels identifying lens type. A second investigator removed the labels from the blister packaging and randomly assigned and labelled two lenses to each subject, ensuring that one was a nitrogen-cured lens and the other an air-cured lens. These lenses were randomly assigned to the subject's right and left eye. The primary investigator and subject knew that the two lens types were being fitted contralaterally but were unaware of the identity of each lens.

2.1.6 Study population

Subjects for this clinical trial were recruited using a bulk e-mail to university staff and students approved by The Committee on the Ethics of Research on Human Beings at The University of Manchester.

2.1.7 Inclusion criteria

To be considered eligible to participate in the clinical investigation, each subject was required to meet the following inclusion criteria:

1. They were of legal age (18 years) and capacity to volunteer.
2. They understood their rights as a research subject and were willing to sign a Statement of Informed Consent.
3. They were willing and able to follow the protocol.
4. They were currently adapted to soft contact lens wear.
5. Keratometry readings were between 7.20mm and 8.30mm.
6. They had a refractive error of between plano and -4.00DS, allowing them to obtain reasonable acuity with the study lenses (-3.00DS).

2.1.8 Exclusion criteria

Subject were not permitted to participate if:

1. They had an ocular disorder which would normally contraindicate contact lens wear.
2. They had a systemic disease affecting ocular health.
3. They had grade 2 or greater of any of the following ocular surface signs: corneal oedema, corneal vascularisation, corneal staining, tarsal conjunctival changes or any other abnormality which would normally contraindicate contact lens wear.
4. They were pregnant or lactating.
5. They had undergone corneal refractive surgery.
6. They were using any topical or systemic medications that could affect ocular health or the performance of the lens.
7. They were current RGP contact lens wearers.
8. They had any corneal distortion resulting from previous hard or rigid lens wear or had keratoconus.

9. They had taken part in any other clinical trial or research, within two weeks prior to starting the study.

2.1.9 Study lenses

The lenses used in this study were manufactured from the same material, in the same mould type and on the same manufacturing line, but the conditions in the curing oven differed with some lenses being polymerised in an air-filled oven (air-cured lenses) and others being polymerised in a nitrogen-purged oven (nitrogen-cured lenses). All lenses were supplied in individual blister packaging containing 0.9% phosphate buffered saline (no surfactants or other additives present). In this study all lenses were applied directly from the blister packaging. Further details of the study lenses are provided in Table 2.1.

Table 2.1: Study lenses.

	Test lens 1	**Test lens 2**
Name	Air-cured	Nitrogen-cured
Manufacturer	CooperVision Inc.	CooperVision Inc.
Polymerisation conditions	Air-filled oven	Nitrogen-purged oven
Manufacturing method	Cast-moulded	Cast-moulded
FDA group	I	I
EWC (%)	46%	46%
Base curve	8.6	8.6
Diameter	14.2	14.2
Spherical power	- 3.00 DS	- 3.00 DS

2.1.10 Screening visit

This visit was conducted to confirm whether the subject was suitable for enrolment onto the study. The study objectives and procedures were explained to the subject. Details were then recorded regarding ocular and personal medical history, family medical and ocular history, medications, allergies, a thorough contact lens history including duration of lens wear, lens types and solutions used and any prior contact lens problems. A full eye examination was then performed including refraction, binocular vision assessment, ophthalmoscopic examination, slit lamp examination, visual field assessment, keratometry and intraocular pressure measurement. If the subject met all the inclusion criteria they

were given a study information form and a copy of the informed consent to review, but not sign. The subject was then discharged and asked to carefully read through the information provided and considered whether they wished to participate in the study. When the subject had confirmed they wanted to take part in the study they were invited to attend for the study visit. The subject was asked to attend for the study visit not having worn their own contact lenses for at least 24 hours.

2.1.11 Initial visit

Before any clinical assessment was performed the subject and investigator discussed and signed the consent form and a study summary form. Copies of the signed forms were issued to the subject. When the subject had signed the consent form, they were considered to be enrolled onto the study. The following procedures were then performed:

1. Corrected distance monocular acuities were recorded.
2. Slit lamp biomicroscopy was carried out for the signs outlined in Appendix A.4.
3. The lenses were fitted according to a randomisation table and allowed to settle for 5 minutes.
4. After 5 minutes the subject was asked to complete the following questionnaire using visual analogue scales (Appendix A.6) where scores were collected for each eye separately:
    - Overall comfort (0-100 scale); where 0 indicates extremely poor comfort and 100 indicates no lens sensation.
    - Sensation of dryness (0-100 scale); where 0 indicates extreme dryness and 100 indicates no sensation of dryness.
    - Burning and stinging (0-100 scale); where 0 indicates extreme burning and stinging and 100 indicates no sensation of burning and stinging.
    - Subjective lens preference (no preference or slightly/strongly prefer right or left lens).
5. Tear film break-up time was measured in seconds using the Keeler Tearscope.

6. Lens surface wettability and lens surface deposition was recorded using 0-4 grading scales (Appendix A.1), where 4 indicates a lens with optimum wetting/no deposition and 0 indicates a non-wetting/extremely deposited surface.

7. The percentage wetting area on the lens surface immediately after blink was recorded, with 100% indicating a lens completely wet by the tear film and 0% indicating a completely non-wetting surface.

8. Lens surface appearance was recorded as a description (e.g. smooth/grainy/non-wetting).

9. Surface defects (if present) were recorded (particles, scratches, fibres, tears, bubbles/blisters, nicks and non-wetting areas).

10. The investigator was asked to record which lens they preferred in terms of the lens surface (no preference or slightly/strongly prefer right or left lens surface).

11. Lens centration was graded for degree of centration (optimal, slight or extreme decentration) and direction if decentred (Appendix A.2).

12. The lens was graded for degree of corneal coverage (either optimal, clinically acceptable or clinically unacceptable).

13. Post-blink movement was measured to the nearest 0.1mm in superior gaze.

14. Lens tightness ('push-up') was recorded using the grading scale (Appendix A.2), with 100% indicating no movement and 0% very excessive movement.

2.1.12 Follow-up visit

After one hour of lens wear the following procedures were then performed:

1. Any subject or investigator comments were noted.

2. The subject was asked to complete the following questionnaire (Appendix A.6) where scores were collected for each eye separately:

    - Overall comfort (0-100 scale), where 0 indicates extremely poor comfort and 100 indicates no lens sensation.

- Sensation of dryness (0-100 scale), where 0 indicates extremely dryness and 100 indicates no sensation of dryness.
- Burning and stinging (0-100 scale), where 0 indicates extreme burning and stinging and 100 indicates no sensation of dryness.
- Subjective lens preference (no preference or slightly/strongly prefer right or left lens).

3. Tear film break-up time was measured in seconds using the Keeler Tearscope.
4. Lens surface wettability and lens surface deposition was recorded using 0-4 grading scales (Appendix A.1), where 4 indicates a lens with optimum wetting/no deposition and 0 indicates a non-wetting/extremely deposited surface.
5. The percentage wetting area on the lens surface immediately after blink was recorded, with 100% indicating a lens completely wet by the tear film and 0% indicating a completely non-wetting surface.
6. Lens surface appearance was recorded as a description (e.g. smooth/grainy/non-wetting).
7. Surface defects (if present) were recorded (particles, scratches, fibres, tears, bubbles/blisters, nicks and non-wetting areas).
8. The investigator was asked to record which lens they preferred in terms of the lens surface (no preference or slightly/strongly prefer right or left lens surface).
9. Lens centration was graded for degree of centration (optimal, slight or extreme decentration) and direction if decentred (Appendix A.2).
10. The lens was graded for degree of corneal coverage (either optimal, clinically acceptable or clinically unacceptable).
11. Post-blink movement was measured to the nearest 0.1mm in superior gaze.
12. Lens tightness ('push-up') was recorded using the grading scale (Appendix A.2), with 100% indicating no movement and 0% very excessive movement.
13. The study lenses were then removed and stored in glass vials containing 0.9% unbuffered saline.

14. Slit lamp biomicroscopy was carried out for the signs outlined in Appendix A.4.

15. Distance corrected monocular visual acuities were recorded.

16. The subject then signed the Study Exit Statement acknowledging that the study was complete. A copy of this signed form was issued to the patient.

The same investigator was used for the examination of all ten subjects.

2.1.13 Data analysis and presentation

Each of the clinical assessment data sets were tested for normality using the Shapiro-Wilks test (Appendix A.9). When data were normally distributed, analysis of variance (ANOVA) was employed to compare variables between subjects for the different lens types, with statistically significant differences further investigated using post-hoc analysis. The Tukey test was used as the post-hoc test of choice. Where the data sets were non-normally distributed, the Krusal-Wallis non-parametric test was applied. Correlations between lens wettability and other recorded variables were tested for significance by regression analysis. Statistical tests were undertaken using JMP 5.0 statistical software for Apple Macintosh. A p-value of 0.05 was taken as the threshold of statistical significance.

2.1.14 Demographics

Demographic data are reported in terms of age, sex, spherical error and cylindrical refractive error for the subjects.

2.1.15 Standard lens fit measures

Each of the standard lens fit measures were compared using a two-way repeated measures ANOVA with the Tukey post-hoc test applied where appropriate. Here, the factors investigated were 'lens type', 'visit' and where required 'lens type x visit' interaction.

2.1.16 Lens surface

Each of the three lens surface measures (surface quality, wettability and front surface deposition) were compared using the statistical approach outlined in section 2.1.15.

Table 2.2: Study demographics. Variables are expressed as a mean ± standard deviation.

Parameter	Females	Males	Total
Number of subjects	4	6	10
Age	31.5 ± 7.9	29.8 ± 3.5	30.5 ± 5.6
Sphere	-2.7 ± 1.4	-1.9 ± 2.1	-2.2 ± 2.2
Cylinder	-1.0 ± 1.0	-0.4 ± 0.6	-0.7 ± 0.8

2.1.17 Biomicroscopy

Biomicroscopy scores were compared using the statistical approach outlined in section 2.1.15.

2.1.18 Subjective reactions

Subjective scores assessed with a 0-100 visual analogue scale were compared using the statistical approach outlined in section 2.1.15.

2.1.19 Results

2.1.19.1 Demographics

Ten subjects were recruited with the demographic details shown in Table 2.2.

2.1.19.2 Serious or significant adverse events

There were no serious or significant adverse events reported during this study.

2.1.19.3 Discontinuations

There were no discontinuations during the course of this study.

2.1.19.4 Lens fitting characteristics

Data for lens fitting characteristics are shown in Table 2.3 and Figure 2.1 [1]. There was no difference in centration or corneal coverage between the two study lens types, with all 20 lenses worn exhibiting optimal centration and corneal coverage on insertion and after 1 hour of wear. A two-way repeated measures ANOVA showed no statistically

[1] For all box and whisker plots used in this thesis, the cross refers to the mean, the line the median and the whiskers show the full range of the data.

significant difference between the lenses for post-blink movement (F=0.92, p=0.34) or push-up tightness (F=0.05, p=0.81). There was also no statistically significant difference between the study visits for post-blink movement (F=2.57, p=0.12) or push-up tightness (F=0.006, p=0.94). No 'visit x lens' interactions were statistically significant for any of the lens fitting characteristics.

Table 2.3: Lens fitting characteristics.

	Nitrogen-cured (Avg.)	**Air-cured (Avg.)**
Centration (initial)	Optimum	Optimum
Centration (1 hour)	Optimum	Optimum
Coverage (initial)	Optimum	Optimum
Coverage (1 hour)	Optimum	Optimum
Post-blink movement (initial)	0.3 ± 0.1	0.3 ± 0.3
Post-blink movement (1 hour)	0.2 ± 0.1	0.3 ± 0.2
Push-up tightness (initial)	50.0% ± 3.3%	50.5% ± 12.1%
Push-up tightness (1 hour)	50.0% ± 7.1%	55.0% ± 10.5%

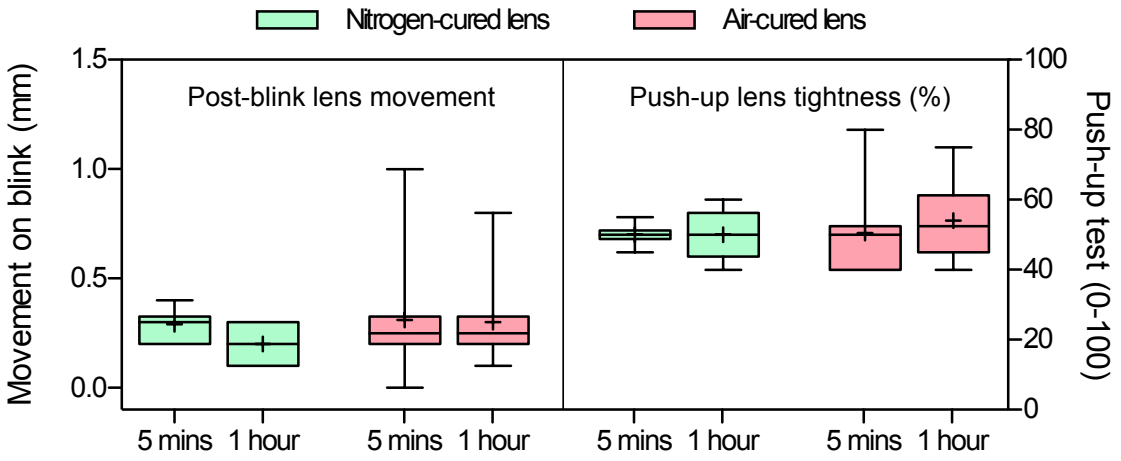

Figure 2.1: Lens fitting data after 5 minutes and 1 hour of lens wear.

2.1.19.5 Lens surface characteristics

Figure 2.2 shows typical slit lamp images of the nitrogen-cured and air-cured contact lenses. The lens surface characteristics are shown in Table 2.4 and Figure 2.3. Since the lens wettability and lens deposition grading scales were ordinal in nature and the % wet-

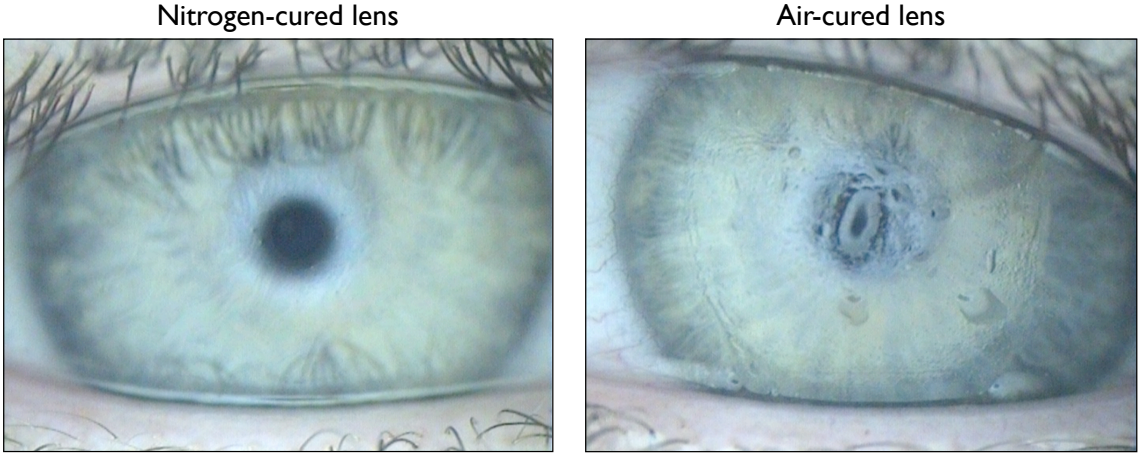

Figure 2.2: Typical slit lamp images of the nitrogen-cured and air-cured study contact lenses.

ting area on the lens surface was shown to differ significantly from a normal distribution (nitrogen-cured W=0.57, p<0.001; air-cured W=0.95, p=0.037), non-parametrical statistics were performed on these data.

A Kruskal Wallis test showed a statistically significant difference between the lenses (χ^2=34.59, p<0.0001) for the wettability grading scale data, but not between the study visits (χ^2=0.06, p=0.81). The percentage wetting area was also shown to differ significantly between the study lenses (χ^2=30.98, p<0.0001), but not between study visits (χ^2=0.02, p=0.88). Lens surface deposition showed a statistically significant difference between the

Table 2.4: Lens surface characteristics.

	Nitrogen-cured (Avg.)	**Air-cured (Avg.)**
Wettability grading scale (initial)	3.0 (0.2)	0.0 (0.0)
Wettability grading scale (1 hour)	3.05 (0.2)	0.0 (0.0)
% Wetting area (initial)	98.5% (2.4%)	50.0 % (17.0%)
% Wetting area (1 hour)	99.0% (2.1%)	50.5 % (17.1%)
Surface appearance (initial)	grainy	non-wetting
Surface appearance (1 hour)	grainy	non-wetting
Deposits (initial)	0.3 (0.2)	3.0 (0.7)
Deposits (1 hour)	0.4 (0.1)	3.5 (0.3)
Deposit type (initial)	lipid	lipid / mucin
Deposit type (1 hour)	lipid	lipid / mucin
Surface preference (initial)	strong yes	strong no
Surface preference (1 hour)	strong yes	strong no

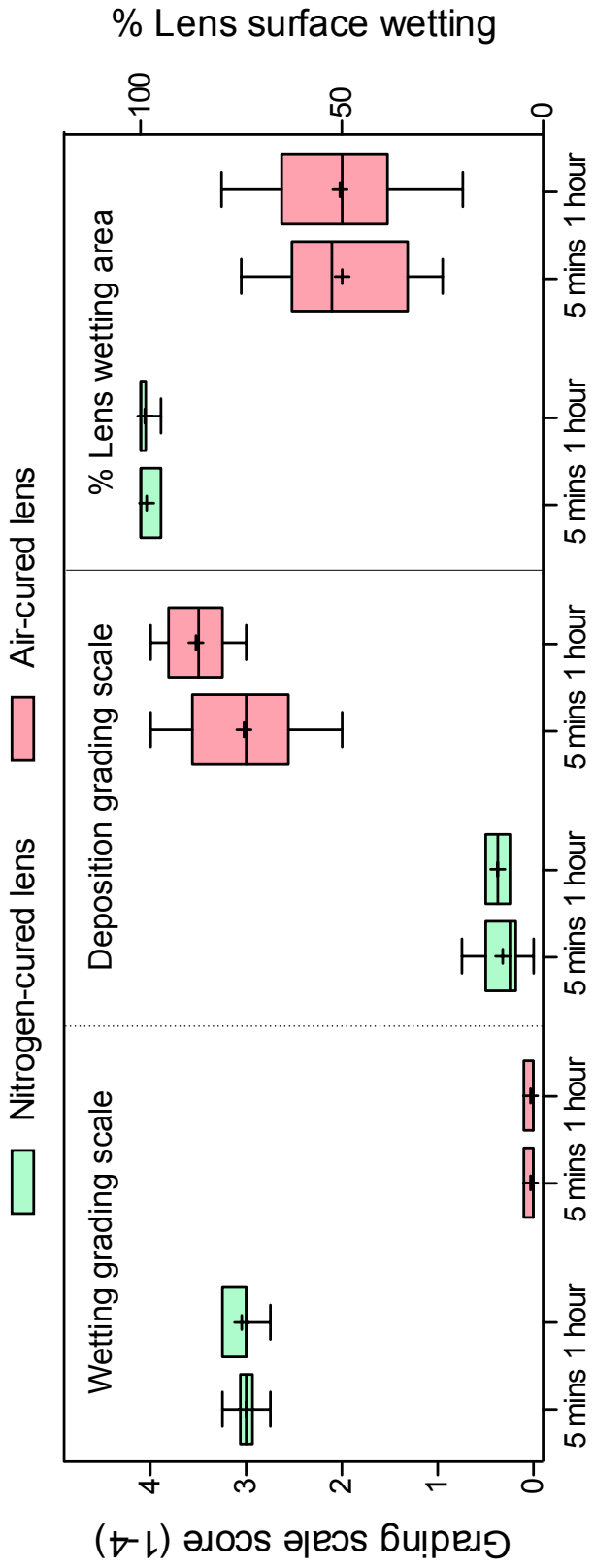

Figure 2.3: Biomicroscopy findings after 5 minutes and 1 hour of lens wear.

lenses (χ^2=29.96, p<0.0001), but not between the study visits (χ^2=0.79, p=0.37). The surface appearance for the nitrogen-cured lenses was graded as smooth (30%) or grainy (70%), whereas the air-cured lenses in all cases were graded as non-wetting. Tear film deposition on the nitrogen-cured lens surface was minimal and, if present, was in the form of a film, whereas the deposition on the air-cured lens was primarily composed of discrete regions of marked deposition on the non-wetting regions of the lens surface. The investigator strongly preferred the nitrogen-cured lens surface over the air-cured lens surface for all ten subjects at both study visits. No lens surface defects, with exception of the non-wetting regions, were observed on any of the 20 study lenses investigated.

Figure 2.4 shows the time following a blink for the non-invasive tear film to break-up (NITBUT) on the anterior surface of a contact lens. The tear film break-up was immediate for all ten air-cured lenses and an average of around nine seconds for the ten nitrogen-cured contact lenses. A Kruskal Wallis test showed a statistically significant difference between the lenses for the NITBUT (χ^2=33.44, p<0.001), but not between the study visits (χ^2=0.01, p=0.91).

2.1.19.6 Biomicroscopy

The biomicroscopy data at the initial and follow-up visits are shown in Table 2.5 and Figure 2.5. The two way repeated measures ANOVA showed a statistically significant difference between the lenses (F=10.99, p=0.002), study visits (F=27.8, p<0.01) and 'lens x visit'

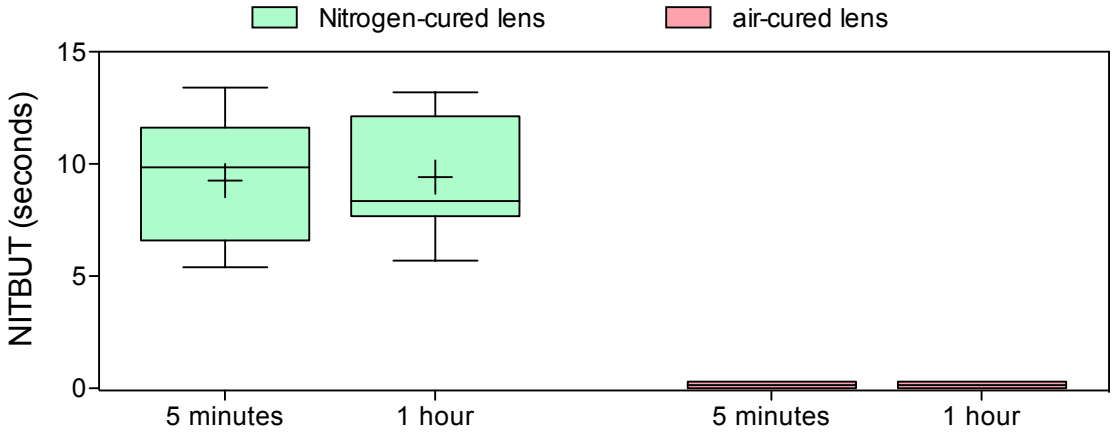

Figure 2.4: Non-invasive tear film break-up time.

Table 2.5: Mean biomicroscopy findings with standard deviation in parenthesis.

	Nitrogen-cured	Air-cured)
Conjunctival (pre-wear)	0.6 (0.2)	0.5 (0.2)
Conjunctival (1 hour)	0.7 (0.1)	1.4 (0.5)
Limbal hypereamia (pre-wear)	0.4 (0.2)	0.4 (0.1)
Limbal hypereamia (1 hour)	0.5 (0.2)	0.8 (0.3)
Corneal vascularisation (pre-wear)	0.1 (0.2)	0.1 (0.1)
Corneal vascularisation (1 hour)	0.1 (0.2)	0.1 (0.2)
Stomal haze (pre-wear)	0.0 (0.0)	0.0 (0.0)
Stomal haze (1 hour)	0.0 (0.0)	0.0 (0.0)
Tarsal conj. roughness (pre-wear)	0.6 (0.2)	0.5 (0.1)
Tarsal conj. roughness (1 hour)	0.5 (0.2)	0.6 (0.2)
Tarsal conj. hypereamia (pre-wear)	0.6 (0.2)	0.5 (0.2)
Tarsal conj. hypereamia (1 hour)	0.6 (0.2)	0.6 (0.4)

interaction ($F=14.89$, $p<0.01$) for conjunctival hyperaemia. Inspection of the data using a Tukey post-hoc test showed that the conjunctival hyperaemia was significantly greater for the air-cured lens at the one hour follow-up visit, than for the air-cured lens at the initial visit or for the nitrogen-cured lens at either of the visits. There was also a statistically significant difference between the study lenses ($F=6.67$, $p=0.01$) and between study visits ($F=20.99$, $p<0.01$) for limbal hyperaemia, with the grading of limbal hyperaemia higher for the air-cured lens than the nitrogen-cured lens and the grading of limbal hyperaemia higher at one hour visit than prior to lens insertion. All other biomicroscopy findings did not change significantly following 1 hour of lens wear ($p > 0.05$ in all cases).

2.1.19.7 Corneal & conjunctival staining

Grading scale scores for corneal and conjunctival staining at the initial fitting and at the follow-up visit are presented in Table 2.6 and Figure 2.6. The two-way repeated measures ANOVA showed no statistically significant difference between conjunctival staining for lens type ($F=0.11$, $p<0.74$) or 'lens x visit' interaction ($F=0.44$, $p=0.51$), but a statistically significant difference was observed between study visits ($F=5.95$, $p=0.02$), where at the one hour visit grading of conjunctival staining was higher for both lens types than prior to lens insertion. Corneal staining showed no statistically significant differences between the lenses ($F=0.11$, $p=0.74$) and 'lens x visit' interaction ($F=0.44$, $p=0.51$), but a statistically significant difference was observed between the visits ($F= 5.95$, $p=0.02$), where at the one hour visit grading of corneal staining was higher for both lens types than prior to lens

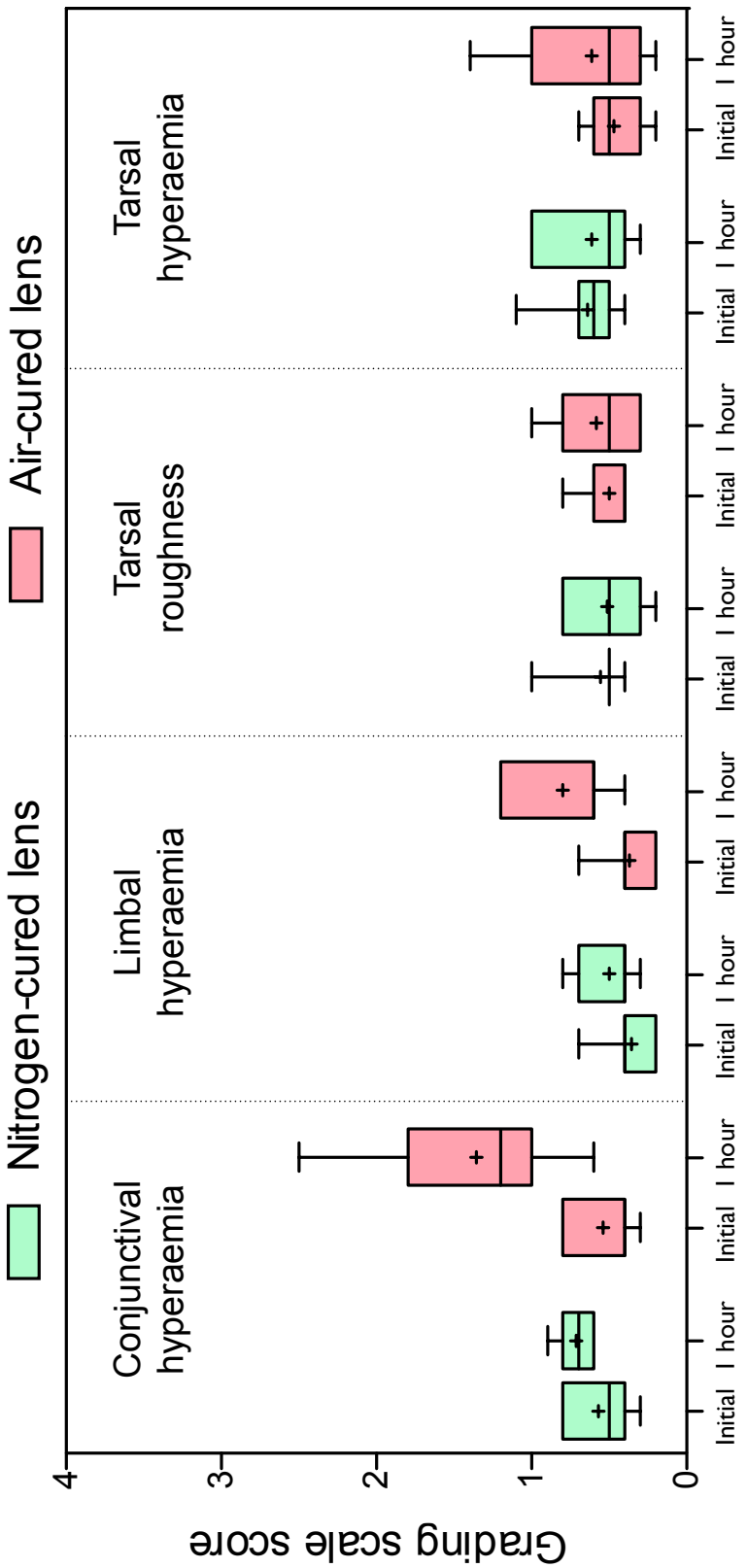

Figure 2.5: Biomicroscopy findings.

Table 2.6: Average corneal and conjunctival staining scores with standard deviation in parenthesis.

	Nitrogen-cured	Air-cured
Corneal staining (pre-wear)	0.3 (0.2)	0.4 (0.3)
Corneal staining (1 hour)	0.6 (0.3)	0.5 (0.3)
Conjunctival staining (pre-wear)	0.5 (0.2)	0.4 (0.2)
Conjunctival staining (1 hour)	0.7 (0.3)	0.8 (0.3)

insertion.

2.1.19.8 Subjective ratings

Scores for subjective ratings at the initial and follow-up visits are presented in Table 2.7 and Figure 2.7. In all cases the subjects gave poorer subjective scores for the air-cured lens over the nitrogen-cured lens when grading for comfort, dryness and burning and stinging. There were statistically significant differences between the lenses for comfort ($F=132.5$, $p<0.01$), dryness ($F=25.9$, $p<0.01$) and burning and stinging ($F=61.8$, $p<0.01$). There were no statistically significant differences between the visits, for comfort ($F=0.20$, $p=0.66$) or dryness ($F=4.02$, $p=0.053$), but there was for burning and stinging ($F=6.11$, $p=0.02$),

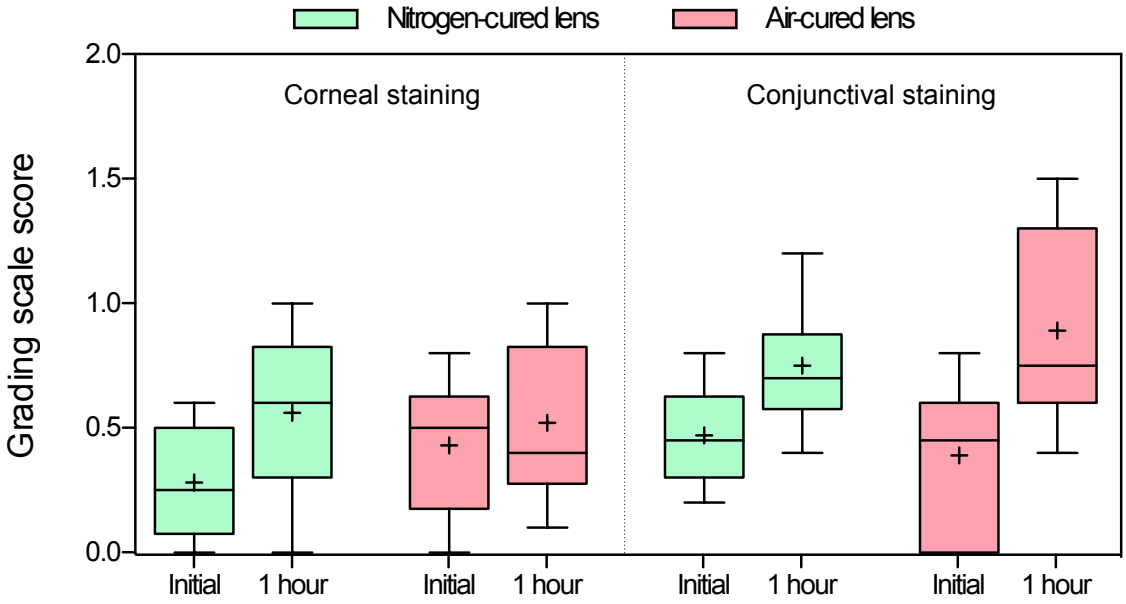

Figure 2.6: A box and whisker plot of the corneal and conjunctival grading scale scores prior to lens wear and after 1 hour of lens wear for both study lenses.

Table 2.7: Average subjective scores for study lenses with standard deviation in parenthesis.

	Nitrogen-cured	Air-cured
Comfort (initial)	82.0 (10.3)	44.0 (11.7)
Comfort (1 hour)	86.0 (7.8)	35.0 (17.0)
Comfort preference	strong yes	strong no
Dryness (initial)	89.0 (6.6)	66.5 (24.0)
Dryness (1 hour)	85.0 (7.8)	46.5 (27.4)
Burning & stinging (initial)	85.5 (8.6)	65.0 (12.2)
Burning & stinging (1 hour)	89.0 (8.8)	39.5 (22.2)

which showed an increase in symptoms of burning and stinging at the one hour visit. The interaction term 'lens x visit' was shown not to be significant for comfort (F=1.46, p=0.23) or dryness (F=1.79, p=0.19), but was found to be significant for burning and stinging (F=10.6, p=0.003). Inspection of the interaction using a Tukey post-hoc test showed that the burning and stinging subjective symptoms were split into three statistically similar groups. The group with the greatest sensation of burning and stinging was the air-cured lens at the 1 hour visit, the second group was the air-cured lens at the 5 minute visit and the group with the least symptoms of burning and stinging contained the nitrogen-cured lens at both the 5 minute and 1 hour study visits.

2.1.19.9 Relationship between clinical parameters

Table 2.8 shows a correlation matrix for the various parameters in the study. Inspection of the matrix inicates that the correlation coefficients are high within the general groups of subjective responses (comfort, dryness and burning and stinging), lens surface wetting (wettability grading scale, % surface wetting, NITBUT and deposition grading scale) and also between these two groups of parameters. Other high correlation coefficients were also observed for:

1. Lens movement parameters except push-up tightness.
2. Limbal and bulbar conjunctiva with subjective comfort parameters.
3. Reduced surface wetting (excluding NITBUT) and increased deposition with bulbar conjunctival redness.
4. Bulbar and limbal conjunctiva.

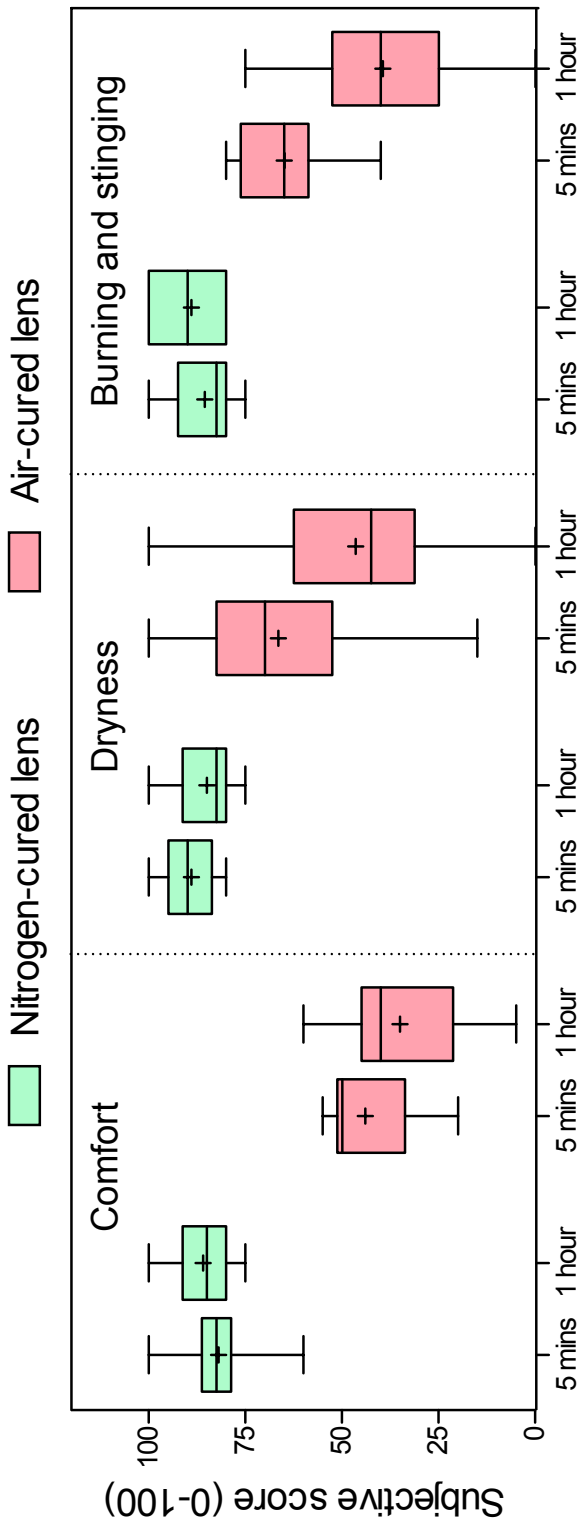

Figure 2.7: Subjective responses (0-100) after 5 minutes and 1 hour of lens wear.

5. Tarsal roughness and tarsal redness.

6. Tarsal roughness/redness and limbal conjunctiva but not bulbar conjunctival changes.

7. Conjunctival staining and bulbar/limbal conjunctiva.

8. Conjunctival staining and %burning & stinging and %dryness, but not % subjective comfort.

Principle component analysis showed that the first principle component was comprised of all lens surface wettability and deposition indicators and the subjective symptoms (dryness, comfort, burning and stinging) (accounting for 36% of the variance). The second component was comprised of lens movement indicators (post-blink, up-gaze lag and primary gaze lag) and corneal staining (accounting for 16% of the variance). The third component was related to conjunctival grading (accounting for 16% of the variance) and the forth was related to conjunctival staining and push-up tightness (accounting for 8% of the variance). In total these four components accounted for 76% of the total variance.

2.1.19.10 Entrance and exit visual acuity

No statistically significant difference was noted between entrance and exit visual acuity (F= 0.08, p=0.85).

2.1.20 Discussion

The interaction between the contact lens and the ocular environment is likely to be heavily influenced by the surface characteristics of the contact lens. With conventional hydrogel materials, both the material from which a contact lens is produced and the method of manufacture have been shown to influence the contact lenses subsequent clinical performance (Grobe *et al.*, 1996; Maldonado-Codina & Efron, 2004, 2005; Maldonado-Codina *et al.*, 2004a). Many studies have looked at the clinical performance of silicone hydrogel lenses (Brennan *et al.*, 2002; Dumbleton *et al.*, 2006; Guillon & Maissa, 2007; Maldonado-Codina *et al.*, 2004b; Morgan & Efron, 2002), but there is little in the published literature on the effect of method of manufacture on the subsequent clinical performance of silicone hydrogel contact lenses.

		LENS WETTING & DEPOSITION				LENS MOVEMENT				SUBJECTIVE SCORES			OCULAR SURFACE GRADING					
		NITBUT	Wettability	% Wetting Area	Deposits	Post-Blink Movement	Primary Gaze Lag	Upgaze Lag	Push-Up Tightness (%)	% Comfort	% Dryness	% Burning and Stinging	Bulbar Conj.	Limbal Conj.	Tarsal Roughness	Tarsal Redness	Corneal Staining	Conj Staining
LENS WETTING & DEPOSITION	NITBUT		0.9317	0.8437	-0.8949	-0.0972	-0.2082	0.0719	-0.0325	0.8127	0.5746	0.6910	-0.3055	-0.2753	0.0192	0.2137	0.0169	-0.1606
	Wettability	0.9317		0.9011	-0.9626	-0.1605	-0.2488	-0.0296	-0.0430	0.8782	0.6192	0.7380	-0.3481	-0.2969	-0.0362	0.1478	-0.0582	-0.0923
	% Wetting Area	0.8437	0.9011		-0.8671	-0.0610	-0.1755	0.1073	-0.1412	0.8967	0.7307	0.7649	-0.4490	-0.3545	-0.0372	-0.0072	-0.0935	-0.0525
	Deposits	-0.8949	-0.9626	-0.8671		0.1431	0.2444	-0.0288	0.1136	-0.8357	-0.5489	-0.7335	0.3893	0.3103	0.0320	-0.1320	0.0427	0.1160
LENS MOVEMENT	Post-Blink Movement	-0.0972	-0.1605	-0.0610	0.1431		0.4400	0.5392	-0.1530	0.0307	0.0673	0.2293	-0.1805	0.0042	0.1056	0.1179	-0.3682	-0.0931
	Primary Gaze Lag	-0.2082	-0.2488	-0.1755	0.2444	0.4400		0.6074	0.0501	-0.0965	-0.0020	0.0336	-0.0566	-0.0120	0.0992	0.0970	-0.2573	0.0484
	Upgaze Lag	0.0719	-0.0296	0.1073	-0.0288	0.5392	0.6074		-0.3064	0.1008	0.1070	0.2352	-0.2424	-0.1651	0.1260	0.0959	-0.3221	0.0545
	Push-Up Tightness (%)	-0.0325	-0.0430	-0.1412	0.1136	-0.1530	0.0501	-0.3064		0.0467	0.0480	-0.0867	0.2634	0.1299	0.1138	0.0069	0.0699	-0.0975
SUBJECTIVE SCORES	% Comfort	0.8127	0.8782	0.8967	-0.8357	0.0307	-0.0965	0.1008	0.0467		0.7991	0.8559	-0.5203	-0.3914	-0.0347	0.0086	-0.1107	-0.1326
	% Dryness	0.5746	0.6192	0.7307	-0.5489	0.0673	-0.0020	0.1070	0.0480	0.7991		0.7228	-0.6915	-0.5714	-0.2667	-0.2225	-0.2650	-0.3756
	% Burning and Stinging	0.6910	0.7380	0.7649	-0.7335	0.2293	0.0336	0.2352	-0.0867	0.8559	0.7228		-0.6711	-0.5029	-0.0414	-0.0095	-0.1741	-0.3201
OCULAR SURFACE GRADING	Bulbar Conj.	-0.3055	-0.3481	-0.4490	0.3893	-0.1805	-0.0566	-0.2424	0.2634	-0.5203	-0.6915	-0.6711		0.7986	0.2308	0.2499	0.2446	0.4101
	Limbal Conj.	-0.2753	-0.2969	-0.3545	0.3103	0.0042	-0.0120	-0.1651	0.1299	-0.3914	-0.5714	-0.5029	0.7986		0.4330	0.4520	0.1318	0.4595
	Tarsal Roughness	0.0192	-0.0362	-0.0372	0.0320	0.1056	0.0992	0.1260	0.1138	-0.0347	-0.2667	-0.0414	0.2308	0.4330		0.8124	-0.0425	0.1304
	Tarsal Redness	0.2137	0.1478	-0.0072	-0.1320	0.1179	0.0970	0.0959	0.0069	0.0086	-0.2225	-0.0095	0.2499	0.4520	0.8124		-0.0928	0.1261
	Corneal Staining	0.0169	-0.0582	-0.0935	0.0427	-0.3682	-0.2573	-0.3221	0.0699	-0.1107	-0.2650	-0.1741	0.2446	0.1318	-0.0425	-0.0928		0.0849
	Conj Staining	-0.1606	-0.0923	-0.0525	0.1160	-0.0931	0.0484	0.0545	-0.0975	-0.1326	-0.3756	-0.3201	0.4101	0.4595	0.1304	0.1261	0.0849	

Figure 2.8: Correlation coefficients of the various parameter combinations for the clinical study (blue data (sig. = 0.05) and red data (sig. = 0.01)).

2.1.20.1 Lens fitting characteristics

The air-cured and nitrogen-cured contact lenses showed no significant difference in lens movement when assessed with post-blink movement and push-up tightness test, with the level of movement in agreement with that generally observed for a soft silicone hydrogel lens (Wolffsohn *et al.*, 2009). Previous studies in the literature have shown a noticeable reduction in lens movement following the initial lens settling period (Golding *et al.*, 1995b; Martin & Holden, 1983), but comparison of the 5 minute and 1 hour data shows no difference with this lens type. The lack of a difference may be associated with the lens material (higher modulus than pHEMA materials), lens design or the use of experienced subjects (with minimal reflex tearing compared with an inexperienced wearer); although it may also reflect the relatively small number of subjects in this study. Given the hydrophobic nature of the air-cured lens surface and the increased subjective awareness of the air-cured lens, it is perhaps surprising that lens movement is not greater with this lens, especially given the lacrimation observed and higher expected levels of friction between the superior lid and lens surface, although these may to some extent cancel each other out. Other factors, such as increased blink rate and blink intensity (Golding *et al.*, 1995a), may have resulted in increased expulsion of the post-lens tear film, thus reducing lens movement. The air-cured and nitrogen-cured contact lenses showed no significant difference in lens coverage and centration. All 20 study lenses showed optimal corneal coverage and the majority of lenses showed optimum centration, with any slight decentration occurring nasally, with no significant vertical decentration observed for either lens type. There appears little in the literature regarding the enfilcon A material, due to its relatively recent introduction as a lens material, but a clinical study of CooperVision's sister product comfilcon A (Brennan *et al.*, 2007) suggests comparable lens fitting characteristics. Given the similarity in the lens design and the bulk material these lens are manufactured from, the similarity of the lens fitting characteristics is perhaps not unexpected. The study therefore suggests that surface wetting characteristics do not play a major role in dictating lens fitting characteristics and this is more likely influence by factors such as lens design and material properties, in addition to patient-dependant characteristics.

2.1.20.2 Lens surface characteristics

A marked difference in lens surface characteristics was observed between the two study materials. While the nitrogen-cured lens showed good clinical surface characteristics, the air-cured lens exhibited large regions (often several millimetres in diameter) of non-wetting with rapid deposition occurring almost immediately after lens insertion. These regions of non-wetting on the surface of the air-cured lenses were clearly demarcated and appeared to be consistent in size and shape over the wearing period, occupying on average around half of the anterior lens surface, although this varied substantially between lenses. The areas of non-wetting appeared randomly distributed with no preference for the lens edge or centre. Minimal tear film deposition was observed on the nitrogen-cured surface and where present produced a mild film, typical of that described as lipoidal in the literature (Lorentz & Jones, 2007). Rapid tear film deposition was observed on the non-wetting regions of the air-cured study contact lenses (Figure 2.2). The deposition encounter on the non-wetting regions of the air-cured lens appeared to be similar in nature to that observed on silicone elastomer lenses, which has been described by Ruben & Guillon (1979) as being composed of lipids and mucous in isolated areas and by Fanti & Holly (1980) as calcium-containing lipo-proteinaceous deposits. The wetting regions on the air-cured lens had an appearance similar to that of the nitrogen-cured lens. The observation of primarily lipid deposition on the surface of the study lenses is in agreement with other studies (Guillon *et al.*, 2009; Jones *et al.*, 2003; Lorentz *et al.*, 2007; Ruben & Guillon, 1979), which have suggested that silicone hydrogel contact lenses deposit less protein, but are prone to lipid and possibly mucin deposition. The marked deposition observed on the non-wetting regions of the air-cured lens appeared similar to deposition observed on the surface of PDMS-based silicone elastomer lenses (Huth & Wagner, 1981; Ruben & Guillon, 1979), where it was suggested a migration of silicone moieties towards the lens surface results in the attraction of the polar head groups of the tear film lipid molecules leaving their non-polar tails extended away from the lens surface leading to evaporation and/or dewetting. Further laboratory analysis of the study contact lenses is required to confirm the composition of the tear film deposition.

Non-invasive tear break-up time for the nitrogen-cured lenses (around 9 seconds) appears to be within the normal range (5 to 15 seconds) for that observed with other commercial lenses with the Tearscope (Guillon *et al.*, 1990; Peterson *et al.*, 2006; Young & Efron,

1991). No difference was observed in NITBUT between the five minute and one hour lens assessments for either study lens, in agreement with a similar study by Faber *et al.* (1991), suggesting the tear film stabilises within five minutes for experienced contact lens wearers. The immediate break-up of the tear film on the air-cured lens limited the ability of the tear film to deposit hydrophilic material on these regions of the lens surface, as has been observed previously on commercial lens materials (Rogers & Jones, 2005; Tonge *et al.*, 2001). The size and location of the non-wetting regions on the study lens appeared similar over the wearing period, although as these lenses had no markings and were of a spherical design they tended to rotate making accurate recording difficult.

Given the highly hydrophobic nature of the air-cured lenses surface, it was apparent that some of the grading scales were only able to discriminate between contact lens surfaces over a limited range. An example of such scales are the clinical wettability and deposition grading scales which rapidly become saturated at an extreme end of the scale. This is likely related to the fact that these scales are usually used to evaluate commercial contact lenses, where their clinical performance is over a much narrower range. Future studies on such materials might benefit from clinical scales which have a more extreme end point than those used here, to allow more accurate clinical details to be recorded.

2.1.20.3 Biomicroscopy

Biomicroscopy grading scores were similar for both lens types, with the exception of conjunctival and limbal hyperaemia which were graded higher for the air-cured lens. Post-hoc analysis suggested no significant change in limbal or conjunctival hyperaemia from baseline for eyes having worn the nitrogen-cured lenses for 1 hour, but a significant increase in limbal and conjunctival hyperaemia was observed for the air-cured lens after 1 hour of lens wear. The exact mechanism by which contact lens wear influences limbal and conjunctival hyperaemia is not known, but factors such as lens design (Løfstrøm & Kruse, 2005) and material oxygen transmissibility (Dumbleton *et al.*, 2001; Papas, 2003) are thought to be important factors. Given that these lens parameters were matched in the two study lenses, the probable cause for the increased vascular response in this study is mechanical irritation of the conjunctiva due to poor lubrication between the eye lids, the contact lens and the ocular surface. It should be noted that no difference in the grading for either the tarsal conjunctival redness or texture was observed. Mechanical irritation of the con-

junctival surface is thought to be a primary cause for the development of contact lens associated papillary conjunctivitis, in addition to an antigenic response (Skotnitsky *et al.*, 2002, 2005). Therefore if the reduction in comfort observed with these lenses is related to increase friction, and thus a mechanical interaction with the tarsal conjunctiva, a clinical response might have been expected. The lack of tarsal response is likely associated with the short lens wearing time and if the cause was mechanical, it would involve an inflammatory response where there would be a delay in biological response (Donshik *et al.*, 2008). Observing the tarsal conjunctiva over a longer lens wearing period might have given a better insight into the cause of the discomfort associated with these lenses, but due to the restricted power range and high levels of discomfort this was not possible. Even if it had been possible, the high level of deposition observed in these regions would have made differentiating a mechanical and deposit-related response difficult.

2.1.20.4 Subjective ratings

For all ten subjects the nitrogen-cured lens was preferred over the air-cured lens. Subjective scores for comfort, dryness and burning and stinging for the nitrogen-cured lens were significantly higher than the air-cured lens, both after five minutes and one hour of lens wear. Subjective scores did not change significantly over the wearing period, except for the air-cured lens where the sensation of burning and stinging increased. This might suggest that the sensation of burning and stinging is more related to a delayed inflammatory type response rather than the more immediate subjective sensation seen for subjective comfort or dryness of the lens. The subjective comfort of a contact lens is normally attributed to potential factors such as lens design, lens material characteristics (friction/water content/modulus/wettability) and patient characteristics (tear film quantity/blink rate/tear chemistry). In this investigation the study contact lenses were identical in design, with matching modulus and water content and were fitted on a contralateral basis for each subject. The disparity in the levels of comfort between the lens types can therefore be directly related to factors such as the surface wetting characteristics and surface friction.

It was observed that the superior and inferior tear film meniscus changed in shape depending whether they overlay a hydrophobic or hydrophilic region (Figure 2.9). When the patient blinked, the tear film meniscus on the air-cured lens (although narrower than the nitrogen-cured lens) was seen to initially advance across the hydrophobic region of the lens

surface generating an apparent layer of tear fluid between the anterior lens surface and the palpebral conjunctiva. The speed of the blink and the obscured view of the meniscus by the lid margin unfortunately meant that the presence of the tear meniscus over the non-wetting region, later in the blinking process, could not be assessed. Tighe (2004) has suggested that a tear film layer present between the contact lens and the palpebral conjunctival lubricates the relative high speed movement of the lid across the lens surface and minimises any frictional forces present. The apparent presence of a tear film layer between the hydrophobic regions on the air-cured lens and the tarsal conjunctiva might then be expected to 'cushion' the conjunctival surfaces from significant frictional forces, thus suggesting that comfort levels with this material would be acceptable. There are two possible reasons why the air-cured lens results in such dramatically reduced levels of subjective comfort. The first possible reason is that direct contact may occur between the anterior lens surface and the tarsal conjunctiva due to tangential flow of the tear film under the lid, associated with surface tension gradients on the lens surface and/or irregular lid forces (i.e. the tear film is acting as a boundary lubricant between two surfaces in contact). The other possible reason is that a thinning of the 'cushioning' tear film results in greater frictional shearing forces transferred through the fluid film by coupling forces (i.e. the tear film is acting as a hydrodynamic lubricant, with the two surfaces separated by a film). In the later case the frictional shearing forces are related to the thickness of the tear film and therefore a thin or irregular tear film over the hydrophobic regions would result in a greater transfer of frictional forces to palpebral conjunctiva and thus potentially more subjective discomfort. In either case it is likely that this abnormal pre-lens tear film results in a transfer of excessive forces to the marginal conjunctival epithelium that wipes the ocular surface resulting in subjective discomfort. Korb *et al.* (2002) have describe the use of fluorescein and rose bengal stains to highlight regions of apparent physical trauma and mechanical abrasion on these marginal lid regions. They termed the clinical condition lid wiper epitheliopathy and showed correlation between symptomatic and asymptomatic contact lens wearer and lid-wiper epitheliopathy was highly significant.

During the inter-blink period the two study materials experienced very different conditions, with the nitrogen-cured lens remaining enveloped by the tear film while the non-wetting regions on the air-cured lens were near constantly exposed to the environment. This is likely to result in a greater material dehydration in the non-wetting regions than on the

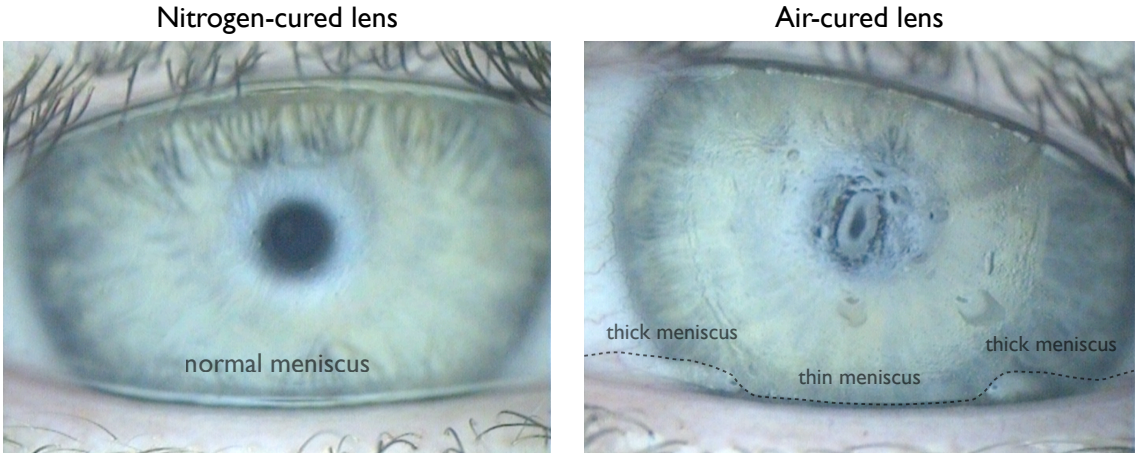

Figure 2.9: Differences in tear film meniscus for the nitrogen-cured and air-cured contact lens.

nitrogen-cured lenses, which has been linked by some with increased contact lens related dry eye symptoms (Brennan, 1988), although this is somewhat disputed in the literature (Fonn *et al.*, 1999; Pritchard & Fonn, 1995b).

In addition to the subjective data at the five minutes and one hour time point, the investigator noted that on initial insertion the patient was immediately aware that one contact lens was uncomfortable (the air-cured lens), whereas the other contact lens settled quickly (the nitrogen-cured lens). This immediate response suggests that the primary cause of the initial discomfort is unlikely to be related to either deposition or dehydration as neither occur immediately. This therefore suggests that the primary cause of the contact lens discomfort is associated with surface characteristics of the non-wetting regions on the air-cured lens surface.

2.1.21 Conclusion

This clinical work has demonstrated marked differences in the surface wetting and deposition characteristics between the two study lens types. The air-cured lens presents a heterogeneous wetting surface, with regions which possess poor clinical performance, in contrast to the acceptable surface wetting present on the nitrogen-cured lens surface. These differences appear to be related purely to the different polymerisation conditions present during the manufacture of these two lens types, as lens designs and component monomers were identical. These regions of non-wetting and heavy deposition on the air-

cured lenses have no clear distribution, occurring seemingly randomly on the anterior lens surface. No differences were observed in lens fit between the two lens types and given the identical lens design and material this similarity is perhaps expected. Conjunctival and limbal redness were shown to be significantly increased following wear of the air-cured lens compared with the nitrogen-cured lens, likely as a result of increased irritation resulting from reduced lubrication between the lids and the lens surface. Subjective responses showed a marked difference between lens types with the air-cured lens giving poor levels of comfort in all subjects. This clinical study is therefore in agreement with the findings of the manufacturer that the lenses cured in moulds surrounded by an air environment have much poorer clinical performance than the same material cured in moulds surrounded by an environment purged with nitrogen.

2.2 Development of the thin film wettability analyser

2.2.1 Introduction

Given the findings of the clinical study, it was apparent that there were clear clinical differences between the air-cured and nitrogen-cured contact lens surfaces. If a central or otherwise defined region of an air-cured lens was investigated with a surface analysis technique, it would be impossible to know whether the area of analysis fell on a wetting or non-wetting region of the lens surface. To understand how the surface characteristics differed between these regions, it was therefore necessary to identify these regions prior to analysis. Given the differences observed in the clinical study, the wetting and non-wetting regions of the air-cured contact lens could have been mapped out during clinical wear. The problem with this approach was that immediately after insertion of the contact lens, the surface underwent rapid deposition by tear film components which effectively contaminated the surface of the contact lens. Even with the use of cleaning agents, such as surfactants, the surface would likely remain heavily contaminated by the tear film components and, in addition, the surfactants might damage or contaminate the highly sensitive hydrogel surface. A technique therefore needed to be developed, which would allow identification of these wetting and non-wetting regions on the contact lens surface, without the need for the contact lens to be worn.

2.2.2 Purpose

To develop a laboratory technique to identify non-wetting regions on a contact lens surface whilst minimising contamination of the lens surface.

2.2.2.1 Development of thin film wettability analyser

The principle behind this new instrument was that when a contact lens is removed from an aqueous solution a thin film of water forms on the lens surface. The formation of a liquid film on the contact lens surface, by emergence of the contact lens from solution, looked to mimic the opening of the eye lids and the subsequent thin tear film formation on the lens surface following a blink. Following immersion from a fluid bath the film is likely to gradually change in thickness as a result of evaporation and tangential flow. It was predicted that relatively hydrophobic regions on the lens surface would drive a tangential flow of fluid away from these regions, towards the more hydrophilic regions of the lens

surface. The effect of evaporation would also thin the aqueous film, eventually resulting in breaks of the fluid layer which would be visualised due to a lack of specular reflection from these regions. It was therefore hypothesised that these areas of fluid break-up would therefore represent the more hydrophobic regions on the lens surface.

The contact lens was removed from its blister packaging, using tweezers and placed anterior surface upwards onto a convex acrylic mount (Figure 2.10 (a)). The lens and acrylic mount were then lowered into a 0.9% phosphate buffered saline bath (Sigma-Aldrich, UK) and left for 5 minutes. The lens and mount were then slowly removed (approximately 1mm/sec), lens apex first, from the water bath (Figure 2.10 (b)) and placed on a dark base. A machine vision lighting tube was then rapidly lower down around acrylic mount and a firewire digital camera and associated optics (Edmunds Optical, York, UK) pre-positioned to view the contact lens anterior surface (Figure 2.10 (c)). The lighting tube was illuminated using LED panels and the light was diffused using a frosted plastic tube. A digital movie was captured of the specular reflection from the fluid film on the contact lens surface for 1 minute, following removal of the lens from the saline bath. The thin film wetting analysis was carried out under standard laboratory conditions (22±2 ^{o}C and 25±5% humidity). The 30 second frame was chosen for analysis as it gave sufficient time for non-wetting regions to appear, but was sufficiently rapid to avoid the entire lens drying, due to evaporation from the lens surface. The 30 second frame was then imported into image analysis software (MATLAB, Natick, MA), where the lens edge and the boundary of the non-wetting regions were traced using a drawing tool (Figure 2.11). From initial testing of the thin film wettability analyser, it was apparent that the instrument was able to identify non-wetting regions on the lens surface, as shown in Figure 2.11. When similar testing was performed on the nitrogen-cured study lenses, an apparently stable water film was observed on the lens surface, with no non-wetting regions observed. For this technique to be a useful measure of contact lens surface wettability, it was important that these non-wetting regions, identified by this technique, were in the same location as regions that were observed to be non-wetting during *in vivo* contact wear. A study was therefore conducted to validate this instrument.

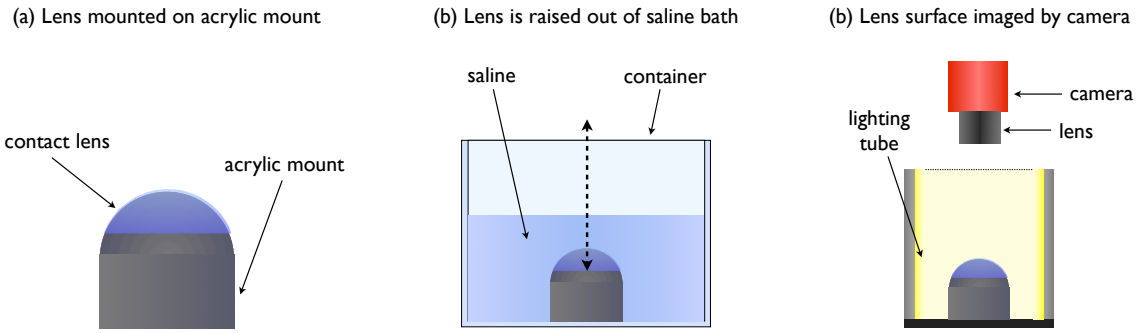

Figure 2.10: Schematic of the thin film wettability analyser

2.2.3 Instrument validation study

2.2.3.1 Purpose

To investigate the validity and repeatability of the thin film wettability analyser to predict clinical non-wetting regions on the contact lens surface.

2.2.3.2 Materials and methods

Ten air-cured and ten nitrogen-cured study contact lenses were used in this study. Each lens was removed from its blister packaging solution using sterile tweezers and placed anterior surface upwards on a sterilised convex acrylic mount (radius of curvature 8.4mm). A Sharpie marker (Sanford Inc., USA) was then used to draw three radial lens orientation markers (LOM's) onto the anterior lens surface at three, six and nine o'clock (Figure 2.11). The lens and mount were then soaked in a 0.9% phosphate-buffered saline bath for five minutes. The lens and mount were then slowly removed from the saline bath (approxi-

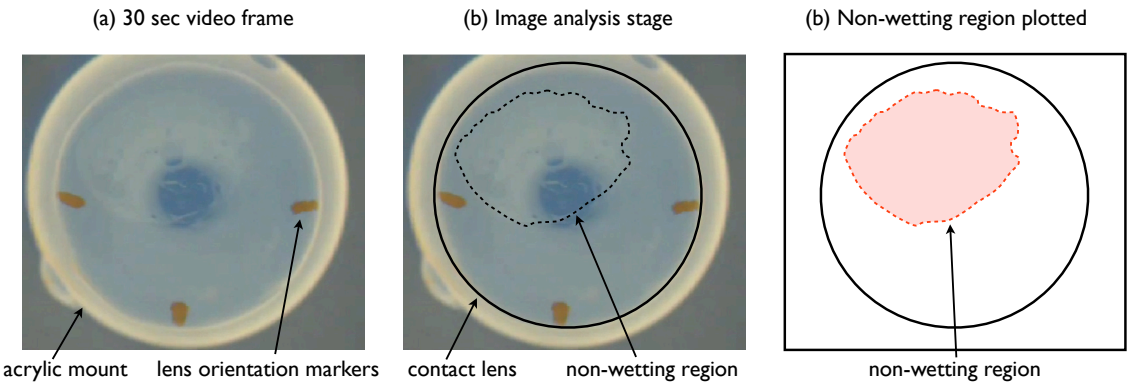

Figure 2.11: Image analysis of the 30 second frame from the thin film wettability analyser

mately 1mm/sec) and rapidly placed onto a dark coloured surface. The lighting tube was then rapidly lowered over the mounted lens with a digital camera already prepositioned to image the lens surface, where a one minute movie of the lens surface was captured. The lens was then returned to the saline bath for five minutes before the process was repeated until five measurements had been completed. In total 100 one minute videos were captured (five measurements on each of the ten nitrogen-cured and ten air-cured lenses). The experiment was performed under laboratory conditions (22±2 ^{o}C and 25±5% humidity). All lenses were then placed into saline filled glass vials which were sealed and autoclaved (Prestige Medical, UK) (121^{o}C for 20 minutes at 15 PSI) to sterilise the lenses.

The 30 second frame of each movie was converted to an image and the boundary of the lens and non-wetting region was plotted using image analysis software. The five repeated measurements for each lens were then plotted onto the same contact lens boundary to compare the agreement. The sterilised contact lenses were then worn by a subject for five minutes and a investigator, who was masked from the *in vitro* measurement, drew the position of the LOM's and the non-wetting regions, if present, on the lens surface. The validity of the thin film wettability analyser was then assessed by comparison of the clinical non-wetting regions and the non-wetting regions identified by the thin film wettability analyser.

2.2.3.3 Results

Figure 2.12 shows the non-wetting areas plotted for the ten air-cured contact lenses following thin film wettability analysis. All 10 of the nitrogen-cured contact lenses showed no non-wetting regions at the 30 second frame with the thin film wettability analyser. For each lens in Figure 2.12 five measurements were taken and the area of non-wetting was recorded in a different colour. Figure 2.13 compares the non-wetting regions identified by the thin film wettability analyser on the surface of the air-cured lenses, with the non-wetting regions observed when these lenses were subsequently worn clinically. This shows a similar pattern between the non-wetting regions from the laboratory technique and from the clinical analysis.

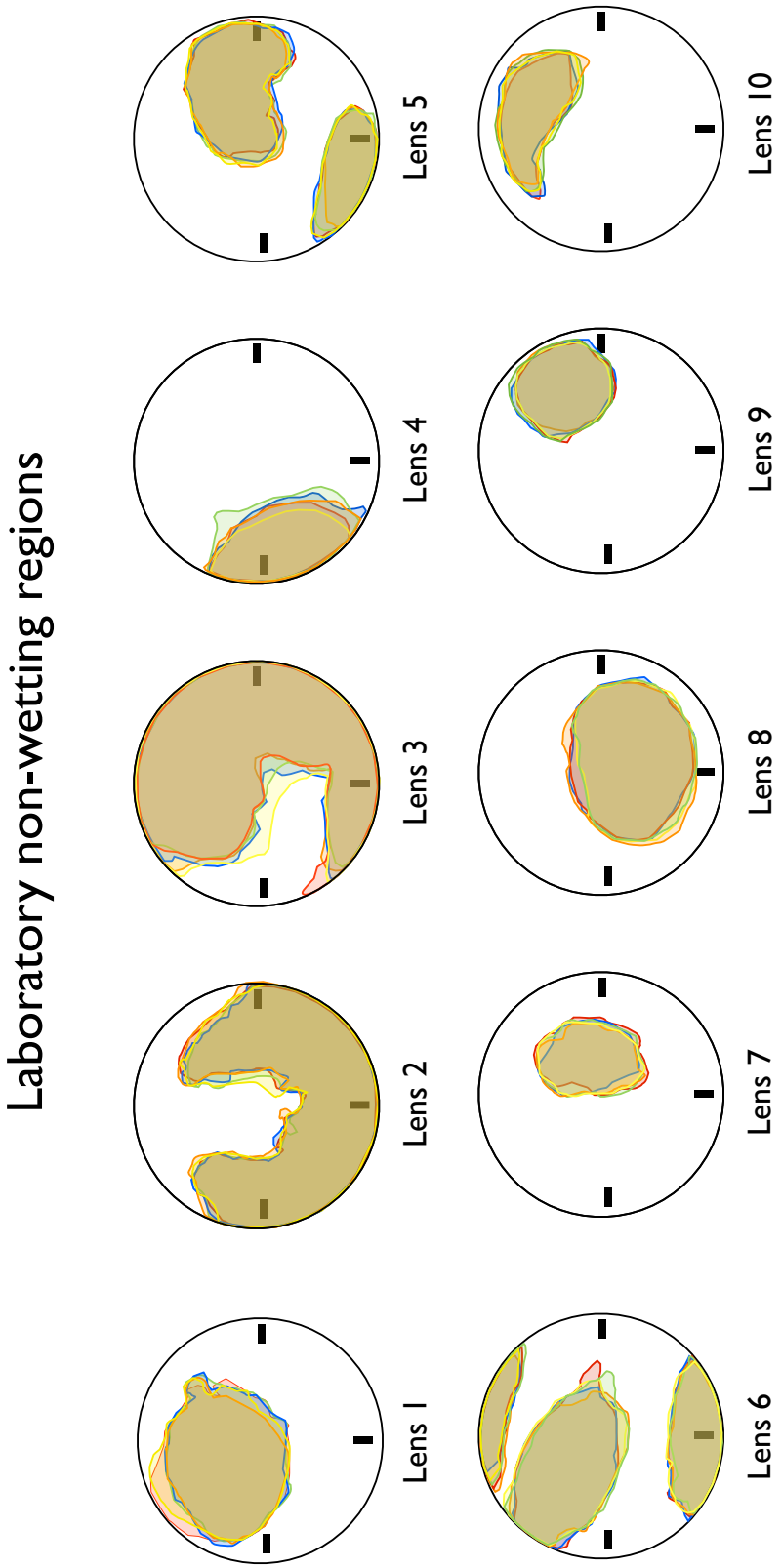

Figure 2.12: Laboratory non-wetting regions measured by the thin film wettability analyser on the air-cured study contact lenses, with repeated measurement represented by the five different colours

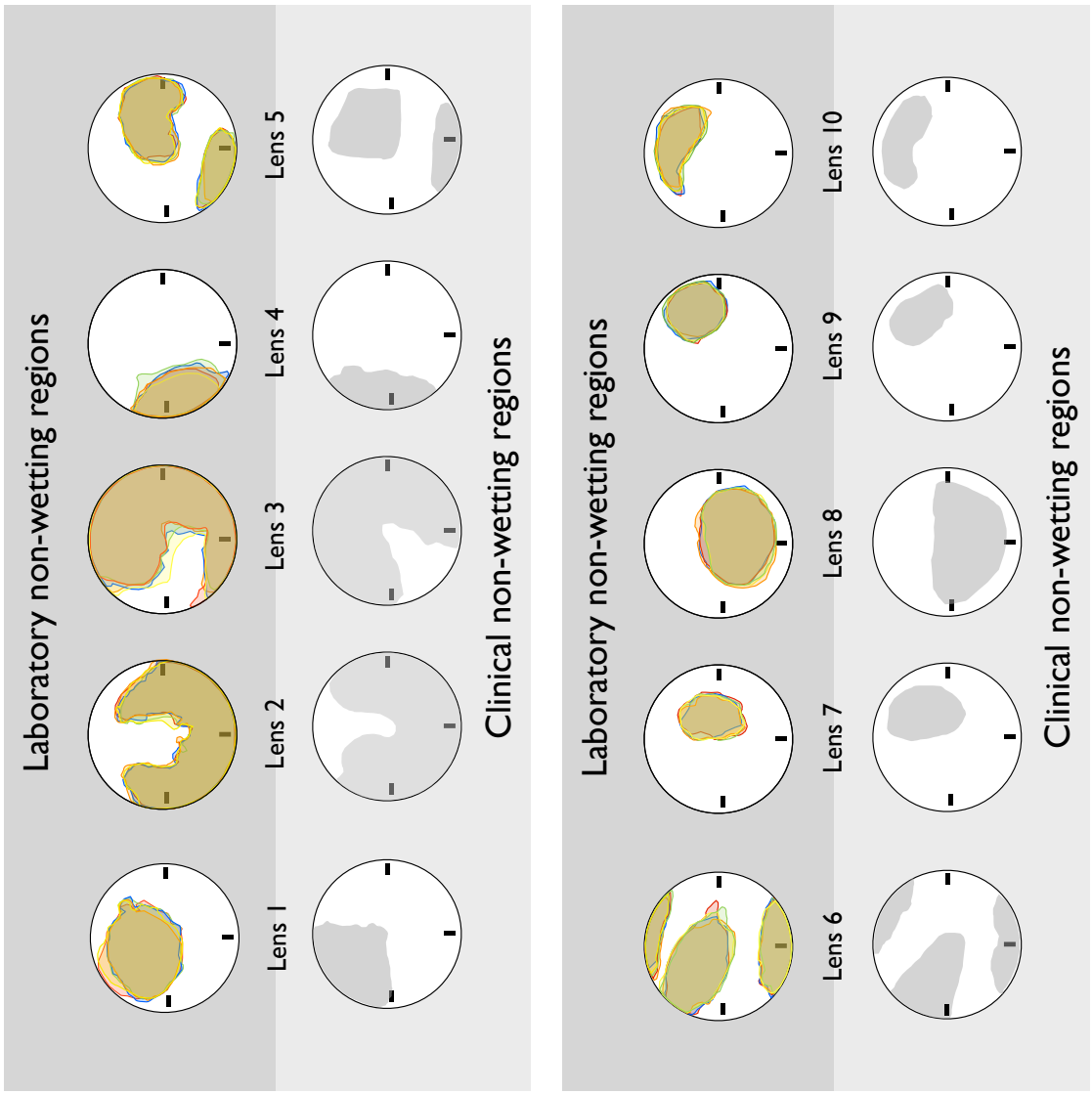

Figure 2.13: Comparison of the non-wetting regions identified by the thin film wettability analyser and the clinical investigation.

2.2.3.4 Discussion

Good agreement between repeated measurements using the *in vitro* thin film wettability analyser (overlap of the different coloured regions on each lens in Figure 2.12) suggests that the instrument has high repeatability in detecting non-wetting regions on the air-cured lenses surface. These non-wetting regions appear to be hydrophobic in nature due to the tangential flow of the saline away from these regions. As with clinical observations, no non-wetting regions were identified on the nitrogen-cured lens surface using the *in vitro* wettability analyser. The lack of non-wetting regions on the nitrogen-cured lens surface suggests that the surface has relatively homogenous wetting characteristics, with the evaporative loss of saline not sufficient, over the 30 seconds following immersion, to result in the formation of any dry spots on the lens surface. Figure 2.13 highlights the similarity in location of the non-wetting regions detected by the laboratory and clinical testing for each air-cured lens, confirming that these relatively hydrophobic regions appear to be in the same location on the lens surface when observed with both techniques. It is also apparent that the non-wetting regions appear to be random in size and location, in agreement with the initial clinical study (Figure 2.1).

2.2.3.5 Conclusion

The thin film wettability analyser appeared able to predict the regions of clinical non-wetting without the need for *in vivo* clinical assessment, allowing subsequent surface analysis on these regions of interest without contamination by tear film components. The thin film wettability analysis technique has therefore been used to identify regions of wetting and non-wetting on the air-cured contact lens surface and confirm the lack of hydrophobic regions on the nitrogen-cured lens surface, prior to further investigation of the surface characteristics of these regions. This chapter has therefore characterised the clinical differences between the two study lens types and developed a technique to identify non-wetting regions on a contact lens surface. The following chapters will now aim to characterise the surface of the study lenses with a range of analysis techniques, focusing particularly on surface wetting (Chapter 2), surface chemistry (Chapter 3) and surface topography (Chapter 4).

Chapter 3

Contact angle analysis of contact lens materials

3.1 Static contact angle measurements on contact lens materials

3.1.1 Introduction contact angle analysis on contact lens materials

Wettability is particularly relevant to contact lenses because the lens surface needs to support a stable ocular tear film layer, and failure to achieve this is likely to adversely affect the visual performance, increase lens surface deposition, and reduce comfort (Jones *et al.*, 2006). A potential negative consequence of the inclusion of silicone into contact lenses is the inherent hydrophobicity it imparts to the material (Kunzler, 1996), resulting in poor *in vivo* wettability (Brennan *et al.*, 2006; Maldonado-Codina *et al.*, 2004b). In an attempt to alleviate clinical problems related to this hydrophobicity, contact lens manufacturers have utilised a range of fabrication techniques, including plasma surface treatments (Weikart *et al.*, 1999, 2001) and the inclusion of hydrophilic monomers (Iwata *et al.*, 2001; Maiden *et al.*, 2002; McCabe *et al.*, 2004) to the bulk material which serve to mask surface hydrophobicity and improve ocular biocompatibility (Kunzler, 1996; Tighe, 2004; Weikart *et al.*, 1999, 2001). In common with all scientific evaluations, repeated measures of contact angles will necessarily vary due to factors such as instrument fluctuation or non-uniformity within or between samples (Bland & Altman, 1996). Such variation can be termed measurement error. Measurement error can be reported by giving (i) the average standard deviation of multiple sets of repeated measurements, (ii) the coefficient of

repeatability (COR), which is defined as the maximum difference likely to occur between two successive measurements ($2\sqrt{2s}$) (where s is the standard deviation of measurements), or (iii) the coefficient of variation (COV) (s), which contextualises the magnitude of the error by comparison of the standard deviation of measurements (s) with the mean (x). This study therefore was designed to allow a comprehensive investigation of the measurement error associated with contact angle assessment of hydrogel contact lens surfaces was therefore undertaken. An understanding of these errors is fundamentally important due to the growing interest in the wetting behaviour of silicone hydrogel lenses and the increasingly widespread use of contact angles by contact lens manufacturers (Maldonado-Codina & Morgan, 2007; Menzies & Jones, 2010; Vermeltfoort *et al.*, 2006). Additionally, such an analysis would allow identification of which factors contribute toward measurement error in this area and provide an indication of the confidence which can be placed on a single published contact angle measurement. Specifically, the study was designed to determine the contact angle COR associated with three measurement conditions using the sessile drop and captive bubble methods:

1. **Image analysis COR**: an estimate of the variability of the repeated use of semi-automated image analysis software on the same image.

2. **Intralens COR**: an estimate of the variability when taking repeated measurements on the same lens.

3. **Interlens COR**: an estimate of the variability when taking repeated measurements on different lenses of the same type.

The COR was chosen as the estimate of measurement error as it provides an immediately meaningful index in the relevant units (degrees), against which absolute measures of contact angle can be judged.

3.1.2 Materials and methods

3.1.2.1 Commercial study lenses

Three silicone hydrogel contact lenses and one conventional hydrogel (i.e. a hydrogel not containing siloxane species) control lens were used in this work (Table 3.1). The back vertex power of all lenses was -3.00 DS. All contact lenses were sourced via normal commercial channels and supplied in their standard blister packaging.

Table 3.1: Properties of the commercial study contact lenses.

USAN[1]	Brand name	Principle monomers[2]	Dk[3]	EWC (%)[3]	Surface treatment
balafilcon A	PureVision	NVP, TPVC, NVA, PBVC.	91	33	Plasma oxidation
lotrafilcon A	Night & Day	DMA, TRIS, fluorine-containing siloxane macromer.	140	24	Plasma coating
senofilcon A	Acuvue Oasys	MPDMS, DMA, HEMA, siloxane macromer, TEGDMA, PVP.	103	38	None (internal wetting agent, PVP)
etafilcon A	1 Day Acuvue	HEMA, MMA.	21	58	None

3.1.2.2 Contact angle analysis technique

Of the three main contact angle analysis techniques discussed in the introduction (sessile drop, captive bubble and Wilhelmy plate) it was decided to use the sessile droplet and captive bubble technique in this investigation. These techniques were selected over the Wilhelmy plate technique as (i) no prior sample preparation (e.g. lens cutting) was required, thus minimising surface contamination, (ii) the testing is surface specific (i.e. analysis of the front lens surface only), (iii) the lens is allowed to remain in a curve state and (iv) specific regions on the lens surface could be targeted for testing, which was critical for the heterogeneous surface observed clinical on the study lenses.

3.1.2.3 Sessile drop method

Contact angles were measured at room temperature ($25^oC \pm 1^oC$) and humidity (35% ± 5%) with an OCA-20 contact angle analyzer (DataPhysics Instruments, Filderstadt, Germany). This instrument is essentially a conventional goniometer featuring automated drop delivery, digital image capture, and semi-automated image analysis software. All lenses were analysed following a 48 hour saline soak in 0.9% phosphate-buffered saline solution (PBS) (Sigma-Aldrich, Germany), which was changed every 12 hours, to remove any surfactant present in the blisters. The lenses were then blotted to remove excess surface liquid. This was achieved by first removing the lens from the saline solution with

[1]United States adopted name.

[2]PVP, polyvinyl pyrrolidone; MPDMS, monofunctional polydimethylsiloxane; DMA, N,M-dimethylacrylamide; HEMA, hydroxyethyl methacrylate; MAA, methacrylic acid; TEGDMA, tetraethyleneglycol dimethacrylate; TRIS, trimethyl siloxysilyl; NVP, N-vinyl pyrrolidone; TPVC, tris-(trimethyl siloxysilyl) propylvinyl carbamate; NVA, N-vinyl amino acid; PBVC, poly(dimethysiloxy)-di(silylbutanol)-bis(vinyl carbamate).

[3]Manufacturer-reported values.

silicone tipped tweezers, touching only the lens edge. The back surface of the lens was then carefully placed onto a custom-made PMMA lens holder (radius of curvature 8.7 mm), and the lens front surface was lowered onto a Supraclean microfibre cloth (Pentax, Slough, UK) suspended over a glass beaker. The lens was briefly held in contact with the cloth (3 seconds), and then this procedure was repeated until excess surface liquid had been removed (no dark mark left on the cloth). This typically required two to three repetitions. This technique was adopted to achieve even blotting across the lens surface. The lens and PMMA mount were then immediately placed onto the OCA-20 instrument, under the needle of the microsyringe (Hamilton 500 lL DS 500/GT) using a customised positioning guide which allowed dosing within 5 seconds of lens blotting. This approach minimised the dehydration of the lens surface during the procedure. A 3 μL drop of deionized water was formed at the tip of the dosing needle at a rate of 2 μL/s and was then lowered until the water and the lens surface made contact. An optical trigger immediately captured a 20 second digital movie clip of the water drop on the lens surface at a rate of 25 frames per second and at a resolution of 768 x 576 pixels. The lens was then returned to the PBS to soak for at least 10 min before the process was repeated on six further occasions, giving a total of seven measurement runs for each individual lens. This procedure was undertaken for 10 lens samples per lens type, and the order of analysis of these lenses was randomized. This gave a total of 280 movie clips (7 measurement runs x 10 lens samples x 4 lens types).

3.1.2.4 Captive Bubble Method

The OCA-20 instrument was also used to determine the contact angles using the captive bubble method. After a 48 hour soaking, as described earlier 3.1.2.3, the back surface of the lens was carefully placed onto a custom-made PMMA lens holder and lowered into a PBS-filled glass chamber to rest on a submerged stand. A curved needle was positioned directly below the centre of the lens from which a 3 μL air bubble was dispensed. The needle was then advanced toward the lens surface, and on contact, the bubble was detached from the needle at the apex of the lens. A movie was captured as detailed earlier after which the bubble was dislodged from the lens surface. The procedure was then repeated on six further occasions on the same lens with at least five minutes between measurements. The saline within the glass chamber was emptied and refilled prior to testing each lens. This procedure was undertaken for 10 lens samples per lens type, and the order of analysis

of these lenses was randomised. This gave a total of 280 movie clips (7 measurement runs x 10 lens samples x 4 lens types).

3.1.2.5 Image Analysis

Each movie clip was analysed using the SCA-20 (version 3.7.4) software supplied with the OCA-20 instrument. As the contact lenses had a curved surface, the automated contact angle analysis mode could not be used and the semi-automated image analysis-drawing tool was utilised. Frame zero was defined as the movie frame on which the sessile droplet/captive bubble was first formed on the lens surface. The movie was then advanced 10 seconds to a time point at which the contact angle had reached equilibrium. This single frame at 10 seconds was analysed using the semi-automated software. The elliptical curve-fitting tool was used to (a) define the contact lens surface and (b) define the droplet/bubble surface. Once the two surfaces were defined, the SCA-20 software automatically calculated the contact angle on both sides of the droplet/bubble (Figures 3.1 and 3.2). Each 10-second frame contact angle image was reanalysed after 24 hours by the same investigator. This process was fully masked and randomised by assigning a random number to each frame from 1 to 560. These frames were then analysed in a different random order on two separate occasions. Once all of the frames had been measured twice, the data were brought together and the masking was broken.

3.1.2.6 Determination of Measurement Errors

1. **Image Analysis Coefficient of Repeatability.**

   Following the testing for normality of the differences between analysis/reanalysis contact angles with the Kolmogorov-Smirnov test, image analysis COR was calculated using the method recommended by Bland & Altman (1986). In brief, the COR is 2.77 x the average standard deviation of the sets of two repeated measurements. This COR value estimates the maximum difference likely to occur between 95% of pairs of successive contact angle measurements on the same image. COR values were calculated separately for the sessile drop and captive bubble methods. In addition, paired t-tests were performed to compare the first and second contact angle measurements. The mean of the analysis/reanalysis contact angles was plotted against the difference between these two measurements using the approach suggested by Bland and Altman to explore the relationship between measurement error and mea-

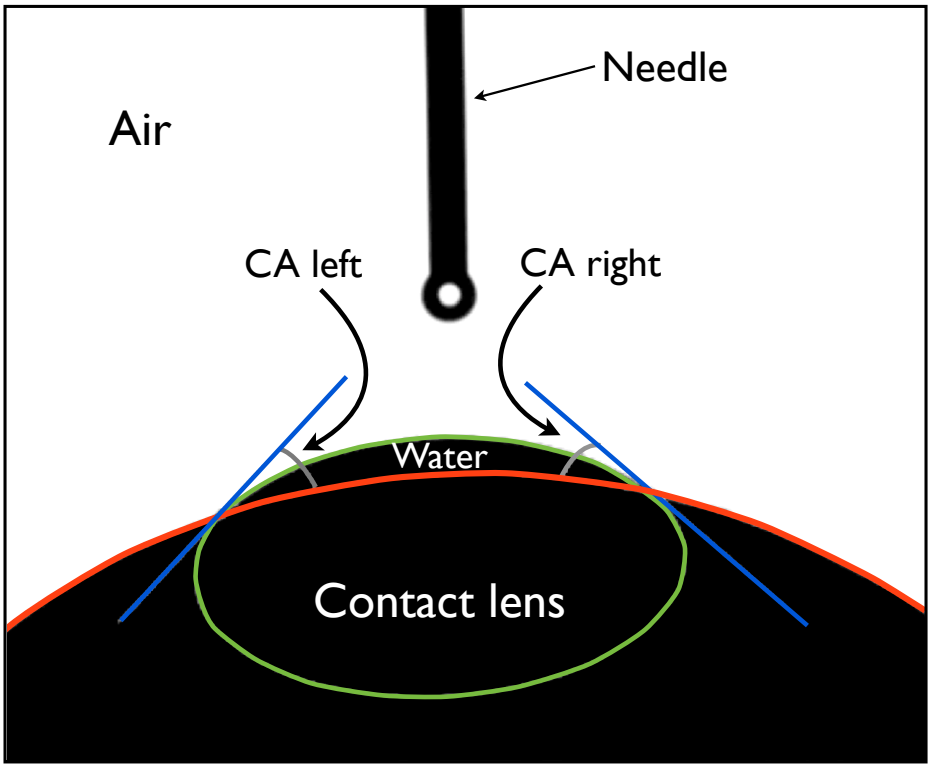

Figure 3.1: Image analysis of a typical sessile drop frame.

surement magnitude and to derive the 95% limits of agreement (Bland & Altman, 1986).

2. **Intralens Coefficient of Repeatability.** Prior to the calculation of intralens and interlens COR, an analysis of covariance model was constructed with lens type as a between factor and measurement sequence number as the covariant to investigate the potential for systematic errors being introduced by repeated measurements on the same sample. The intralens COR was then calculated as 2.77 x the average standard deviation of the 10 sets of seven within-lens repeated measurements. This COR value estimates the maximum difference likely to occur between 95% of successive contact angle measurements on the same lens surface. COR values were calculated for each of the four lens types, separately for the sessile drop and captive bubble methods.

3. **Interlens Coefficient of Repeatability.** The interlens COR was calculated as 2.77 x the average standard deviation of the seven sets of 10 between-lens repeated measurements. This COR value estimates the maximum difference likely to occur between 95% of successive contact angle measurements on different lenses of the same

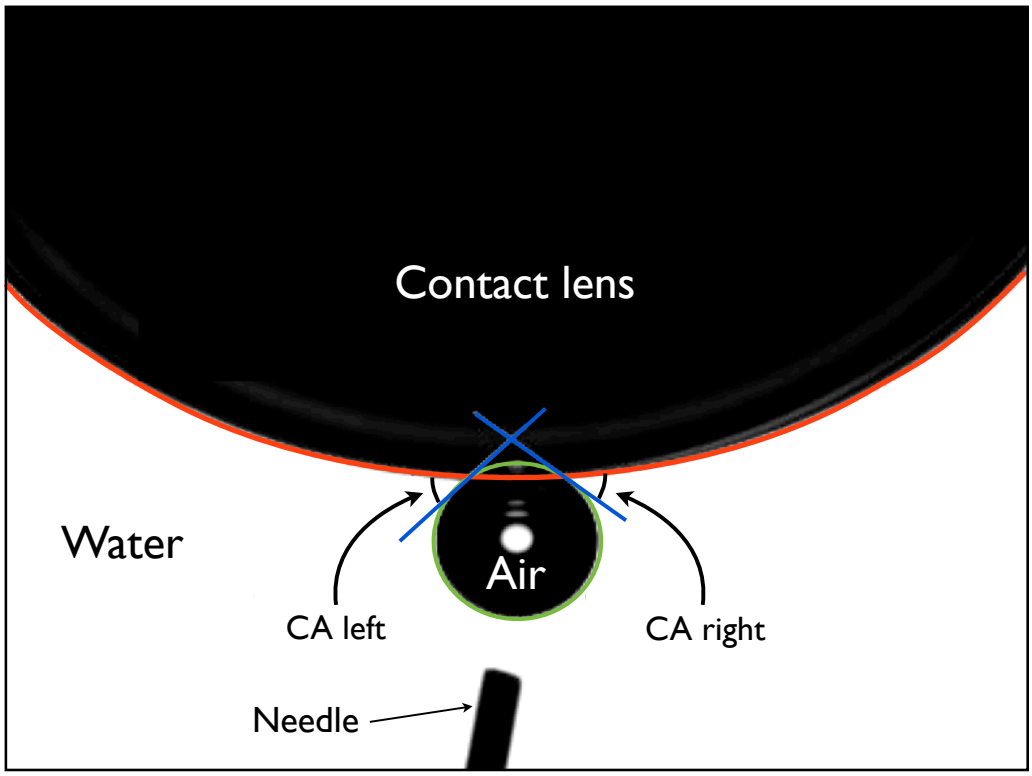

Figure 3.2: Image analysis of a typical captive bubble frame.

type. COR values were calculated for each of the four lens types, separately for the sessile drop and captive bubble methods. Ninety-five percent confidence intervals were calculated for all COR values. Measurements were deemed to be statistically significantly different when there was no overlap between the relevant 95% confidence intervals.

3.1.2.7 Contact angle assessment of study contact lenses

In addition to the commercial study contact lenses, ten air-cured and ten nitrogen-cured experimental study contact lenses were assessed using both the sessile drop and captive bubble technique. These lenses were prepared and analysed as described previously for the four commercial contact lenses (Section 3.1.2.3 and 3.1.2.4), with each lens analysed seven times. The investigator was masked from the lens type and analysis was performed in a randomised lens order. Following completion of the experiment the masking was broken and the magnitude of the sessile drop and captive bubble contact angle was calculated. The intralens and interlens coefficients of repeatability were also calculated along with

their 95% confidence intervals. Measurements were deemed to be statistically significantly different when there was no overlap between the relevant 95% confidence intervals.

3.1.3 Results

3.1.3.1 Commercial contact lenses

There was no significant difference between the distribution of differences in image analysis/reanalysis values and that of a normal distribution (sessile drop: K=1.0, p=0.50; and captive bubble: K=1.0, p=0.51), justifying the subsequent parametric statistical treatment of the data. Table 3.2 shows the absolute contact angles and image analysis COR values for each lens type. The overall image analysis COR value was 2.18^o for both the sessile drop and captive bubble methods. Contact angle measurements were not significantly different for the first and second image analysis measurements for both the sessile drop (t=0.4, p=0.72) and captive bubble methods (t=0.4, p=0.71). Bland-Altman plots for the image analysis/reanalysis data are shown for both the sessile drop (Figure 3.3) and captive bubble methods (Figure 3.4). The 95% limits of agreement were 22.18^o to 12.28^o for both the sessile drop and captive bubble methods. Both Bland-Altman plots showed no apparent relationship between the analysis/reanalysis differences and the magnitude of the contact angle measured. Measurement sequence number was demonstrated not to have a significant influence on the measured contact angle values (F=0.0, p=0.89) suggesting that sequential measures on an individual sample were not a confounding factor in our quantification of lens COR. Intralens COR values for all lens type/method combinations ranged between 4.08^o and 10.28^o. Inter-lens COR values for all lens type/method combinations ranged between 4.58^o and 16.58^o . The combined data are shown in Figure 3.5.

3.1.3.2 Experimental study contact lenses

Absolute contact angle values for the two study contact lens types are shown in Table 3.3. The air-cured lenses showed a significantly higher sessile drop contact angle (F=555.20, p0.0001) and a significantly higher captive bubble contact angle (F=9.52, p=0.0025) than the nitrogen-cured lenses. Figure 3.6 shows the intra-lens and inter-lens COR values along with their 95% confidence intervals. Intra and inter-lens COR values for the study contact lenses differed statistically only during sessile drop analysis on the air-cured lenses.

Table 3.2: Absolute Contact Angle Values and Image Analysis COR Values. The 95% confidence intervals appear in parentheses.

	Contact angle		COR	
Lens Type	Sessile Drop (^{o})	Captive Bubble (^{o})	Sessile Drop (^{o})	Captive Bubble (^{o})
Senofilcon A	80.0 (78.2, 81.8)	27.8 (27.3, 28.3)	2.0 (1.8, 2.2)	1.4 (0.9, 1.9)
Balafilcon A	86.5 (85.6, 87.4)	27.8 (27.4, 28.2)	2.2(1.4, 3.0)	2.0 (1.3, 2.7)
Lotrafilcon A	50.2 (49.5, 50.9)	25.3 (24.9, 25.7)	1.9 (1.2, 2.6)	2.4 (1.5, 3.3)
Etafilcon A	15.3 (14.8, 15.8)	24.9 (24.3, 25.5)	2.5 (1.6, 3.4)	2.6 (1.7, 3.5)

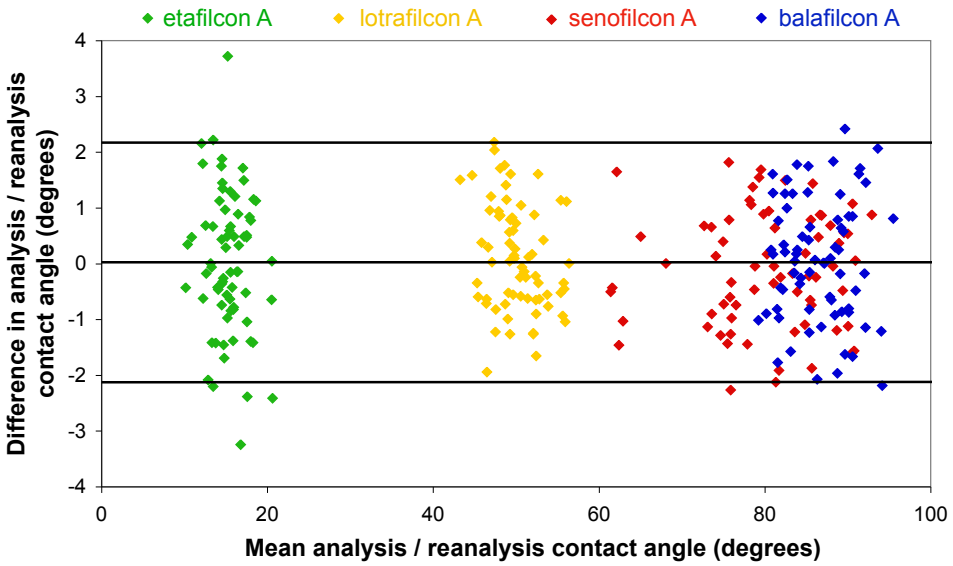

Figure 3.3: Bland-Altman plots for repeated contact angle measurement with SCA-20 image analysis software, for sessile droplet data with 95% confidence intervals.

Table 3.3: Absolute Contact Angle Values for the air and nitrogen-cured contact lenses. The 95% confidence intervals appear in parentheses.

	Contact angle	
Lens Type	Sessile Drop (^{o})	Captive Bubble (^{o})
Air-cured	88.0 (4.8)	26.5 (2.4)
Nitrogen-cured	72.8 (3.3)	22.4 (2.3)

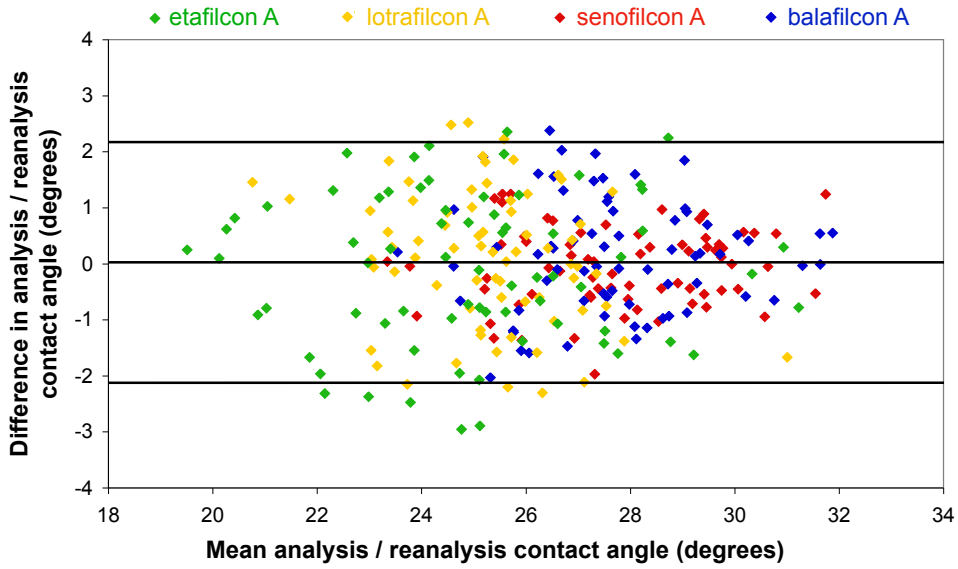

Figure 3.4: Bland-Altman plots for repeated contact angle measurement with SCA-20 image analysis software, for captive bubble data with 95% confidence intervals.

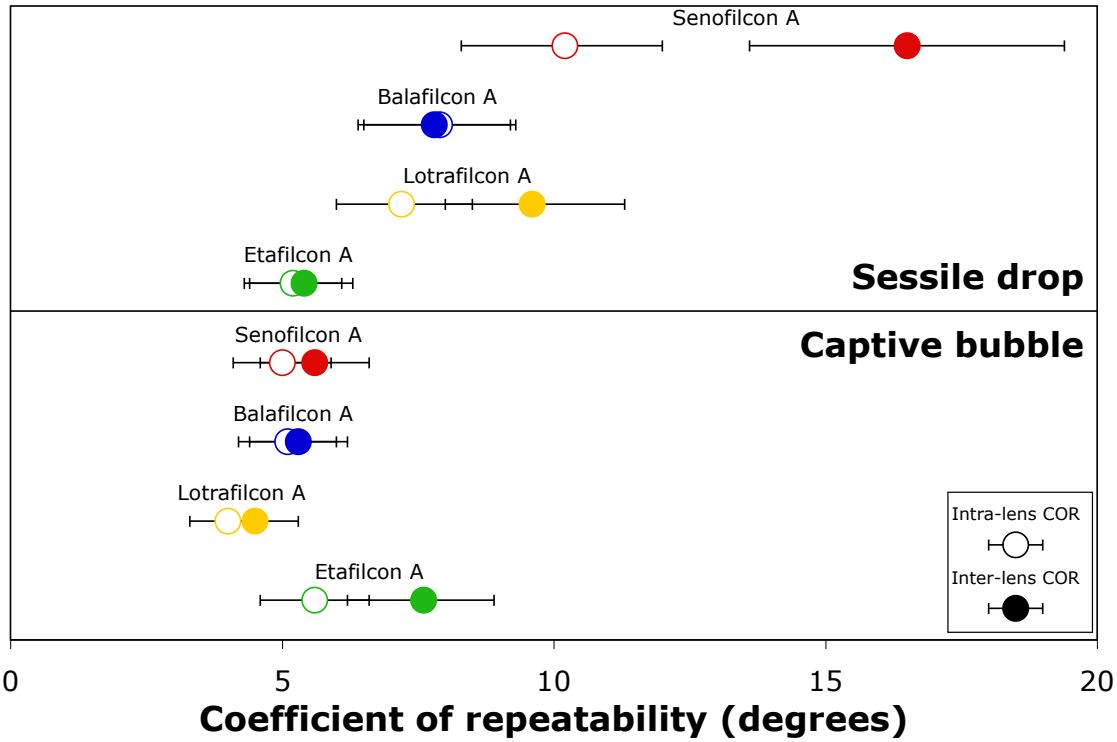

Figure 3.5: Intralens and interlens COR values. Error bars represent the 95% confidence intervals.

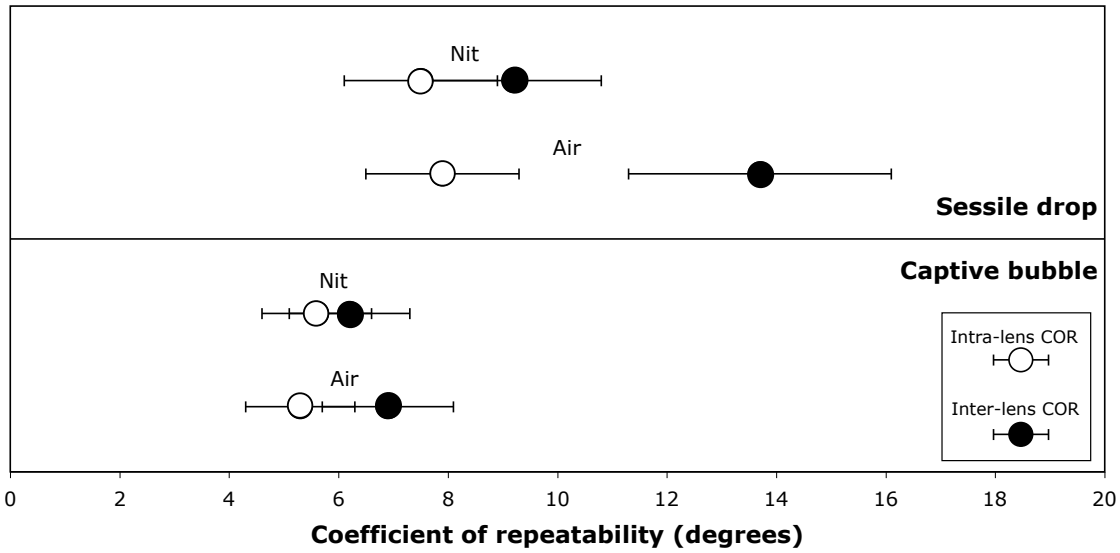

Figure 3.6: Intralens and interlens COR values for the air-cured and nitrogen-cured study contact lenses. Error bars represent the 95% confidence intervals.

3.1.4 Discussion

Contact angle analysis is commonly used in an attempt to predict the clinical wetting of the contact lens by the tear film. Since the launch of silicone hydrogel contact lenses in the late 1990s, wettability has been at the forefront of clinical and material science research in this area, and an increasing number of publications have reported the contact angles of these lenses (Bruinsma *et al.*, 2001; Cheng *et al.*, 2004; Lorentz *et al.*, 2007; Santos *et al.*, 2008; Vermeltfoort *et al.*, 2006; Willis *et al.*, 2001). However, the measurement of a contact angle on a hydrogel surface is problematic due to the inherent variabilities introduced at the sample preparation stage and the sensitivity of the surface to changes in its local environment. As such, understanding the magnitude of measurement error in the assessment of hydrogel contact angles is particularly important.

3.1.4.1 Commercial contact lenses

The image analysis COR values found in this work were small (about 2^o) when considered as absolute measures and were not related to contact angle magnitude. However, these measurement errors become more significant for materials with low contact angles. For example, the COR for sessile drop assessment of etafilcon A was 2.5^o with a mean

value of 15.3^o (16%) when compared with a COR of 2.2^o and mean value of 86.5^o (3%) for the balafilcon A lens. In general, we consider these values to be small and that the semi-automated image analysis software used in this work was repeatable. In instruments where software is fully automated, this aspect of measurement error is likely to be reduced (with the added benefit of faster analysis), and this will be discussed further in Section 3.2.3.3.

Repeatability was poorer (i.e. higher COR values) for silicone hydrogel sessile drop measures when compared with those from captive bubble assessment. This is likely to be due to differences in surface dehydration between consecutive sessile drop measurements as a result of small variations in preparation time as well as differences in the amount of surface liquid removed during the blotting procedure. Contact angle measures on silicone hydrogel materials may be more sensitive to changes in surface dehydration because of the increased rotational mobility of silicon-oxygen bonds when compared with carbon-carbon bonds (present in conventional hydrogel materials), leading to a less uniformly wetting surface as a result of hydrophobic moieties migrating to the lens/air interface. This hypothesis is further supported by the similarity of (a) repeatability values for the conventional hydrogel lens (etafilcon A) for the two methods and (b) all the captive bubble COR data.

The results also show a greater inter-lens COR value when compared with the intra-lens COR value for the senofilcon A lens for sessile drop measures. This finding presumably relates to the material characteristics of this lens which, unlike the other silicone hydrogel lenses investigated, is not surface treated. Instead, this lens material incorporates high-molecular-weight PVP in the bulk polymer (Maiden *et al.*, 2002; McCabe *et al.*, 2004) to mask the hydrophobic siloxane groups from the tear film. Variation in the distribution of PVP across a lens surface may give rise to increased COR values, as a slightly different part of the lens surface may be sampled during repeated measurements; our finding of greater inter-lens COR compared with intra-lens COR could represent an indirect indication of greater variation in PVP distribution between lenses than across a single lens surface, although a more direct analytical approach would be required to confirm this. Another possible reason for this finding is that the senofilcon A lens surface might be unpredictably influenced by the blotting process, resulting is a high level of variability for

the sessile drop contact angle. This discrepancy between inter-lens and intra-lens COR values for the senofilcon A lens is not evident for captive bubble measurements for the same lens material which supports the hypothesis that surface dehydration occurring during sessile drop measures increases the presentation of hydrophobic moieties at the contact lens surface. In contrast, the other two commercial silicone hydrogel lenses used in this work undergo surface treatment to improve their clinical wettability characteristics. The lotrafilcon A lens undergoes a plasma surface treatment resulting in a homogenous, dense, 25-nm thick coating. The coating possesses low molecular mobility which in turn has the effect of minimising the migration of hydrophobic silicone groups toward the surface (Weikart *et al.*, 1999, 2001). The balafilcon A lens has an incomplete plasma oxidation surface treatment, resulting in hydrophilic silicone islands surrounded by the hydrophobic silicone-based bulk material (Kunzler, 1996). Such surface treatments appear to give rise to more repeatable sessile drop values for these lenses when compared with the non surface-treated senofilcon A lens, inferring a reduced susceptibility to surface dehydration during *in vitro* contact angle assessment.

3.1.4.2 Experimental study contact lenses

The nitrogen-cured study lens material exhibited comparable sessile drop and captive bubble wetting characteristics to the senofilcon A material with contact angles of 79^o and 25^o respectively. In contrast, the air-cured lens surface displayed a significantly elevated captive bubble contact angle ($\sim 4^o$ greater) and sessile drop contact angle ($\sim 15^o$ greater). The sessile drop technique is analogous to an advancing contact angle and a relative increase in the angle suggests the presence of more hydrophobic regions on the air exposed lens surface. In addition, significant differences were observed between the intra and inter-lens COR values for the sessile drop technique on the air-cured lens surface (no overlap of the 95% confidence intervals) which was not observed on the surface of the nitrogen-cured lenses suggesting potentially heterogeneous surface wetting characteristics. This static contact angle study preceded the clinical study and was the first indication that the surface was heterogeneous in nature. The clinical study has subsequently shown the relatively random nature of these hydrophobic domains on the anterior lens surface (see Section 2.2.3.3) which is the probable cause of the increased variability observed between air-cured lenses.

3.1.4.3 Comparison of study findings with the literature

The measurement errors reported here are relatively small in comparison with the differences in absolute contact angle values found between the various published studies in this area. Although the ranking of the contact angles values found in this work is in agreement with previous reports, which have adopted similar experimental methodology (Bruinsma *et al.*, 2001; Lorentz *et al.*, 2007; Maldonado-Codina & Morgan, 2007), there are clear discrepancies in the absolute values obtained. These differences are likely to be due to some or all of the following:

1. Different instruments and software (e.g. Dataphysics OCA 20 instrument (Maldonado-Codina & Morgan, 2007) versus a custom-made instrument (Vermeltfoort *et al.*, 2006)).

2. Variations in sample preparation (e.g. blotting the lens on a flat surface using lens paper (Lorentz *et al.*, 2007) versus blotting using a microfiber cloth on a curved surface as described in this investigation).

3. Changes to material formulations and blister packaging solutions over time (e.g. recent enhancements to balafilcon A and lotrafilcon A lenses (Pence, 2008)).

4. Inter-investigator variability.

3.1.5 Conclusion

This study has compared the static contact angles measured for both commercially-available and experimental study contact lenses using both the sessile droplet and captive bubble technique. In addition, it has presented a detailed description of the measurement errors that occur during the measurement of contact angles on curved hydrogel contact lens surfaces while using the sessile drop and captive bubble methods. These measurement errors are influenced by (a) the subjective elements introduced by using semi-automated software, (b) methodology-dependant variables, and (c) surface-related material variables. Measurement error associated with image analysis was shown to be small as an absolute measure, although more significant for lenses with low contact angle. Overall, the captive bubble method was subject to smaller measurement errors than the sessile drop method, which is thought to be due to the sensitivity of the lens surfaces to dehydration. All such measurement errors should be taken into account when considering any published contact

angle data for hydrogel contact lenses. Contact angle analysis was also able to detect differences in the advancing contact angle between the two experimental study materials, with the air-cured lens possessing a relatively hydrophobic surface and measurements of repeatability suggesting heterogenous wetting characteristics across the surface of the air-cured lens.

3.2 Development of a dynamic captive bubble technique

3.2.1 Introduction

Static contact angle assesment using the sessile drop and captive bubble techniques can provide useful information about the surface wetting properties of a contact lens surface, but these techniques have limitations. It has been suggested that the sessile drop technique is analogous to an advancing contact angle and the captive bubble technique is analogous to a receding contact angle (Maldonado-Codina & Morgan, 2007), as the contact lens surface is exposed to very different environmental conditions during analysis. The wetting process that occurs at the lens surface during clinical wear is a highly dynamic one, where the lens is usually surrounded by a tear film envelope. The relatively strong forces associated with an eye lid blink, drive the tear film meniscus across the anterior contact lens surface. Following completion of the lid blink, a thin pre-lens tear film forms across the lens surface. The presence of a contact lens is known to destabilise the tear film (Guillon *et al.*, 1997) and it is hypothesised that the inability of the tear film to be maintained across the lens surface might result in reduced vision (associated with a loss of the smooth refractive surface offered by a stable tear film (Thai *et al.*, 2002a)), increased deposition (associated with increased surface heterogeneity associated with exposure of the lens material to an air environment (Tighe & Franklin, 1997)) and reduced comfort (associated with reduced lubrication between the eye lid and anterior lens surface (Jones *et al.*, 2006)). To better model the ocular environment, an analysis technique should therefore ideally maintain the contact lens in a hydrate stated and allow the investigation of both the stability of a fluid film present on the lens surface during exposure to an air environment and the subsequent ease with which the fluid is then able to spread back across the previously air exposed surface.

3.2.2 Aim

To develop a dynamic captive bubble technique which maintains the contact lens in its fully hydrated state and allows the measurement of the dynamic advancing and receding contact angles in a rapid and repeatable manner.

3.2.3 Methods and materials

The Dataphysics OCA-20 instrument is a video-based device for the measurement and analysis of the static and dynamic contact angle according to the sessile and captive drop method. Software-controlled automation of a syringe allows the dispensing or retraction of a fluid in a highly controlled and repeatable manner. The variable optics and high resolution camera allow the imaging of a sessile droplet or captive bubble which is then captured as either an image or video. The OCA-20 instrument fulfils many of the requirements of a system to dynamically characterise surface wetting properties, but two problems limited its application to contact lens surfaces. One of these problems was that the supplied contact lens mounting stand was relatively poor at holding the contact lens in position in a saline water bath. The other more significant problem was that the OCA-20 automated contact angle analysis software could only be applied to a flat surface. This meant that a manual curve fitting tool had to be used to calculate the contact angle, which although acceptable for static contact angle measurements (where only one measurement required), proved extremely time consuming for even a short dynamic movie (i.e. manual image analysis took up to 1 hour for an 80 second movie at 1 frame per second).

3.2.3.1 Captive bubble lens holder design

Figure 3.7 shows a schematic diagram of the redesigned lens mount which cradles the contact lens in position while allowing the apex of the contact lens to be analysed. The lens was lowered anterior surface facing downwards into the convex-shaped polypropylene mount. 20ml of PBS was then syringed into the convex contact lens cavity, which stabilised the lens and formed a smooth anterior lens surface which protruded out beneath the aperture of the lens mount. The contact lens and mount were then slowly lowered into a glass chamber filled with PBS solution until the mount rested on either side of the chamber and the lens was submerged. The contact lens was then left in solution to settle for 5 minutes, while atmospheric air (35% humidity $\pm$ 15%) was drawn into the automated OCA-20 syringe.

3.2.3.2 Captive bubble experimental procedure

Contact angles were measured at room temperature (25 ^{o}C $\pm$ 1^{o}C) and humidity (35% $\pm$ 5%) with the OCA-20 contact angle analyser using a dynamic captive bubble method. An

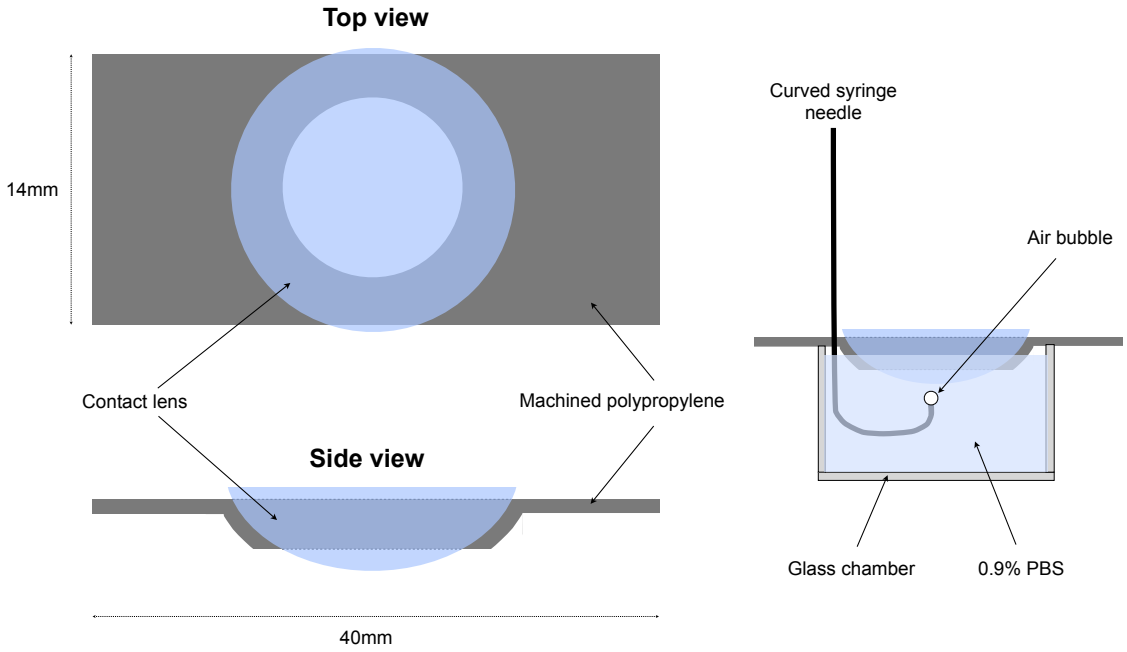

Figure 3.7: A schematic of the contact lens holder developed for the dynamic captive bubble technique.

air bubble was dispensed from a curved 1.65 mm outer diameter blunt-ended steel needle positioned 2 mm directly below the lens apex. The size of the air bubble was slowly increased by 0.1μl per second using the OCA-20 automated bubble delivery function until contact was made with the lens surface. Assessment of the receding and advancing contact angles was achieved by first enlarging the air bubble at a rate of 0.12 μl per second until it increased in volume by 3 μl and then shrinking its volume (at a rate of 0.12 μl per second) until the bubble detached from the lens surface. This entire process was captured as a digital movie.

3.2.3.3 Automated contact angle analysis on curved substrate using MATLAB

The Dataphysics DCA-20 software has the ability to perform automated contact angle analysis on a flat sample surface, but is unable to automatically analyse a curved sample surface, such as the anterior surface of a contact lens. In a previous study, Cheng *et al.* (2004) flattened the contact lens surface by clamping the lens periphery while using a plunger to flatten the central lens surface. Although this technique allowed automated contact angle measurements, the contact lens underwent significant deformation which

potentially influenced the surface characteristics of the lens surface. By choosing to keep the contact lens in its curved form, it became apparent that the manual nature of the semi-automated contact angle analysis would be too time consuming to perform on any large scale studies. It was therefore decided to develop fully automated image analysis software which would rapidly and repeatably measure the contact angle formed by the captive bubble technique on a curved lens surface. To perform dynamic captive bubble analysis, an air bubble was placed in contact with the apex of a soft contact lens and the volume of the bubble was increased and then subsequently reduced until the bubble detached from the lens surface, as highlighted in Figure 3.8.

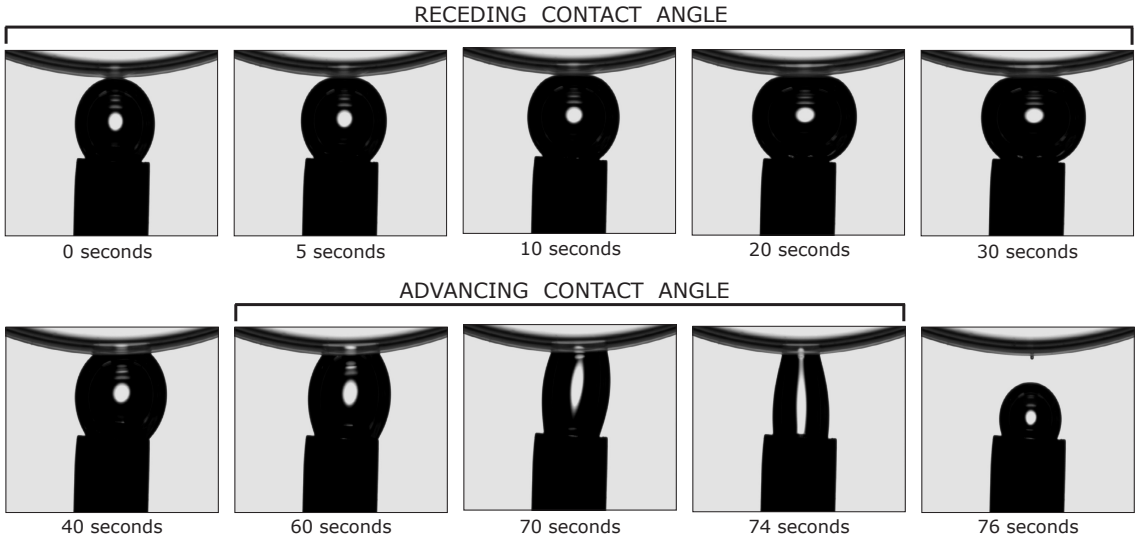

Figure 3.8: A series of frames from a dynamic captive bubble movie showing the enlargement and contraction of the air bubble against a contact lens surface, with the advancing and receding phases highlighted.

A MATLAB script (The MathWorks, Natick, MA) was developed which applied a customised, fully automated image analysis routine to each side of the bubble for all frames in the captured movie clip (Figure 3.9). This routine employed a tracing technique used to identify the boundary of the contact lens and bubble surfaces around the three-phase interface (Figure 3.9 (Step 3 & 4)). The three-phase interface point on each side of the bubble was identified from which contact angle (using the intersection of the two linear approximations of the local contact lens and bubble surfaces) and contact diameter (the distance between the two three-phase interfaces) were calculated (Figure 3.9 (Step 5)). The mean of the two contact angles for each frame and the contact diameter were plotted

versus frame number in order to identify the advancing and receding contact angle phases (Figure 3.10). The development of this automated analysis technique therefore allowed contact angle measurements to be taken in a few seconds, rather than the one hour taken to obtain these measurements manually.

3.2.4 Validation of the MATLAB image analysis technique

3.2.4.1 Aim

To investigate the validity of the automated contact angle analysis software by comparison with the OCA-20 manual imaging analysis software tool for a range of contact lens materials.

3.2.4.2 Method

The automated contact angle analysis software was used to process a captured captive bubble video for three contact lens materials. The three contact lens types (balafilcon A, senofilcon A and lotrafilcon A) were chosen as they are known to possess different surface wetting characteristics (Read *et al.*, 2009). Two lenses were analysed for each lens type (6 lenses in total), using the methodology described in Section 3.2.3.2. The lenses underwent a 48 hours PBS soak (with saline changed every 12 hours) prior to analysis. The resulting captive bubble contact angle movies were analysed both automatically by the customised software and manually using the OCA-20 software. Calibrated images were also used to validated the MATLAB automated contact angle image analysis software (Figure 3.11). The limits of agreement and mean difference between the manual and automated contact angle analysis techniques were calculated using the method described by Bland & Altman (1986).

3.2.4.3 Results

Comparison of the contact angle measurements using the manual and automated contact angle analysis techniques showed generally good agreement (Figure 3.12) with differences in contact angle measurements uninfluenced by the magnitude of the contact angle being measured (Figure 3.13). For all three contact lens materials, contact angle limits of agreement values were less than ± 6 degrees (Table 3.5). Automated contact angle measurements for the calibrated images were in all cases within 2 degrees of the expected value (Table 3.4).

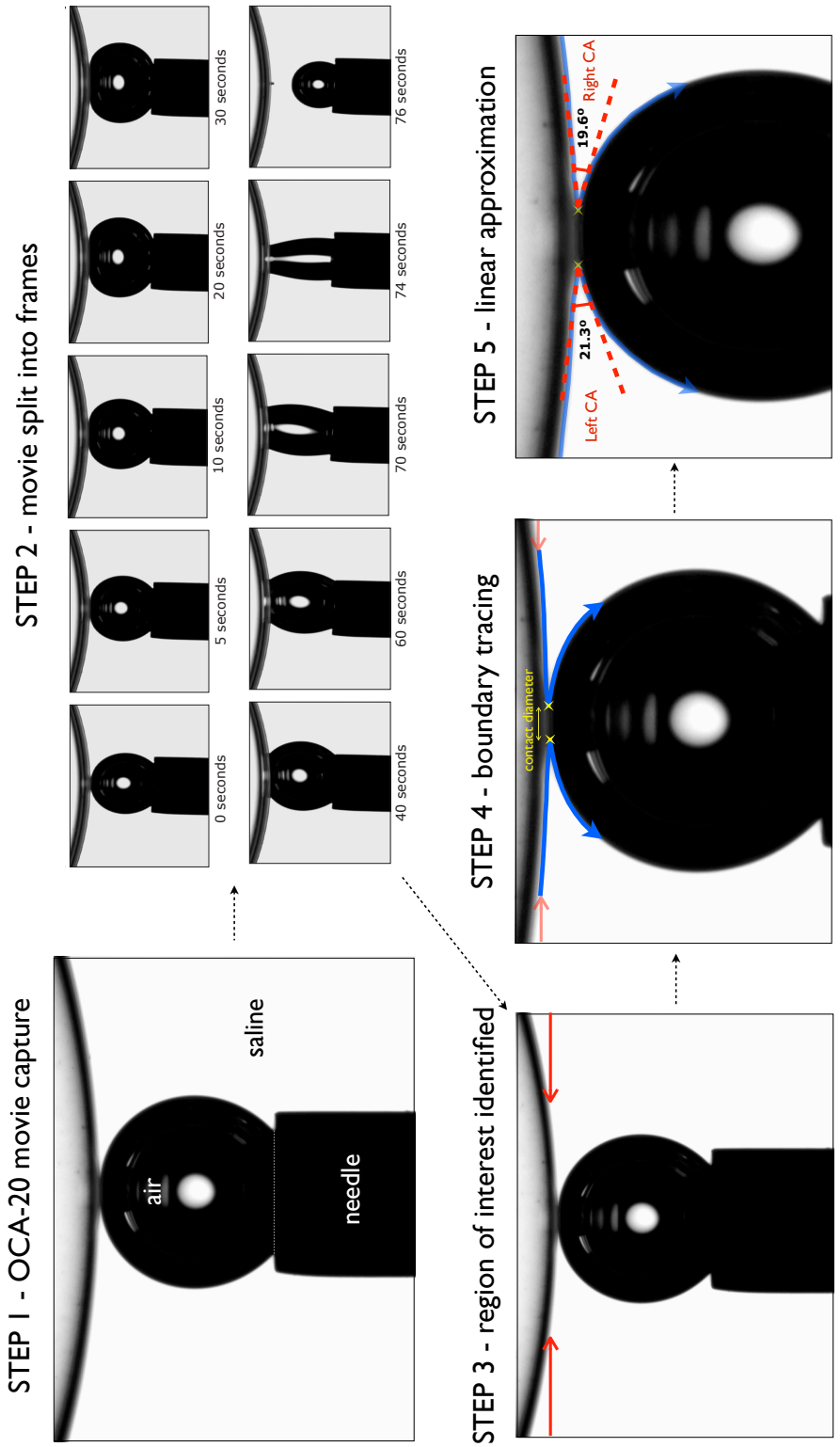

Figure 3.9: MATLAB image analysis routine for a typical captive bubble movie.

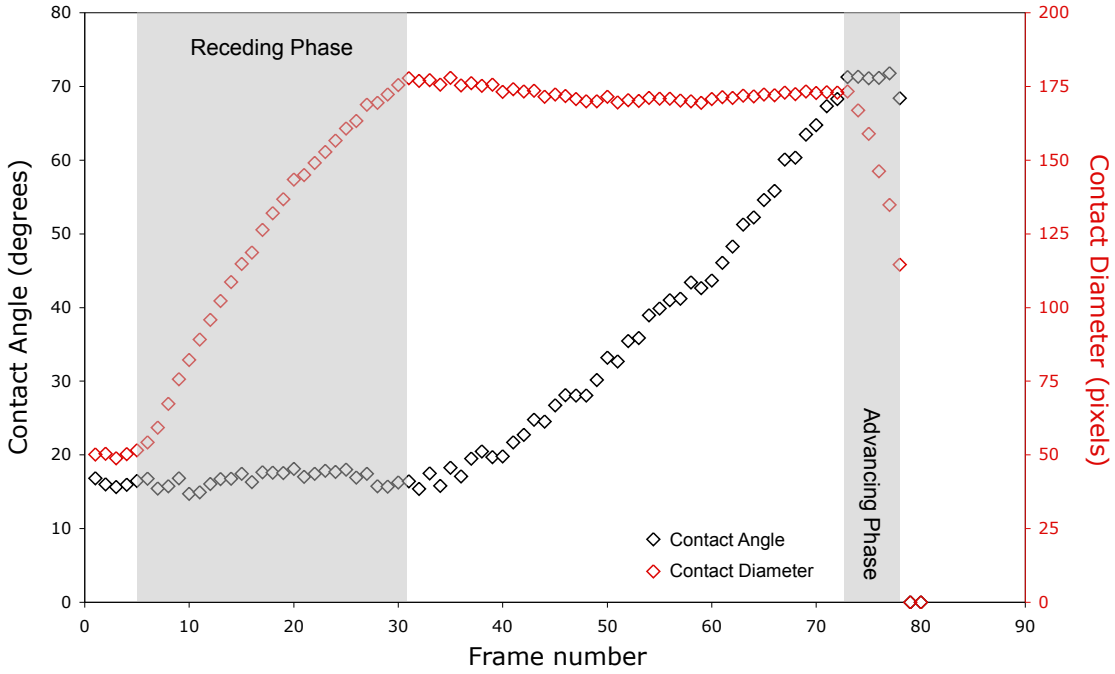

Figure 3.10: Contact angle and contact diameter vs frame number for a balafilcon lens. The advancing and receding phases are highlighted.

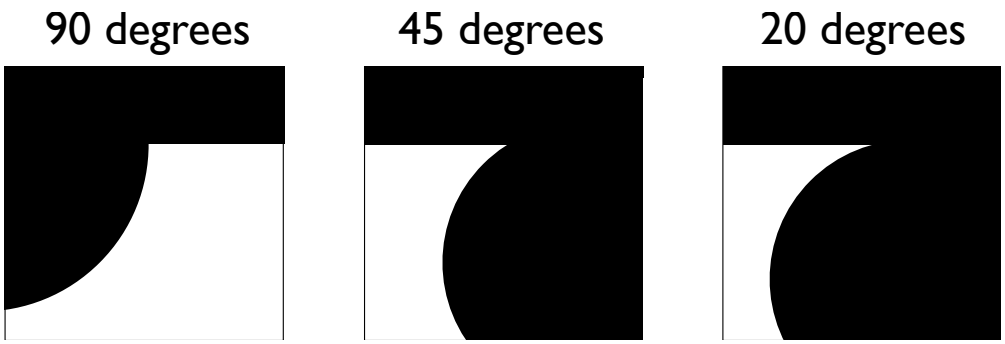

Figure 3.11: Images with calibrated angles to validate the automated contact angle analysis software

Table 3.4: Agreement between contact angle measurements using both the automated and manual technique on three different lens types

Calibrate image angle	90^o	45^o	20^o
Automated angle analysis software	90.1^o	46.2^o	19.8^o

Table 3.5: Comparison of the manual and automated contact angle measurement techniques on three different contact lens materials.

	Mean difference (degrees)	Limits of agreement (degrees)
etafilcon A	0.3	4.8
lotrafilcon A	-0.3	4.6
balafilcon A	-0.2	5.1

3.2.4.4 Discussion

The small differences observed between the manual and automated contact angle analysis techniques were likely associated with measurement errors in both techniques. Measurement errors in the automated contact angle analysis method are likely associated with linear curve fitting approximations and limited image contrast and resolution, in addition to those observed for the manual contact angle analysis method (Section 3.1.4). These results suggest that the automated contact angle analysis software does allow rapid contact angle measurements to be made on curved contact lens surfaces and that these measurements are in good agreement with both manual contact angle measurements and calibrated images.

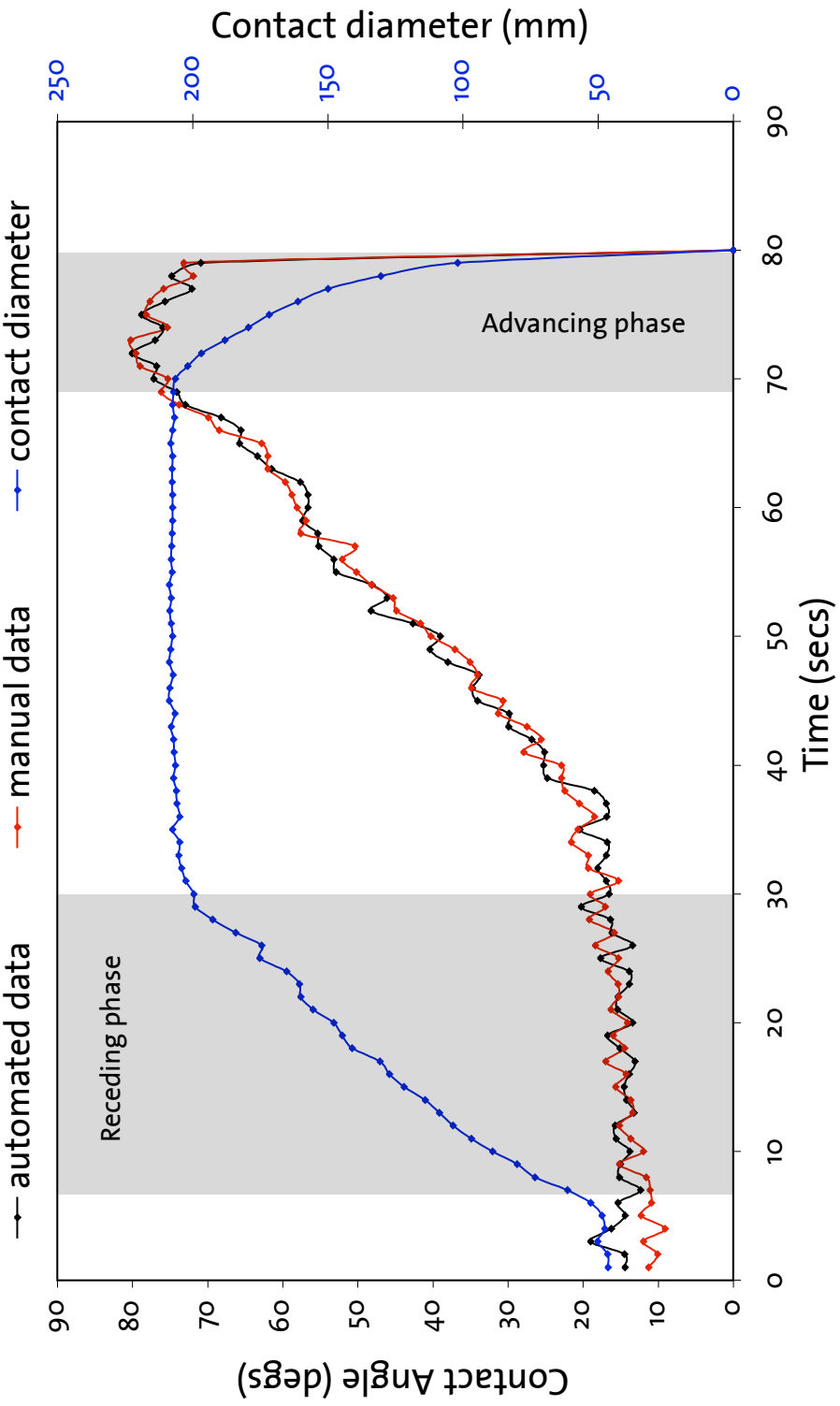

Figure 3.12: A graph of contact angle against time for the balafilcon A material, with the dynamic contact angle movie analysed using a manual and automated technique.

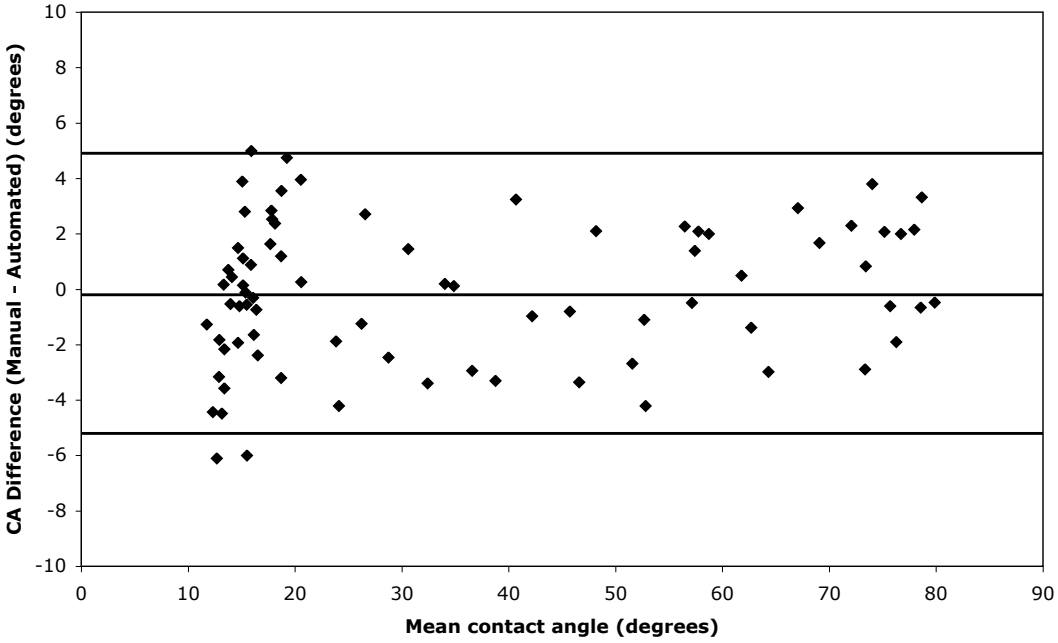

Figure 3.13: Bland-Altman plot of agreement between the automated and manual method of contact angle analysis for dynamic captive bubble data on balafilcon A lens material.

3.3 Dynamic captive bubble analysis on silicone hydrogel contact lenses

3.3.1 Introduction

The development of the automated contact angle analysis technique (Section 3.2) allowed the rapid sampling of a far greater number of lenses than was possible with the manual technique. Although contact angle analysis has been used for many years in the investigation of contact lens wetting characteristics, the development and commercial introduction of silicone hydrogel materials has brought this field back into the spotlight. Numerous studies have investigated the wetting characteristics of these lenses, but direct comparison of their findings is often difficult due to the differences in lens preparation prior to testing, type of contact angle analysis performed, type of probe liquid and speed of analysis as well as other experimental factors. This study therefore sort to investigate the wetting characteristics for a wide range of silicone hydrogel contact lenses (both commercially available lenses and the experimental study lenses) using a consistent methodology to better understand what surface wetting characteristics are required for successful clinical lens wettability.

3.3.2 Materials and methods

3.3.2.1 Lenses

Eleven commercially available silicone hydrogel contact lenses and the two experimental study contact lenses (air-cured and nitrogen-cured study lenses) were used in this investigation. Details of these lenses including public domain information on their chemical composition are provided in Figure 3.14. All commercial contact lenses were sourced from individual manufacturing batches via normal commercial channels and supplied in their standard blister packaging. All lenses were coded by a second investigator in order that the primary investigator (who conducted all measurements throughout the study) remained masked to the lenses being evaluated.

Lens type[a]	Brand name	Manufacturer	Principal monomers	Oxygen permeability (Barrers)[b]	Water content (%)	Modulus (MPa)[b]	Surface treatment
Asmofilcon A	PremiO	Menicon	silicone methacrylates, silicone acrylates, DMA, pyrrolidone derivative	129	40	0.91	Plasma coating & plasma oxidation
Balafilcon A	Purevision	Bausch & Lomb	NVP, TPVC, NVA, PBVC	91	33	1.06	Plasma oxidation
Clariti	Clariti	Sauflon	alkyl methacrylates, silicone acrylates, siloxane monomers, NVP	60	58	0.50	None (inherently wettable)
Comfilcon A	Biofinity	CooperVision	M3U, FMM, TAIC, IBM, VMA, NVP, HOB	128	48	0.75	None (inherently wettable)
Enfilcon A	Avaira	CooperVision	M3U, TEGMA, MMA NMNVA, AOE	100	46	0.50	None (inherently wettable)
Galyfilcon A	Acuvue Advance	Johnson & Johnson	mPDMS, DMA, EGDMA, HEMA, siloxane macromer, PVP	60	47	0.43	None (internal wetting agent, PVP)
Lotrafilcon A	Air Optix Night & Day	Ciba Vision	DMA, TRIS, fluorine-containing siloxane macromer	140	24	1.50	Plasma coating
Lotrafilcon B	Air Optix	Ciba Vision	DMA, TRIS, fluorine-containing siloxane macromer	110	33	1.22	Plasma coating
Narafilcon A	1 Day Acuvue TruEye	Johnson & Johnson	hydroxy-functionalised mPDMS, DMA, HEMA, siloxane macromer, TEGDMA, PVP	101	46	0.66	None (internal wetting agent, PVP)
Senofilcon A	Acuvue Oasys	Johnson & Johnson	mPDMS, DMA, HEMA, siloxane macromer, TEGDMA, PVP	103	38	0.72	None (internal wetting agent, PVP)
Silfilcon A	Air Optix Individual	Ciba Vision	DMA, TRIS, fluorine-containing siloxane macromer, styrene	82	32	1.10	Plasma coating
Nitrogen-cured study lens	N/A	N/A	M3U, TEGMA, MMA, NVA, AOE	100	46	0.5	None (inherently wettable)
Air-cured study lens	N/A	N/A	M3U, TEGMA, MMA, NVA, AOE	100	46	0.5	None (inherently wettable)

[a] United States Adopted Name.

[b] Manufacturer-reported values.

PVP: polyvinyl pyrrolidone; mPDMS: monofunctional polydimethylsiloxane; DMA: N,M-dimethylacrylamide; HEMA: hydroxyethyl methacrylate; MAA: methacrylic acid; EGDMA: ethyleneglycol dimethacrylate; TEGDMA: tetraethyleneglycol dimethacrylate; TRIS: trimethyl siloxysilyl; NVP: N-vinyl pyrrolidone; TPVC: tris-(trimethyl siloxysilyl) propylvinyl carbamate; NVA: N-vinyl amino acid; PBVC: poly(dimethysiloxy) di (silylbutanol) bis (vinyl carbamate), M3U: $\alpha\omega$-bis(methacryloyloxyethyl iminocarboxy ethyloxypropyl)-poly(dimethylsiloxane)-poly(trifluoropropylmethylsiloxane)-poly(methoxy-poly(ethyleneglycol)propylmethyl-siloxane, FMM: α-methacryloyloxyethyl iminocarboxyethyloxypropyl-poly(dimethylsiloxy)-butyldimethylsilane, TAIC: 1,3,5-triallyl-1,3,5-triazine-2,4,6(1H,3H,5H)-trione, IBM: isobornyl methacrylate, VMA: N-vinyl-N-methylacetamide, HOB: 2-hydroxybutyl methacrylate, NMNVA: N-methyl-N-vinyl acetamide, MMA: methyl methacrylate, TEGDMA: tetraethyleneglycol dimethacrylate, AOE: 2-allyloxyethanol

Figure 3.14: Study contact lenses.

3.3.2.2 Surface Tension Measurement

The surface tension of the blister contact lens packaging solutions was measured in order to determine the presence of any surface active agents since such components will have a significant effect on the magnitude of any contact angle measured (Maldonado-Codina & Morgan, 2007). Surface active agents are often added to contact lens blisters in order to prevent the lenses adhering to the blister material (particularly at high temperatures, e.g., during sterilisation) and in an apparent attempt to aid initial wearer comfort of the

lenses (Tonge *et al.*, 2001). Surface tension measurement was performed using the pendant drop technique with an OCA-20 (DataPhysics Instruments, Filderstadt, Germany) contact angle analyser, which comprises a conventional goniometer with automated drop delivery and digital image capture. The pendant drop method has previously been well documented (Alvarez *et al.*, 2009); in brief, the surface tension was derived by fitting the Young-Laplace equation to the digitised outline of the largest possible liquid drop suspended from a 2.41mm outer diameter blunt-ended steel needle. Prior to contact angle measurement, all lenses underwent a 48 hour saline soak in PBS solution (Sigma-Aldrich, Germany), which was changed every 12 hours in an attempt to remove any surface active agents adsorbed onto the lens surfaces or absorbed into the lens polymer bulk. The effectiveness of this strategy was tested by comparing the surface tension of the final (fourth) post-soak PBS to that of freshly prepared PBS.

3.3.2.3 Dynamic Contact Angle Analysis

Contact angles were measured at room temperature (25.0^{o}C $\pm$ 1^{o}C) and humidity (35% $\pm$ 5%) with the OCA-20 contact angle analyser using a dynamic captive bubble method. The captive bubble methodology applied has previously been described in Section 3.2.3.2 and utilises the customised contact lens holder and MATLAB automated contact angle analysis software. For each contact lens a digital movie of the dynamic captive bubble process was captured and the measurement procedure was repeated on four further occasions on the same lens, with at least 5 minutes between measurements. The PBS within the glass chamber was emptied and refilled prior to testing each different lens. This procedure was undertaken for 10 lens samples per lens type, and the order of analysis of these lenses was randomised. This gave a total of 650 movie clips (5 measurement runs x 10 lens samples x 13 lens types).

3.3.2.4 Image Analysis

Receding and advancing contact angles were derived for each movie. This was achieved by applying the customised, fully automated image analysis routine (MATLAB, The MathWorks, Natick, MA) to each side of the bubble for all frames in the captured movie clip (Section 3.2.3.3). The receding contact angle was defined as the mean angle in five frames at the midpoint of the receding phase and the advancing contact angle as the mean angle in the first five frames of the advancing phase.

3.3.2.5 Data Analysis

Given the normal distribution of the data sets (advancing and receding contact angles, and hysteresis data for each of the 13 lens types, Kolmogorov-Smirnov test, all $p>0.14$), a linear regression model was constructed to investigate the overall study findings. Specifically, the factors of interest were lens type, contact angle type (advancing or receding), measurement run (as a covariant), and lens sample (as a random effect) with contact angle magnitude as the dependent variable. This was then followed by separate linear regression models for advancing contact angle, receding contact angle, and magnitude of hysteresis as the dependent variable in order to investigate differences between lens types.

3.3.3 Results

3.3.3.1 Surface Tension Measurement

The surface tension measurements of the lens blister packaging solutions and the post-soak PBS are shown in Table 3.6. The post-soak surface tension of the PBS was within 0.2 dynes/cm (0.0002 N/m) of the pre-soak saline in all cases confirming that any surface active agents were removed by the soaking process.

3.3.3.2 Dynamic Contact Angle Analysis

Advancing and receding contact angles for the lenses are shown in Table 3.7 and Figure 3.15. The hysteresis values of the lenses are also shown in Table 3.7. The results of the overall linear regression model showed a significant interaction for lens type x contact angle type ($F=678.7$, $p<0.0001$). Measurement run was not significant ($F=1.1$, $p=0.29$). Given the significant interaction term above, separate analyses for advancing and receding contact angles and hysteresis were undertaken. Lens types were significantly different for advancing angles ($F=964.5$, $p<0.0001$). Post-hoc analysis using the Tukey HSD test divided the lenses into the following seven groups within which statistically similar advancing contact angles were measured (in descending order of contact angle magnitude): (1) air-cured study lens (2) balafilcon A/asmofilcon A, (2) enfilcon A/nitrogen-cured study lens,(3) Clariti/lotrafilcon B, (4) galyfilcon A/narafilcon A/senofilcon A, (5) silfilcon A/comfilcon A, and (6) lotrafilcon A.

Lens type	Blister packaging solution	Post-soak PBS
Air-cured	72.6 (0.5)	72.7 (0.1)
Asmofilcon A	67.5 (0.4)	72.7 (0.2)
Balafilcon A	72.0 (0.1)	72.7 (0.1)
Clariti	54.4 (0.6)	72.6 (0.1)
Comfilcon A	68.5 (0.1)	72.6 (0.2)
Enfilcon A	65.1 (1.2)	72.6 (0.2)
Galyfilcon A	51.3 (0.7)	72.6 (0.1)
Lotrafilcon A	71.8 (0.1)	72.5 (0.2)
Lotrafilcon B	72.2 (0.1)	72.6 (0.1)
Nit-cured	72.3 (0.3)	72.6 (0.2)
Narafilcon A	52.6 (0.6)	72.7 (0.2)
Senofilcon A	52.1 (0.8)	72.5 (0.2)
Silfilcon A	72.5 (0.1)	72.6 (0.4)

Table 3.6: Surface tension (mN/m) of blister packaging solution and post-soak PBS solution. The standard deviations appear in parentheses.

Differences were also demonstrated between the lens types for receding angle ($F=23.8$, $p<0.0001$). Post-hoc analysis using the Tukey HSD test divided the lenses into four statistically similar groups with some overlap between them. They were in descending order of contact angle magnitude: (1) air-cured study lens (2) galyfilcon A, narafilcon A and senofilcon A (3) nitrogen-cured study lens, enfilcon A, lotrafilcon B, asmofilcon A, silfilcon A, comfilcon A, and balafilcon A (4) silfilcon A, comfilcon A, balafilcon A, Clariti, and lotrafilcon A.

Hysteresis was also different for the various lens brands ($F=868.7$, $p<0.0001$). In general, each lens type was different to all the others with the exception of (1) galyfilcon A, narafilcon A, and senofilcon A, (2) nitrogen-cured study lens and enfilcon A (3) senofilcon A, silfilcon A, and comfilcon A, where within each group the lenses were statistically similar.

Lens type	Advancing CA	Receding CA	CA hysteresis
Air-cured	88.2 (2.5)	30.2 (1.5)	60.0 (2.0)
Asmofilcon A	71.2 (1.5)	19.6 (0.7)	51.6 (1.4)
Balafilcon A	71.5 (1.1)	18.3 (0.6)	53.3 (1.3)
Clariti	42.2 (0.9)	17.5 (0.4)	24.7 (1.1)
Comfilcon A	29.6 (1.2)	18.6 (0.5)	11.1 (1.3)
Enfilcon A	68.3 (1.5)	19.7 (0.7)	48.7 (1.7)
Galyfilcon A	37.5 (1.9)	21.8 (1.1)	15.8 (1.4)
Lotrafilcon A	19.9 (0.9)	17.1 (0.5)	2.8 (0.7)
Lotrafilcon B	41.3 (1.0)	19.6 (0.9)	21.7 (1.3)
Nit-cured	66.7 (1.8)	20.1 (1.1)	46.6 (1.5)
Narafilcon A	37.0 (0.7)	22.1 (1.0)	14.9 (0.7)
Senofilcon A	35.4 (0.5)	22.1 (0.6)	13.3 (0.6)
Silfilcon A	30.5 (1.4)	18.6 (0.7)	12.0 (1.5)

Table 3.7: Advancing and receding contact angles. The standard deviations appear in parentheses.

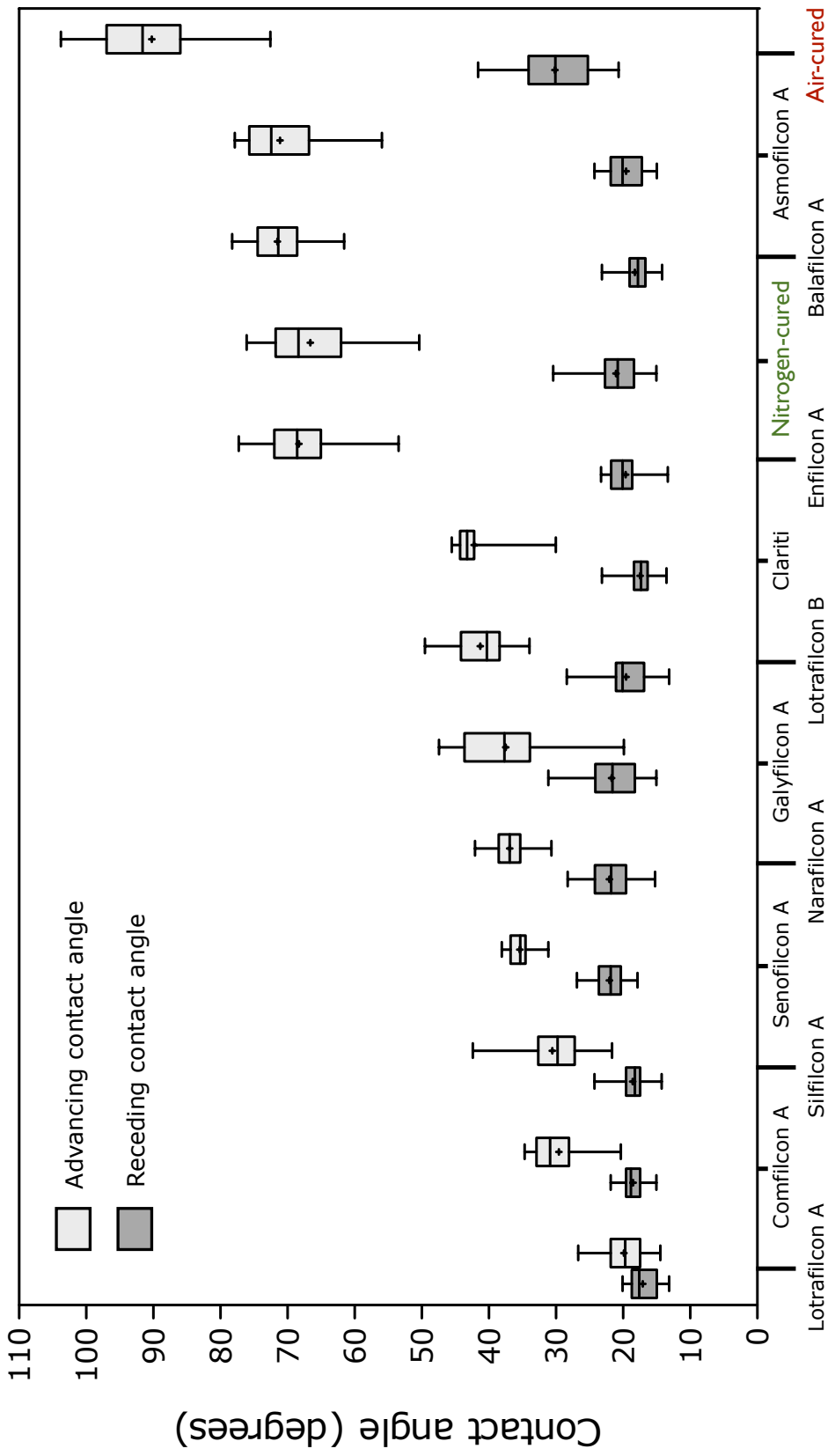

Figure 3.15: Advancing and receding contact angles for all the silicone hydrogel lenses investigated. The boxes represent the 25th and 75th centiles, and the whiskers indicate the full extent of the data set. The median is represented by a horizontal line within the box and the mean by a cross.

3.3.4 Discussion

This work has provided data for advancing and receding contact angles for a wide range of silicone hydrogel lenses obtained using consistent methodology and a single investigator. A review of the literature shows that there are relatively few published reports detailing the contact angles of unworn, silicone hydrogel lenses. Only one report has documented a dynamic captive bubble methodology similar to that used in our current investigation (Cheng *et al.*, 2004). This work by Cheng and coworkers noted that the balafilcon A lens demonstrated a receding contact angle of 24^o and an advancing contact angle of 80^o when saline was used as the probe liquid. These values are reasonably similar to those found in the present investigation (18^o and 72^o). Their data for the lotrafilcon A lens (21^o and 60^o) were markedly different to our own findings (17^o and 20^o). When comparing our data with those of Cheng and coworkers, the differences obtained may be due to the following:

1. Different instruments: In this study the OCA 20 instrument was used, whereas Cheng and coworkers used a customised setup based around the Kruss DSA-10 instrument with semi-automated angle analysis software.

2. Differences in sample preparation: Cheng and coworkers stretched their lens samples over a Teflon holder in order to present a flat surface for analysis. In comparison, this PhD study assessed the lenses without deformation and without a holder applied to the lens back surface.

3. Differences to lens material formulations and packaging solutions: Both the balafilcon A and the lotrafilcon A lenses have undergone refinements since Cheng and coworkers carried out their work (Pence, 2008).

4. Different investigators: Subtle differences in measurement technique may introduce variability in the data obtained.

These differences serve to highlight the difficulties of inter-laboratory comparison of data in this area. The findings of this study have shown key differences between advancing contact angles for the different lenses investigated. Advancing contact angles ranged from 20^o to 88^o, and for some of the lenses, it is possible to relate the magnitude of these angles to the surface chemical properties of the lenses. For example, the two lenses that undergo a surface oxidation process (balafilcon A and asmofilcon A) have the largest advancing

contact angles. It has been well documented that such a surface treatment can result in glassy islands of hydrophilic silicate material surrounded by areas of hydrophobic bulk (Teichroeb *et al.*, 2008; Tighe, 2004). Within these hydrophobic areas, when the lens surface is exposed to air, the siloxane groups within the polymer are able to migrate, unimpeded, to the surface in order to minimise the surface energy, which in turn increases the measured advancing contact angle. A large advancing contact angle was observed for the enfilcon A lens despite the lens not undergoing any kind of surface modification following cast moulding, while the comfilcon A lens that is fabricated by the same manufacturer (CooperVision Inc) has a much smaller advancing contact angle, which may be due to its somewhat different chemical formulation (Figure 3.14). The Clariti and lotrafilcon B lenses had similar advancing contact angles despite different compositions and surface treatments (Figure 3.14). Surprisingly, the lotrafilcon A, lotrafilcon B, and silfilcon A lenses (manufactured by CIBA Vision) all had advancing contact angles which were significantly different to each other despite the lenses being based on similar polymer chemistry and undergoing an apparently similar surface plasma coating process. It is likely that these discrepancies are due to the following: (a) differences in plasma coating, (b) variation in the bulk chemical composition (such as the addition of styrene in silfilcon A, or differing ratios of siloxane monomer present in lotrafilcon A and lotrafilcon B materials), which may influence the surface characteristics of the lenses despite the presence of a coating, or (c) a combination of (a) and (b). The three lenses manufactured by Johnson & Johnson (galyfilcon A, senofilcon A, and narafilcon A) demonstrated comparable advancing contact angles despite apparent differences in formulation. The information available in the public domain (Figure 3.14) suggests that the chemical compositions of the galyfilcon A and the senofilcon A materials are similar, and considering the differences in the water content of the materials, it is reasonable to assume that the ratios of the components differ between them, with more PVP being incorporated into the senofilcon A material (McCabe *et al.*, 2004). The narafilcon A material contains the same hydrophilic monomers used in the senofilcon A and galyfilcon A formulations, but it contains only one rather than two silicone-containing monomers. This silicone monomer is of a lower molecular weight than that used in the galyfilcon A and senofilcon A materials (Rathore *et al.*, 2008). An obvious difference was observed in advancing contact angle for the experimental contact lenses, with the air-cured lens have a mean advancing contact angle more than 20 degrees higher than the nitrogen-cured lens. Given the similarity in bulk chemical composition it is clear

that the polymerisation conditions have influenced the surface wetting characteristics, resulting in these differences. In addition to composition-based differences and variations in surface treatment of lenses described above, there are other processing related factors, which could affect the resultant contact angles; these include polymerisation conditions, solvents used to cast the lenses, and hydration/extraction methods. However, there is almost no information about these factors available in the public domain.

When comparing the dynamic contact angle results with the static results found in Section 3.1, it is apparent that for some materials there are significant differences between the findings. One such example is the contact lens material etafilcon A, which when assessed with the static sessile droplet technique (thought to be analogous to an advancing contact angle) gave a contact angle of around 20 degrees, whereas when assessed using the captive bubble technique, the advancing contact angle was found to be around 80 degrees. Other studies have presented similar findings (Cheng *et al.*, 2004; Lorentz *et al.*, 2007), suggesting genuine differences in contact angle values associated with the measurement technique used. A potential factor is the need for surface blotting which removes water from the surface of the hydrogel to allow accurate testing of the material. Immediately following blotting, the water within the material may be redistributed from the bulk to rehydrate the surface and potentially form a surface film. The rate at which the water is redistributed within the material is likely to be important; as conventional hydrogel materials typically possess a higher ion permeability when compared with silicone hydrogels materials (Austin, 2009). It is hypothesised that this allows the surface of conventional hydrogel materials to regain a fully hydrated nature almost immediately after blotting, with a possible surface water film generated. This water swollen surface is likely sufficient to resist reorganisation of the chemical groups at the surface and therefore predominately hydrophilic (hydroxyl) groups are presented as the droplet is placed onto the surface, giving a low sessile drop (advancing) contact angle (Figure 3.16). In the captive bubble technique, the constant pressure exerted by the air bubble appears sufficient to result in removal of the surface water layer between the air bubble and the lens surface. This results in a reorganisation of the functional groups at the lens surface (methyl groups dominating the surface), therefore presenting a relatively hydrophobic surface and resisting the advancing water phase as observed during dynamic contact angle testing (Figure 3.16).

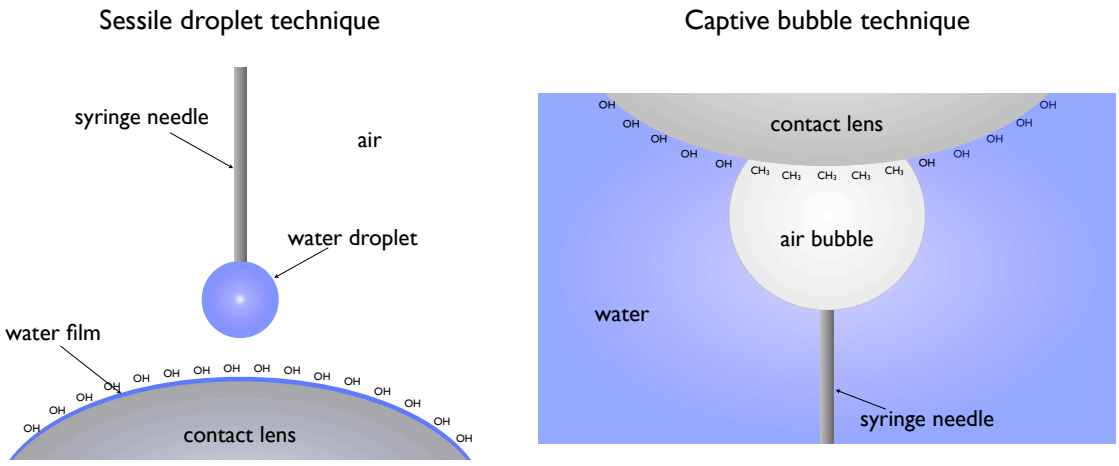

Figure 3.16: A schematic diagram of sessile drop and captive bubble analysis on etafilcon A showing the apparent difference in presentation of the hydroxyl (OH) and methyl (CH_3) functional groups. Based on diagrams from Holly & Refojo (1975).

A significant difference was also observed between the static sessile drop contact angle and the advancing contact angle measured using the dynamic captive bubble technique for the senofilcon A material. The contact angle for sessile drop technique is much higher (around 80 degrees) than the advancing contact angle for the dynamic captive bubble technique technique (around 40 degrees). It has been proposed that the surface of the senofilcon A material has hydrophilic PVP chains which protrude out from the surface (Yañez *et al.*, 2008), presenting a relatively hydrophilic surface during captive bubble testing. However, when the surface is disturbed by an invasive blotting technique, such as that typically used for the sessile droplet technique, the PVP chains are likely to be flattened against the polymer surface. This is thought to result in greater expression of the hydrophobic species within the material, resulting in the elevated contact angle seen for the sessile droplet technique. When assessing the advancing contact angle of a lens material, the key variable appears to be whether air exposure prior to measurement is sufficient to result in reorganisation of the chemical groups and if so, to what degree this occurs. This is dependant on factors such as the speed of the contact angle boundary during testing, the number of hydration/dehydration cycles, the ion permeability of the material, the temperature of both the material and the probe liquid, the humidity of the probe air, the blotting technique employed (if any) and perhaps most importantly the contact angle analysis technique used. Given that these factors vary significantly between research

groups and to a lesser extent within research groups, this probably accounts for the wide range of contact angle values reported in the literature.

This dynamic captive bubble study has shown that the receding contact angles for all the lenses investigated were restricted to a narrower range (17^o to 30^o) compared with the advancing contact angle (20^o to 88^o). The air-cured lens possessed by far the highest receding contact angle, suggesting a more hydrophobic tendency, even when in an aqueous environment. All three of the Johnson & Johnson lenses along with the nitrogen-cured lenses demonstrated larger receding contact angles than the other lenses studied. The hysteresis of the lenses followed a similar pattern to that of the advancing angles given that the receding angles of all of the lenses were numerically similar. Our results suggest that the magnitude of hysteresis and the advancing contact angle appear not to be indicative of the clinical performance of commercially available contact lens since all of the lenses investigated in this work are currently on the market, and those with either large (Brennan *et al.*, 2007; Lakkis & Vincent, 2009) or small (Maldonado-Codina *et al.*, 2004b; Young *et al.*, 2007) levels of hysteresis have been demonstrated to have clinically acceptable levels of wettability. The results showed a clear difference between the two experimental lens types for both the advancing and receding contact angle and in the contact angle hysteresis. As differences are present in all three contact angle measurements it is therefore difficult to conclude which if any is primarily responsible for the clinical non-wetting observed in Chapter 2.

3.4 Investigation of wetting heterogeneity across a contact lens surface

3.4.1 Introduction

Following the comparative clinical study (Section 2.1) and the development of the *in vitro* wettability analyser (Section 2.2.2.1), it became apparent that although the static and dynamic contact angle studies provided useful information regarding the surface wettability of the study contact lenses, only the apex of the contact lenses had been investigated. The assumption that the peripheral lens surface would possess similar wetting characteristics to that of the apex, might have seemed logical for the commercial contact lenses with their relatively homogenous wetting characteristics, but for the air-cured study lenses with their heterogenous wetting characteristics this seemed highly unlikely. This study therefore sort to further develop the dynamic captive bubble technique to allow an assessment of wettability at any point across the lens surface, and subsequently to apply this across the surface of both the nitrogen-cured and air-cured contact lenses following assessment with the *in vitro* contact lens wettability analyser (Section 2.2.2). By combining both these techniques the study aimed to investigate how the wetting characteristics of the different regions on the air-cured and nitrogen-cured contact lenses differed and in doing so potentially highlight the critical *in vitro* wetting characteristics which are associated with acceptable clinical lens performance.

3.4.2 Materials and methods

3.4.2.1 Lenses

Ten nitrogen-cured study lenses and ten air-cured study lenses were used in this investigation (Section 1.9). These lenses were supplied in their standard blister packaging and all lenses underwent a 48 hour soaking in PBS (with the saline changed every 12 hours) prior to analysis.

3.4.2.2 Modified lens mount

Figure 3.17 shows the design of the modified lens mount. It consisted of a 17mm diameter steel ball bearing with a flat surface. The ball bearing was then coated (Plasti-Kote, UK) and attached to a small acrylic sheet. A 15mm diameter neodymium magnetic disc was

then carefully machined to form a ring magnet with an internal chamfer matching that of the ball bearing curvature. The ring magnet was then also coated. Both the magnetic ring and the mounted ball bearing were soaked for prolonged periods in 0.9% PBS without showing any change in the surface tension of the soaking liquid.

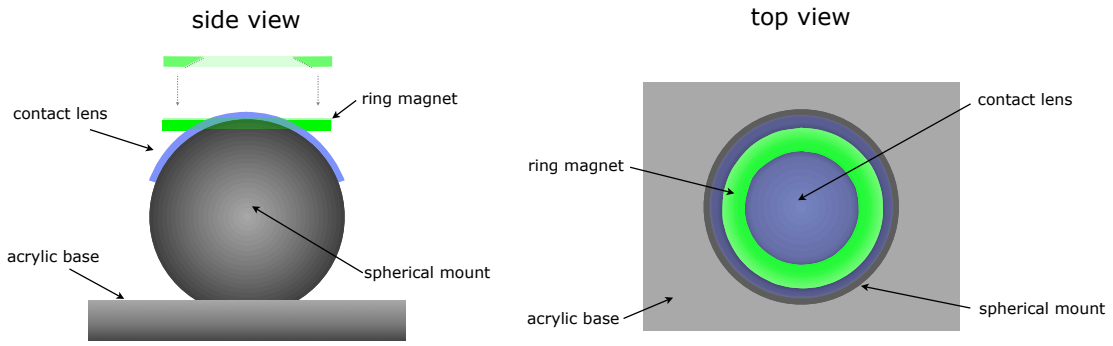

Figure 3.17: A schematic diagram of the lens mount used to allow dynamic contact angles to be measured across a lens surface

3.4.2.3 *In vitro* wetting analysis

Each air-cured contact lens was removed from its PBS filled vial and placed onto the spherical lens mount (figure 3.18 - step 1). The lens and mount were then placed into a saline bath and left there for 5 minutes. The lens and mount were then removed and analysed using the *in vitro* lens wetting analyser (Section 2.2.2), before being returned to the saline bath. This was repeated on four further occasions to allow the non-wetting regions to be identified. The lens was then moved on the mount until the hydrophobic or hydrophilic region was positioned at the apex of the mount (Figure 3.18 - step 2). The ring magnet was then placed over the region of interest where it gently clamped the lens in position (Figure 3.18 - step 3). The mount and lens were then turned over and lowered into the PBS filled captive bubble analysis chamber (figure 3.18 - step 4). The nitrogen-cured lenses were also analysed using the *in vitro* lens wetting analyser.

3.4.2.4 Dynamic Contact Angle Analysis

Contact angles were measured at room temperature (25.0^{o}C $\pm$ 1^{o}C) and room humidity (35% $\pm$ 5%) with the OCA-20 contact angle analyser using a dynamic captive bubble method. The dynamic captive bubble experimental procedure followed that previously

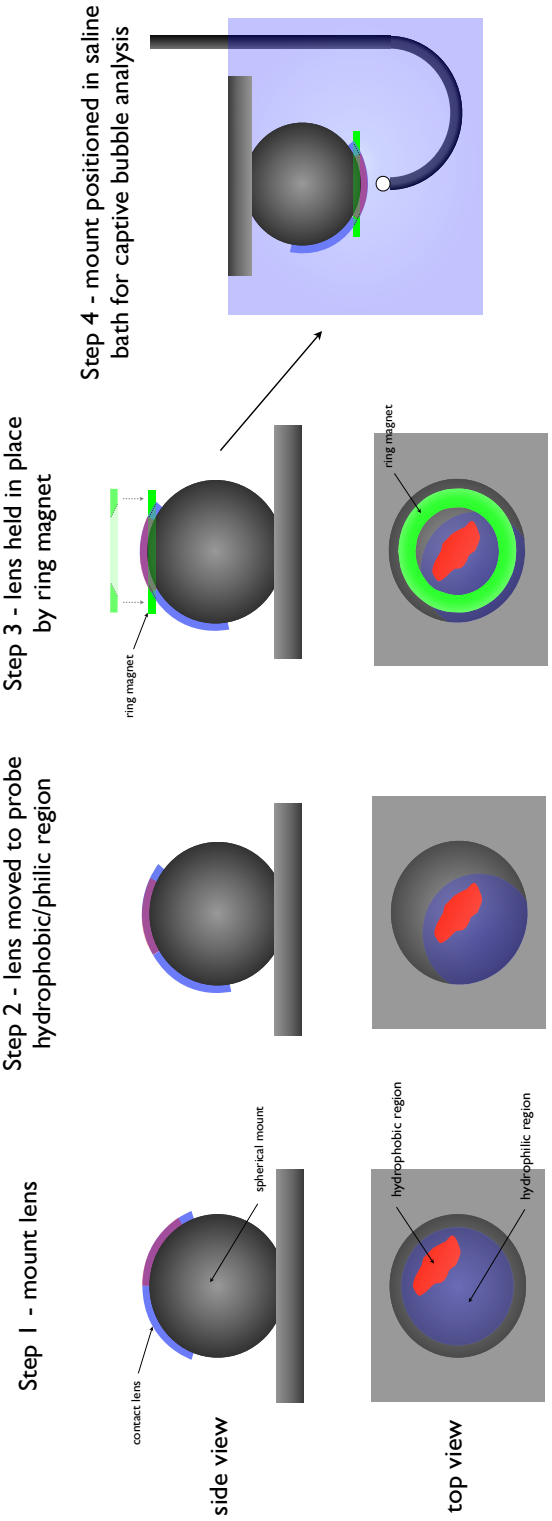

Figure 3.18: A schematic diagram showing the experimental procedure required to analyse hydrophobic and hydrophilic regions on a contact lens surface.

described in Section 3.2.3.2 with the use of the magnetic contact lens holder and MATLAB automated contact angle analysis software. For each contact lens region a digital movie of the dynamic captive bubble process was captured and the measurement procedure was repeated on four further occasions on the same lens, with at least 5 minutes PBS soaking between measurements. The PBS within the glass chamber was emptied and refilled prior to testing each different lens. This procedure was undertaken for ten air-cured lens samples in both a region of non-wetting and a region of wetting (as identified by the *in vitro* lens wetting analyser), with the order of analysis between regions randomised. Ten nitrogen-cured lenses were then also analysed using the captive bubble technique in regions corresponding to those found on the air cured lens in a randomised order (Figure 3.19). This gave a total of 200 movie clips (5 measurement runs x 10 lens samples x 2 lens types x 2 regions of interest).

3.4.2.5 Data analysis

Following the testing for normality of the contact angle data with the Kolmogorov-Smirnov (KS) test, a linear regression model was constructed to investigate the overall study findings. Specifically, the factors of interest were lens type, lens region, contact angle type (advancing or receding), measurement run (as a covariant), and lens sample (random effect) with contact angle magnitude as the dependent variable. This was then followed by separate linear regression models for advancing contact angle, receding contact angle, and magnitude of hysteresis as the dependent variable in order to investigate differences between the two lens types.

3.4.3 Results

There was no significant difference between the distribution of contact angle values and that of a normal distribution (sessile drop: K=1.4, p=0.32; and captive bubble: K=3.7, p=0.64), justifying the subsequent parametric statistical treatment of the data. Advancing and receding contact angles for the lenses are shown in Table 3.4.3. The results of the overall linear regression model showed a significant interaction for lens type x contact angle type (F=137.2, p<0.0001). Measurement run was not significant (F=0.7, p=0.40). Given the significant interaction term above, separate analyses for advancing and receding contact angles were undertaken.

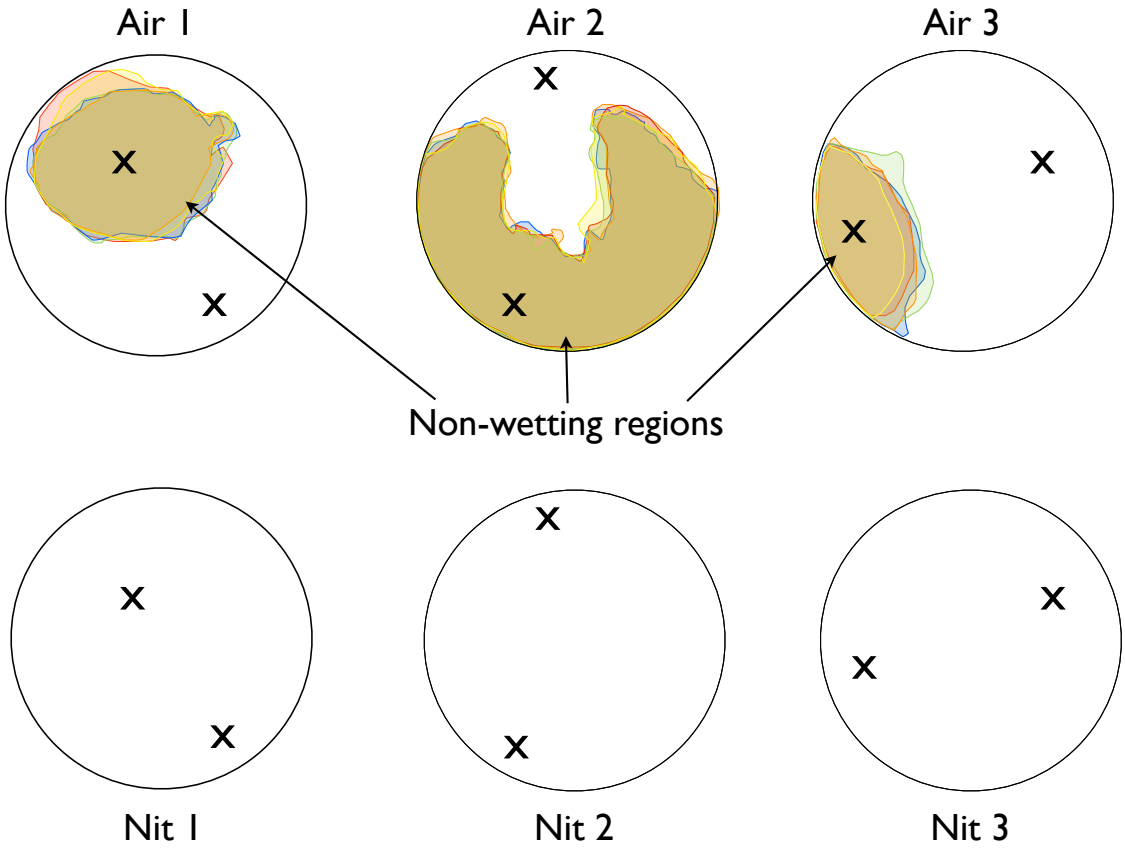

Figure 3.19: A schematic diagram showing the locations of dynamic captive bubble analysis (X) on three of the ten air-cured study contact lenses (above) and the corresponding regions analysed on the nitrogen-cured lenses (below).

Lens type	Lens Region	Mean advancing CA	Mean receding CA
Air-cured	Non-wetting	87.2^o (4.6^o)	31.7^o (4.9^o)
Air-cured	Wetting	77.5^o (9.0^o)	18.2^o (2.0^o)
Nitrogen-cured	(Non-wetting)	65.4^o (4.6^o)	17.9^o (1.7^o)
Nitrogen-cured	(Wetting)	64.2^o (3.4^o)	18.5^o (2.0^o)

Table 3.8: The mean advancing and receding contact angles for the wetting and non-wetting regions on the air-cured and nitrogen-cured lens types. The standard deviation appears in parentheses.

For the advancing contact angle data there was a significant difference between the two lens types ($F=639.2$, $p<0.0001$), with the air-cured lens having a higher mean value (82.3 degrees) than the nitrogen-cured lens (64.8 degrees). There was also a significant difference between the two lens regions ($F=42.8$, $p<0.0001$), with the non-wetting regions having a higher mean contact angle (75.1 degrees) than the wetting regions (70.1 degrees). A significant interaction was observed for lens type x lens region ($F=35.4$, $p<0.0001$) with post hoc analysis using Tukey HSD test dividing the lens type/lens region combinations into the following three groups within which statistically similar advancing contact angles were measured: (1) non-wetting region on air-cured lens, (2) wetting region on air-cured lens, (3) both regions analysed on the nitrogen-cured lens.

For the receding contact angle data there was a significant difference between the two lens types ($F=212.7$, $p<0.0001$), with the air-cured lens having a higher mean value (25.0 degrees) than the nitrogen-cured lens (18.5 degrees). There was also a significant difference between the two lens regions ($F=221.4$, $p<0.0001$), with the non-wetting regions having a higher mean contact angle (25.0 degrees) than the wetting regions (18.4 degrees). A significant interaction was observed for lens type x lens region ($F=35.4$, $p<0.0001$) with post hoc analysis using Tukey HSD test dividing the lens type/lens region combinations into the following two groups within which statistically similar advancing contact angles were measured: (1) non-wetting region on air-cured lens, (2) wetting region on air-cured lens and both regions on the nitrogen-cured lens.

Figure 3.20 shows the change in advancing and receding contact angle between the regions of wetting and non-wetting on the air-cured lenses and the matching areas on the nitrogen-cured lenses. The nitrogen-cured study lenses showed little change in either advancing or receding contact angle between the regions, whereas the air-cured lenses showed a general reduction in both advancing and receding contact angles. The absolute difference in contact angle between the wetting and non-wetting regions on the air-cured lens was 9.7 degrees for the advancing contact angle and 13.6 degrees for the receding contact angle, with a percentage reduction of 12% and 43% respectively.

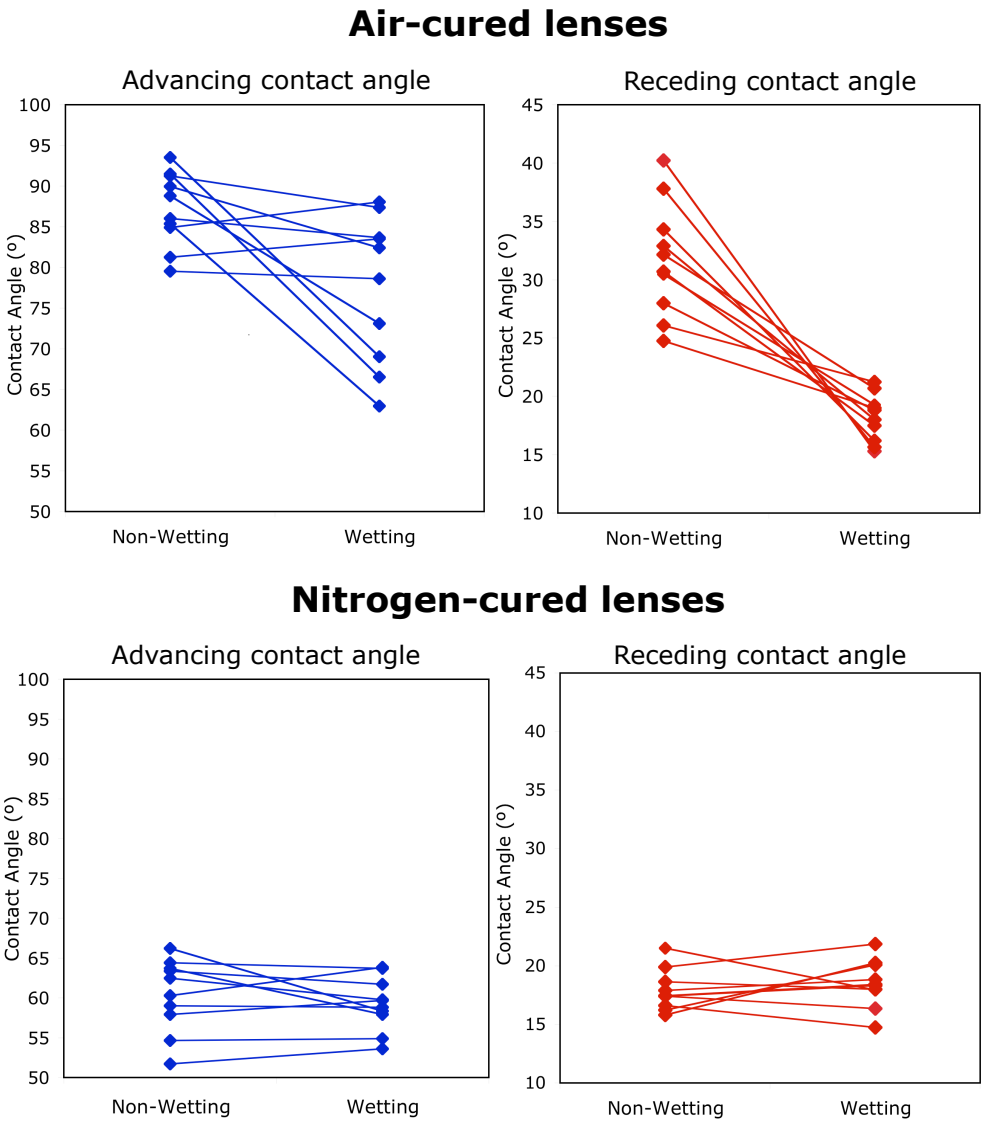

Figure 3.20: The change in advancing (blue) and receding (red) contact angle between wetting and non-wetting regions on the air-cured lenses (above) and respective areas on the nitrogen-cured lens (below)

3.4.4 Discussion

The clinical relevance of the advancing and receding contact angle to contact lens wear has been debated in the literature. Some studies have suggested that the advancing contact angle is the most relevant clinical measure as it describes the ability of a tear film to form over a contact lens surface, whereas others have stressed the importance of the receding contact angle in maintaining a stable tear film across the lens surface. The data from the comparative clinical study in this PhD study (Section 2.1) showed that a contact lens cured in an air-filled oven (air-cured lens) had regions of very poor *in vivo* wetting along with regions of acceptable lens wetting. The contact lenses cured in a nitrogen-purged oven (nitrogen-cured lens) in contrast demonstrated a relatively homogenous clinical wetting surface. This contact angle work therefore sort to investigate the wetting properties of these regions and in doing so allow a improved understanding of the clinical importance of these *in vitro* measurements.

When analysing the results for the nitrogen-cured lens it was apparent that there was little difference in the dynamic wetting characteristics across the lens surface. The receding contact angle data showed no significant difference between the wetting regions on the air-cured lenses and the nitrogen-cured lenses suggesting similarities in these surfaces, whereas the advancing contact angle data showed a significant difference between these surfaces. This suggests that more hydrophobic domains were present on the surface of the wetting region of the air-cured lens compared with the nitrogen-cured lens when exposed to an air environment, whereas on exposure to an aqueous environment both surfaces reorganised to present similarly hydrophilic surfaces. The wetting region of the air-cured lens therefore appears to have a greater concentration of hydrophobic material at the surface than the nitrogen-cured lens, while still having sufficient hydrophilic species to allow reorganisation of the polymer structure at the surface, thus masking the relatively materials hydrophobic nature.

The advancing and receding contact angle data highlight significant differences between the non-wetting regions on the air-cured lenses and both the wetting regions of the air-cured lens and the nitrogen-cured lens. The elevated advancing contact angle suggests that when the material is exposed to an air environment the hydrophobic species are able to present more efficiently at the lens surface than for in the other lens regions. The

elevated receding contact angle suggested that when in an aqueous environment the surface in this region presents relatively hydrophobic species in comparison with other lens regions. These findings suggest an increased presence of the hydrophobic species to a degree where the lens surface is dominated by the silicone material and even when exposed to a hydrophilic environment the surface is unable to reorganise sufficiently to fully mask its hydrophobic nature, due to the lack of hydrophilic material in the surface / sub-surface.

The difference in both the advancing and receding contact angle between the non-wetting and wetting regions on the air-cured lens and respective regions on the nitrogen-cured lens show marked differences between the lens types. The nitrogen-cured lenses show minimal change in the measured advancing and receding contact angle between the two regions suggesting the presence of a surface with homogenous wetting characteristics. For the air-cured lens both the advancing and receding contact angles differed significantly between the wetting and non-wetting regions, confirming the presence of a heterogeneous lens surface. Although statistical analysis of the data on the air-cured lens showed both the advancing and receding contact angle values were significantly higher in the non-wetting region, observation of the individual measurements suggests that not all lenses follow that trend (Figure 3.20). Four of the ten air-cured lenses gave measurements which showed no apparent reduction between the two regions (with two lenses actually recording a higher advancing contact for the wetting region). In contrast the receding contact angle measurements for all the air-cured lenses showed a difference between the wetting and non-wetting regions, with the wetting region always giving the lower receding contact angle value. Another interesting observation from Figure 3.20 is an apparent trend suggesting that the higher the receding contact angle value in the non-wetting region, the lower the value in the wetting region. By plotting the receding contact angle for the non-wetting region against the receding contact angle for the wetting region, Figure 3.21 is obtained. By adding a line of best fit it is apparent that there is a trend of reducing receding contact angle on the wetting region with an increasing receding contact angle on the non-wetting region. A possible cause for this finding is macro-scale phase separation at the surface of the air-cured study lenses. Where this phase separation is most marked, the non-wetting regions would be primarily composed of hydrophobic siloxane macromer, whereas the wetting regions would be composed primarily of hydrophilic monomer. Given the ability of hydrogel materials to reorganise and present a hydrophilic surface when fully hydrated, it

suggests that these materials with elevated receding contact angles are relative rich in the siloxane macromer, to the point where insufficient hydrophilic polymer components are present to mask its underlying hydrophobic nature.

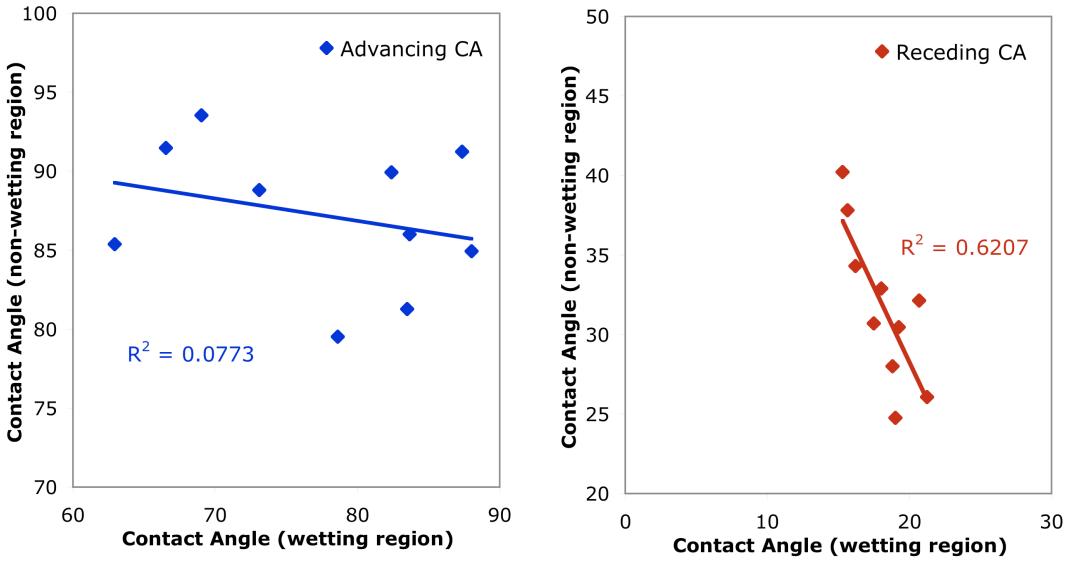

Figure 3.21: Receding contact angle (non-wetting region) against receding contact angle (wetting region) and advancing contact angle (non-wetting region) against receding contact angle (wetting region).

The advancing contact angle results appear to present a less clear trend with some lenses showing no reduction and other air-cured lenses showing large reductions in advancing contact angle between the two study regions. Given the increased levels of siloxane macromer likely present at the surface of the non-wetting regions it is perhaps surprising that a less clear trend is observed, as the advancing contact angle is more typically associated with the presence of the more hydrophobic components in the material. The results may be complicated by other factors such as the molecular weight and the cross linking density of the polymer in these regions as well as the extent of surface dehydration of the material during the advancing phase. What is apparent is that the receding contact angle appears more sensitive to the subtle changes between both lens type and lens region in this study and is more consistently able to differentiate between regions which possess markedly different clinical performance.

Although the air-cured experimental contact lenses exhibited obviously different surface properties to commercial contact lenses, they allowed an investigation into the critical factors for the surface wetting characteristics of contact lens materials. There is little in the literature which has looked at the wetting characteristics of poorly wettable contact lenses. Hiratani *et al.* (2003) looked at the use of water-soluble moulds to manufacture silicone elastomer lenses and showed that unmodified PDMS-related materials manufactured in polypropylene moulds produced a relatively hydrophobic surface with a captive bubble static contact angle in the 30 to 40 degrees range. Their value is in agreement with the findings of this study where the mean receding contact angle for the air-cured non-wetting was 31.7 degrees. Hiratani *et al.* (2003) also used XPS analysis to show that the lens surface was dominated by the PDMS-based material, in agreement with the conclusion of this PhD study, where the air-exposed non-wetting regions on the air-cured lens appear composed predominantly of the siloxane macromer (Section 4.1.1.3). The nitrogen-cured lens, in contrast, was shown to have properties similar to many of the commercially-available lenses with a receding contact angle value typically in the 16^o to 24^o range and a mean receding contact angle of around 18^o. The advancing contact angle measured on the nitrogen-cured lens material is also within the range of commercially-available materials, although there appears a greater measurement variability than that observed for the receding contact angle data. The non-wetting region of the air-cured lens, in contrast, falls outside the contact angle range typically observed for commercially-available lens material with respect both to the advancing and receding contact angle, thus making it difficult to interpret which is the most significant *in vitro* predictor of clinical contact lens wetting.

In vitro contact angle measurements are commonly used to characterise polymeric materials, but their application to biomaterials is complicated by the fact that these materials surface characteristics are often altered by contact with the biological system. When a contact lens material is placed onto the ocular surface and into the tear film, the material is rapidly deposited with tear film components. These tear film components have been shown to result in changes to the surface wetting properties of contact lens materials both *in vitro* (Cheng *et al.*, 2004) and *in vivo* (Tonge *et al.*, 2001). Future work should therefore investigate not only the lens material in a virgin state, but also the wetting characteristics of the lens material following wear to better understand how this deposition process influences subsequent clinical performance.

In summary, the development of the dynamic captive bubble contact angle analyser allows rapid and repeatable contact angle measurements to be made in a hydrated environment at any point across the surface of a contact lens. The nitrogen-cured lens gave consistent advancing and receding contact angle measurements across its lens surface and these measurements were within the range shown by commercially available contact lenses. In contrast, both the advancing and receding contact angle values for the non-wetting region on the air-cured study lenses were greater than that found for commercial contact lenses. When the wetting and non-wetting regions on the air-cured lenses were compared the difference in the receding contact angle was greater both as a absolute and a percentage change, in comparison with that observed for advancing contact angle between the two regions. The wetting regions on the air-cured lenses possessed similar receding contact angle measurements but larger advancing contact angle measurements ompared with the nitrogen-cured lenses, suggesting intermediate wetting characteristics between the non-wetting regions on the air-cured lens and the nitrogen lens. The receding contact angle is shown in this study to be the most consistent *in vitro* predictor of initial clinical performance, although it is likely the advancing contact angle also provides useful information relating to the surface properties of the contact lens when in an air-exposed state.

3.4.5 Conclusion

The ability of a contact lens material to allow a tear film to spread and maintain itself across the anterior surface of a contact lens during wear is critical in providing the wearer with clear vision, high levels of comfort and in minimising significant tear film deposition (Jones *et al.*, 2006). Contact angle analysis is a standard laboratory method employed to investigate the wetting characteristics of surfaces and was applied in this study to analyse a range of commercially available and experimental contact lens materials. Static contact angle measurements on contact lens materials gave a wide range of advancing contact angles (15^o to 90^o), whereas receding contact angles were within a much more limited range (15^o to 25^o) and were generally in good agreement with the literature. The high levels of contact angle hysteresis observed for some of these these materials have been reported in the literature and are thought to relate to the ability of the hydrogel surface to change its free energy through reorientation of the polymer side chains and chain segments depending on the nature of the environment adjacent to the polymer surface. Where contact lenses undergo a surface treatment which limit this reorganisation, the hysteresis was found to be

comparatively low (Maldonado-Codina & Morgan, 2007), supporting this general theory. The inclusion of siloxane-related polymers into contact lens materials has the tendency of increasing hysteresis due to the highly flexible silicon-oxygen polymer backbone, which readily allows reorganisation of the surface. This reorganisation is driven by the nature of the environment surrounding the polymer, where when exposed to a non-polar fluid such as air, the surface reorganises to present the hydrophobic methyl groups extremely efficiently, whereas when exposed to an aqueous fluid the surface readily reorganises to present more hydrophilic species at the surface. The challenge for contact manufactures has been to develop materials with sufficient siloxane material to boost oxygen transmission, while maintaining acceptable levels of surface wettability typical by either surface treatment or inclusion of hydrophilic monomers.

In an attempt to better understand how the *in vitro* surface wetting characteristics of a contact lens material influence its clinical performance, this PhD has looked to investigate the repeatability of the existing contact angle methodology and where necessary has sought to develop new instrumentation to overcome experimental limitations and to subsequently apply these techniques to a range of both commercially-available and experimental study contact lenses.

Although contact angle measurements have been used for many years to characterise the surface wetting properties of polymer materials a through investigation of the repeatability of these measurements on hydrogel contact lens materials had not been undertaken. This PhD study therefore sought to improve understanding in this area and to refine methodology to minimise these errors. The results of this study not only suggest the level of confidence that can be achieved for these measurements, but also informs us about factors such as the effect of repeated measurements on a sample surface and the relative influence of blotting on different contact lens surfaces and thus allows improved understanding of these techniques and how these tests should be applied to hydrated materials.

Static contact angle measurements, although useful, are limited in the information they provide and the process of lens surface blotting was shown to influence the measurements obtained. A dynamic captive bubble technique was therefore developed which maintained the contact lens in a fully hydrated state while allowing the dynamic wetting properties of a

contact lens to be investigated. This involved the development of both the instrumentation and computer software to allow automated data analysis, required for rapid and repeatable dynamic contact angle measurements. By analysing a wide range of commercially-available silicone hydrogel contact lens materials the measurement of dynamic contact angle values was possible for a wide range of commercially-available materials, allowing direct comparison of these measurements with the results from the experimental study contact lenses. Following analysis of data from the clinical study (Section 2.1), it became apparent that the wetting properties of the air-cured study lens varied across the lens surface, requiring the development of the *in vitro* contact angle analyser to map out areas of non-wetting on the anterior surface of the air-cured study contact lens. Following this development, the instrument was further modified to allow analysis at any point across the lens surface, allowing targeted regions to be analysed. This targeted dynamic contact angle technique has been able to show clear differences between the three regions of interest on the study contact lenses and has answered, in part, the role these *in vitro* measurements can play in predicting the clinical performance of contact lenses.

This PhD work suggests that an elevated receding contact angle may be considered a more consistent predictor of poor initial clinical wettability, than the advancing contact angle. This is likely associated with the relatively powerful blinking action of the eye which forces the tear film, primarily present in the tear meniscus, across and into contact with the anterior surface of the contact lens. The process which then dictates whether the tear film remains stable over the lens surface or results in the formation of dry spots is more analogous to the development of a receding contact angle, as described by Cheng *et al.* (2004). This is not to suggest that the advancing contact angle is not also an important factor, as a value substantially higher than that observed for commercial lenses may still result in an incomplete coverage of the anterior lens surface during the blinking process and thus may influence factors such as the quality of the tear film or the ease with which the lids pass over the anterior lens surface (potentially influencing factors such as comfort). The *in vitro* wetting characteristics of a lens material is only likely to influence the lens clinical wetting for a short period, as the lens undergoes deposition by the tear film within the first few minutes of wear (Tonge *et al.* (2001)). The subsequent wetting process is then likely dominated by patient dependant variables (such as blink rate, tear production and drainage and tear chemistry) and the interaction of tear film

components with the lens surface and the associated bioconversion of the lens surface. A stable initial tear film, is likely critical in allowing advantageous tear film deposition on to the contact lens surface while minimising the deposition of hydrophobic components.

Improvements in the understanding of contact angle measurements and the development of new instrumentation during this PhD study has allowed a thought investigation to be performed on the experimental study contact lens. It is evident that in the non-wetting regions on the air-cured study lenses both the advancing and receding contact angle measurements seemed higher (mean difference 10^o) than that found on both the nitrogen-cured lens surface and on all commercially available contact lenses investigated. The nitrogen-cured contact lens surface gave values for advancing and receding contact angles within the range of commercially available contact lenses and consistent across the lens surface, although the magnitude of the hysteresis was similar to that found for the air-cured contact lens. The wetting regions on the air-cured lens seem to possess characteristics between those of the other two lens regions with receding contact angle measurements similar to the nitrogen-cured lens and advancing contact angle measurement between the values found for the nitrogen-cured lenses and the non-wetting region on the lens surface. An apparent trend when comparing the wetting and non-wetting regions on the air-cured lens is that when the receding contact angle is elevated on the non-wetting region, it is typically lower on the wetting region and *vice versa*. When this finding is considered in conjunction with the contact angle values for the non-wetting region of the air-cured lens, which were similar to that of a primarily siloxane-related polymer, there is a suggestion that what is being observed is a degree of phase separation of the polymer components on a macro scale across regions of the surface of the air-cured lens. In contrast, the nitrogen-cured lens appears to exhibit no such macroscopic phase separation. The cause of this apparent phase separation at the polymer surface is clearly associated with the presence of one of the gases in the atmospheric air, which subsequently influences the polymer during the curing process. Atmospheric air is composed primarily of nitrogen (approximately 70%) and oxygen (approximately 20%) and as a nitrogen-purged environment results in no surface wetting problems, it is obvious that the likely component in air influencing the radical polymerisation process is oxygen. The interaction of atmospheric oxygen during the polymerisation of the contact lens material is clearly influencing the distribution of the components within the polymer, resulting in the seemingly random distribution of non-

wetting regions across the surface of these air-cured contact lens. In future chapters of this thesis a range of surface analysis tools are utilised in an attempt to better understand this process and improve understanding of how polymerisation conditions influence the clinical performance of the contact lenses produced.

Chapter 4

Chemical characterisation of contact lens materials

4.1 Introduction to the XPS studies

Given that the study lenses were shown to possess poor clinical and laboratory wetting properties (Chapter 2), the lens surface chemistry was an important characteristic to investigate.

Given the poor clinical (Chapter 2) and laboratory wetting properties (Chapter 3) of the study lenses, it was apparent that lens surface chemistry was an important characteristic to investigate. This is because the wetting characteristics of a surface are determined soley by the chemistry within the first few molecular layers (Johnson & Dettre, 1993). In addition to analysing a range of contact lens materials, the moulds used to manufacture the experimental study lens were also investigated as they formed the surface of the study lenses. XPS analysis was therefore used to investigate the surface chemistry of virgin (unused) and used moulds in an attempt to understand how they might influence the surface chemistry of the contact lens. Perhaps as important as the initial contact lens surface chemistry is the surface chemistry of the lens following a period of wear. This is due to deposition of tear film components onto the lens surface which can significantly change its surface chemistry (McArthur *et al.*, 2001) and wetting properties (Tonge *et al.*, 2002). The surface chemistry following a period of wear was therefore investigated as part of the XPS study. A drawback of XPS analysis on polymeric materials is that the surface must be exposed to a ultra high vacuum environment. XPS analysis of hydrogel materials

therefore typically requires the sample material to be in a dehydrated state, often resulting in significant changes to the surface chemistry of the sample (Hook *et al.*, 2006). Part of this study therefore looked to develop a cryogenic handling technique which would allow the lens sample to remain in a hydrated frozen state and therefore minimise any changes in the surface chemistry resulting from exposure to a high vacuum environment.

The XPS analysis was divided into three discrete experiments:
Study 1 - XPS analysis of both commercially-available and experimental contact lenses in a dehydrated state.
Study 2 - XPS analysis of (i) polypropylene contact lens moulds used to manufacture the experimental contact lenses and (ii) worn study contact lenses.
Study 3 - XPS analysis of unworn study contact lenses using a cryo-sampling handling technique.

4.1.1 General materials and methods

4.1.1.1 Study materials

The samples analysed using the XPS system included commercially-available and experimental contact lenses and the moulds used in the manufacture of these experimental lenses. All contact lenses were provided in plastic blister containers covered with a heat sealed aluminium foil. All contact lenses were soaking in buffered saline (0.9% sodium chloride) solution, with the commercially-available contact lenses also including additional agents such as surfactants and viscosity agents.

4.1.1.2 XPS instrumentation

XPS analysis was undertaken using a Kratos Axis Ultra instrument (Kratos Ltd, Manchester, UK) located in the School of Materials at The University of Manchester. This instrument utilises a magnetic immersion/electrostatic lens, spherical mirror analyser for energy filtered imaging and a channel plate/delay line detector for pulse-counting electrons. Charge build-up at the sample surface was minimised using a low-energy electron flood source. Spectra were acquired using a monochromatic Al Kα X-ray source operating at 150 W. The base pressure of the instrument was 2 x 10^{-9} Torr.

4.1.1.3 XPS analysis

Wide scan spectra were acquired for elemental quantification, and high energy resolution spectra for chemical state determination were recorded through the C 1s, O 1s, N 1s, Si 2p and F1s photoelectron regions. Wide scan spectra were acquired for a 500 μm by 500 μm analysis area, at a pass energy of 160 eV and for a binding energy range of 1100 eV to 0 eV, with a 0.4 eV step size and with a dwell time of 500 ms. The spectroscopic data were quantified by measuring the photoelectron peak areas after correcting for the intensity/energy response of the instrument determined using the NPL procedure (Seah, 2003). Theoretically determined relative sensitivity factors (Walton & Fairley, 2006b) were applied to the XPS data. Curve fitting was carried out on the high energy resolution spectra from the C 1s, O 1s and Si 2p photoelectron regions to resolve overlapping peaks, and the data were corrected for charging effects by reference to the carbon peak at 285.0eV binding energy. All data processing was performed using CasaXPS version 2.3.11.7. Statistical analysis of the data were performed using multivariate ANOVA with significance taken at $P < 0.05$.

4.1.1.4 Procedures to minimise surface contamination

In all three XPS studies precautions were taken to minimise surface contamination. Powder-free nitrile gloves (Sempermed, USA) were worn during sample preparation and handling. The tweezers and punching instrument used to handle the contact lens samples were cleaned with 100% ethanol, rinsed copiously with HPLC grade water (Sigma-Aldrich) and left to air dry. Prior to analysis, the XPS instrument was dismantled and carefully cleaned internally. The instrument was then rebuilt and baked out for 12 hours to reduced to a minimum any contamination of the vacuum.

4.2 Study 1 - XPS analysis on dehydrated lens samples

4.2.1 Study 1 - Materials and methods

Three commercially-available contact lenses types were analysed, two silicone hydrogel materials and one polyHEMA material. The two silicone hydrogel contact lenses studied were balafilcon A and lotrafilcon A. The polyHEMA contact lens used in the study was polymacon A. The chemical composition of these contact lens materials are proprietary,

but the USAN registered components of balafilcon A, lotrafilcon A and polymacon A are highlighted in Table 4.1. All three lens materials are cast moulded with both of the silicone hydrogel materials requiring plasma surface modification to enhance their surface wetting characteristic. Lotrafilcon A undergoes a nitrogen-based plasma surface coating and balafilcon A a plasma oxidation surface treatment (Tighe, 2004), whereas polymacon A does not require surface treatment. These lenses were chosen as they have previously undergone investigation with XPS (Karlgard *et al.*, 2004) and therefore could act as control materials and allow comparison of expected chemistry with experimental findings. The selection of several commercial lenses also allowed comparison of lens materials known to possess good clinical performance (i.e. the commercial and nitrogen-cured lenses) with that of a lens material known to possess poor clinical performance (air-cured study contact lenses), in an attempt to better understand the critical surface chemistry requirements of a contact lens material, required to provide advantageous clinical wetting properties. Each lens was removed from its packaging with tweezers, touching only the very edge of the lens, and soaked in HPLC grade water (Sigma-Aldrich Ltd., UK) for 24 hours to remove the saline solution and any other blister packaging solution additives to avoid contamination of the surface following dehydration. A round lens sample (4mm diameter) was then punched from the centre of each commercial contact lens and from the three regions of interest on the experimental study lenses, identified using the laboratory technique detailed in Section 2.2.3.3. Each punched sample was then mounted on the XPS sample bar using PDMS-free double-sided adhesive tape, with the front lens surface facing upwards. For each commercial lens type, one sample was analysed and for each study lens region, three lens samples were analysed, giving a total of nine experimental contact lens samples (nitrogen-cured x 3; air-cured 'wetting region' x 3; air-cured 'non-wetting region' x 3). A minimum amount of adhesive tape and contact lens material was used to reduce the amount of water within the chamber allowing a vacuum to be achieved more rapidly. Once the specimens were mounted, the sample bar was locked into position in the preparation chamber and then pumped down to $1x10^{-8}$ torr. The samples were left in the preparation chamber overnight to ensure a high vacuum was present prior to introduction into the analysis chamber. Analysis was then performed as detailed in Section 4.1.1.3 using the Kratos Axis Ultra instrument. Statistical analysis was performed as detailed in Section 4.1.1.3.

Table 4.1: Properties of the commercial study contact lenses.

Lens type	Brand name	Principle monomers	Dk	EWC (%)	Surface treatment
balafilcon A	PureVision	NVP, TPVC, NVA, PBVC[1]	91	33	Plasma oxidation
lotrafilcon A	Night & Day	DMA, TRIS, fluorine-containing siloxane macromer[2]	140	24	Plasma coating
polymacon	Sauflon 38	HEMA	38	38	None

4.2.2 Study 1 - Results

4.2.2.1 Commercially available contact lenses

Figure 4.1 shows the wide spectrum surveys for the surface of polymacon A, lotrafilcon A and balafilcon A materials, highlighting the characteristic peaks in the spectrum associated with different elements on the contact lens surface. The polymacon A lens surface, as expected, showed strong peaks characteristic of C 1s (285 eV) and O 1s (530 eV) and also smaller peaks related to Si 2p (103 eV) and N 1s (400 eV). The balafilcon A and lotrafilcon A materials both showed prominent photoelectron peaks for C 1s, O 1s and N 1s. The Si 2p peak was observed for both balafilcon A and lotrafilcon A samples, although for the latter this was less prominent. A small Na 1s photoelectron peak was also observed on the surface of both silicone hydrogel materials, but not on surface of polyHEMA. Table 4.2 shows the elemental surface composition expressed as an atomic percentage, with the elements not in the theoretical composition of the material, highlighted in red. The C:O ratio for polymacon A, lotrafilcon A and balafilcon A using the XPS elemental data was 3.06, 5.40 and 3.38 respectively.

High resolution scans of the elemental peak regions were also performed and analysed. Figure 4.2 shows the high resolution spectrum (red line) of the C 1s envelope for polymacon A, with the contributing components from different functional groups highlighted (black peaks). Figure 4.3 shows the high energy resolution C 1s envelope overlaid for lotrafilcon A, balafilcon A and polymacon A. The polymacon A spectrum shows characteristic peaks at around 287 eV and 289 eV in addition to the major peak at 285 eV which relate to the single and double bonding of carbon to oxygen as well as the saturated carbon atom

[1]NVP: N-vinyl pyrrolidone; TPVC: tris-(trimethyl siloxysilyl); NCVE: N-carboxyvinyl ester; PBVC: poly(dimethysiloxy)di(silylbutanol)bis(vinyl carbamate).

[2]DMA: N, M-dimethylacrylamide; TRIS: tris-(trimethyl siloxysilyl).

Table 4.2: Elemental surface composition (atomic percentage) of soft contact lens materials by XPS analysis, with elements not theoretical present in red.

	C 1s	O 1s	N 1s	Si 2p	F 1s	Na 1s
polymacon A	73.5	24.0	0.6	1.9	0.0	0.0
lotrafilcon A	75.0	13.9	9.3	1.4	0.0	0.4
balafilcon A	65.3	19.3	6.9	7.2	0.0	0.5

(Figure 4.2). In contrast the balafilcon A and lotrafilcon A samples show a lesser peak in these regions with a peak more evident at around 288 eV, highlighting the differences in the carbon bonding between the materials. Figure 4.4 shows the high resolution C 1s XPS spectra for balafilcon A where the envelope has been fitted using 4 component curves labeled C1 to C4. The C1 peak at 284.9 relates primarily to C-C, C-H and C-Si, the C2 peak at 286.2 relates to C-O and C-N, the C3 peak is related to CNO and the C4 peak relates to COO, CNOO and COOO. The C 1s chemical shifts observed are in general agreement with that expected for balafilcon A from its known composition (Karlgard *et al.*, 2004). Figure 4.4 also shows the high resolution C 1s XPS spectra for lotrafilcon A where the envelope has been fitted using five component curves labelled C1 to C5. The C1 peak at 285.0 eV relates to C-C, C-H and C-Si, the C2 peak at 285.9 eV relates to C-N, the C3 peak at 286.7 relates to C-O, the C4 peak at 288.0 eV relates to CNO and the C5 peak relates to CNOO and COO.

4.2.2.2 Experimental contact lenses

Figure 4.5 shows the wide scan XPS spectra for the nitrogen-cured lens and for the wetting and non-wetting regions of the air-cured contact lens. It is apparent that all three lens surface types produced similar spectra, with strong peaks characteristic of C 1s (285 eV) and O 1s (530 eV) and also smaller peaks related to Si 2p (103 eV) and F 1s (689 eV). Figure 4.6 shows the percentage elemental surface composition for the three different lens regions. A multivariate ANOVA showed no significant difference in elemental composition between the three lens regions for any of the elements ($F=0.0259$, $p = 0.97$). High resolution data for the carbon, oxygen and silicon elements is shown in Appendix C (Figure C.1 and C.2). Statistical analysis of the high resolution data showed no significant difference between the three lens regions ($F=0.0381$, $p=0.968$).

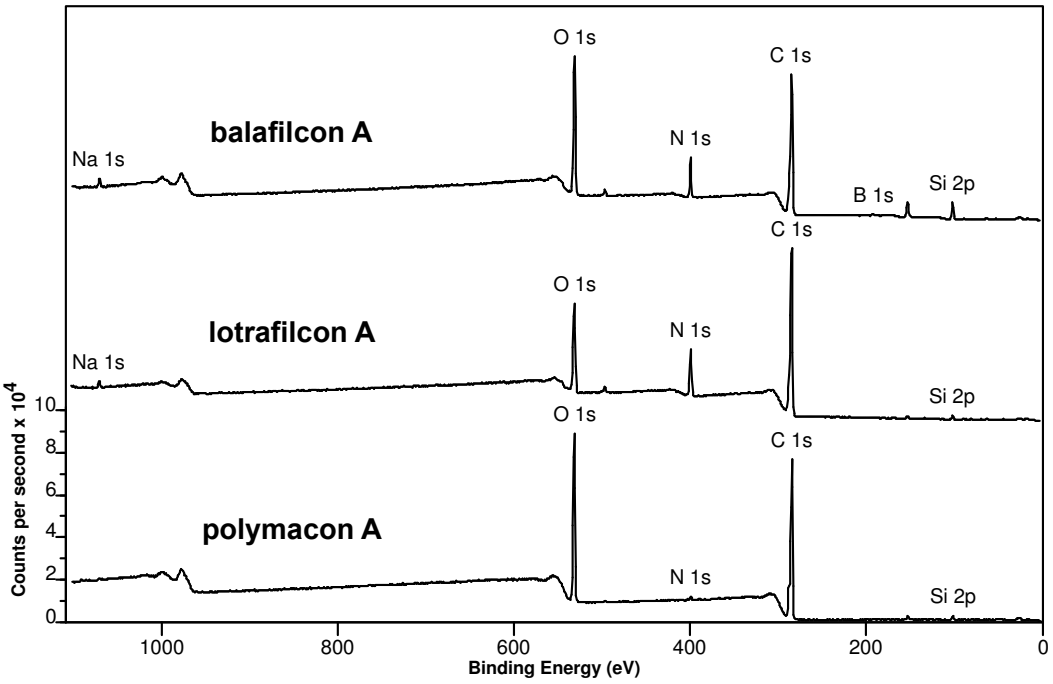

Figure 4.1: Wide scan survey photoelectron spectrum for polymacon A, balafilcon A and lotrafilcon A contact lens materials (data overlaid to allow comparison).

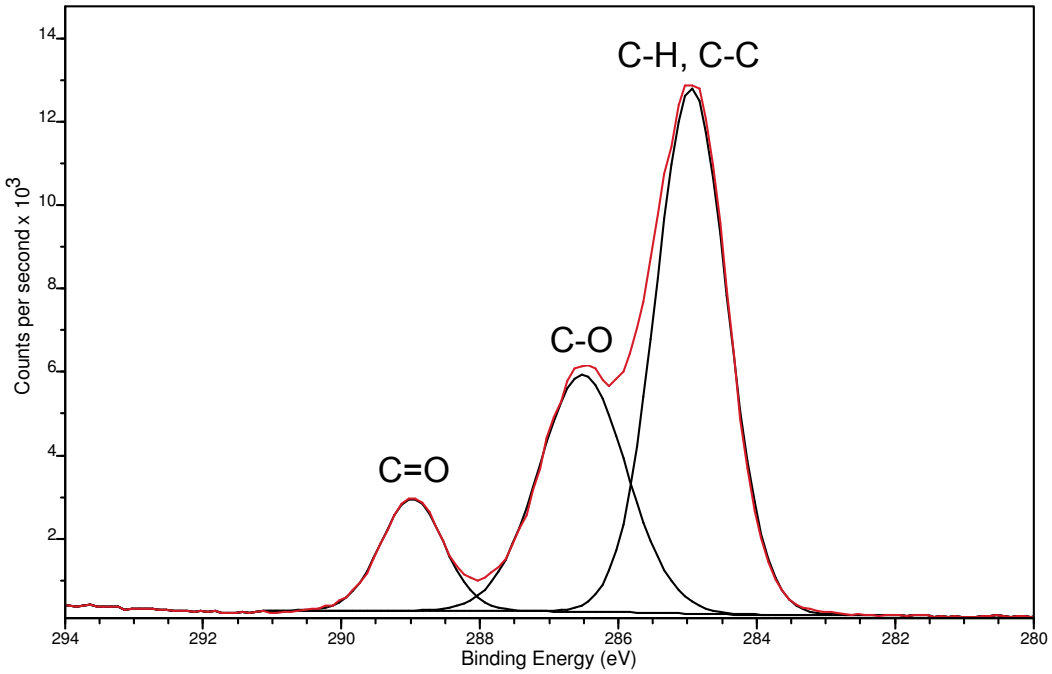

Figure 4.2: High resolution C 1s spectrum for polymacon A (red line) with peak fitting performed (black lines).

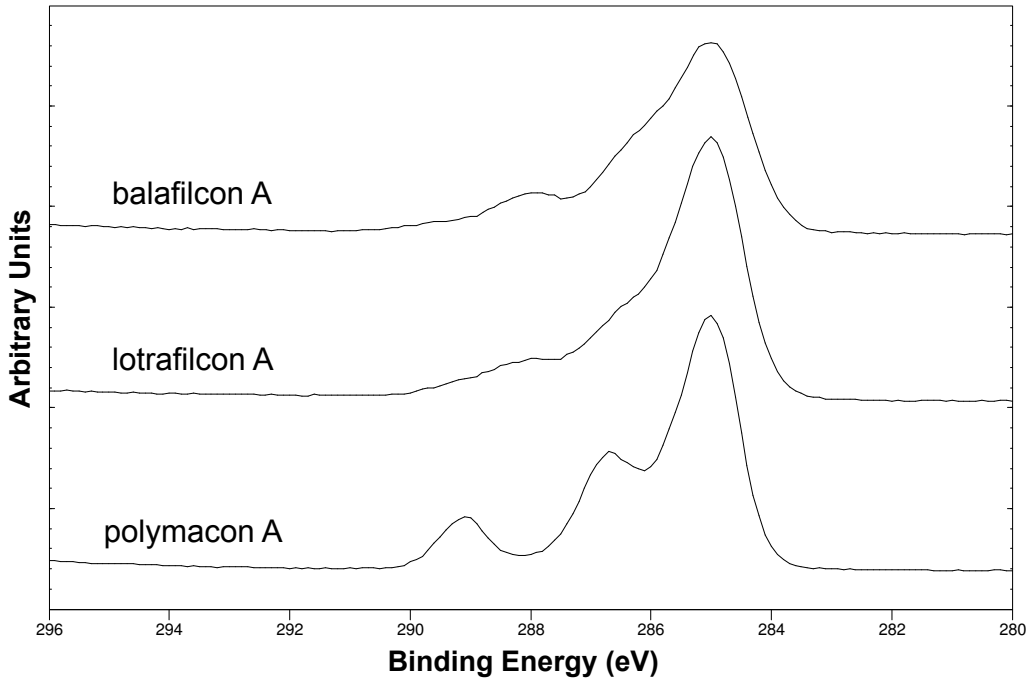

Figure 4.3: High resolution C 1s XPS spectra for polymacon A, lotrafilcon A and balafilcon A (data overlaid to allow comparison).

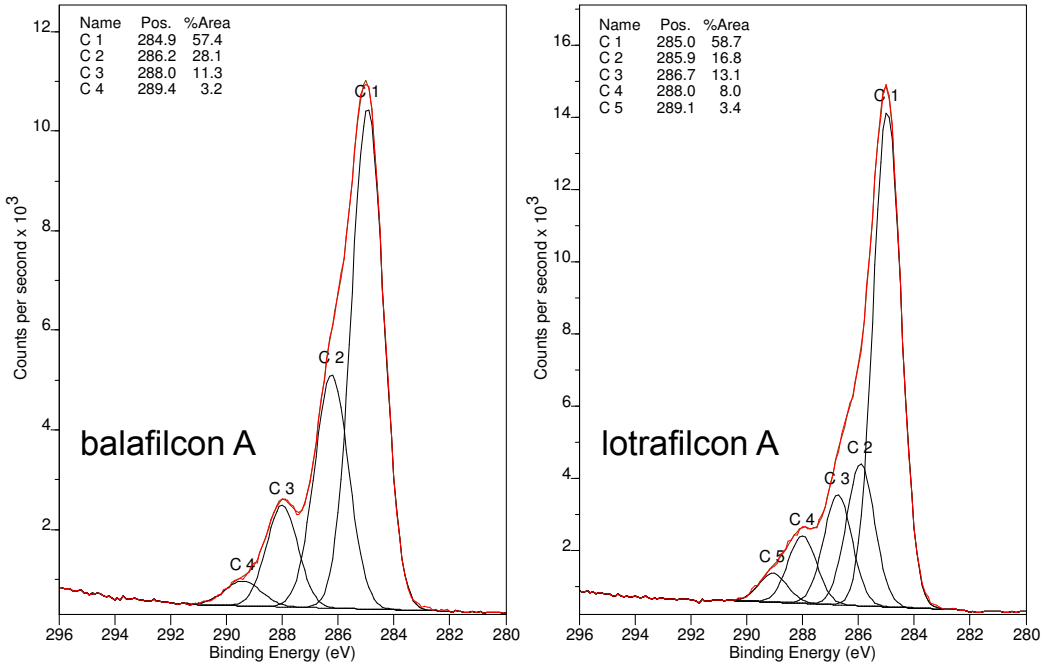

Figure 4.4: High resolution XPS spectra in the C 1s region (red line) for balafilcon A and lotrafilcon A with curve fitting applied and components highlighted (C1-C5).

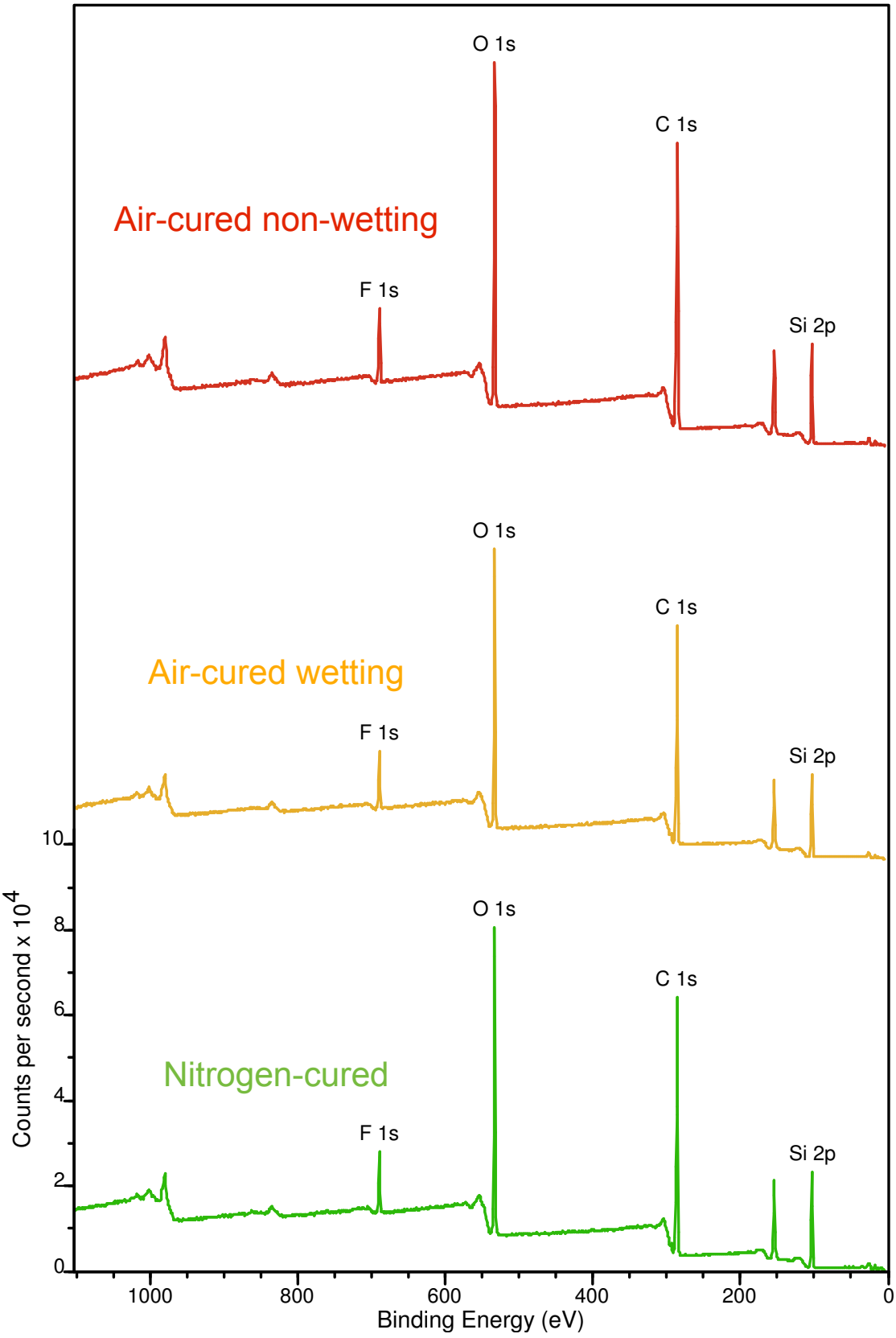

Figure 4.5: Wide scan XPS spectra for the nitrogen-cured and wetting and non-wetting regions of the air-cured lens (data overlaid to allow comparison).

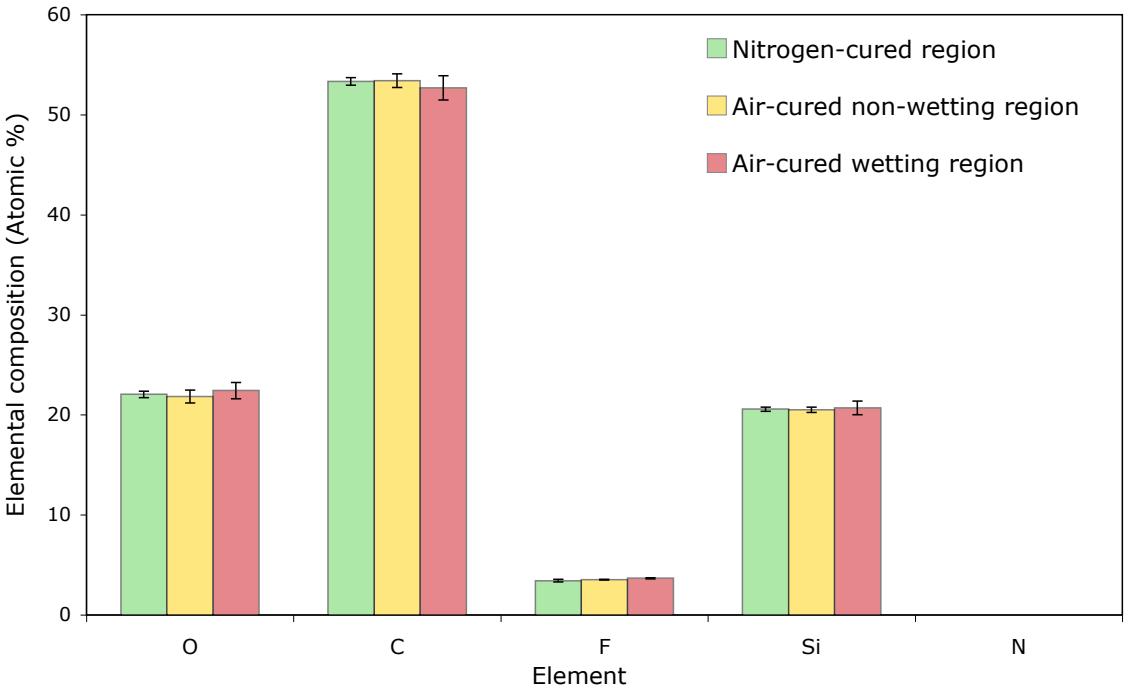

Figure 4.6: Percentage elemental composition for the three regions of interest on the experimental study contact lenses (± SD).

4.2.3 Study 1 - Discussion

4.2.3.1 Commercially available contact lenses

Both balafilcon A and lotrafilcon A materials undergo a surface treatment following cast moulding to improve their surface wetting characteristics (Tighe, 2004). The elemental composition detected at the surface of these contact lenses is therefore not in agreement with what we might expect to find given their known bulk polymer chemistry (Table 4.1). The lotrafilcon A material undergoes a nitrogen-based plasma coating process which results in a 25nm thick polymer film on the surface of the lens matrix. Although the elemental surface composition of lotrafilcon A detected using XPS is in agreement with what is expected given what is known about the material (Tighe, 2004), it appears to differ in percentage terms to a much greater extent than might be expected compared with the results of previous XPS studies (Karlgard *et al.*, 2004). This apparent difference may relate to changes in lens design or manufacture since the previous paper was published or may be associated with differing experimental methodologies. This PhD study also showed a low concentration of silicon present at the lens surface for the commercial lenses in agree-

ment with the literature (Bruinsma *et al.*, 2001; Karlgard *et al.*, 2004; Maldonado-Codina *et al.*, 2004a). No carbon-fluorine bonding was evident in the C 1s envelope, which was in agreement with the lack of fluorine in the calculated surface elemental composition, but different to that expected given the known composition of the material. The absence of a fluorine signal on the lens surface is likely due to the plasma surface polymer coating, which masks the underlying fluorine-containing contact lens bulk. This also explains why for a material which is known to contain relatively high levels of a siloxane-based polymer (due to the high oxygen transmissibility of the material), very little silicon is present on the lens surface. The balafilcon A material undergoes a plasma oxidation process, resulting in increased surface cross-linking and the formation of glassy islands where the organic silicone is converted into inorganic silicate (González-Méijome *et al.*, 2009). These highly wettable silicate islands therefore partially mask the underlying hydrophobic bulk, although they do not cover the entire surface of the material, leaving regions of unmodified or partially modified silicone at the surface (Tighe, 2004). The silicon found at the surface of balafilcon is therefore likely to be a combination of unmodified silicone and inorganic silicate, seen in the XPS data as the complex multiple peak fitting in the high resolution Si 2p spectrum (Appendix C.2). The presence of silicone at the surface (although reduced by the plasma oxidation process) is the likely reason for the larger advancing contact angle values measured in the laboratory for balafilcon A (Maldonado-Codina & Morgan, 2007), although clinical wetting with this material has been shown to be clinically acceptable (Brennan *et al.*, 2002). Previous XPS analysis of the balafilcon A material (Karlgard *et al.*, 2004) gave similar findings to this PhD study with elemental surface composition differing by less than 2%. The lotrafilcon A (nDMA and nitrogen-based plasma coating) and balafilcon A (NVP) materials both contain monomer components which are nitrogen-based explaining the presence of nitrogen on the surface of these lenses. The presence of sodium is likely to be related to the saline (sodium chloride) solution which these lenses were soaked prior in to analysis. The boron peak present for the balafilcon A material is probably related to the borate-buffered saline used in the packaging solution of balafilcon (both lotrafilcon and polymacon use a phosphate buffered saline). The detection of elements from the packaging solution on the surface of the silicone hydrogel contact lens materials following soaking in pure water, is probably related to the lower ion-permeability of these materials in comparison with polyHEMA type materials (Austin, 2009). This may result in ions taking longer to migrate out of the materials during soaking and thus if still present within

the material during dehydration may be detected on the lens surface. To minimise this effect a longer soaking time should be considered to allow more complete removal of the soaking solutions. Nitrogen was also found at a much lower concentration on the surface of the polyHEMA lenses where it is not an intended component and is likely related to an additive from the mould, such as N,N-ethylene bis stearamide, which is often used as an antistatic agent in polypropylene (Cotton *et al.*, 1991). The presence of trace levels of nitrogen in polymacon A materials has also been reported by others (Hart *et al.*, 1993; McArthur *et al.*, 2001). Although in theory no silicon should be present in polymacon A, previous studies have shown silicon is present on the surface of conventional HEMA-based hydrogels which is usually attributed to impurities in the manufacturing process (Grobe *et al.*, 1996; Hart *et al.*, 1993; Maldonado-Codina *et al.*, 2004a). In agreement with these findings, this study detected similar levels of silicon on the surface of polymacon samples.

High resolution C 1s spectra for the three commercial contact lens materials demonstrated a markedly different shape (Figure 4.3), due to the different contributing components from different functional groups. Peak fitting in the C 1s region for the polymacon A material resulted in a three peak assignment with the major peak at 285.0 eV relating to C-C and C-H, and a secondary peak relating to C-O at 286.6 eV and C=O at 289.0 eV. The theoretical ratio of atomic concentration is 3:2:1 for C-C/C-H:C-O:C=O respectively, thus the actual percentage ratio should be 50% : 33% : 16%. The actual data from the polymacon material in this study showed a ratio of 59% : 31% : 10%. Reports in the literature are conflicting with some studies finding the exact 3:2:1 ratio (Griesser *et al.*, 1990), whereas others have found significant variations from the theoretical ratio (Karlgard *et al.*, 2004). These differences may be due in part to the differences in the purity of monomer components used for polymer preparation (i.e. some samples are produced commercially, such as these lenses, whereas other samples are produced using highly purified analytical grade components and moulded against extremely clean surface). Another factor may be that the surface is often not representative of the bulk chemistry and contaminants are most likely to segregate towards the surface of the polymer material.

Surface elemental concentrations of the different chemical states of C 1s for the balafilcon and lotrafilcon materials were determined by multiplying the fractional relative intensity by the carbon elemental concentration determined by the wide scan. The peak fit concen-

Table 4.3: Carbon peak fitting concentrations (atomic percentage) for lotrafilcon A and balafilcon A contact lens materials.

	Curve fitting data				
	C1	C2	C3	C4	C5
	C-C & C-H	**C-N**	**C-O**	**CNO & CNOO**	**COO**
lotrafilcon A	44.0	12.6	9.8	6.0	2.6
balafilcon A	37.5	18.3	7.4	2.1	0.0

trations are as detailed in Table 4.3. The carbon present on the surface of the lotrafilcon A material is primarily bonded to hydrocarbon material, although there is significant C-N, C-O, CNO, CNOO and COO bonding. Although similar in nature, the results of peak fitting in balafilcon suggest a lower concentration of carbon bonded to hydrocarbons, C-O and CNOO and a higher concentration of C-N bonding at the surface than lotrafilcon A.

4.2.3.2 Experimental contact lenses

XPS analysis of the dehydrated experimental contact lenses gave surface elemental composition somewhat different from their known bulk chemistry. The composition of the study contact lens material (Section 1.9) suggests that around 40% (by weight) of the polymer is composed of the macromer M3U, 40% (by weight) is composed of the monomer VMA and around 20% (by weight) composed of the monomer MMA. The element nitrogen is present both in the siloxane-based polymer M3U macromer and also in the hydrophilic monomer, VMA. It is evident that as elemental silicon was detected on the surface of all experimental study lenses, at levels much higher than the contamination levels observed on the other commercial contact lenses, M3U must be present on the surface (as M3U is the only monomer to contain silicon) and therefore elemental nitrogen would also be expected. The level of nitrogen in M3U can be estimated by studying the molecular formula in the Section 1.9. Here the F:N ratio should be 12:1 and the F:Si atomic ratio should be 1:5.75. From the XPS quantification data, the F 1s:Si 2p is as expected. From the F and Si concentrations the amount of nitrogen is expected to be about 0.3%. This is a relative small amount and on the limits of what an XPS instrument can detect, meaning that if there was any contamination over-layer, the nitrogen may no longer be detected. From the compositional information for the study contact lens material it would also be expected that the lens material was composed of around 40% (by weight) of VMA. Given the rel-

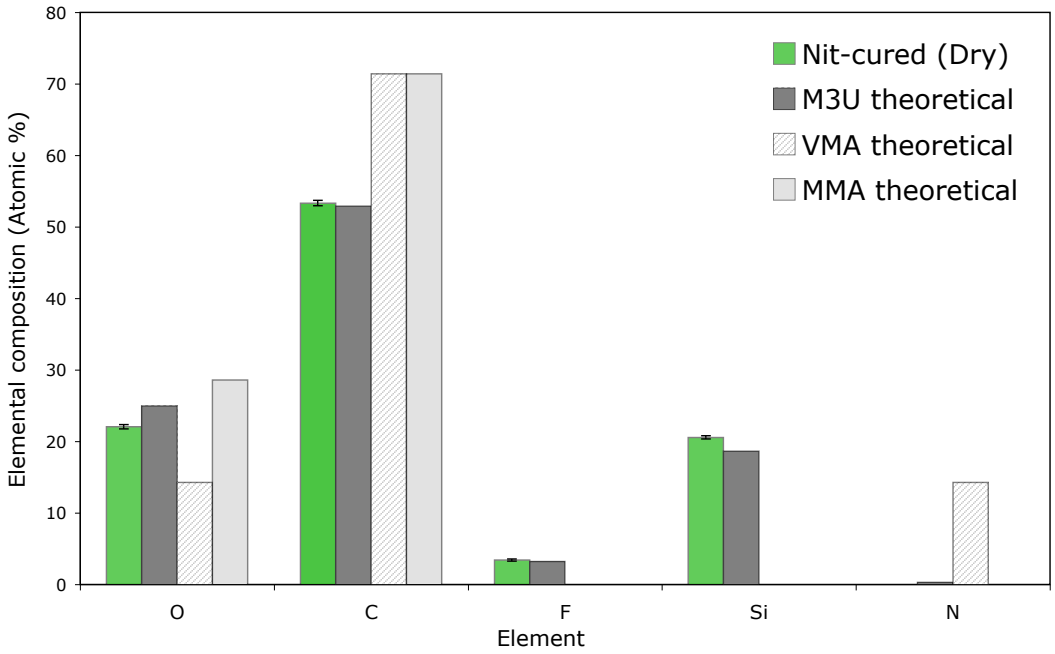

Figure 4.7: Comparison of experimental XPS elemental composition and theoretical values for three component monomers.

ative high levels of nitrogen-containing VMA it is surprising that no nitrogen is found on the surface of any of the experimental lens materials. VMA is the primary hydrophilic monomer present in these experimental contact lenses and low levels suggest a surface dominated by the more hydrophobic components such as M3U and/or MMA. Figure 4.7 is a comparison of the elemental composition of the nitrogen-cured lens surface with the theoretical elemental composition of the three major component monomers M3U, VMA and MMA. The only monomer to contain either silicon or fluorine is the monomer M3U. Figure 4.7 shows an experimental concentration of silicon and fluorine at similar levels to that of a surface composed entirely of M3U. In addition, no nitrogen was detected on any of the experiment lenses following dehydration suggesting no significant level of VMA was present at the surface. The concentration of carbon and oxygen at the surface of the experimental lens is more complex to interpret, since these elements are present in all the component monomers, but the composition is also similar to that for theoretical M3U composition.

The high resolution peak fitting in the C 1s, O 1s and Si 2p regions showed little difference for the three regions of interest on the surface of the study contact lenses (Appendix C.1).

The Si1 peak is associated with an electron emitted from Si $2p_{1/2}$ and the Si2 peak is from an electron emitted from Si $2p_{3/2}$. Thus the Si2 peak has half the intensity of the Si1 peak. Both of these peaks are associated with silicon bound to oxygen and in enfilcon A, this is found only in the silicone macromer (M3U). Dehydrated analysis of the nitrogen-cured lens surface (highly wettable surface), the wetting region of the air-cured lens (wettable surface) and the non-wetting region of the air-cured lens (non-wetting surface) using XPS appears unable to differentiate between these surfaces. This was an unexpected finding, given that the wetting properties are thought to be controlled by the chemistry of the very outer surface layers. It would therefore be expected that a highly surface-sensitive tool, such as XPS, would identify these differences either from the elemental or chemical state information it is able to provide. A clue as to why these surfaces appear so similar is given by the dominate siloxane signal, with a high silicon and fluorine signal detected and no detectable nitrogen signal. The chemical state data is also dominated by C-Si, and O-Si species, present only in the siloxane containing monomer. When comparing these experimental values to the theoretical values for the component polymers it is apparent that the experimental data closely resembles that of the silicone macromer M3U, with little evidence of the other component polymers being present at the contact lens surface in any significant quantity. As both clinical (Chapter 2) and laboratory wetting studies (Chapter 4) have shown that the wetting properties of these lens surface regions appear to vary significantly, this would indicate that their surface chemistry differs between these regions when in a hydrated state. This suggests the possibility that the siloxane macromer migrates to the surface during dehydration, as has been observed in previous studies on siloxane containing materials (Bousquet *et al.*, 2007; Oran *et al.*, 2004; Selby *et al.*, 1994). To investigate this more fully a cryogenic handling technique was developed to maintain and stabilise the surface in an attempt to avoid the possibility of polymer migration and this is discussed later in Section 4.4.

4.3 Study 2 - XPS analysis of lens moulds and worn lenses

4.3.1 Study 2 - Materials and methods

During the clinical study, heavy tear film deposition was observed on the non-wetting regions of the air-cured experimental contact lenses (Section 2.1.19.5). Figure 4.8 shows that for these experimental air-cured lenses deposition was clearly visible on the lens after

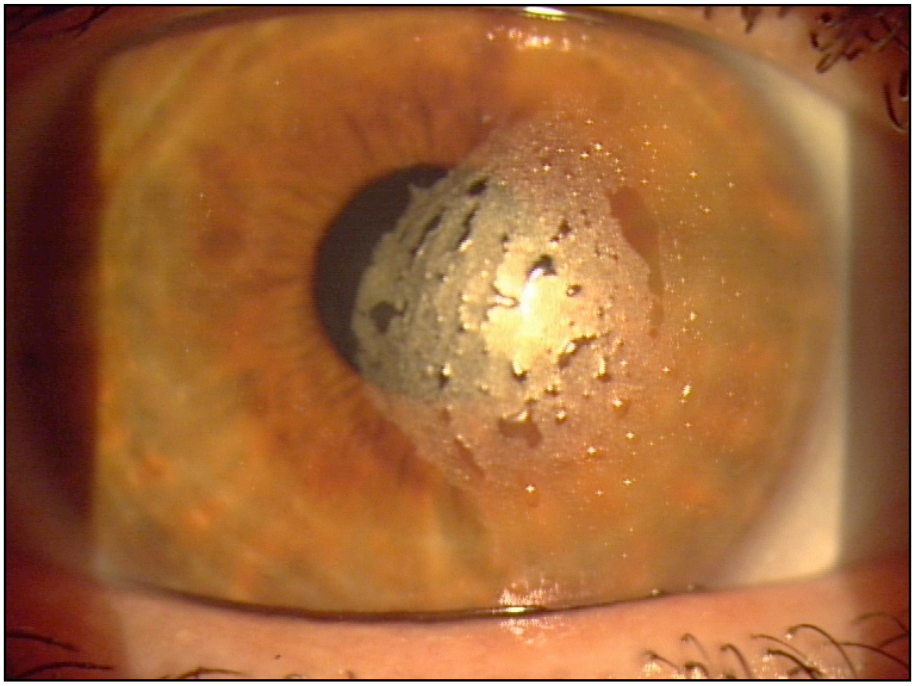

Figure 4.8: A non-wetting and heavily deposited region on an air-cured contact lens after 10 minutes of wear.

only 10 minutes of wear. Given this high level of tear film deposition on specific areas of the air-cured lens surface it was proposed to compare these deposited regions with the surface of worn nitrogen-cured lenses using the XPS instrument. A nitrogen-cured lens and air-cured lens were worn on a contralateral basis by an experienced contact wearer for 1 hour. The contact lenses were removed using powder-free nitrile gloves, touching only the very edge of the lens and following observation on a stereo microscope a 4mm punch was immediately taken from a heavily deposited area on the air-cured lens and a corresponding region on the nitrogen-cured lens. Three worn air-cured lens samples and three worn nitrogen-cured lens samples were analysed. These punched lens specimens were attached to the sample bar with PDMS-free double-sided adhesive tape. The sample bar was then loaded into the preparation chamber and pumped down to 1 x 10^{-8} torr overnight to ensure complete dehydration of the samples. Wide scan and high resolution XPS spectra were then obtained using the instrumentation and methodology detailed in Section 4.1.1.3. Statistical analysis involved a linear regression model with a Tukey post-hoc test applied where required.

Previous surface analysis studies have shown that the surface of a contact lens is inherently associated with that of the mould used in its manufacture (Rabke *et al.*, 1995). During polymerisation the mould is in direct contact with the forming lens surface and therefore any interaction, especially during the demoulding process, may result in altered lens surface properties. Differences in the chemical composition of the two used mould surface types (nitrogen-cured and air-cured lens moulds) might be expected as it has been reported (Biswal & Hilt, 2009) that polymeric lens materials cured in the present of oxygen (such as the air-cured lenses) tend to have a tackier surface and thus might cause a greater amount of lens material to adhere to the lens mould. Differences in lens/mould adhesion is therefore a possible reason for the clinical differences in surface wettability observed in the clinical study, due to greater exposure of the underlying relatively hydrophobic bulk on the air-curded lens surface. Chemical analysis of the lens moulds was performed to investigate whether adhesion between the mould and the lens surface differed between the two lens types by comparing the chemical composition of the surface of the two study lens mould types. In addition to imaging the moulds (Chapter 5) it was decided to also chemically characterise the surface of both the virgin (unused) moulds and the used moulds which had been used to manufacture both the air-cured and nitrogen-cured lenses. A central 5mm by 5mm section of the female lens mould was obtained by fracturing the plastic to minimise surface contamination. The female mould surface was analysed as it was the surface used to create the front surface of the contact lens. Used moulds analysed with the XPS system were from both the air-cured and nitrogen-cured contact lenses. For each mould type three samples were analysed (3 x virgin moulds, 3 x nitrogen-cured lens moulds and 3 x used air-cured lens moulds), giving a total of nine lens moulds analysed in total. The moulds were mounted on the XPS sample bar using PDMS-free double sided adhesive tape and loaded into the XPS instrument. Wide scan and high resolution XPS spectra were then obtained as described in Section 4.1.1.3. Statistical analysis involved a linear regression model with a Tukey post-hoc test applied where required.

4.3.2 Study 2 - Results

4.3.2.1 Study lens moulds

Figure 4.9 shows a comparison of the wide scan spectra for both virgin moulds and used contact lens moulds. The blue spectrum is from a virgin mould where the major elemental

peak present was C 1s (285 eV) with small peaks at O 1s (533 eV) and Si 2p (103 eV). This is in a agreement with the expected polypropylene composition of the moulds. The two other spectra are associated with used contact lens moulds from both the air-cured and nitrogen-cured lenses. In these two spectra an additional elemental peak is visible at F 1s (689 eV) and the size of the Si 2p and O 1s are significantly greater, with an associated reduction in the C 1s peak. No nitrogen signal was detected on any of the contact lens moulds.

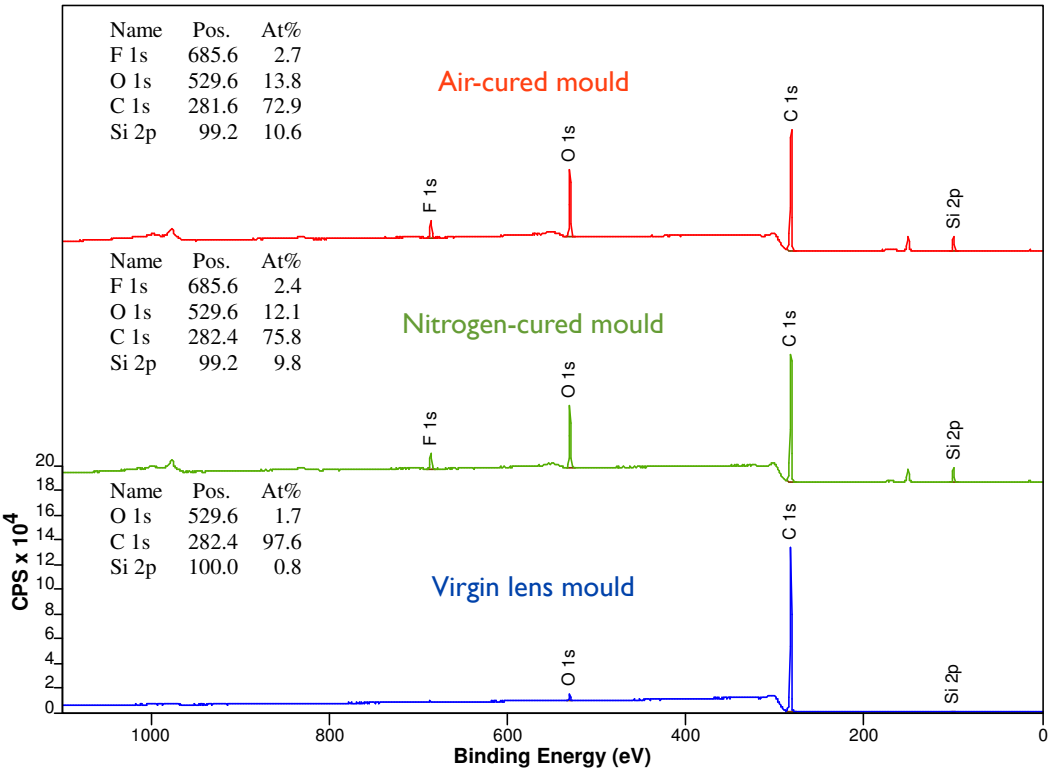

Figure 4.9: Representative wide-scan XPS spectra for both virgin and used air-cured and nitrogen-cured contact lens moulds (data overlaid to allow comparison).

Figure 4.10 shows a histogram of percentage atomic concentration following peak fitting for the carbon 1s, oxygen 1s and silicon 2p peaks. For the virgin moulds the majority of the carbon is found in the C2 peak which is associated with saturated carbon, being bonded either to another carbon or hydrogen. The remaining carbon is bonded to trace amounts of silicone (C1 curve) or oxygen (C3 and C4 curves). This finding was also mirrored in the O 1s and Si 2p peaks with both peaks associated primarily with carbon bonding. Differences in peak fitting concentrations between the mould types for the high resolution curve fitting

for the carbon 1s peak (F= 20.15, p<0.0001), oxygen 1s peak (F=122.08, p<0.0001) and silicon 2p peak (F=14.15, p<0.0001). Post-hoc analysis showed no significance difference between the nitrogen-cured and air-cured lens moulds for either the C1s, O1s or Si2p peaks, but a significant differences between these moulds and the virgin lens moulds for all the C1s, O1s and Si2p peaks. A significant interaction term (curve fit*mould type) was observed for the C1s (F=48.41, p<0.0001), O1s (F=40.70, p<0.0001) and Si2p (F=62.37, p=<0.0001) XPS data. Post-hoc analysis showed the concentration of saturated carbon (C2 curve) was significantly reduced in the used moulds (both nitrogen and air-cured), with a much greater concentration of C-Si bonding (C1 curve), compared with the virgin moulds. Post-hoc analysis also showed significantly greater concentration of oxygen in O1 and O2 curves for the used moulds compared with the virgin moulds, primarily related to the greater than six-fold increase in oxygen as can be observed in Figure 4.9. Post-hoc analysis of the data from the Si 2p region showed a greater concentration of Si1 and Si2 curves for the used contact lens moulds compred with the virgin moulds, again associated with a ten fold increase in the atomic concentration of silicon as identified by the wide-scan data (Figure 4.9).

4.3.2.2 *Ex vivo* study contact lenses analysis

Table 4.4 gives the elemental concentration of carbon, oxygen, nitrogen, silicon and fluorine for both the *ex vivo* nitrogen-cured and air-cured study contact lenses. These values were compared with the elemental composition of unworn lenses of the same type from the earlier XPS study (Section 4.2.2.1). Although the changes in the elemental composition are small in absolute value (<2% in all cases) there are two statistically significant differences in elemental concentrations following wear. Following one hour of wear the nitrogen-cured lenses showed a significant decrease (F=8.33, p=0.0005) in carbon concentration (from 53.9% to 52.8%) and a significant increase (F=6.35, p=0.007) in oxygen concentration (from 22.1% to 22.5%). The atomic ratio for nitrogen:carbon (N:C) and oxygen:carbon (O:C) were also calculated showing a significant higher (F=34.75, p=0.0041) O:C ratio for the air-cured lens compared with the nitrogen-cured lens following 1 hour of lens wear. No nitrogen was found on any of the *ex vivo* study contact lenses. Analysis of the curve fitting for the high resolution C 1s (F=0.1341, p=0.7152), O 1s (F=0.083, p=0.774) and Si 2p (F=0.60, p=0.455) spectra showed no significant difference between the air-cured and nitrogen-cured lens types following 1 hour of lens wear.

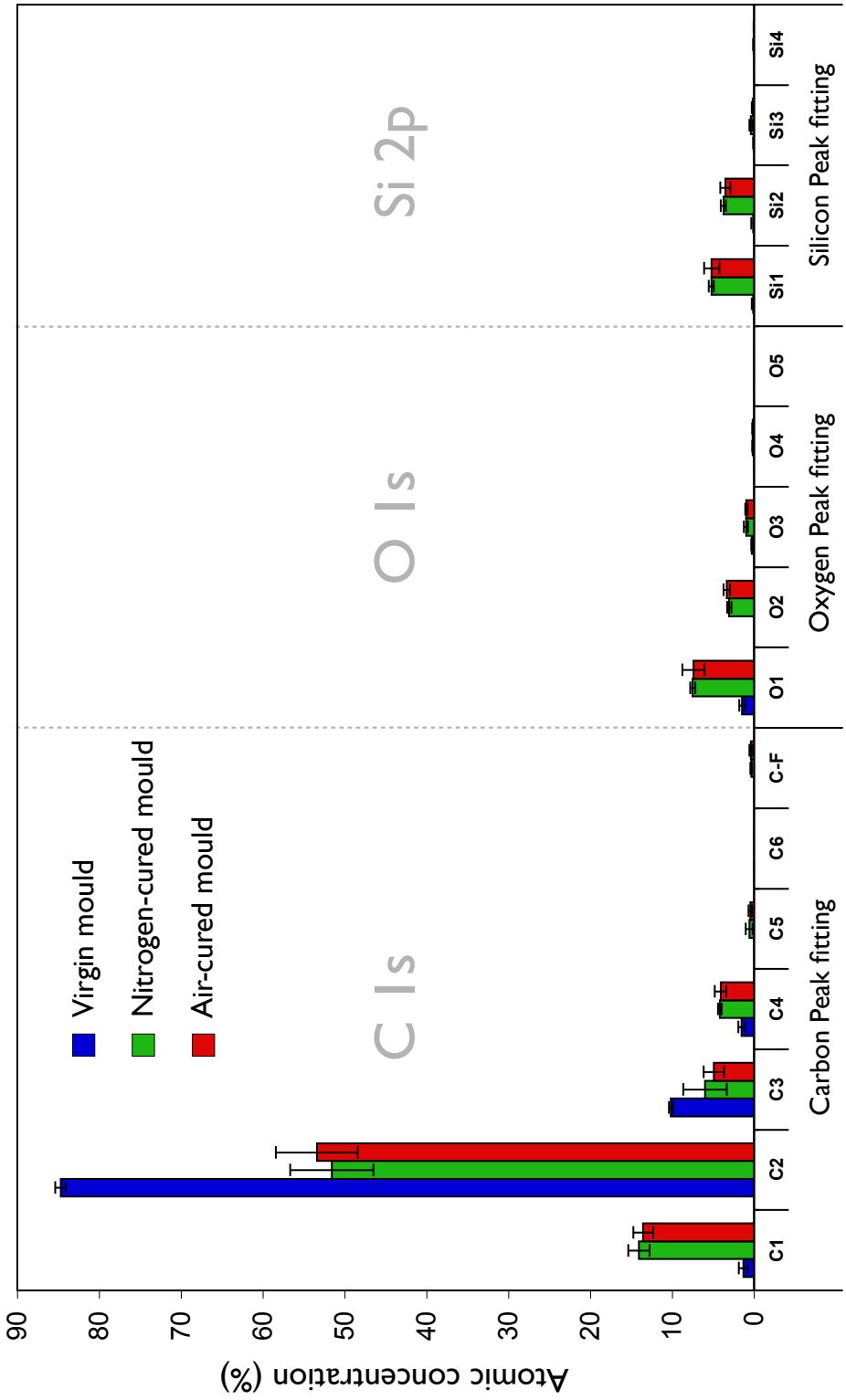

Figure 4.10: Atomic percentage concentration obtained by peak fitting of the high resolution XPS spectra associated with C 1s, O 1s and Si 2p peaks (error bars indicate standard deviation) for used and unused lens moulds.

4.3.3 Study 2 - Discussion

4.3.3.1 XPS analysis of study contact lens moulds

Following polymerisation of the study contact lens, the polypropylene moulds were separated and the lens demoulded. One possible cause for the non-wetting regions on the air-cured lens surface was adhesion between the lens material and the mould, resulting in a disturbed or damaged surface. In addition to imaging of the contact lens moulds (Section 1.14.1), a chemical analysis was performed on the surface of virgin and used contact lens moulds (air-cured and nitrogen-cured moulds). This analysis confirmed that the virgin lens moulds were made from polypropylene due to the very high carbon signal, with trace levels of oxygen related to surface oxidation which is commonly observed with polypropylene (Rjeb *et al.*, 2000) and the presence of silicon which is a common surface contaminant found in many polymeric materials (Oran *et al.*, 2004). Analysis of used contact lens moulds showed significant levels of contact lens material on both the air-cured and nitrogen-cured lens moulds. The relative amount of lens material on the used moulds was not statistically different between the lens types ($F=0.72$, $p=0.45$). The amount of contact lens polymer left on the mould was less than the depth of analysis of the XPS instrument as the silicon, fluorine and oxygen signals were significantly lower in intensity than that observed for the lens surface itself, suggesting the XPS instrument was also detecting the underlying polypropylene mould material. The deposited material appears to be primarily related to the silicone macromer (M3U) as no nitrogen signal is evident in the wide scan XPS spectrum for either the air-cured or nitrogen-cured moulds, but significant levels of fluorine and silicone were detected. Comparison of the high resolution XPS scans for C 1s, O 1s and Si 2p showed no difference in the material adhered to the lens moulds. These findings confirmed that only a thin layer of lens-related material was deposited on the moulds and that it was of the same chemical composition for the air and nitrogen-cured

Table 4.4: XPS atomic concentrations of worn and unworn study contact lenses polymerised in an air or nitrogen environment. Standard deviations are in parentheses.

	Atomic concentration					Atomic ratios	
	C	**O**	**N**	**Si**	**F**	**N:C**	**O:C**
Nitrogen-cured unworn	53.9 (0.4)	22.1 (0.3)	0.0 (0.0)	20.7 (0.2)	3.4 (0.1)	0.00 (0.00)	0.410 (0.01)
Nitrogen-cured 1 hour	52.8 (0.2)	22.5 (0.1)	0.0 (0.0)	20.8 (0.6)	3.4 (0.2)	0.00 (0.00)	0.426 (0.01)
Air-cured unworn	53.8 (1.1)	22.0 (1.0)	0.0 (0.0)	20.4 (0.3)	3.5 (0.1)	0.00 (0.00)	0.410 (0.03)
Air-cured 1 hour	54.2 (0.4)	21.9 (0.3)	0.0 (0.0)	20.4 (0.2)	3.4 (0.1)	0.00 (0.00)	0.404 (0.01)

lens moulds, being based primarily of the silicone macromer. The presence of hydrophobic silicone macromer on the surface is expected as polypropylene is a relatively hydrophobic non-polar material which is expected to attract hydrophobic polymeric materials to the surface, such as M3U, and repel more hydrophilic materials, such as VMA. It is therefore apparent that the difference in lens surface wetting properties between the two study lens types is not related to greater adhesion between the lens surface and the mould.

4.3.3.2 XPS analysis of worn study contact lenses

Comparison of the elemental composition of the worn (*ex vivo*) contact lenses and the unworn study contact lenses show only very small differences in any of the key elements. When considering the type of materials likely to deposit on the surface of the lens following wear, the likely candidates are proteins, lipids and mucins from the tear film. Much work in the literature has focused on understanding the process of deposition and the influence it has on both the surface properties of lens materials and the resulting clinical performance (Bruinsma *et al.*, 2002; Cheng *et al.*, 2004; Green-Church & Nichols, 2008; Pritchard & Fonn, 1995b; Tonge *et al.*, 2001). It is clear from the literature that on silicone hydrogel materials the level of deposition associated with tear film proteins is generally lower than that observed with conventional hydrogels, especially those with ionic charge (Subbaraman *et al.*, 2006). In contrast, the deposition of lipid is reportedly higher on silicone hydrogels (Lorentz & Jones, 2007). Comparison of worn and unworn study contact lenses showed surprisingly little difference in surface chemistry, with only the nitrogen-cured lens showing a difference following wear, with a slight (1%) but statistically significant increase in oxygen and reduction in concentration of carbon. The lack of any nitrogen signal would suggest a lack of significant protein deposition, as McArthur *et al.* (2001) have shown that tear film proteins contain a significant amount of nitrogen, which would have been detected if present. McArthur *et al.* (2001) also suggested that monitoring the carbon:oxygen ratio following wear can allow the differentiation of mucin from lipid deposition as lipids are typically carbon rich and therefore lower the O:C, whereas mucins are relatively oxygen rich increasing the O:C ratio. For both the nitrogen-cured and the air-cured contact lenses a significant change in the O:C was observed indicating that the nitrogen-cured lens was being deposited primarily by mucins and other carbohydrate-rich species (increasing O:C), whereas the air-cured lens appears to be deposited primarily by lipids (reducing O:C). These results are in line with other research (Huth & Wagner, 1981; Lorentz &

Jones, 2007), which suggests that more hydrophobic surfaces tend to be more lipophilic, whereas deposition on hydrophilic surfaces favour mucin type tear film components. The similar high resolution XPS spectra for the unworn and worn study lenses suggest minimal chemical state changes, with the dominant signal associated with the underlying contact lens material. This is likely due to both the relatively short period of lens wear and the relative depth of XPS analysis in comparison with the thickness of the tear film deposits on the lens surface. This assessment of tear film deposition assumes that the surface which is exposed to deposition is the same surface that undergoes analysis. It is evident that this may not be the case, especially if, as the previous study suggested (Section 4.2.3.2), the surface in all of the three study regions appears altered by a migration of the hydrophobic M3U siloxane macromer towards the surface. This has the potential to mask the true deposited components as they are potentially engulfed by the siloxane macromer. This seems increasingly probable as these non-wetting regions on the air-cured surface, on visual examination, appeared to show heavy deposition on the lenses surface (Figure 4.8) which might be expected to change the XPS spectra in a far more significant way to that which was observed in the XPS data for these dehydrated samples. Indeed, work by McArthur *et al.* (2001) suggested far more significant changes to the XPS spectra from much less obvious deposition, with conventional hydrogels, where the thermodynamic drive for polymeric reorganisation at the surface is much lower than in these siloxane-containing polymers. To better understand this process, cryo-XPS analysis could be utilised in an attempt to stabilise the polymeric surface structure and avoid the possibility that tear film related deposition is masked. The remaining XPS analysis therefore focused on minimising potential surface reorganisation using cryogenic handling techniques.

4.4 Study 3 - Cryogenic XPS handling technique for study contact lenses

4.4.1 Study 3 - Materials and methods

An air-cured and nitrogen-cured study contact lens were soaked in HPLC grade water for 24 hours and then a round sample (4mm diameter) was punched from the nitrogen-cured lens, and from both a wetting region and non-wetting region on the air-cured lens (as described in Section 2.2.3.3). Each sample was then placed, anterior surface downwards, over one of three apertures on a copper mask (3 mm diameter) which was then turned

over and lowered down onto the copper XPS cryo-stub where it was fixed with a central clamping screw (Figure 4.11). The anterior surface of the contact lens was then visible through the aperture in the copper mask and therefore available for analysis. The copper stub was then partially lowered into liquid nitrogen, which rapidly cooled the copper stub and indirectly froze the lens samples. The stub was held in liquid nitrogen for 5 minutes and then rapidly transferred to a liquid nitrogen cooled stage in the preparation chamber (Figure 4.12). The preparation chamber was purged with nitrogen gas and then pumped down to $1x10^{-8}$ torr where it was held for 2 hours. The sample transfer arm was then brought through into the preparation chamber and attached to the stub where it was left for 15 minutes to allow it to cool. The stub was then removed from the cooling stage using the pre-cooled transfer arm and moved through into the analysis chamber where the stub was mounted on the liquid nitrogen cooled analysis stage. The stage temperature was then maintained at between -160^{o}C and -170^{o}C during XPS analysis. Wide scan and high resolution XPS spectra were then obtained as described in Section 4.1.1.3. Following XPS analysis in the frozen state, the stage was allowed to warm up to room temperature overnight allowing the samples to dehydrate in the ultra high vacuum conditions. The wide and high resolution XPS scans were then repeated on the same contact lens samples to monitor changes in surface chemistry following dehydration. In total three lens samples were analysed using the cryo-XPS technique (1 x nitrogen-cured lens sample, 1 x 'wetting' region on air-cured lens and 1 x 'non-wetting' region on air-cured lens). The number of samples used in this study were limited to an individual sample for each study lens region, as cryogenic XPS analysis is time consuming (two days instrument use for three samples) and very expensive. This was thought to be acceptable due to the high repeatability of XPS analysis compared with other surface analysis techniques, where a greater number of samples are required to confirm a difference between materials. No formal statistics were performed on the study data due to the low number of samples analysed in this experiment.

4.4.2 Study 3 - Results

4.4.2.1 Cryogenic temperature results

Figure 4.13 shows the wide scan XPS spectra for the nitrogen-cured contact lens sample and both the wetting and non-wetting regions of an air-cured contact lens sample. Table

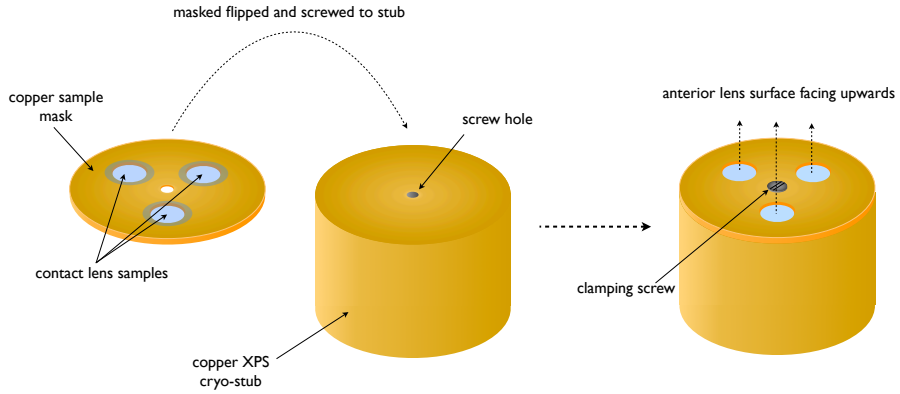

Figure 4.11: Schematic of sample mounting process for the XPS cryo-stub.

4.14 presents the elemental data from these XPS spectra in percentage form. The elements carbon, oxygen, silicon, nitrogen and fluorine were detected on the surface of all lenses. The concentration of silicon and fluorine was higher on the air-cured wetting lens compared with the nitrogen-cured lens, and even higher on the air-cured non-wetting lens. In contrast, the nitrogen-cured lens had the highest concentration of the nitrogen, reducing for the air-cured wetting and non-wetting regions. Neither carbon nor oxygen showed a clear trend for increasing or reducing concentration in relation to the apparent variation in wettability. The concentration of the carbon was highest for the air-cured wetting region followed by nitrogen-cured and lowest for the air-cured non-wetting region. Oxygen showed highest concentration in the nitrogen-cured sample, decreasing for the air-cured wetting region and again for the air-cured wetting region.

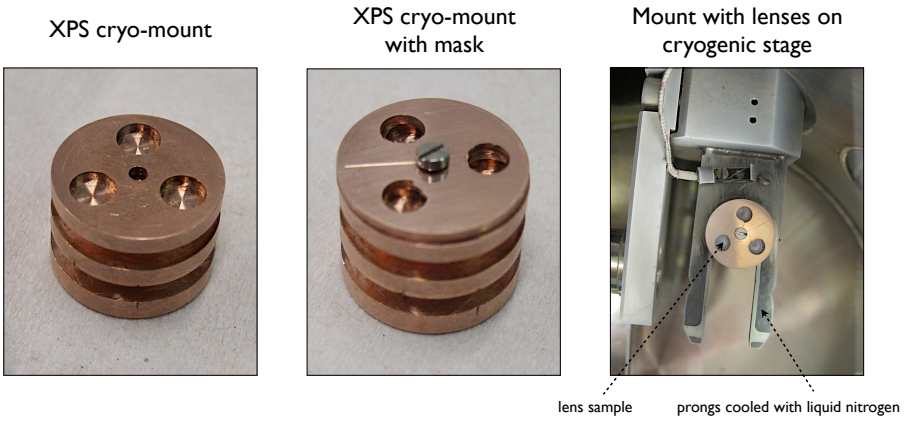

Figure 4.12: Photographs of customised cryo-XPS lens mount.

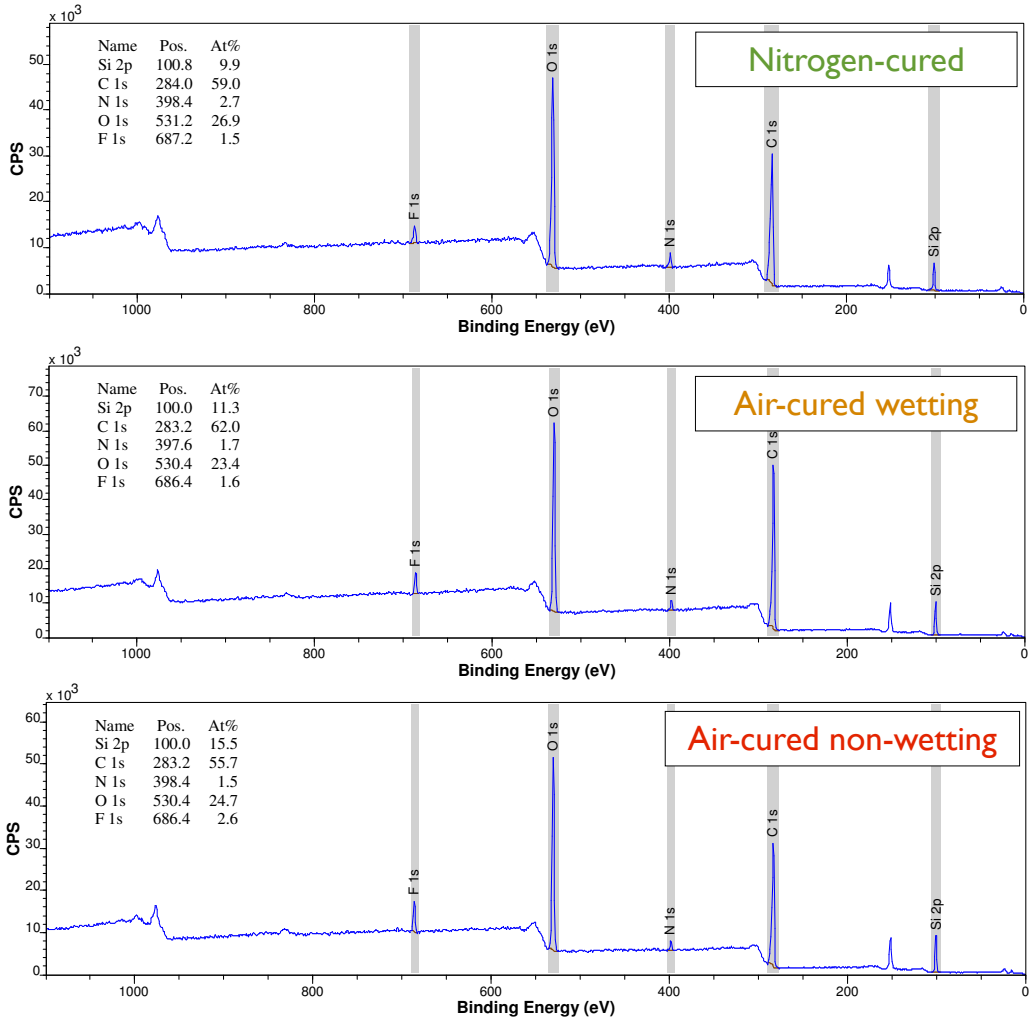

Figure 4.13: Wide survey cryo-XPS scans for the three lens regions of interest.

	C 1s	O 1s	Si 2p	F 1s	N 1s
Nitrogen-cured	59.0	26.9	9.9	1.5	2.7
Air-cured wetting	62.0	23.4	11.3	1.6	1.7
Air-cured non-wetting	55.7	24.7	15.5	2.6	1.5

Figure 4.14: Comparison of elemental composition (%) for the three study lens regions at cryogenic temperature.

Figure 4.15 shows the high resolution C 1s XPS spectra for the three study contact lens regions. Curve fitting was performed using six component curves (C1 to C6). C1 concentration was highest for the air-cured non-wetting region and reduced for the air-cured wetting region, with lowest concentration for the nitrogen-cured region. In contrast the C2 peak increased in concentration from the air-cured non-wetting region, to the air-cured wetting region and was greatest for the nitrogen cured lens. No clear trends were apparent for peaks C3 to C6. Figure 4.16 shows the high resolution O 1s XPS spectra for the three study contact lens regions. Curve fitting was performed using five component curves (O1 to O6). O1 concentration was highest for the air-cured non-wetting region reducing for the air-cured wetting region and lowest for the nitrogen-cured region. O3 shows the opposite trend with the lowest concentration on the air-cured non-wetting region and highest on the nitrogen-cured region. C2 and C5 also appear to alter in concentration between the regions, with a greater than two times increase in the nitrogen-cured lens compared with either of the air-cured regions for the C2 peak, and a greater than ten times increase in intensity for the C5 peak in the nitrogen-cured lens when compared to that observed on either of the air-cured regions. In contrast to differences observed between the contact lens regions in the O 1s and C 1s high resolution spectra there was very little difference noted in the Si 2p spectra, with all peaks varying in intensity by less than 5%.

4.4.2.2 Room Temperature Results

Table 4.17 shows the elemental composition from wide scan spectra for the cryo-XPS samples after they had been allowed to warm up to room temperature overnight. When comparing these results with those from the frozen samples in Figure 4.14, there was a clear trend for the elemental composition of the samples to be higher in oxygen, silicon and fluorine, but lower in carbon and nitrogen at room temperature. Figure 4.18 shows the high energy resolution data for C 1s, O1s and Si 2p with peak fitting performed to determine overlapping peaks. The air-cured wetting data is not presented here as an additional peak was present in the high resolution data to the left of the elemental peaks, resulting in problems with relative analysis and quantification. This is likely associated with differential charging as a result of distortion of the surface following dehydration of the material. The C 1s high-resolution spectra for the samples at room temperature follow at similar trend to that of the samples when at a cryogenic temperature, with the

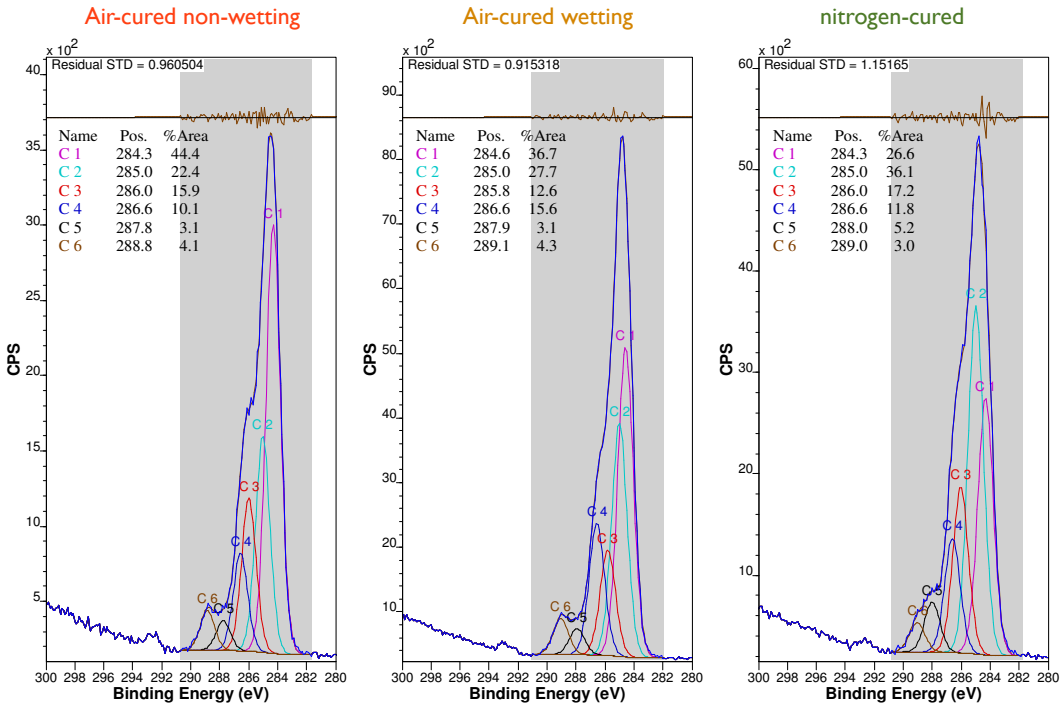

Figure 4.15: Comparison of the high resolution C 1s spectra with curve fitting for the three study contact lens regions.

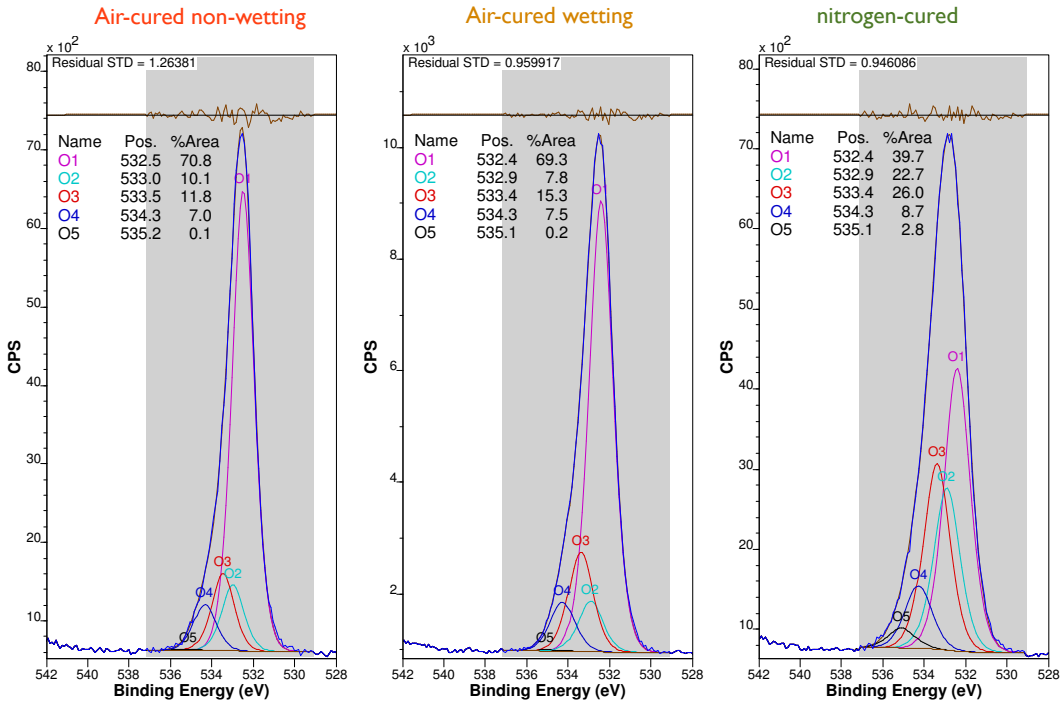

Figure 4.16: Comparison of the high resolution O 1s spectra with curve fitting for the three study contact lens regions.

	C 1s	O 1s	Si 2p	F 1s	N 1s
Nitrogen-cured	60.1	21.3	13.8	2.5	2.4
Air-cured wetting	56.3	22.4	17.6	3.2	0.6
Air-cured non-wetting	53.1	24.8	18.2	3.4	0.5

Figure 4.17: Comparison of elemental composition (%) for the three regions on the experimental contact lenses at room temperature.

C1 and C-F peaks having a lower peak intensity and the C2 and C3 peaks having a higher intensity for the nitrogen-cured lens in comparison with the air-cured non-wetting region. The C4 peak intensity appears similar for both samples and the C5 and C6 peak appears to show a slightly higher intensity for the nitrogen-cured lens. The O 1s high resolution spectra is dominated by the O1 and O2 peaks in similar ratios in the air-cured non-wetting and nitrogen-cured regions. The Si 2p high resolution spectra show similar peak fitting patterns for both the nitrogen-cured and air-cured non-wetting regions.

4.4.3 Study 3 - Discussion

The use of a cryogenic handling technique during XPS analysis highlighted significant differences between the hydrated frozen surface spectra and the dehydrated sample spectra. During analysis of the cryogenically frozen samples, a nitrogen signal became detectable suggesting the presence of VMA at the lens surface (as VMA is the only monomer to contain significant amounts of nitrogen) and silicone and fluorine levels significantly reduced suggesting less silicone macromer at the surface. Differences in the elemental composition were also apparent for the three study contact lens regions, with a significant increase in the intensity of nitrogen for the nitrogen-cured surface in comparison with the air-cured wetting and to a greater extent the air-cured non-wetting region, suggesting a greater concentration of the hydrophilic monomer VMA at the surface in the more wettable regions. In addition, the most wettable surface (nitrogen-cured) had the lowest concentration of silicone and fluorine, with increased levels found for air-cured wetting and greater still for the air-cured non-wetting regions, suggesting a greater concentration of silicone macromer (M3U) at the surface in the relative hydrophobic contact lens surfaces. As carbon and oxygen are found in all the monomers present, the interpretation is more complex, with no

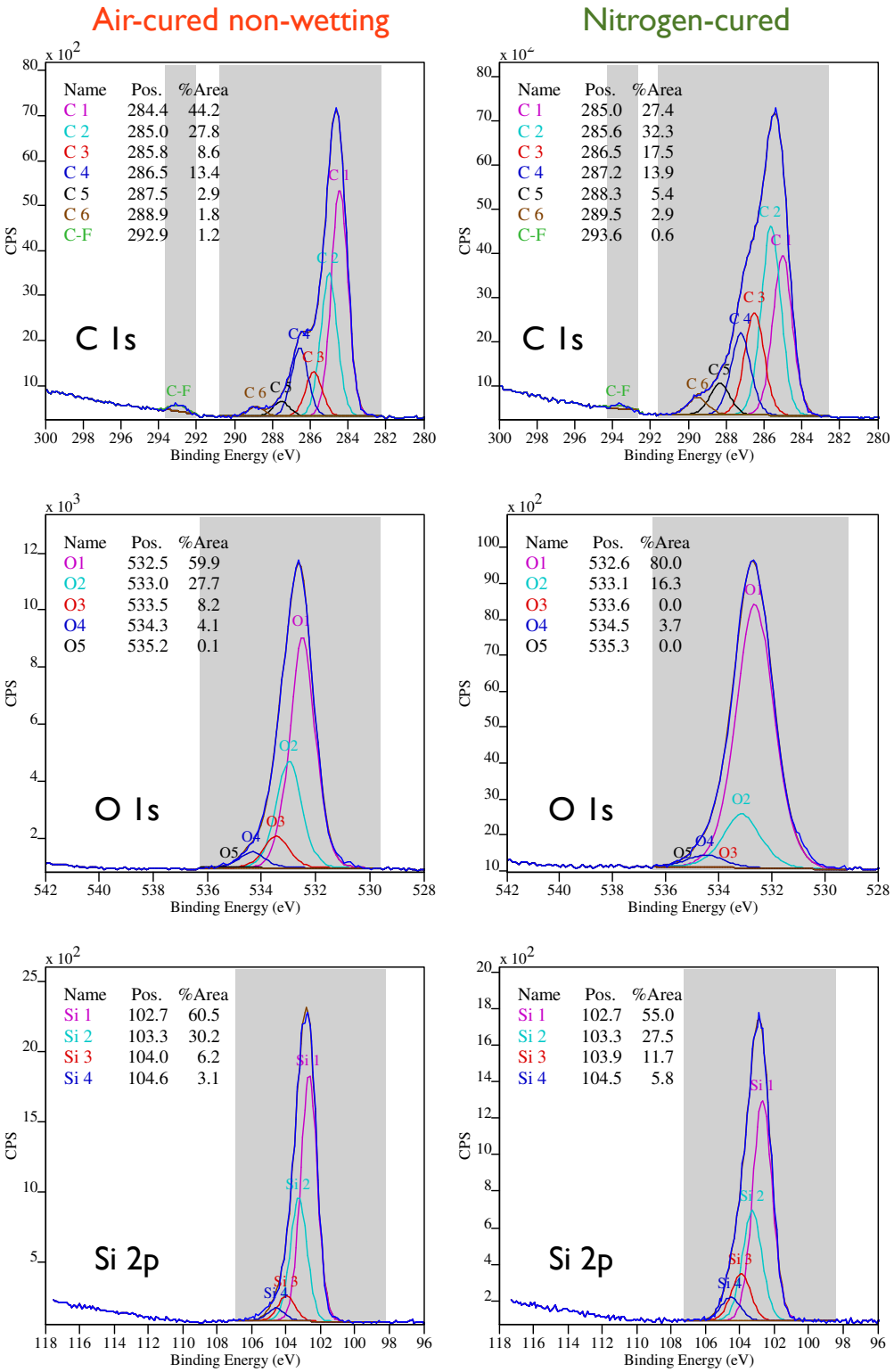

Figure 4.18: Comparison of the high resolution C 1s, O 1s and Si 2p spectra with curve fitting for the nitrogen-cured and air-cured non-wetting lens regions at room temperature.

obvious trends apparent when comparing the XPS data to the known clinical wettability of the lens surfaces (Section 2.1). Chemical state analysis of carbon and oxygen showed apparent differences in the bonding concentration between the hydrated (cryo-frozen) and dehydrated samples, with a lower concentrations of (a) C-Si bonding (C1) and (b) C-F bonding and a higher concentration of (a) C-C/C-H bonding (C2), (b) C-C-O bonding(C3), (c) O-C-O/C=O bonding (C5) and (d) O-C=O (C6). The lower concentration of C-Si and C-F bonding is in agreement with the elemental findings that the concentration of the silicone macromer is lower in the hydrated state than in the dehydrated state. The increased concentration of the hydrocarbon and oxygen-carbon bonding suggests an increase in the more hydrophilic elements of the polymer along with the suggestion of higher levels of the monomer MMA at the surface using the cryogenic handling technique. This suggests that during dehydration the siloxane macromer migrates to the surface and forms a silicone rich layer. This process appears to occur in all three regions of interest on the study contact lens surface suggesting that it is a property of the polymer rather than related to the differences in polymerisation conditions. Differences were also present when the elemental composition of the three frozen regions of interest were compared, with higher concentrations of silicone and fluorine found on the more hydrophobic study lens surface (air-cured non-wetting) and high levels of nitrogen on the more hydrophilic study lens surface. Chemical state analysis of the frozen samples also shows changes in the C 1s regions with a greater level of carbon-silicon and carbon-fluorine bonding in the air-cured non-wetting (hydrophobic) region with decreasing levels in the air-cured wetting (intermediate wetting) region and less still for the nitrogen-cured lens region (hydrophilic). Chemical state changes in the O 1s region also changed across the three regions with a reduction in the concentration of oxygen-silicon bonding in the nitrogen-cured (highly wettable) region and an increase in oxygen-carbon bonding levels. Both these findings suggested that the hydrophobic (air-cured wetting) region has a higher concentration of siloxane polymer, whereas the nitrogen-cured region has a higher concentration of the hydrocarbon-based polymers (based on the MMA and VMA monomers). The difference in the polymer composition at the surface of the contact lens material suggests that phase separation may be occurring in the more hydrophobic regions of the study lenses with a dominance of the siloxane-containing polymer at the surface.

Given that the elemental composition of the three study lens regions was shown not to dif-

fer when the samples were air dehydrated (Section 4.2.2.1), it was expected that following cryogenic freezing and subsequent vacuum dehydration the lens would also have similar elemental composition. Contrary to expectation, differences were observed following vacuum dehydration, although these differences were less marked than for the lens samples in a frozen state. A possible cause for the different findings may be the small number of lens samples used in this cryo-XPS study, although the findings of the dehydrated lens sample study were consistent across nine lens samples. Other possible reasons for the difference may relate to the difference in material temperature during dehydration (-150^{o}C for post cryo-XPS dehydration versus 25^{o}C for air dehydrated lens sample) or the type of dehydration occurring (water evaporation for air dehydration versus sublimation for post cryo-XPS dehydration). Future studies should therefore looking to investigate a greater number of samples to clarify these results.

4.5 XPS conclusions

The highly surface sensitive nature of the XPS technique has allowed investigation of the surface chemistry for a range of contact lens materials and moulds used to manufacture contact lenses. In general, investigation of the surface of dehydrated commercial contact lenses was similar to that previously reported in the literature. Analysis of the lens moulds showed a thin film of lens material remained on the moulds following use, although this did not differ between the two study lens manufacturing conditions. Dehydration of the study contact lenses in an ultra high vacuum prior to XPS analysis resulted in a substantial reorganisation of the lens surface, leading to a surface dominated by the siloxane macromer. The use of a cryogenic handling technique reduced this reorganisation and allowed the surface chemistry of the hydrated lens to be analysed. This showed differences in surface chemistry between regions on the study contact lenses, with silicone macromer enrichment in the non-wetting regions and a greater degree of hydrophilic polymer in the wetting regions. On heating the sample to room temperature the surface partially reorganised, resulting in a surface chemistry which was richer in silicone macromer. When assessing the surface chemistry of hydrogel materials it is therefore critical to avoid dehydration of the material, as this can result in surface reorganisation. This is even more critical when assessing silicone-containing materials as they are readily able to reorganise due to their highly flexible nature, indicated by the low glass transition temperature of the materials.

Careful cryogenic freezing of the sample below its glass transition temperature has been shown to limit this reorganisation and allow hydrated surface chemistry to be assessed. Future XPS work should therefore focus on cryogenic analysis as dehydrated analysis is likely to be misleading, particularly with non-surface treated silicone hydrogel materials, where reorganisation is highly probable.

4.6 Introduction to ToF-SIMS analysis of the study contact lenses

This work aimed to investigate the surface chemistry of three regions of interest on the study contact lenses using ToF-SIMS. Surface chemistry is known to play a critical role in influencing the wetting properties of a material and given the tendency of the study lenses to wet poorly during both clinical and laboratory assessment, characterising the surface chemistry of the study contact lens regions was of primary concern. Previous work within this research group has investigated the surface chemistry of commercial hydrogel and silicone hydrogel contact lenses with a ToF-SIMS instrument (Maldonado-Codina *et al.*, 2004a). The current study therefore focused on the experimental study contact lens materials in both a dehydrated and hydrated state in an attempt to understand the differences in surface chemistry between these regions. ToF-SIMS depth profiling was also performed to investigate how the lens chemistry changed from the surface towards the bulk. The three sample types analysed were identified using the *in vitro* wettability analyser (Section 2.2.3.3). The ToF-SIMS investigation was therefore separated into three discrete studies:

Study 1 - To investigate the differences in surface chemistry between the three regions of interest on the study contact lenses in a dehydrated state.

Study 2 - To investigate the differences in surface chemistry between the three regions of interest on the study contact lenses in a cryo-frozen hydrated state.

Study 3 - To investigate the differences in surface chemistry during a depth profile into the three regions of interest in both a hydrated and dehydrated state.

4.7 Study 1 - ToF-SIMS analysis of dehydrated study lenses

4.7.1 Materials and Methods

4.7.1.1 Study lenses

The two study contact lenses used in this study were custom-manufactured in the same manufacturing facility, specifically for this experiment, using identical component monomers (Section 1.9). During manufacture, half of the study contact lenses were cured in an air-filled oven and half were cured in a nitrogen-purged oven. When these lenses were polymerised in the nitrogen-purged oven they possessed acceptable *in vivo* wetting characteristics, whereas when polymerised in an air-filled oven *in vivo* wetting appeared unacceptable, with regions of wetting and non-wetting across the lens surface (Section 2.1.19.5). Four experimental silicone hydrogel contact lenses were investigated in this study (2 x nitrogen-cured lenses and 2 x air-cured lenses). Lenses were supplied in blister packaging containing only PBS solution with no surfactants or other additives.

4.7.1.2 Sample preparation

Each lens was removed from its blister packaging using stainless steel tweezers touching only the very edge of the lens. The lenses were then soaked in HPLC grade water (Sigma-Aldrich Ltd., UK) for 24 hours (with the water changed after 12 hours) in an attempt to remove the saline blister packaging solution from the lens (Figure 4.19a). The development of the *in vitro* wettability analyser detailed in Section 2.2.2.1 allowed identification of the wetting and non-wetting regions on the air-cured lens surface without the need for *in vivo* inspection. All lenses used in the ToF-SIMS investigation underwent this laboratory wetting analysis and were then subsequently soaked for a further 12 hours in HPLC grade water. Each lens was then removed from the water using tweezers and placed, anterior lens surface upwards, onto a clean glass surface. A 3.5mm medical biopsy punch (Kai Industries Inc., Gifu, Japan) was used to remove a round sample from the wetting and non-wetting regions identified on the air-cured lens surface and an area on the nitrogen-cured lens corresponding to the area of non-wetting on the air-cured lens (Figure 4.19b). Each sample was then placed onto an inverted stainless steel mask with the anterior lens surface facing downwards (Figure 4.19c). Once all samples had been mounted the mask was turned over and screwed down onto the copper base leaving the anterior surface of the lens samples exposed for analysis (Figure 4.19d). The copper-mounting stub was then

introduced into the entry chamber and the pressure lowered to 1 x 10^{-7} torr. After being held in this chamber for 30 minutes the copper stub was transferred to the main analytical chamber where the pressure was lowered to 1x10^{-9} torr. The stage was then adjusted to centre the sample and an area of 200 μm^2 selected. Each lens sample was analysed in three different 200 μm^2 regions. For each region of interest (nitrogen/air wetting/air non-wetting) there were two samples, with each sample analysed in three different 200μm^2 areas (**two** samples x **three** lens regions x **three** 200 μm^2 scans), giving a total of 18 positive and 18 negative spectra obtained in this study.

4.7.1.3 ToF-SIMS Instrumentation

ToF-SIMS analysis was performed using a Bio-ToF SIMS instrument, the design of which has been described previously (Braun *et al.*, 1998). Data was collected using a 20 kV C_{60}^+ ion gun (Ionoptika Ltd., UK) with a 15ns pulse width and a beam current of approximately 0.35 nA rastered over a 200x200 μm area. The spectra consisted of 200,000 shots for each

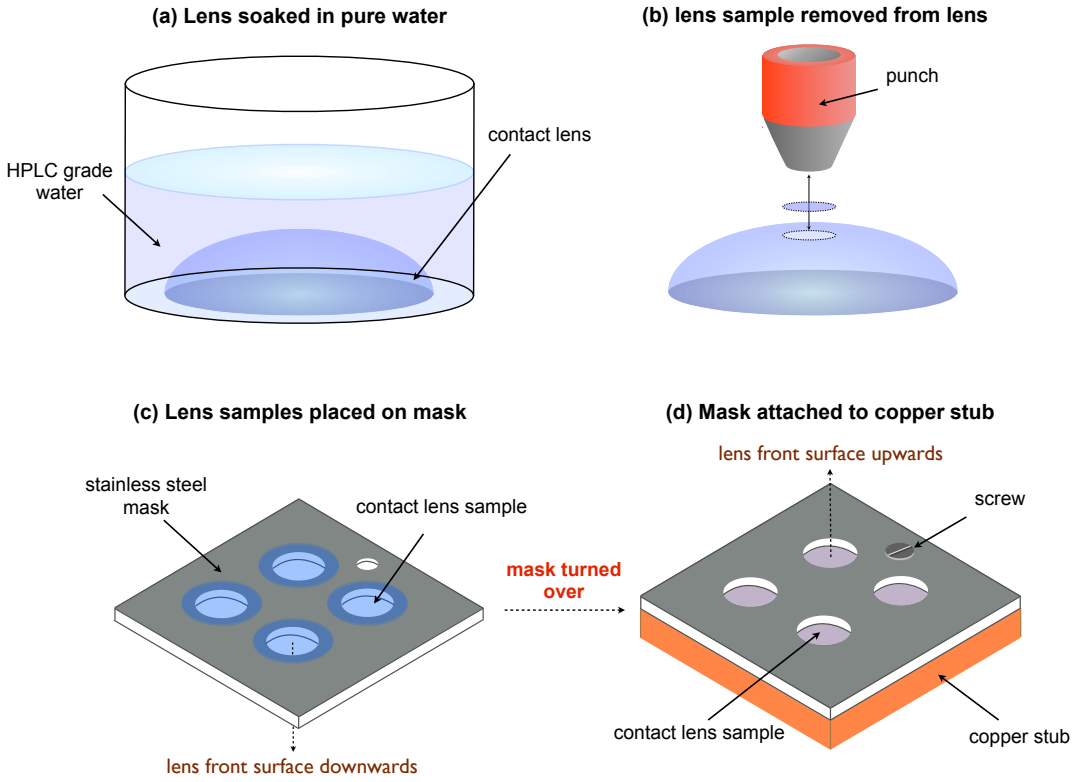

Figure 4.19: Sample preparation prior to ToF-SIMS analysis

acquisition and had an average mass resolution of 900 at m/z 28. Secondary ion yields reported correspond to the number of secondary ions detected per primary ion impact. Data was collected from three regions on each film to provide an error assessment of the values presented. Low energy (25 eV) electrons were flooded onto the sample between primary ion pulses to limit any effects from sample charging. The sample stage was held at ground during ion impact, and the secondary ions were directed into a two-stage reflectron by applying a delayed extraction pulse of 2.5 kV to the stage. The ions were post-accelerated to 20 KeV and detected using a dual micro channel plate assembly with the flight times being recorded on a 1 ns time-to-digital converter (Fast Comtec, GmbH). The data were analyzed using the ToFPak software program from Physical Electronics (Eden Prarie, MN). This applies multivariate techniques, including principle component analysis (PCA), to identify differences in the spectra between the study lens samples.

4.7.1.4 Avoidance of sample contamination

All lens preparation and sample handling was carried out using tools cleaned with 99.9%+ grade ethanol (Sigma Aldrich, UK) and rinsed copiously with pure water. In addition, the operator wore powder-free nitrile gloves to avoid sample contamination. Hook *et al.* (2006) suggested possible contamination from 'old' de-ionised water used for sample preparation, therefore fresh ultra pure water was used in this study. In addition, prior to analysis the ToF-SIMS instrument was stripped down and the analysis chamber cleaned with ethanol, then reassembled and baked out for 24 hours to ensure a clean analysis environment.

4.7.2 Results

4.7.2.1 Positive-ion SIMS

This study primarily focused on identifying differences in the molecular composition of the three regions on the study lenses rather than attempting to specifically infer the lens materials chemical composition. The positive ion ToF-SIMS spectrum for the nitrogen-cured lens is shown in Figure 4.20. The great majority of the positive ions are of a mass to charge ratio (m/z) less than 500Da. Figure 4.21 therefore presents the same spectrum on a 0-300Da scale allowing easier observation of the major peaks. There is a large amount of siloxane in the SIMS spectrum, which is expected, based on the monomer composition of these lenses (Section 1.9). Masses at: m/z 45, 59, 73, 147 and 207 are the major peaks

detected which relate to a siloxane fragmentation pattern (Table 4.5). All three lens regions contain similar peak patterns and peak ratios. The positive ion ToF-SIMS spectra for the nitrogen-cured lens sample and for both the wetting and non-wetting regions on the air-cured lens are shown in Figure 4.22. The spectra for the wetting and non-wetting regions on the air-cured sample and for the nitrogen sample were similar in both intensity and ions detected. Each spectrum analysed, regardless of lens region, contained the same peaks (ions) with the exception of the nitrogen-cured lens, which contained a peak at m/z 7 which corresponds to lithium (both the air-cured lens regions had no detectable peak at this mass). There are slight differences in peak intensities, which can be directly compared since all films were analysed at the same time and under identical conditions. For the positive ion spectra, the most notable differences between the study lens regions relate to increased intensity in the nitrogen-cured and air-cured wetting lens films (factors of 2 to 7) at peak locations of m/z 7, 23, 39, 41, 56, and 65. Resolved peaks were detected above m/z 320, however no differences in intensity or peak ratios of statistical relevance were observed other than those mentioned. The peak at m/z 7 is due to the presence of Li^+; the peak at m/z 23 is due to the presence of Na^+. The peak at m/z 39 is likely associated with the presence of K^+, but could also be attributed to $C_3H_3^+$. The other major isotope of potassium, $^{41}K^+$, is also observed to increase in intensity in the nitrogen-cured sample, suggesting that both peaks are related to the increase in intensity in the nitrogen-cured lens. It should be noted that the intensity of m/z 41 is greater than that of m/z 39 and therefore cannot be solely related to potassium. Instead it is likely overlapping peaks from $^{41}K^+$ and $C_3H_3^+$ which are unresolved in the spectra collected. The peak detected at m/z 56 may be due to the presence of Fe^+. Iron has a significant isotope at m/z 54, for which there is also a slight increase in intensity for the nitrogen-cured lens spectra. A stainless steel mask was used during the acquisition of the spectra, which may be the source of these peaks. An increase in peak intensity is also observed at m/z 65, which may be related to the presence of copper. The sample stub used in this experiment was made of copper.

4.7.2.2 Negative-Ion SIMS

Figure 4.23 shows the negative-ion spectra for the nitrogen-cured and air-cured non-wetting regions. As with the positive-ion spectra, no new peaks were detected when comparing the two air-cured lens regions with the nitrogen-cured lens region. There were some slight intensity differences between the air-cured and nitrogen-cured regions. Major

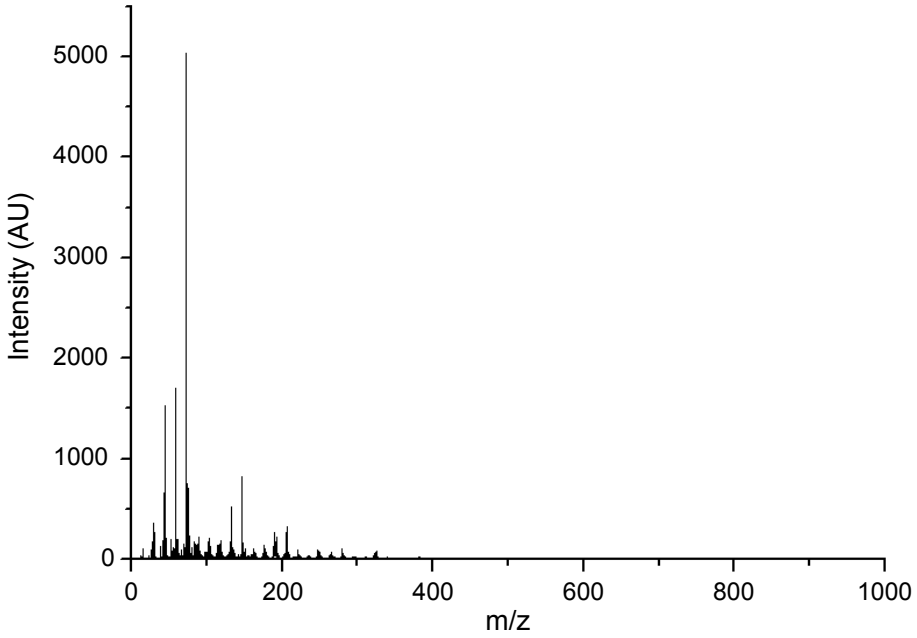

Figure 4.20: Positive ion ToF-SIMS spectra for the dehydrated nitrogen-cured lens samples in the 0-1000Da region.

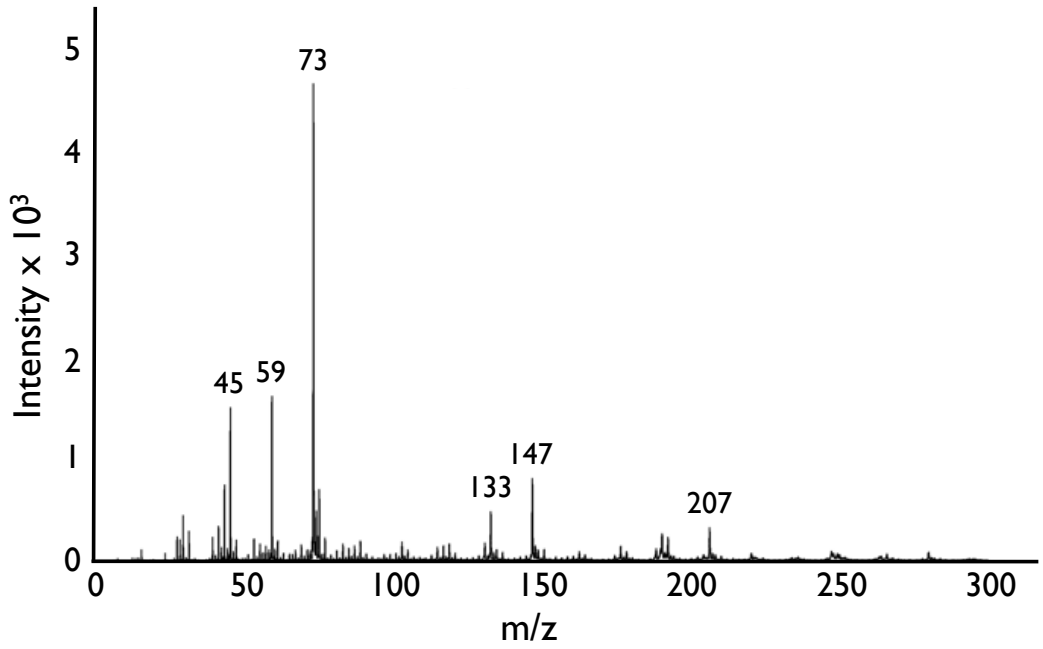

Figure 4.21: Positive ion ToF-SIMS spectra for the dehydrated nitrogen-cured lens samples in the 0-300Da region.

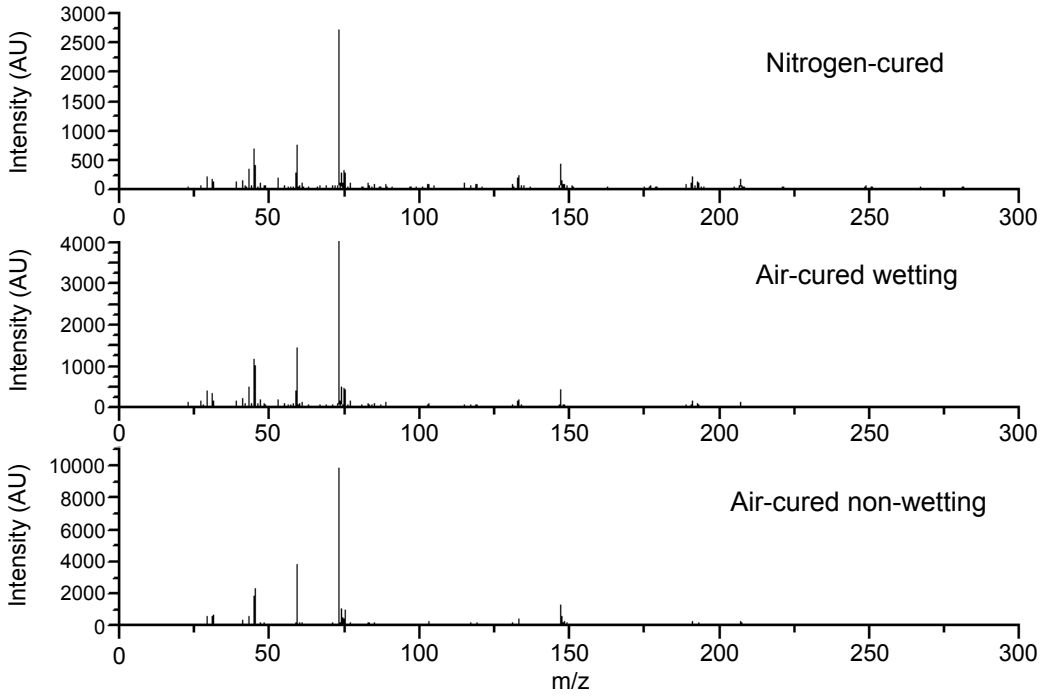

Figure 4.22: Comparison of the positive ion ToF-SIMS spectra for the three study lens samples.

Table 4.5: Probable chemical formulas for the major positive ion peaks detected with ToF-SIMS.

Peak location (m/z)	Probable formula
45	$SiOH^+$ or $C_2H_5O^+$
59	$SiOCH_3{}^+$
73	$SiC_3H_9{}^+$ or $SiC_2H_6O^+$
133	$C_4H_{13}OSi_2{}^+$
147	$C_5H_{15}OSi_2{}^+$
207	$C_5H_{13}O_3Si_3{}^+$

peaks for the spectra were detected at m/z 25, 61, 69, 75, 149 and 223. Peaks at m/z 61, 75, 149 and 223 are related to the siloxane molecule. The ions at m/z 25 and 69 are likely $C_2H_5{}^-$ and $CF_3{}^-$, respectively. Intensity differences were noted for peaks at m/z 26 and 42. The ion at m/z 26 is CN^-, which has a six-fold increase for the nitrogen-cured and air-cured wetting region over the air-cured non-wetting region. The ion at m/z 42 has a two-fold increase for the nitrogen-cured and air-cured wetting region over the air-cured non-wetting region and is due to the CNO^- ion. As with the positive data, resolved peaks are observed up to about m/z 320 however, peak intensities other than those mentioned do not change appreciably.

4.7.3 Discussion

The positive-ion and negative-ion spectra for the three contact lens regions suggest very similar major ion peaks at similar intensity levels. Where intensity levels were seen to vary between lens regions these differences were often associated with ions related to contaminants such as Fe^+ or Cu^+ from the mounting stub or from the saline blister packaging solution, such as Na^+ or K^+. The notable exception here relates to the negative-ion spectra where differences were observed in the ion intensity associated with elemental nitrogen on the contact lens surface. Nitrogen is primarily found in the monomer component VMA (although a small component is also present in M3U) and was present at significantly higher levels in the wettable surfaces (the nitrogen-cured and air-cured wetting regions) compared to the surface with poor wetting properties (air-cured non-wetting region). This finding suggests higher levels of VMA at the surface of the nitrogen-cured and air-cured wetting

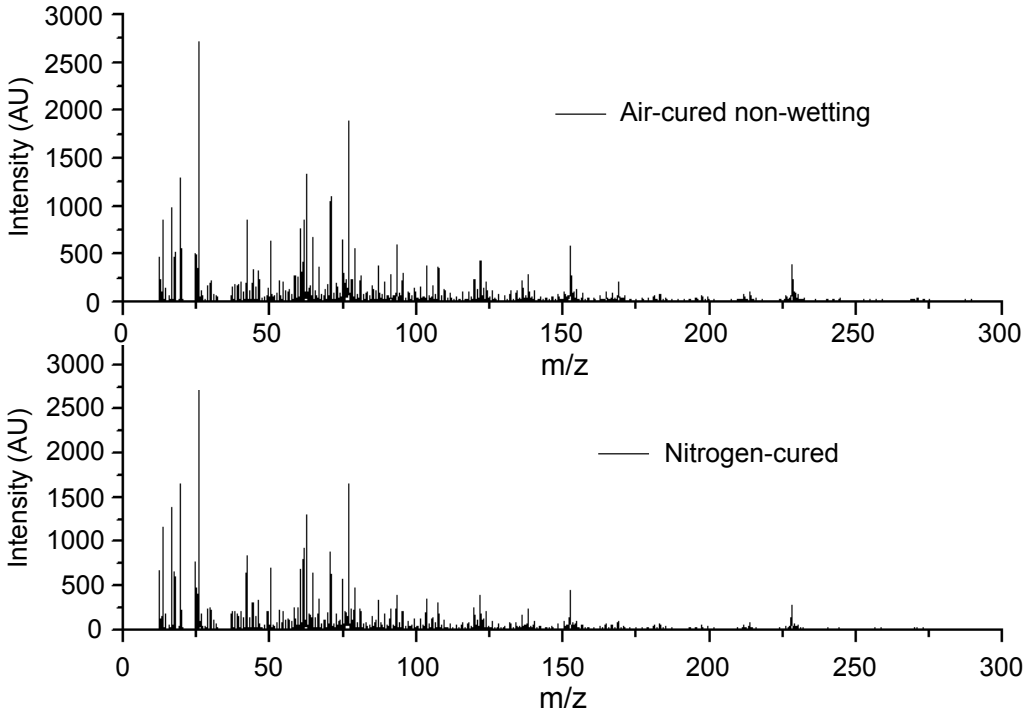

Figure 4.23: Negative Ion ToF-SIMS spectra of dehydrated (a) air-cured non-wetting (above) and (b) nitrogen-cured (below) contact lens regions in the 0-300Da region.

surface and as VMA is the primary hydrophilic component in the study lens monomer, it goes some way to explain the difference in clinical performance, although these differences appear very small given the dramatic differences in clinical wetting properties.

These findings are in general agreement with other studies investigating the surface chemistry of silicone hydrogel contact lens materials (Hook *et al.*, 2006; Maldonado-Codina *et al.*, 2004a), although the surface of the present study lenses appear more obviously dominated by siloxane-based material and contain lower levels of hydrocarbon-ions than was the case for balafilcon A or lotrafilcon A (Maldonado-Codina *et al.*, 2004a). A possible reason for these differences is that both balafilcon A and lotrafilcon A lens materials undergo a plasma surface treatment (unlike the study contact lenses) which increases polymer cross-linking and results in a surface which is less able to reorganise when dehydrated. This surface treatment is incomplete on the balafilcon A material and this may be the reason why a greater siloxane signal is observed for this material compared with lotrafilcon A. When the positive ion spectrum from nitrogen-cured study lenses is compared with a reference sample of PDMS (Figure 4.24) there is obvious similarity in the major ion peaks detected, suggesting a surface dominated by siloxane.

Given that the study contact lens is composed of around 30% M3U (the only component monomer which contains siloxane) the results suggest that the surface of all three lens regions is enriched with M3U in the dehydrated state. Several other ToF-SIMS studies have shown that surface enrichment can occur in polymer blends containing siloxane, both in hydrogel (Hook *et al.*, 2006) and non-hydrogel materials (Chen & Gardella, 1998; Selby *et al.*, 1994). In hydrogel materials the surface is able to reorganise in response to the surrounding environment, in order to minimise its surface free energy (Holly & Refojo, 1975). This ability of the surface to reorganise has been demonstrated in the literature using a variety of surface analysis technique (contact angle (Holly & Refojo, 1975), AFM (Kim *et al.*, 2002), ToF-SIMS (Hook *et al.*, 2006) and XPS (Chen *et al.*, 2008)).

When a hydrated contact lens material is exposed to an air environment it is advantageous for the surface to reorganise with the hydrophobic species exposed at the surface, while the hydrophilic species bury themselves into the bulk of the material (Holly & Refojo, 1975). ToF-SIMS analysis, as with many other surface chemical characterisation techniques, re-

quires analysis to be performed in an ultra high vacuum (in the order of 1x10^{-9} torr). Thermodynamic laws dictate that when a surface is exposed to a non-polar fluid such as air or a vacuum, at a temperature above the polymer's glass transition temperature (T_g), then a reorganisation of the material at the surface can occur. This can be especially marked in amphiphillic hydrogel materials containing a PDMS-type component due to its low glass transition temperature of around -127°C (Owen, 1993). These materials possess a low glass transition temperatures due to their highly flexible silicon-oxygen backbone. If the material is above this temperature, these PDMS-based components are likely to reorganise with the resultant surface being the most thermodynamically stable configuration. In contrast, other non-PDMS based components, such as VMA and MMA present in the study contact lens polymer, are likely to possess significantly higher glass transition tem-

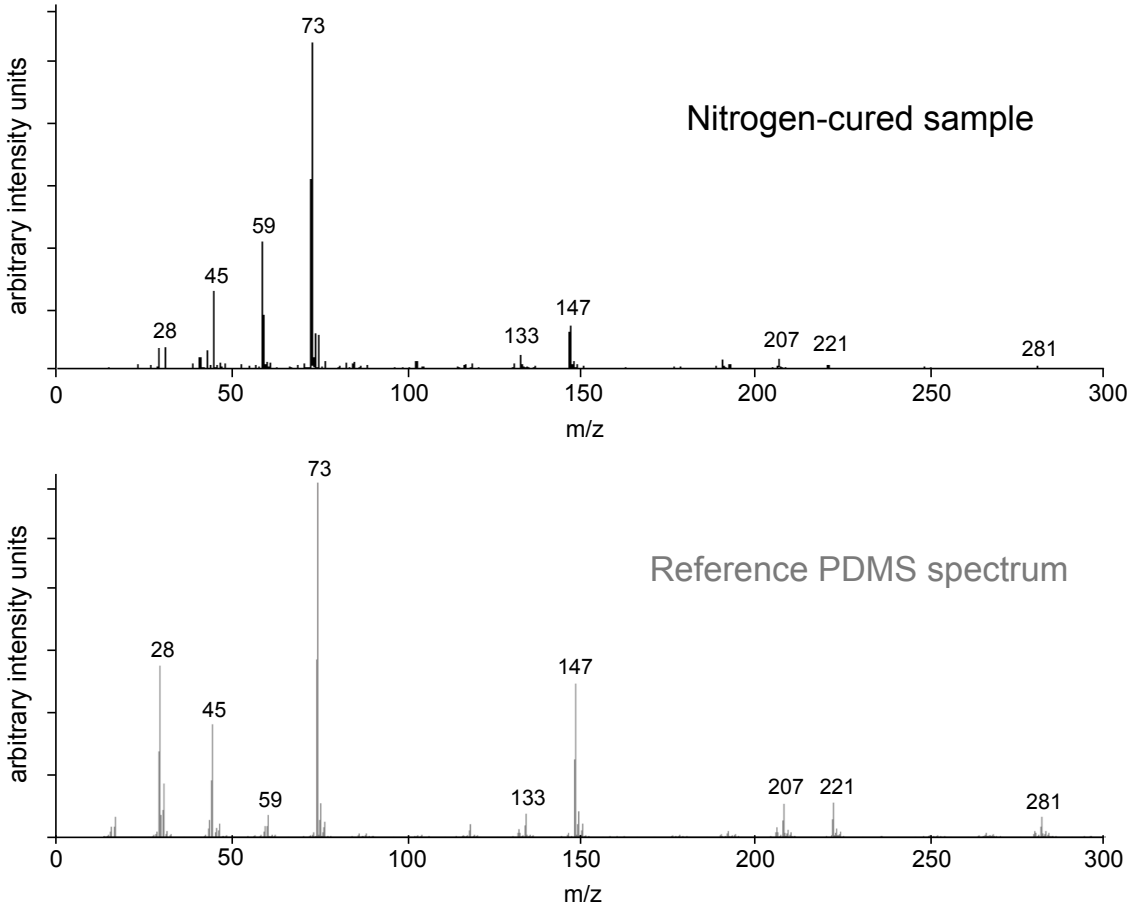

Figure 4.24: Comparison of the positive-ion SIMS spectra from the nitrogen-cured lens sample and a reference PDMS sample (from the Static SIMS library (version 4.0.1.35) by Surface Spectra Ltd).

peratures and thus are unable to significantly reorganise. Hydration of a hydrogel cannot be maintained in a vacuum as water is rapidly drawn out of the material and removed from the chamber to allow the instrument to reach it operational vacuum. The removal of the water molecules is essential otherwise the primary and secondary ions would collide with water particles in the chamber resulting in a poor signal from the surface. This thermodynamically driven process of reorganisation is thought to be the reason why the surface of all of the contact lens regions studied here are dominated by the siloxane signal. The samples were exposed to a pressure in the main chamber of around 1 x 10^{-9} torr and were at room temperature during analysis. This temperature is well above the T_g for the siloxane containing polymer, but lower than the T_g for hydrophilic polymers with a carbon backbone. The likely reason why little difference is found in the surface chemistry using ToF-SIMS is that the initial surface structure when in the hydrated state may be subsequently masked by a preferential reorganisation of the hydrophobic siloxane phase during dehydration of the sample. The wetting properties a material exhibits are usually dictated by the composition of only the first few molecular layers at the interface between the hydrogel material and the wetting liquid (Johnson & Dettre, 1993). It is therefore critical that the surface is preserved in its hydrated state during ToF-SIMS analysis to allow identification of the chemical characteristics responsible for the non-wetting regions. In an attempt to preserve the hydrated surface composition for these materials in a UHV environment it was decided to develop a cryogenic handling technique which is detailed in the following study.

4.8 Study 2 - ToF-SIMS analysis using a cryogenic handling technique

4.8.1 Methods

The lens sample preparation for this study was similar to that described previously in Section 4.7.1.1. In brief, this involved the use of a laboratory instrument, detailed in Section 2.2.2.1, to identify three regions of interest on the study lenses (i) air-cured wetting, (ii) air-cured non-wetting and (iii) nitrogen-cured. Following lens soaking in HPLC grade water (for 24 hours), a 3.5mm stainless steel punch was used to cut lens samples in these regions (Figure 4.25b). In contrast to the previous study the cryogenic sample handling technique required the samples to be mounted and analysed individually on a copper stub.

Each lens sample was placed onto a copper stub and partially lowered into liquid nitrogen where the sample was rapidly frozen indirectly through the conducting copper block (figure 4.25 d). After 5 minutes in liquid nitrogen the copper stub was rapidly transferred onto the pre-cooled ToF-SIMS arm and moved through into the introduction chamber where it was placed into a temperature controllable fork, itself cooled by circulating liquid nitrogen. The chamber was pumped down to a ultra high vacuum (1 x 10^{-7} torr) while maintaining the lens sample in a frozen state. After 1 hour in the UHV preparation chamber, the sample was transferred into the main chamber, where it was maintained at cryogenic temperatures at a pressure of (1x10^{-9} torr). The $C60^{+}$ primary ion source was used to etch through the frozen water layer over a 200 μm^2 area until a non-water signal was detected. ToF-SIMS analysis was then performed on the exposed hydrated lens surface over a 100 μm^2 area. This process was used to analyse the wetting and non-wetting regions of the air-cured lenses and the nitrogen-cured study contact lenses. For each region of interest (nitrogen-cured/air-cured wetting region/air-cured non-wetting region) there were two samples, with each sample analysed in three different 200μm^2 areas (**2** samples x **3** lens regions x **3** 200 μm^2 scans), giving a total of 18 positive and 18 negative spectra obtained in this study. The ToF-SIMS instrument has been described previously in Section 4.7.1.3 and the precautions taken to avoid sample contamination were described in Section 4.7.1.4.

4.8.2 Results

The spectra from the frozen hydrated samples contained substantially less total counts than those run at room temperature making the spectral comparison challenging (Figure 4.26). Figure 4.27 shows the spectra for the nitrogen-cured and both the wetting and non-wetting regions of the air-cured study lenses. The comparison of the sum normalised data shows few differences in the main peaks observed and the appearance of no new peaks. The two largest differences observed in the frozen-hydrated samples are that the air-cured non-wetting region has a higher intensity at m/z 39, which based on the presence of two shoulder peaks, would likely make this from K^{+}, and m/z 23 which indicates the presence of Na^{+}. However the presence of these two ions can come from several outside sources, such as the saline solution, and are not likely to be sample dependent. Another difference was observed at m/z 15, where the signal was much stronger for the air-cured wetting region than both the nitrogen-cured and air-cured non-wetting regions. This ion

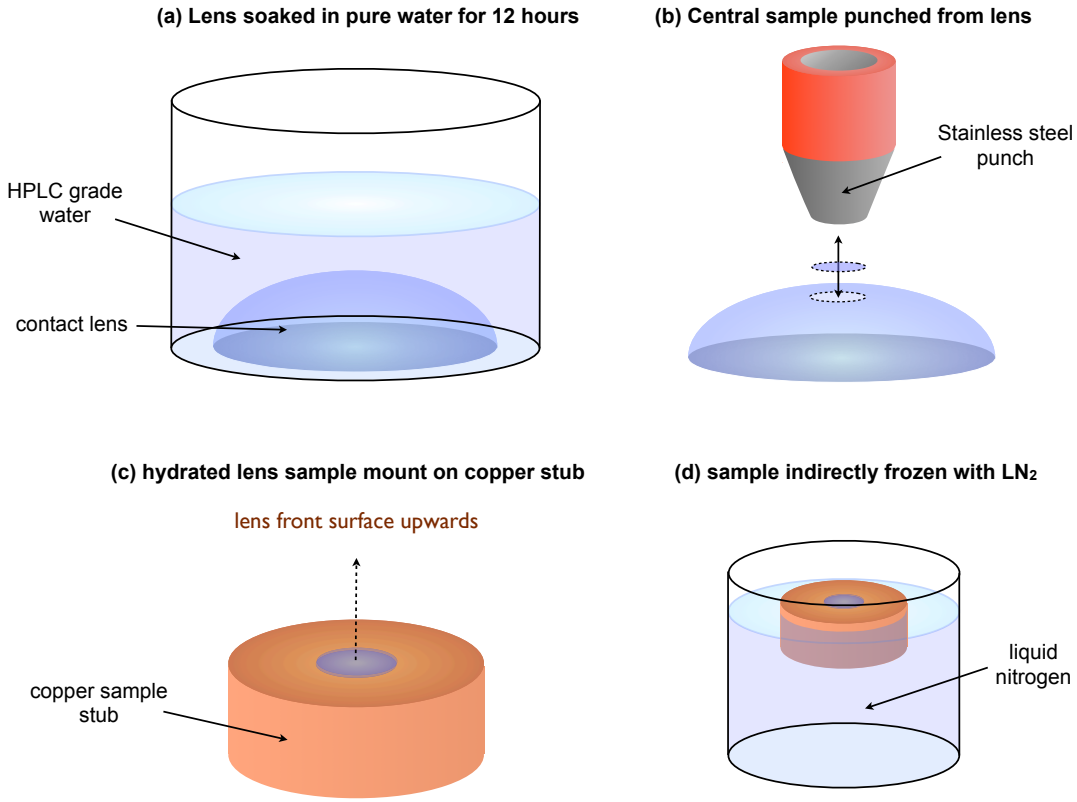

Figure 4.25: ToF-SIMS sample preparation using a cryogenic handling technique.

is likely associated with $CH3^+$. Differences were also observed at m/z 43, 45 and 59 with these ions most probably associated with silicone containing ions (CH_3Si^+, $SiOH^+$ and $(CH_3)_2SiH^+$) where higher ion signals were detected for the nitrogen-cured study lenses as detailed in Table 4.6.

4.8.3 Discussion

The data set obtained for the cryo-analysis of the study lens regions had a relatively low secondary ion signal count, making interpretation difficult. The main difference between the data sets in this study and those in the previous ToF-SIMS studies, related to the frozen-hydrated sample handling technique. The presence of water at the lens surface can lead to a charging effect, which can reduce the secondary ion signal. In addition, the use of the $C60^+$ source to remove the protective water layer can result in an increase in the amount of water in the vacuum which can both raise the chamber pressure and interfere with both the movement of the primary and secondary ions. The presence of the water therefore caused the secondary ion signal to have a reduced peak height (see Figure 4.26), making peaking assignment and spectral comparison much more challenging. Although the SIMS spectra for the different lens regions suggested a very similar composition for the cryogenically frozen lens samples, there were differences in intensity for some of the secondary ions peaks observed. The nitrogen-cured lenses showed a relative high intensity for the peaks associated with siloxane (m/z 43, 45 59), compared with the air-cured non-wetting lens regions. Increased levels of siloxane-containing species at the surface might seem counterintuitive as this is likely to result in a surface with a relatively high surface free energy (due to the highly flexible silicone/oxygen polymer backbone) and therefore would be expected to display relatively poor wetting characteristics. In contrast, we know that

Table 4.6: Relative intensity of silicon-containing ion peaks during cryo ToF-SIMS analysis.

Peak location (m/z)	**Relative Intensity**
43	nitrogen > air wetting > air non-wetting
45	nitrogen > air wetting **and** air non-wetting
59	nitrogen **and** air wetting > air non-wetting

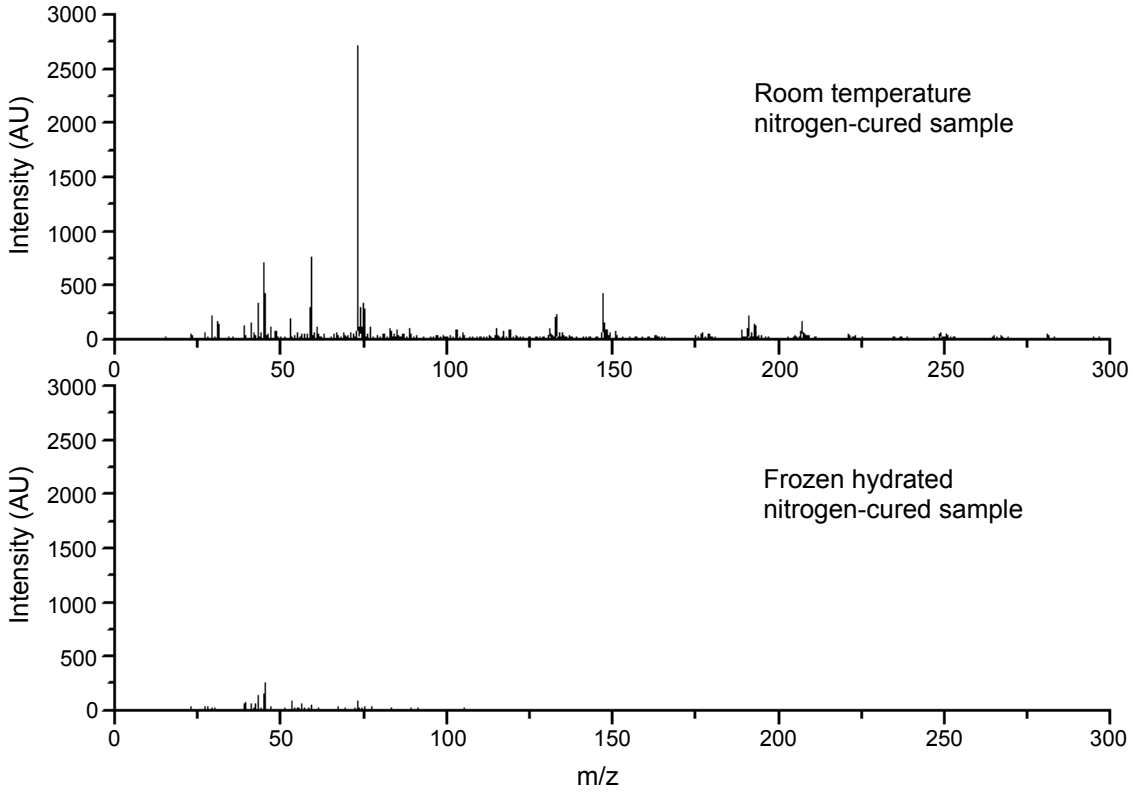

Figure 4.26: Positive-Ion ToF-SIMS spectra for (i) a dehydrated nitrogen-cured sample and (ii) a hydrated frozen nitrogen-cured sample.

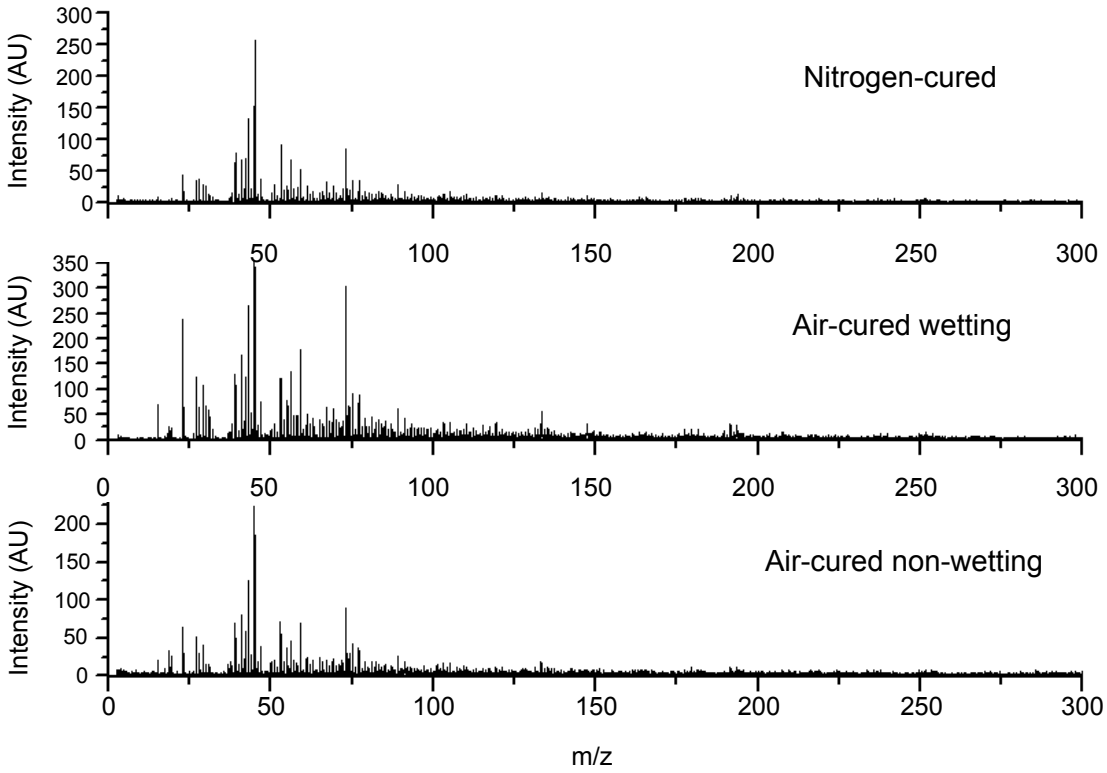

Figure 4.27: ToF-SIMS spectra using cryo-analysis for (a) nitrogen-cured sample, (b) air-cured wetting region and (c) air-cured non-wetting region.

the nitrogen-cured lenses have better wetting characteristics compared with the air-cured non-wetting lens regions. This may be due to the analysed film not being the lens surface, but sub-surface. Ideally the protective surface water layer would be sublimed away, exposing a frozen hydrated lens surface. In the experimental methodology used here the vacuum and temperature controls were not sensitive enough to allow sublimation to occur in the required temperature range (<-127°C). Therefore, the frozen surface water film was removed by primary ion etching of the surface until the secondary ion signal changed from water to that of a polymer surface. With this technique it is difficult to ensure that all the water is removed, while ensuring that none of the polymer surface is removed, prior to analysis. It may well be that the very surface of the lens was removed by etching prior to analysis. Other possible reasons for the finding of more apparent siloxane on the surface of the nitrogen-cured lens may include changes in the surface chemistry related to the etching ion beam or that the etching ion beam influenced the local temperature of the sample, allowing reorganisation of the polymer components to reduce the free energy at the apparent lens surface.

The reduction in the secondary ion signal is likely associated with the presence of water interference as the surface was etched to expose the contact lens. The presence of the water molecules tends to increase the pressure, making it more difficult to maintain an adequate vacuum. The problems associated with low secondary ion signal count could be minimised in future studies by:

1. The use of a cold finger (an extremely cold probe placed into the main chamber) allowing water molecules to condense on it removing them from possible interference with the ions. Chen (2008) describes the used a modified sample holder with cold finger in their analysis, which provides improved secondary ion signal in SIMS analysis.

2. Leaving the sample in an UHV for a prolonged period to allow the surface water to slowly sublimate.

3. After ion etching with the $C60^{+}$ source, the chamber could be left for a prolonged period allowing time for the water molecules to be removed from the vacumm.

Improvements which could be applied to future studies could also include the mounting of all three study lenses on the sample analysis stub, as used for the XPS study (Figure 4.12),

to ensure the samples are prepared in a similar manner. Another possible improvement to the study would be to replace the liquid nitrogen used in this study with liquid propane which would allow more rapid cooling of the lens samples. Even with the problems experienced using the cryogenic handling technique it is clear that the hydrated lens surface has a very different chemical character to the same surface following dehydration. Figure 4.26 compares the positive-ion SIMS spectra for the nitrogen-cured lens surface when in a hydrated and dehydrated state. It is evident that the major ion peaks differ for the two conditions, in agreement with the findings of the XPS studies, both of which suggest surface segregation of the siloxane polymer following dehydration in all three study lens regions.

4.9 Study 3 - Ion beam etching of study lens materials

4.9.1 Introduction to C_{60}^+ ion beam etching

In an attempt to understand the differences in the surface and sub-surface chemistry between the three lens regions, a depth profiling technique was applied. This involved the initial capture of a ToF-SIMS surface spectrum, followed by use of the C_{60}^+ primary ion source to etch a layer of polymer material away, before capturing another spectrum and then etching again. Previous studies have shown significant variation in the chemical distribution between the surface and sub-surface of a polymer which has been shown to be related both to phase separation (Lee *et al.*, 2008), surface segregation (Hook *et al.*, 2006) or to surface treatment processes (Braun *et al.*, 2007). The C_{60}^+ source was chosen as it has been shown to etch material with much less damage than other primary ion sources (Ga^+ /Cs^+), therefore minimising chemical characterisation artefacts observed following etching (Szakal *et al.*, 2004).

4.9.2 Materials and methods

The contact lens samples were prepared in both a dehydrated (described in section 4.7.1.2) and a hydrated frozen state (described in section 4.8). The etching procedure involved using the C_{60}^+ primary ion source at much higher energy levels that that used for standard ToF-SIMS analysis to remove layers of material. Between each etching phase a ToF-SIMS spectrum was captured, allowing the distribution of the polymer chemistry to be analysed as a function of depth into the material. For the depth profile, spectra were acquired up to

a dose of 2.5 x 10^{14} ions/cm^2. It is generally accepted that a dose of 1.0 x 10^{13} ions/cm^2 would impact nearly 100% of the sample surface. A dose 25 times greater is likely to remove several layers of material, but is still near-surface analysis. The etching technique used here was estimated to etch to a total depth of around 25 - 50nm, although this is sample dependant. For each region of interest (nitrogen-cured region, air-cured wetting region and air-cured non-wetting region), one dehydrated sample and one hydrated frozen samples were analysed, giving a total of six depth profiles performed. For the data comparison, the spectra were normalised to total counts so an absolute intensity comparison could take place. Data comparison therefore involved visually inspecting the spectra to observe if any new peaks formed or if relative intensities for the peaks change noticeably (>10%).

4.9.3 Results

4.9.3.1 Depth profiling data for dehydrated samples

Figure 4.28 provides positive secondary ion intensity profiles from select ion species plotted as a function of sputter ion dose (C_{60}^+/cm^2). The ion species chosen are believed to best represent the components present in the study contact lens materials. It should be noted that fragments consistent with the same chemistry as those chosen for the plots showed similar intensity variations, as highlighted in Figure 4.29. The M3U-based intensity distribution (m/z 73 & 147 in figure 4.28) shows a steady decline for all three lens regions, with a more immediate reduction for primary ion dose densities of less than 2 x 10^{13} ions/cm^2 for the two air-cured lenses regions. In the deeper sub-surface layers (primary ion dose 2 to 10 x 10^{13}) the air-cured wetting regions shows a less marked intensity reduction than the air-cured non-wetting region. The intensity variation of the sodium ions differ between the lens regions, with the nitrogen-cured and air-cured wetting regions showing a relatively small variation in sodium intensity, whereas the air-cured non-wetting region showed a small reduction in intensity for a primary ion dose up to 3 x 10^{13} ions/cm^2, followed by a rapid increase in intensity for the remainder of the depth profile. Figure 4.30 shows the overlay of the three ion intensities for each of the three lens regions analysed. The intensity variation of the 53 m/z peak with depth, differs to the 73 m/z and 147 m/z peaks (Figure 4.28), suggesting that this signal is not associated with the siloxane macromer. Given the lack of a nitrogen signal, the 53 m/z peak is not likely to be associated with the VMA and more likely associated with either the MMA, EGDMA or AOE monomer components.

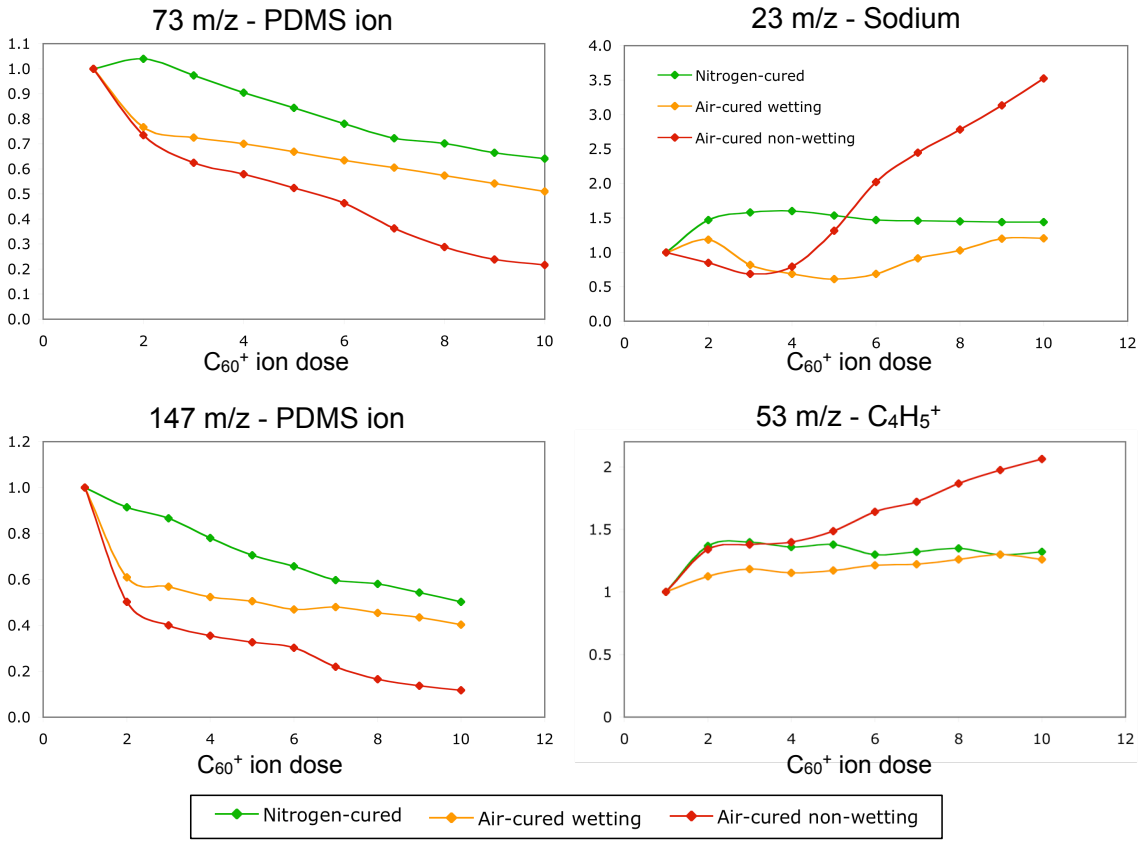

Figure 4.28: Secondary ion intensities for three dehydrated lens regions as a function of sputter ion beam fluence for selected ion species of interest. Intensity profiles allow comparison of the distribution of components between the study lens regions.

4.9.3.2 Sub-surface spectral analysis for dehydrated samples

The spectra from the final depth profiling cycle for each of the three lens regions of interest was then compared to look for differences in chemistry of the sub-surface. Figure 4.31 shows the representative spectra for the air-cured non-wetting region, air-cured wetting region and nitrogen-cured lens samples normalised to total counts. Figure 4.31(a) shows a relatively high intensity for the air-cured non-wetting region over the air-cured wetting region and the nitrogen-cured lens for m/z 53 and 55. Figure 4.31(b) shows the general agreement in the data for several masses from m/z 103 to 113 indicating that differences in intensity for the other ions are significant. Figures 4.31(c) and 4.31(d) show two of the main fragment ions from PDMS; m/z 147 and m/z 73. Both of these ions show a higher intensity in the air-cured wetting region and nitrogen-cured lens compared to the air-cured non-wetting region. The slight shift in peak location is due to differences in the calibration and

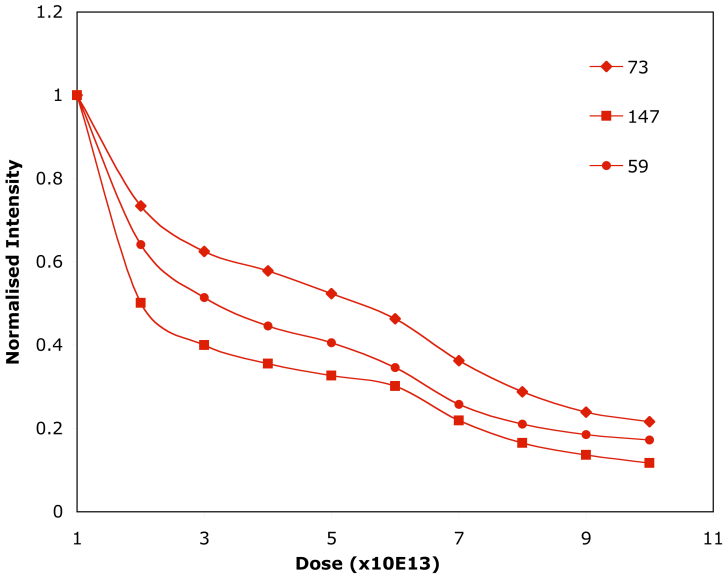

Figure 4.29: Secondary ion intensities for PDMS-related species as a function of sputter ion beam fluence, highlighting the similar intensity variations.

is not representative of ion mass shifts. From this analysis, there were no new peaks which formed, indicating that the three samples analysed are similar in composition. There are, however, some relative peak intensities differences with the air-cured non-wetting regions having a higher relative intensity for m/z 27, 39, 41, 43, 53, 55, 57, 67 and 69, whereas the air-cured wetting and nitrogen-cured regions have a higher relatively intensity for m/z 73, 147, 207 (siloxane peaks) as well as m/z 191 and 193. In addition the nitrogen-cured lens has a higher intensity at m/z 115 compared to the air-cured non-wetting and air-cured wetting regions. Based on the experimental setup and the number of samples which were run, it is possible only to suggest general ion assignments based on the masses observed. This experiment did not attempt to achieve high mass accuracy, which would be needed for a proper diagnosis of the peaks mentioned above. In addition, the sample comparison is for one sample from each type of lens, so no statistical analysis could be preformed. Therefore, we can only speculate at their molecular structures, of which there are several possibilities. For this reason, the first chemical structure which is listed in bold type is the primary assignment of an ion to that peak mass based on certain trends. The other structure(s) suggest possible other ions with a similar mass which are equally possible. It is possible that there is even an overlap from several of these ions. For the air-cured non-wetting region: m/z 27 ($\mathbf{C_2H_3}^+$, Al^+), m/z 39 ($\mathbf{C_3H_3}^+$, K^+), m/z 41 ($\mathbf{C_3H_5}^+$), m/z 43 ($\mathbf{C_3H_7}^+$, CH_3Si^+, $C_2H_3O^+$), m/z 53 ($\mathbf{C_4H_5}^+$), m/z 55 ($\mathbf{C_4H_7}^+$, Mn^+), m/z 57

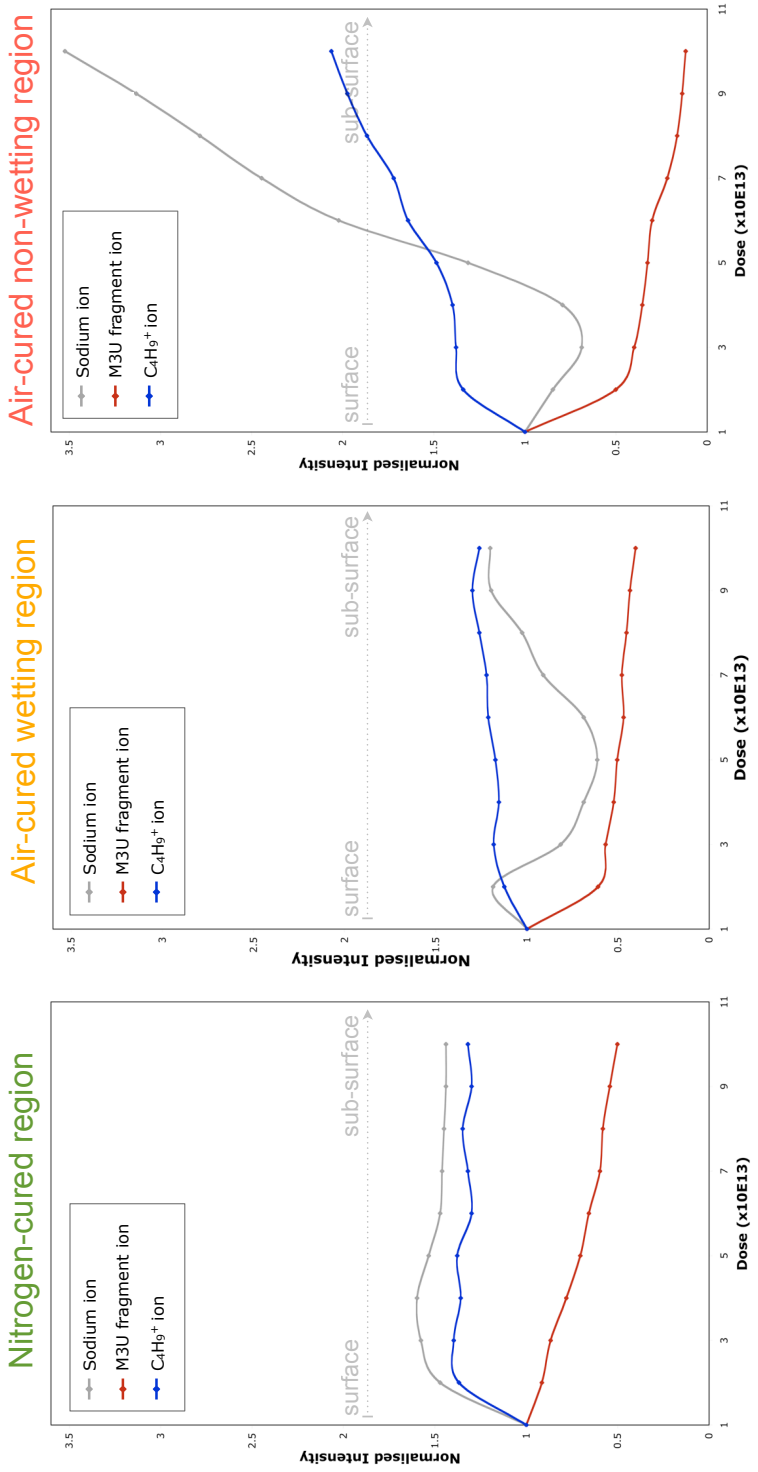

Figure 4.30: Secondary ion intensity depth profiles for three select ions species as a function of ion beam fluence for the dehydrated study contact lens regions. Intensity profiles show the relative distribution of components at the surface vs the sub-surface of the lens

($\mathbf{C_4H_9}^+$), m/z 67 ($\mathbf{C_5H_7}^+$) and m/z 69 ($\mathbf{C_5H_9}^+$, $C_4H_5O^+$). The assignments in bold all correspond to major hydrocarbon fragments. This may indicate that subsurface, the air-cured non-wetting region contains a slightly higher proportion of material that contains hydrocarbon groups or produces hydrocarbon fragments. For the air-cured non-wetting region ions at m/z 73 ($\mathbf{Si(CH_3)_3}^+$), 147 ($\mathbf{Si_2O(CH_3)_5}^+$) and 207 ($\mathbf{Si_3O_3(CH_3)_5}^+$) when observed together almost certainly arise from the presence of a siloxane. Signals from these peaks are all of higher intensity for the air-cured wetting region and the nitrogen lens compared to the air-cured non-wetting region, indicating a relatively higher abundance of this type of material in the subsurface region of the air-cured wetting region and nitrogen-cured lenses. Ions at m/z 191 and 193 are unassigned, but may be related to polyethylene terephthalate, as identified in the chemical database (J.C. Vickerman & Henderson, 2006). For the nitrogen-cured lens, m/z 115 brings up a number of possible ions and is difficult to assign with no other peak trends, with the database suggesting $C_5H_7O_3^+$, $C_6H_11O_2$ or $C_9H_7^+$.

4.9.3.3 Depth profiling data for cryo-frozen samples

Figure 4.32 shows the normalised secondary ion intensity for the H_3O^+, $C_4H_9^+$ and M3U fragment ions during the C_{60}^+ depth etching process for the three lens regions. In all three lens regions a H_3O^+ ion signal suggests the presence of an ice layer on the lens surface. The varying amount of C_{60}^+ ion etching required to bring about a significant reduction in the H_3O^+ ion signal (a dose of 4 x 10^{13} for nitrogen-cured lens region compared with 7 x 10^{13} for the air-cured wetting lens region), suggests a difference in the ice film thickness between the lens regions. In the early stages of the depth profile the mixture of ion signals originating both from the contact lens material and the ice film suggest that the etching process is not completely removing the ice and then etching though the contact lens surface, but rather etching some of the lens surface at the same time as some of the ice layer. Possible reasons for this include an uneven ice film thickness, a uneven distribution of the etching process or a rough/uneven contact lens surface. Analysis of the contact lens surface with an ice layer partially present is clearly not ideal and a goal of future studies would be to remove the ice film either by sublimation or by obtaining better control of the etching process. Highlighted on Figure 4.32 is the point where the H_3O^+ signal falls to a near zero value suggesting the complete removal of the ice film for each lens. Associated with the initial minimum H_3O^+ signal is a peak for the M3U fragment ion for all three lens

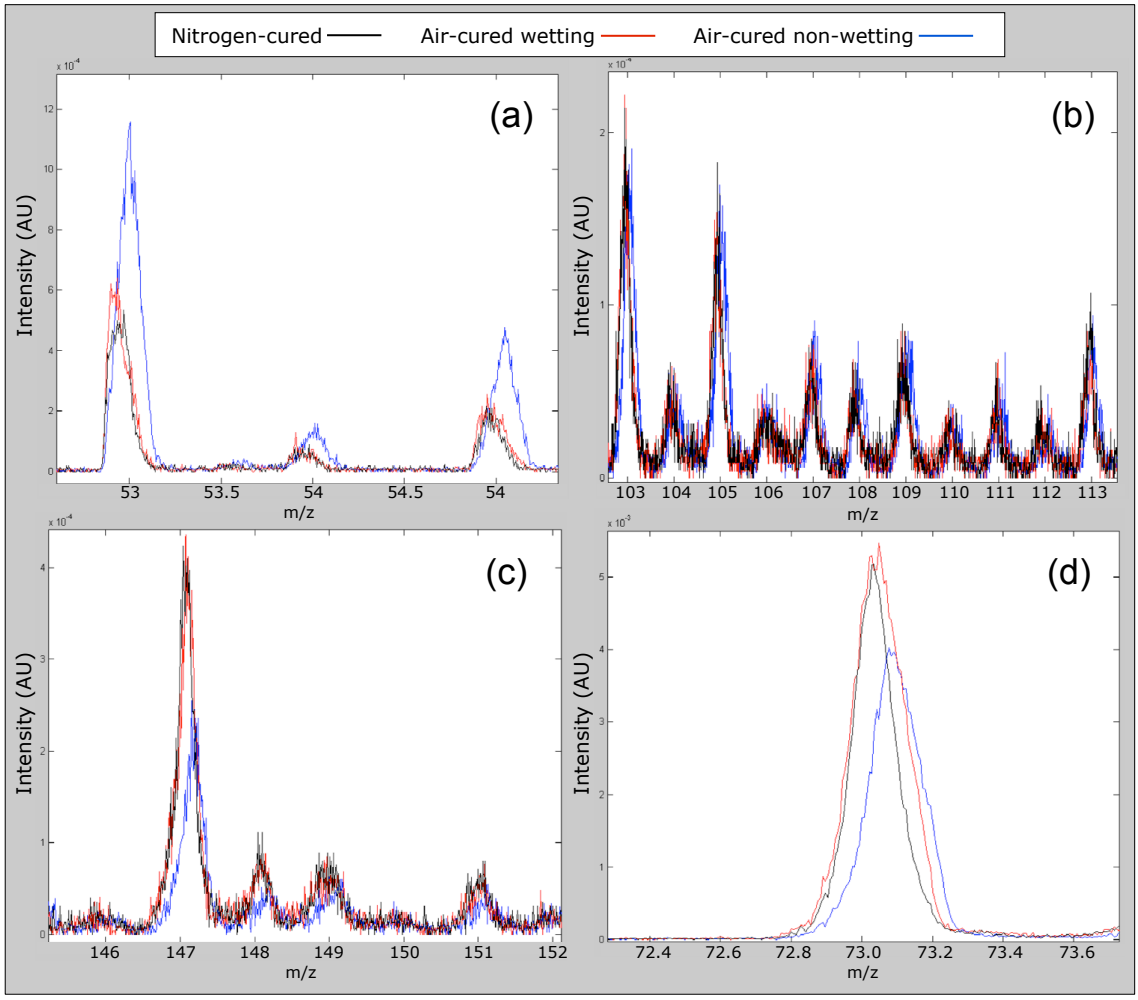

Figure 4.31: Room temperature ToF-SIMS spectra for the three study lens regions for (A) 52 - 54 m/z, (B) 103 - 113 m/z, (C) 145 - 152 m/z, (D) 72 - 74 m/z) following completion of the etching process. These spectra describe the sub-surface chemical composition.

regions. This pattern was observed for all the M3U-related peaks (m/z 43, 73 and 207) on all three lens regions. The $C_4H_9^+$ ion showed a similar intensity trend near the surface, with peak intensity just below the polymer surface. Due to apparent charging effects a negative ion spectrum was not able to be captured for any of the three lens regions. The $C_4H_9^+$ ion intensity showed a reducing signal with depth, as was observed for the M3U-related peak, but at a slower rate. The cryogenic depth profiles suggest a surface enrichment in all three contact lens regions for both $C_4H_9^+$ related material and to a much greater extent M3U-related material. As with the dehydrated lens samples there was little evidence of a significant nitrogen-based ion signal, suggesting that the levels of VMA in the surface and sub-surface regions are relatively low. Given the variable thickness of ice on the surface of the samples, comparison is difficult, therefore Figure 4.33 shows the same data but with the results normalised to first data point with minimal H_3O^+ signal for each lens region, to allow the surfaces to be more readily compared.

4.9.4 Discussion

When a hydrogel material is exposed to a hydrophobic environment it is thermodynamically advantageous to structurally reorganise to present a surface with a high surface free energy (Holly & Refojo, 1975). This potential reorganisation only occurs if the material is above its T_g. When the hydrogel is a blend of polymers, there can be preferential surface reorganisation for those with a low T_g compared to those with a high T_g. For siloxane-containing hydrogel polymers such as the study contact lens materials this process can be particularly marked as the silicone-oxygen polymer backbone is especially flexible, giving it an extremely low glass transition temperature of around -127°C. By freezing and maintaining the contact lens sample below its T_g it was expected that the chemical differences presumed to be present when hydrated and at room temperature would be preserved. The use of the depth profile allowed the observation of the chemical distribution at the surface and sub-surface when the lens was in both a hydrated and dehydrated state.

4.9.4.1 Depth profile at room temperature

Depth profiling using a C_{60}^+ primary ion source has been able to obtain information on the variation of composition with depth below the initial surface for both dehydrated and hydrated (frozen) lens sample. In both the hydrated and dehydrated studies, the spectra have been composed primarily of ions associated with siloxane polymers, although hydro-

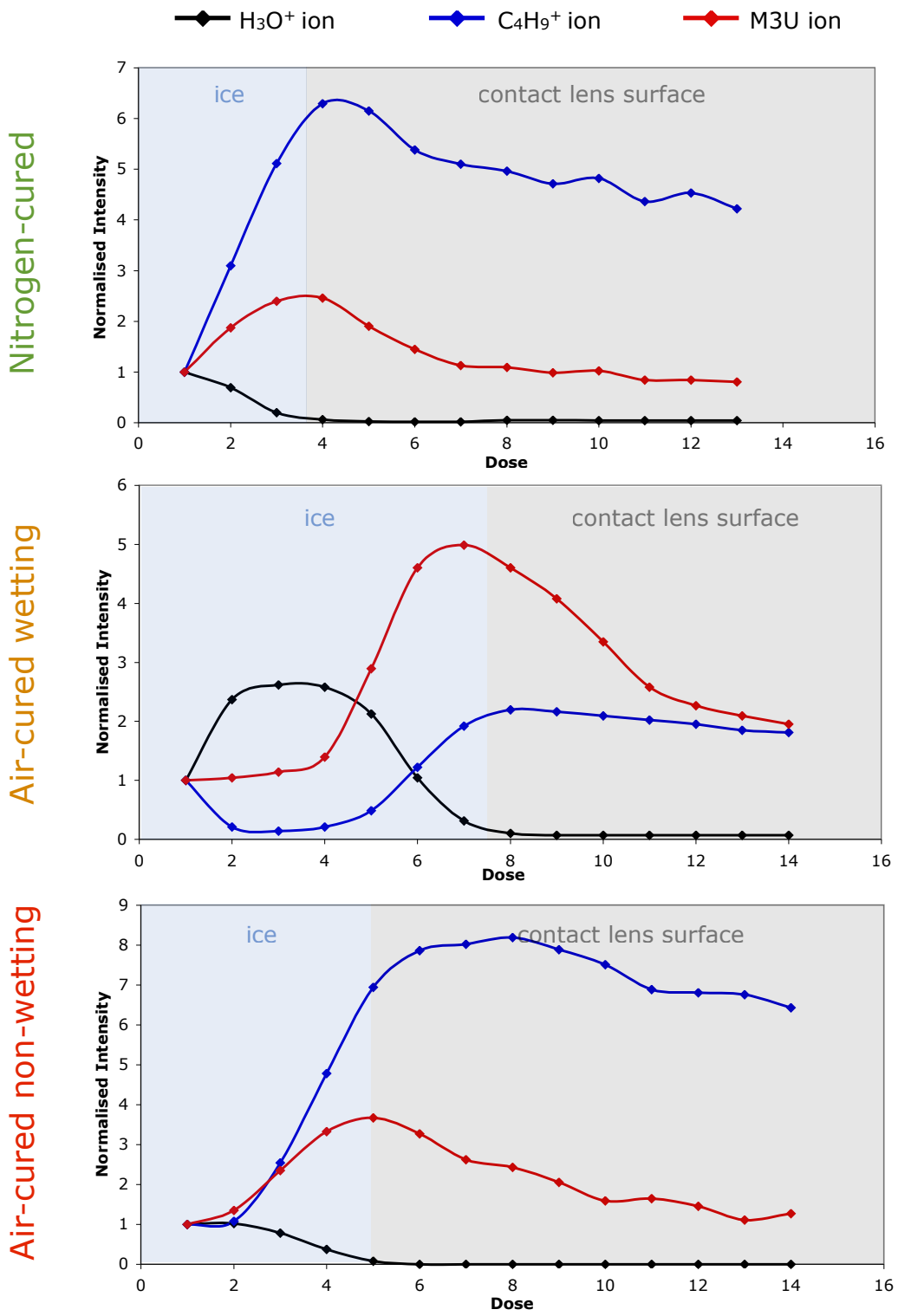

Figure 4.32: Secondary ion intensity depth profile for three ion species as a function of ion beam fluence for the cryogenically frozen study contact lens regions. Intensity profiles show the relative distribution of components at the surface vs the interior of lens.

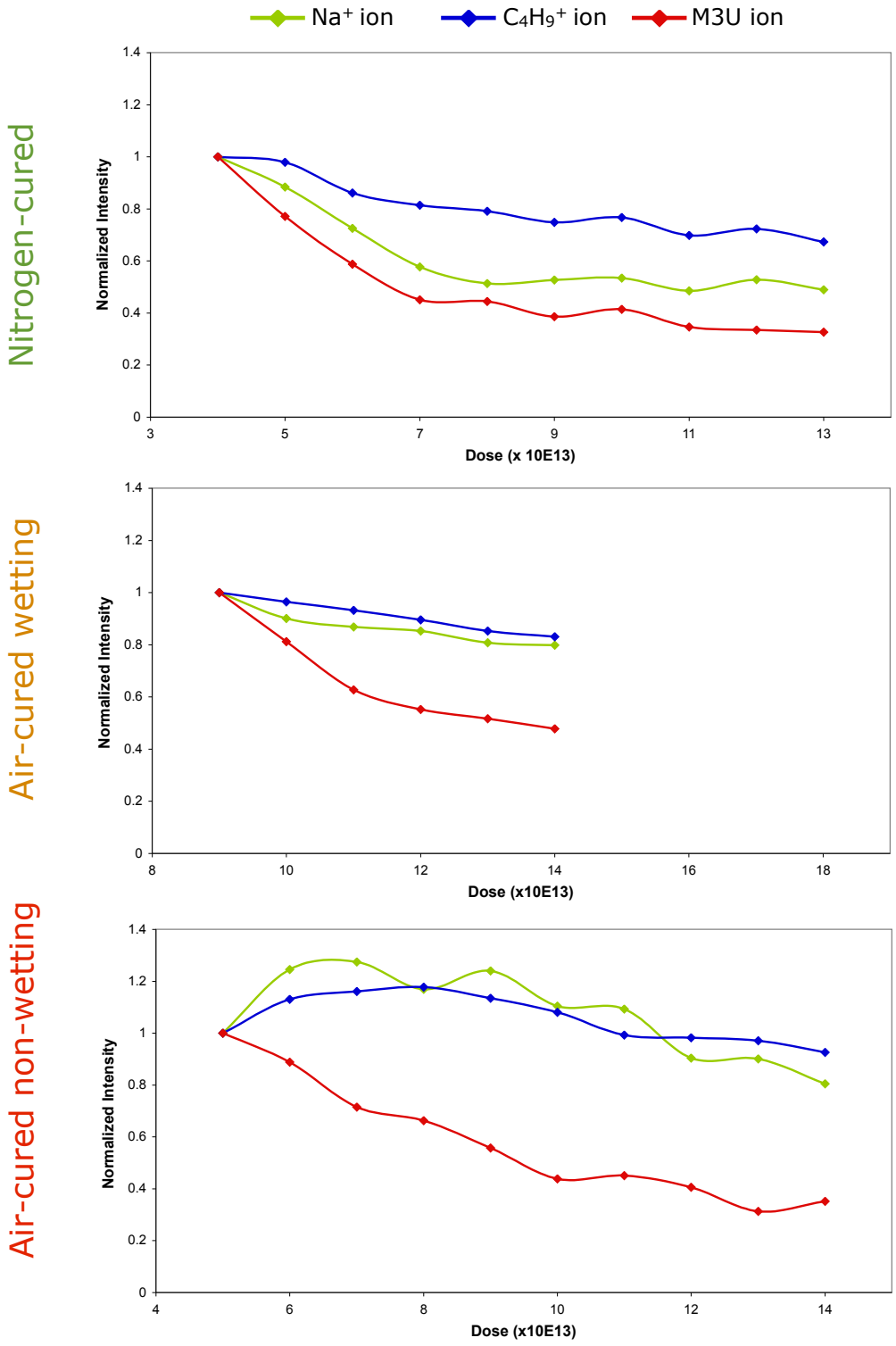

Figure 4.33: Secondary ion intensity depth profile for three ion species as a function of ion beam fluence for the cryogenically frozen study contact lens regions. The data is normalised to a point where there has been a substantial signal decrease from the m/z 19 signal for each material to allow a more direct comparison.

carbon ion species have been identified. This indicates the presence primarily of the M3U silicone macromer at the surface of these materials, along with other components such as methyl methacrylate. Interestingly, there was little evidence, in either the hydrated or dehydrated state, of any ion signal associated with the nitrogen-containing hydrophilic component, VMA. When studying the intensity of the M3U related ions with depth, it became clear that all ions followed similar patterns, with a peak intensity at the sample surface followed by a rapid reduction in intensity with depth to a relatively steady state intensity by the tenth etching cycle. The change in intensity of the siloxane-related ion was greatest for the two air-cured lens regions compared to the nitrogen-cured region. The hydrocarbon ions appear associated with the component monomer methyl methacrylate and followed a similar pattern in both dehydrated and hydrated state, suggesting it reached an intensity peak slightly below the sample surface where it either remained at a steady state or reduced to a relatively steady state with increasing depth. All lens samples showed the presence of significant levels of sodium, likely associated with the saline (sodium chloride) soaking solution, even though they had undergone 24 hours of soaking in pure water. The intensity of the sodium ion signal appeared similar to that observed in previous ToF-SIMS depth profiling studies (Braun *et al.*, 2007). Interestingly, the air-cured non-wetting region showed a rapidly increasing Na^+ signal with depth, unlike the other lens regions, suggesting that saline clearance in this region may have been restricted possibly as a result of poor ion permeability in this region, due to a lack of hydrophilic polymer present, although further work is required to confirm if this is the case. These findings suggest an enrichment of M3U-related material in the top surface layers of all three lens regions in their dehydrated state, with the concentration gradient for the M3U component greater for the air-cured non-wetting and least for the nitrogen-cured lens region. In contrast, the hydrocarbon species consistent with the hydrophilic component monomers possess intensity variations that were relatively low at the surface before rising to a relatively steady state for the nitrogen-cured and air-cured wetting region, but saw a continued increased across the profiling depth for the non-wetting region.

Comparison of the sub-surface ToF-SIMS spectra showed differences in the chemistry between the three lens regions, with the non-wetting region from the air-cured lens showing a higher relative intensity for hydrocarbon fragments while the wetting region from the air-cured lens and the nitrogen-cured lens show a higher relative intensity for the siloxane-

related ion peaks. These findings rather counter intuitively suggest that the sub-surface of the non-wetting regions have a higher abundance of material that produces hydrocarbon fragments, whereas the regions with good clinical wetting properties have a higher abundance of siloxane type material in the sub-surface region. The hydrocarbon fragments detected are unlikely to originate from the VMA due to a lack of nitrogen ion signal in the spectra or TEGDMA given the low level of TEGDMA in the material (approximately 1%) and is therefore likely to originate from the MMA lens component. The MMA component is included in the material both to improve compatibility of the siloxane and hydrophilic lens components and possibly to reduce the ion permeability of the material in an attempt to reduce clinical complications, such as conjunctival staining. The relatively high levels of MMA in the sub-surface below the non-wetting regions may be resulting in regions with poor ion permeability and a relative low surface water content, which might increase the hydrophobic nature of the lens surface. An alternative hypothesis is that when the lens surface is exposed to an air environment at room temperature, the material at the surface and in the sub-surface regions is likely to reorganise in an attempt to lower the surface free energy of the material. For polymers with a hydrocarbon backbone this results in a reorganisation of the pendant groups, but in siloxane type polymers this can result in a reorganisation of the entire polymer due to its highly flexible silicon-oxygen backbone. Factors such as the extent of polymer cross-linking or the molecular weight of the polymer are likely to influence the degree to which this reorganisation occurs. Given the presence of oxygen during the polymerisation of the air-cured lens it is likely that this may have resulted in the premature termination of the free radical polymerisation. Oxygen inhibition has been shown to result in surface regions which are less heavily crosslinked and typically with a lower molecular weight (Biswal & Hilt, 2009). The lack of siloxane in the sub-surface of the air-cured non-wetting region may be as a result of the reorganisation of this material towards the surface leaving the sub-surface region relatively rich in hydrocarbon material. For the nitrogen-cured and air-cured wetting regions the siloxane component may be more heavily cross linked and be of a higher molecular weight with greater entanglement leading to a reduced ability to reorganise, resulting in the comparatively high intensity for the siloxane fragments observed in the sub-surface region.

4.9.4.2 Depth profile at cryogenic temperatures

The depth profiles obtained for the cryogenically frozen samples were complicated by the presence of an ice film over the lens surface. The use of the C_{60}^{+} ion source to etch though this ice layer allowed a SIMS spectra for the frozen lens surface to be captured, but resulted in a lowering of the vacuum pressure and presented problems associated with capturing of negative ion data. Figure 4.32 shows that prior to etching, a significant water layer was present on each sample which was of variable depth. Figure 4.33 shows the same data, but in this case the starting point of acquisition is defined as the point at which the m/z 19 signal first became negligible and at this point the data was normalised for all the lens regions. This allowed the lens regions to be readily compared and overcomes the problems associated with different ice layer thicknesses. The M3U-related ion intensity was seen to reduce in a similar manner to that observed in the dehydrated samples, with M3U surface enrichment which rapidly fell to a near steady state with increasing depth. The hydrocarbon fragment ions also followed a similar pattern to the dehydrated lens samples with the greatest ion intensity at the surface or in the immediate sub-surface region with a steady reduction in intensity with depth. As was observed for the dehydrated lens samples, the air-cured non-wetting region showed a higher relative intensity for the hydrocarbon fragment ions than the other two lens regions in the sub-surface region, reducing less markedly in intensity with depth. The sodium signal associated with the saline solution was seen to follow the ion intensity distribution of the hydrocarbon fragments, suggesting that this hydrocarbon element may be resulting in reduced ionic permeability and therefore a reduced ability for the sodium to soak out of the material in these regions.

Few ToF-SIMS studies have investigated hydrogel materials using a cryogenic depth profiling technique. Sosnik *et al.* (2006) described the use of a deep freezing ToF-SIMS approach to study the surface of collagen/poloxamine hydrogels. They also observed problems with the formation of a thin ice layer even when using a nitrogen-purged preparation chamber. Their subsequent methodology involved warming the UHV chamber up to around -70^{o}C to allow sublimation of the water. This methodology appears acceptable for their sample types, but with siloxane-containing materials this may induce reorientation as this is substantially above the expected T_g of the siloxane macromer. Braun *et al.* (2007) performed a depth profiling ToF-SIMS technique on dehydrated conventional contact lenses. Although the lens materials differ to those in this study, similar trends were observed

with the intensity distribution of the multiple polymer components varying, with some components showing evidence of lens surface enrichment while other components show enrichment beneath the top layer of the lens surface. In agreement with our study, these intensity differences were typically seen to reduce with depth, suggesting that they may be caused, at least in part, by differences in surface free energies of the polymer components. On exposure to a vacuum environment it might be reasonable to expect the most hydrophobic species to be driven towards the vacuum/surface interface while the more hydrophilic components are more stable deeper within the lens bulk.

One of the major general advantages of ToF-SIMS is its surface sensitivity (∼2nm) and it therefore seemed an obvious tool to probe the molecular composition of the wetting and non-wetting regions on the study contact lens surfaces. The main problem involved in applying this technique to hydrogel materials is the need for UHV analysis chamber conditions. To avoid potential reorganisation at the lens surface associated with dehydration of the lens material, a cryogenic handling technique was used. This still seemed unable to identify substantial molecular differences between the wetting and non-wetting regions of the air-cured samples and between either of these and the nitrogen-cured lenses. The inability of ToF-SIMS to identify substantial differences in the surface chemistry, in contrast to the differences highlighted by the XPS analysis (Section 4.4.3), is likely related to the very high surface sensitivity of the SIMS instrument, which means that any surface contamination or surface segregation can result in the true surface of the material being masked.

4.10 Conclusion

This study has used ToF-SIMS to highlight differences in the surface chemistry of silicone hydrogel contact lenses manufactured using different polymerisation conditions. ToF-SIMS surface characterisation of the dehydrated lens samples showed surfaces dominated by the siloxane fragmented ions, suggesting a large degree of surface segregation for the siloxane-containing M3U macromer. Small differences were observed in the negative ion spectra suggesting a greater concentration of the hydrophilic VMA at the surface of the nitrogen-cured and air-cured wetting lens regions. Depth profiling of the dehydrated lens samples using the C_{60}^{+} primary ion source confirmed the presence of surface segregation

for the M3U polymer although this was similar for all three lens regions. Relatively high intensity was observed for ions apparently associated with the polymer component MMA in the sub-surface region, along with an elevated sodium ion signal for the air-cured non-wetting lens region, suggesting the possibility of reduced ion permeability in these regions. The use of a cryogenic sample handling technique during ToF-SIMS analysis showed that the spectra produced by a hydrated (frozen) lens sample was far less dominated by the siloxane ion peaks than when dehydrated, highlighting the thermodynamically driven surface reorganisation that occurs during sample dehydration, with this material. Even when frozen, the surface shows evidence of some surface segregation for the siloxane macromer M3U in all three lens regions. The non-wetting regions on the air-cured lens surface also showed an elevated intensity for MMA and sodium in the sub-surface, indicating that MMA may also play a role in the formation of the non-wetting regions. No hydrophilic VMA-related ions were seen in any of the spectra during surface analysis or depth profiling, for any of the lens samples. The secondary ion signal intensity was significantly reduced compared to that observed for the dehydrated lens sample which is likely related to water ions in the analysis chamber.

The use of the ToF-SIMS instrument to probe the study materials in both a dehydrated and hydrated state and at varying depths has allowed a greater understanding of the surface and sub-surface chemistry in these regions. This work has also highlighted the importance, particularly for siloxane containing materials, of analysing the surface chemistry of the contact lens in a hydrated state to avoid characterising a surface that could have substantially reorganised during sample dehydration. The ToF-SIMS instrument is a highly sensitive surface chemical characterisation tool which provides information about only the outermost layers of the sample material ($\sim$2nm), but by its nature it is highly susceptible to the detection of contamination and/or unintended surface segregation. Further work is required to develop both the methodology and the instrumentation to optimise cryogenic ToF-SIMS analysis for hydrated contact lens samples.

Chapter 5

Contact Lens Surface Topography

5.1 Selection of imaging techniques

In this PhD investigation it was decided to image the study contact lenses with both the atomic force microscope and the environment scanning electron microscope. This decision was made as the techniques are seen as complementary with the AFM providing true topographical data for the surface, whereas the ESEM instrument has the capability to image the surface over a much wider magnification range. Therefore to capture the most information possible regarding the surface characteristics of the study contact lenses, both imaging techniques were applied to characterise these surfaces.

5.2 Study 1 - AFM imaging on dehydrated contact lenses

5.2.1 Study Aim

To investigate the topography across the surface of the two experimental study contact lenses (air-cured and nitrogen-cured contact lens samples) along with commercially available contact lenses, in a dehydrated state, using an atomic force microscope.

5.2.2 Materials and methods

5.2.2.1 Contact lenses

The anterior surface of the experimental study contact lenses and commercially available contact lenses were examined using an atomic force microscope. The laboratory technique described in Section 2.2.2.1 was used to investigate the surface wetting properties of five

air-cured and five nitrogen-cured study lenses. All air-cured lenses were shown to have wetting and non-wetting regions on the anterior lens surface, whereas all nitrogen-cured lenses exhibited complete surface wetting. All lenses were then subsequently soaked in pure water for 48 hours with the water changed every 12 hours. A 3.5mm medical biopsy punch (Kai Inc., CA) was used to remove a round lens sample from the wetting and non-wetting regions identified on the air-cured lens surface and for corresponding regions on the nitrogen-cured lens (Figure 5.1). The posterior surface of the lens sample was then blotted with filter paper and mounted on a metal AFM specimen disk (Pelco Inc., CA) using double sided tape (Figure 5.2). The mounted samples were then left in a desiccating jar overnight to dehydrate the lens material prior to analysis. In addition to the study contact lenses, a conventional hydrogel contact lens (etafilcon A) and a silicone hydrogel contact lens (balafilcon A) were also mounted as described and imaged using the atomic force microscope.

5.2.2.2 AFM instrumentation

The AFM instrument used in this work was a Nanoscope III model (Digital Instruments, Santa Barbara, CA). The instrument was operated in Tapping Mode using oxide sharpened Si_3N_4 cantilever tips (0.06 N/m spring constant) in an air environment at room temperature. The topographic, amplitude and phase data were captured for three randomly selected regions on each of the contact lens samples. The scanning range was varied to allow different image magnification of the lens surface. The probe scanned a sample area of 20μm x 20μm, 10μm x 10μm, 5μm x 5μm and 2μm x 2μm. The images obtained were flattened using a second-order algorithm to correct for the piezo-derived differences between the scan lines. Mean-square-roughness (Rms), mean roughness (R_a) and maximum roughness (R_{max}) values were obtained from the roughness analysis facility of the Scanning Probe Image Processor, SPIP^{TM}, version 4.2.2.0 software. A linear regression model was constructed to investigate the overall study findings. Specifically, the factors of interest were study lens region (nitrogen, air-cured non-wetting or air-cured wetting), roughness metric (Ra, Rmax or Rms), and lens sample (as a random effect) with magnitude of roughness as the dependent variable. Post-hoc analysis was performed using the Tukey HSD test. Statistical tests were undertaken using JMP 5.0 statistical software for Apple Macintosh. A p-value of 0.05 was taken as the threshold of statistical significance.

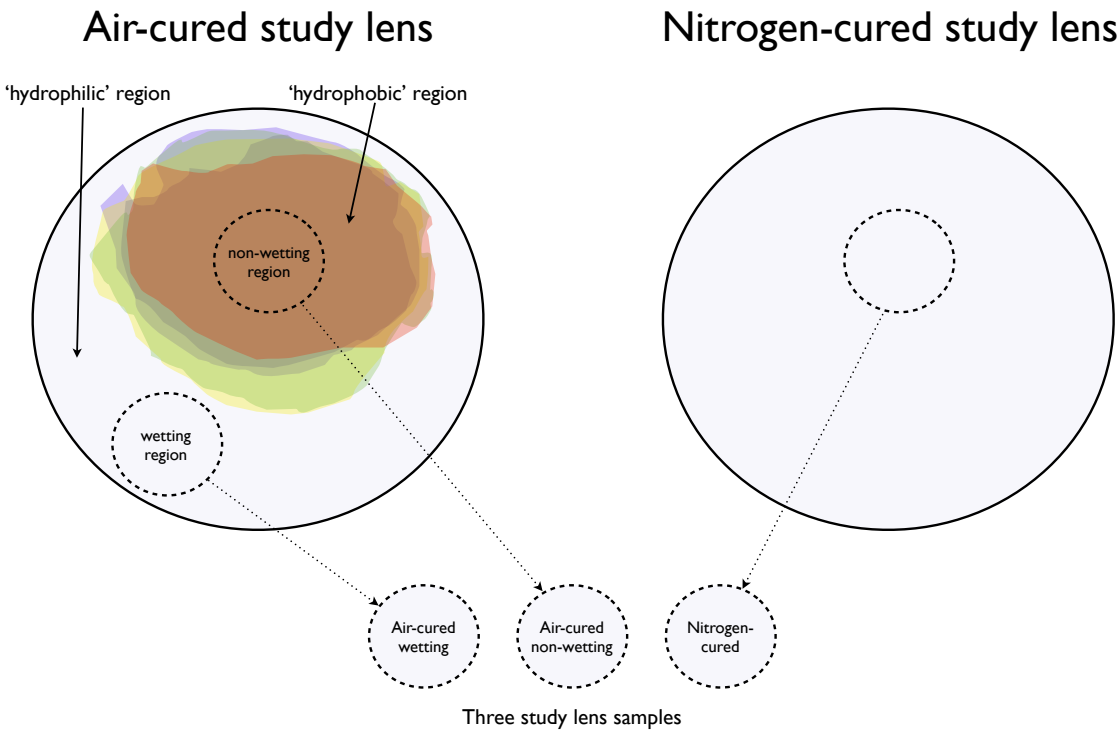

Figure 5.1: Lens sample preparation following laboratory wettability analysis.

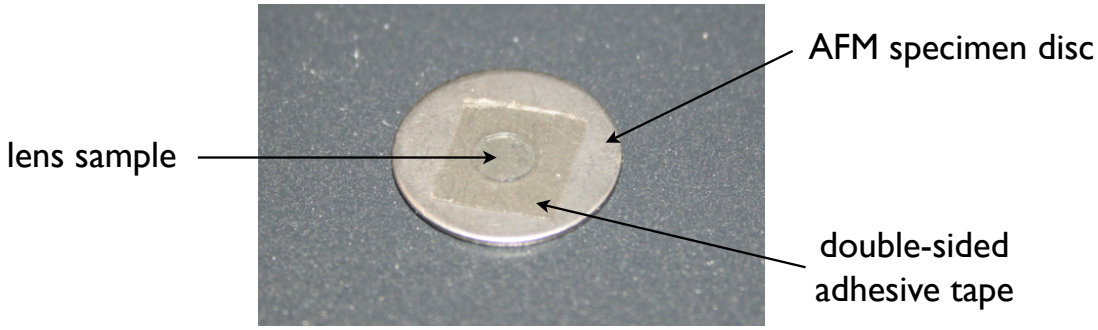

Figure 5.2: Lens sample mounted on metal AFM specimen holder.

5.2.3 Results

5.2.3.1 Conventional and silicone hydrogel contact lens materials

Figure 5.3 shows representative topographic and phase AFM images for the dehydrated polyHEMA and balafilcon A samples. The polyHEMA sample presents a smooth, regular surface with a multitude of very small peaks. Large peaks observed on the polyHEMA surface were attributed to contamination by dust particles which are electrostatically attracted to the lens surface and have been observed in previous hydrogel contact lens studies, especially on high water content lens containing MAA (Baguet *et al.*, 1992). The lens surface showed no signs of surface defects associated with polishing or lathing marks transferred from the lens mould, which have been observed in other AFM studies on contact lens materials (Baguet *et al.*, 1992). Figure 5.4 shows apparent holes in the pHEMA surface which varied in size from 10-25nm with a depth of at least 5nm, in addition to apparent surface contamination. These surface features have been observed previously on contact lenses (Lira *et al.*, 2008; Lopez-Alemany *et al.*, 2002) and are likely associated with the porous nature of hydrogel materials. The surface roughness values for polyHEMA and balafilcon A are presented in Table 5.1. The balafilcon A material showed elevated 'island like' regions on the lens surface which were surrounded by lower lying polymeric material. The transition between these regions is abrupt giving relatively high levels of surface roughness as shown in Table 5.1. The accompanying phase image shows little change in comparison with the topographical image.

Table 5.1: Roughness measurements for the 10μm x 10μm scan.

	polyHEMA	**balafilcon A**
Roughness (RMS)	0.60 nm	14.97 nm
Roughness (Ra)	0.34 nm	11.67 nm
Roughness range (Rmax)	11.13 nm	158.32 nm

5.2.3.2 Study contact lens regions

Figure 5.5 shows three 25μm^2 AFM scans of the anterior surface of the nitrogen-cured lens present in both 2D and 3D format. The lens presents a relatively flat surface with a multitude of very small peaks comparable with that observed for polyHEMA. Two of

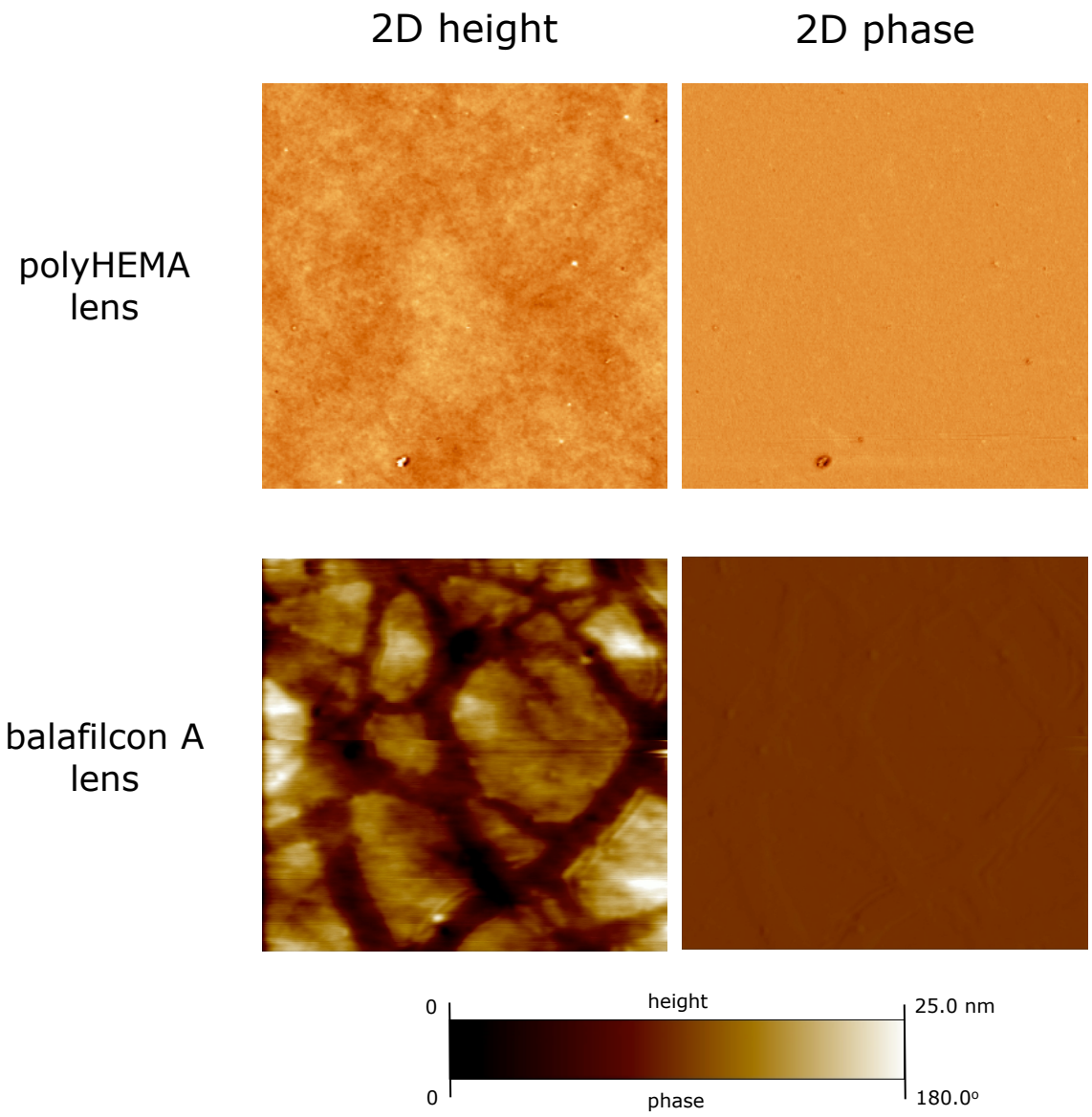

Figure 5.3: Height and phase AFM images for polyHEMA and balafilcon A contact lens materials (10μm x 10μm scan).

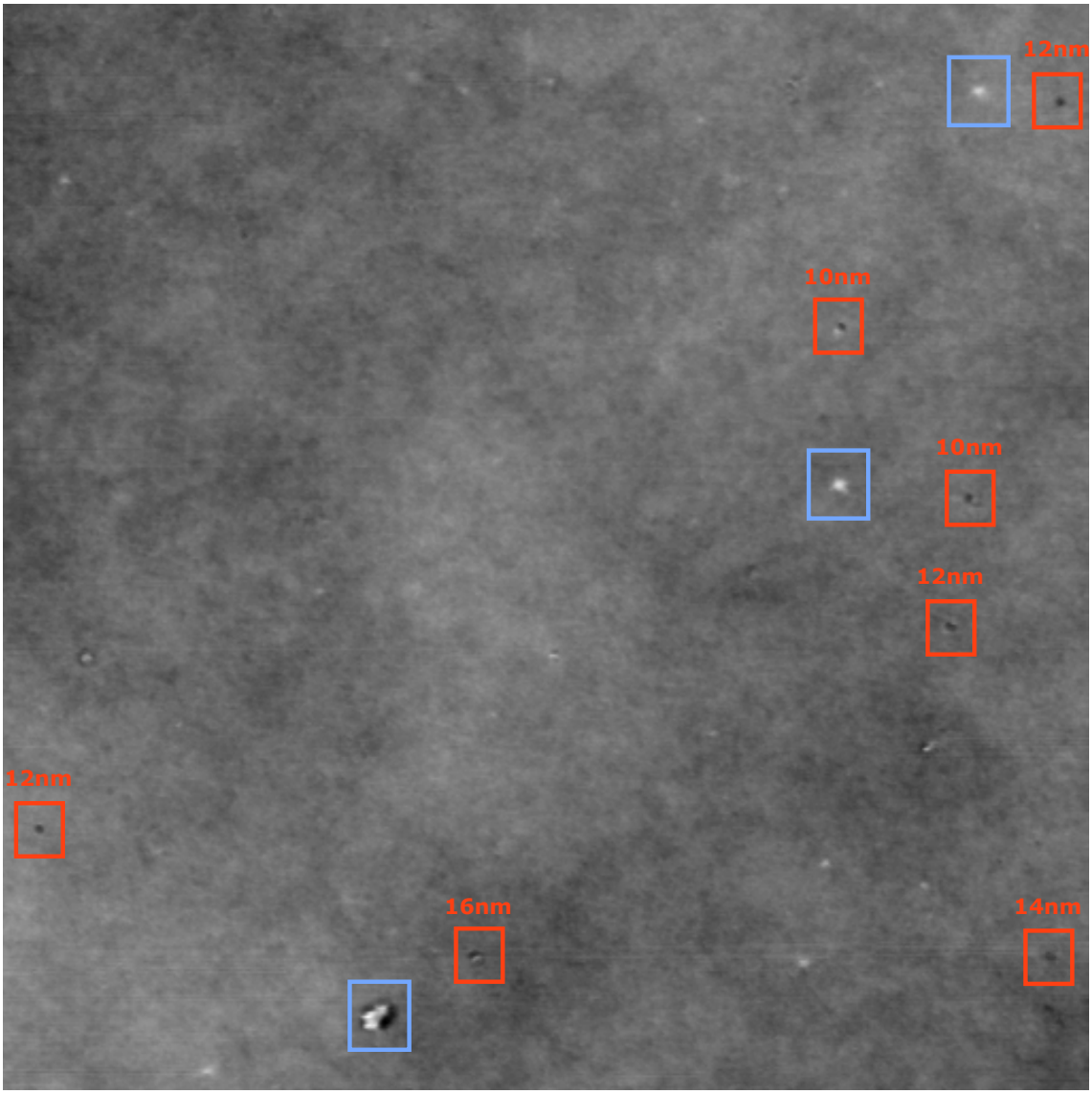

Figure 5.4: Apparent pores (red boxes) and contamination (blue boxes) on the anterior surface of a polyHEMA contact lens (10μm x 10μm scan).

the three AFM image show tall peaks elevated from the surface which appear related to surface contamination. All three regions demonstrate small (∼10 to 20nm in diameter), deep depressions in the polymer surface suggesting a porous nature to the lens material. Figure 5.6 shows three $25\mu m^2$ AFM scans of the anterior surface of the wetting regions on the air-cured lenses. The majority of the surface topography is similar to that observed for the nitrogen-cured lens with a relatively flat surface made up of a multitude of small peaks. Several raised regions are evident on these surfaces which are domed in nature, differentiating them from the contamination type peaks. Where present the pores are of similar size to the nitrogen-cured lens material and observed only on the main surface, with none appearing on the elevated smooth domes.

Figure 5.7 shows three $25\mu m^2$ AFM scans of the anterior surface of the non-wetting regions on the air-cured lenses. It is immediately apparent that a greater part of the surface is composed of the elevated smooth dome shaped regions, with the surrounding relatively flat surface made up of a multitude of small peaks similar to that observed for the nitrogen-cured samples. Several of these domed regions demonstrate a central further elevated peaked region with a textured summit. As with the wetting region of the air-cured lens the pores are only visible in the relatively flat region, with none present in the smooth domed region. The appearance of the relatively flat surface made up of a multitude of small peaks is similar to that of a hydrogel material as observed on the polyHEMA and nitrogen-cured lens surfaces. The nature of the relatively smooth domed regions is not typical of a hydrogel material. These are likely either composed of a phase separated polymeric material or may be a different type of surface contamination to that observed on hydrogel materials previously. These dome shaped regions have a relatively smooth appearance with phase imaging revealing differences in the tip interaction between these regions and the surrounding hydrogel meshwork (Figure 5.8). Table 5.2 shows the surface roughness values for the three regions of the experimental study contact lenses. The linear regression model showed that surface roughness values differed significantly between the lens regions ($F=4.79$, $p=0.0194$), with a post-hoc analysis showing a significant difference between all three lens regions. In addition, the surface roughness values differed significantly between the three different lens metrics ($F=21.07$, $p<0.0001$), with post-hoc analysis showing no significant between RMS and Ra roughness metrics, but a significant difference between both of these metrics and the roughness range (Rmax).

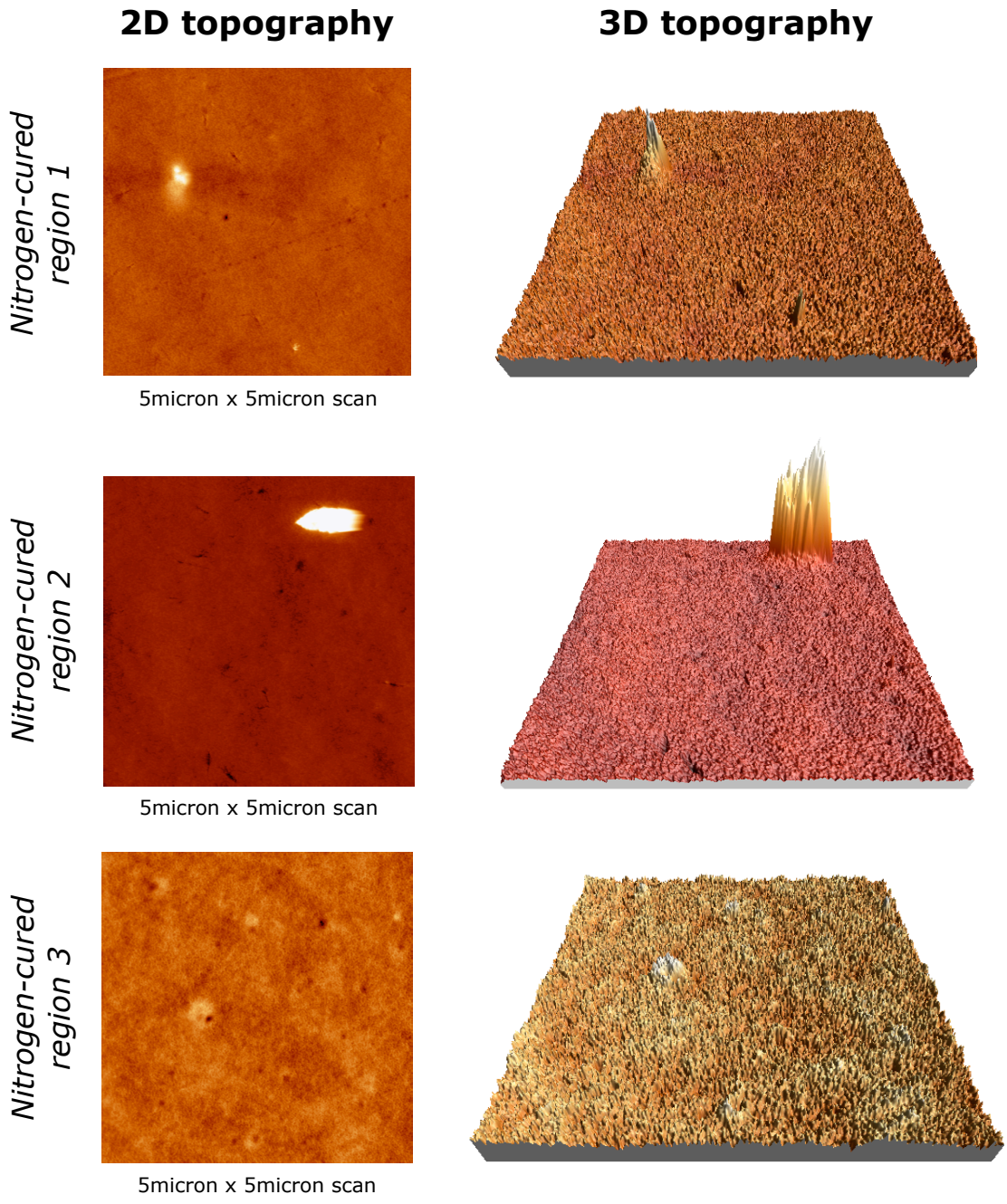

Figure 5.5: AFM surface imaging of three representative regions on the nitrogen-cured study contact lens.

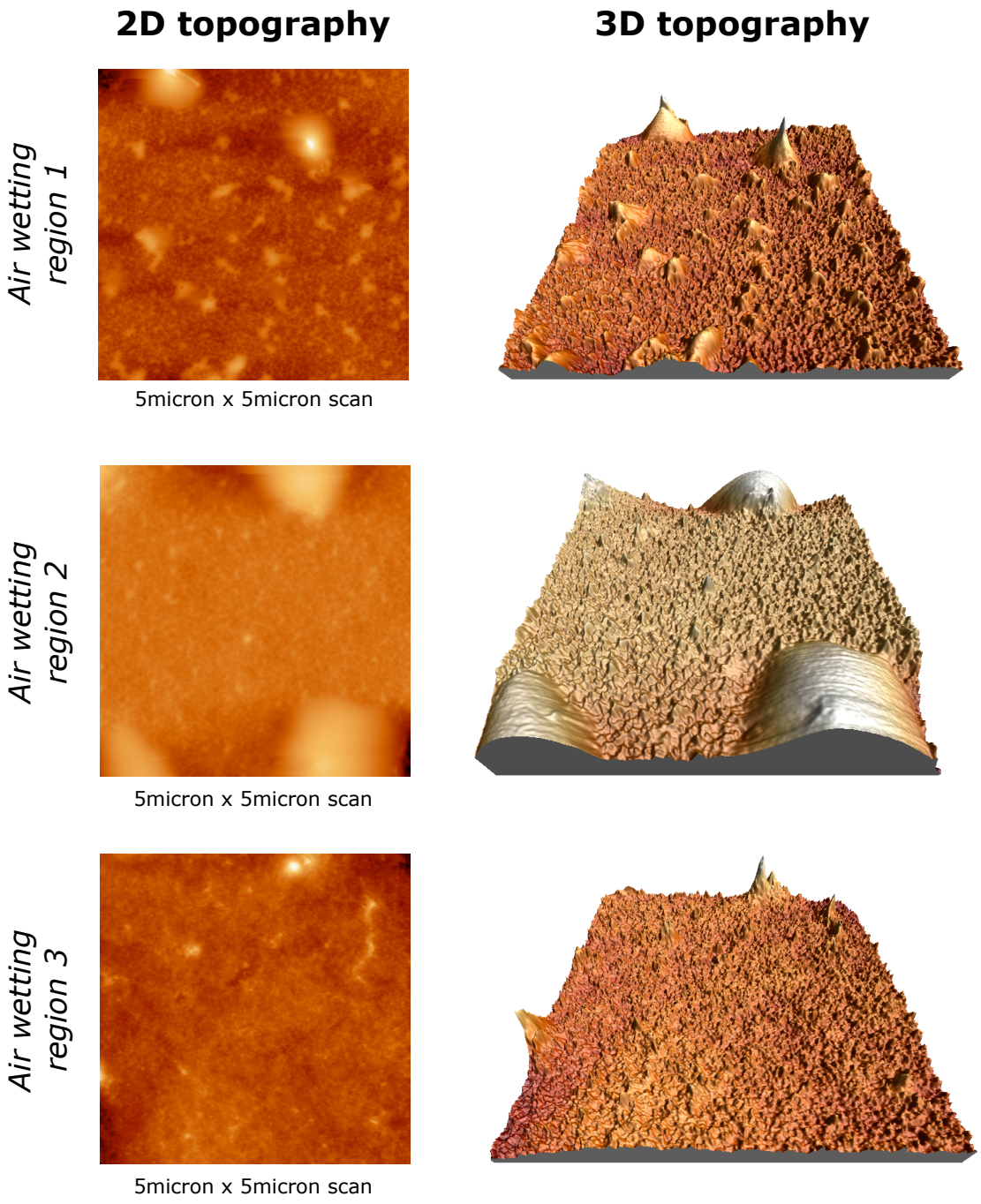

Figure 5.6: AFM surface imaging of three representative images for the wetting region of the air-cured study contact lens.

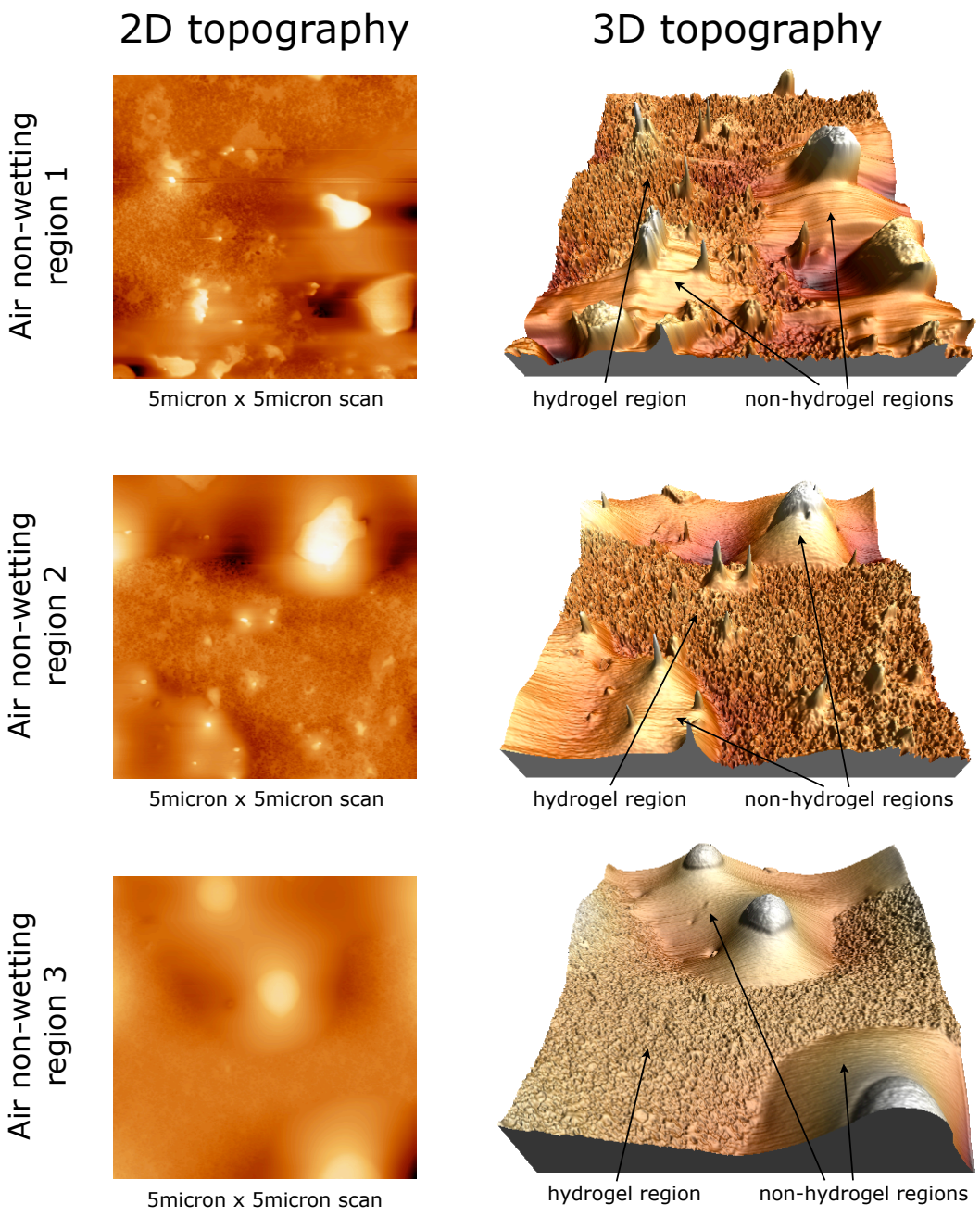

Figure 5.7: AFM surface imaging of three representative images for the non-wetting region of the air-cured study contact lens.

.

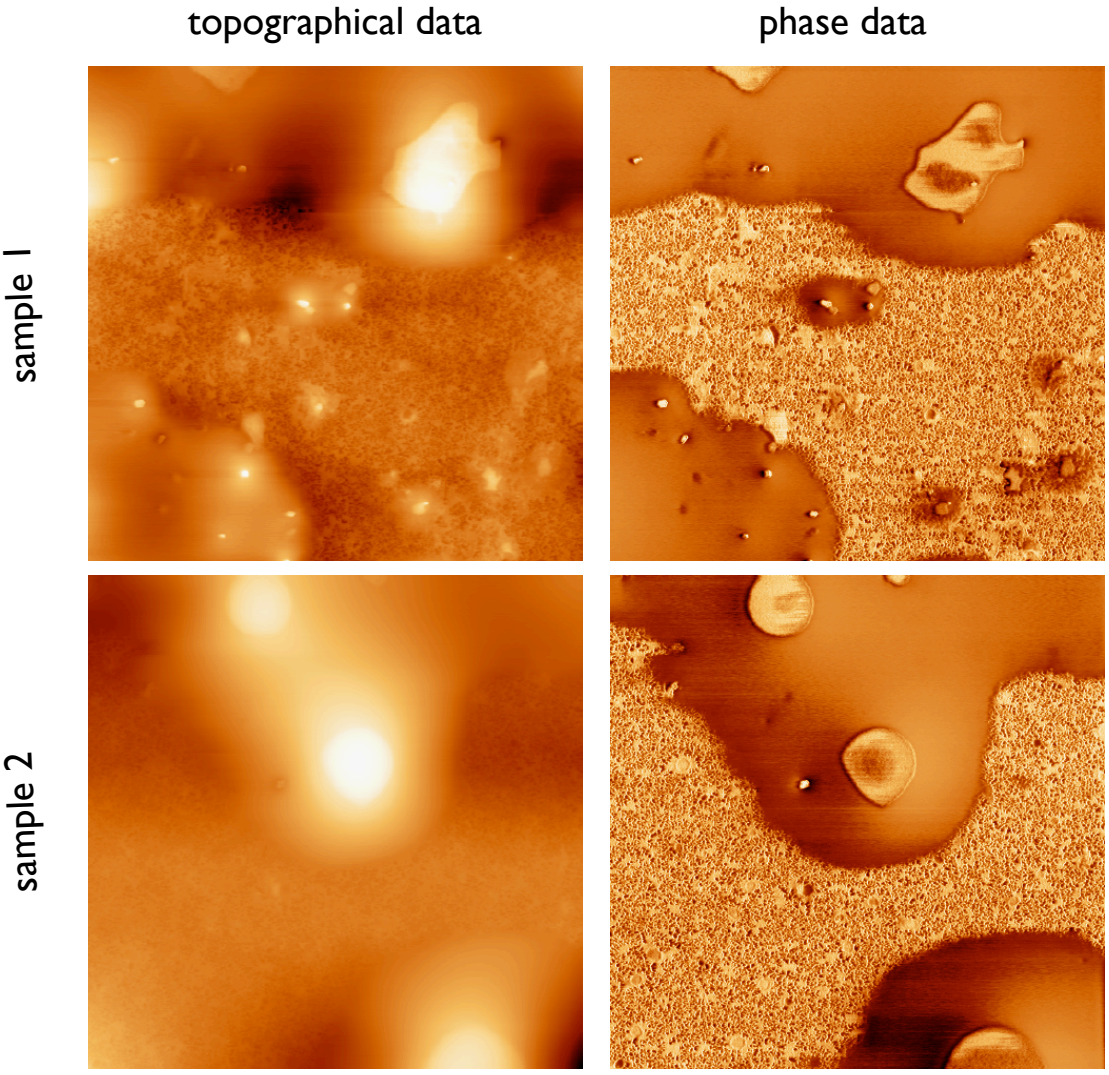

Figure 5.8: Topographical and phase AFM images of the air-cured non-wetting lens region.

Table 5.2: Mean surface roughness measurements for the three study lens regions (± standard deviation).

	Air-cured non-wetting	**Air-cured wetting**	**Nitrogen-cured**
Roughness (RMS)	15.1 ± 6.1	5.3 ± 2.0	2.4 ± 0.4
Roughness (Ra)	10.2 ± 4.2	3.3 ± 1.3	2.1 ± 0.1
Roughness (Rmax)	120.3 ± 53.8	57.1 ± 16.7	38.1 ± 19.5

5.2.4 Discussion

5.2.4.1 Imaging comercial contact lens surfaces using AFM

Imaging of the commercial contact lenses with AFM shows surfaces generally in agreement with hydrogel contact lens materials in the literature (Baguet *et al.*, 1995a; Bruinsma *et al.*, 2001; Kim *et al.*, 2002; Koffas *et al.*, 2004; Opdahl *et al.*, 2003; Teichroeb *et al.*, 2008). Figure 5.9 shows a representative image of the surface of the balafilcon A lenses from this study compared with those from other studies. It has been suggested (Tighe, 2004) that the raised 'islands' are associated with the plasma oxidation coating and are the result of polymeric silicon containing material which has been oxidised, resulting in a glassy hydrophilic inorganic silicone oxide surface. During hydration, it has been suggested that this surface then fractures due to expansion of the polymer substrate resulting in the formation of the depressed regions surrounding the oxidised regions (Lopez-Alemany *et al.*, 2002). In different AFM studies the size and shape of the glassy islands, the size and distribution of the pores and the amount of underlying polymeric material differs as shown in Figure 5.9. This may, to some extent, be related to experimental variables such as the AFM instrument, tip design and hydration of lens, but also suggests a variation either across the surface or between lenses, which might relate to the difficulty in applying a consistent plasma oxidation coating during commercial manufacture. Similarly, variability in contact angle measurements between manufacturing batches has been shown on lenses that require a post-polymerisation surface treatment (Read *et al.*, 2010b).

The polyHEMA samples demonstrated a smooth flat surface with a small number of peaks (thought to be contamination) and holes (thought to be pores) comparable with the results

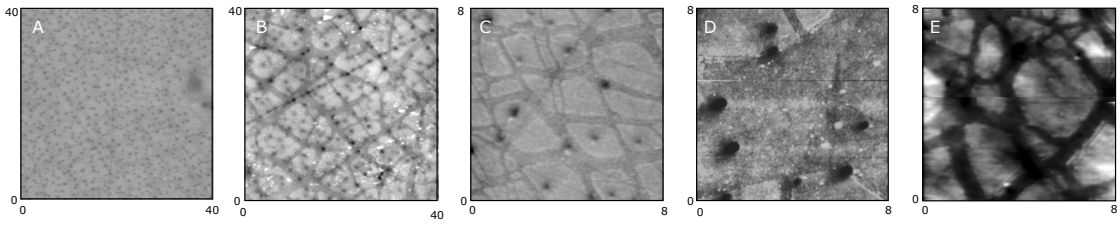

Figure 5.9: Comparison of the surface topography of balafilcon A using AFM from different studies (A (Bruinsma *et al.*, 2001), B (Teichroeb *et al.*, 2008), C (Gonzalez-Meijome *et al.*, 2005), D (Guryca *et al.*, 2007) and E (this PhD study)).

of others (Baguet *et al.*, 1995a; Kim *et al.*, 2001). Although the surface was imaged in a dry state, previous studies have shown little difference in topographic data between wet and dry lens samples (Kim *et al.*, 2001), although frictional and mechanical AFM data is likely to be much more dependant on the level of hydration of the material. The AFM imaging of commercial contact lenses gave results comparable with those in the literature for these materials (Baguet *et al.*, 1995a; Kim *et al.*, 2001; Koffas *et al.*, 2004; Opdahl *et al.*, 2003) giving confidence in the measurements obtained and allowing direct comparison of results with those found in previous studies.

5.2.4.2 Imaging the study contact lens surfaces using AFM

The development of the thin film wettability analyser, described in Section 2.2.2.1 and its subsequent validation as a tool to predict regions of non-wetting on the study contact lenses, has allowed the imaging of the nitrogen-cured lenses and both wetting and non-wetting region of the air-cured lenses. The nitrogen-cured lens presents a regular smooth globular surface similar to conventional hydrogel type materials with an apparently more open meshwork. This surface appearance is typical of a homogeneously distributed hydrogel meshwork with the lack of phase imaging signal suggesting no regions of significant polymer phase separation. The majority of the wetting region on the air-cured lens surface is also composed of this typical hydrogel meshwork, but on several of the AFM images, smooth elevated domed regions of varying size (approximately 0.5 μm to 3 μm in diameter) were also observed. The smooth and shallow transition from the hydrogel meshwork to these domed regions suggests that these were not areas of contamination, but rather true surface features. The lack of surface features even in high resolution scans and the differences in the phase images suggest that these domed regions are not hydrogel in nature, but may be associated with a phase separation of the lens material. Pores are evident in the hydrogel lens surface regions but not on the smooth domed regions, suggesting that this material is non porous in nature. These features are much more evident on the surface of the non-wetting air-cured lens regions, with similar elevated and smooth surface characteristics suggesting a greater degree of phase separation in these regions. This type of separation is not uncommon with polymeric materials (Bates, 1991) and appears associated in this case with the polymerisation conditions within the oven during lens curing.

The findings of this study are limited to the understanding of the material in a dehy-

drated state. While it has been suggested that the surface of polyHEMA contact lenses change very little between the hydrated and dehydrated state (Baguet *et al.*, 1992), it is likely that for silicone hydrogel materials, which are often made up of multiple monomer components, they are more likely to restructure depending on the level of hydration. In addition, mechanical characteristics such as surface modulus and friction are likely to be highly dependant on the degree of hydration.

This study has shown that AFM analysis has the ability to characterise not only the surface topography of a dehydrated contact lenses sample, but also infer some information about the material characteristics using phase imaging. It has shown that the surface differs significantly between the regions on the experimental study lenses. The relatively hydrophobic air-cured non-wetting regions appear rich in raised domes of apparently non-hydrogel material, whereas the relatively hydrophilic nitrogen-cured lens surface was dominated by a smooth hydrogel meshwork appearance. The air-cured wetting lens shows intermediate characteristics with smaller less prominent smooth domes on a primarily hydrogel surface.

5.3 Study 2 - AFM imaging on hydrated contact lenses

5.3.1 Study aim

To investigate the surface topography and mechanical differences across the surface of the two study contact lenses along with commercial contact lenses using an atomic force microscope in a hydrated state.

5.3.2 Materials and Methods

5.3.2.1 Atomic force microscope

The AFM used in this work was a MFP-3D (Asylum Research, Santa Barbara, CA). The instrument was operated in Tapping Mode using oxide sharpened Si_3N_4 cantilever tips (0.06 N/m spring constant) in an 0.9% phosphate buffered saline environment at room temperature. The topographic, amplitude and phase data were captured for three randomly selected regions on each of the contact lens samples. The scanning range was varied to allow different image magnification of the lens surface. The probe scanned a sample area of 40μm x 40μm, 10μm x 10μm and 2μm x 2μm. The images obtained were flattened using a second-order algorithm to correct for the piezo-derived differences between the scan lines. Mean-square-roughness (Rms), mean roughness (R_a) and maximum roughness (R_{max}) were obtained from the roughness analysis facility of the Scanning Probe Image Processor, SPIP^{TM}, version 4.2.2.0 software. A linear regression model was constructed to investigate the overall study findings. Specifically, the factors of interest were study lens region (nitrogen, air-cured non-wetting or air-cured wetting), scan area (40, 10 or 2μm^2), and lens sample (as a random effect) with magnitude of roughness as the dependent variable. Post-hoc analysis was performed using the Tukey HSD test. Statistical tests were undertaken using JMP 5.0 statistical software for Apple Macintosh. A p-value of 0.05 was taken as the threshold of statistical significance.

5.3.2.2 Contact lenses

A 3.5mm medical biopsy punch (Kai Inc., Ca) was used to remove a round lens sample from the wetting and non-wetting regions identified on the air-cured lens surface and for corresponding regions on the nitrogen-cured lens. For each lens region three samples were prepared. The posterior surface of the lens sample was then lightly blotted and mounted

on a metal AFM specimen disk (Pelco Inc., CA) using double sided tape. The mounted samples were then soaked overnight in PBS prior to analysis. In addition to the study contact lenses, two other previously well characterised silicone hydrogel contact lenses (balafilcon A and lotrafilcon A) were also mounted as described and imaged using the atomic force microscope. The samples were placed in a PBS-filled temperature controlled closed fluid cell which was maintained at a constant 30^{o}C and left for 30 minutes to stabilise prior to imaging. In total 11 samples were imaged (3 x air non-wetting, 3 x air wetting, 3 x nitrogen-cured, 1 x balafilcon and 1 x lotrafilcon), with each lens imaged in three randomly selected regions at three different scan ranges (2μm x 2μm, 10μm x 10μm and 40μm x 40μm), giving a total of 99 AFM images captured.

5.3.3 Results

5.3.3.1 Commercial lenses

Figure 5.10 shows representative 2D and 3D surface AFM images in addition to phase information for the balafilcon A lens materials. These images again show the glassy islands observed for the dehydrated lens material, although the gaps between these regions appear narrower than for the dehydrated AFM images in this study (Section 5.2.4.1). The 10μm x 10μm and 40μm x 40 μm scans show very obvious surface pits (around 0.5μm) which are numerous on the lens surface and associated with the porous nature of balafilcon A (Lopez-Alemany *et al.*, 2002). The phase images show small changes in signal associated with the tip scanning over the pores and between the glassy island.

Figure 5.11 shows representative 2D and 3D surface AFM images in addition to phase information for the lotrafilcon A lens materials. The 10μm x 10μm and 40μm x 40μm topographic images show distinctive non-parallel predominantly linear marks on the lens surface. There was little evidence for the presence of pores on the surface of the lotrafilcon material. AFM phase imaging showed a small signal when the probe crossed these lens surface marking.

5.3.3.2 Study lenses

Figure 5.12 shows representative 2D and 3D surface AFM images in addition to phase data for the nitrogen-cured lens surface. The 10μm x 10μm and 40μm x 40μm topographic im-

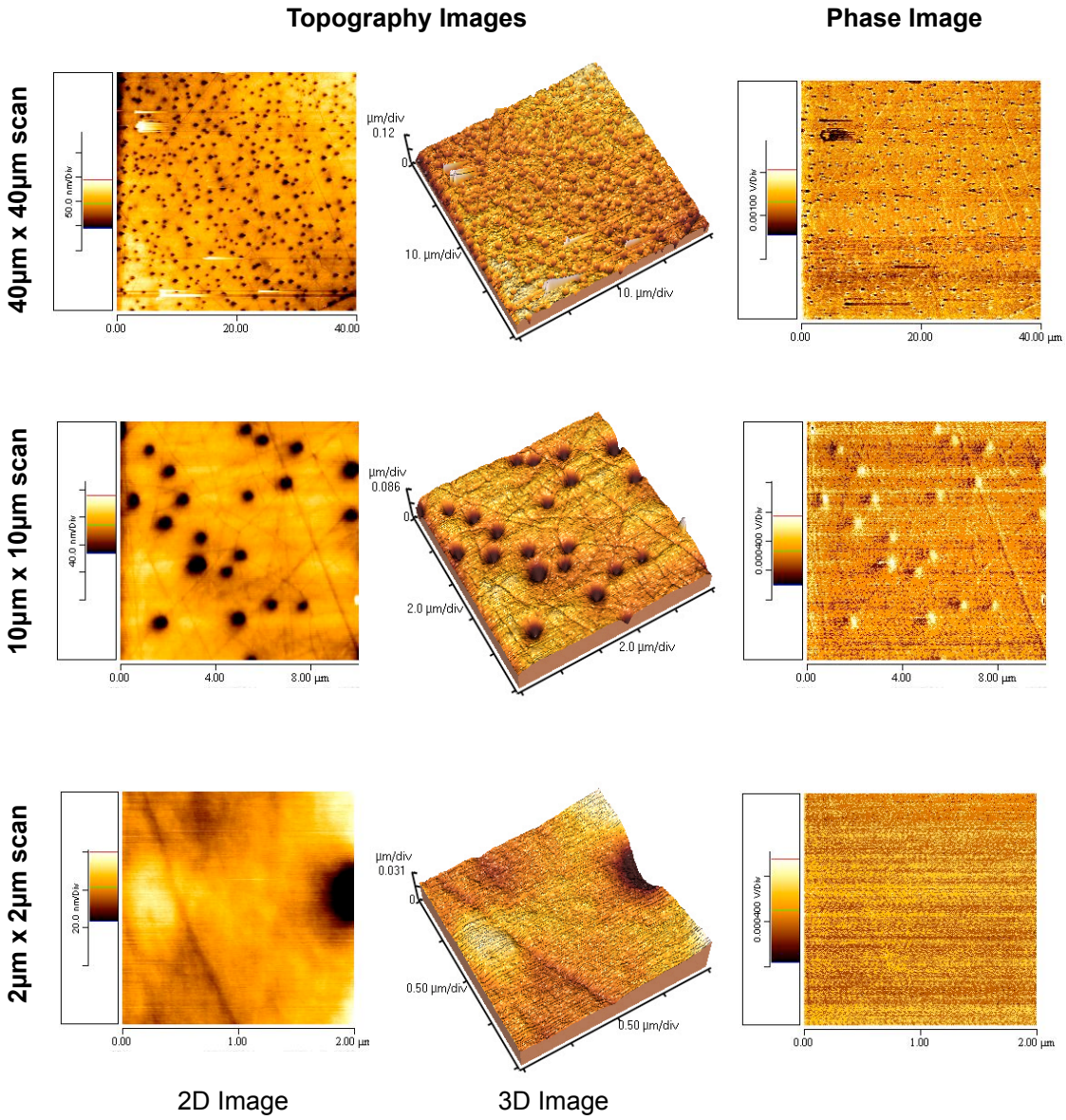

Figure 5.10: Two dimensional and three dimensional topographical images of balafilcon A with phase imaging.

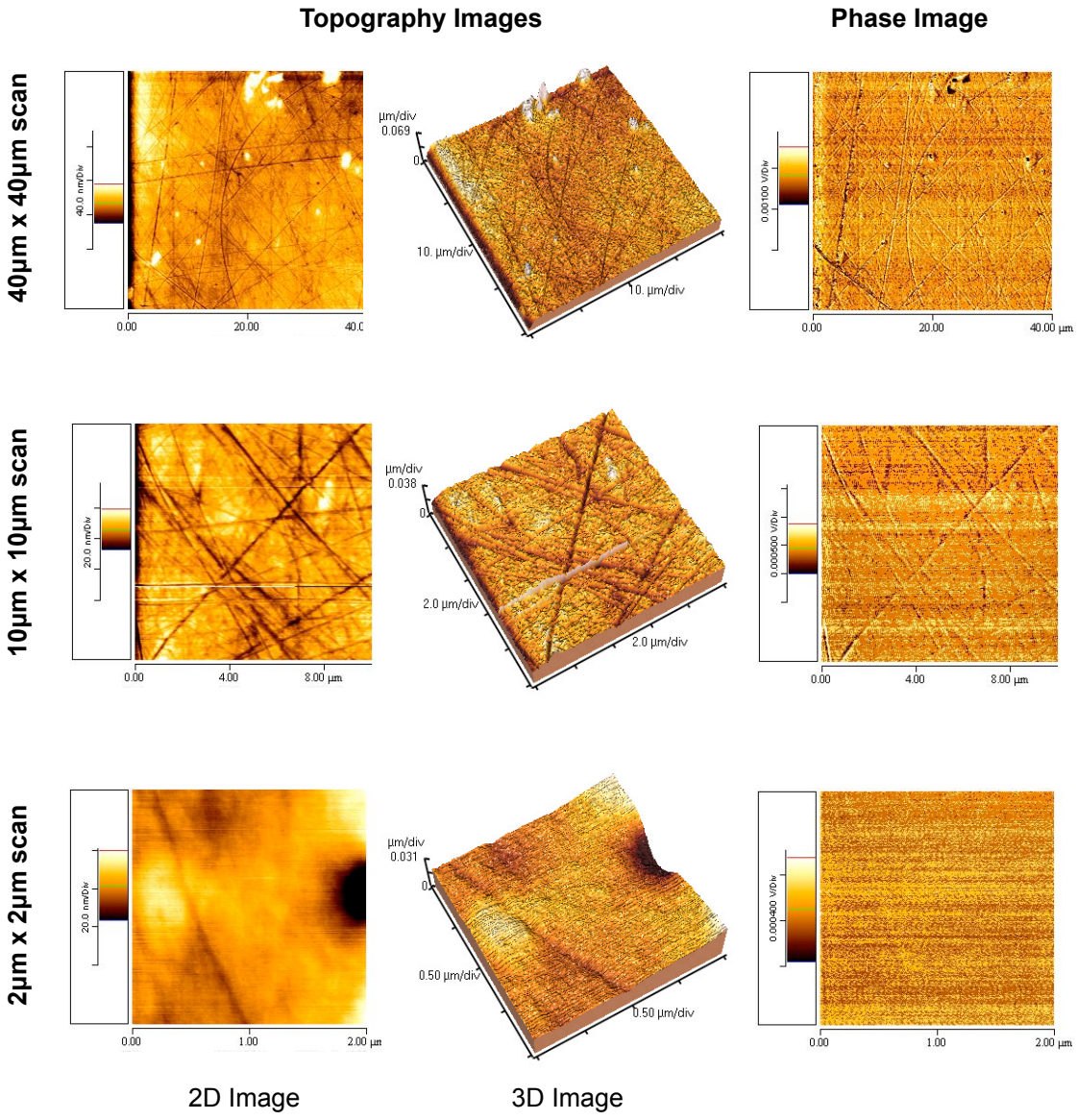

Figure 5.11: Two dimensional and three dimensional topographical images of lotrafilcon A with phase imaging.

ages showed a relatively smooth surface with the presence of parallel and regularly spaced linear marks. In the 10μm x 10μm topographical scan pits were visible along these linear surface marking with relatively regular spacing. Several peaks and pits were observed primarily on the 40μm x 40μm images, with phase imaging suggesting a difference between the mechanical characteristics of these features and the rest of the surface.

Figure 5.13 and 5.14 show representative 2D and 3D surface AFM images in addition to phase information for the wetting region and non-wetting regions on the air-cured lens surface respectively. In the 2μm x 2μm, 10μm x 10μm and 40μm x 40μm topographical images, the surface of these regions appears relatively smooth, but with numerous small peaks across the lens surface. These peaks on the non-wetting air-cured lens region appear more numerous and higher than the wetting region of the air-cured lens. No evidence of linear marks or pits was observed on any of the air-cured lens images. Phase imaging suggested that the mechanical characteristics of the peaks differed to the rest of the surface.

5.3.3.3 Surface roughness

Surface roughness values for both the commercial and study lenses are shown in Table 5.3. The linear regression model showed that surface roughness values (RMS) differed significantly between the lens regions ($F=20.67$, $p<0.0001$), with a post-hoc analysis showing no significant difference between the nitrogen-cured region and wetting region of the air-cured lens, but the non-wetting region was shown to have significantly greater roughness than both these regions. In addition, the surface roughness values differed significantly between the three AFM scan sizes ($F=29.25$, $p<0.0001$). RMS surface roughness values were shown to reduce with a smaller scan size for all lens samples studied, in agreement with the findings of Poon & Bhushan (1995). The nitrogen-cured study lenses had similar roughness characteristics to lotrafilcon A, whereas the air-cured lenses had a rougher surface, more similar to the wetting region on the balafilcon A. The non-wetting region on the air-cured lens had the roughest surface of any of the lens samples.

5.3.4 Discussion

Atomic force microscopy is one of the few surface analysis techniques that can readily be used to investigate hydrogel materials in a hydrated state and at room temperature. Its ability to not only image the lens surface but also to gain information about the three-

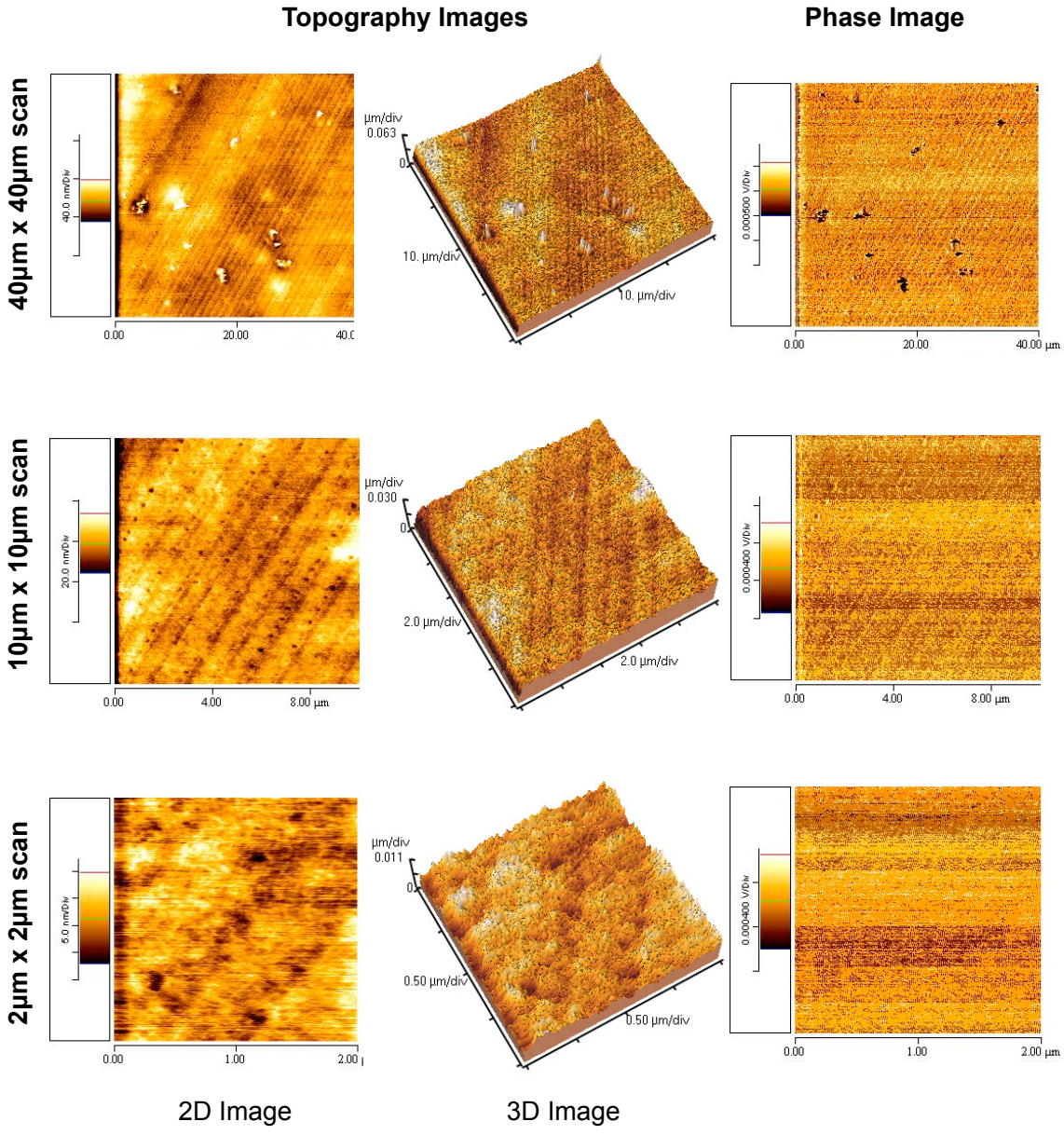

Figure 5.12: Two dimensional and three dimensional topographical images of the nitrogen-cured study lens with phase imaging.

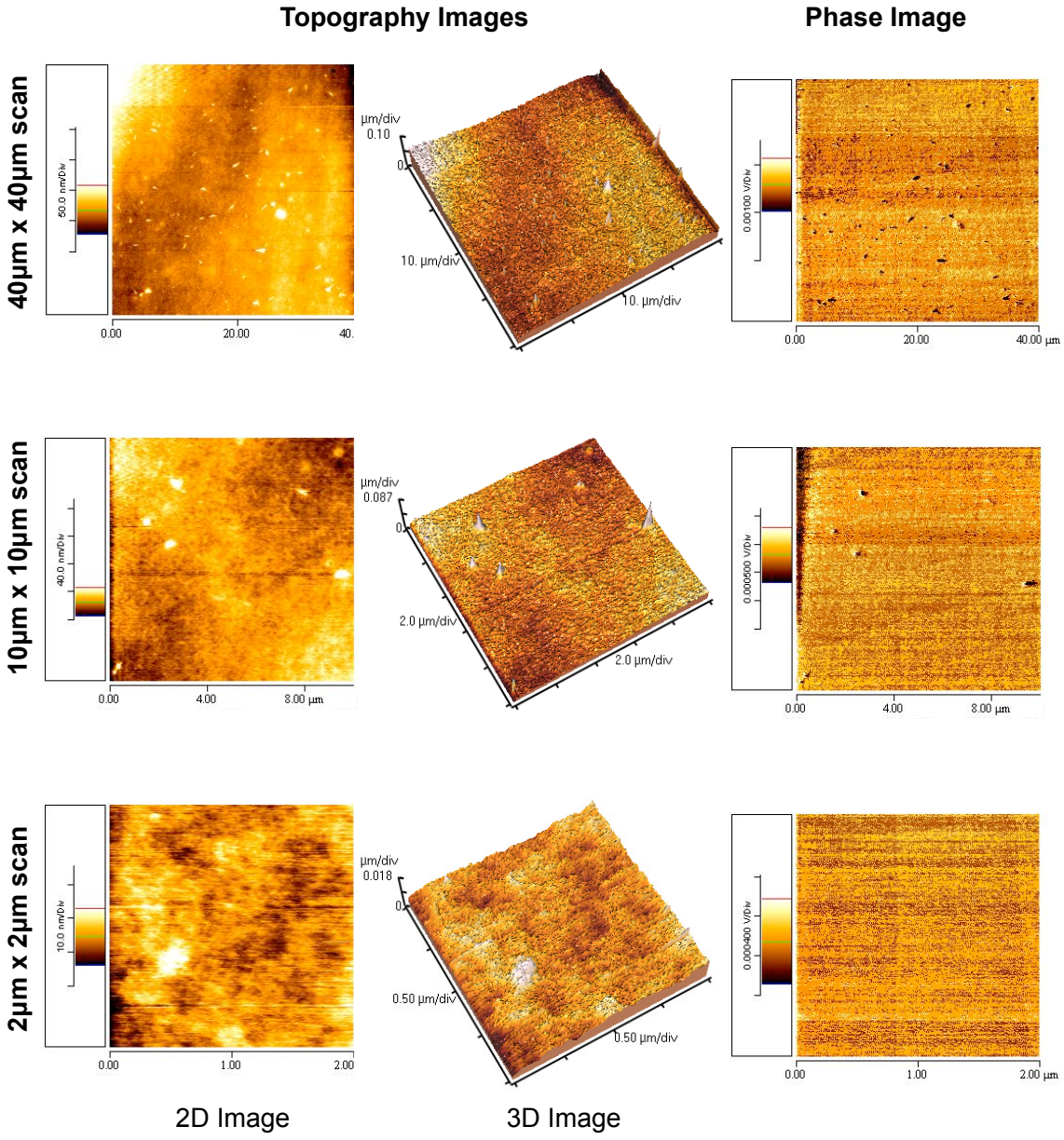

Figure 5.13: Two dimensional and three dimensional topographical images of the wetting region of the air-cured study lens with phase imaging.

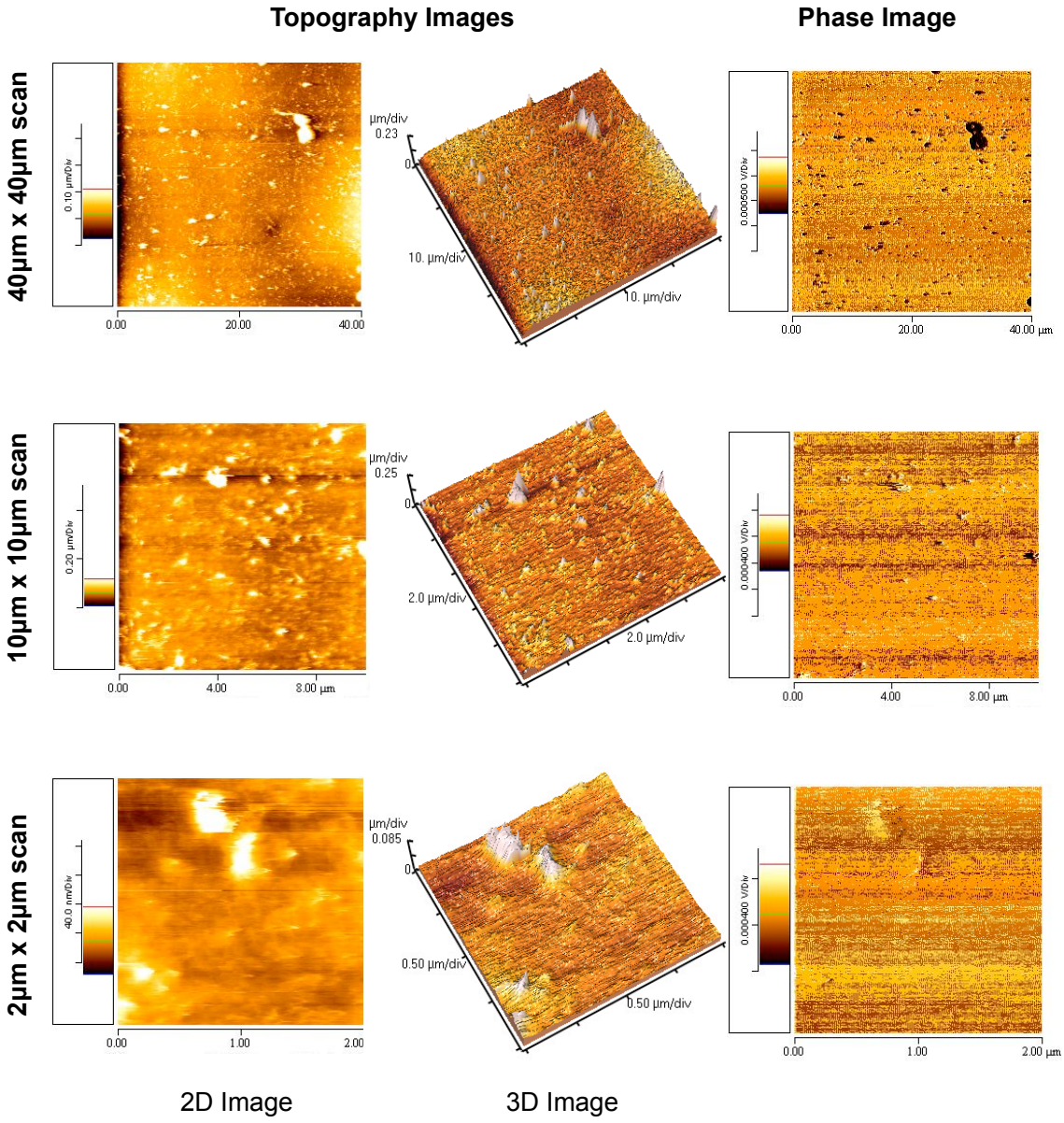

Figure 5.14: Two dimensional and three dimensional topographical images of the non-wetting region of the air-cured study lens with phase imaging.

dimensional surface topography and the mechanical and frictional characteristics of the surface, allow a greater range of information to be gathered than by surface imaging either by optical or electron microscopy which provides only two-dimensional information. The high resolution that AFM provides also allows the hydrogel polymer to be investigated on a microscopic scale, allowing observation of characteristics such as phase separation, surface porosity and surface contamination.

AFM images of the balafilcon A material in a hydrated environment showed a highly porous surface with a crazed surface appearance. When compared to the dehydrated sample the pores were much more evident in the hydrated state, but the gaps between the glassy oxidised silicon islands were less visible. The spacing between the 'islands' is likely to alter when the hydrogel material swells as it was imaged in the hydrated state, but this would normally result in the dehydrated material shrinking in volume and thus causing the gaps between the silicon oxide island to reduced and not increase as apparently found in this study. Instrumentation differences between the two studies such as the different AFM instrument design and tip type used may have influenced these findings. In addition, differences due to using lenses from different manufacturing batches or from sampling slightly different regions on the lens surface may also account for these differences. One of the problems with the AFM instrument is that it is limited to a relative small scanning area (typically 100μm x 100μm) and the capturing of images is a relatively lengthy process, therefore instead of the whole area of interest being investigated, typically several regions are randomly chosen to represent the surface. If the surface is not homogenous in structure, it may be that images captured are not representative of the surface under investigation. It is therefore important to capture as much information as possible before

Table 5.3: RMS roughness measurements for the control and study lens samples at different AFM scan sizes.

	40μm^2	**10μm^2**	**2μm^2**
balafilcon A	16.56 nm	13.98 nm	6.03 nm
lotrafilcon A	7.43nm	4.47nm	3.52 nm
nitrogen-cured	7.51 $\pm$ 0.33nm	4.15 $\pm$ 0.43nm	2.60 $\pm$ 0.47nm
air-cured wetting	14.24 $\pm$ 2.14nm	7.98 $\pm$ 0.91nm nm	3.30 $\pm$ 0.20nm
air-cured non-wetting	33.32 $\pm$ 23.10nm	10.96 $\pm$ 7.27nm	6.57 $\pm$ 5.18nm

drawing conclusions from the data, especially where a heterogenous surface is expected. When comparing the AFM images for the balafilcon A lens material in this study with those in the literature (González-Méijome *et al.*, 2006a, 2009; Guryca *et al.*, 2007; Lira *et al.*, 2008), although there is generally reasonable agreement (Figure 5.9), there are differences between the studies suggesting that the surface of the balafilcon A material may be heterogenous in nature. The porous nature of the balafilcon A is not just of interest from a surface and polymer science perspective, but it is also likely to influence the clinical performance of this lenses. Lopez-Alemany *et al.* (2002) has suggested that the porous nature of balafilcon may prevent adhesion of the lens to the corneal surface by increasing the ion permeability of the material. The porous nature of balafilcon may also influence clinical characteristics such as the uptake and release of drugs (Hui *et al.*, 2008) or other clinical observations such as transient corneal staining associated with certain lenses and lens care solution combinations (Jones *et al.*, 1997b, 2002a). Surface roughness values were found to be higher than the lotrafilcon A material primarily due to the porous nature of the surface.

The surface of the lotrafilcon A contact lens has a large number of predominantly linear marks in varying directions across the lens surface. These have been observed previously in the literature (Gonzalez-Meijome *et al.*, 2005; Guryca *et al.*, 2007) and are thought to be associated with the transfer of lathing and polishing marks from the surface of the mould to the contact lens surface during polymerisation (Grobe *et al.*, 1996). In the AFM images it is clear there are both linear and curved marks on the lens surface, with the linear marks likely caused predominately by the lathing process whereas the curved marks are likely caused by the polishing of the mould or lens surface. Comparison of AFM images from the lotrafilcon A material in this study and a lathed etafilcon material show clear similarities, suggesting this is indeed the cause of the surface markings (Figure 5.15). The thickness of the plasma coating applied to the lens surface has been shown to be between 5 - 50 nm in thickness (Weikart *et al.*, 2001) and appears not to mask these surface markings, although smaller features such as pores in the polymer matrix do appear to become covered (Weikart *et al.*, 2001).

One of the three nitrogen-cured lens samples imaged with AFM showed numerous linear, parallel and equally spaced markings across the lens surface. These markings are typical of lathing marks transferred from the polypropylene lens moulds onto the surface of

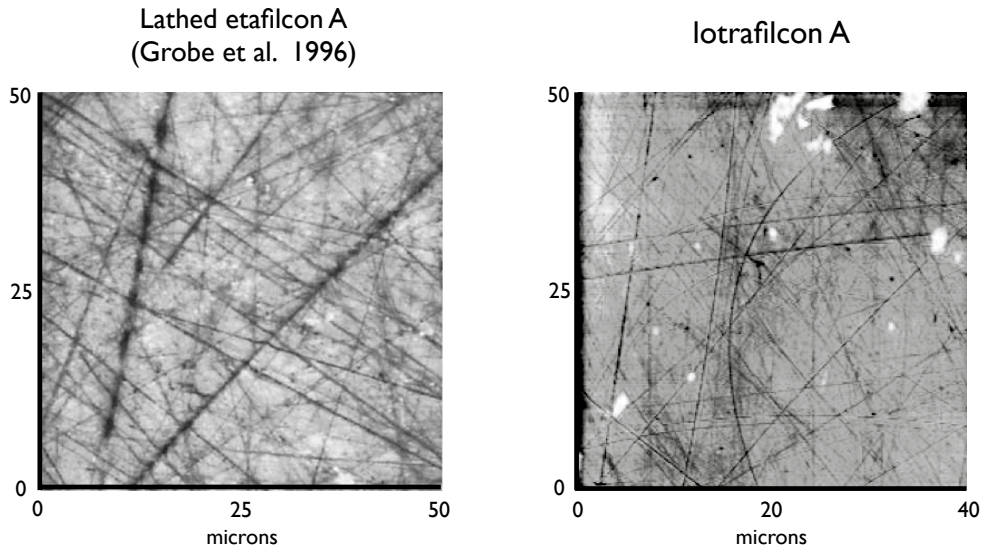

Figure 5.15: Comparison of marks on the surface of the lotrafilcon A material and a lathed etafilcon A lens (Grobe *et al.*, 1996).

the contact lens. These features were only seen on one of the nitrogen-cured lenses and not the others, suggesting that these markings were restricted to only certain regions on the mould surface and therefore transferred to only certain regions on the contact lens surface. In addition to these linear markings, pores/pits were observed which followed the linear surface features. These pits might also be raised features on the lathed mold surfaces that would be transferred to the lens material during polymerisation or that during polymerisation the conditions were such that pores may have formed in this regular arrangement. To better understand these surface features, AFM could be performed with a high aspect ratio tip (Figure 1.34) over a small scan area to allow the topography of these features to be more clearly defined. The majority of the nitrogen-cured lenses were composed of a relatively smooth surface with the surface topography typical of a hydrogel meshwork, with uniformly distributed globular features, thought to be polymer moieties. The raised peaks observed on the nitrogen-cured lens surface are not typical of features found on hydrogel materials and given the contrast in the phase imaging in these regions, it would suggest that these peaks possess different mechanical characteristics compared with hydrogel surface. In the literature similar features have been observed on the surface of contact lenses during AFM and SEM imaging and have been attributed to contaminants on the lens surface (Baguet *et al.*, 1992; Maldonado-Codina *et al.*, 2004a).

AFM imaging on the wetting and non-wetting regions of the air-cured lens surface showed the number and size of the peaks present on these surfaces were higher than those observed on the nitrogen-cured lens surface. The non-wetting regions on the air-cured lens surface possessed a greater number of peaks and with greater magnitude than those observed on the wetting regions. These peaked features were typically 0.1 to 0.5 microns in width and up to 200nm in height and again showed phase contrast suggesting the peaks differed with regard to their mechanical characteristics. These surface features are not typical of those associated with regions of polymer phase-separation suggesting that these peaks are more likely related to contamination of the lens surface. Given that the surface of the study lenses were exposed to the same environment during examination with the *in vitro* thin film analyser, the difference in apparent surface contamination between the lens regions is unexpected. The non-wetting region and to a lesser extent the wetting regions of the air-cured study lenses have surfaces which appear to adhere higher levels of contamination than the nitrogen-cured lens surface. Maldonado-Codina & Efron (2005) reported that when conventional hydrogel contact lenses were cast moulded from a HEMA/GMA (glycerol methacrylate) copolymer in an air-filled oven the surfaces exhibited stickier surfaces than when they were cured anaeorbically (nitrogen-purged oven). The cause of this increased adhesion was thought to be a result of polymerisation being inhibited by the presence of oxygen during curing in the air-filled oven. This resulted in non-crosslinked shorter polymer chains at the lens surface which engulfed contaminant particles more readily. It is likely that a similar process occurs at the surface of the air-cured lenses in this study explaining the greater degree of contaminant particles observed on the wetting and non-wetting regions of the air-cured lens surface. The tendency for the air-cured lens surface to adhere contaminants was also observed during static contact angle analysis, where following lens blotting a sessile droplet was lowered onto the lens surface. Figure 5.16 shows a typical image from both the air-cured and nitrogen-cured contact lenses surface just prior to analysis. It can be clearly seen that the air-cured lens has a greater degree of surface contamination than the nitrogen-cured lens type. This type of lens surface degradation has also been linked with increased tear film deposition (Maldonado-Codina & Efron, 2005), in agreement with the findings of the clinical study in section 2.1.

The AFM images for the dehydrated study lenses showed a more clearly defined hydrogel

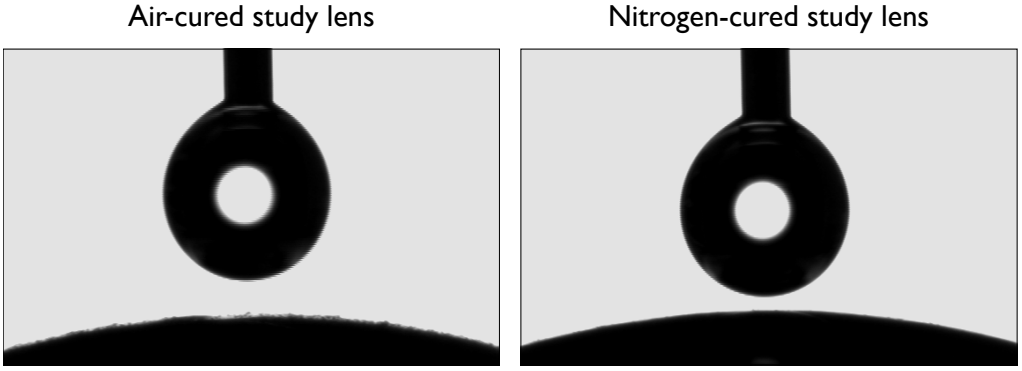

Figure 5.16: Comparison of typical images capture following blotting during contact angle analysis, showing greater contamination on the air-cured lens surface.

meshwork surface appearance than the hydrated lens samples. The nitrogen-cured contact lens appeared relatively featureless for both hydrated and dehydrated AFM, except for the occasional peaks, thought to be associated with surface contaminants. The two air-cured lens regions both showed more significant areas of surface contamination type peaks, but also much larger smooth domed regions, which were quite different in appearance to the contaminant peaks. Although these surface features might be associated with a different type of lens surface contamination, the dome with its smooth transition into the surrounding hydrogel meshwork appeared more characteristic of regions of polymer phase separation. Observation of the AFM phase images also shows differences in the phase signal across these regions, suggesting different material characteristics compared with the hydrogel meshwork elsewhere on the surface. These findings therefore suggest that in addition to the 'tacky' nature of the air-cured lenses surface (in particular the non-wetting regions), there may also be a degree of phase separation on the air-cured lens surface. This only appeared to be present in the dehydrated state, but this may also be present on the hydrated surface, as AFM only probes a very small region of the lens sample with each scan and isolated features can easily be missed. Analysis of the surface using a lower magnification or larger field of view (such as scanning electron microscopy or optical microscopy) is better able to characterise the surface over significantly larger surface regions (Section 1.14.1).

5.3.5 Conclusion

The use of AFM to image the surface of contact lenses in both a hydrated and dehydrated state has allowed not only a better understanding of the material from which the lens is manufactured, but also how the method of manufacture influences these surfaces and how these features might influence its subsequent clinical performance. The commercial contact lenses studied here have been well characterised previously in the literature and the findings of this study are in general agreement with those of previous studies. Imaging of the three regions of interest on the surface of the two study contact lenses, showed marked differences. Although all three lens regions showed a smooth underlying surface, typical of a hydrogel material, the non-wetting lens region and to a lesser extent the wetting region on the air-cured lens showed increased levels of apparent surface contamination. This increased contamination is likely associated with a tackier surface as a result of polymer degradation at the lens surface due to oxygen inhibition of the polymerisation reaction during curing. This means the polymer chains at the surface are likely to be less heavily crosslinked and entrapment may occur more readily than for the comparatively heavily crosslinked nitrogen-cured lens surface. AFM images of the dehydrated air-cured study lens suggest that in addition to the degraded surface there may also be regions of phase separation of the polymer components, most visible on the non-wetting region of the air-cured lens surface.

5.4 ESEM imaging of contact lens materials

5.4.1 Aim

The study aimed to investigate the study contact lens materials using an environmental SEM in a dehydrated, hydrated frozen and fully hydrated state.

5.4.2 Material and methods

ESEM imaging was used to examine the surface topography of the three regions of interest on the experimental study contact lenses. The *in vitro* wettability analyser (Section 2.2.2.1) was used to identify wetting and non-wetting regions on the air-cured study lens. In all cases, the surface of the nitrogen-cured lenses appeared fully wettable. Three samples were punched for each lens region of interest (air-cured non-wetting, air-cured wetting and nitrogen-cured regions) giving a total of nine lens sample. These 3.5mm punched lens samples were then lightly blotted on the posterior lens surface and mounted on a metal disc using double sided tape. These mounted lens samples were then soaked in pure water for 24 hours to fully hydrate the lens samples and to remove salt residue from within the material. Three sets of nine samples were prepared to allow analysis with three different SEM techniques:

1. ESEM in 'wet' mode (fully hydrated analysis)
2. ESEM in low vacuum mode (dehydrated analysis)
3. Cryo-SEM analysis. (frozen hydrated analysis)

For the lens samples undergoing dehydrated analysis, the lenses where removed from the water and placed overnight into a desiccating jar to fully dehydrate the samples. In addition to the lens samples, the female lens moulds (the mould surface responsible for forming the anterior contact lens surface) were also imaged with SEM in three different conditions: (i) unused virgin lens mould, (ii) air-cured lens mould and (iii) nitrogen-cured lens mould. Due to their non-hydrogel structure, the lens moulds were analysed only in the low vacuum SEM mode.

5.4.3 ESEM instrumentation

The samples were imaged using a Philips XL30 ESEM-FEG environmental scanning electron microscope.

5.4.3.1 ESEM in low vacuum mode

Analysis of the dehydrated lens samples and the polypropylene lens mould was performed in low-vacuum environmental mode, employing a gaseous secondary electron detector at 0.5 Torr using an accelerating voltage of 15kV. The use of the low-vacuum environmental mode negated the need for surface coating of specimens as water vapour in the microscope chamber allowed charge neutralisation.

5.4.3.2 ESEM imaging in 'wet' ESEM mode

Analysis of the hydrated lens samples was performed in ESEM / wet mode using a GSE detector using water vapour in the microscope chamber and a Peltier stage to cool the lens samples. The pressure of the water vapour and the temperature of the cooling stage was controlled to maintain saturation conditions (100% RH) allowing the sample to remain hydrated whilst inside the chamber.

5.4.3.3 Cryo SEM imaging

Cryogenic lens sample analysis was performed by removing the mounted lens sample from pure water and rapidly, but indirectly, freezing the sample with liquid nitrogen. The frozen sample was then immediately transferred to a pre-cooled stage in the preparation chamber, where it was then splutter coated with gold palladium. The liquid nitrogen-cooled lens sample was then transferred into the analysis chamber where it was imaged using a secondary electron detector (SE) at 0.5 Torr using an accelerating voltage of 10kV. Images were captured at both the lens / mould centre and periphery for each lens mould.

5.4.4 Results

5.4.5 ESEM imaging of contact lens moulds

Figure 5.17 shows three ESEM images of an unused virgin female mould. The surface appeared relatively smooth with the presence of both parallel linear marks and a random distribution of marks on the mould. Another feature occasionally observed on the virgin mould surface was small regular crystalline-like particles which showed high signal intensity in the ESEM images (Figure 5.18). Figure 5.19 shows the central and peripheral regions of used air-cured lens moulds. Figure 5.19 (A) and (B) clearly show the region of the lens mould where the lens edge is formed by the mould. All ESEM images of the

female lens mould surface show adhered regions of polymeric contact lens material which are of varying dimensions. The regions of adhered polymeric material do not appear to differ substantially between the central and peripheral regions. Figure 5.19 (C) shows in higher magnification apparent lathing marks associated with the lens edge margins. These markings are similar to the markings observed on one of the nitrogen-cured lenses as shown in Figure 5.20.

Figure 5.21 shows images of the central and peripheral regions of the used nitrogen-cured lens moulds. All these images show adhered regions of polymeric contact lens material which do not appear to differ significantly between the central and peripheral regions. Figure 5.21 (C) and (E) show a layer of polymeric material on the surface of the lens in addition to several larger regions of polymeric material, whereas Figure 5.21 (D) appears to show an incomplete polymeric film on the lens mould in addition the larger regions of polymeric material. Comparison of the images from the nitrogen-cured and air-cured used contact lens moulds show little difference in appearance with both mould types showing significant residual polymeric material on the mould surface both in the form of a film and larger hydrogel regions.

5.4.6 ESEM imaging of dehydrated study contact lenses

5.4.6.1 Imaging of nitrogen-cured lens

Figure 5.22 shows ESEM images of the nitrogen-cured lens surface which possess a relatively smooth surface with small 1-10 μm surface features. Figure 5.22 (D) appears to show pores at the lens surface and Figure 5.22 (A), (E) and to a greater extent (C) show regions of differing contrast which may be associated with slight phase separation or a drying artefact.

5.4.6.2 Imaging of wetting region on air-cured lens

Figure 5.23 shows ESEM images of the wetting regions on the air-cured lens showing surfaces that are comparable with the nitrogen-cured lenses, with a relatively smooth surface with 1-10 microns surface features evident. Figure 5.23 (E) and to a lesser extent (B) show regions of differing contrast suggesting either a degree of phase separation or an artefact from drying.

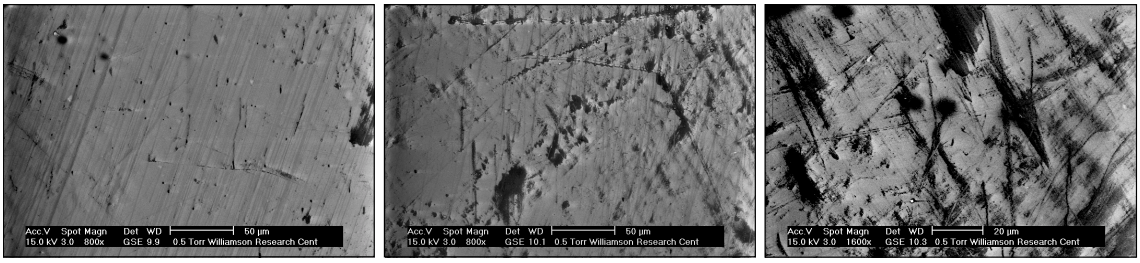

Figure 5.17: Representative ESEM images of virgin study contact lens moulds.

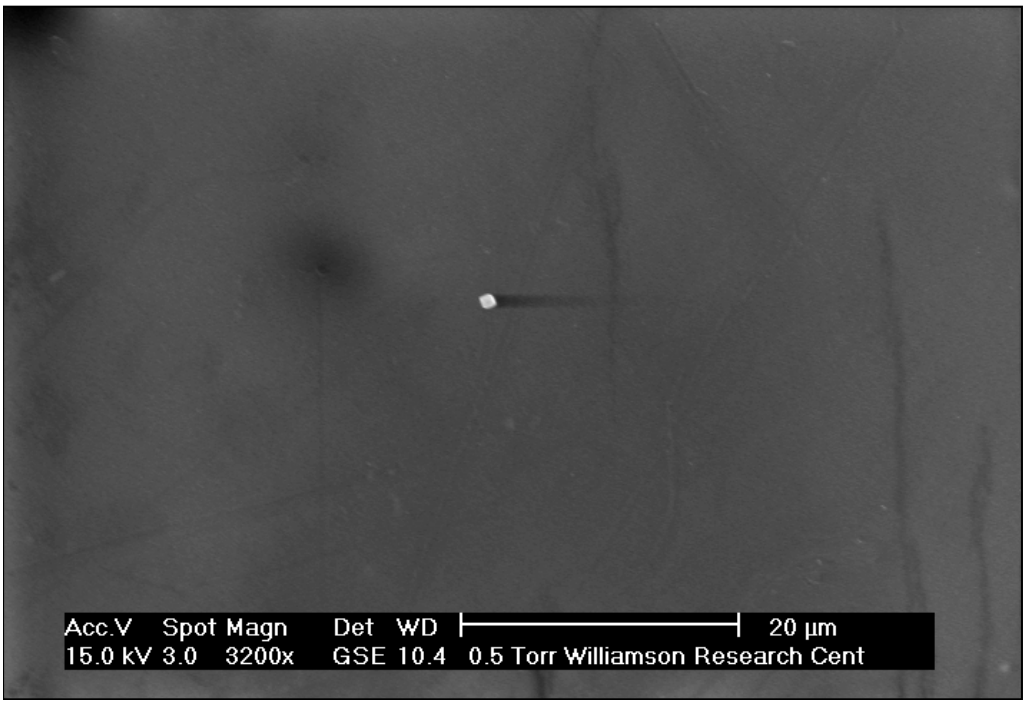

Figure 5.18: Representative ESEM images of crystalline object on virgin study contact lens mould.

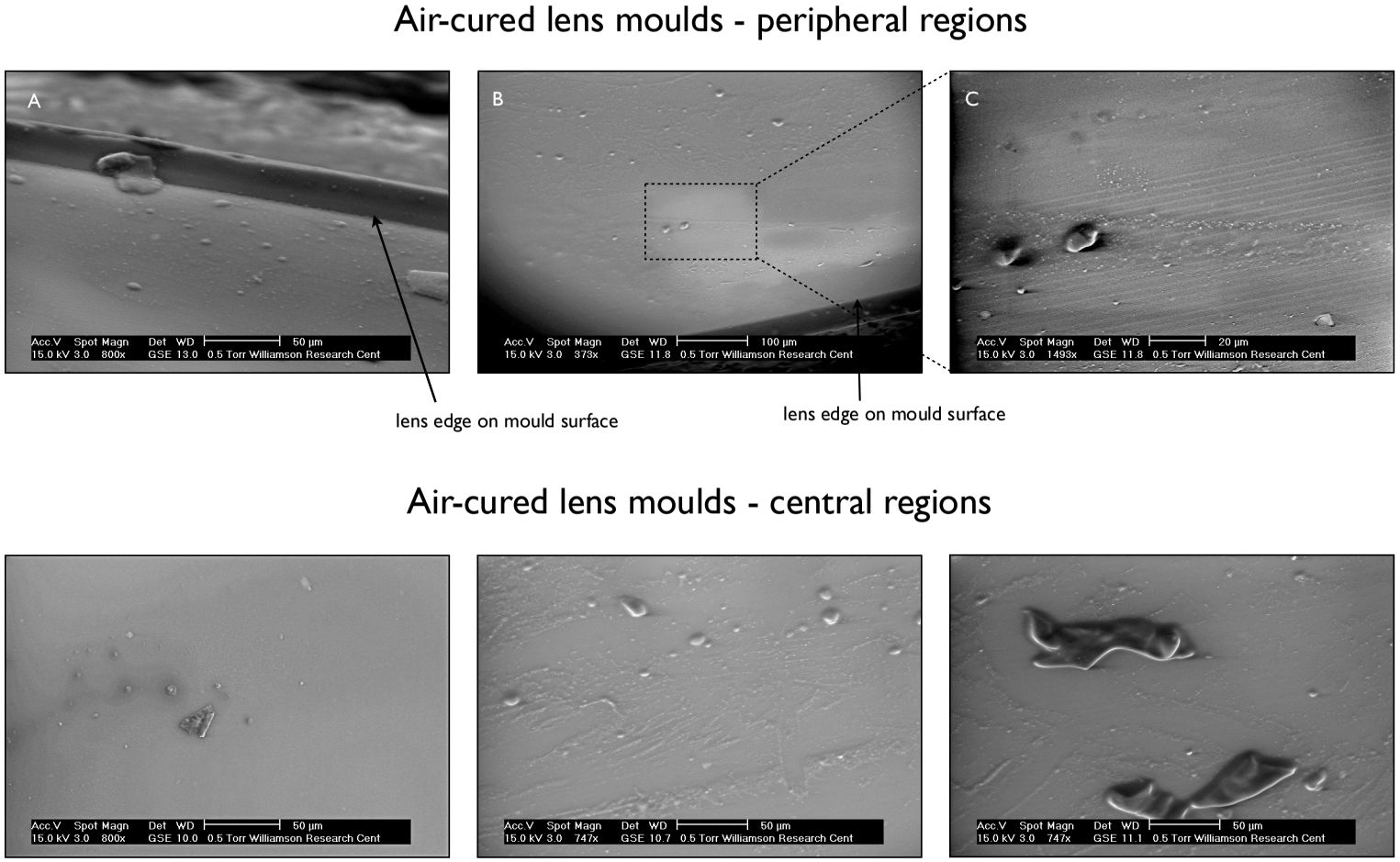

Figure 5.19: Representative ESEM images of peripheral (above) and central (below) regions of the used air-cured contact lens moulds.

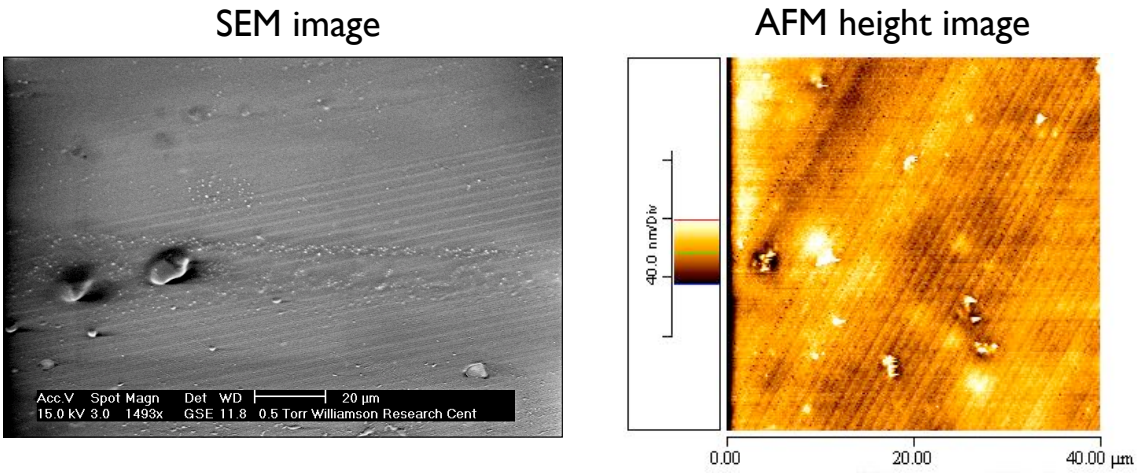

Figure 5.20: Comparison of linear marking observed on the study lens surface using ESEM and AFM.

5.4.6.3 Imaging of non-wetting region on air-cured lens

Figure 5.24 shows SEM images of the non-wetting regions on the air-cured contact lenses. Two of the images (image (A) and (E) from Figure 5.24) show a surface which is comparable with the nitrogen-cured lenses and the wetting region on the air-cured lenses, with a relative smooth surface and relatively few small surface features. In contrast images (B), (C), (D) and (F) from Figure 5.24 show discrete regions within the material, suggesting either some sort of significant phase separation at the surface of the lens material or a surface disturbance associated with material dehydration. Due to the use of the pressure limiting apertures during ESEM image (to avoid having to coat the lens and allow operation in a relative low vacuum (0.5 - 1.0 Torr)) the maximum field of view that could be obtained was around 500 microns. To allow larger areas of the surface to be imaged several images were stitched together to better understand these surface characteristics. Figure 5.25 shows a transition from an area of relatively smooth surface to an area of apparent phase separation/dehydration artefact on a non-wetting region of the air-cured lens. Further imaging of the non-wetting air-cured samples showed that the majority of the surface was composed of apparently phase separated material/dehydration artefact with the surrounding surface composed of a relative smooth surface (Figure 5.26).

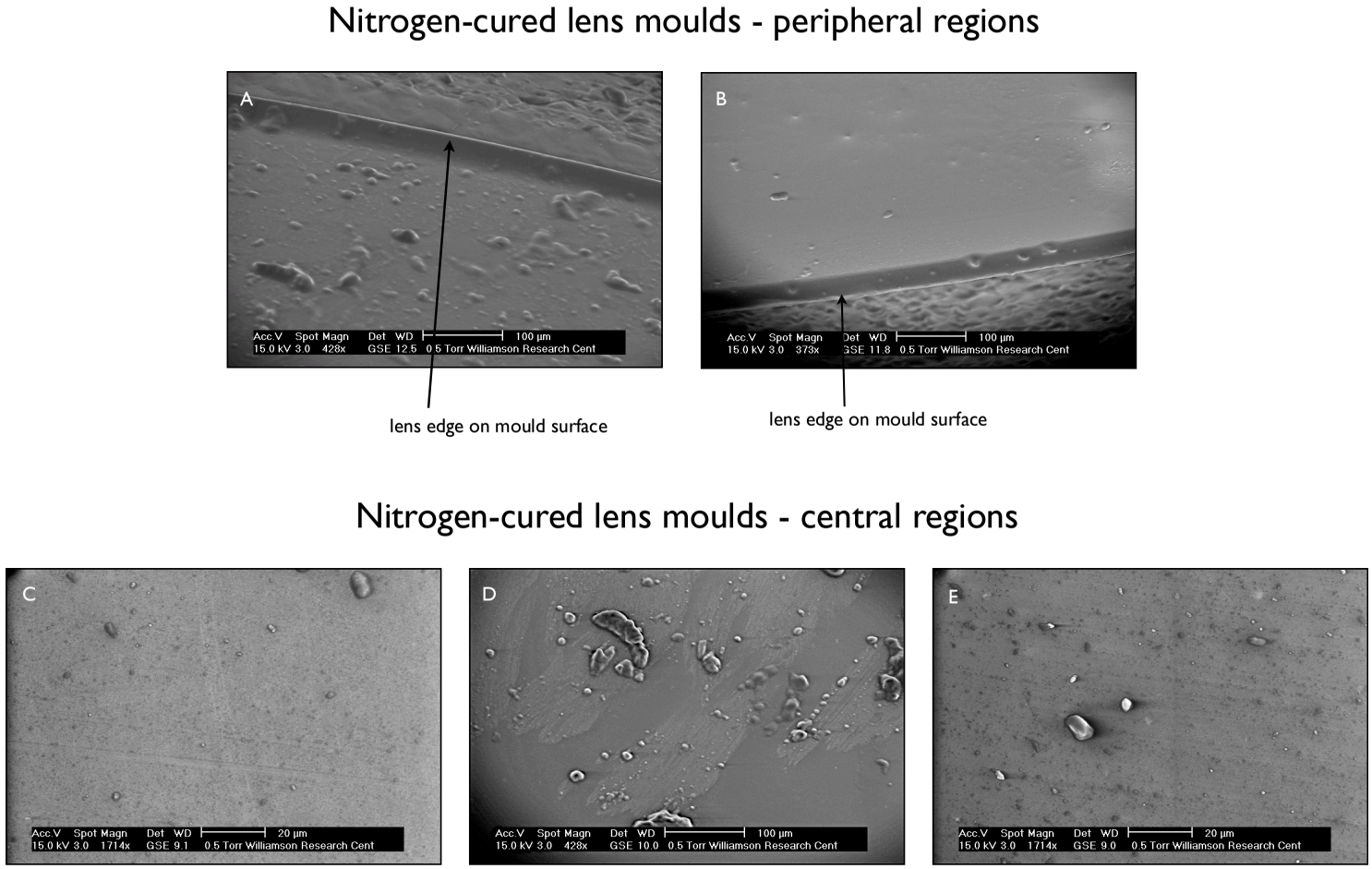

Figure 5.21: Representative ESEM images of peripheral (above) and central (below) regions of the used nitrogen-cured contact lens moulds.

Figure 5.22: Representative ESEM images of nitrogen-cured contact lenses.

Figure 5.23: Representative ESEM images of wetting regions on air-cured contact lenses.

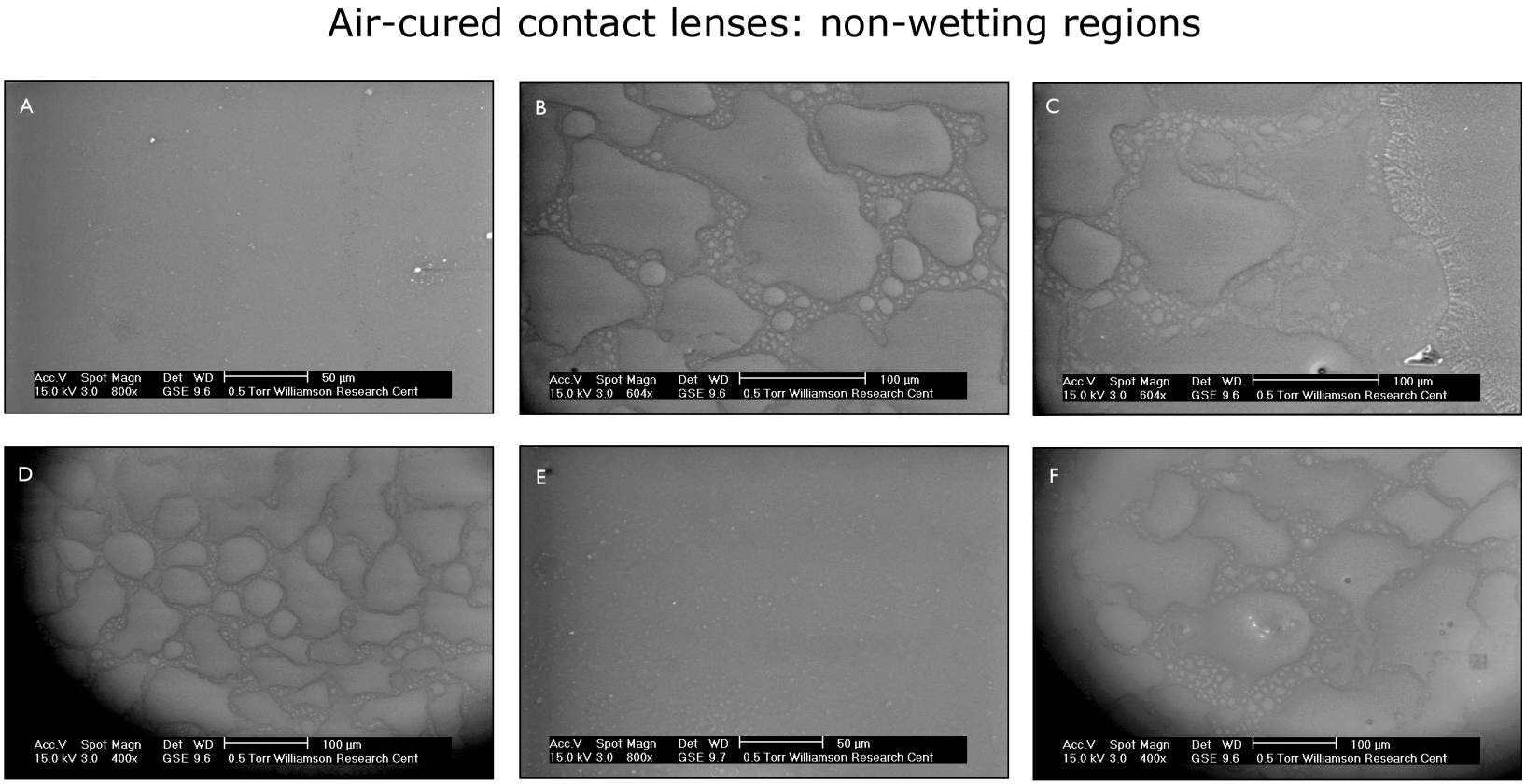

Figure 5.24: Representative ESEM images of wetting regions on air-cured contact lenses. Note: vignetting is observed in some images due to the pressure limiting apertures used during ESEM imaging.

Figure 5.25: Three ESEM images stitched together to show the transition from a relatively smooth surface to an apparently phased separated surface on the non-wetting region of an air-cured lens.

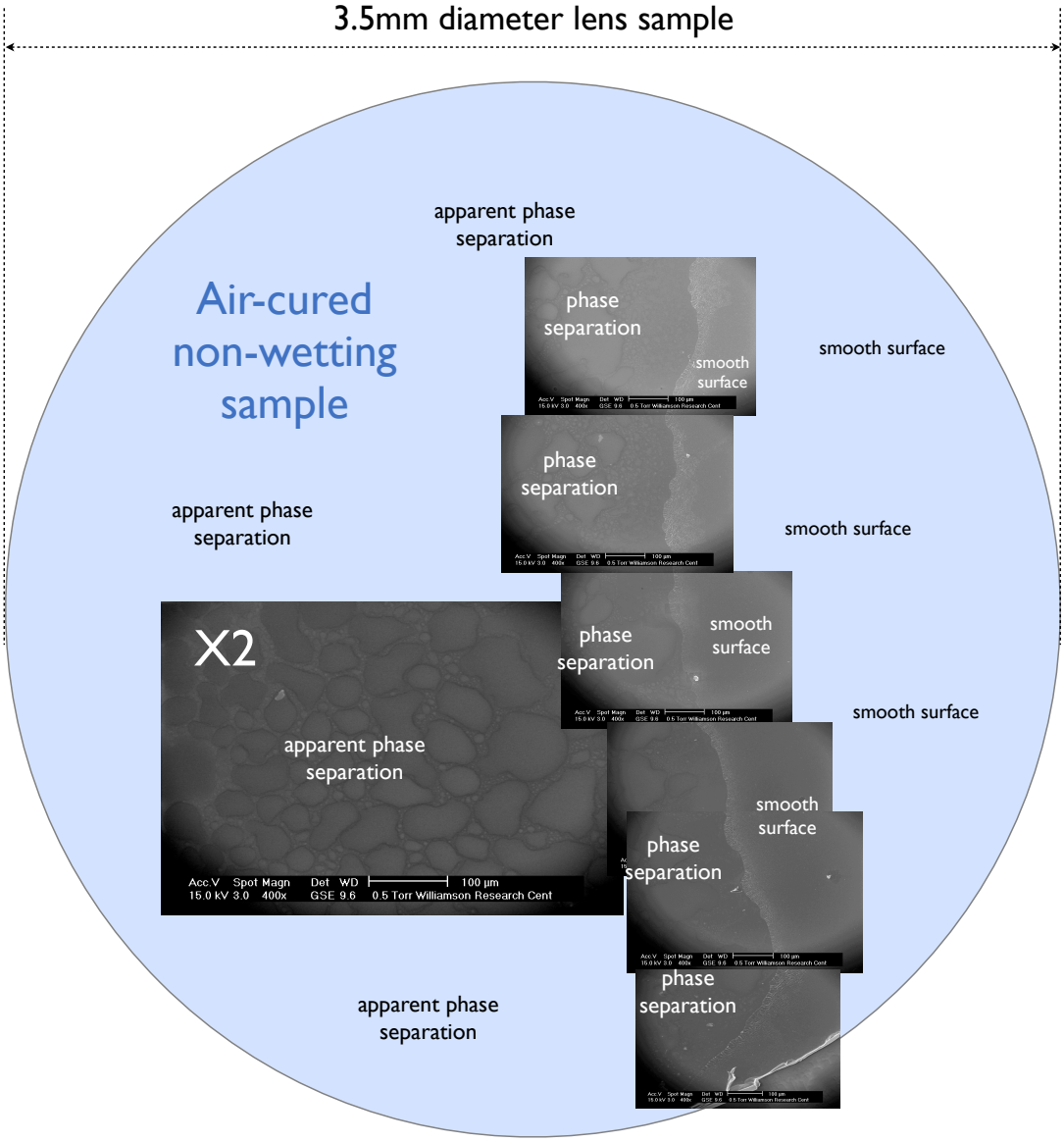

Figure 5.26: Collection of ESEM images showing the transition from a smooth surface to an apparently phased separated surface on the non-wetting region of an air-cured lens.

5.4.7 ESEM imaging of hydrated study contact lenses

Initial imaging of hydrated contact lenses showed no surface features and thus focusing was difficult. By gradually increasing the pressure in the vacuum chamber imaging of the surface was possible, although a clear image was difficult to obtain (Figure 5.27). By continuing to expose the sample to the vacuum environment the surface appeared to further dehydrate allowing the surface features to be identified more easily. The surface features were similar to those identified during imaging of the dehydrated lens surface, but lacked the image clarity of the dehydrated lens samples.

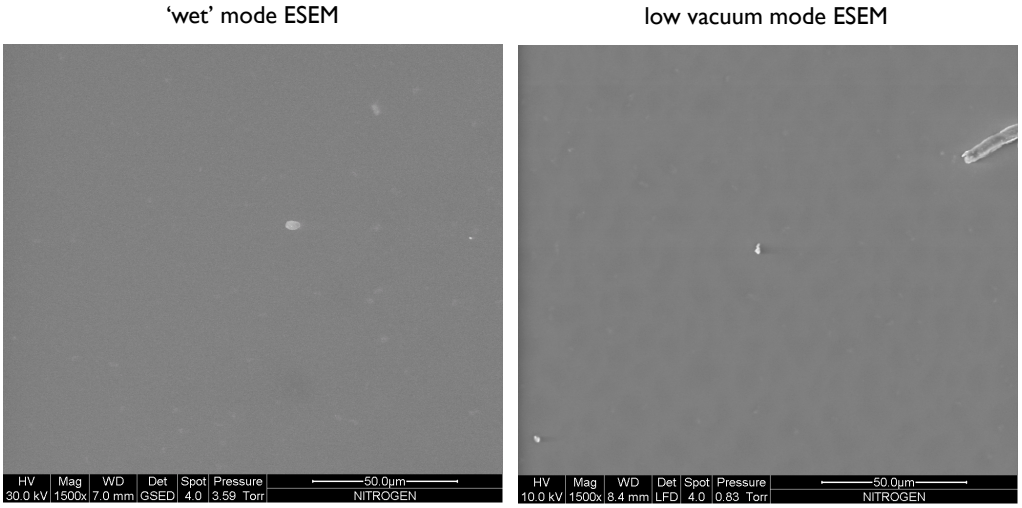

Figure 5.27: ESEM images showing greater surface definition with increasing surface dehydration.

5.4.8 CryoSEM imaging of hydrated study contact lenses

Figure 5.28 shows the cryo-SEM images of the nitrogen-cured study contact lenses, which present a relatively smooth surface typical of a hydrogel material at high magnification (González-Méijome *et al.*, 2006b; Guryca *et al.*, 2007). The image quality is improved at higher magnification compared with the ESEM images, due to the application of a thin gold coating on the surface prior to imaging, which improves the sample conduction and thus image quality. Figure 5.29 shows cryo-SEM images of the non-wetting region on the air-cured lens. One of the three non-wetting air-cured lens samples showed numerous regions of increased roughness which were typically around 3μm in diameter. These regions did not change when the sample was heated suggesting that these surface features were

not associated with ice crystallisation on the contact lens surface and were true surface features.

5.4.9 Discussion

This study has shown that ESEM images of the surface of silicone hydrogel contact lenses and their polypropylene moulds can be obtained both in a hydrated state (either at room temperature or at cryogenic temperatures) and for lenses in a dehydrated state. Imaging of the polypropylene moulds showed evidence of lathing marks (numerous parallel equally spaced lines) used to create the surface and polishing mark (marks of differing size and in differing directions) used to further refine the surface of the metal insert used to manufacture the polypropylene lens moulds (O'Brien & Charman, 2006). Small crystalline objects were also occasionally observed on the surface of unused and used lens moulds, which were of high atomic weight (bright signal during ESEM imaging) suggesting these may be abrasive particles originating from the polish pitch used to finish the metal moulds and then transferred to the mould surface during manufacturing of the polypropylene moulds or contaminants in the polypropylene material, which have been driven to the surface during mould manufacture. These small crystalline objects were never observed on the lens surface suggesting that these objects were bound into the polypropylene mould material. The used lens moulds from both the air-cured and nitrogen-cured lenses showed similar levels of polymeric material adhered to moulds in the form of both a film and larger more significant sections of hydrogel material. There is no evidence to show that de-moulding was more difficult for either study lens type, indicating that the regions of non-wetting on the air-cured lens surface appear not to be associated with any mechanical damage to the lens surface as a result of adhesion to the mould. The surface features of both, the lens mould and the hydrogel material adhered to the mould, are reflected in the final study contact lens surface and agree with other studies which have suggested that the contact lens surface is directly related to the surface of the mould used in its manufacture (Rabke *et al.*, 1995). This study appears to be the first to image contact lens moulds used to manufacture silicone hydrogel lenses. The lack of previous investigation is likely due to the fact that contact lens moulds are difficult to obtain without cooperation of the lens manufacturer. Imaging of conventional hydrogel lens moulds has shown similar surface features with both lathing and polishing marks, which are likely transferred from the metal inserts (moulds) used to manufacture the contact lens moulds (Willis *et al.*, 2001). Polypropylene

Figure 5.28: Representative Cryo-SEM images of nitrogen-cured contact lenses.

Figure 5.29: Representative Cryo-SEM images of non-wetting regions on the air-cured contact lenses.

moulds were used for both the air-cured and nitrogen-cured study contact lenses and are relatively non-polar in nature. The adhesion of hydrogel polymeric material to the mold appears similar for both study lens types suggesting that this adhered polymeric material is primarily associated with the surface chemistry of the lens material and mould rather than the polymerisation conditions within the oven.

Numerous studies in the literature have used SEM imaging to investigate the surface properties of silicone hydrogel (Guryca *et al.*, 2007; Lopez-Alemany *et al.*, 2002; Teichroeb *et al.*, 2008) and conventional hydrogel contact lenses (Deg & Binder, 1986; Guryca *et al.*, 2007; Holden *et al.*, 1974; Lopez-Alemany *et al.*, 2002; Maldonado-Codina, 2001; Teichroeb *et al.*, 2008). These studies have used a range of sample preparation techniques to optimise image quality and minimise surface changes prior to analysis in the UHV chamber, including dehydration in air (Deg & Binder, 1986; Teichroeb *et al.*, 2008), by replacing water with other chemicals (Lopez-Alemany *et al.*, 2002; Maldonado-Codina, 2001) or by freezing the samples (Guryca *et al.*, 2007). The study lenses were analysed in both a hydrated and a dehydrated state to gain a better understanding of both their surface characteristics and to investigate the influence of sample preparation on the surfaces observed. For the contact lenses investigated using 'wet' mode ESEM (hydrated at 4°C) surface imaging proved problematic due to the presence of an adhered water layer which masked any underlying surface features. By gradually increasing the pressure in the chamber the surface water was removed and surface features became evident. These surface features were similar to those observed for fully dehydrated study contact lenses samples, with little if any extra information obtained compared to the dehydrated lens sample. Due to the greater complexity involved in imaging in the 'wet' ESEM mode and due to the reduced image quality it was decided to image the study lens regions solely in the dehydrated state.

The surface images obtained using ESEM are shown to differ depending on the method of sample preparation prior to analysis. Previous studies have suggested that factors such as the polymer structure, strength of bonds, thickness, percent hydration and overall lens tolerance to commonly used SEM dehydration methods should be considered when evaluating the surface morphology of soft lenses (Deg & Binder, 1986). Water is the vehicle for exchange of carbon dioxide and oxygen through conventional hydrogels and as water is removed during the dehydration process, the polymer structure may collapse and

excess gases are not able to flow through or escape from the lens material. After the collapse of the polymer, residual gases are forced to escape in any way possible, causing structural alterations that may appear as deposits. The ability of silicone hydrogel materials to transports gases even without water present suggests that these features might be less evident on silicone hydrogel materials than on conventional polyHEMA materials. By using an ESEM environment in a low vacuum mode it was hoped to minimise these potential surface changes and better maintain the surface structure. More recent studies have suggested that the surface structure of silicone hydrogel lenses appear less influenced by dehydration (likely also related in part to their typically lower water content and high mechanical modulus) meaning that fixation was not required to obtain surface images (Teichroeb *et al.*, 2008).

With the materials in a dehydrated state, images of the surface were easily captured in low vacuum mode, thus avoiding the need for surface coating prior to analysis. The smooth relatively featureless lens surface of the nitrogen-cured lens and wetting region of the air-cured contact lens were similar to that observed on other cast-moulded contact lens surfaces (Lopez-Alemany *et al.*, 2002; Teichroeb *et al.*, 2008) and the findings of the AFM study (Section 5.2). The non-wetting regions of the air-cured lens in contrast differed substantially with large areas of varied topography with a mottled appearance and with a distinct boundary, surrounded by areas of smooth lens surface which was similar in nature to the nitrogen-cured and wetting regions of the air-cured lens.

ESEM images of the nitrogen-cured surface following cryogenic freezing showed a similar surface to the dehydrated nitrogen-cured lens samples (Figure 5.22). The relatively smooth surface of the nitrogen cured lens is similar to other moulded and non-surface treated conventional hydrogel and silicone hydrogel lenses (González-Méijome *et al.*, 2006b; Guryca *et al.*, 2007) although small features are present likely related to regions of adhesion to the lens mould, lathing marks transferred onto the lens surface and/or contamination during sample preparation.

The application of the gold palladium coating following sublimation of the surface ice on the cryo-frozen sample allowed improved resolution at higher magnification. Comparison of dehydrated and cryo-frozen lens surfaces for the nitrogen-cured and wetting region of

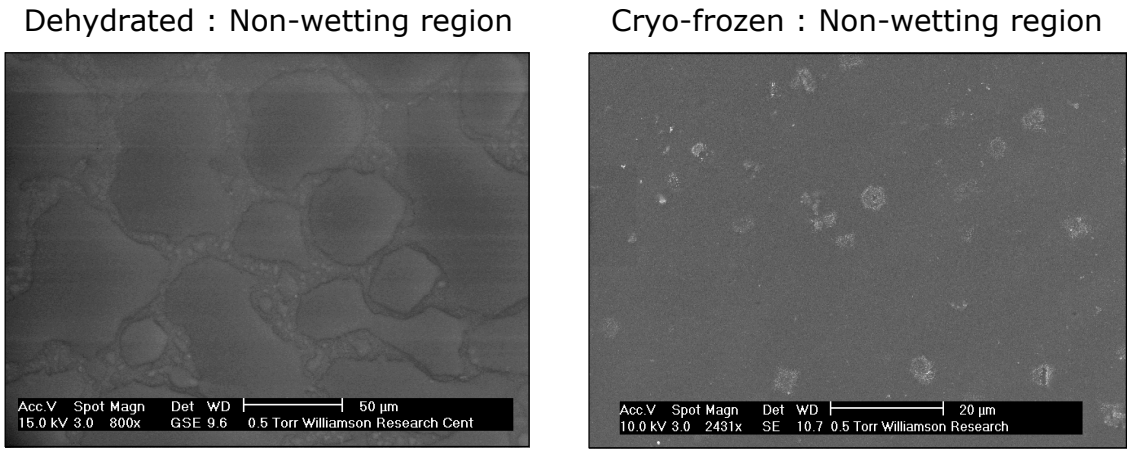

Figure 5.30: Comparison of non-wetting region on the air-cured study lens following (i) dehydration and (ii) cryogenic freezing.

the air-cured lenses showed similar generally smooth surfaces. The SEM images for the dehydrated and cryo-frozen surfaces did differ substantially for the air-cured non-wetting lens surface with the cryo-frozen surface suggesting a relatively smooth surface with small surface features on one of the lens samples (around 3μm in size). A possible cause of these surface features might involve adhesion of the contact lens material to the mould during manufacture, possible regions of phase separation, or damage to the surface related to the freezing process. These surface features remained after the sample was warmed suggesting that they were not associated with ice crystals. In contrast, the dehydrated non-wetting regions on the air-cured lenses showed significant variation in topography giving a mottled appearance (Figure 5.38). These images suggest either a phase separation of the polymeric material or a distortion of the lens surface due to the dehydration process. In either case this mottled surface was observed on all three non-wetting lens samples for the air-cured lens and on none of the other six lens samples (3 x nitrogen-cured samples and 3 x wetting air-cured samples) suggesting that there are key differences in the material at the lens surface and in the way these materials respond to being dehydrated. Given the similarity in the appearance of the contact lens regions in the hydrated state, it either suggests that the surface reorganises to present a similar appearance typical of a hydrogel meshwork or that the material following hydration changes character as it become water swollen.

This ESEM study therefore suggests that although both the nitrogen-cured and wetting

region of the air-cured lenses were shown to be relatively stable following dehydration, all three of the non-wetting regions on the air-cured lenses appear prone to changes in surface structure following dehydration. This difference in surface stability during dehydration suggests that the degree of cross-linking and/or the chemical composition of the surface appears to differ between the study lens types. A possible reason for these topographic differences is phase separation in the non-wetting air-cured surface regions. Phase separation is not an uncommon phenomena and has been shown to occur across a wide range of polymeric materials (Ton-That *et al.*, 2001; Wang & Composto, 2003). The major components of the study contact lens material are VMA (hydrophilic polymer), MMA (non-ion permeable polymer) and M3U (silicone macromer). Given that silicone-containing materials have a tendency to migrate towards the surface (Chen & Gardella, 1994; Ha & Gardella, 2005), especially given the use of non-polar polypropylene moulds, it is likely that the lens surface is at least in part composed of M3U. MMA is also known to have a tendency to undergo phase-separation and surface segregation in polymeric materials (Bates, 1991; Silveira *et al.*, 1995), suggesting this might also be a potential component of a phase separated surface. Lee *et al.* (2003) have shown that a similar co-polymer blend composed of PMMA and PDMS can result in a polymer with a phase separated surface.

The ESEM images of the non-wetting regions of the air-cured lens are similar in appearance to a type of phase separation known as viscoelactic phase separation (Figure 5.31) (Tanaka *et al.*, 1979). This type of network formation is often observed in a polymer blend in which one phase is close to glass transition and typically appears when the two phases have very different viscoelastic properties. The study contact lens monomers have very different glass transition temperatures and viscoelastic properties and this therefore may be a possible cause for the unusual surface structure on the non-wetting region of the air-cured lens following dehydration. Another possible cause for the unusual surface structure may relate to material shrinkage which is likely to accompany material dehydration. This would be even more exaggerated, if indeed there were different phases present at the lens surface as these would have different expansion factors following dehydration (most likely negative), giving a uneven contraction of the lens surface. To fully understand what polymer components make up the phase separated regions, surface chemical imaging techniques using ToF-SIMS (Weng *et al.*, 1998) or XPS (Walton & Fairley, 2004) in a cryo-state could be applied to understand the exact chemical nature of these surface

features.

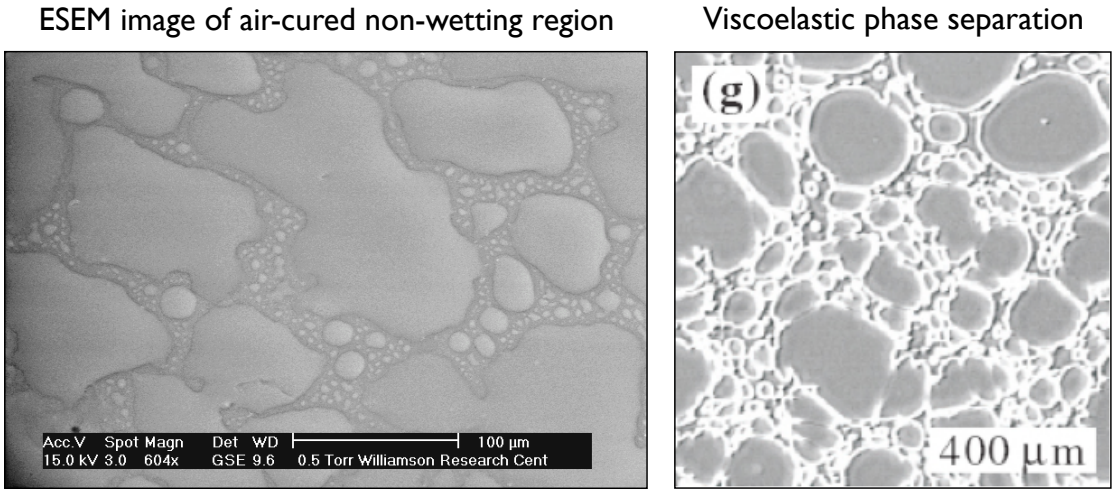

Figure 5.31: Comparison of non-wetting region on the air-cured study lens with an image of viscoelastic phase separation (Tanaka, 2000).

In conclusion, the ESEM study has shown that images can be obtained for silicone hydrogel contact lenses in the instrument's 'wet' mode, although they appear dominated by surface water, which when removed showed an appearance similar to a fully dehydrated lens. The dehydrated study lenses showed relatively smooth surfaces except for the non-wetting regions on the air-cured lenses which consistently showed primarily topographic structures similar to those observed in phase separated materials, although material dehydration cannot be discounted as another possible cause of these topographical features. The cryo-SEM analysis showed the study lens to have a relatively smooth surface except for one of the non-wetting air-cured region samples which showed small areas (several microns in diameter) of increased roughness. In general, the images obtained by ESEM in both 'wet' and low-vacumn mode and by cryo-SEM analysis show a similar surface appearance for the study contact lenses. The surface appearance of the non-wetting air-cured lens region differed between the ESEM imaging types with either phase separation or surface distortion related to the dehydration process, much more marked in the dry state. This increased visibility of the apparent phase separation in the hydrated state is thought to be associated with the different degree of expansion/contraction following dehydration between the different polymer phases. This apparent phase separation appeared consistently

in the lens regions associated with poor surface wetting (the air-cured non-wetting region) suggesting that the polymer surface in these regions is influenced by the polymerisation conditions during lens manufacture. The formation of a micro-scale silicone copolymer network (M3U) with the other non-miscible polymer components (MMA and VMA) is known to be problematic and is highly dependant on the polymerisation conditions during manufacture (Owen, 1993). The presence of air during polymerisation of a polymer material is known to influence the resultant polymer, primarily due to oxygen inhibition (Decker & Jenkins, 1985), resulting in a surface that is typically less heavily crosslinked. The polymer surface is therefore more readily able to reorganise, resulting in the ESEM images that were observed in this study. In addition, the change in material volume following dehydration is likely to differ for the different component polymers, resulting in greater topographical variation in regions of macroscopic phase separation, as observed by ESEM imaging on the dehydrated lens samples.

Chapter 6

General Discussion

6.1 Clinical study

Clinical comparison of the air-cured and nitrogen-cured study lenses has shown clear differences in their *in vivo* performance. The most obvious initial sign of poor clinical performance for the air-cured lens was the inability of the tear film to stably reside on the lens surface, causing the tear film to be rapidly repelled in certain regions. These non-wetting regions appeared randomly distributed on the lens surface and consistent in size and shape through the lens wearing period, suggesting stable hydrophobic surface features. The air-cured lens also showed marked surface deposition during wear, primarily restricted to the non-wetting regions. Lens surface deposition increased throughout the one hour wearing period, with little apparent change in the clinical surface wetting, suggesting a hydrophobic nature to these deposits. The deposited material is therefore unlikely to be composed of hydrophilic mucins or proteins, but more likely lipoidal in nature. This is in agreement with the lack of a nitrogen signal (typically associated with proteins) and a slight increase in the carbon:oxygen ratio (typical of lipids) using the XPS technique (Section 4.3.2.2), although further work is required to confirm the type of deposition present. Xu & Siedlecki (2007) have shown that surface wettability influences protein adhesion onto biomaterial surfaces. Their findings suggest reducing levels of protein deposition on increasingly hydrophobic materials, which is the opposite of that observed in this clinical study, again suggesting that the deposited material is unlikely to be proteinaceous in nature. In addition to the hydrophobic nature of these non-wetting regions, the air-cured lens surface was also shown to have a 'tackier' surface, which readily became contaminated, as observed during AFM imaging (Section 5.3) and contact angle analysis (Section 5.3.4). Oxygen

inhibition during lens manufacture has been shown to result in 'tacky' surfaces due to incomplete polymerisation of the material, resulting in substantially uncross-linked polymer chains at the lens surface (Hagmann *et al.*, 2003). These partially uncured surfaces are prone to greater tear film deposition, as the uncross-linked polymer chains are thought to allow entanglement of tear film components and debris into the lens matrix. Similar 'tacky' surfaces have been observed on conventional hydrogel materials and were associated with the presence of oxygen during lens manufacture, which was thought to have inhibited polymerisation at the lens surface (Maldonado-Codina & Efron, 2004). These conventional hydrogel lenses were shown to have reduced subjective comfort, reduced vision, increased deposition and reduced clinical wettability of the lens surface. In addition, these conventional hydrogel lenses did not possess a hydrophobic surface when analysed by contact angle testing, indicating that excessive tear film deposition was a result of the partially cured surface and not poor surface wetting. The PhD study lenses appear to possess both a partially uncured surface and poor wetting, making identification of the causative factor for excessive tear film deposition difficult. In contrast, contact lens discomfort was found to be associated with poor surface wetting on the study lenses, as poor comfort was apparent immediately following lens insertion (i.e. the poor comfort occurred before any significant surface deposition had taken place). Following one hour of lens wear the level of subjective comfort was unchanged for the air-cured lens (compared with that after five minutes), suggesting that the tear film components deposited had not significantly improved lubrication between the study lens and lid wiper region. Careful observation of the tear film during a blink cycle appears to show the complete surface of the air-cured lens wetting immediately following a blink, followed by a rapid repulsion of the tear film over the non-wetting regions. The tear film repulsion observed on the non-wetting regions is not commonly observed on commercial contact lenses, where a break in the tear film appears to be more evaporative in nature. Similar wetting characteristics are more commonly observed on poorly wettable materials such as waxes or silicone surfaces, suggesting that these non-wetting regions are very hydrophobic in nature. Careful observation of the wetting and immediate dewetting of these regions suggested that the wetting characteristics were likely to be associated with the receding contact angle (given the hydrophilic environment prior to the formation of the non-wetting spots). In contrast to the air-cured lens, the nitrogen-cured lens showed levels of deposition and surface wettability comparable with commercially contact lenses (Brennan *et al.*, 2007).

An area that is of increasing interest is contact lens surface friction (Kim *et al.*, 2001; Ngai *et al.*, 2005; Rennie *et al.*, 2005). Surface friction might appear to be primarily associated with surface roughness, but this only has a small effect on friction in most cases (Blau, 2009). The primary cause of friction with soft materials is related to molecular adhesion and deformation due to the compliant nature of the material. During wear, the surface friction of a contact lens is influenced massively by the presence of the tear film which acts as a lubricating fluid (Guillon & Maissa, 2007). In addition, the adsorption of tear film components onto the lens surface has been shown to influence the frictional characteristics of the surface (Ngai *et al.*, 2005). Regions of poor wetting are therefore likely to have a reduced lubricating tear film layer, potentially allowing direct contact between the lid wiper region of the eyelid and the lens surface. In addition, the deposition of tear film components may result in increased lens surface roughness (Teichroeb *et al.*, 2008). This combination of events increases friction between the contact lens surface and the blinking eye lid, resulting in greater subjective lens awareness. Therefore, a contact lens surface ideally needs to possess a relatively smooth surface (comparable with current commercially available contact lenses), maintain a tear film layer across the lens surface and display a low coefficient of friction to minimise irritation to the lid wiper region. Development of better *in vitro* and possibly *in vivo* models to assess both contact lens surface friction and contact lens surface wettability are required to allow the rapid optimisation of future lens materials.

6.1.1 Future work: clinical study

- Tear film deposition onto the lens surface during wear has been shown to influence the wetting characteristics of commercial contact lens. It may therefore be benificial to investigate the *ex vivo* wetting properties of the three study lens regions to observe how this bioconversion process is influenced by these differing surfaces.

- Recent clinical studies have highlighted an apparent relationship between lid wiper epitheliopathy and reduced subjective comfort (Korb *et al.*, 2002; Shiraishi *et al.*, 2009; Yeniad *et al.*, 2010). Future studies could monitor the incidence of lid wiper epitheliopathy over a range of patients and lens materials (both experimental and commercial lens types) to better understand whether lid wiper epitheliopathy is

primarily patient dependant, lens dependant or a combination of both.

- In an attempt to better understand the aetiology of subjective lens discomfort, potential objective lens performance indicators such as *in vivo* contact angle, *ex vivo* contact angle, surface chemistry of *ex vivo* contact lens, lid wiper epitheliopathy and non-invasive tear film break-up, should be studied for a range of subjects and lens types to better understand the relative importance of these objective measures.

- Clinical studies typically use commercial lenses to investigate the influence of lens design and material characteristics on clinical performance of these lenses. Unfortunately, these lenses differ in numerous aspects and it is often near impossible to infer which of these differences are influencing clinical performance. Future studies should therefore look to introduce independent changes in modulus, water content, wetting characteristics, lens thickness, lens edge and surface friction to allow more controlled investigation into how these characteristics influence contact lens performance.

- Deposition of tear film components onto the lens surface clearly influences several important characteristics, such as bacterial binding, surface wettability and surface friction. Future studies should investigate the differences in tear film deposition between the regions of interest on the study lenses.

6.2 Surface wetting characteristics

6.2.1 Study lens surface wetting characteristics

The performance of a contact lens material depends not only on its bulk characteristics, but also on its interfacial behaviour. Controlling the surface characteristics of a contact lens is critical in the development of new materials with improvements in properties such as adhesion, wettability, friction and biocompatibility (Bousquet *et al.*, 2007). The surface composition of a polymer is often markedly different from its bulk and the methods by which the material is processed can also be critical to its subsequent performance (Maldonado-Codina, 2001). The surface characteristics of wetting and non-wetting silicone hydrogel lenses were investigated in this PhD work, in addition to a number of commercial hydrogel contact lenses, in an attempt to better understand how these surface properties relate to their clinical performance.

6.2.2 Contact angle measurements

Given the marked difference in clinical wetting between the two study lenses, it is not surprising that contact angle analysis also showed significant differences between the materials. Assessment of the air-cured and nitrogen-cured contact lenses with static contact angle analysis showed differences in both the sessile drop and captive bubble contact angle, with the nitrogen-cured lens displaying the lower contact angle in each case.

Cheng *et al.* (2004) have suggested that the advancing contact angle is analogous to the spreading of the tear film on the lens surface, whereas the receding contact angle is analogous to the formation of non-wetting spots on the lens surface. If this is indeed the case, it would suggest that the formation of non-wetting regions observed here is related to the surface properties measured by the receding contact angle. This is in contrast to the results typically presented in both the literature and by contact lens manufactures, which primarily focuses on the advancing/sessile drop contact angle. One disadvantage of the sessile droplet technique is the need to blot the lens to remove the excess surface water. The advancing angle is therefore highly dependant on the degree of lens blotting, with least blotting giving a lower angle. The greater the degree of blotting, the greater is the likelihood for reorientation of the functional groups, with more hydrophobic species being presented at the lens surface. The blotting technique is also likely to adversely influence surfaces with a more delicate structure (such as materials with brush polymer surfaces), in contrast to more robust surfaces (such as those having undergone a plasma treatment). The difficulty in performing lens blotting repeatably and without significantly influencing the surface, led to the development of the dynamic captive bubble technique, which allowed measurement of both the advancing and receding contact angle, while maintaining the lens in a hydrated state.

Dynamic captive bubble analysis of the study lenses showed similar advancing and receding contact angle values to that recorded by the static sessile drop technique, although significant differences were observed for other commercial lenses (Section 3.2). It was apparent for both the static and dynamic contact angle techniques, that the repeatability of the contact angle measurements on the air-cured lens appeared poor, especially between lenses.

Following the clinical study, it became apparent that the surface of the air-cured lens was not uniformly wettable, but rather had regions of wetting and non-wetting randomly distributed on the surface. This explained the greater variability observed between different air-cured lenses (Section 3.1), as only the lens apex was sampled. In contrast, the nitrogen-cured lens appeared to possess relatively homogenous wetting characteristics across the surface. With the development of the *in vitro* thin film analyser and its ability to map out the non-wetting regions on air-cured lens, it was therefore possible to analyse the contact angle wetting characteristics on both the wetting and non-wetting regions on the air-cured lens. This was of interest, as the wetting regions clearly allowed a stable tear film to form, whereas the non-wetting regions destabilised the tear film. By analysing the wetting and non-wetting regions it was hoped to better understand which *in vitro* wettability measurements best predicted clinical lens performance. To allow this type of analysis, a modified lens holder was developed to enable captive bubble analysis at any desired point on the surface of the contact lens. This allowed analysis of the wetting and non-wetting regions on the air-cured surface and highlighted the differences in laboratory wetting characteristics between these regions.

It was apparent, even with the static sessile drop data, that when exposed to an air environment the air-cured lens tended to present a more hydrophobic surface than the nitrogen-cured lens. This suggested that the surface of air-cured lens had a greater concentration of hydrophobic species than the nitrogen-cured lens surface, during analysis. Dynamic contact angle analysis confirmed this finding with the nitrogen-cured lens displaying a significantly lower advancing contact angle than both the air-cured lens regions. Comparison of the advancing contact angle on the wetting and non-wetting regions showed significant differences between the contact angle values with the non-wetting regions typically giving the higher contact angle (poorer wettability). This suggests that when these surfaces are exposed to an air environment a greater degree of hydrophobic material is expressed on the non-wetting surface, indicating a higher concentration of siloxane-related material at the surface.

Contact angle analysis on silicone elastomer (PDMS) has been shown to result in an advancing contact angle of around 120 degrees (Chen *et al.*, 2005). This suggests that although the non-wetting regions are relatively hydrophobic (advancing contact angle of

around 87 degrees), there are hydrophilic species present even when air exposed. In comparison with the low level of hysteresis observed for the PDMS surface (around 30 degrees) (Cordeiro *et al.*, 2009), all three study lenses showed a much greater degree of hysteresis (around 55 degrees), highlighting the substantial surface reorganisation in these study lens regions. As wetting characteristics are influenced only by the material at the polymer's surface, it suggests that both hydrophobic and hydrophilic species are present at or near the surface for all lens types.

Where the advancing contact angle describes the wetting characteristics of an air-exposed lens surface, the receding contact angle describes the wetting characteristics of a water-exposed lens surface. Static and dynamic captive bubble results both showed a significant difference between the air-cured and nitrogen-cured lens regions, although increased variability was again observed for the air-cured lens, due to its heterogeneous wetting characteristics. Dynamic contact angle analysis using the captive bubble technique on the wetting and non-wetting regions of the air-cured lens showed that the receding contact angle measured on the wetting region was similar to that on the nitrogen-cured lens surface. This suggests that when exposed to water, similar hydrophilic species were dominant on the surface of both the nitrogen-cured lens and the wetting region of the air-cured lens. In contrast, the receding contact angle measured on the non-wetting region of the air-cured lens was significantly elevated, suggesting significant hydrophobic species were present at the lens surface even in a aqueous environment. Given the ability the surface normally has to reorganise, this suggests that the non-wetting regions on the air-cured lens surface are dominated by hydrophobic material, with insufficient hydrophilic material to completely mask its hydrophobic nature. In contrast, sufficient hydrophilic material appears to be present in the surface/sub-surface region of both the nitrogen-cured and wetting regions of the air-cured lens material to allow any hydrophobic material to be effectively masked in an aqueous environment. This is in agreement with the findings of the cryo-XPS study, which showed the non-wetting region of the air-cured lens possessed an elevated concentration of M3U-related elements (fluorine and silicone), whereas the nitrogen-cured and to a lesser extent the wetting region of the air-cured lens showed a higher elemental concentration of a hydrophilic-related element (nitrogen). This type of reorganisation at a polymer surface is well documented (Holly & Refojo, 1975) and has been shown by others with a range of surface analysis techniques, such as SFG (Koffas *et al.*, 2004), ToF-SIMS

(Hook *et al.*, 2009) and AFM (Kim *et al.*, 2002).

Another observation made during contact angle analysis analysis was that the surface of the air-cured lens tended to rapidly become contaminated. This was particularly marked following blotting where the air-cured lens surface was visible more contaminated than the nitrogen-cured lens surface (Figure 5.16). This was supported by the AFM images which showed similar apparent contamination on the non-wetting regions of the air-cured lens during hydrated analysis. This increased contamination is likely to be a result of oxygen inhibition during polymerisation, which has been shown to result in a less heavily crosslinked surface, which is tacky (Biswal & Hilt, 2009) and prone to contamination (Maldonado-Codina & Efron, 2004) . Silicone-containing materials are particularly prone to this due to the high oxygen permeability of the material. In contrast, the lenses manufactured in the nitrogen-purged environment are unaffected, as nitrogen does not interfere with the free radical polymerisation process and therefore the surface are fully cured and do not possess a tacky surface.

Differences in the wetting characteristics between regions are therefore likely as a result of variation in relative concentrations of the hydrophobic and hydrophilic species. This difference in concentration between the lens regions is possibly related to phase separation and/or surface segregation of the hydrophilic/hydrophobic components and may also indicate a less heavily crosslinked polymer network at the surface of the air-cured lens, due to oxygen inhibition during polymerisation.

6.2.3 Commercial lens surface wetting characteristics

The magnitude of the advancing contact angle has been shown to vary widely across a range of commercially-available contact lens materials. Given that all these contact lens materials have been shown to perform well clinically, the advancing contact angle does not appear to be a good predictor of clinical performance, at least over the range assessed (20 - 80 degrees). As the advancing contact angle has been likened to the process of the tear film spreading across the lens surface during blinking (Cheng *et al.*, 2004), it is perhaps surprising that this laboratory measure does not relate, in some way, to the clinical performance of the lens. There appears to be two reasons why this is not the case. Firstly, the formation of the tear film across the lens surface is not a simple spreading process.

The tear meniscus is driven across the lens surface by the eyelids and it appears relatively independent of the angle the tear film forms with the lens surface, as the motion of the lids force it to spread across the lens surface (Wong *et al.*, 1996). The second reason is that tear film components adsorb almost immediately to the contact lens surface, rapidly enhancing its wetting characteristics, with a reducing *ex vivo* advancing contact angle measured (Read *et al.*, 2010b; Tonge *et al.*, 2001). The *in vitro* advancing contact angle measurements therefore appear to be a poor predictor of clinical performance on commercial contact lenses. However, if a lens surface possessed a substantially elevated advancing contact angle (> 90 degrees), it would be likely to result in poor clinical performance. This is due to the hydrophobic nature of the surface, which would adversely influence tear film adsorption and restrict the ability of the tear film to be spread over these extremely hydrophobic regions. Such disruption to the tear film would expose the lens surface to the hydrophobic lipids, which usually reside on the anterior tear film surface, resulting in adsorption to the lens surface and driving further hydrophobic deposition. This deposition is likely to reduce visual acuity, increase mechanical and biological interaction with the lids and further destabilise the tear film, potentially causing reduced subjective comfort (Jones & French, 2009).

The receding contact angle values for commercial lenses are typically much more similar between the different analysis techniques. This likely relates to the fact that this contact angle measurement is taken when the surface is in its most hydrophilic arrangement and direct contact exists between the region of the surface being tested and the probe liquid. Indeed the variation in receding contact angle between different lens types is typically small, varying by less than five degrees across a wide range of silicone hydrogel materials. The lack of difference highlights the similarity in the character of the hydrophilic groups present at the lens surface of these materials. Cheng *et al.* (2004) have suggested that when the lens surface is in its most hydrophilic arrangement (during the receding phase), it is completely wettable (i.e. a contact angle of 0 degrees) and that the angle measured is a limitation of the captive bubble technique in being able to differentiate between an angle of 0 degrees and 20 degrees. Given that in this study a consistent, although small, difference was observed between commercial lens types, it appears that this is a true measurement of the surface chemistry rather than a value limited by the ability to measure. It is apparent that a captive bubble measurement of around 20-25 degrees (measured with

the captive bubble technique in our laboratory) is sufficient to maintain acceptable clinical performance, with these values changing little with contact lens wear (Tonge *et al.*, 2001). On investigation of experimental materials with known poor clinical performance within our laboratory (including the experimental study lenses used in this PhD study) a consistently elevated receding contact angle (30-40 degrees) has always been present for these materials. It therefore appears that a substantially elevated receding contact angle may indicate a contact lens material with potentially poor clinical wetting, although this is often accompanied by an increased advancing contact angle, making identification of the causative factor difficult. Comparison of the advancing and receding contact angle data for commercial lenses with the results of contact lens clinical trials, shows no obvious link with comfort (Brennan & Morgan, 2009). This suggests that although the receding contact angle appears able to predict non-wetting regions on the lens surface, there is no evidence to suggest it is able to predict *in vivo* comfort or wettability. As with the advancing contact angle, this is likely to be, at least in part, associated with *in vivo* tear film deposition which influences the wetting characteristics of the contact lens material, although for the receding contact angle the changes appear to be minimal (Read *et al.*, 2010a). Further studies investigating the wetting characteristics of lens materials should include both experimental lenses with poor clinical characteristics and commercial contact lenses, in an attempt to gain a better understanding of the importance of these laboratory values and the critical values for each measurement type. These studies should include contact angle measurements on unworn and worn contact lenses, while also carefully recording subjective and objective lens performance data.

Contact angle hysteresis gives a measure of the ability of the contact lens surface to reorganise under different environmental conditions. Ideally a lens material should resist the tendency to become more hydrophobic when exposed to an air environment, otherwise hydrophobic regions can be generated across the lens surface in the inter-blink period. Various different manufacturing methods have been developed in an attempt to mask the hydrophobic species from the lens surface (Jones *et al.*, 2006). Dynamic captive bubble data suggest minimal hysteresis for plasma coated lenses, whereas uncoated and plasma oxidised surfaces show greater levels of hysteresis (Section 3.3). It should be noted, that even lens materials with high levels of apparent hysteresis have very acceptable clinical performance (Brennan *et al.*, 2007; Lakkis & Vincent, 2009; Maldonado-Codina & Morgan,

2004; Young *et al.*, 2007), likely associated with the reducing advancing contact angle and thus hysteresis following lens wear (Read *et al.*, 2010a). The work of this PhD therefore suggests that for a contact lens to have acceptable clinical wetting, the material should have an advancing contact angle (measured by dynamic captive bubble technique) of less than 90 degrees and a receding contact angle of no more than around 25 degrees. However, contact angle measurements have been shown to be highly dependant on experimental methodology and therefore care should be taken when comparing these values with those produced experimentally using other techniques or methodologies. There appears to be little apparent clinical advantage to a material with a low advancing contact angle or low contact angle hysteresis over the range observed for commercial contact lens materials. Indeed, in a recent study looking at the data obtained from a number of fully masked and randomised studies, Brennan (2009) found that the lens type with the lowest advancing contact angle and hysteresis in this PhD study had on average one of the lowest levels of subjective comfort. It is therefore clear that surface wetting is only one of a range of lens surface features that must be considered when developing contact lens materials, with other potential clinical factors, such as roughness, friction, deposition and material dehydration, also likely to be of key importance.

6.2.4 Thin Film Wettability Analyser

The consistency with which the *in vitro* thin film wettability analyser was able to identify the regions of non-wetting on the lens surface, even after prolonged periods of soaking, indicate that these regions are crosslinked into the lens structure and are not mobile (Appendix C). The accuracy with which this laboratory instrument could consistently identify the clinical non-wetting regions suggest that a similar process may be occurring in the ocular environment. As the thin liquid film was generated by submersion and emersion of the contact lens in a saline bath, the lens surface was continuously exposed to a polar liquid which would drive the presentation of hydrophilic species at the lens surface. The formation of a non-wetting region is likely a result of hydrophobic species present on the surface of the non-wetting region, even in the hydrophilic environment, which drive this tangential flow of liquid. Surprisingly, given the lower surface tension of the tear film, the development of non-wetting spots occured much quicker clinically ($<$ 1 second) than in the laboratory instrument (approximately 5-15 seconds). The formation of a saline film by passing it through the water/air interface is clearly different to the blinking process

and likely leads to a different film thickness. Such differences in the film thickness and differences in the chemistry of the probe liquids are thought to influence the time taken for the film to destabilise and expose the underlying polymer surface. Given that the lens surface was initially exposed to water prior to the formation of the non-wetting region, this suggests that the receding angle values may be a better predictor of contact lens clinical performance. This is in agreement with the findings of the dynamic contact angle study (Section 3.4), where the receding contact angle was more consistently able to differentiate the wetting and non-wetting air-cured lens surfaces, than the advancing contact angle. In contrast, others have proposed that the advancing angle is the more relevant measure of clinical performance (Tonge *et al.*, 2001). This may, in part, relate to the fact that differences in the advancing contact angle are observed between the commercial materials (unlike the receding contact angle) and therefore an assumption that a difference must in some way be clinically relevant. In agreement with this PhD study, others have suggested that the receding contact angle is an important wetting characteristic which cannot be ignored (Cheng *et al.*, 2004). Better understanding of the *in vivo* wetting process is further complicated by factors such as the adhesion of tear film components to the lens surface. Future research should therefore focus on the bioconversion of the lens surfaces during wear and the influence this has on both wetting characteristics and clinical lens performance.

6.2.5 Future work: Contact angle analysis / lens surface wettability

- Contact angle values are commonly used in the contact lens industry and beyond to compare surface wetting properties of materials. These values are primarily intended to allow estimation of the surface energy of a material. Techniques such as that described by Owens & Wendt (1969) allow calculation of the free energy of a surface by testing the material with a range of well characterised liquids. A similar technique has also been described for the captive bubble method by Hamilton (1972). Therefore, future studies should consider characterisation of contact lens materials, both with respect to free energy of the surface and the polar/dispersive nature of the surface free energy. This may improve understanding of the wetting properties and adhesion of tear film components and/or bacteria to the lens surface during wear.

- It is often assumed that lenses of the same brand type will have identical properties. Future studies should investigate the repeatability of contact angle measurements, both within and between manufacturing batches, for a range of contact lens types to better understand variability in surface wetting.

- Differences in methodology commonly lead to significant variation in contact angle measurements. One possible reason for this is the difference in surface curvature, with some lenses analysed in a curved state (Ketelson *et al.*, 2005; Maldonado-Codina & Morgan, 2007) and some analysed in a flattened state (Cheng *et al.*, 2004; Tonge *et al.*, 2001). Future work should therefore investigate the influence of surface curvature for both sessile droplet and captive bubble techniques.

- Future work could also use the difference in contact angle on either side of the bubble/droplet during dynamic contact angle testing to assess surface heterogeneity, for a range of commercial contact lens materials.

- Contact angles have traditionally been performed at laboratory temperature. A possible reason why *in vitro* contact angle measurements are unable to predict clinical performance, might be associated with the difference in temperature between the two conditions. A future study could therefore investigate the influence of temperature on wetting characteristics for a range of commercial contact lenses.

- It is evident that tear film adsorption rapidly changes contact lens wetting characteristics. Future studies should investigate how *ex vivo* contact angle measurements compare with subjective and objective grades of lens performance, in an attempt to better understand how the bioconversion of the lens surface influences clinical lens performance.

- When testing the contact angle of a surface we often attempt to simulate *in vivo* conditions. Recent work by Haddad (2010) has performed contact angle analysis on eye, therefore negating the need to simulate these conditions. This small clinical study has suggested a link between the rate of spread of a droplet and the subjective comfort experienced by the lens wearer. Future work should further develop this technique to investigate the apparent link between subjective comfort and surface wetting.

6.3 Study lens surface chemistry

The chemistry of the contact lens surface influences important clinical factors such as wettability, tear film deposition and bacterial adhesion. The use of techniques such as XPS and ToF-SIMS has allowed a detailed investigation of both the lens surface chemistry (Garrett *et al.*, 1999; Griesser *et al.*, 1990; Karlgard *et al.*, 2004) and tear film deposition onto the lens surface following wear (Bruinsma *et al.*, 2002; McArthur *et al.*, 2001). These studies highlighted the ability of XPS to investigate the elemental composition (% of each chemical element) and chemical bonding state (what each element is bond to) of the surface. XPS studies on rigid gas permeable contact lens materials have shown good agreement between chemical composition of the surface and contact angle wetting data (Fakes *et al.*, 1988), although this is less clear with hydrogel contact lens and especially problematic with siloxane-containing materials (Migonney *et al.*, 1995). XPS data are often influenced by the presence of surface active compounds, which can surface segregate during dehydration (Migonney *et al.*, 1995). This has been observed for a range of siloxane-containing polymers (Hook *et al.*, 2006; Lee *et al.*, 2003; Selby *et al.*, 1994) and appears to occur following dehydration for both study lens types (Section 4.4). Dehydrated XPS and ToF-SIMS analysis of the study lens regions showed a surface dominated by silioxane material for all study lens regions. The surface of all regions on the study lenses were similar in elemental and molecular composition to pure M3U and given the known differences in wetting characteristics, this indicated M3U-related surface segregation. In view of the different clinical and laboratory wetting characteristics for the three regions, the apparent similarity in surface chemistry suggested the possibility that significant surface reorganisation had occurred during dehydration, thus masking the true differences in hydrated surface chemistry. *Ex vivo* XPS analysis of worn study contact lenses also showed unexpected surface chemistry, with the lens surface showing minimal evidence of tear film deposition, in contrast to that observed in previous studies (McArthur *et al.*, 2001), again supporting the theory of surface reorganisation.

Cryogenic techniques were therefore developed in an attempt to minimise surface reorganisation prior to analysis in ultra high vacuum conditions by maintaining the lens samples in a frozen hydrated state. Both XPS and ToF-SIMS cryo-analysis showed much lower levels of siloxane-related material on the lens surface than was observed for the dehy-

drated lens samples. Cryo-XPS showed differences between the study lens regions with the highest levels of elemental nitrogen on the nitrogen-cured lens samples and lowest levels on the non-wetting region of the air-cured lens surface. The silicon and oxygen signals, in contrast, were at lower levels on the nitrogen-cured sample and higher levels on non-wetting region of the air-cured lens. In agreement with the results for the elemental composition analysis, the chemical state XPS analysis showed high levels of carbon-silicon and silicon-oxygen bonding on the non-wetting regions of the air-cured lens in comparison with the lower levels seen on the nitrogen-cured lens surface. All these results indicated greater levels of the siloxane-containing polymer (M3U) at the surface of the non-wetting region and to a lesser extent the wetting region of the air-cured lens, in comparison with the nitrogen-cured lenses, which in turn was more dominated by the hydrophilic nitrogen-based polymer (VMA). Comparison of the results from the XPS and contact angle studies showed that study lens regions with greater siloxane macromer expression, tended to present a more hydrophobic surface, as expected given the typically hydrophobic nature of the siloxane material. This is in agreement with work by Weikart *et al.* (1999, 2001), who showed that lenses with a higher concentration of silicone at the surface tend to have poorer laboratory wettability. The hydrophobic regions on the surface of the air-cured lenses appeared unable to allow the stable formation of a tear film over the lens surface during clinical lens wear, with immediate tear film break-up following blinking. Similar studies have shown that high silicone expression on silicone hydrogel materials is related to poorer clinical performance (Lai & Friends, 1997). In addition, a rapid deposition of tear film components onto these non-wetting regions was observed. Given the hydrophobic and lipophilic nature of siloxane materials (Abbasi *et al.*, 2001) it is assumed that this initial deposition is primarily lipoidal in nature, although further investigation is required to better understand this deposition process.

In contrast to the XPS data, cryogenic ToF-SIMS analysis showed little difference in composition between the three study lens regions. The obvious differences in both clinical and laboratory wetting characteristics indicated differences in the surface chemistry between the study lens regions. The apparent lack of sensitivity of the ToF-SIMS instrument is likely associated with (i) the ion etching required to removed the surface ice, making identification of the surface difficult (ii) surface reorganisation, due to possible brief periods of sample warming during sample transfer (iii) possible surface contamination during sample

preparation and (iv) low secondary ion signal count during cryo-analysis. Lewis & Ratner (1993) also observed that surface contamination was a major issue at cryogenic temperatures, due to the increased rate of condensation of contaminants on the sample surface in both air and vacuum. Colliver *et al.* (1997) noted similar problems during frozen-hydrated analysis where water vapour in the vacuum became a major source of interference. It has been shown both in this XPS study (Section 4.4) and by others (Colliver *et al.*, 1997; Severs & Shotton, 1995; Willison & Rowe, 1980) that carefully controlled sublimation of surface water, can be less invasive at removing surface ice, producing a relatively artefact free polymer surface. For polymers containing materials with a low glass transition temperature, such as siloxane-containing materials, care must be taken during sublimation to avoid warming the sample above its glass transition temperature. If this occurs substantial surface reorganisation is likely to occur (Selby *et al.*, 1994). Hook *et al.* (2009) have recently shown that by carefully sublimating the surface ice on siloxane-containing polymers, cryogenic ToF-SIMS analysis can minimise surface reorganisation and allow investigation of the hydrated surface chemistry. As the surface of silicone hydrogel lenses has been shown to reorganise and become dominated by hydrophilic material, care must be taken when interpreting surface chemistry data from dehydrated samples and ideally these materials should be analysed in a hydrated state. Future studies should therefore look to improve the ToF-SIMS cryogenic sample handling technique to optimise signal quality and minimise contamination, while maintaining the lens sample below the glass transition temperature of the siloxane polymer to avoid chemical reorganisation at the surface.

In the development of future contact lens materials the ideal surface would exhibit minimal siloxane-related material and be primarily composed of hydrophilic groups (such as hydroxyl / carboxyl / amino and/or phosphate functional groups). The lens surfaces should avoid reorganisation in the clinical environment, either by heavily cross linking the hydrophilic components and/or by enrichment with hydrophilic species, to limit the thermodynamic drive of siloxane components towards the surface. Care must also be taken during lens surface optimisation to maintain optical clarity, minimise bacterial adhesion/activity, minimise surface friction and provide sufficient oxygen and ion permeability through the material. The cost of manufacture is another important consideration and where possible additional processing steps such as surface treatment should be avoided.

6.3.1 Future work: study lens surface chemistry

- The ToF-SIMS instrument needs to be further developed to improve cryogenic analysis. Required features include continuous sample cooling within the instrument, the addition of a cold finger probe to condense water vapour in the chamber and an improved sublimation technique to remove surface ice while maintaining the surface in a hydrated frozen state.

- Differences in polymerisation between the two study lens types could be further investigated by analysing the lenses both pre and post-extraction or by analysing the extraction liquid of the two study lens types to identify differences in the material removed from the surface during extraction.

- Analysis of dehydrated worn contact lenses using XPS gave an unexpectedly low signal associated with adsorbed tear film components. Future studies should compared hydrated and dehydrated worn samples using XPS, to better understand if surface reorganisation resulted in the masking of the chemistry associated with the tear film components.

- The ability of XPS and ToF-SIMS to be operated in an imaging mode (Ton-That *et al.*, 2001; Walton & Fairley, 2006a,b) allows the monitoring of chemical homogeneity across the sample surface. Future studies could apply these techniques to the cryo-frozen study lens regions to investigate the possible presence of phase separation on the lens surfaces or distribution of adsorbed tear film components on worn lenses.

- Given the difference in surface chemistry between the three study lens regions, there are likely to be differences in the water content of the material at the lens surface. Future studies could therefore investigate the water content of the three study lens regions to better understand the relative water content in these surface regions.

- In addition to XPS and ToF-SIMS, another technique that should be considered when analysing the surface chemistry of lens materials is sum frequency generation (SFG) vibrational spectroscopy. SFG can be used in a hydrated environment and has been shown able to monitor changes in surface chemistry during dehydration (Koffas *et al.*, 2004), without the need for a high vacuum environment.

- Commercial contact lens materials often show significant contact angle hysteresis (Tonge *et al.*, 2001), thought to be associated with surface chemical reorganisation (Holly & Refojo, 1975). Comparison of the surface chemical composition in both an air exposed and water exposed hydrated (frozen) state for a range of commercial materials, would allow investigation of this theory.
- Use of a depth profiling technique (XPS and SIMS) or angle resolved technique (XPS) on a range of cryogenically frozen commercial contact lenses, would give important information about the chemical structure of the lens surface. Similar analysis on worn lenses would also allow investigation of the tear film components deposited on the surface and within the sub-surface of the material.
- Both XPS and mass spectrometry techniques have been shown to be able to monitor tear film deposition on the lens surface following wear (Green-Church & Nichols, 2008; Kingshott *et al.*, 1997; McArthur *et al.*, 2001). By monitoring the surface chemistry of the lens following wear, for symptomatic and asymptomatic groups of contact lens wearers, it may be possible to identify advantageous and non-advantegous deposits on the lens surface.

6.4 Contact lens surface topography

Several studies have shown the importance of surface topography to wettability (Miller *et al.*, 1996), bacterial adhesion (Giraldez *et al.*, 2010) and deposition (Baguet *et al.*, 1995b) of biomaterials. Investigation of surface roughness on contact lens materials can be problematic as it is often difficult to differentiate between true surface roughness and contamination (Fakes *et al.*, 1988). There is little in the literature to suggest at what point a contact lens surface becomes too rough, either with respect to subjective comfort or optical performance. Comparison of roughness findings from several studies, measured using AFM, suggest that a wide range of surface roughness values provide acceptable clinical performance (Baguet *et al.*, 1995b; González-Méijome *et al.*, 2009; Guryca *et al.*, 2007; Kim *et al.*, 2002; Teichroeb *et al.*, 2008). Comparison of lathe cut and cast moulded contact lenses has indicated that lathe cut lenses typically have a rougher surface, although this is not thought to affect subjective lens performance (Maldonado-Codina & Efron, 2005). A study by O'Brien & Charman (2006) showed minimal change in clinical performance following lens polishing for a lathe cut lens, implying that surface roughness

is not a critical factor for subjective lens comfort with modern manufacturing techniques. Although surface roughness does not appear to directly affect subjective comfort, it has been shown to play a important role in bacterial (Bruinsma *et al.*, 2003) and tear film component adhesion (Baguet *et al.*, 1995b). Much of this research has been performed by comparing commercial contact lenses where the surfaces typically differ in numerous ways, meaning that the exact cause of the increased adhesion or lens comfort is difficult to assess.

AFM and ESEM imaging of the hydrated study lenses showed surface features typical of a porous hydrogel material. AFM imaging showed greater surface roughness for the air-cured lens, than the nitrogen-cured lens, with the non-wetting region having the highest surface roughness. These levels of surface roughness are within the normal range for commercially available contact lenses (Baguet *et al.*, 1992; Bruinsma *et al.*, 2001; Giraldez *et al.*, 2010; González-Méijome *et al.*, 2006a, 2009; Guryca *et al.*, 2007; Lira *et al.*, 2008; Santos *et al.*, 2008; Teichroeb *et al.*, 2008) and appear insufficient to result in the subjective discomfort observed with the air-cured lenses. The features which increased the surface roughness on the air-cured lens do not appear typical of a polymeric surface and are more typical of surface contamination (Baguet *et al.*, 1992). Given that these air-cured lenses underwent the same sample preparation as the nitrogen-cured contact lenses, it suggests that the air-cured lens surface attracted greater levels of environmental contamination. This greater contamination appears to be the result of the air-cured lens having a 'tacky' surface. During manufacture the lenses are cured in polypropylene moulds in either an air-filled or nitrogen-filled oven. Although polypropylene has a relative low oxygen permeability, oxygen is still able to be transported through the mould during curing, especially at the elevated temperature the mould experiences in the ovens (Maier & Calafut, 1998). The presence of oxygen during polymerisation has been shown to strongly inhibit radical-induced polymerisation because of its high reactivity toward radical species (Decker & Jenkins, 1985). The oxygen molecules scavenge the the initiator radicals reducing polymerisation rates, increasing induction periods, decreasing conversion, decreasing polymer kinetic chain length and creating 'tacky' surface properties (Biswal & Hilt, 2009). Initially when the monomer mix is injected into the female polypropylene moulds there is a rapid uptake of oxygen by the highly oxygen permeable siloxane-containing material. As the male and female moulds are sealed together the oxygen within the monomer mix is likely to be evenly distributed throughout the material. As polymerisation is initiated by the

heat of the ovens, the oxygen will be rapidly depleted by the free radical initiators. At this point the only source of oxygen is from diffusion through the polypropylene mould material (Müller *et al.*, 2003). The oxygen diffusion through the lens mould reacts immediately with the free radical initiators and therefore this inhibition process is primarily associated with the lens surface (Biswal & Hilt, 2009). Kim *et al.* (2003) have shown that oxygen inhibition of the surface is typically greater with siloxane-containing polymers as oxygen is freely soluble in the material and exhibits a high diffusion coefficient, resulting in a lower degree of cross-linking of the material at the polymer surface. Others in the literature have described surface oxygen inhibition during contact lens polymerisation, suggesting this can result in a more slippery surface (Hagmann *et al.*, 2003) and increased deposition (Maldonado-Codina & Efron, 2005), primarily associated with an inhibition of cross-linking during polymerisation. Lens manufacturers have investigated several techniques to avoid problems related to oxygen inhibition, such as using mold materials with oxygen scavenging components (Lawton *et al.*, 2009), using alternative mould materials (Liu *et al.*, 2009; Martin *et al.*, 1998), varying the amount of initiator (Biswal & Hilt, 2009), varying the curing temperature (Gauthier *et al.*, 2005) or most commonly polymerising the contact lens in an inert environment, such as nitrogen (Atkinson *et al.*, 2008; Martin *et al.*, 1998) or carbon dioxide (Studer *et al.*, 2003a,b). A contact lens cured in a nitrogen-purged environment is therefore likely to possess a more heavily cross-linked polymer surface, than that of an air-cured lens. Maldonado-Codina & Efron (2005) investigated the surface chemistry of conventional soft contact lenses produced using different manufacturing techniques. They found that HEMA/GMA lenses polymerised in aerobic conditions within polypropylene moulds, showed unsaturated and/or aromatic hydrocarbon species present on the lens surface, indicative of surface degradation. These lenses were shown to have sticky surfaces, resulting in poor handling, marked contamination during SEM imaging and rapid *in vivo* tear film deposition. These findings are remarkably similar to the observations of this PhD study, suggesting that in both cases the presence of oxygen during polymerisation is likely to have promoted short non-crosslinked chains at the polymer surface. Such non-crosslinked polymer chains have been shown to protrude out from the lens surface when in a hydrated state (Kim *et al.*, 2002) and may interact to a greater extent with the surrounding environment, resulting in 'tackier' surfaces and a greater degree of surface contamination, associated with entrapment of particles.

Hydrated AFM imaging of the study contact lenses showed the nitrogen-cured lens was less prone to contamination than the the air-cured lens surface (Section 5.3). Comparison of the two regions on the air-cured study lens showed that the non-wetting regions were more heavily contaminated than the wetting regions. These findings are in agreement with the greater surface contamination observed during contact angle analysis and the greater tear film deposition observed during the clinical study. This suggests that the non-wetting regions are more significantly influenced by the oxygen inhibition during polymerisation and thus less heavily crosslinked at the surface, resulting in greater contamination. The lack of any obvious pattern for the non-wetting regions on the air-cured lens surface, suggest that the oxygen inhibition is not consistently influenced by factors such as mould parameters, but appears a more random process. Given that the oxygen is dissolved primarily in the siloxane-containing material, it may be that any slight differences in the distribution of the siloxane phase may also influence oxygen distribution and subsequent inhibition.

Cryogenic ESEM imaging for the nitrogen-cured lens surface showed a uniform surface with a typical hydrogel appearance similar to that observed for the hydrated AFM imaging. The non-wetting region of the air-cured sample showed a similar uniform hydrogel surface with occasional small surface features. These features may be related to surface contamination during sample preparation or related to mild surface damage during freezing. The lack of significant damage to the lens surface on cryogenic freezing, observed by other cryogenic lens imaging studies (González-Méijome *et al.*, 2006b), suggested that the cryogenic handling technique was well optimised to minimise damage and allowed confidence in the findings of the cryogenic surface chemistry studies. Dehydrated AFM and ESEM imaging of the wetting regions of the air-cured lens and the nitrogen-cured lens in their dehydrated state showed a similar hydrogel appearance to that observed in their hydrated state, with a uniform hydrogel meshwork with occasional pores. In contrast, the ESEM images of the non-wetting region of the air-cured lens in a dehydrated state showed a markedly different appearance, with large areas on these samples composed of small apparent islands surrounded by 'sponge-like' domains. One possible reason for this dramatic change in surface appearance is a type of polymer phase separation known viscoelastic phase separation. Viscoelastic phase separation describes the behaviour of a dynamically asymmetric mixture, which is composed of fast and slow components (Tanaka, 2000). In a polymer system this asymmetry can be induced by a difference in glass transition tem-

perature between the components of a mixture. Given the marked differences between the glass transition temperature of the component polymers this might have resulted in these phase separated regions on drying. Another possible reasons for the markedly different surface appearance on dehydration is the formation of polyethylene oxide (PEO) crystallites following sample dehydration, which melt and become clear on rehydration (Sung *et al.*, 1990). Perhaps a simpler possible explanation is that the lens surface became distorted due to differential shrinking on the polymer components upon dehydration. Independent of the exact cause, there is clearly a consistent difference between the material in the non-wetting region of the air-cured lens and the other two study lens regions. This difference suggests a degree of phase separation at the surface of the polymeric material, in addition to the observed surface reorganisation shown by cryo-XPS.

In the dehydrated state, AFM imaging on the non-wetting region of the air-cured lens showed non-uniform surface topography, in agreement with that observed with ESEM imaging. Imaging of the non-wetting region proved difficult due to interaction of the AFM tip with the lens surface, which was not observed on the nitrogen-cured lens surface. Initially it was assumed this was related to a thin water layer on the lens surface, but this interaction was present even under a flow of nitrogen gas or following alcohol washing. Problems associated with AFM tip interaction are commonly observed on tacky polymeric materials (Revenko *et al.*, 2001), especially in the dehydrated state where the interaction forces are greater than in the hydrated state. This occurs as AFM imaging in a liquid media reduces the capillary forces between tip and sample (Wadu-Mesthrige *et al.*, 2001). The probable cause for this 'tacky' surface, given the findings of the other studies, is that oxygen inhibition during curing results in the surface of the air-cured lens not having undergone complete polymerisation. This led to greater tip interaction, due to adhesion of the tip by the surface, resulting in poor surface topography data. The optical microscope used for tip alignment on the AFM instrument showed an appearance similar to that observed with dehydrated ESEM imaging, with an interlinking 'sponge-like' material surrounding relative smooth surface regions. Imaging on the 'sponge-like' regions was possible with AFM, but imaging the smooth regions proved very difficult with excessive tip interaction making imaging near impossible. In comparison with the ESEM images, the AFM images are at a much higher magnification and appear to give details primarily related to the 'sponge-like' regions identified in the ESEM images (Figure 6.1), although

this is difficult to confirm. The phase imaging showed marked differences between the smooth and textured regions on the air-cured lens surface, suggesting different polymeric materials or differences in the degree of polymerisation are present in these regions. The difference between the hydrated and dehydrated surface topography is thought to relate to a reorganisation of the surface moieties and polymer chains at the surface. If this is indeed the case then it would be expected that the non-wetting air-cured regions would alter more significantly due to the reduced polymer cross-linking in these region, associated with surface oxygen inhibition. Holly & Refojo (1975) described the reorganisation that occurs at an air exposed hydrogel surface due to the asymmetrical molecular force field at the gel-air interface, where the molecular force field of the water molecules in the gaseous phase is much weaker than in the liquid phase. It is therefore more energetically favourable for the polymer chain segments to orient in such a way as to expose the hydrophobic (non-polar) groups towards the gaseous phase and to bury the hydrophilic (polar) groups within the gel. When the hydrogel is then immersed in water, its structure becomes unfavourable due to the high interfacial tension against the water. The polymer segments therefore reorient, with hydrophobic groups buried into the bulk and hydrophilic groups exposed at the surface, in order to achieve minimal interfacial tension. This process is typically more marked with siloxane-containing materials, as the polymer backbone is highly mobile, allowing extensive reorganisation of the polymer structure when thermodynamically favourable. This hydrogel surface reorganisation was originally suggested to explain contact angle hysteresis (Holly & Refojo, 1975), with these findings corroborated by SFG studies (Chen *et al.*, 1999). For the non-wetting region of the air-cured surface, the polymer chains near the surface appear less heavily cross-linked, due to oxygen inhibition. The resulting reorganisation of the surface is therefore likely to be more extensive, due to the higher concentration of siloxane in these regions (shown by XPS analysis) and lower cross linking density (suggested by the hydrated AFM study). The ESEM images of the non-wetting regions on the air-cured lens may therefore relate to this more substantial reorganisation, potentially exposing sub-surface features or resulting in phase separation following dehydration, as observed in other polymer materials (Huraux *et al.*, 2007; Saraf *et al.*, 1998). Further investigation of these surface changes during the drying process, with techniques such as SFG and imaging cryo-XPS and ToF-SIMS, is required to better understand the dehydrated ESEM images, as such topography does appear to be a marker for poor clinical lens wetting.

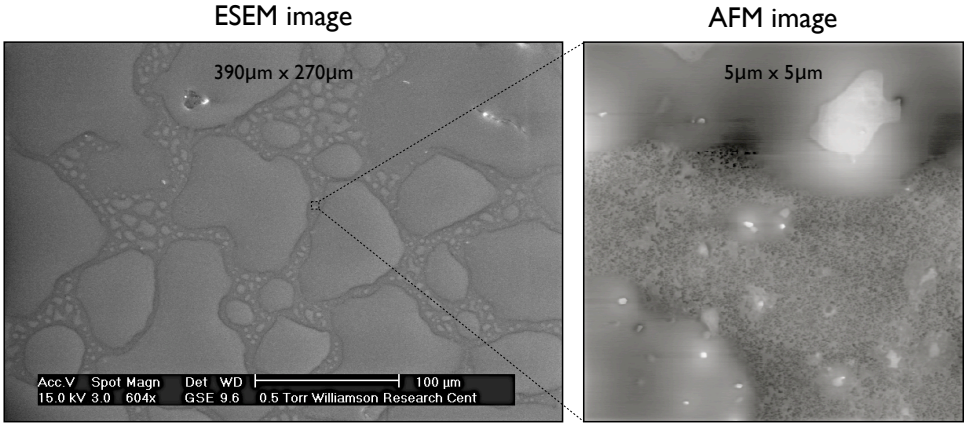

Figure 6.1: Comparison of the ESEM and AFM images of the dehydrated non-wetting region of the air-cured contact lens.

6.4.1 Future work: study lens surface topography

- AFM has the ability to assess the frictional forces present as the tip moves across the lens surface. Future studies could investigate the frictional characteristics of contact lens materials when analysed with a range of AFM tip types. This frictional data could then be compared with clinical data in an attempt to better understand if these surface features influence *in vivo* lens performance.

- Oxygen inhibition of polymerisation at the lens surface is likely to influence its mechanical properties. Future studies could therefore investigate the modulus/mechanical properties of the three study lens regions, using a technique such as nanoindentation.

- AFM tips can be functionalised to allow the investigation of chemistry across a polymer surface by monitoring interaction forces (Anantawaraskul, 2005). Future studies could apply this technique to the three study lens regions in order to compare their surface chemistry.

- AFM imaging of worn contact lens allows the monitoring of tear film deposition on the lens surface. Given the marked differences in tear film deposition between the study lens regions, AFM could image these surfaces in an attempt to better understanding this surface bioconversion process.

- SEM images obtained in this study were either from a lens sample in a fully hydrated (frozen) state or in a dehydrated state. Given the difference between hydrated and

dehydrated images, a future ESEM study could begin with a frozen sample, which would then be slowly warmed while images were captured to observe any changes to the surface structure with dehydration.

- In addition to imaging the lens surface, many SEM instruments are equipped with energy-dispersive X-ray spectroscopy (EDS), which allows chemical characterisation of regions of the SEM image. Use of this technique on the study lenses would allow chemical characterisation of the lens regions identified using ESEM and perhaps focusing on the different structures evident on the non-wetting region of the air-cured lens.

- During wear the lens surface is likely exposed to both a predominately aqueous tear film and on occasions an air environement. This environment is likely different to both the fully hydrated conditions in a wet cell or the dehydrated analysis, and therefore likely to result in different surface features. Kim *et al.* (2002) developed a technique using a humidity chamber during AFM analysis which showed changes in polymer structure with different environmental conditions. Analysis of silicone hydrogel materials and in particular the study lens regions in a similar manner would allow a better understanding of their surface and how they are influenced by these changing environmental conditions.

It is clear that many of the key hurdles that still need to be addressed in the development of the ideal contact lens material are associated with the lens surface. Many contact lens users cease wear primarily due to discomfort (Fonn, 2007), therefore contact lens development should focus on surface features such as wettability, dehydration and friction, in addition to other factors such as lens design. As contact lens wear still significantly increases the risk of corneal infection (Stapleton *et al.*, 1995), development should also focus on minimising the adhesion and activity of bacteria on the lens surface, in addition to optimisation of lens care solutions. This PhD work set out to improve understanding of lens surface characteristics and their impact on the clinical performance of silicone hydrogel materials, using both commercial and experimental contact lenses. In part, it looked to investigate the cause of a specific manufacturing problem, but also used the unusual properties of these lenses to better understand the importance of surface characteristics with regard to the clinical performance of contact lenses. The work has therefore looked to improve methodology where necessary to better characterise these silicone hydrogel materials in

order to better understand the influence of these surface characteristics on the contact lenses clinical performance.

6.5 Conclusion

The clinical study has shown marked differences between the study lenses, particularly with respect to surface wetting, tear film deposition and subjective comfort. The air-cured lens showed regions of wetting and non-wetting on the lens surface, whereas the nitrogen-cured lens showed generally acceptable clinical performance. The regions of non-wetting on the air-cured lens were shown to have a higher concentration of silicone-containing material and an apparently 'tackier' surface, due to oxygen inhibition of the polymerisation process during manufacture. These hydrophobic non-wetting regions appeared to induce discomfort by mechanical interaction with the lid wiper region, due to insufficient lubrication by the tear film, although further work is need to confirm this. The increased deposition observed on the air-cured surface is likely a combination of the hydrophobic silicone-rich surface composition and the 'tacky' nature of the surface which causes attraction and entrapment of tear film components. In addition, surface imaging has suggested a degree of surface phase separation of the polymer material on the non-wetting regions of the air-cured lens, which is likely to adversely influence the materials clinical characteristics.

Given the wide range of surface analysis techniques undertaken in this PhD investigation, it is clear that some methods were more suited to the investigation of contact lens surfaces than others. Perhaps the instrument which provided the least useful data in this thesis was that of the ToF-SIMS instrument. This is likely due to the high sensitivity of the technique which made its findings highly susceptible to surface segregation and contamination. For future studies to gain meaningful results from this technique, further improvements are required in the cryogenic sample handling methodology. AFM and ESEM imaging of contact lens surfaces are well established techniques and their ability to image contact lens surface in a hydrated state gives them a great advantage as tools for probing the lens surface. Sessile drop contact angle measurements were shown able to characterise the wetting characteristics of contact lenses, but these values appeared unrelated to the contact lenses known clinical performance. The receding contact angle measured using the dynamic captive bubble techniques appeared to discriminate between

the regions of the study lens, although for commercial lenses these values appeared very similar. Contact angle measurements therefore seem relatively poor predictors of clinical performance for commercial contact lens, likely due to tear film deposition which rapidly alters the wetting characteristics of the contact lens with wear. Future contact angle studies analysing worn contact lenses, may provide insight into the changes in surface wetting characteristics with wear and allow a better understanding of the relationship between *in vitro* contact angle measurements and *in vivo* clinical observations. XPS analysis provide the most convincing data regarding the chemical reorganisation of the contact lens surface following dehydration. These findings suggest that the cryogenic handling technique has a potential application in aiding the development of future contact lens materials and in better understand the clinical behaviour of contact lenses.

Many of the surface analysis techniques used in this PhD were unable to detect differences between the materials in a dehydrated state and therefore much of the work in this PhD has involved the development of methodologies to allow hydrate analysis of these materials. Hydrated analysis appears especially important for silicone hydrogel materials due to the high flexible nature of the silicon-oxygen polymer backbone which allows rapid surface segregation when exposed to an air/vacuum environment. Future studies investigating soft contact lens surface characteristics should therefore maintain sample hydration where possible, to preserve the true surface characteristics of the lens surface.

Appendix A

Paperwork associated with Chapter 2

Clinical Study Grading & Measurement Scales

Wettability Grading Scale

White light, diffuse and/or broad beam, low-medium magnification. Grade degree of wettability in 0.25 steps.

0	**VERY POOR**	Immediately displaying non-wetting areas on the lens surface, immediate drying time.
1	**POOR**	Irregular surface appearance, drying time << blink time.
2	**ACCEPTABLE**	Smooth surface appearance immediately after blink becoming irregular after awhile, drying time < blink time.
3	**GOOD**	Typical soft lens appearance with long drying time.
4	**EXCELLENT**	Appearance of a healthy cornea with very long drying time.

Appearance of Lens Surface

White light, diffuse and/or broad beam, low-medium magnification.
Description of lens surface, such as: **Smooth / Grainy / Non-Wetting.**

Front Surface Deposition

White light, diffuse and/or broad beam, low-medium magnification. Grade degree of deposits in 0.25 steps.

0	Clean, no deposits.
1	5 or less small deposits (<0.1mm).
2	>5 deposits of <0.1mm size or film covering 25-50% of surface.
3	Deposits of between 0.1 and 0.5mm or film covering 50-75% of surface.
4	Deposits of 0.5mm or larger or film covering more than 75% of surface.

Deposit Type

White light, diffuse and/or broad beam, low-medium magnification. Grade type of deposits.

Lipid
Mucous
Protein
Other (describe)

Investigator Surface Preference

White light, diffuse and/or broad beam, low-medium magnification. Investigator is asked which lens surface they prefer, if any and whether the preference is slight ot strong.

Strongly prefer right lens
Slightly prefer right lens
No preference
Slightly prefer left lens
Strongly prefer left lens

Figure A.1: Clinical Study Grading Scales - Page 1

Lens Centration
Assessed in primary gaze, white light, diffuse, low-medium magnification. Grade degree of centration and indicate direction if decentred.

Optimal	A lens symetrical about the centre of the cornea.
Slight Decentration	A lens which is slighly decentred, but the limbus is not exposed.
Extreme Decentration	A lens which is extremely decentred leaving the limbus exposed

Post Blink Movement
Assessed in primary gaze. If necessary, lower lid depressed for better observation. Amount of movement (to the nearest 0.1mm) immediately after the blink.

Primary Gaze Lag
Assessed observing lens movement.
The amount of lens drop in mm that occurs in primary gaze when the lower lid is pulled down.

Up Gaze Lag
Assessed observing lens movement.
The amount of lens drop in mm that occurs when the eye moves from primary gaze to upgaze.

Push-Up Test
Assessed by digital push-up test using 0%-100% continuous scale in 5% steps.

0%	Falls from cornea without lid support
50%	Optimum
100%	No movement

Subject Comfort Preference
The subject was asked “In terms of lens comfort, do you prefer the lens in your right eye or left eye? Is this preference strong or slight?”

1 Strongly prefer right lens
2 Slightly prefer right lens
3 No preference
4 Slightly prefer left lens
5 Strongly prefer left lens

Figure A.2: Clinical Study Grading Scales - Page 2

Objective Clinical Grading

Objective clinical grading of the ocular surface was recorded using an Efron Grading Scale (see Appendix A) in 0.1 steps.

0-100 Subjective Grading Scales

Subjective grading scales were used to assess (i) **Comfort**, (ii) **Dryness and Burning**, (iii) **Lens Dehydration** (see Appendix A).

Figure A.3: Clinical Study Grading Scales - Page 3

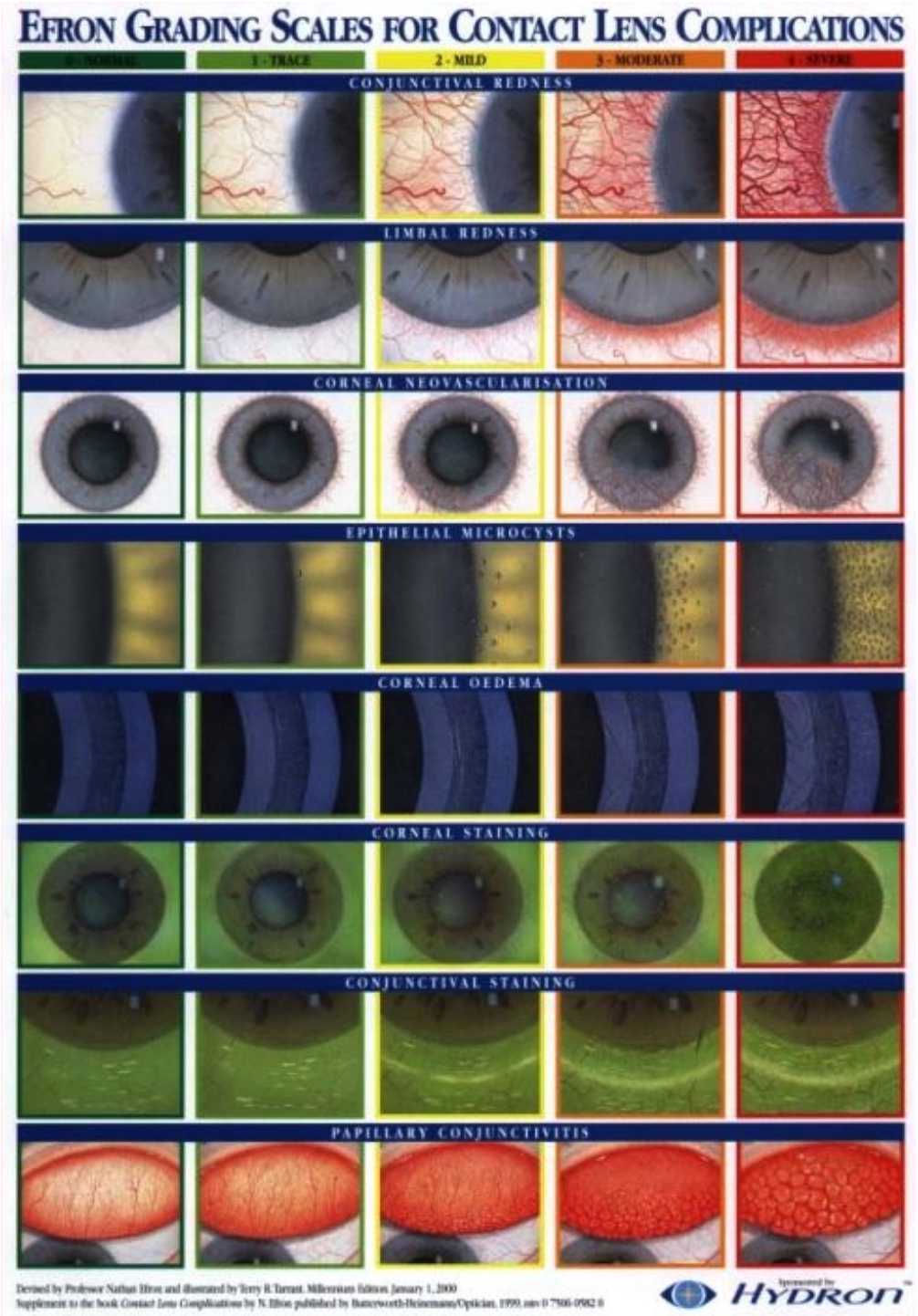

Figure A.4: Efron Grading Scale - Part 1

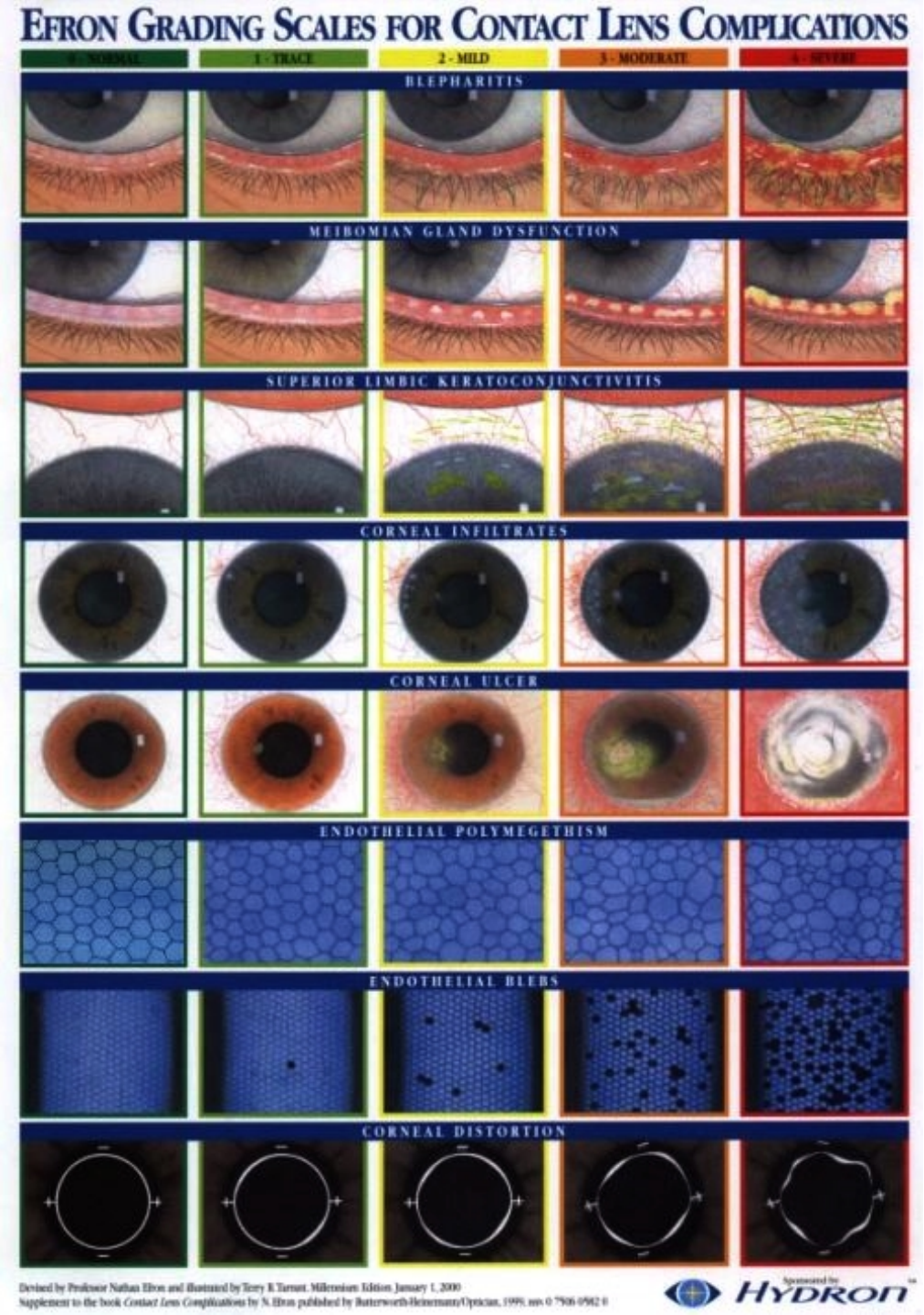

Figure A.5: Efron Grading Scale - Part 2

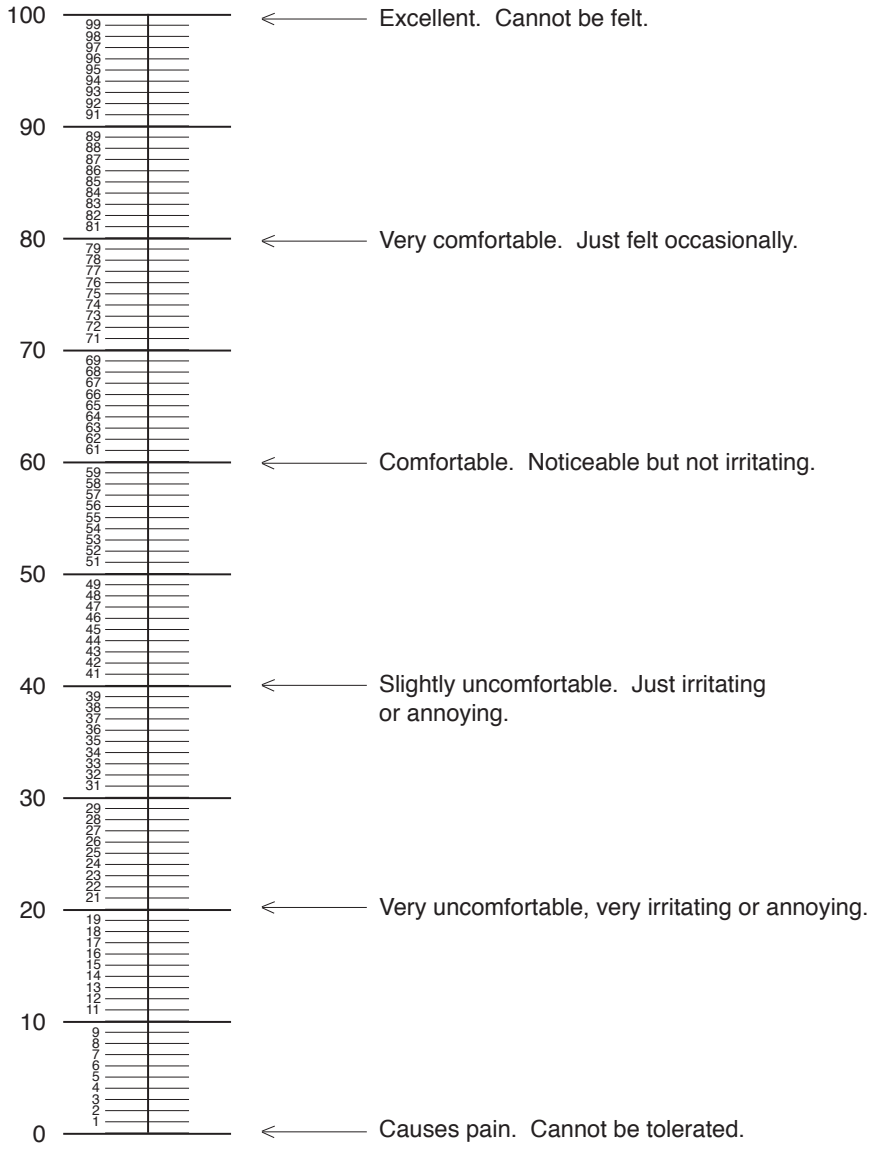

Figure A.6: 0-100 Visual Analogue Scales - Comfort

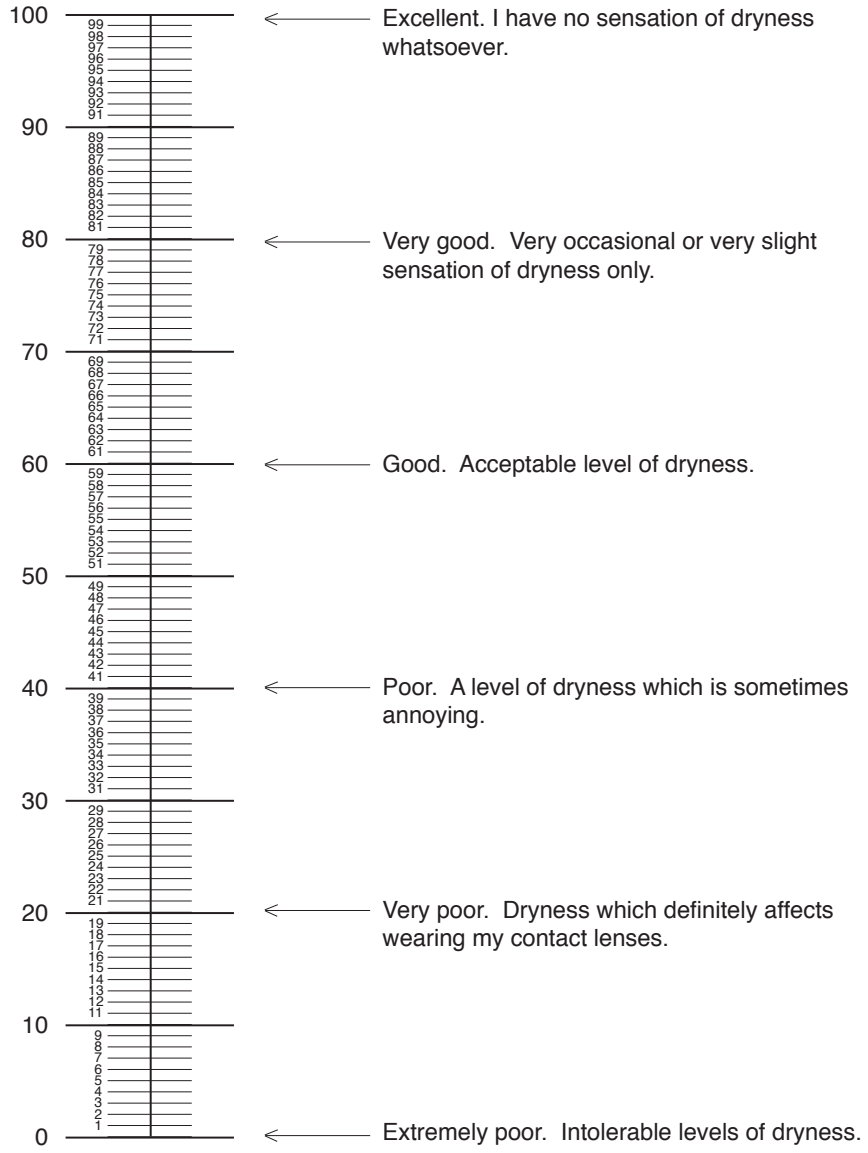

Figure A.7: 0-100 Visual Analogue Scales - Sensation of dryness

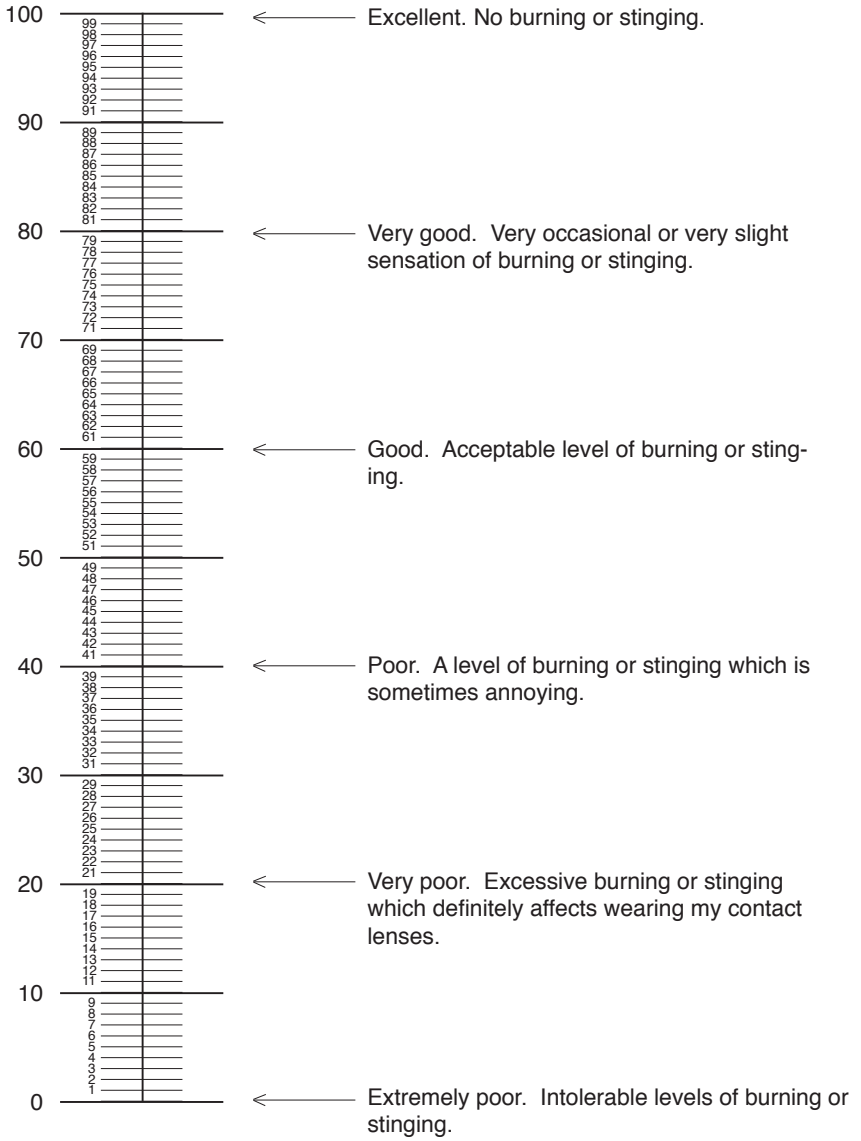

Figure A.8: 0-100 Visual Analogue Scales - Burning and stinging

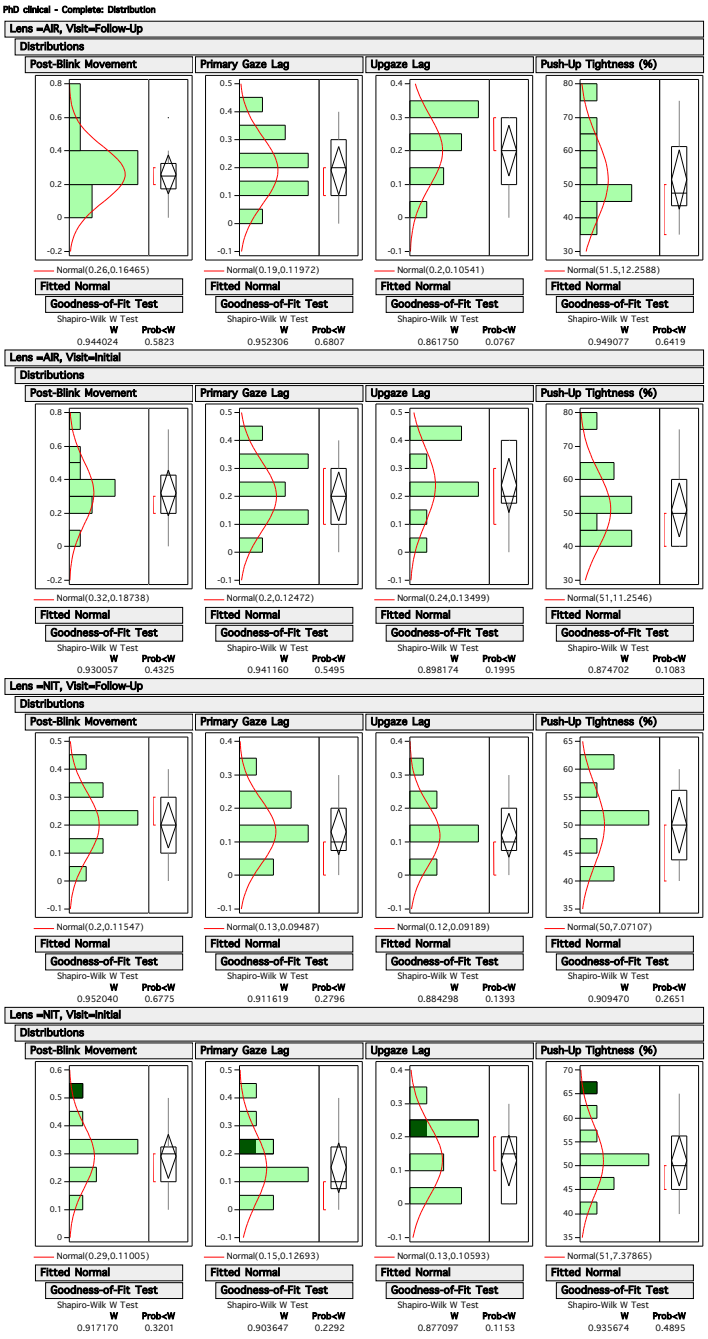

Figure A.9: Test for normality of the lens fitting characteristics data with a Shapiro Wilks test

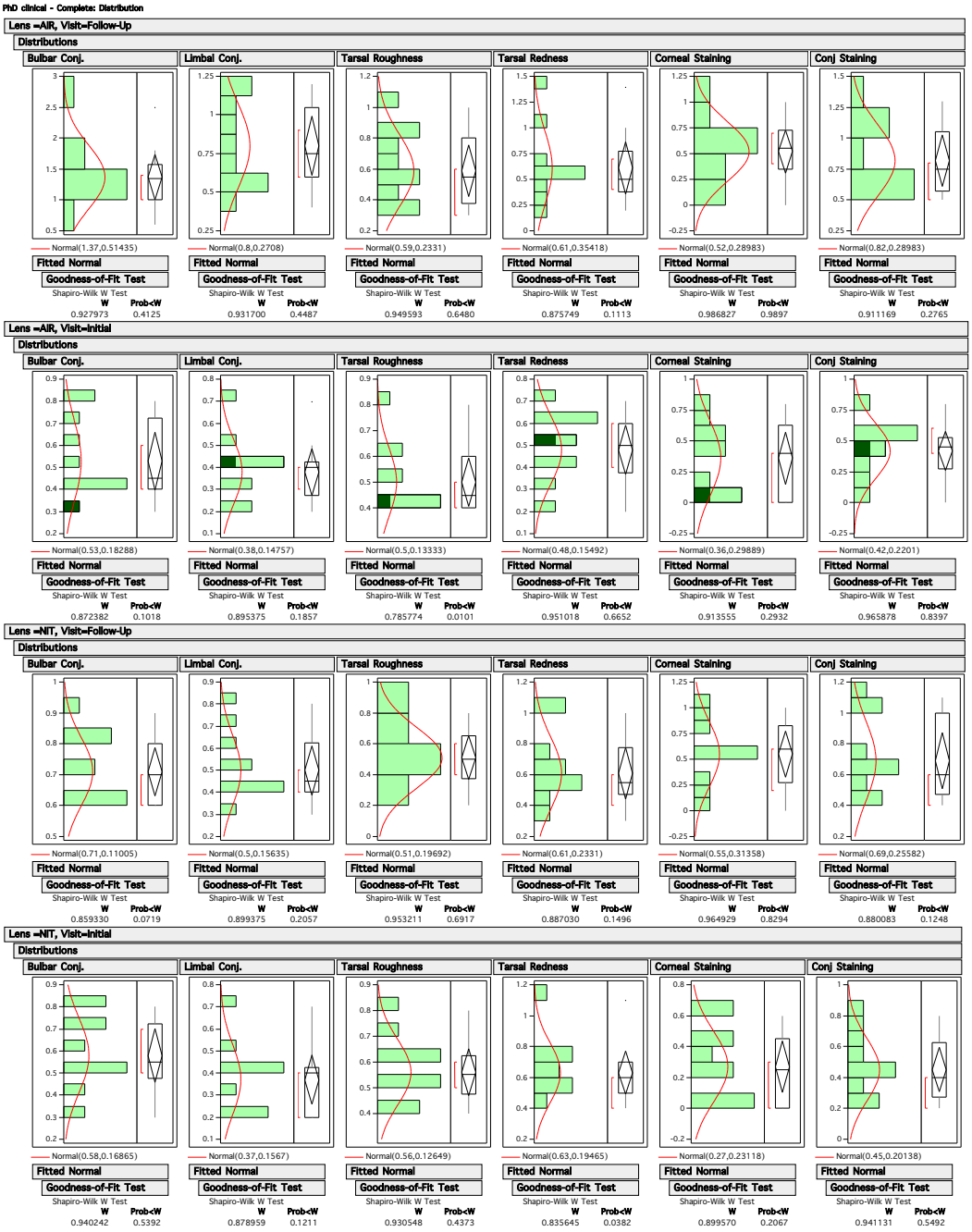

Figure A.10: Test for normality of the biomicroscopy data with a Shapiro Wilks test

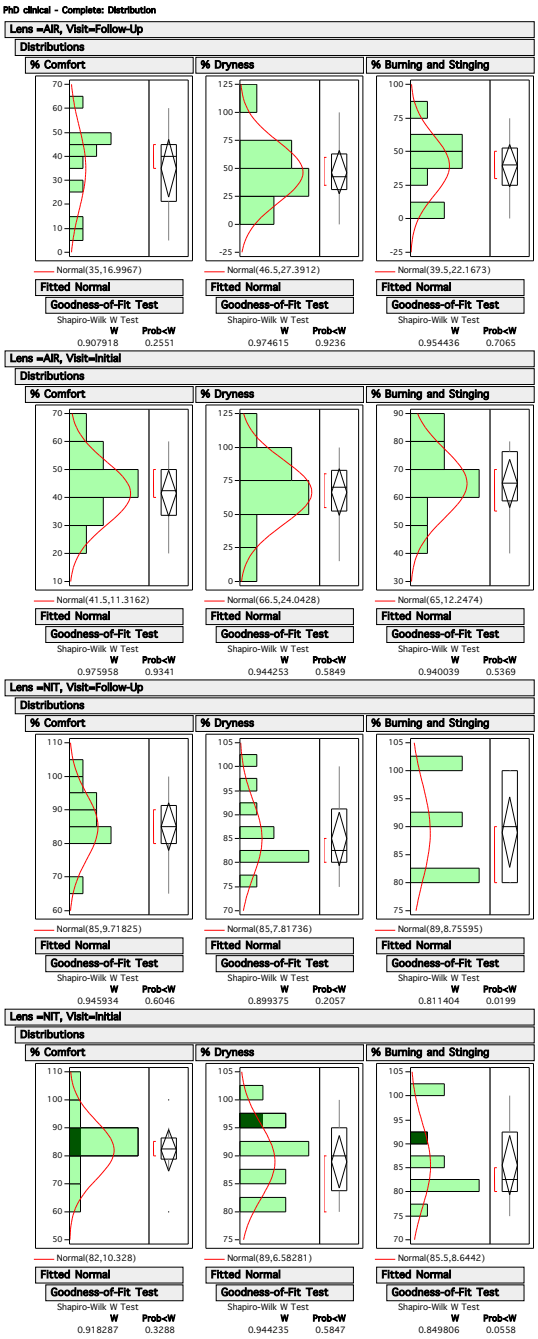

Figure A.11: Test for normality of the subjective data with a Shapiro Wilks test

Appendix B

Investigating stability of the non-wetting regions on the air-cured lens

B.1 Aim

To investigate whether the non-wetting regions identified by the thin film wettability analyser were stable or mobile on the lens surface.

B.2 Method

Three air-cured and three nitrogen-cured study contact lenses were removed from their blister packaging and soaked for 24 hours. The laboratory surface wetting properties were then investigated using the thin film wettability analyser as described in Section 2.2.2.1. Following three analysis cycles for each lens, the lenses were place in 0.9% PBS for 24 hours. The lenses were then removed from saline and again analysed by the thin film analyser. The lenses were then soaked in 0.9% PBS for 1 week and reanalysed with the thin film wettability analyser.

B.3 Results

No non-wetting regions were identified on the nitrogen-cured lenses. In contrast, the air-cured lenses always presented non-wetting regions when analysed. These non-wetting

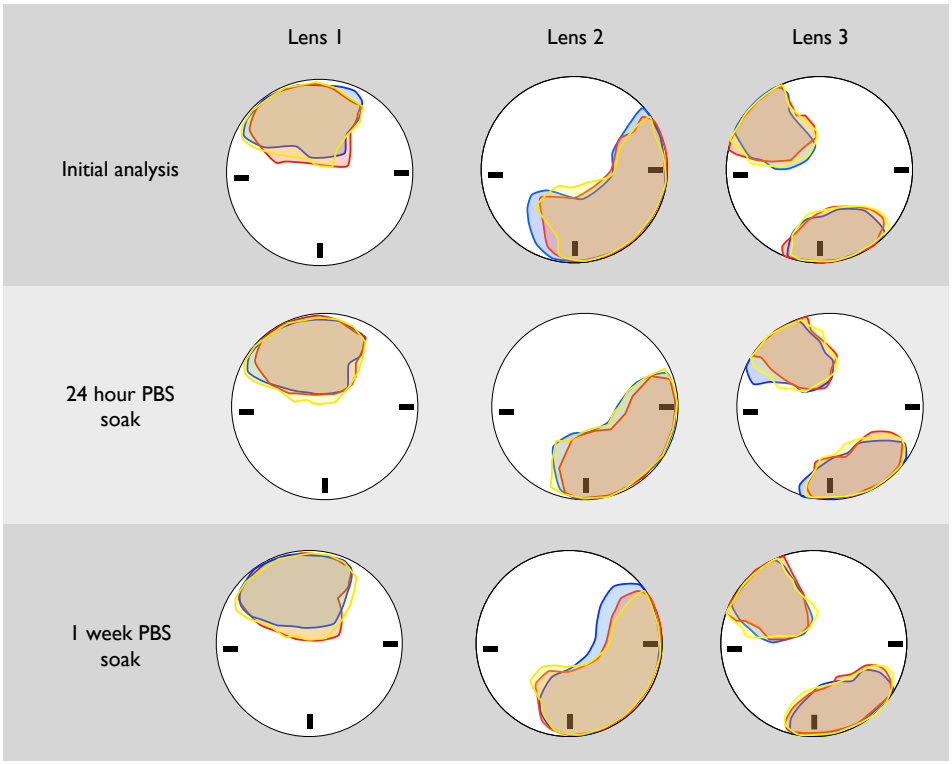

Figure B.1: Non-wetting regions identified by the thin film wettability analyser for three air-cured study contact lens.

regions for the three air-cured lenses at the three visits are shown in Figure B.1. Comparison of the non-wetting regions for each lens at each time point suggests that the non-wetting region does not change significantly in shape, size or location.

B.4 Conclusion

The non-wetting regions on the air-cured lens surface appear stable in shape, size and location over the eight day soaking period suggesting that whatever is causing these non-wetting regions is either substantially adhered to the lens surface or bound within the material. This is in agreement with the findings of the clinical study comparison and when clinical non-wetting regions were compared with the thin film wettability analyser where the location of non-wetting appeared stable over time.

Appendix C

XPS data

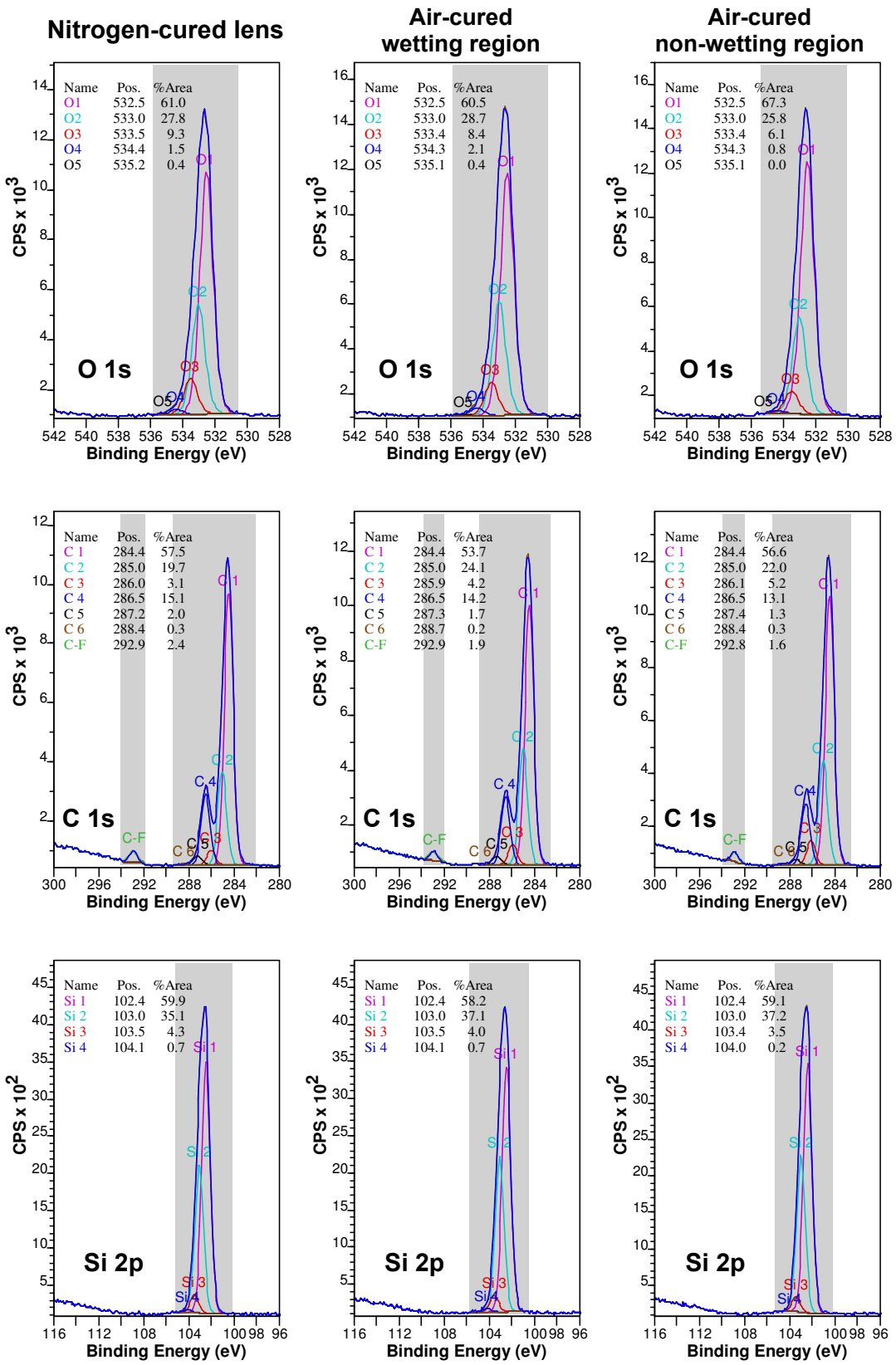

Figure C.1: High resolution XPS sepctra for carbon, oxygen and silicon on the dehydrated study lens regions.

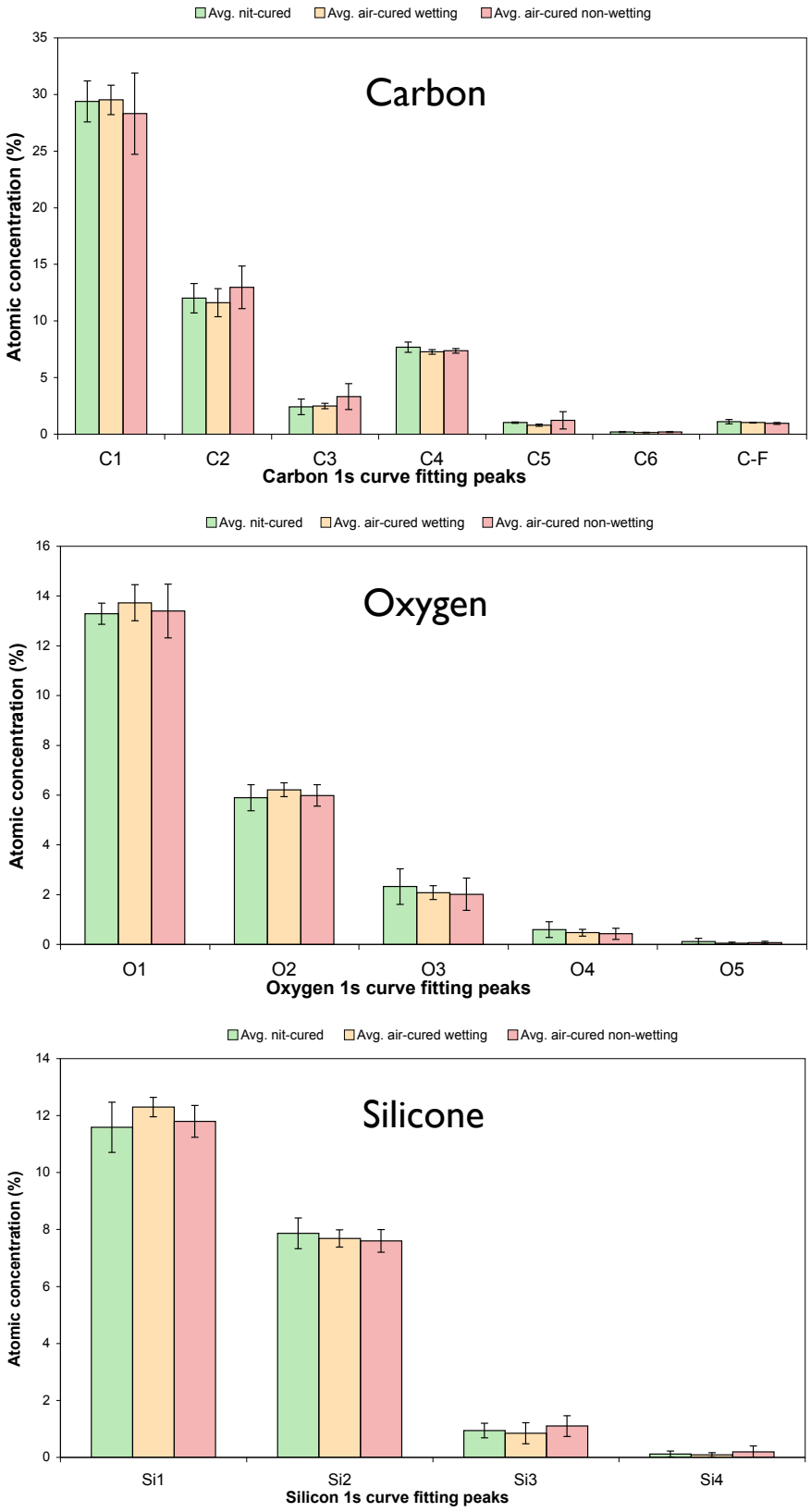

Figure C.2: High resolution XPS fitting data for carbon, oxygen and silicon on the dehydrated study lens regions.

Appendix D

Published paper - Measurement Errors Related to Contact Angle Analysis of Hydrogel and Silicone Hydrogel Contact Lenses

Measurement Errors Related to Contact Angle Analysis of Hydrogel and Silicone Hydrogel Contact Lenses

Michael L. Read, Philip B. Morgan, Carole Maldonado-Codina

Eurolens Research, Faculty of Life Sciences, The University of Manchester, Manchester, United Kingdom

Received 20 January 2009; revised 22 April 2009; accepted 27 April 2009
Published online 6 July 2009 in Wiley InterScience (www.interscience.wiley.com). DOI: 10.1002/jbm.b.31442

Abstract: This work sought to undertake a comprehensive investigation of the measurement errors associated with contact angle assessment of curved hydrogel contact lens surfaces. The contact angle coefficient of repeatability (COR) associated with three measurement conditions (image analysis COR, intralens COR, and interlens COR) was determined by measuring the contact angles (using both sessile drop and captive bubble methods) for three silicone hydrogel lenses (senofilcon A, balafilcon A, lotrafilcon A) and one conventional hydrogel lens (etafilcon A). Image analysis COR values were about 2°, whereas intralens COR values (95% confidence intervals) ranged from 4.0° (3.3°, 4.7°) (lotrafilcon A, captive bubble) to 10.2° (8.4°, 12.1°) (senofilcon A, sessile drop). Interlens COR values ranged from 4.5° (3.7°, 5.2°) (lotrafilcon A, captive bubble) to 16.5° (13.6°, 19.4°) (senofilcon A, sessile drop). Measurement error associated with image analysis was shown to be small as an absolute measure, although proportionally more significant for lenses with low contact angle. Sessile drop contact angles were typically less repeatable than captive bubble contact angles. For sessile drop measures, repeatability was poorer with the silicone hydrogel lenses when compared with the conventional hydrogel lens; this phenomenon was not observed for the captive bubble method, suggesting that methodological factors related to the sessile drop technique (such as surface dehydration and blotting) may play a role in the increased variability of contact angle measurements observed with silicone hydrogel contact lenses. © 2009 Wiley Periodicals, Inc. J Biomed Mater Res Part B: Appl Biomater 91B: 662–668, 2009

Keywords: contact angle; contact lens; hydrogel; silicone hydrogel; measurement error; coefficient of repeatability

INTRODUCTION

The term "wettability" is traditionally used to describe the tendency for a liquid to spread over a solid surface.[1] This process is influenced by both the cohesion between liquid molecules and the adhesion between liquid and solid molecules.[2] Despite the widespread use of the term wettability, no physical measurement exists that can completely quantify it. Despite this limitation, contact angle analysis has become a widely accepted method to investigate the wetting properties of a solid surface.[3,4] These measurements represent the angle formed by a liquid at a three-phase boundary where a liquid, gas, and solid intersect. Contact angle measurement techniques include "sessile drop" (where a liquid drop is placed onto a solid surface), "captive bubble" (where a gas bubble is placed in contact with a solid which is immersed in a liquid), and "Wilhelmy plate" (where a solid sample is immersed and withdrawn from a liquid).

Wettability is particularly relevant to contact lenses because the lens surface needs to support a stable ocular tear film layer, and failure to achieve this is likely to adversely affect the visual performance, increase lens surface deposition,[5] and reduce comfort.[6] This consideration applies to all forms of contact lenses, but in particular to siloxane-containing soft contact lens materials, termed "silicone hydrogels." In recent years, these lenses have seen a significant increase in the worldwide market share[7] because of their enhanced ability to deliver oxygen to the ocular surface, which in turn has resolved a number of clinical complications seen with non-siloxane-containing hydrogels.[5,8,9] A potential negative consequence of the inclusion of silicon into contact lenses is the inherent hydrophobicity it imparts to the material[10] resulting in poor *in vivo* wettability.[5,11] In an attempt to alleviate clinical problems related to this hydrophobicity, contact lens manufacturers have utilized a range of fabrication techniques, including plasma surface treatments and the

Correspondence to: C. Maldonado-Codina (e-mail: c.m-codina@manchester.ac.uk)
Contract grant sponsors: CooperVision Inc. and the Medical Research Council at The University of Manchester

TABLE I. Study of Contact Lenses

Brand Name	Acuvue Oasys	PureVision	Air Optix Night and Day	1 Day Acuvue
Manufacturer	Johnson & Johnson Vision Care	Bausch & Lomb	CIBA Vision	Johnson & Johnson Vision Care
USAN[a]	Senofilcon A	Balafilcon A	Lotrafilcon A	Etafilcon A
Water content (%)[b]	38	36	24	58
Oxygen permeability (Barrers)[b]	103	99	140	21
Modulus (MPa)[b]	0.72	1.1	1.52	0.28
Surface treatment	None (internal wetting agent, PVP)	Plasma oxidation	Plasma coating	None
Principal monomers[c]	MPDMS, DMA, HEMA, siloxane macromer, TEGDMA, PVP	NVP, TPVC, NVA, PBVC	DMA, TRIS, siloxane monomer	HEMA, MAA

PVP, polyvinyl pyrrolidone; MPDMS, monofunctional polydimethylsiloxane; DMA, N,M-dimethylacrylamide; HEMA, hydroxyethyl methacrylate; MAA, methacrylic acid; EGDMA, ethyleneglycol dimethacrylate; TEGDMA, tetraethyleneglycol dimethacrylate; TRIS, trimethyl siloxysilyl; NVP, *N*-vinyl pyrrolidone; TPVC, tris-(trimethyl siloxysilyl) propylvinyl carbamate; NVA, *N*-vinyl amino acid; PBVC, poly(dimethysiloxy)-di(silylbutanol)-bis(vinyl carbamate).

[a] United States adopted name.

[b] Manufacturer-reported values.

[c] From Jones and Dumbleton[21] and Teichroeb et al.[22]

inclusion of hydrophilic monomers to the bulk material which serve to mask surface hydrophobicity and improve ocular biocompatibility.[10,12–14]

In common with all scientific evaluations, repeated measures of contact angles will necessarily vary due to factors such as instrument fluctuation or nonuniformity within or between samples.[15] Such variation can be termed "measurement error." Measurement error can be reported by giving (i) the average standard deviation of multiple sets of repeated measurements, (ii) the coefficient of repeatability (COR), which is defined as the maximum difference likely to occur between two successive measurements ($2\sqrt{2}s$) (where s is the standard deviation of measurements), or (iii) the coefficient of variation (COV) ($\frac{s}{\bar{x}}$), which contextualizes the magnitude of the error by comparison of the standard deviation of measurements (s) with the mean ($\bar{x}$).[16]

We sought to undertake a comprehensive investigation of the measurement error associated with contact angle assessment of hydrogel contact lens surfaces. An understanding of these errors is fundamentally important due to the growing interest in the wetting behavior of silicone hydrogel lenses[17–19] and the increasingly widespread use of contact angles by contact lens manufacturers. Additionally, such an analysis will allow identification of which factors contribute toward measurement error in this area and provide an indication of the confidence which can be placed on a single published contact angle measurement.

Specifically, we set out to determine the contact angle COR[20] associated with three measurement conditions using the sessile drop and captive bubble methods:

1. Image analysis COR: an estimate of the variability of the repeated use of semiautomated image analysis software on the same image.
2. Intralens COR: an estimate of the variability when taking repeated measurements on the same lens.
3. Interlens COR: an estimate of the variability when taking repeated measurements on different lenses of the same type.

COR was chosen as our estimate of measurement error as this provides an immediately meaningful index in the relevant units (degrees), against which absolute measures of contact angle can be judged.

MATERIALS AND METHODS

Lenses

Three silicone hydrogel contact lenses and one conventional hydrogel (i.e., a hydrogel not containing siloxane species) control lens were used in this work (Table I). The back vertex power of all lenses was −3.00 DS. All contact lenses were sourced via normal commercial channels and supplied in their standard blister packaging.

Sessile Drop Method

Contact angles were measured at room temperature (25.0°C ± 1.0°C) and humidity (35% ± 5%) with an OCA-20 contact angle analyzer (DataPhysics Instruments, Filderstadt, Germany). This instrument is essentially a conventional goniometer featuring automated drop delivery, digital image capture, and semiautomated image analysis software.

All lenses were analyzed following a 48-h saline soak in 0.9% phosphate-buffered saline solution (PBS) (Sigma-Aldrich, Germany), which was changed every 12 h, to remove any surfactant present in the blisters. The lenses were then blotted to remove excess surface liquid. This was achieved by first removing the lens from the saline solution with silicone tipped tweezers, touching only the edge. The back surface of the lens was then carefully placed onto a

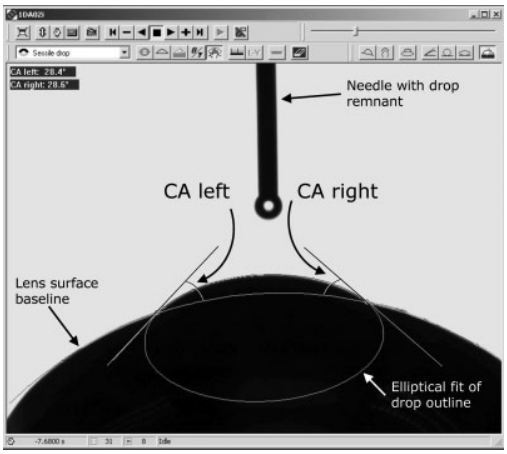

Figure 1. Image analysis of a typical sessile drop frame. From Maldonado-Codina and Morgan.[23]

custom-made poly(methymethacrylate) (PMMA) lens holder (radius of curvature 8.7 mm), and the lens front surface was lowered onto a Supraclean microfibre cloth (Pentax, Slough, UK) suspended over a glass beaker. The lens was briefly held in contact with the cloth (3 s), and then this procedure was repeated until excess surface liquid had been removed (no dark mark left on the cloth). This typically required two to three repetitions. This technique was adopted to achieve even blotting across the lens surface.

The lens and PMMA mount were then immediately placed onto the OCA-20 instrument, under the needle of the microsyringe (Hamilton 500 μL DS 500/GT) using a customized positioning guide which allowed dosing within 5 s of lens blotting. This approach minimized the dehydration of the lens surface during the procedure. A 3 μL drop of deionized water was formed at the tip of the dosing needle at a rate of 2 μL/s and was then lowered until the water and the lens surface made contact. An optical trigger immediately captured a 20-s digital movie clip of the water drop on the lens surface at a rate of 25 frames per second and at a resolution of 768 $\times$ 576 pixels. The lens was then returned to the PBS to soak for at least 10 min before the process was repeated on six further occasions, giving a total of seven measurement runs for each individual lens. This procedure was undertaken for 10 lens samples per lens type, and the order of analysis of these lenses was randomized. This gave a total of 280 movie clips (7 measurement runs $\times$ 10 lens samples $\times$ 4 lens types).

Captive Bubble Method

The OCA-20 instrument was also used to determine the contact angles using the captive bubble method. After a 48-h soaking, as described earlier, the back surface of the lens was carefully placed onto a custom-made PMMA lens holder and lowered into a PBS-filled glass chamber to rest on a submerged stand. A curved needle was positioned directly below the center of the lens from which a 3 μL air bubble was dispensed. The needle was then advanced toward the lens surface, and on contact, the bubble was detached from the needle at the apex of the lens. A movie was captured as detailed earlier after which the bubble was dislodged from the lens surface. The procedure was then repeated on six further occasions on the same lens with at least 5 min between measurements. The saline within the glass chamber was emptied and refilled prior to testing each lens. This procedure was undertaken for 10 lens samples per lens type, and the order of analysis of these lenses was randomized. This gave a total of 280 movie clips (7 measurement runs $\times$ 10 lens samples $\times$ 4 lens types).

Image Analysis

Each movie clip was analyzed using the SCA-20 (version 3.7.4) software supplied with the OCA-20 instrument. As the contact lenses had a curved surface, the automated contact angle analysis mode could not be used and the semiautomated image analysis-drawing tool was utilized. Frame zero was defined on which the surface droplet/detached bubble was first formed on the lens surface. The movie was then advanced 10 s to a time point at which the contact angle had reached equilibrium. This single frame at 10 s was analyzed using the semiautomated software. The elliptical curve-fitting tool was used to (a) define the contact lens surface and (b) define the droplet/bubble surface. Once the two surfaces were defined, the SCA-20 software automatically calculated the contact angle on both sides of the droplet/bubble (Figures 1 and 2). Each 10-s frame contact angle image was reanalyzed after 24 h by the same investigator. This process was fully masked and randomized by assigning a random number to each frame from 1 to 560. These frames were then analyzed in a different random order on two separate occasions. Once all of the

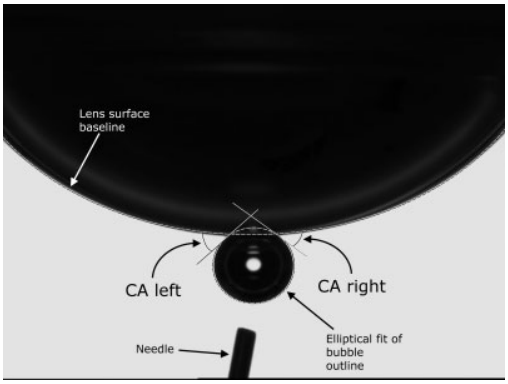

Figure 2. Image analysis of a typical captive bubble frame. From Maldonado-Codina and Morgan.[23]

TABLE II. Absolute Contact Angle Values and Image Analysis COR Values

	Contact Angle		COR	
Lens Type	Sessile Drop (°)	Captive Bubble (°)	Sessile Drop (°)	Captive Bubble (°)
Senofilcon A	80.0 (78.2, 81.8)	27.8 (27.3, 28.3)	2.0 (1.8, 2.2)	1.4 (0.9, 1.9)
Balafilcon A	86.5 (85.6, 87.4)	27.8 (27.4, 28.2)	2.2 (1.4, 3.0)	2.0 (1.3, 2.7)
Lotrafilcon A	50.2 (49.5, 50.9)	25.3 (24.9, 25.7)	1.9 (1.2, 2.6)	2.4 (1.5, 3.3)
Etafilcon A	15.3 (14.8, 15.8)	24.9 (24.3, 25.5)	2.5 (1.6, 3.4)	2.6 (1.7, 3.5)

The 95% confidence intervals appear in parentheses.

frames had been measured twice, the data were brought together and the masking was broken.

Determination of Measurement Errors

Image Analysis Coefficient of Repeatability. Following the testing for normality of the differences between analysis/reanalysis contact angles with the Kolmogorov-Smirnov (KS) test, image analysis COR was calculated using the method recommended by Bland and Altman.[16] In brief, the COR is 2.77 × the average standard deviation of the sets of two repeated measurements. This COR value estimates the maximum difference likely to occur between 95% of pairs of successive contact angle measurements on the same image. COR values were calculated separately for the sessile drop and captive bubble methods. In addition, paired *t*-tests were performed to compare the first and second contact angle measurements. The mean of the analysis/reanalysis contact angles was plotted against the difference between these two measurements using the approach suggested by Bland and Altman[16] to explore the relationship between measurement error and measurement magnitude and to derive the 95% limits of agreement.[16]

Intralens Coefficient of Repeatability. Prior to the calculation of intralens and interlens COR, an analysis of covariance model was constructed with "lens type" as a between factor and "measurement sequence number" as the covariant to investigate the potential for systematic errors being introduced by repeated measurements on the same sample.

The intralens COR was then calculated as 2.77 × the average standard deviation of the 10 sets of seven "within-lens" repeated measurements. This COR value estimates the maximum difference likely to occur between 95% of successive contact angle measurements on the same lens surface. COR values were calculated for each of the four lens types, separately for the sessile drop and captive bubble methods.

Interlens Coefficient of Repeatability. The interlens COR was calculated as 2.77 × the average standard deviation of the seven sets of 10 "between-lens" repeated measurements. This COR value estimates the maximum difference likely to occur between 95% of successive contact angle measurements on different lenses of the same type. COR values were calculated for each of the four lens types, separately for the sessile drop and captive bubble methods.

Ninety-five percent confidence intervals were calculated for all COR values. Measurements were deemed to be statistically significantly different when there was no overlap between the relevant 95% confidence intervals.

RESULTS

There was no significant difference between the distribution of differences in image analysis/reanalysis values and that of a normal distribution (sessile drop: $K = 1.0$, $p = 0.50$; and captive bubble: $K = 1.0$, $p = 0.51$), justifying the subsequent parametric statistical treatment of the data. Table II shows the absolute contact angles and image analysis COR values for each lens type. The overall image analysis COR value was 2.1° for both the sessile drop and captive bubble methods. Contact angle measurements were not significantly different for the first and second image analysis measurements for both the sessile drop ($t = 0.4$, $p = 0.72$) and captive bubble methods ($t = 0.4$, $p = 0.71$). Bland-Altman plots for the image analysis/reanalysis data are shown for both the sessile drop (Figure 3) and captive bubble methods (Figure 4). The 95% limits of agreement were −2.1° to +2.2° for both the sessile drop and captive bubble methods. Both Bland-Altman plots showed no apparent relationship between the analysis/reanalysis differences and the magnitude of the contact angle measured.

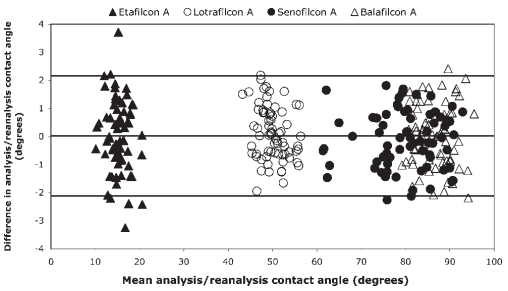

Figure 3. Bland-Altman plot for image analysis/reanalysis of the sessile drop data. Lines on the plot show the 95% limits of agreement.

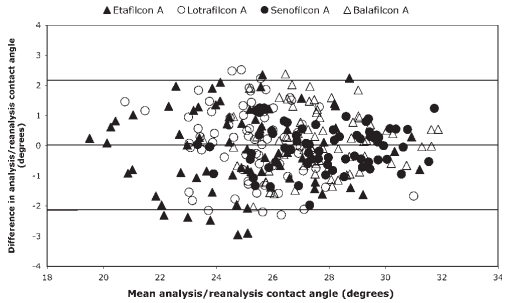

Figure 4. Bland-Altman plot for image analysis/reanalysis of the captive bubble data. Lines on the plot show the 95% limits of agreement.

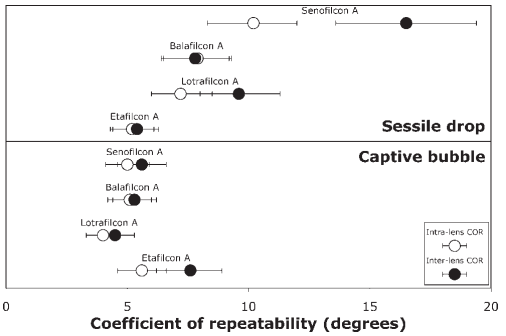

Figure 5. Intralens and interlens COR values. Error bars represent the 95% confidence intervals.

"Measurement sequence number" was demonstrated not to have a significant influence on the measured contact angle values ($F = 0.0$, $p = 0.89$) suggesting that sequential measures on an individual sample were not a confounding factor in our quantification of lens COR.

Intralens COR values for all lens type/method combinations ranged between 4.0° and 10.2°. Interlens COR values for all lens type/method combinations ranged between 4.5° and 16.5°. The combined data are shown in Table III and Figure 5.

DISCUSSION

Contact angle analysis is commonly used to predict the on-eye wettability (tear film stability) of contact lenses and in particular, hydrogel contact lenses. Since the launch of silicone hydrogel contact lenses in the late 1990s, wettability has been at the forefront of clinical and material science research in this area, and an increasing number of publications have reported the contact angles of these lenses.[17–19,24–26] However, the measurement of a contact angle on a hydrogel surface is problematic due to the inherent variabilities introduced at the sample preparation stage and the sensitivity of the surface to changes in its local environment. As such, understanding the magnitude of measurement error in the assessment of hydrogel contact angles is particularly important.

TABLE III. Intralens and Interlens COR Values

		Method	
	Lens Type	Sessile Drop (°) (95% Confidence Intervals)	Captive Bubble (°) (95% Confidence Intervals)
Intralens	Senofilcon A	10.2 (8.4, 12.1)	5.0 (4.1, 5.9)
	Balafilcon A	7.9 (6.5, 9.3)	5.1 (4.2, 6.0)
	Lotrafilcon A	7.2 (5.9, 8.4)	4.0 (3.3, 4.7)
	Etafilcon A	5.2 (4.3, 6.1)	5.6 (4.6, 6.6)
Interlens	Senofilcon A	16.5 (13.6, 19.4)	5.6 (4.6, 6.6)
	Balafilcon A	7.8 (6.4, 9.2)	5.3 (4.4, 6.2)
	Lotrafilcon A	9.6 (7.9, 11.2)	4.5 (3.7, 5.2)
	Etafilcon A	5.4 (4.5, 6.4)	7.6 (6.3, 9.0)

The image analysis COR values found in this work were small (about 2°) when considered as absolute measures and were not related to contact angle magnitude. However, these measurement errors become more significant for materials with low contact angles. For example, the COR for sessile drop assessment of etafilcon A was 2.5° with a mean value of 15.3° (16%) when compared with a COR of 2.2° and mean value of 86.5° (3%) for the balafilcon A lens. In general, we consider these values to be small and that the semiautomated image analysis software used in this work was repeatable. In instruments where software is fully automated, this aspect of measurement error is likely to be reduced (with the added benefit of faster analysis), and this will be the subject of a future publication.[27]

Repeatability was poorer (i.e., higher COR values) for silicone hydrogel sessile drop measures when compared with those from captive bubble assessment. This is likely to be due to differences in surface dehydration between consecutive sessile drop measurements as a result of small variations in preparation time as well as differences in the amount of surface liquid removed during the blotting procedure. Contact angle measures on silicone hydrogel materials may be more sensitive to changes in surface dehydration because of the increased rotational mobility of silicon–oxygen bonds when compared with carbon–oxygen bonds (present in conventional hydrogel materials), leading to a less uniformly wetting surface as a result of hydrophobic moieties migrating to the lens/air interface. This hypothesis is further supported by the similarity of (a) repeatability values for the conventional hydrogel lens (etafilcon A) for the two methods and (b) all the captive bubble COR data.

Our results show a greater interlens COR value when compared with the intralens COR value for the senofilcon A lens for sessile drop measures. This finding presumably

relates to the material characteristics of this lens which, unlike the other silicone hydrogel lenses investigated, is not surface treated. Instead, this lens material incorporates high-molecular-weight poly(vinyl pyrrolidone) (PVP) in the bulk polymer[28,29] to mask the hydrophobic siloxane groups from the tear film. Variation in the distribution of PVP across a lens surface may give rise to increased COR values because a slightly different part of the lens surface may be sampled during repeated measurements; our finding of greater interlens COR compared with intralens COR could represent an indirect indication of greater variation in PVP distribution between lenses than across a single lens surface, although a more direct analytical approach would be required to confirm this. This discrepancy between interlens and intralens COR values for the senofilcon A lens is not evident for captive bubble measurements for the same lens material which supports the hypothesis that surface dehydration occurring during sessile drop measures increases the presentation of hydrophobic moieties at the contact lens surface.

In contrast, the other two silicone hydrogel lenses used in this work undergo surface treatment to improve their clinical wettability characteristics. The lotrafilcon A lens undergoes a plasma surface treatment resulting in a homogenous, dense, 25-nm thick coating. The coating possesses low molecular mobility which in turn has the effect of minimizing the migration of hydrophobic silicone groups toward the surface.[13,14] The balafilcon A lens has an incomplete plasma oxidation surface treatment, resulting in hydrophilic silicone "islands" surrounded by the hydrophobic silicone-based bulk material.[10] Such surface treatments appear to give rise to more repeatable sessile drop values for these lenses when compared with the nonsurface-treated senofilcon A lens, inferring a reduced susceptibility to surface dehydration during *in vitro* contact angle assessment.

We note that the measurement errors reported here are relatively small in comparison with the differences in absolute contact angle values found between the various published studies in this area. Although the ranking of the contact angles values found in this work is in agreement with previous reports, which have adopted similar experimental methodology,[18,23,25] there are clear discrepancies in the absolute values obtained. These differences are likely to be due to some or all of the following:

1. Different instruments and software (e.g., Dataphysics OCA 20 instrument[23] *versus* a custom-made instrument[25]).
2. Variations in sample preparation (e.g., blotting the lens on a flat surface using lens paper[18] *versus* blotting using a microfiber cloth on a curved surface as described in this investigation).
3. Changes to material formulations and blister packaging solutions over time (e.g., recent enhancements to balafilcon A and lotrafilcon A lenses[30]).
4. Interinvestigator variability.

CONCLUSIONS

This work has presented a detailed description of the measurement errors that occur during the measurement of contact angles on curved hydrogel contact lens surfaces while using the sessile drop and captive bubble methods. These measurement errors are influenced by (a) the subjective elements introduced by using semiautomated software, (b) methodology-dependant variables, and (c) surface-related material variables. Measurement error associated with image analysis was shown to be small as an absolute measure, although more significant for lenses with low contact angle. Overall, the captive bubble method was subject to smaller measurement errors than the sessile drop method, which is thought to be due to the sensitivity of the lens surfaces to dehydration. All such measurement errors should be taken into account when considering any published contact angle data for hydrogel contact lenses.

REFERENCES

1. Johnson RE, Dettre RH. Wettability. New York: CRC Press; 1993.
2. Padday JF. Spreading, wetting and contact angles. J Adhes Sci Technol 1992;6:1347–1358.
3. Carre A, Woehl P. Spreading of silicone oils on glass in two geometries. Langmuir 2006;22:134–139.
4. Molina R, Comelles F, Julia MR, Erra P. Chemical modification on human hair studied by means of contact angle determination. J Biomed Mater Res 2001;237:40–46.
5. Maldonado-Codina C, Morgan PB, Schnider CM, Efron N. Short-term physiologic response in neophyte subjects fitted with hydrogel and silicone hydrogel contact lenses. Optom Vis Sci 2004;81:911–921.
6. Guillon M, Maissa C. Use of silicone hydrogel material for daily wear. Contact Lens Anterior Eye 2007;30:5–10.
7. Morgan PB, Woods CA, Knajian R, Jones D, Efron N, Tan K-O, Pesinova A, Grein H-J, Marx S, Santodomingo J, Runberg S-E, Tranoudis IG, Chandrinos A, Itoi M, Bendoriene J, van der Worp E, Helland M, Phillips G, Gonzalez-Meijome JM, Belousov V, Mack CJ. International contact lens prescribing in 2007. Contact Lens Spectrum 2008;23: 36–41.
8. Papas EB, Vajdic CM, Austen R, Holden BA. High-oxygen-transmissibility soft contact lenses do not induce limbal hyperaemia. Curr Eye Res 1997;16:942–948.
9. Dumbleton K. Noninflammatory silicone hydrogel contact lens complications. Eye Contact Lens 2003;29 (1, Suppl): S186–S189.
10. Kunzler J. Silicone hydrogels for contact lens applications. Trends Polym Sci 1996;4:52–59.
11. Brennan NA, Coles ML, Ang JH. An evaluation of silicone-hydrogel lenses worn on a daily wear basis. Clin Exp Optom 2006;89:18–25.
12. Tighe B. Silicone hydrogels: structure, properties and behaviour. In: Sweeney D, editor. Silicone Hydrogels: Continuous Wear Contact Lenses. London: Butterworth-Heinemann; 2004. pp 1–21.
13. Weikart CM, Matsuzawa Y, Winterton L, Yasuda HK. Evaluation of plasma polymer-coated contact lenses by electrochemical impedance spectroscopy. J Biomed Mater Res 2001;54:597–607.
14. Weikart CM, Miyama M, Yasuda HK. Surface modification of conventional polymers by depositing plasma polymers of

trimethylsilane and of trimethylsilane $+O_2$. I. Static wetting properties. J Colloid Interface Sci 1999;211:28–38.
15. Bland JM, Altman DG. Statistics notes: Measurement error. BMJ 1996;313:744.
16. Bland JM, Altman DG. Statistical methods for assessing agreement between two methods of clinical measurement. Lancet 1986;1:307–310.
17. Cheng L, Muller SJ, Radke CJ. Wettability of silicone-hydrogel contact lenses in the presence of tear-film components. Curr Eye Res 2004;28:93–108.
18. Lorentz H, Rogers R, Jones L. The impact of lipid on contact angle wettability. Optom Vis Sci 2007;84:946–953.
19. Santos L, Rodrigues D, Lira M, Oliveira MECDR, Oliveira R, Vilar EYP, Azeredo J. Bacterial adhesion to worn silicone hydrogel contact lenses. Optom Vis Sci 2008;85:520–525.
20. BSI. Precision of test methods, part 1: guide for the determination of repeatability and reproducibility for a standard test method. BS 5497, Part 1. London: British Standards Institute; 1979.
21. Jones L, Dumbleton K. Contact lens fitting today. Silicone hydrogels, Part 1: Technological developments. Optom Today 2005;18:23–29.
22. Teichroeb JH, Forrest JA, Ngai V, Martin JW, Jones L, Medley J. Imaging protein deposits on contact lens materials. Optom Vis Sci 2008;85:1151–1164.
23. Maldonado-Codina C, Morgan PB. *In vitro* water wettability of silicone hydrogel contact lenses determined using the sessile drop and captive bubble techniques. J Biomed Mater Res Part A 2007;83:496–502.
24. Bruinsma GM, van der Mei HC, Busscher HJ. Bacterial adhesion to surface hydrophilic and hydrophobic contact lenses. Biomaterials 2001;22:3217–3224.
25. Vermeltfoort PB, Rustema-Abbing M, de Vries J, Bruinsma GM, Busscher HJ, van der Linden ML, Hooymans JM, van der Mei HC. Influence of day and night wear on surface properties of silicone hydrogel contact lenses and bacterial adhesion. Cornea 2006;25:516–523.
26. Willis SL, Court JL, Redman RP, Wang JH, Leppard SW, Obyrne VJ, Small SA, Lewis AL, Jones SA, Stratford PW. A novel phosphorylcholine-coated contact lens for extended wear use. Biomaterials 2001;22:3261–3272.
27. Read ML, Kelly JM, Maldonado-Codina C, Morgan PB. Automated contact angle measurements of a curved contact lens surface. Poster presented at 14th Symposium on the Material Science and Chemistry of Contact Lenses, New Orleans, 2008.
28. Maiden AC, Vanderlaan DG, Turner DC, Love RN, Ford D, Molock FF, Steffen RB, Hill GA, Alli A, McCabe KP. Hydrogel with internal wetting agent. US Patent 6,367,929 (2002).
29. McCabe KP, Molock FF, Hill GA, Alli A, Maiden AC, Steffen RB, Vanderlaan DG, Young KA. Biomedical devices containing internal wetting agent. US Patent 6,822,016 (2004).
30. Pence N. Lens material enhancements: different but the same. Contact Lens Spectrum 2008;23:24.

Appendix E

Published paper - Dynamic Contact Angle Analysis

Dynamic Contact Angle Analysis of Silicone Hydrogel Contact Lenses

MICHAEL LEONARD READ, PHILIP BRUCE MORGAN,
JEREMIAH MICHAEL KELLY AND CAROLE MALDONADO-CODINA*
Eurolens Research, Faculty of Life Sciences
The University of Manchester, Manchester, UK

ABSTRACT: Contact angle measurements are used to infer the clinical wetting characteristics of contact lenses. Such characterization has become more commonplace since the introduction of silicone hydrogel contact lens materials, which have been associated with reduced *in vivo* wetting due to the inclusion of siloxane-containing components. Using consistent methodology and a single investigator, advancing and receding contact angles were measured for 11 commercially available silicone hydrogel contact lens types with a dynamic captive bubble technique employing customized, fully automated image analysis. Advancing contact angles were found to range between 20° and 72° with the lenses falling into six statistically discrete groupings. Receding contact angles fell within a narrower range, between 17° and 22°, with the lenses segregated into three groups. The relationship between these laboratory measurements and the clinical performance of the lenses requires further investigation.

KEY WORDS: contact angle, contact lens, silicone hydrogel, wettability, hysteresis.

INTRODUCTION

Wettability can be defined as the tendency for a liquid to spread over a solid surface [1–3] and is particularly relevant to contact lenses because the lens surface needs to support a stable ocular tear film

*Author to whom correspondence should be addressed.
E-mail: c.m-codina@manchester.ac.uk

0885-3282/10/00 0001–15 $10.00/0 DOI: 10.1177/0885328210363505

layer and failure to achieve this is likely to adversely affect visual performance, increase lens surface deposition [4], and reduce comfort [5]. This consideration applies to all forms of contact lenses, but in particular to siloxane-containing soft contact lens materials, termed 'silicone hydrogels'. In recent years, these lenses have seen a significant increase in the worldwide market share [6] because of their enhanced ability to deliver oxygen to the ocular surface, which in turn has resolved a number of clinical complications seen with non-siloxane-containing hydrogels [7–9]. A potential negative consequence of the inclusion of silicon into contact lenses is the inherent hydrophobicity this imparts to the material [10] which can result in poor *in vivo* wettability [8,11]. In an attempt to alleviate clinical problems related to this hydrophobicity, contact lens manufacturers have used a range of fabrication techniques, including plasma surface treatments [12,13] and the inclusion of hydrophilic monomers [14–16] to the bulk material, which serve to mask surface hydrophobicity and improve ocular biocompatibility [10,12,13,17].

Contact angle analysis has become a widely accepted method with which to infer the wetting characteristics of contact lenses [18–21]. In this context, it involves measuring the angle between a liquid and the lens surface at the three-phase boundary where a liquid, gas, and solid intersect. Contact angles can be described as 'dynamic' or 'static' dependent on whether or not the three-phase boundary is in motion. Dynamic assessment can be further subdivided into 'advancing' measures where, in the case of the analysis of contact lenses, a probe liquid moves across an air-exposed lens surface, or 'receding' in which the probe liquid moves across a liquid-exposed lens surface. The difference in magnitude between the advancing and receding angles is termed 'hysteresis'. Hydrogels typically demonstrate large levels of hysteresis, which can be explained by rapid mobility of the macromolecules at the lens surface resulting in reorientation of hydrophilic and hydrophobic functional groups [22].

Contact angle measurement techniques, which have been used for the assessment of contact lenses include 'sessile drop' [19,23] (where a liquid drop is placed onto the lens surface), 'captive bubble' [18,24] (where an air bubble is placed in contact with a lens immersed in a liquid), and 'Wilhelmy plate' [20] (where a lens sample is immersed and withdrawn from a liquid). Although the majority of published studies have investigated contact lenses using static sessile drop or captive bubble techniques, a potentially more clinically meaningful approach is to obtain advancing and receding contact angles by means of a dynamic contact angle technique. In the eye, the tear film spreads over a contact lens

surface via the mechanical opening and closing of the eyelids. As the eyelids close, they push or 'advance' the tear film over the contact lens. Some authors have postulated that the advancing contact angle is important in modeling the initial spreading of the prelens tear film over a dry or partially dry lens surface [18]. This prelens tear film layer (approximately 3 μm thick [25]) will then tend to break to form dry spots over the lens surface, which in turn stimulates another blink to take place. The receding angle is thought to be an important measure of the likelihood of the prelens tear film to break ('recede') and may be an indicator of prelens tear film stability. Although the Wilhelmy plate method measures both advancing and receding angles [26], the sample preparation is complex [20,27], which can impact significantly on the results obtained. The sessile drop method has been widely adopted for hydrogel lens contact angle analysis but is not ideal for this application since the lens surface needs to be blotted in order to allow a contact angle to form [24] (which inherently alters the surface under investigation), and additionally, the lens surface will undergo significant dehydration during the procedure since the lens is being measured in air. The captive bubble technique, on the other hand, is widely considered the best suited to the investigation of hydrogels since the material is immersed in a liquid throughout the process and therefore does not undergo dehydration. A potential disadvantage of any dynamic technique is that the analysis of contact angles over many seconds of examination can be very time consuming. Fully automating the analysis of captured digital movies has allowed us to obtain data very quickly and has streamlined our methodology into an accurate and rapid technique for obtaining dynamic contact angle data on curved contact lens surfaces [28,29].

Contact angles are often quoted by manufacturers in their marketing literature, but it is impossible to compare these angles since they will vary widely depending on (1) which method has been used to obtain the angle, (2) which probe liquid has been used, and (3) whether static or dynamic contact angles have been investigated. The aim of this work was therefore to provide independent measures for advancing and receding contact angles using standardized methodology for the most widely prescribed silicone hydrogel contact lenses currently on the market.

MATERIALS AND METHODS

Lenses

Eleven commercially available silicone hydrogel contact lenses were used in this investigation. Details of these lenses including public domain

Table 1. Study contact lenses.

Lens type[a]	Brand name	Manufacturer	Principal monomers	Oxygen permeability (Barrers)[b]	Water content (%)	Modulus (MPa)[b]	Surface treatment
Asmofilcon A	PremiO	Menicon	Silicone methacrylates, silicone acrylates, DMA, pyrrolidone derivative	129	40	0.91	Plasma coating and plasma oxidation
Balafilcon A	Purevision	Bausch & Lomb	NVP, TPVC, NVA, PBVC	91	33	1.06	Plasma oxidation
Clariti[c]	Clariti	Sauflon	Alkyl methacrylates, silicone acrylates, siloxane monomers, NVP	60	58	0.50	None (inherently wettable)
Comfilcon A	Biofinity	CooperVision	M3U, FMM, TAIC, IBM, NMNVA NVP, HOB	128	48	0.75	None (inherently wettable)
Enfilcon A	Avaira	CooperVision	M3U, TEGMA, MMA NMNVA, AOE	100	46	0.50	None (inherently wettable)
Galyfilcon A	Acuvue Advance	Johnson & Johnson	mPDMS, DMA, HEMA, SiGMA EGDMA, PVP	60	47	0.43	None (internal wetting agent, PVP)
Lotrafilcon A	Air Optix Night & Day	CIBA Vision	DMA, TRIS, fluorine-containing siloxane macromer	140	24	1.50	Plasma coating
Lotrafilcon B	Air Optix	CIBA Vision	DMA, TRIS, fluorine-containing siloxane macromer	110	33	1.22	Plasma coating
Narafilcon A	1-Day Acuvue TruEye	Johnson & Johnson	Hydroxy-functionalized mPDMS, DMA, HEMA, TEGDMA, PVP	101	46	0.66	None (internal wetting agent, PVP)
Senofilcon A	Acuvue Oasys	Johnson & Johnson	mPDMS, DMA, HEMA, SiGMA, TEGDMA, PVP	103	38	0.72	None (internal wetting agent, PVP)
Silfilcon A	Air Optix Individual	CIBA Vision	DMA, TRIS, fluorine-containing siloxane macromer, styrene	82	32	1.10	Plasma coating

[a]United States Adopted Name (USAN).
[b]Manufacturer-reported values.
[c]This lens currently has no USAN name. The brand name is used throughout this work.
PVP: poly(vinyl pyrrolidone); mPDMS: monofunctional methacryloxypropyl terminated polydimethylsiloxane; DMA: N,Ndimethylacrylamide; HEMA: hydroxyethyl methacrylate; EGDMA: ethyleneglycol dimethacrylate; TEGDMA: tetraethyleneglycol dimethacrylate; TRIS: methacryloxypropyl tris(trimethyl siloxy)silyane; NVP: N-vinyl pyrrolidone; TPVC: tris-(trimethyl siloxysilyl) propylvinyl carbamate; NVA: N-vinyl amino acid; PBVC: poly(dimethysiloxy) di (silylbutanol) bis (vinyl carbamate); M3U: αω-bis(methacryloyloxyethyl iminocarboxy ethyloxypropyl)-poly(dimethylsiloxane)-poly(trifluoropropylmethylsiloxane)-poly(methoxy-poly(ethyleneglycol)propylmethyl-siloxane; FMM: α-methacryloyloxyethyl iminocarboxyethyloxypropyl-poly(dimethylsiloxy)-butyldimethylsilane; TAIC: 1,3,5-triallyl-1,3,5-triazine-2,4,6(1H,3H,5H)-trione; IBM: isobornyl methacrylate; HOB: 2-hydroxybutyl methacrylate; NMNVA: N-methyl-N-vinyl acetamide; MMA: methyl methacrylate; AOE: 2-allyloxyethanol; SiGMA: 2-propenoic acid, 2-methyl, 2-hydroxy-3-(3-(1,3,3,3-tetramethyl-1-(trimethylsilyl)oxy)disiloxanyl)propoxypropyl ester.

information on their chemical composition are provided in Table 1. The back vertex power of all lenses was −3.00DS. All contact lenses were sourced from individual manufacturing batches via normal commercial channels and supplied in their standard blister packaging. All lenses were coded by a second investigator in order that the primary investigator (who conducted all measurements throughout the study) remained masked to the lenses being evaluated.

Surface Tension Measurement

The surface tension of the blister contact lens packaging solutions was measured in order to determine the presence of any surface active agents since such components will have a significant effect on the magnitude of any contact angle measured [24]. Surface active agents are often added to contact lens blisters in order to prevent the lenses adhering to the blister material (particularly at high temperatures, e.g., during sterilization) and in an apparent attempt to aid initial wearer comfort of the lenses [20]. Surface tension measurement was performed using the pendant drop technique with an OCA-20 (DataPhysics Instruments, Filderstadt, Germany) contact angle analyzer, which comprises a conventional goniometer with automated drop delivery and digital image capture. The pendant drop method has previously been well documented [30]; in brief, we derived surface tension by fitting the Young-Laplace equation to the digitized outline of the largest possible liquid drop suspended from a 2.41 mm outer diameter blunt-ended steel needle.

Prior to contact angle measurement, all lenses underwent a 48 h saline soak in 0.9% phosphate buffered saline (PBS) solution (Sigma-Aldrich, Germany), which was changed every 12 h in an attempt to remove any surface active agents adsorbed onto the lens surfaces or absorbed into the lens polymer bulk. The effectiveness of this strategy was tested by comparing the surface tension of the final (fourth) postsoak PBS to that of freshly prepared PBS.

Dynamic Contact Angle Analysis

Contact angles were measured at room temperature ($25.0^{\circ}C \pm 1^{\circ}C$) and humidity ($35\% \pm 5\%$) with the OCA-20 contact angle analyzer using a dynamic captive bubble method.

Following the soaking procedure described above, the lens was carefully suspended circumferentially in a custom-made lens holder so that the anterior lens surface faced downward directly into a PBS-filled,

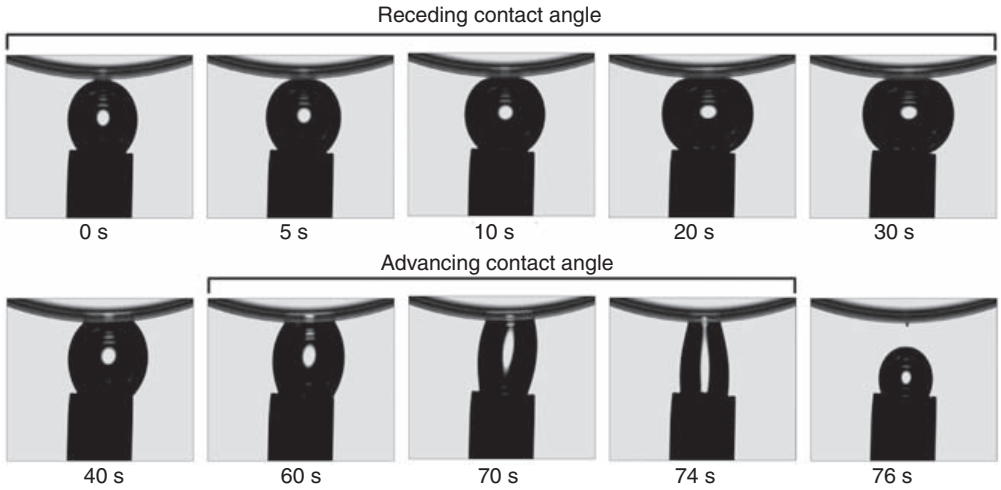

Figure 1. Image sequence for the expansion and contraction of the air bubble demonstrating the advancing and receding phases.

optically clear chamber. An air bubble was dispensed from a curved 1.65 mm outer diameter blunt-ended steel needle positioned 2 mm directly below the lens apex. The size of the bubble was slowly increased by 0.1 $\mu L\,s^{-1}$ using the OCA-20 automated bubble delivery function until contact was made with the lens surface. Assessment of the receding and advancing contact angles was achieved by first enlarging the air bubble at a rate of 0.12 $\mu L\,s^{-1}$ until it increased in volume by 3 μL and then shrinking its volume until the bubble detached from the lens surface (Figure 1). This entire process was captured as a digital movie. The procedure was then repeated on four further occasions on the same lens with at least 5 min between measurements. The saline within the glass chamber was emptied and refilled prior to testing each different lens. This procedure was undertaken for 10 lens samples per lens type, and the order of analysis of these lenses was randomized. This gave a total of 550 movie clips (5 measurement runs $\times$10 lens samples $\times$11 lens types).

Image Analysis

Receding and advancing contact angles were derived for each movie. This was achieved by applying a customized, fully automated image analysis routine (MATLAB, The MathWorks, Natick, MA) to each side of the bubble for all frames in the captured movie clip. This routine employed a tracing technique used to identify the boundary of the contact lens and bubble surfaces around the three-phase interface (Figure 2). The three-phase interface point on each side of the bubble was identified

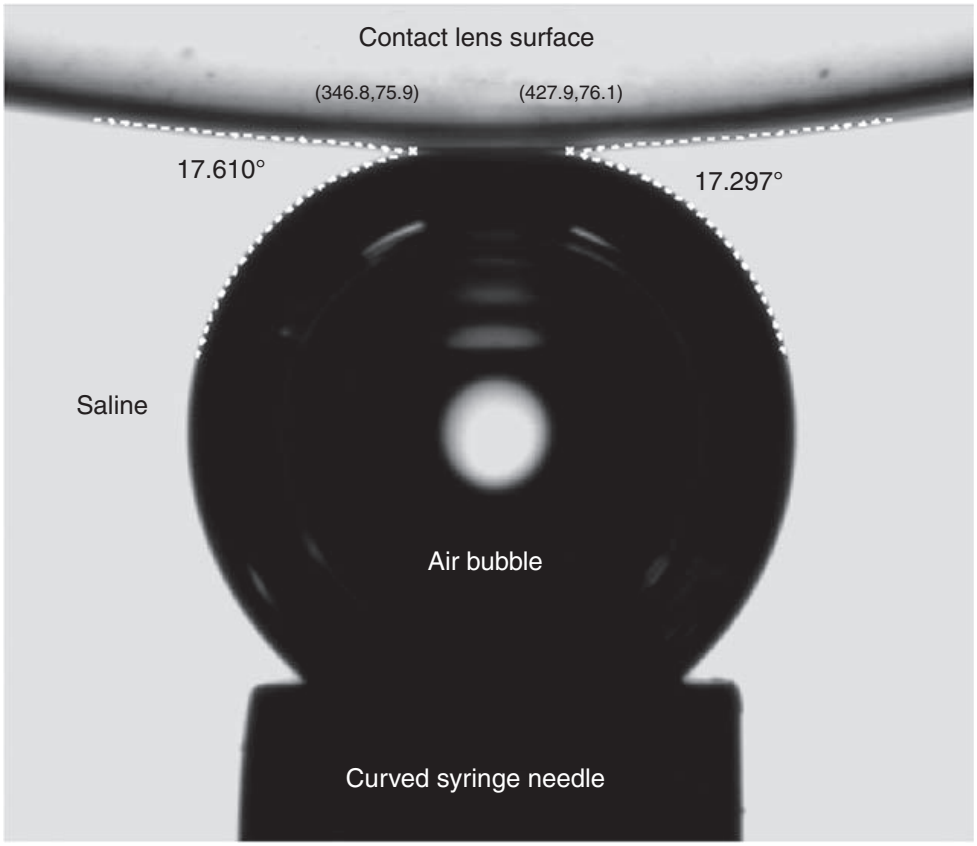

Figure 2. Image analysis of a typical captive bubble frame. The magnitude of the calculated contact angles are shown (in degrees) to the left and right of the bubble.

from which contact angle (using the intersection of the two linear approximations of the local contact lens and bubble surfaces) and contact diameter (the distance between the two three-phase interfaces) were calculated. The mean of the two contact angles for each frame and the contact diameter were plotted versus frame number in order to identify the advancing and receding contact angle phases (Figure 3). We defined the receding contact angle as the mean angle in five frames at the midpoint of the receding phase and the advancing contact angle as the mean angle in the first five frames of the advancing phase.

Data Analysis

Given the normal distribution of the data sets (advancing and receding contact angles, and hysteresis data for each of the 11 lens types, Kolmogorov-Smirnov test, all $p > 0.14$), a linear regression model was constructed to investigate the overall study findings. Specifically, the

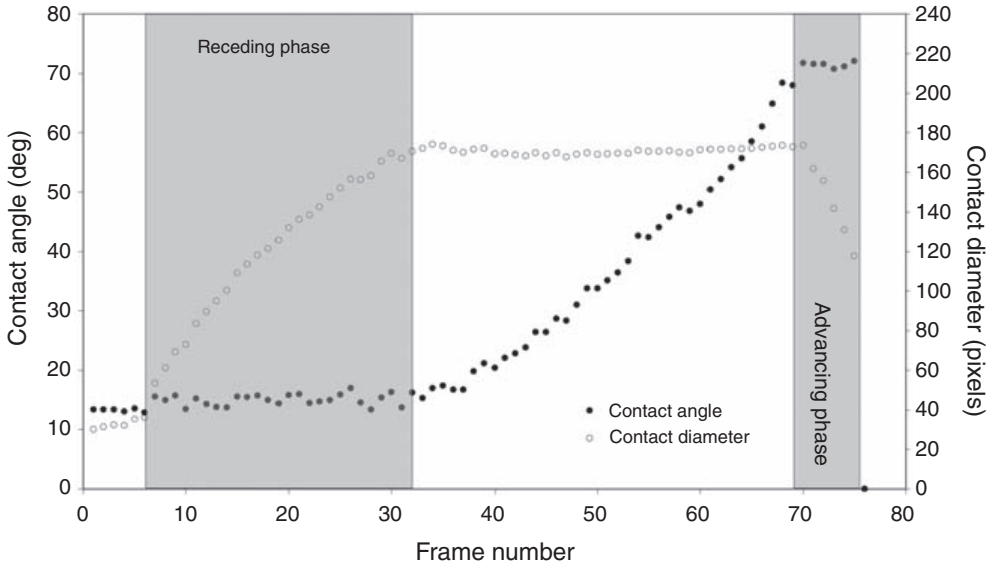

Figure 3. Contact angle and contact diameter vs frame number for a balafilcon A lens. The advancing and receding phases are highlighted.

factors of interest were lens type, contact angle type (advancing or receding), measurement run (as a covariant), and lens sample (as a random effect) with contact angle magnitude as the dependent variable. This was then followed by separate linear regression models for advancing contact angle, receding contact angle, and magnitude of hysteresis as the dependent variable in order to investigate differences between lens types.

RESULTS

Surface Tension Measurement

The surface tension measurements of the lens blister packaging solutions and the postsoak PBS are shown in Table 2. The postsoak surface tension of the PBS was within 0.2 dynes/cm (0.0002 N/m) of the presoak saline in all cases confirming that any surface active agents were removed by the soaking process.

Dynamic Contact Angle Analysis

Advancing and receding contact angles for the lenses are shown in Table 3 and Figure 4. The hysteresis values of the lenses are also shown in Table 3. The results of the overall linear regression model showed a

Table 2. Surface tension of the blister packaging solutions.

	Surface tension (dynes/cm)	
Lens type	Blister packaging solution	Postsoak PBS
Asmofilcon A	67.5 (0.4)	72.7 (0.2)
Balafilcon A	72.0 (0.1)	72.7 (0.1)
Clariti	54.4 (0.6)	72.6 (0.1)
Comfilcon A	68.5 (0.1)	72.6 (0.2)
Enfilcon A	65.1 (1.2)	72.6 (0.2)
Galyfilcon A	51.3 (0.7)	72.6 (0.1)
Lotrafilcon A	71.8 (0.1)	72.5 (0.2)
Lotrafilcon B	72.2 (0.1)	72.6 (0.1)
Narafilcon A	52.6 (0.6)	72.7 (0.2)
Senofilcon A	52.1 (0.8)	72.5 (0.2)
Silfilcon A	72.5 (0.1)	72.6 (0.4)

The 95% confidence intervals appear in parentheses.

Table 3. Advancing and receding contact angles.

Lens type	Advancing contact angle (deg)	Receding contact angle (deg)	Hysteresis (deg)
Asmofilcon A	71.2 (1.5)	19.6 (0.7)	51.6 (1.4)
Balafilcon A	71.5 (1.1)	18.3 (0.6)	53.3 (1.3)
Clariti	42.2 (0.9)	17.5 (0.4)	24.7 (1.1)
Comfilcon A	29.6 (1.2)	18.6 (0.5)	11.1 (1.3)
Enfilcon A	68.3 (1.5)	19.7 (0.7)	48.7 (1.7)
Galyfilcon A	37.5 (1.9)	21.8 (1.1)	15.8 (1.4)
Lotrafilcon A	19.9 (0.9)	17.1 (0.5)	2.8 (0.7)
Lotrafilcon B	41.3 (1.0)	19.6 (0.9)	21.7 (1.3)
Narafilcon A	37.0 (0.7)	22.1 (1.0)	14.9 (0.7)
Senofilcon A	35.4 (0.5)	22.1 (0.6)	13.3 (0.6)
Silfilcon A	30.5 (1.4)	18.6 (0.7)	12.0 (1.5)

The 95% confidence intervals appear in parentheses.

significant interaction for lens type $\times$ contact angle type ($F = 678.7$, $p < 0.0001$). Measurement run was not significant ($F = 1.1$, $p = 0.29$).

Given the significant interaction term above, separate analyses for advancing and receding contact angles and hysteresis were undertaken. Lens types were significantly different for advancing angles ($F = 964.5$, $p < 0.0001$). Post hoc analysis using the Tukey HSD test divided the lenses into the following six groups within which statistically similar advancing contact angles were measured (in descending order of contact angle magnitude): (1) balafilcon A/asmofilcon A, (2) enfilcon A,

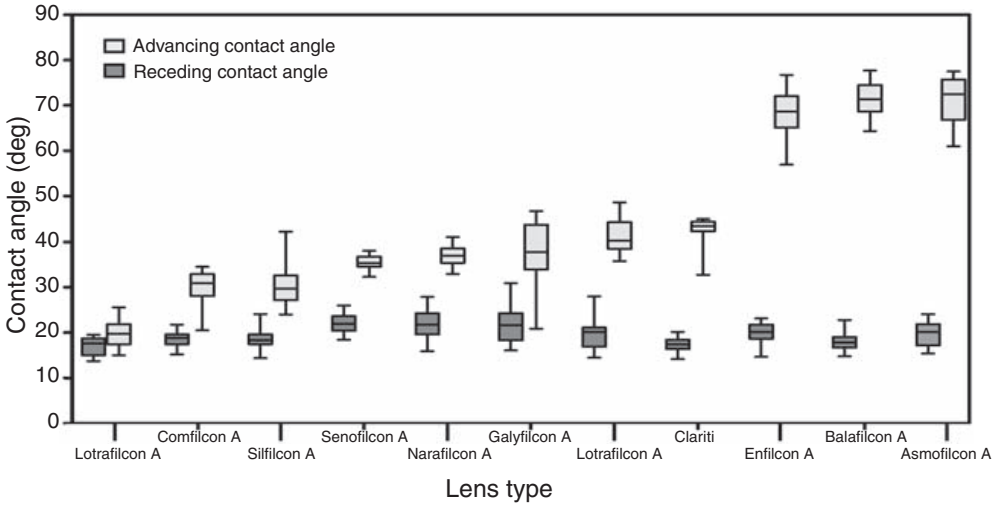

Figure 4. Advancing and receding contact angles for all the silicone hydrogel lenses investigated. The boxes represent the 25th and 75th centiles, and the whiskers indicate the full extent of the data set. The mean is represented by a horizontal line within the box.

(3) Clariti/lotrafilcon B, (4) galyfilcon A/narafilcon A/senofilcon A, (5) silfilcon A/comfilcon A, and (6) lotrafilcon A.

Differences were also demonstrated between the lens types for receding angle ($F = 23.8$, $p < 0.0001$). Post hoc analysis demonstrated larger angles for three lenses (senofilcon A, narafilcon A, and galyfilcon A) compared with the other lens types. The remaining eight brands were statistically divided into two groups with some overlap between them. One group included enfilcon A, lotrafilcon B, asmofilcon A, silfilcon A, comfilcon A, and balafilcon A; the other group comprised silfilcon A, comfilcon A, balafilcon A, Clariti, and lotrafilcon A.

Hysteresis was also different for the various lens brands ($F = 868.7$, $p < 0.0001$). In general, each lens type was different to all the others with the exception of galyfilcon A, narafilcon A, and senofilcon A, which were grouped together and senofilcon A, silfilcon A, and comfilcon A, which were also statistically similar.

DISCUSSION

This work has provided data for advancing and receding contact angles for a wide range of silicone hydrogel lenses obtained using consistent methodology and a single investigator.

A review of the literature shows that there are relatively few published reports detailing the contact angles of unworn, silicone hydrogel lenses. Only one report has documented a dynamic captive bubble methodology

similar to that used in our current investigation [18]. This work by Cheng and coworkers noted that the balafilcon A lens demonstrated a receding contact angle of 24° and an advancing contact angle of 80° when saline was used as the probe liquid. These values are reasonably similar to those found in the present investigation (18° and 72°). Their data for the lotrafilcon A lens (21° and 60°) were markedly different to our own findings (17° and 20°). We have previously documented the reasons why different investigations of contact angles may produce discrepant results [29]. When comparing our data with those of Cheng and coworkers, the differences obtained may be due to the following:

(a) Different instruments: We used the OCA 20 instrument, whereas Cheng and coworkers used a customized setup based around the Kruss DSA-10 instrument with semiautomated angle analysis software.
(b) Differences in sample preparation: Cheng and coworkers stretched their lens samples over a Teflon holder in order to present a flat surface for analysis. In comparison, we assessed the lenses without deformation and without a holder applied to the lens back surface.
(c) Differences to lens material formulations and packaging solutions: Both the balafilcon A and the lotrafilcon A lenses have undergone refinements since Cheng and coworkers carried out their work [31].
(d) Different investigators: Subtle differences in measurement technique may introduce variability in the data obtained.

These differences serve to highlight the difficulties of inter-laboratory comparison of data in this area.

Our data have shown key differences between advancing contact angles for the different lenses investigated. Advancing contact angles ranged from 20° to 72°, and for some of the lenses, it is possible to relate the magnitude of these angles to the surface chemical properties of the lenses. For example, the two lenses that undergo a surface oxidation process (balafilcon A and asmofilcon A) have the largest advancing contact angles. It has been well documented that such a surface treatment can result in glassy islands of hydrophilic silicate material surrounded by areas of hydrophobic bulk [17,32]. Within these hydrophobic areas, when the lens surface is exposed to air, the siloxane groups within the polymer are able to migrate, unimpeded, to the surface in order to minimize the surface energy, which in turn increases the measured advancing contact angle. We note a large advancing contact angle for the enfilcon A lens despite the lens not undergoing any kind of surface modification following cast moulding, while the comfilcon A lens that is fabricated by the same manufacturer

(CooperVision Inc) has a much smaller advancing contact angle, which may be due to its somewhat different chemical formulation (Table 1).

The Clariti and lotrafilcon B lenses had similar advancing contact angles despite different compositions and surface treatments (Table 1). Surprisingly, the lotrafilcon A, lotrafilcon B, and silfilcon A lenses (manufactured by CIBA Vision) all had advancing contact angles which were significantly different to each other despite the lenses being based on similar polymer chemistry and undergoing an apparently similar surface plasma coating process. We speculate that these discrepancies may be due to the following: (a) differences in plasma coating, (b) variation in the bulk chemical composition (such as the addition of styrene in silfilcon A, or differing ratios of siloxane monomer present in lotrafilcon A and lotrafilcon B materials), which may influence the surface characteristics of the lenses despite the presence of a coating, or (c) a combination of (a) and (b).

The three lenses manufactured by Johnson & Johnson (galyfilcon A, senofilcon A, and narafilcon A) demonstrated comparable advancing contact angles despite apparent differences in formulation. The information available in the public domain (Table 1) suggests that the chemical compositions of the galyfilcon A and the senofilcon A materials are similar (Table 1), and considering the differences in the water content of the materials, it is reasonable to assume that the ratios of the components differ between them, with more poly(vinyl pyrrolidone) being incorporated into the senofilcon A material [16]. The narafilcon A material contains the same hydrophilic monomers used in the senofilcon A and galyfilcon A formulations, but it contains only one rather than two silicone-containing monomers. This silicone monomer is of a lower molecular weight than that used in the galyfilcon A and senofilcon A materials [33].

In addition to composition-based differences and variations in surface treatment of lenses described above, there are other processing related factors, which could affect the resultant contact angles; these include polymerization conditions, solvents used to cast the lenses, and hydration/extraction methods. However, there is almost no information about these factors available in the public domain.

The receding contact angles for all the lenses investigated were restricted to a narrower range (17°–22°) than that of the advancing angles (20°–72°). All three of the Johnson & Johnson lenses demonstrated larger receding contact angles than the other lenses studied. The hysteresis of the lenses followed a similar pattern to that of the advancing angles given that the receding angles of all of the lenses were numerically similar.

CONCLUSIONS

Our results suggest that the magnitude of hysteresis and the advancing contact angle appear not to be indicative of the clinical performance of a contact lens since all of the lenses investigated in this work are currently on the market, and those with either large [34,35] or small [8,36] hysteresis have been demonstrated to have clinically acceptable levels of wettability. Differences between clinical and laboratory observations may be explained by the rapid deposition of tear film components over the lens, which in turn reduces the disparity between the various surfaces. Further investigation is required to determine more fully the relationship between laboratory measurements of contact angle and the clinical wetting behavior of these hydrogel contact lenses.

ACKNOWLEDGMENTS

This work is part of a PhD program supported by a grant from CooperVision Inc. and a Doctoral Training Award from the Medical Research Council at The University of Manchester. We thank Andy Broad at Sauflon CL Ltd. for useful comments on Table 1.

REFERENCES

1. Carre, A. and Woehl, P. Spreading of Silicone Oils on Glass in Two Geometries, *Langmuir*, 2006: **22**: 134–139.
2. Johnson, R.E. and Dettre, R.H. (1993). Wetting of Low-Energy Surfaces, In: Berg, J.C. (ed.), *Wettability (Surfactant Science Series)*, New York, CRC Press, Vol. 49, pp. 1–73.
3. Molina, R., Comelles, F., Julia, M.R. and Erra, P. Chemical Modification on Human Hair Studied by Means of Contact Angle Determination, *J. Biomed. Mater. Res.*, 2001: **237**: 40–46.
4. Jones, L., Senchyna, M., Glasier, M.A., et al. Lysozyme and Lipid Deposition on Silicone Hydrogel Contact Lens Materials, *Eye Contact Lens*, 2003: **29**: S75–S79.
5. Guillon, M. and Maissa, C. Use of Silicone Hydrogel Material for Daily Wear, *Cont. Lens Anterior. Eye*, 2007: **30**: 5–10.
6. Morgan, P.B., Woods, C.A., Knajian, R., et al. International Contact Lens Prescribing in 2007, *Contact Lens Spectrum*, 2008: **23**: 36–41.
7. Dumbleton, K.A. Noninflammatory Silicone Hydrogel Contact Lens Complications, *Eye Contact Lens*, 2003: **29**: S186–S189.
8. Maldonado-Codina, C., Morgan, P.B., Schnider, C.M. and Efron, N. Short-Term Physiological Response in Neophyte Subjects Fitted With Hydrogel and Silicone Hydrogel Contact Lenses, *Optom. Vis. Sci.*, 2004: **81**: 911–921.

9. Papas, E.B., Vajdic, C.M., Austen, R. and Holden, B.A. High Oxygen-Transmissibility Soft Contact Lenses do Not Induce Limbal Hyperaemia, *Curr. Eye Res.*, 1997: **16**: 942–948.
10. Kunzler, J.F. Silicone Hydrogels for Contact Lens Applications, *Trends Polym. Sci.*, 1996: **4**: 52–59.
11. Brennan, N.A., Coles, M.L. and Ang, J.H. An Evaluation of Silicone-Hydrogel Lenses Worn on a Daily Wear Basis, *Clin. Exp. Optom.*, 2006: **89**: 18–25.
12. Weikart, C.M., Matsuzawa, Y., Winterton, L. and Yasuda, H.K. Evaluation of Plasma Polymer-Coated Contact Lenses by Electrochemical Impedance Spectroscopy, *J. Biomed. Mater. Res.*, 2001: **54**: 597–607.
13. Weikart, C.M., Miyama, M. and Yasuda, H.K. Surface Modification of Conventional Polymers by Depositing Plasma Polymers of Trimethylsilane and of Trimethylsilane + O2, *J. Colloid Interface Sci.*, 1999: **211**: 28–38.
14. Iwata, J., Hoki, T. and Ikawa, S. (2004). Long Wearable Soft Contact Lens, US Patent Application No. 4004/0192872.
15. Maiden, A.C., Vanderlaan, D.G., Turner, D.C., et al. (2002). Hydrogel With Internal Wetting Agent, US Patent No. 6367929.
16. McCabe, K.P., Molock, F.F., Hill, G.A., et al. (2004). Biomedical Devices Containing Internal Wetting Agents, US Patent No. 6822016.
17. Tighe, B. (2004). Silicone Hydrogels: Structure, Properties and Behaviour, In: Sweeney, D.F. (ed.), *Silicone Hydrogels: Continuous Wear Contact Lenses*, Edinburgh, Butterworth-Heinemann, pp. 1–27.
18. Cheng, L. and Radke, C.J. Wettability of Silicone-Hydrogel Contact Lenses in the Presence of Tear-Film Components, *Curr. Eye Res.*, 2004: **28**: 93–108.
19. Ketelson, H.A., Meadows, D.L. and Stone, R.P. Dynamic Wettability Properties of a Soft Contact Lens Hydrogel, *Colloids Surf. B Biointerfaces*, 2005: **40**: 1–9.
20. Tonge, S., Jones, L., Goodall, S. and Tighe, B. The Ex Vivo Wettability of Soft Contact Lenses, *Curr. Eye Res.*, 2001: **23**: 51–59.
21. Willis, S.L., Court, J.L., Redman, R.P., et al. A Novel Phosphorylcholine-Coated Contact Lens for Extended Wear Use, *Biomaterials*, 2001: **22**: 3261–3272.
22. Tretinnikov, O.N. and Ikada, Y. Dynamic Wetting and Contact Angle Hysteresis of Polymer Surfaces Studies with the Modified Wilhelmy Balance Method, *Langmuir*, 1994: **10**: 1606–1614.
23. Lorentz, H., Rogers, R. and Jones, L. The Impact of Lipid on Contact Angle Wettability, *Optom. Vis. Sci.*, 2007: **84**: 946–953.
24. Maldonado-Codina, C. and Morgan, P.B. In Vitro Water Wettability of Silicone Hydrogel Contact Lenses Determined Using Sesile Drop and Captive Bubble Techniques, *J. Biomed. Mater. Res. A*, 2007: **83**: 496–502.
25. King-Smith, P.E., Fink, B.A., Hill, R.M., Koelling, K.W. and Tiffany, J.M. The Thickness of the Tear Film, *Curr. Eye Res.*, 2004: **29**: 357–368.
26. Uyama, Y., Inoue, H., Ito, K., Kishida, A. and Ikada, Y. Comparison of Different Methods for Contact Angle Measurement, *J. Colloid Interface Sci.*, 1991: **141**: 275–279.

27. Davies, J. and Davies, T. A General Equation for the Determination of the Dynamic Contact Angle of a Disc, *J Colloid Interface Sci*, 1993: **159**: 383–391.
28. Read, M.L., Kelly, J.M., Maldonado-Codina, C. and Morgan, P.B. (2008). Automated Contact Angle Measurements of a Curved Contact Lens Surface, In: *Poster Presented at 14th Symposium on the Material Science and Chemistry of Contact Lenses*, Astor Crowne Plaza Hotel, New Orleans, Louisiana, USA, 19–21 November.
29. Read, M.L., Morgan, P.B. and Maldonado-Codina, C. Measurement Errors Related to Contact Angle Analysis of Hydrogel and Silicone Hydrogel Contact Lenses, *J. Biomed. Mater. Res. Part B Appl. Biomater.*, 2009: **91**: 662–668.
30. Alvarez, N.J., Walker, L.M. and Anna, S.L. A Non-Gradient Based Algorithm for the Determination of Surface Tension from a Pendant Drop: Application to Low Bond Number Drop Shapes, *J Colloid Interface Sci*, 2009: **333**: 557–562.
31. Pence, N. Lens Material Enhancements: Different But the Same, *Contact Lens Spectrum*, 2008: **23**: 24.
32. Teichroeb, J.H., Forrest, J.A., Ngai, V., Martin, J.W., Jones, L. and Medley, J. Imaging Protein Deposits on Contact Lens Materials, *Optom. Vis. Sci.*, 2008: **85**: 1151–1164.
33. Rathore, O., Mahadevan, S., Molock, F., et al. (2008). Wettable Hydrogels Comprising Acyclic Polyamides, US Patent Application, US 2008/0045612 A1.
34. Brennan, N.A., Coles, M.-L.C., Connor, H.R.M. and McIlroy, R.G. A 12-Month Prospective Clinical Trial of Comfilcon A Silicone-Hydrogel Contact Lenses Worn on a 30-Day Continuous Wear Basis, *Cont. Lens Anterior Eye*, 2007: **30**: 108–118.
35. Lakkis, C. and Vincent, S. Clinical Investigation of Asmofilcon A Silicone Hydrogel Lenses, *Optom. Vis. Sci.*, 2009: **86**: 350–356.
36. Young, G., Riley, C.M., Chalmers, R.L. and Hunt, C. Hydrogel Lens Comfort in Challenging Environments and the Effect of Refitting with Silicone Hydrogel Lenses, *Optom. Vis. Sci.*, 2007: **84**: 302–308.

Appendix F

Comparison of lens parameters for the air-cured and nitrogen-cured study lenses

F.1 Aim

To investigate whether the the air-cured and nitrogen-cured study lenses differed in total diameter, base curve or centre thickness.

F.2 Method

Five air-cured and five nitrogen-cured study contact lenses were removed from their blister packaging and soaked for 24 hours in 0.9% PBS. The lens diameter and base curve were then assessed using an Optimec JCF (Optimec Ltd, UK) and the centre thickness measured using a Rehder ET-3 (Rehder Development Company, CA) following ISO 18369-3:2006 standards. The lenses were measured three times for each parameter. A linear regression model was constructed to compare the lens parameters for the two study lens types.

F.3 Results

Table F.1 shows the mean lens diameter, base curve and centre thickness values for the nitrogen-cured and air-cured lenses. No significant differences were observed between the air-cured and nitrogen-cured study lenses for any of the lens parameters assessed.

Table F.1: Mean parameters for the air-cured and nitrogen-cured study lenses (standard deviation in parenthesis).

	Nitrogen-cured	Air-cured lens	Significant difference?
Centre Thickness (microns)	75.07 (1.0)	75.33 (1.0)	**No** p=0.58, F=0.45
BOZR (mm)	8.34 (0.04)	8.35 (0.04)	**No** p=0.45, F=0.58
Lens Diameter (mm)	14.18 (0.04)	14.19 (0.03)	**No** p=0.64, F=0.23

F.4 Conclusion

The findings of this study clearly indicate that the physical parameters of the two study lens types do not differ significantly. This finding is perhaps expected given that the study lenses are manufactured from the same polymer and mould design. Differences in clinical performance between the two lens types are therefore unlikely to be attributed to differences in lens design.

References

Abbasi, F., Mirzadeh, H. & Katbab, A. (2001). Modification of polysiloxane polymers for biomedical applications: a review. *Polymer International*, **50**, 1279–1287. 340

Adamson, A.W. (1976). *Physical Chemistry of Surfaces*. Wiley-Interscience, New York, 3rd edn. 84

Alvarez, N.J., Walker, L.M. & Anna, S.L. (2009). A non-gradient based algorithm for the determination of surface tension from a pendant drop: application to low bond number drop shapes. *J Colloid Interface Sci*, **333**, 557–62. 184

Alvord, L., Court, J., Davis, T., Morgan, C.F., Schindhelm, K., Vogt, J. & Winterton, L. (1998). Oxygen permeability of a new type of high dk soft contact lens material. *Optom Vis Sci*, **75**, 30–6, 1040-5488 (Print) Journal Article. 51

Anantawaraskul, S. (2005). *Polymer analysis, polymer theory*. Advances in polymer science, Springer. 349

Andrade, J., Smith, L. & Gregonis, D. (1985a). *The contact angle and interface energetics*. Plenum Press, New York. 87

Andrade, J.D., Gregonis, D.E. & Smith, L.M. (1985b). Polymer surface dynamics. In J.D. Andrade, ed., *Surface and Interfacial Aspects of Biomedical Polymers*, vol. 1, 15, Plenum Press, New York. 47

Andrasko, G. & Ryen, K. (2008). Corneal staining and comfort observed with traditional and silicone hydrogel lenses and multipurpose solution combinations. *Optometry*, **79**, 444–54. 64

Andrasko, G.J. & Ryen, K.A. (2007). A series of evaluations of mps and silicone hydrogel lens combinations. *Review of Cornea Contact Lenses*, 36 – 42. 64

Assender, H., Bliznyuk, V. & Porfyrakis, K. (2002). How surface topography relates to materials properties. *Science*, **297**, 973–976. 103, 104

Atkinson, H., Riggs, P., Gibson, J., Warren, T., Dover, R., Williams, A., Cowden, J. & Gunner, M. (2008). Thermal curing methods and systems for forming contact lenses. 345

Austin, D.T.R. (2009). *An investigation of water and ion mobility in the aqeous phase of soft contact lens hydrogels*. Ph.D. thesis, Anglia Ruskin University. 191, 220

Baba, M. & Watanabe, T. (2005). Lens material for contact lens, contains compound(s) having ethylene-type unsaturated group and polydimethyl siloxane structure bonded through urethane bond, and pyrrolidone derivative(s) having methylene group as polymerizable group. 55, 56

Baguet, J., Sommer, F. & Duc, T. (1992). Imaging surfaces of hydrophilic contact lenses with atomic force microscopy. *Biomaterials*, **14**, 279–284. 111, 114, 279, 289, 300, 344

Baguet, J., Sommer, F., Claudon-Eyl, V. & Duc, T.M. (1995a). Characterization of lacrymal component accumulation on worn soft contact lens surfaces by atomic force microscopy. *Biomaterials*, **16**, 3–9, 0142-9612 (Print) Comparative Study Journal Article Research Support, Non-U.S. Gov't. 104, 111, 112, 114, 120, 287, 288

Baguet, J., Sommer, F., Claudon-Eyl, V. & Duc, T.M. (1995b). Characterization of lacrymal component accumulation on worn soft contact lens surfaces by atomic force microscopy. *Biomaterials*, **16**, 3–9. 343, 344

Bambury, R. & Seelye, D. (1991). Novel vinyl carbonate and vinyl carbamate contact lens material monomers. *US Patent 5,070,215*. 51

Barbieri, R., Quaglia, M., Delfini, M. & Brosio, E. (1998). Investigation of water dynamic behaviour in poly(hema) and poly(hema-co-dhpma) hydrogels by proton t2 relaxation time and self-diffusion coefficient n.m.r. measurements. *Polymer*, **39**, 1059–1066. 115

Baselt, D. (1993). *The tip-sample interaction in atomic force microscopy and its implications for biological applications*. Ph.D. thesis. 14, 110

Bates, F., FS (1991). Polymer-polymer phase-behavior. *Science*, **251**, 898–905. 288, 323

Bennett, J. (1992). Recent developments in surface-roughness characaterisation. *Measurement Science Technology*, **3**, 1119–1127. 104

Binning, G., Quate, C. & Gerber, C. (1986). Atomic force microscopy. *Phys Rev Lett*, **56**, 930–933. 106

Biswal, D. & Hilt, J.Z. (2009). Analysis of oxygen inhibition in photopolymerizations of hydrogel micropatterns using ftir imaging. *Macromolecules*, **42**, 973–979. 81, 82, 226, 272, 333, 344, 345

Bland, J.M. & Altman, D.G. (1986). Statistical methods for assessing agreement between two methods of clinical measurement. *Lancet*, **1**, 307–10, 0140-6736 (Print) Clinical Trial Comparative Study Journal Article Randomized Controlled Trial. 162, 163, 177

Bland, J.M. & Altman, D.G. (1996). Statistics notes: Measurement error. *BMJ*, **313**, 744. 158

Blau, P.J. (2009). *Friction science and technology: from concepts to applications*. CRC Press, Boca Raton, FL, 2nd edn. 328

Borazjani, R.N., Levy, B. & Ahearn, D.G. (2004). Relative primary adhesion of pseudomonas aeruginosa, serratia marcescens and staphylococcus aureus to hema-type contact lenses and an extended wear silicone hydrogel contact lens of high oxygen permeability. *Cont Lens Anterior Eye*, **27**, 3–8, 1367-0484 (Print) Journal Article. 113

Bousquet, A., Pannier, G., Ibarboure, E., Papon, E. & Rodriguez-Hernandez, J. (2007). Control of the surface properties in polymer blends. *Journal of Adhesion*, **83**, 335–349. 224, 329

Braun, R., Blenkinsopp, P., Mullock, S., Corlett, C., Willey, K., Vickerman, J. & Winograd, N. (1998). Performance characteristics of a chemical imaging time-of-flight mass spectrometer. *Rapid Communications In Mass Spectrometry*, **12**, 1246–+. 245

Braun, R.M., Ingham, S.J., Harmon, P.S. & Hook, D.J. (2007). Surface and depth profile investigation of a phosphorylcholine-based contact lens using time of flight secondary ion mass spectrometry. *J. Vac. Sci. Technol.*, **25**, 866–871. 261, 271, 273

Brennan, N.A. (1988). A survey of wearers of low water content hydrogel contact lenses. *J Clinical and Experimental Optometry*, **71**, 86–90. 65, 66, 149

Brennan, N.A. (2009). Key factors influencing contact lens comfort, presented at AAO 2009 - Orlando. 66, 336

Brennan, N.A. & Morgan, P.B. (2009). Clinical highs and lows of dk/t. part 2 - modulus, design and surface - more than just fresh air. *Optician*, 16 – 20. 65, 335

Brennan, N.A., Coles, M.L., Comstock, T.L. & Levy, B. (2002). A 1-year prospective clinical trial of balafilcon a (purevision) silicone-hydrogel contact lenses used on a 30-day continuous wear schedule. *Ophthalmology*, **109**, 1172–7, 0161-6420 (Print) Clinical Trial Comparative Study Evaluation Studies Journal Article Multicenter Study Randomized Controlled Trial Research Support, Non-U.S. Gov't. 64, 142, 220

Brennan, N.A., Coles, M.L. & Ang, J.H. (2006). An evaluation of silicone-hydrogel lenses worn on a daily wear basis. *Clin Exp Optom*, **89**, 18–25, 0816-4622 (Print) Comparative Study Journal Article Multicenter Study Randomized Controlled Trial Research Support, Non-U.S. Gov't. 65, 158

Brennan, N.A., Coles, M.L.C., Connor, H.R.M. & McIlroy, R.G. (2007). A 12-month prospective clinical trial of comfilcon a silicone-hydrogel contact lenses worn on a 30-day continuous wear basis. *Cont Lens Anterior Eye*, **30**, 108–18. 61, 144, 193, 327, 335

Broad, R.A. (2009). Contact lens are formed of a composition comprising reaction product of silicone-containing monomer; 3-methacryloxypropyl tris(trimethylsiloxy)silane; n-vinyl pyrrolidone; and other non-ionic hydrophilic monomer. 56

Brook, M.A. (2000). *Silicon in organic, organometallic, and polymer chemistry*. J. Wiley. 46, 47

Bruce, A.S., Mainstone, J.C. & Golding, T.R. (2001). Analysis of tear film breakup on etafilcon a hydrogel lenses. *Biomaterials*, **22**, 3249–56, 0142-9612 (Print) Comparative Study Journal Article. 67

Bruinsma, G., Rustema-Abbing, M. & Vries, J.D. (2003). Multiple surface properties of worn rgp lenses and adhesion of pseudomonas aeruginosa. *Biomaterials*. 344

Bruinsma, G.M., van der Mei, H.C. & Busscher, H.J. (2001). Bacterial adhesion to surface hydrophilic and hydrophobic contact lenses. *Biomaterials*, **22**, 3217–24, 0142-9612 (Print) In Vitro Journal Article. 19, 114, 168, 171, 220, 287, 344

Bruinsma, G.M., Rustema-Abbing, M., de Vries, J., Stegenga, B., van der Mei, H.C., van der Linden, M.L., Hooymans, J.M. & Busscher, H.J. (2002). Influence of wear and overwear on surface properties of etafilcon a contact lenses and adhesion of pseudomonas aeruginosa. *Invest Ophthalmol Vis Sci*, **43**, 3646–53, 0146-0404 (Print) Journal Article. 112, 114, 120, 231, 339

Cain, J.B., Francis, D.W., Venter, R.D. & Neumann, A.W. (1983). Dynamic contact angles on smooth and rough surfaces. *Journal of Colloid and Interface Science*, **94**, 123. 90

Carnt, N., Jalbert, I., Stretton, S., Naduvilath, T. & Papas, E. (2007). Solution toxicity in soft contact lens daily wear is associated with corneal inflammation. *Optom Vis Sci*, **84**, 309–15. 64

Chen, H., Chen, Y., Sheardown, H. & Brook, M. (2005). Immobilization of heparin on a silicone surface through a heterobifunctional peg spacer. *Biomaterials*, **26**, 7418–7424. 331

Chen, J. & Gardella, J.A. (1998). Solvent effects on the surface composition of poly(dimethylsiloxane)-co-polystyrene/polystyrene blends. *Macromolecules*, **31**, 9328–9336. 252

Chen, L. (2008). *X-ray photoelectron spectroscopy studies of water-induced surface reorganization of amphiphilic poly(2-hydroxyethyl methacrylate-g-dimethylsiloxane) copolymers using cryogenic sample handling techniques*. Ph.D. thesis, The State University of New York at Buffalo. 260

Chen, L., Hook, D.J., Paul L. Valint, J.J.A.G. & Jr (2008). X-ray photoelectron spectroscopy studies of water-induced surface reorganization of amphiphilic poly(2-hydroxyethyl methacrylate-g-dimethylsiloxane) copolymers using cryogenic sample han-

dling techniques. *Journal of Vacuum Science Technology A: Vacuum, Surfaces, and Films*, **26**, 616–623. 252

Chen, Q., Zhang, D., Somorjai, G. & Bertozzi, C. (1999). Probing the surface structural rearrangement of hydrogels by sum-frequency generation spectroscopy. *J. Am. Chem. Soc.* 348

Chen, X. & Gardella, J. (1994). Surface modification of polymers by blending siloxane block-copolymers. *Macromolecules*, **27**, 3363–3369. 323

Cheng, L., Muller, S.J. & Radke, C.J. (2004). Wettability of silicone-hydrogel contact lenses in the presence of tear-film components. *Curr Eye Res*, **28**, 93–108, 0271-3683 (Print) Journal Article. 33, 72, 74, 90, 91, 92, 122, 168, 175, 189, 191, 204, 207, 231, 330, 333, 334, 337, 338

Cheung, S., Cho, P., Chan, B., Choy, C. & Ng, V. (2007a). A comparative study of biweekly disposable contact lenses: silicone hydrogel versus hydrogel. *Clinical and Experimental Optometry*, **90**, 124–131. 73

Cheung, S.w., Cho, P., Chan, B., Choy, C. & Ng, V. (2007b). A comparative study of biweekly disposable contact lenses: silicone hydrogel versus hydrogel. *Clinical and Experimental Optometry*, **90**, 124–131. 62

Cho, P., Ho, K.Y., Huang, Y.C., Chui, H.Y. & Kwan, M.C. (2004). Comparison of noninvasive tear break-up time measurements from black and white background instruments. *Optom Vis Sci*, **81**, 436–41, 1040-5488 (Print) Comparative Study Journal Article. 67

Colas, A. & Curtis, J. (2004). *Biomaterials Science: An Introduction to Materials in Medicine*, chap. 7.19 - Medical applications of silicones, 697–707. Elsevier. 31

Coles-Brennan, C., Brennan, N., Connor, H. & McIlroy, R. (2006). Do silicone-hydrogels really solve end-of-day comfort problems? *Invest Ophthalmol Vis Sci*, **47**. 65

Colliver, T., Brummel, C., Pacholski, M., Swanek, F., Ewing, A. & Winograd, N. (1997). Atomic and molecular imaging at the single-cell level with tof-sims. *Anal Chem*, **69**, 2225–2231. 341

Cordeiro, A.L., Nitschke, M., Janke, A., Helbig, R., D'Souza, F., Donnelly, G.T., Willemsen, P.R. & Werner, C. (2009). Fluorination of poly(dimethylsiloxane) surfaces by low pressure cf4 plasma – physicochemical and antifouling properties. *eXPRESS Polymer Letters*, **3**, 70–83. 332

Cotton, N., Bartle, K. & Clifford, A. (1991). Analysis of low molecular weight constituents of polypropylene and other polymeric materials using on-line sfe-sfc. *Journal of High Resolution Chromatography*. 221

Covey, M., Sweeney, D.F., Terry, R., Sankaridurg, P.R. & Holden, B.A. (2001). Hypoxic effects on the anterior eye of high-dk soft contact lens wearers are negligible. *Optom Vis Sci*, **78**, 95–9, 1040-5488 (Print) Clinical Trial Journal Article Research Support, Non-U.S. Gov't. 59

Cowie, J. (1991). *Polymers: chemistry physics of modern materials*. Blackie academic professional, Glasgow, second edition edn. 13, 38

Curtis, A. & Wilkinson, C. (1997). Topographical control of cells. *Biomaterials*, **18**, 1573–1583. 104

Dalton, K., Subbaraman, L.N., Rogers, R. & Jones, L. (2008). Physical properties of soft contact lens solutions. *Optom Vis Sci*, **85**, 122–8. 76

Danilatos, G.D. (1988). Foundations of environmental scanning electron-microscopy. *Advances In Electronics and Electron Physics*, **71**, 109–250. 120

Danilatos, G.D. (1990). Theory of the gaseous detector device in the environmental scanning electron microscope. *Advances in electronic and electron physics*, **78**, 1–102. 120

Dart, J., Radford, C., Minassian, D., Verma, S. & Stapleton, F. (2008). Risk factors for microbial keratitis with contemporary contact lenses: A case-control study. *Ophthalmology*, **115**, 1647–54. 63

Decker, C. & Jenkins, A.D. (1985). Kinetic approach of oxygen inhibition in ultraviolet- and laser-induced polymerizations. *Macromolecules*, **18**, 1241–1244. 325, 344

Deg, J.K. & Binder, P.S. (1986). Electron microscopic features of never-worn soft contact lenses: deposits or artifacts? *Curr Eye Res*, **5**, 27–36, 0271-3683 (Print) Comparative Study Journal Article. 122, 320

Dillehay, S.M. (2007). Does the level of available oxygen impact comfort in contact lens wear?: A review of the literature. *Eye Contact Lens*, **33**, 148–55. 65

Dilly, P.N. (1994). Structure and function of the tear film. *Adv Exp Med Biol*, **350**, 239–47, 0065-2598 (Print) Journal Article Review. 72

Donshik, P.C., Ehlers, W.H. & Ballow, M. (2008). Giant papillary conjunctivitis. *Immunology and Allergy Clinics of North America*, **28**, 83–103. 147

Dumbleton, K. (2003). Noninflammatory silicone hydrogel contact lens complications. *Eye Contact Lens*, **29**, S186–9, 1542-2321 (Print) Journal Article Review. 60

Dumbleton, K., Jones, L., Chalmers, R., Williams-Lyn, D. & Fonn, D. (2000). Clinical characterization of spherical post-lens debris associated with lotrafilcon high-dk silicone lenses. *Clao J*, **26**, 186–92, 0733-8902 (Print) Comparative Study Evaluation Studies Journal Article Research Support, Non-U.S. Gov't. 61

Dumbleton, K., Keir, N., Moezzi, A., Feng, Y., Jones, L. & Fonn, D. (2006). Objective and subjective responses in patients refitted to daily-wear silicone hydrogel contact lenses. *Optom Vis Sci*, **83**, 758–68. 64, 142

Dumbleton, K., Woods, C., Jones, L., Richter, D. & Fonn, D. (2010). Comfort and vision with silicone hydrogel lenses: effect of compliance. *Optom Vis Sci*, **87**, 421–5. 64

Dumbleton, K.A., Chalmers, R.L., Richter, D.B. & Fonn, D. (2001). Vascular response to extended wear of hydrogel lenses with high and low oxygen permeability. *Optom Vis Sci*, **78**, 147–51. 146

Dumbleton, K.A., Chalmers, R.L., McNally, J., Bayer, S. & Fonn, D. (2002). Effect of lens base curve on subjective comfort and assessment of fit with silicone hydrogel continuous wear contact lenses. *Optom Vis Sci*, **79**, 633–7, 1040-5488 (Print) Journal Article Research Support, Non-U.S. Gov't. 59, 60, 65

Dumbleton, K.A., Woods, C.A., Jones, L.W. & Fonn, D. (2008). Comfort and adaptation to silicone hydrogel lenses for daily wear. *Eye Contact Lens*, **34**, 215–23. 64, 65, 73

Edmondson, L. & Edmondson, W. (2003). Masking astigmatism: Ciba focus night and day vs focus monthly. *Optom Vis Sci*, **80**, 184. 59

Epstein, A. (2002). Spk with daily wear of silicone hydrogel lenses and mps. *Contact Lens Spectrum*, **17**, 30. 63

Faber, E., Golding, T.R., Lowe, R. & Brennan, N.A. (1991). Effect of hydrogel lens wear on tear film stability. *Optom Vis Sci*, **68**, 380–4. 146

Fakes, D., Davies, M., Brown, A. & Newton, J. (1988). The surface analysis of a plasma modified contact lens surface by ssims. *Surface and Interface Analysis*, **13**, 233–236. 103, 339, 343

Fanti, P. & Holly, F.J. (1980). Silicone contact lens wear. ii. clinical experience. *Eye Contact Lens*, **6**, 25–32. 145

Fatt, I. (1984). Prentice medal lecture: contact lens wettability–myths, mysteries, and realities. *Am J Optom Physiol Opt*, **61**, 419–30, 0093-7002 (Print) Journal Article. 77, 84, 85, 87, 88

Fatt, I. & Chaston, J. (1982). Relation of oxygen transmissibility to oxygen tension or eop under the lens. *Int. Contact Lens Clin.*, **9**. 31

Flemming, C., Austen, R. & Davies, S. (1994). Pre-corneal deposits during soft contact lens wear. *Optom Vis Sci*, **71**, 152–153. 61

Fonn, D. (2007). Targeting contact lens induced dryness and discomfort: what properties will make lenses more comfortable. *Optom Vis Sci*, **84**, 279–85. 64, 71, 350

Fonn, D. & Dumbleton, K. (2003). Dryness and discomfort with silicone hydrogel contact lenses. *Eye Contact Lens*, **29**, S101–4; discussion S115–8, S192–4. 65

Fonn, D. & Pritchard, N. (2000). Factors affecting the success of silicone hydrogels. In D.F. Sweeney, ed., *Silicone Hydrogels: The Rebirth of Continuous Wear Contact Lenses*, 214–234, Butterworth-Heinemann, Oxford. 59, 61, 65

Fonn, D., Situ, P. & Simpson, T. (1999). Hydrogel lens dehydration and subjective comfort and dryness ratings in symptomatic and asymptomatic contact lens wearers. *Optom Vis Sci*, **76**, 700–4. 64, 66, 149

Fowler, S. & Allansmith, M. (1980). The surface of the continuously worn contact lens. *Archives of Ophthalmology*, **98**, 1980. 114

Franklin, V., Bright, A. & Tighe, B. (1993). Hydrogel polymers and ocular spoilation processes. *Trends Polym Sci*, **1**, 9. 114

French, K. (2005). Contact lens materials: Part 1 - wettability. *Optician*, **230**, 20–28. 32, 72, 75

Garofalo, R.J., Dassanayake, N., Carey, C., Stein, J., Stone, R. & David, R. (2005). Corneal staining and subjective symptoms with multipurpose solutions as a function of time. *Eye Contact Lens*, **31**, 166–74. 63, 64

Garrett, Q., Garrett, R.W. & Milthorpe, B.K. (1999). Lysozyme sorption in hydrogel contact lenses. *Invest Ophthalmol Vis Sci*, **40**, 897–903. 339

Gauthier, M., Stangel, I. & Ellis, T. (2005). Oxygen inhibition in dental resins. *Journal of Dental Research*. 345

Gaylord, N. (1974). Method for correcting visual defects, compositions and articles of manufacture useful therein. 48

Gellatly, K.W., Brennan, N.A. & Efron, N. (1988). Visual decrement with deposit accumulation of hema contact lenses. *Am J Optom Physiol Opt*, **65**, 937–41. 62

Giraldez, M.J., Resua, C.G., Lira, M., Oliveira, M.E.C.D.R., Magariños, B., Toranzo, A.E. & Yebra-Pimentel, E. (2010). Contact lens hydrophobicity and roughness effects on bacterial adhesion. *Optom Vis Sci*, **87**, E426–31. 63, 105, 343, 344

Goldbeck-Wood, G., Bliznyuk, V., Burlakov, V., Assender, H., Briggs, G., Tsukahara, Y., Anderson, Y. & Windle, A. (2002). Surface structure of amorphous polystyrene: Comparison of sfm imaging and lattice chain simulations. *Macromolecules*, **35**, 5283–5289. 104

Golding, T.R., Bruce, A.S., Gaterell, L.L., Little, S.A. & Macnamara, J. (1995a). Soft lens movement: Effect of blink rate on lens settling. *Acta Ophthalmologica Scandinavica*, **73**, 506–511. 144

Golding, T.R., Harris, M.G., Smith, R.C. & Brennan, N.A. (1995b). Soft lens movement: effects of humidity and hypertonic saline on lens settling. *Acta Ophthalmologica Scandinavica*, **73**, 139–144. 144

Gonzalez-Meijome, J., Lopez-Alemany, A., Almeida, J., Parafita, M. & Refojo, M.F. (2005). Microscopic observations of unworn siloxane-hydrogel soft contact lenses by atomic force microscopy. *J Biomed Mater Res Part B: Appl Biomater*, **76B**, 412–418. 19, 51, 111, 112, 113, 121, 287, 299

González-Méijome, J.M., López-Alemany, A., Almeida, J.B., Parafita, M.A. & Refojo, M.F. (2006a). Microscopic observation of unworn siloxane-hydrogel soft contact lenses by atomic force microscopy. *J Biomed Mater Res B Appl Biomater*, **76**, 412–8. 51, 54, 299, 344

González-Méijome, J.M., López-Alemany, A., Almeida, J.B., Parafita, M.A. & Refojo, M.F. (2006b). Microscopic observations of superficial ultrastructure of unworn siloxane-hydrogel contact lenses by cryo-scanning electron microscopy. *J Biomed Mater Res B Appl Biomater*, **76**, 419–23. 316, 321, 346

González-Méijome, J.M., López-Alemany, A., Almeida, J.B. & Parafita, M.A. (2009). Surface afm microscopy of unworn and worn samples of silicone hydrogel contact lenses. *J Biomed Mater Res B Appl Biomater*, **88**, 75–82. 122, 220, 299, 343, 344

Good, R. (1992). Contact-angle, wetting, and adhesion - a critical review. *Journal of Adhesion Science and Technology*, **6**, 1269–1302. 86

Green-Church, K.B. & Nichols, J.J. (2008). Mass spectrometry-based proteomic analyses of contact lens deposition. *Mol Vis*, **14**, 291–7. 231, 343

Griesser, H.J., Meijs, G. & Mcausian, B. (1990). Xps analysis of acid etched poly (2-hydroxyethyl methacrylate) surfaces. *Journal of Bioactive and Compatible Polymers*, **5**, 179–193. 221, 339

Grobe, G.I. & Kunzler, J. (1999). Silicone hydrogels for contact lens applications. *Polymeric Materials Science and Engineering*, 108–109. 51

Grobe, G.I., Valiant, P. & Ammon, D. (1996). Surface chemical structure for soft contact lenses as a function of polymer processing. *Journal of Biomedical Materials Research*, **32**, 45–54. 20, 41, 95, 111, 122, 142, 221, 299, 300

Guillon, J.P., Guillon, M. & Malgouyres, S. (1990). Corneal desiccation staining with hydrogel lenses: tear film and contact lens factors. *Ophthalmic Physiol Opt*, **10**, 343–50. 145

Guillon, M. (1994). *Contact Lens Pracice*. Chapman Hall, London. 44, 68, 71

Guillon, M. & Maissa, C. (2007). Use of silicone hydrogel material for daily wear. *Cont Lens Anterior Eye*, **30**, 5–10, 1367-0484 (Print) Journal Article. 73, 74, 75, 124, 142, 328

Guillon, M., Allary, J.C., Guillon, J.P. & Orsborn, G. (1992). Clinical management of regular replacement: Part i. selection of replacement frequency. *International Contact Lens Clinic*, **19**, 104. 71, 75

Guillon, M., Styles, E., Guillon, J.P. & Maissa, C. (1997). Preocular tear film characteristics of nonwearers and soft contact lens wearers. *Optometry & Vision Science*, **74**. 173

Guillon, M., Maissa, C., Garofalo, R.J., Lemp, J.M. & Deng, L. (2009). Determination of lipid deposition on contact lenses worn extended wear. *Optometry - Journal of the American Optometric Association*, **80**, 291 – 291. 145

Guryca, V., Hobzová, R., Prádný, M., Sirc, J. & Michálek, J. (2007). Surface morphology of contact lenses probed with microscopy techniques. *Cont Lens Anterior Eye*, **30**, 215–22. 19, 287, 299, 316, 320, 321, 343, 344

Ha, C. & Gardella, J. (2005). X-ray photoelectron spectroscopy studies on the surface segregation in poly(dimethylsiloxane) containing block copolymers. *Journal of Macromolecular Science-Polymer Reviews*, **C45**, 1–18. 323

Haddad, M. (2010). *An investigation of in vivo contact lens wettability*. Ph.D. thesis, The University of Manchester. 74, 338

Hagmann, P., Heinrich, A. & Hoerner, W. (2003). Plastic casting molds. 327, 345

Hall, B., Jones, S., Young, G. & Coleman, S. (1999). The on-eye dehydration of proclear compatibles lenses. *CLAO J*, **25**, 233–7. 65

Hamilton, W. (1972). A technique for the characterization of hydrophilic solid surfaces. *Journal of Colloid and Interface Science*, **40**, 219–222. 337

Hart, D.E., DePaolis, M., Ratner, B.D. & Mateo, N.B. (1993). Surface analysis of hydrogel contact lenses by esca. *Clao J*, **19**, 169–73, 0733-8902 (Print) Comparative Study Journal Article Research Support, U.S. Gov't, P.H.S. 221

Harvitt, D.M. & Bonanno, J.A. (1999). Re-evaluation of the oxygen diffusion model for predicting minimum contact lens dk/t values needed to avoid corneal anoxia. *Optom Vis Sci*, **76**, 712–9. 45

Henriques, M., Sousa, C., Lira, M., Elisabete, M., Oliveira, R., Oliveira, R. & Azeredo, J. (2005). Adhesion of pseudomonas aeruginosa and staphylococcus epidermidis to silicone-hydrogel contact lenses. *Optom Vis Sci*, **82**, 446–50. 63

Hiratani, H., Baba, M., Yasui, T., Ito, E. & Yung, L. (2003). Surface wettability improvement of silicone elastomers synthesized with water-soluble polyacrylic acid molds. *Journal of Applied Polymer Science*, **89**, 3786–3789. 204

Hirji, N., Patel, S. & Callander, M. (1989). Human tear film pre-rupture phase time (tp-rpt)–a non-invasive technique for evaluating the pre-corneal tear film using a novel keratometer mire. *Ophthalmic Physiol Opt*, **9**, 139–42, 0275-5408 (Print) Journal Article. 67

Hoffman, A.S. & Ratner, B.D. (2004). *Biomaterials science: an introduction to materials in medicine*. Academic Press, 2nd edn. 82, 83

Holden, B.A. & Mertz, G.W. (1984). Critical oxygen levels to avoid corneal edema for daily and extended wear contact lenses. *Invest Ophthalmol Vis Sci*, **25**, 1161–7, 0146-0404 (Print) Journal Article Research Support, Non-U.S. Gov't. 31, 45

Holden, B.A., Pain, P. & Zantos, S. (1974). Observations on sem of hydrohphilic contact lenses. *Aust J Optom*, **57**, 100–106. 120, 320

Holden, B.A., Williams, L., Sweeney, D.F. & Swarbrick, H.A. (1986). The endothelial response to contact lens wear. *Clao J*, **12**, 150–2, 0733-8902 (Print) Journal Article. 43

Holden, B.A., Stephenson, A., Stretton, S., Sankaridurg, P.R., O'Hare, N., Jalbert, I. & Sweeney, D.F. (2001). Superior epithelial arcuate lesions with soft contact lens wear. *Optom Vis Sci*, **78**, 9–12, 1040-5488 (Print) Journal Article Research Support, Non-U.S. Gov't Review. 60

Holly, F.J. (1981). Tear film physiology and contact lens wear. i -pertinent aspects of tear film physiology. *Am J Optom Physiol Opt*, **58**, 330–42. 67

Holly, F.J. & Refojo, M.F. (1975). Wettability of hydrogels. i. poly (2-hydroxyethyl methacrylate). *J Biomed Mater Res*, **9**, 315–26, 0021-9304 (Print) Journal Article Research Support, U.S. Gov't, P.H.S. 16, 32, 83, 87, 192, 252, 268, 332, 343, 348

Holly, F.J. & Refojo, M.F. (1976). *Water wettability of protein adsorbed at the hydrogel-water interface*, 267–282. ACS Symposium. 74

Hook, D., Valint, P., Chin, L. & Gardella, J. (2006). Quantitative and high mass tof-sims studies of siloxane segregation in hydrogel polymers using cryogenic sample handling techniques. *Applied Surface Science*, **252**, 6679–6682. 102, 211, 246, 252, 261, 339

Hook, D.J., Chen, L., Valint, P.L. & Gardella, J.A. (2009). Time of flight secondary ion mass spectroscopy studies of poly(allyl methacrylate-g-dimethylsiloxane) copolymers using cryogenic sample handling techniques: Effects of hydration on surface chemical structure and surface chain length distribution. *J Vac Sci Technol A*, **27**, 1281–1288. 333, 341

Hui, A., Boone, A. & Jones, L. (2008). Uptake and release of ciprofloxacin-hcl from conventional and silicone hydrogel contact lens materials. *Eye Contact Lens*, **34**, 266–71. 64, 299

Huraux, K., Narita, T., Fretigny, C. & Lequeux, F. (2007). Solution drying and phase separation morphology of polyacrylamide/poly(ethylene glycol)/water system. *Macromolecules*, **40**, 8336–8341. 348

Huth, S. & Wagner, H. (1981). Identification and removal of deposits on polydimethylsiloxane silicone elastomer lenses. *Int Contact Lens Clin*, 19–26. 33, 47, 62, 145, 231

Hwang, S.T., Tang, T.E.S. & Kammermeyer, K. (1971). Transport of dissolved oxygen through silicone rubber membrane. *Journal of Macromolecular Science, Part B,*, **5**, 1–10. 31

Ilhan, B., Irkec, M., Orhan, M. & Celik, H. (1998). Surface deposits on frequent replacement and conventional daily wear soft contact lenses: a scanning electron microscopic study. *Clao J*, **24**, 232–5, 0733-8902 (Print) Clinical Trial Comparative Study Controlled Clinical Trial Journal Article. 121

Iwata, J., Hoki, T. & Ikawa, S. (2001). Soft contact lens capable of being worn for a long period. 33, 55, 158

Jalbert, I., Sweeney, D.F. & Holden, B.A. (2001). Epithelial split associated with wear of a silicone hydrogel contact lens. *Clao J*, **27**, 231–3, 0733-8902 (Print) Case Reports Journal Article Research Support, Non-U.S. Gov't. 60

J.C. Vickerman, D.B. & Henderson, A. (2006). The static sims library version 4. Cd-rom, SurfaceSpectra. 266

Johnson, R. & Dettre, R. (1993). Wetting of low-energy surfaces. In J. Berg, ed., *Wettability*, 1–74, CRC Press, New York, 1st edn. 32, 210, 254

Jones, L. & Dumbleton, K. (2002). silicone hydrogel lenses: Fitting procedures and in-practice protocols for continuous wear lenses. *Optician*, **223**, 37–45. 60

Jones, L. & French, K. (2009). A decade with silicone hydrogels: Part 2. 1–10. 61, 75, 334

Jones, L., Evans, K., Sariri, R., Franklin, V. & Tighe, B. (1997a). Lipid and protein deposition of n-vinyl pyrrolidone-containing group ii and group iv frequent replacement contact lenses. *Clao J*, **23**, 122–6, 0733-8902 (Print) Clinical Trial Journal Article Randomized Controlled Trial. 98

Jones, L., Jones, D. & Houlford, M. (1997b). Clinical comparison of three polyhexanide-preserved multi-purpose contact lens solutions. *Cont Lens Anterior Eye*, **20**, 23–30, 1367-0484 (Print) Journal Article. 299

Jones, L., Fcoptom, Mann, A., Evans, K., Franklin, V. & Tighe, B. (2000). An in vivo comparison of the kinetics of protein and lipid deposition on group ii and group iv frequent-replacement contact lenses. *Optom Vis Sci*, **77**, 503–10. 62

Jones, L., MacDougall, N. & Sorbara, L.G. (2002a). Asymptomatic corneal staining associated with the use of balafilcon silicone-hydrogel contact lenses disinfected with a polyaminopropyl biguanide-preserved care regimen. *Optom Vis Sci*, **79**, 753–61. 63, 64, 299

Jones, L., May, C., Nazar, L. & Simpson, T. (2002b). In vitro evaluation of the dehydration characteristics of silicone hydrogel and conventional hydrogel contact lens materials. *Cont Lens Anterior Eye*, **25**, 147–56, 1367-0484 (Print) Journal Article. 59, 65, 116

Jones, L., Senchyna, M., Glasier, M.A., Schickler, J., Forbes, I., Louie, D. & May, C. (2003). Lysozyme and lipid deposition on silicone hydrogel contact lens materials. *Eye Contact Lens*, **29**, S75–9, 1542-2321 (Print) Comparative Study Journal Article Research Support, Non-U.S. Gov't. 32, 62, 145

Jones, L., Subbaraman, L., Rogers, R. & Dumbleton, K. (2006). Surface treatment, wetting and modulus of silicone hydrogels. *Optician*, **232**, 28–34. 32, 33, 59, 73, 92, 158, 173, 205, 335

Karlgard, C.C.S., Sarkar, D.K., Jones, L.W., Moresoli, C. & Leung, K.T. (2004). Drying methods for xps analysis of purevision(tm), focus(r) nightday(tm) and conventional hydrogel contact lenses. *Applied Surface Science*, **230**, 106. 73, 95, 122, 213, 215, 219, 220, 221, 339

Keay, L., Sweeney, D.F., Jalbert, I., Skotnitsky, C. & Holden, B.A. (2000). Microcyst response to high dk/t silicone hydrogel contact lenses. *Optom Vis Sci*, **77**, 582–5, 1040-5488 (Print) Clinical Trial Comparative Study Journal Article Randomized Controlled Trial Research Support, Non-U.S. Gov't. 59

Keay, L., Willcox, M.D., Sweeney, D.F., Morris, C.A., Harmis, N., Corrigan, K. & Holden, B.A. (2001). Bacterial populations on 30-night extended wear silicone hydrogel lenses. *CLAO J*, **27**, 30–4. 63

Ketelson, H.A., Meadows, D.L. & Stone, R.P. (2005). Dynamic wettability properties of a soft contact lens hydrogel. *Colloids and Surfaces B: Biointerfaces*, **40**, 1–9. 338

Kim, H., Ju, H. & Hong, J. (2003). Characterization of uv-cured polyester acrylate films containing acrylate functional polydimethylsiloxane. *European Polymer Journal*, **39**, 2235–2241. 345

Kim, J., Marmo, C. & Somorjai, G.A. (2001). Friction studies of hydrogel contact lenses using afm: non-crosslinking polymers of low friction at the surface. *Biomaterials*, **22**, 3285–3294. 116, 288, 328

Kim, S.H., Opdahl, A., Marmo, C. & Somorjai, G.A. (2002). Afm and sfg studies of phema-based hydrogel contact lens surfaces in saline solution: adhesion, friction, and the presence of non-crosslinked polymer chains at the surface. *Biomaterials*, **23**, 1657–66, 0142-9612 (Print) Journal Article Research Support, Non-U.S. Gov't Research Support, U.S. Gov't, Non-P.H.S. 252, 287, 333, 343, 345, 350

Kingshott, P., St John, H., Chatelier, R. & Griesser, H.J. (1997). Study of protein adsorption onto polysaccharide contact lens coatings by maldi-tof-ms and xps. *Abstr Pap Am Chem Soc*, 48. 343

Kodjikian, L., Casoli-Bergeron, E., Malet, F., Janin-Manificat, H., Freney, J., Burillon, C., Colin, J. & Steghens, J.P. (2008). Bacterial adhesion to conventional hydrogel and new silicone-hydrogel contact lens materials. *Graefes Arch Clin Exp Ophthalmol*, **246**, 267–73. 63

Koffas, T.S., Amitay-Sadovsky, E., Kim, J. & Somorjai, G.A. (2004). Molecular composition and mechanical properties of biopolymer interfaces studied by sum frequency generation vibrational spectroscopy and atomic force microscopy. *J Biomater Sci Polym Ed*, **15**, 475–509, 0920-5063 (Print) Journal Article Research Support, Non-U.S. Gov't Research Support, U.S. Gov't, Non-P.H.S. 115, 116, 287, 288, 332, 342

Kohler, J. & Flanagan, G. (1985). Clinical dehydration of extended wear contact lenses. *Int Contact Lens Clinic*, **12**, 152. 116

Korb, D.R., Greiner, J.V., Herman, J.P., Hebert, E., Finnemore, V.M., Exford, J.M., Glonek, T. & Olson, M.C. (2002). Lid-wiper epitheliopathy and dry-eye symptoms in contact lens wearers. *CLAO J*, **28**, 211–6. 33, 148, 328

Kuk, Y. & Silverman, P. (1989). Scanning tunnelling microscope instrumentation. *Rev. Istrum.*, **60**, 165. 106

Kunzler, J. (1996). Silicone hydrogels for contact lens applications. *Trends Polym Sci*, **4**, 52–59. 32, 33, 158, 170

Kunzler, J. & Ozark, R. (1994). Fluorosilicone hydrogels. 51, 77

Kunzler, J. & Seelye, D. (2007). Hydrogel that is hydrated polymerization product of monomer mixture, comprising hydrophilic monomer, and of vinyl carbonate end-capped polysiloxane containing fluorinated side chain, useful for contact lenses, and medical devices. 77

Lai, Y.C. & Friends, G.D. (1997). Surface wettability enhancement of silicone hydrogel lenses by processing with polar plastic molds. *J Biomed Mater Res*, **35**, 349–56, 0021-9304 (Print) Comparative Study Journal Article. 115, 340

Lakkis, C. & Vincent, S. (2009). Clinical investigation of asmofilcon a silicone hydrogel lenses. *Optom Vis Sci*, **86**, 350–6. 193, 335

Larke, J., Pedley, D., Smith, P. & Tighe, B. (1973). A semi-rigid contact lens. *Ophthal. Optician*, 1065–1067. 92

Lawton, B., Johnston, S. & Vaquero, E. (2009). Molds for production of ophthalmic devices. 345

Leahy, C.D., Mandell, R.B. & Lin, S.T. (1990). Initial in vivo tear protein deposition on individual hydrogel contact lenses. *Optom Vis Sci*, **67**, 504–11, 1040-5488 (Print) Comparative Study Journal Article. 98, 114

Lee, J.W., Jeong, E.D., Cho, E.J., Jr., J.A.G., Jr., W.H., Hard, R. & Bright, F.V. (2008). Surface-phase separation of peo-containing biodegradable plla blends and block copolymers. *Applied Surface Science*, **255**, 2360 – 2364. 261

Lee, Y., Akiba, I. & Akiyama, S. (2003). The study of surface segregation and the formation of gradient domain structure at the blend of poly(methyl methacrylate)/poly(dimethyl siloxane) graft copolymers and acrylate adhesive copolymers. *Journal of Applied Polymer Science*, **87**, 375–380. 323, 339

Lemp, M.A. (2003). Contact lenses and associated anterior segment disorders: dry eye, blepharitis, and allergy. *Ophthalmol Clin North Am*, **16**, 463–9. 67, 71

Levy, B., McNamara, N., Corzine, J. & Abbott, R. (1997). Prospective trial of daily and extended wear disposble contact lenses. *Cornea*, 274–276. 60

Lewis, K.B. & Ratner, B.D. (1993). Observation of surface rearrangement of polymers using esca. *Journal of Colloid And Interface Science*, **159**, 77–85, cited By (since 1996) 78. 341

Lin, S.T., Mandell, R.B., Leahy, C.D. & Newell, J.O. (1991). Protein accumulation on disposable extended wear lenses. *Clao J*, **17**, 44–50, 0733-8902 (Print) Clinical Trial Comparative Study Journal Article Randomized Controlled Trial. 98

Lira, M., Santos, L., Azeredo, J., Yebra-Pimentel, E. & Oliveira, M.E.C.D.R. (2008). Comparative study of silicone-hydrogel contact lenses surfaces before and after wear using atomic force microscopy. *J Biomed Mater Res B Appl Biomater*, **85**, 361–7. 279, 299, 344

Little, S. & Bruce, A.S. (1995). Enviromental influences on hydrogel lens deydration and the post-lens tear film. *ICLC*, **22**, 148–155. 115

Liu, A.W., Lipscomb, L.K., Schaub, M. & Smith, D.A. (2009). Method for cast moding contact lenses. 345

Løfstrøm, M. & Kruse, A. (2005). A conjunctival response to silicone hydrogel lens wear. 146

Long, B., Robirds, S. & Grant, T. (2000). Six months of in-practice experience with a high dk lotrafilcon a soft contact lens. *Cont Lens Anterior Eye*, **23**, 112–8, 1367-0484 (Print) Journal Article. 60

Lopez-Alemany, A., Compan, V. & Refojo, M.F. (2002). Porous structure of purevision versus focus nightday and conventional hydrogel contact lenses. *J Biomed Mater*

Res, **63**, 319–25, 0021-9304 (Print) Comparative Study Journal Article. 51, 64, 112, 115, 121, 279, 287, 291, 299, 320, 321

Lorentz, H. & Jones, L. (2007). Lipid deposition on hydrogel contact lenses: how history can help us today. *Optom Vis Sci*, **84**, 286–95. 145, 231

Lorentz, H., Rogers, R. & Jones, L. (2007). The impact of lipid on contact angle wettability. *Optom Vis Sci*, **84**, 946–53. 62, 145, 168, 171, 191

Maiden, A., Vanderlaan, D., Turner, D., Love, R., Ford, D., Molock, F., Steffen, R., Hill, G., Alli, A. & McCabe, K. (2002). Hydrogel with internal wetting agent. 33, 158, 169

Maier, C. & Calafut, T. (1998). *Polypropylene: the definitive user's guide and databook*. William Andrews Inc., New York. 344

Maissa, C., Franklin, V., Guillon, M. & Tighe, B. (1998). Influence of contact lens material surface characteristics and replacement frequency on protein and lipid deposition. *Optom Vis Sci*, **75**, 697–705, 1040-5488 (Print) Journal Article. 62, 98

Maldonado-Codina, C. (2001). *Impact of manufacturing technology on the physicochemical properties and clinical performance of soft contact lenses*. Ph.D. thesis, University of Manchester. 320, 329

Maldonado-Codina, C. & Efron, N. (2003). Hydrogel lenses - materials and manufacture: A review. *Optometry in Practice*, **4**, 101–115. 37, 41, 43, 44, 45

Maldonado-Codina, C. & Efron, N. (2004). Impact of manufacturing technology and material composition on the clinical performance of hydrogel lenses. *Optom Vis Sci*, **81**, 442–54, 1040-5488 (Print) Clinical Trial Journal Article Randomized Controlled Trial Research Support, Non-U.S. Gov't. 47, 82, 142, 327, 333

Maldonado-Codina, C. & Efron, N. (2005). Impact of manufacturing technology and material composition on the surface characteristics of hydrogel contact lenses. *Clin Exp Optom*, **88**, 396–404. 122, 142, 301, 343, 345

Maldonado-Codina, C. & Efron, N. (2006). Dynamic wettability of phema-based hydrogel contact lenses. *Ophthalmic Physiol Opt*, **26**, 408–18, 0275-5408 (Print) Journal Article Research Support, Non-U.S. Gov't. 87, 88, 89, 92

Maldonado-Codina, C. & Morgan, P. (2004). Short-term physiologic response in neophyte subjects fitted with hydrogel and silicone hydrogel contact lenses. *Optometry & Vision ...*. 335

Maldonado-Codina, C. & Morgan, P. (2007). In vitro water wettability of silicone hydrogel contact lenses determined using the sessile drop and captive bubble techniques. *Journal of Biomedical Materials Research Part A*, **83A**, 496–502, 1552-4965 10.1002/jbm.a.31260. 73, 76, 88, 159, 171, 173, 183, 206, 220, 338

Maldonado-Codina, C., Morgan, P.B., Efron, N. & Canry, J.C. (2004a). Characterization of the surface of conventional hydrogel and silicone hydrogel contact lenses by time-of-flight secondary ion mass spectrometry. *Optom Vis Sci*, **81**, 455–60, 1040-5488 (Print) Journal Article. 14, 51, 99, 101, 102, 122, 142, 220, 221, 243, 252, 300

Maldonado-Codina, C., Morgan, P.B., Schnider, C.M. & Efron, N. (2004b). Short-term physiologic response in neophyte subjects fitted with hydrogel and silicone hydrogel contact lenses. *Optometry and Vision Science*, **81**, 911–21, 1040-5488 (Print) Clinical Trial Journal Article Randomized Controlled Trial Research Support, Non-U.S. Gov't. 32, 73, 142, 158, 193

Mandell, R. & Polse, K. (1969). Corneal thickness changes as a contact lens fitting index-experimental results and a proposed model. *Am. J. Optom. Arch. Acad. Optom*, **46**, 479–491. 31

Mandell, R., Polse, K. & Fatt, I. (1970). Corneal swelling caused by contact lens wear. *Archives of Ophthalmology*, **83**, 3–&. 31

Marmur, A. (2003). Wetting on hydrophobic rough surfaces: To be heterogeneous or not to be? *Langmuir*, **19**, 8343–8348. 86

Martin, D.C. & Holden, B.A. (1983). Variations in tear fluid osmolality, chord diameter and movement during wear of high water content hydrogel contact lenses. *ICLC*, **10**, 332–342. 144

Martin, W., Adams, J., Enns, J. & Kindt-Larsen, T. (1998). Low oxygen molding of soft contact lenses. 345

McArthur, S.L., McLean, K.M., St John, H.A. & Griesser, H.J. (2001). Xps and surface-maldi-ms characterisation of worn hema-based contact lenses. *Biomaterials*, **22**,

3295–304, 0142-9612 (Print) Journal Article Research Support, Non-U.S. Gov't. 95, 98, 114, 210, 221, 231, 232, 339, 343

McCabe, K., Molock, F., Hill, G., Alli, A., Maiden, A., Steffen, R., Vanderlaan, D. & Young, K. (2004). Biomedical devices containing internal wetting agent. 33, 158, 169, 190

McConville, P. & Pope, J.M. (2000). A comparison of water binding and mobility in contact lens hydrogels from nmr measurements of the water self-diffusion coefficient. *Polymer*, **41**, 9081. 115

McKenney, C. & Becker, N. (1998). Lens deposits with a high dk hydrophilic soft lens. *Optom Vis Sci*, **75**, 276. 62

McMahon, T.T. & Zadnik, K. (2000). Twenty-five years of contact lenses: the impact on the cornea and ophthalmic practice. *Cornea*, **19**, 730–40. 43

Meagher, L. & Griesser, H.J. (2002). Interactions between adsorbed lactoferrin layers maesured directly with the atomic force microscopy. *Colloids and Surfaces B: Biointerfaces*, **23**, 125–140. 114

Meeten, G.H. (1986). *Optical properties of polymers*. Elsevier Applied Science Publishers, London. 104

Menzies, K.L. & Jones, L. (2010). The impact of contact angle on the biocompatibility of biomaterials. *Optom Vis Sci*, **87**, 387–99. 75, 76, 159

Merindano, M.D., Canals, M., Saona, C. & Costa, J. (1998). Rigid gas permeable contact lenses surface roughness examined by interferential shifting phase and scanning electron microscopies. *Ophthalmic Physiol Opt*, **18**, 75–82, 0275-5408 (Print) Journal Article. 112

Meyer, E., Hug, H.J. & Bennewitz, R. (2004). *Scanning probe microscopy: the lab on a tip*. Springer, Berlin. 109

Migonney, V., Lacroix, M.D., Ratner, B.D. & Jozefowicz, M. (1995). Silicone derivatives for contact lenses: functionalization, chemical characterization, and cell compatibility assessment. *J Biomater Sci Polym Ed*, **7**, 265–75. 339

Miller, J., Veeramasuneni, S. & Drelich, J. (1996). Effect of roughness as determined by atomic force microscopy on the wetting properties of ptfe thin films. *Polymer Engineering and science*. 343

Miller, M.J., Wilson, L.A. & Ahearn, D.G. (1988). Effects of protein, mucin, and human tears on adherence of pseudomonas aeruginosa to hydrophilic contact lenses. *J Clin Microbiol*, **26**, 513–7, 0095-1137 (Print) Journal Article. 113

Millodot, M. & O'Leary, D.J. (1980). Effect of oxygen deprivation on corneal sensitivity. *Acta Ophthalmol (Copenh)*, **58**, 434–9. 65

Mobilia, E., Yamamoto, G. & Dohlman, C. (1980). Corneal wrinkling induced by ultra-thin soft contact lenses. *Ann Ophthalmol*, **12**, 371–5. 43

Mondino, B.J., Salamon, S.M. & Zaidman, G.W. (1982). Allergic and toxic reactions of soft contact lens wearers. *Surv Ophthalmol*, **26**, 337–44. 62

Montero Iruzubieta, J., Nebot Ripoll, J.R., Chiva, J., Fernández, O.E., Rubio Alvarez, J.J., Delgado, F., Villa, C. & Traverso, L.M. (2001). Practical experience with a high dk lotrafilcon a fluorosilicone hydrogel extended wear contact lens in spain. *CLAO J*, **27**, 41–6. 60

Morgan, P.B. (2001). Is the uk contact lens market healthy? *Optician*, **5795**, 22–26. 33, 64

Morgan, P.B. & Efron, N. (1998). The oxygen performance of contemporary hydrogel contact lenses. *Cont Lens Anterior Eye*, **21**, 3–6, 1367-0484 (Print) Journal Article. 43

Morgan, P.B. & Efron, N. (2002). Comparative clinical performance of two silicone hydrogel contact lenses for continuous wear. *Clin Exp Optom*, **85**, 183–92, 0816-4622 (Print) Clinical Trial Comparative Study Journal Article Randomized Controlled Trial Research Support, Non-U.S. Gov't. 61, 142

Morgan, P.B. & Efron, N. (2003). In vivo dehydration of silicone hydrogel contact lenses. *Eye Contact Lens*, **29**, 173–6, 1542-2321 (Print) Clinical Trial Controlled Clinical Trial Journal Article Research Support, Non-U.S. Gov't. 59, 65, 115

Morgan, P.B., Efron, N., Hill, E.A., Raynor, M.K., Whiting, M.A. & Tullo, A.B. (2005). Incidence of keratitis of varying severity among contact lens wearers. *Br J Ophthalmol*, **89**, 430–6. 63

Morgan, P.B., Woods, C.A., Knajian, R., Jones, D., Efron, N., Tan, K.O., Pesinova, A., Grein, H.J., Marx, S., Santodomingo, J., Runberg, S.E., Tranoudis, I.G., Chandrinos, A., Itoi, M., Bendoriene, J., van der Worp, E., Helland, M., Phillips, G., Gonzalez-Meijome, J.M., Belousov, V. & Mack, C.J. (2008). International contact lens prescribing in 2007. *Contact Lens Spectrum*, **23**, 36–41. 31, 54, 63

Morgan, P.B., Brennan, N.A., Maldonado-Codina, C., Quhill, W., Rashid, K. & Efron, N. (2010). Central and peripheral oxygen transmissibility thresholds to avoid corneal swelling during open eye soft contact lens wear. *J Biomed Mater Res B Appl Biomater*, **92**, 361–5. 48

Morra, M., Occhiello, E. & Garbassi, F. (1990). Knowledge about polymer surfaces from contact angle measurements. *Advances in Colloid and Interface Science*, **32**, 79. 87

Morris, C.A., Holden, B.A., Papas, E., Griesser, H.J., Bolis, S., Anderton, P. & Carney, F. (1998). The ocular surface, the tear film, and the wettability of contact lenses. *Adv Exp Med Biol*, **438**, 717–22, 0065-2598 (Print) Journal Article. 73

Müller, U., Jockusch, S. & Timpe, H.J. (2003). Photocrosslinking of silicones. vi. photocrosslinking kinetics of silicone acrylates and methacrylates. 345

Ngai, V., Medley, J., Jones, L., Forrest, J. & Teichroeb, J. (2005). Friction of contact lenses: Silicone hydrogel versus conventional hydrogel. In G.D. D. Dowson M. Priest & A. Lubrecht, eds., *Life Cycle Tribology - Proceedings of the 31st Leeds-Lyon Symposium on Tribology Held at Trinity and All Saints College, Horsforth, Leeds, UK 7th–10th September 2004*, vol. 48 of *Tribology and Interface Engineering Series*, 371 – 379, Elsevier. 122, 328

Nichols, J.J. (2006). Deposition rates and lens care influence on galyfilcon a silicone hydrogel lenses. *Optom Vis Sci*, **83**, 751–7. 62

Nichols, J.J. & Sinnott, L.T. (2006). Tear film, contact lens, and patient-related factors associated with contact lens-related dry eye. *Invest Ophthalmol Vis Sci*, **47**, 1319–28. 71

Nicholson, P., Baron, R., Chabrecek, P., Court, J., Domschke, A., Griesser, H., Ho, A., Hoepken, J., Laycock, B., Liu, Q., Lohmann, D., Meijs, G., Papaspiliotopoulos, E., Terry, W., Vogt, J. & Winterton, L. (1996). Extended wear ophthalmic lenses. 49

Nicholson, P.C. & Vogt, J. (2001). Soft contact lens polymers: an evolution. *Biomaterials*, **22**, 3273. 124

Nick, J., Winterton, L. & Lally, J.M. (2005). Enhancing comfort with a lubricating daily disposable. *Optician*, 30–32. 76

Novicky & Hill, R. (1981). Oxygen measurements: Dks and eops. *Int. Contact Lens Clin*, **8**, 41–43. 43

O'Brien, C. & Charman, W.N. (2006). Relative performance of soft contact lenses having lathe-cut posterior surfaces with and without additional polishing. *Cont Lens Anterior Eye*, **29**, 101–7. 317, 343

Opdahl, A., Kim, S.H., Koffas, T.S., Marmo, C. & Somorjai, G.A. (2003). Surface mechanical properties of phema contact lenses: viscoelastic and adhesive property changes on exposure to controlled humidity. *J Biomed Mater Res A*, **67**, 350–6, 1549-3296 (Print) Journal Article Research Support, Non-U.S. Gov't Research Support, U.S. Gov't, Non-P.H.S. 89, 115, 116, 287, 288

Oran, U., Unveren, E., Wirth, T. & Unger, W. (2004). Poly-dimethyl-siloxane (pdms) contamination of polystyrene (ps) oligomers samples: a comparison of time-of-flight static secondary ion mass spectrometry (tof-ssims) and x-ray photoelectron spectroscopy (xps) results. *Applied Surface Science*, **227**, 318–324. 224, 230

Orsborn, G.N. & Zantos, S.G. (1988). Corneal desiccation staining with thin high water content contact lenses. *CLAO J*, **14**, 81–5. 71

Owen, M.J. (1993). *Siloxane Polymers*. Prentice Hall, Englewood Cliffs, NJ. 32, 46, 78, 253, 325

Owen, M.J. (2000). Surface properties and applications. In R.G. Jones, W. Ando & J. Chojnowski, eds., *Silicon-Containing Polymers - The Science and Technology of Their Synthesis and Applications*, chap. 8, 213 – 229, Springer - Verlag. 46, 47

Owens, D. & Wendt, R. (1969). Estimation of the surface free energy of polymers. *Journal of Applied Polymer Science*, **13**, 1741–1747. 337

Ozark, R. & Kunzler, J. (1995). Fluorinated siloxane polymers for contact lenses prodn. - using mixture of fluorinated siloxane contg monomer, vinyl or acryl contg. hydrophilic monomer and initiator. 77

Ozdemir, M. & Temizdemir, H. (2010). Age- and gender-related tear function changes in normal population. *Eye (Lond)*, **24**, 79–83. 75

Papas, E. (1998). On the relationship between soft contact lens oxygen transmissibility and induced limbal hyperaemia. *Exp Eye Res*, **67**, 125–31. 31

Papas, E.B. (2003). The role of hypoxia in the limbal vascular response to soft contact lens wear. *Eye Contact Lens*, **29**, S72–4; discussion S83–4, S192–4. 146

Papas, E.B., Vajdic, C.M., Austen, R. & Holden, B.A. (1997). High-oxygen-transmissibility soft contact lenses do not induce limbal hyperaemia. *Current Eye Research*, **16**, 942–948, informa Healthcare 0271-3683 59

Parvin, A., Mirzadeh, H. & Khorasani, M.T. (2008). Physicochemical and biological evaluation of plasma-induced graft polymerization of acrylamide onto polydimethylsiloxane. *Journal of Applied Polymer Science*, **107**, 2343–2349. 56

Pence, N. (2008). Lens material enhancements: different but the same. *Contact Lens Spectrum*, **23**, 24. 171, 189

Penn, L.S. & Miller, B. (1980). A study of the primary cause of contact angle hysteresis on some polymeric solids. *Journal of Colloid and Interface Science*, **78**, 238. 87

Peterson, R. (2010). Reduced sics following lens rubbing. In *BCLA 2010*. 64

Peterson, R.C., Wolffsohn, J.S., Nick, J., Winterton, L. & Lally, J. (2006). Clinical performance of daily disposable soft contact lenses using sustained release technology. *Cont Lens Anterior Eye*, **29**, 127–34. 145

Plesnarski, A.M. (2004). 510(k) lotrafilcon b soft contact lenses. Summary of safety and substantial equivalence, Food and Drug Administration. 54

Plowright, A., Morgan, P.B., Maldonado-Codina, C. & Moody, K. (2008). An investigation of ocular comfort in contact lens wearers, spectacle wearers and non-wearers. *American Academy of Optometry Meeting*. 13, 65

Poggio, E.C., Glynn, R.J., Schein, O.D., Seddon, J.M., Shannon, M.J., Scardino, V.A. & Kenyon, K.R. (1989). The incidence of ulcerative keratitis among users of daily-wear and extended-wear soft contact lenses. *N Engl J Med*, **321**, 779–83, 0028-4793 (Print) Comparative Study Journal Article Research Support, Non-U.S. Gov't. 45

Polse, K. & Mandell, R. (1970). Critical oxygen tension at the corneal surface. *Arch. Ophthalmol*, **84**, 41–43. 43

Poon, C. & Bhushan, B. (1995). Comparison of surface roughness measurements by stylus profiler, afm and non-contact optical profiler. *Wear*, **190**, 76–88. 294

Pritchard, N. & Fonn, D. (1995a). Dehydration, lens movement and dryness ratings of hydrogel contact lenses. *Ophthalmic Physiol Opt*, **15**, 281–6, 0275-5408 (Print) Clinical Trial Journal Article Randomized Controlled Trial Research Support, Non-U.S. Gov't. 64, 115

Pritchard, N. & Fonn, D. (1995b). Dehydration, lens movement and dryness ratings of hydrogel contact lenses. *Ophthalmic Physiol Opt*, **15**, 281–6. 149, 231

Pritchard, N., Fonn, D. & Weed, K. (1996). Ocular and subjective responses to frequent replacement of daily wear soft contact lenses. *CLAO J*, **22**, 53–9. 62

Putman, C., DeGrooth, B., Van Hulst, N. & Greve, J. (1992). A detailed analysis of the optical beam deflection technique for use in atomic force microscopy. *J. App. Phys.*, **72**, 6–12. 106

Rabke, C., Valint, P. & Ammon, D. (1995). Ophthalmic applications of atomic force microscopy. *ICLC*, **22**, 32–41. 106, 111, 112, 114, 226, 317

Rae, S.T. & Huff, J.W. (1991). Studies on initiation of silicone elastomer lens adhesion in vitro: binding before the indentation ring. *Clao J*, **17**, 181–6, 0733-8902 (Print) Journal Article Research Support, Non-U.S. Gov't. 47

Ramamoorthy, P., Sinnott, L.T. & Nichols, J.J. (2008). Treatment, material, care, and patient-related factors in contact lens-related dry eye. *Optom Vis Sci*, **85**, 764–72. 76

Rathore, O., Mahadevan, S. & Molock, F. (2008). Wettable hydrogels comprising acyclic polyamides. 190

Read, M.L., Maldonado-Codina, C. & Morgan, P.B. (2009). Mesaurements errors related to contact angle analysis of hydrogel and silicone hydrogel contact lenses. *Journal of Biomedical Materials Research Part B: Applied Biomaterials*, **91B**, 662–668. 177

Read, M.L., Maldonado-Codina, C. & Morgan, P.B. (2010a). The influence of wear on contact lens surface wetting characteristics. 74, 114, 335, 336

Read, M.L., Morgan, P.B. & Maldonado-Codina, C. (2010b). The influence of manufacturing batch on the repeatability of dynamic contact angle measurements on hydrogel contact lenses. Poster presentation at ARVO. 287, 334

Rennie, A., Dickrell, P. & Sawyer, W. (2005). Friction coefficient of soft contact lenses: measurements and modeling. *Tribology Letters*, **18**, 499–504. 328

Revenko, I., Tang, Y. & Santerre, J. (2001). Surface structure of polycarbonate urethanes visualized by atomic force microscopy. *Surface Science*. 347

Rieger, G. (1992). The importance of the precorneal tear film for the quality of optical imaging. *Br J Ophthalmol*, **76**, 157–8. 32

Riley, C., Young, G. & Chalmers, R. (2006). Prevalence of ocular surface symptoms, signs, and uncomfortable hours of wear in contact lens wearers: the effect of refitting with daily-wear silicone hydrogel lenses (senofilcon a). *Eye Contact Lens*, **32**, 281–6. 53

Rjeb, A., Letarte, S., Tajounte, L., El Idrissi, M., Adnot, A., Roy, D., Claire, Y. & Kaloustian, J. (2000). Polypropylene natural aging studied by x-ray photoelectron spectroscopy. *Journal of Electron Spectroscopy and Related Phenomena*, **107**, 221–230. 230

Robertson, J., Su, K., Goldenburg, M. & Mueller, K. (1991). Wettable, flexible, oxygen permeable contact lens containing block copolymer polysiloxane-polyoxyalkylene backbone units and use thereof. 50

Rogers, R. & Jones, L. (2005). In vitro and ex vivo wettability of phema and siloxane-based contact lens polymers. *Invest Ophthalmol Vis Sci*, **46**. 146

Ruben, M. & Guillon, M. (1979). 'silicone rubber' lenses in aphakia. *Br J Ophthalmol*, **63**, 471–4. 145

Sanchez, M., Mateo, J., Colomer, F. & Ribelles, J. (2006). Nanoindentation and tapping mode afm study of phase separation in poly(ethyl acrylate-co-hydroxyethyl methacrylate) copolymer networks. *European Polymer Journal*, **42**, 1378–1383. 14, 109

Sankaridurg, P.R., Holden, B.A. & Jalbert, I. (2004). Adverse events and infections: which ones and how many? In D.F. Sweeney, ed., *Silicone Hydrogels - continuous wear contact lenses*, 217–274, Butterworth-Heinmann, Oxford, second edition edn. 60

Santodomingo-Rubido, J., Barrado-Navascués, E., Rubido-Crespo, M.J., Sugimoto, K. & Sawano, T. (2008). Compatibility of two new silicone hydrogel contact lenses with three soft contact lens multipurpose solutions. *Ophthalmic Physiol Opt*, **28**, 373–81. 76

Santos, L., Rodrigues, D., Lira, M., Real Oliveira, M.E.C.D., Oliveira, R., Vilar, E.Y.P. & Azeredo, J. (2008). Bacterial adhesion to worn silicone hydrogel contact lenses. *Optom Vis Sci*, **85**, 520–5. 63, 168, 344

Saraf, R., Ostrander, S. & Feenstra, R. (1998). Surface-influenced phase separation in organic thin films on drying. *Langmuir*, **14**, 483–489. 348

Schein, O.D., Glynn, R.J., Poggio, E.C., Seddon, J.M. & Kenyon, K.R. (1989). The relative risk of ulcerative keratitis among users of daily-wear and extended-wear soft contact lenses. a case-control study. microbial keratitis study group. *N Engl J Med*, **321**, 773–8. 45

Schultz, C., Kunert, K. & White, R. (2000). Bacterial coloniztion of rigid gas permeable and hydrogel contact lenses by staphylococcus aureus. *J Ind Microbiol Biotechnol.*, **24**, 113–115. 113

Seah, M.P. (1980). The quantitative analysis of surfaces by xps: A review. *Surf. Interface Anal.*, **2**, 222–239. 93

Seah, M.P. (2003). Quantification in aes and xps. In D. Briggs & J.T. Grant, eds., *Surface Analysis by Auger and X-Ray Photoelectron Spectroscopy*, chap. 7, SurfaceSpectra Ltd/I M Publications. 212

Selby, C.E., Stuart, J.O., Clarson, S.J., Smith, S.D., Sabata, A., Ooij, W.J. & Cave, N.G. (1994). Surface segregation in blends containing poly(dimethylsiloxane)-polystyrene block copolymers. *Journal of Inorganic and Organometallic Polymers*, **4**, 85–93. 224, 252, 339, 341

Senchyna, M., Jones, L., Louie, D., May, C., Forbes, I. & Glasier, M.A. (2004). Quantitative and conformational characterization of lysozyme deposited on balafilcon and etafilcon contact lens materials. *Current Eye Research*, **28**, 25 – 36, informa Healthcare 0271-3683 18, 2007. 62, 65, 114

Severs, N. & Shotton, D. (1995). *An introduction to freeze fracture and deep etching.*, chap. 1. Rapid freezing, freeze fracture and deep etching., Wiley Liss. 341

Sferrazza, M., Xiao, C., Jones, R., Bucknall, D., Webster, J. & Penfold, J. (1997). Evidence for capillary waves at immiscible polymer/polymer interfaces. *Physical Review Letters*, **78**, 3693–3696. 103

Shiobara, M., Schnider, C.M., Back, A. & Holden, B.A. (1989). Guide to the clinical assessment of on-eye wettability of rigid gas permeable lenses. *Optom Vis Sci*, **66**, 202–6, 1040-5488 (Print) Journal Article Research Support, Non-U.S. Gov't. 68, 70

Shiraishi, A., Yamanishi, S., Yamamoto, Y., Yamaguchi, M. & Ohashi, Y. (2009). [lid-wiper epitheliopathy in patients with dry eye symptoms]. *Nippon Ganka Gakkai Zasshi*, **113**, 596–600. 328

Silveira, K., Yoshida, I. & Nunes, S. (1995). Phase-separation in pmma silica sol-gel systems. *Polymer*, **36**, 1425–1434. 323

Simmons, P.A., Donshik, P.C., Kelly, W.F. & Vehige, J.G. (2001). Conditioning of hydrogel lenses by a multipurpose solution containing an ocular lubricant. *Clao J*, **27**, 192–4, 0733-8902 (Print) Clinical Trial Comparative Study Journal Article Randomized Controlled Trial. 76, 77

Sindt, C.W. (2010). What's in your blister pack? *Review of cornea and contact lenses*. 75

Skotnitsky, C., Sankaridurg, P.R., Sweeney, D.F. & Holden, B.A. (2002). General and local contact lens induced papillary conjunctivitis (clpc). *Clin Exp Optom*, **85**, 193–7, 0816-4622 (Print) Case Reports Journal Article Research Support, Non-U.S. Gov't. 60, 147

Skotnitsky, C., Sweeney, D., Naduvilath, T. & Sankaridurg, P. (2005). The Incidence of Local and General Contact Lens Induced Papillary Conjunctivitis in Silicone Hydrogel Contact Lenses. *Invest. Ophthalmol. Vis. Sci.*, **46**, 2064–. 147

Sosnik, A., Sodhi, R.N., Brodersen, P.M. & Sefton, M.V. (2006). Surface study of collagen/poloxamine hydrogels by a 'deep freezing' tof-sims approach. *Biomaterials*, **27**, 2340 – 2348. 273

St John, H., Kingshott, P. & Griesser, H.J. (1997). Surface characteristics of worn hydrogel contact lenses. *Abstr Pap Am Chem Soc*, 83. 101

Stahl, U., Willcox, M.D.P., Naduvilath, T. & Stapleton, F. (2009). Influence of tear film and contact lens osmolality on ocular comfort in contact lens wear. *Optom Vis Sci*, **86**, 857–67. 71

Stapleton, F., Dart, J.K., Seal, D.V. & Matheson, M. (1995). Epidemiology of pseudomonas aeruginosa keratitis in contact lens wearers. *Epidemiol Infect*, **114**, 395–402. 350

Stapleton, F., Keay, L., Edwards, K., Naduvilath, T., Dart, J.K.G., Franzco, G. & Holden, B.A. (2008). The incidence of contact lens-related microbial keratitis in australia. *Ophthalmology*, **115**, 1655 – 62. 63

Steffen, R. & Schnider, C.M. (2004). A next generation silicone hydrogel lens for daily wear. *Optician*, **227**, 23–25. 60, 73

Stokes, D. (2003). Recent advances in electron imaging, image interpretation and applications: environmental scanning electron microscopy. *Philosophical Transactions of the Royal Society of London Series A-Mathematical Physical and Engineering Sciences*, **361**, 2771–2787. 120

Stout, K.J. & Dong, W.P. (1994). *Three dimensional surface topography: measurement, interpretation, and applications : a survey and bibliography*. Penton Press, London. 105

Studer, K., Decker, C., Beck, E. & Schwalm, R. (2003a). Overcoming oxygen inhibition in uv-curing of acrylate coatings by carbon dioxide inerting, part i. *Progress In Organic Coatings*, **48**, 92–100. 345

Studer, K., Decker, C., Beck, E. & Schwalm, R. (2003b). Overcoming oxygen inhibition in uv-curing of acrylate coatings by carbon dioxide inerting: Part ii. *Progress In Organic Coatings*, **48**, 101–111. 345

Subbaraman, L.N., Glasier, M.A., Senchyna, M., Sheardown, H. & Jones, L. (2006). Kinetics of in vitro lysozyme deposition on silicone hydrogel, pmma, and fda groups i, ii, and iv contact lens materials. *Curr Eye Res*, **31**, 787–96. 62, 76, 231

Subbaraman, L.N., Woods, J., Teichroeb, J.H. & Jones, L. (2009). Protein deposition on a lathe-cut silicone hydrogel contact lens material. *Optom Vis Sci*, **86**, 244–50. 57

Sung, C., Sobarvo, M. & Merrill, E. (1990). Synthesis and characterization of polymer networks made from poly(ethylene oxide) and polysiloxane. *Polymer*, **31**, 556–563. 347

Sweeney, D. (2004). *Silicone Hydrogels - continuous-wear contact lenses*. Elsevier, London, 2nd edn. 53

Sweeney, D.F. & Naduvilath, T.J. (2007). Are inflammatory events a marker for an increased risk of microbial keratitis? *Eye Contact Lens*, **33**. 64

Sweeney, D.F., Du Toit, R., Keay, L., Jalbert, I. & al., e. (2004). Clinical performance of silicone hydrogel lenses. In D.F. Sweeney, ed., *Silicone Hydrogels - continuous wear contact lenses*, 164–216, Butterworth-Heinemann, London, second edition edn. 61, 65, 73

Szakal, C., Sun, S., Wucher, A. & Winograd, N. (2004). C60 molecular depth profiling of a model polymer. *Applied Surface Science*, **231-232**, 183 – 185, proceedings of the Fourteenth International Conference on Secondary IOn Mass Spectrometry and Related Topics. 261

Tadmor, Z. & Gogos, C. (2006). *Principles of polymer processing*. Wiley-Interscience. 104

Tan, J., Keay, L., Jalbert, I., Naduvilath, T.J., Sweeney, D.F. & Holden, B.A. (2003). Mucin balls with wear of conventional and silicone hydrogel contact lenses. *Optom Vis Sci*, **80**, 291–7, 1040-5488 (Print) Clinical Trial Comparative Study Controlled Clinical Trial Journal Article Research Support, Non-U.S. Gov't. 60, 61

Tanaka, H. (2000). Viscoelastic phase separation. 21, 324, 346

Tanaka, K., Takahashi, K. & Kanada, M. (1979). Copolymer for soft contact lens, it preperation and soft contact lens made from therefrom. 48, 51, 53, 323

Teichroeb, J.H., Forrest, J.A., Ngai, V., Martin, J.W., Jones, L. & Medley, J. (2008). Imaging protein deposits on contact lens materials. *Optom Vis Sci*, **85**, 1151–64. 19, 190, 287, 320, 321, 328, 343, 344

Thai, L.C., Tomlinson, A. & Ridder, W.H. (2002a). Contact lens drying and visual performance: the vision cycle with contact lenses. *Optom Vis Sci*, **79**, 381–8. 32, 124, 173

Thai, L.C., Tomlinson, A. & Simmons, P.A. (2002b). In vitro and in vivo effects of a lubricant in a contact lens solution. *Ophthalmic Physiol Opt*, **22**, 319–29, 0275-5408 (Print) Clinical Trial Journal Article Randomized Controlled Trial Research Support, Non-U.S. Gov't. 76, 77

Tighe, B. (2002). Soft lens materials. In N. Efron, ed., *Contact lens practice*, 71–84, Butterworth-Heinmann, Oxford. 41, 42, 43, 44, 50, 58

Tighe, B. (2004). Silicone hydrogels: structure, properties and behaviour. In D. Sweeney, ed., *Silicone Hydrogels: continuous wear contact lenses*, pp 1–21, Butterworth-Heinemann, London. 33, 48, 50, 51, 52, 60, 124, 148, 158, 190, 213, 219, 220, 287

Tighe, B. (2006). Trends and developments in silicone hydrogel materials. Silicone Hydrogels. 53, 55

Tighe, B. & Franklin, V. (1997). Lens deposition and spoilation. In J. Larke, ed., *The Eye in Contact Lens Wear*, 49–100, Butterworth-Heinemann, Oxford. 173

Tighe, B.J., Jones, L., Evans, K. & Franklin, V. (1998). Patient-dependent and material-dependent factors in contact lens deposition processes. *Adv Exp Med Biol*, **438**, 745–51, 0065-2598 (Print) Clinical Trial Journal Article Randomized Controlled Trial. 98

Timberlake, G.T., Doane, M.G. & Bertera, J.H. (1992). Short-term, low-contrast visual acuity reduction associated with in vivo contact lens drying. *Optom Vis Sci*, **69**, 755–60. 124

Tomlinson, A. (1989). Comparitive evalution of surface deposits on high water content contact lens polymers. *Clao J*, **16**, 121–127. 120

Tomlinson, A. (2006). *Epidemiology of dry eye disease*. Thieme, 1st edn. 71

Tomlinson, A., Khanal, S., Ramaesh, K., Diaper, C. & McFadyen, A. (2006). Tear film osmolarity: determination of a referent for dry eye diagnosis. *Invest Ophthalmol Vis Sci*, **47**, 4309–15. 71

Ton-That, C., Shard, A., Teare, D. & Bradley, R. (2001). Xps and afm surface studies of solvent-cast ps/pmma blends. *Polymer*, **42**, 1121–1129. 323, 342

Tonge, S., Jones, L., Goodall, S. & Tighe, B. (2001). The ex vivo wettability of soft contact lenses. *Curr Eye Res*, **23**, 51–9, 0271-3683 (Print) Clinical Trial Journal Article Randomized Controlled Trial Research Support, Non-U.S. Gov't. 74, 90, 92, 114, 146, 184, 204, 207, 231, 334, 335, 337, 338, 343

Tonge, S., Rebeix, V., Young, R. & Tighe, B. (2002). Dynamic surface activity of biological fluids, ophthalmic solutions and nanostructures. *Adv Exp Med Biol*, **506**, 593–9, 0065-2598 (Print) Journal Article. 210

Troy, D.B. (2005). *Remington: the science and practice of pharmacy*. Lippincott Williams Wilkins, 21st edn. 75

Tutt, R., Bradley, A., Begley, C. & Thibos, L.N. (2000). Optical and visual impact of tear break-up in human eyes. *Invest Ophthalmol Vis Sci*, **41**, 4117–23. 124

Vermeltfoort, P., van der Mei, H., Busscher, H., Hooymans, J. & Bruinsma, G. (2004). Physicochernical factors influencing bacterial transfer from contact lenses

to surfaces with different roughness and wettability. *Journal of Biomedical Materials Research Part B-Applied Biomaterials*, **71B**, 336–342. 104

Vermeltfoort, P.B., Rustema-Abbing, M., de Vries, J., Bruinsma, G.M., Busscher, H.J., van der Linden, M.L., Hooymans, J.M. & van der Mei, H.C. (2006). Influence of day and night wear on surface properties of silicone hydrogel contact lenses and bacterial adhesion. *Cornea*, **25**, 516–23, 0277-3740 (Print) Comparative Study Journal Article. 63, 113, 114, 159, 168, 171

Wadu-Mesthrige, K., Amro, N. & Garno, J. (2001). Contact resonance imaging-a simple approach to improve the resolution of afm for biological and polymeric materials. *Applied Surface ....* 347

Walton, J. & Fairley, N. (2004). Quantitative surface chemical-state microscopy by x-ray photoelectron spectroscopy. *Surface and Interface Analysis*, **36**, 89–91. 323

Walton, J. & Fairley, N. (2006a). Characterisation of the kratos axis ultra with spherical mirror analyser for xps imaging. *Surface and Interface Analysis*, **38**, 1230–1235. 342

Walton, J. & Fairley, N. (2006b). Transmission-function correction for xps spectrum imaging. *Surface and Interface Analysis*, **38**, 388–391. 212, 342

Wang, H. & Composto, R. (2003). Wetting and phase separation in polymer blend films: Identification of four thickness regimes with distinct morphological pathways. *Interface Science*, **11**, 237–248. 323

Wang, J., Fonn, D., Simpson, T.L. & Jones, L. (2003). Precorneal and pre- and postlens tear film thickness measured indirectly with optical coherence tomography. *Invest Ophthalmol Vis Sci*, **44**, 2524–8. 67

Wang, J., Aquavella, J., Palakuru, J., Chung, S. & Feng, C. (2006). Relationships between central tear film thickness and tear menisci of the upper and lower eyelids. *Invest Ophthalmol Vis Sci*, **47**, 4349–55. 75

Ward, K.W. (2008). Superficial punctate fluorescein staining of the ocular surface. *Optometry and Vision Science*, **85**, 8–16. 64

Weikart, C.M., Miyama, M. & Yasuda, H.K. (1999). Surface modification of conventional polymers by depositing plasma polymers of trimethylsilane and of trimethylsilane

+ o2: I. static wetting properties. *J Colloid Interface Sci*, **211**, 28–38, 0021-9797 (Print) Journal article. 33, 158, 170, 340

Weikart, C.M., Matsuzawa, Y., Winterton, L. & Yasuda, H.K. (2001). Evaluation of plasma polymer-coated contact lenses by electrochemical impedance spectroscopy. *J Biomed Mater Res*, **54**, 597–607, 0021-9304 (Print) Comparative Study Journal Article. 33, 51, 158, 170, 299, 340

Weng, L., Smith, T., Feng, J. & Chan, C. (1998). Morphology and miscibility of blends of ethylene-tetrafluoroethylene copolymer poly(methyl methacrylate) studied by tof sims imaging. *Macromolecules*, **31**, 928–932. 323

Whyman, G., Bormashenko, E. & Stein, T. (2008). The rigorous derivation of young, cassie-baxter and wenzel equations and the analysis of the contact angle hysteresis phenomenon. *Chemical Physics Letters*, **450**, 355 – 359. 86

Wichterle, O. & Lim, D. (1960). Hydrophilic gels for biological use. *Nature*, 117–118. 41

Wichterle, O. & Lim, D. (1961). Method of producing shaped articles from three-dimensional hydrophilic polymers. 41

Willis, S.L., Court, J.L., Redman, R.P., Wang, J.H., Leppard, S.W., O'Byrne, V.J., Small, S.A., Lewis, A.L., Jones, S.A. & Stratford, P.W. (2001). A novel phosphorylcholine-coated contact lens for extended wear use. *Biomaterials*, **22**, 3261. 95, 168, 317

Willison, J.H.M. & Rowe, A.J. (1980). *Practical Methods in Electron Microscopy*, vol. 8. ELSEVIER SCIENTIFIC. 341

Wolffsohn, J.S., Hunt, O.A. & Basra, A.K. (2009). Simplified recording of soft contact lens fit. *Contact Lens and Anterior Eye*, **32**, 37 – 42. 144

Wong, H., Fatt, I.I. & Radke, C.J. (1996). Deposition and thinning of the human tear film. *J Colloid Interface Sci*, **184**, 44–51, 0021-9797 (Print) Journal article. 72, 334

Xu, L.C. & Siedlecki, C.A. (2007). Effects of surface wettability and contact time on protein adhesion to biomaterial surfaces. *Biomaterials*, **28**, 3273–83. 326

Yañez, F., Concheiro, A. & Alvarez-Lorenzo, C. (2008). Macromolecule release and smoothness of semi-interpenetrating pvp-phema networks for comfortable soft contact lenses. *Eur J Pharm Biopharm*, **69**, 1094–103. 53, 192

Yeniad, B., Beginoglu, M. & Bilgin, L.K. (2010). Lid-wiper epitheliopathy in contact lens users and patients with dry eye. *Eye Contact Lens*, **36**, 140–3. 33, 328

Young, G. (2004). Why one million contact lens wearers dropped out. *Cont Lens Anterior Eye*, **27**, 83–5. 33, 64

Young, G. & Efron, N. (1991). Characteristics of the pre-lens tear film during contact lens wear. *Ophthalmic Physiol Opt*, 53–8. 75, 145

Young, G., Bowers, R., Hall, B. & Port, M. (1997). Six month clinical evaluation of a biomimetic hydrogel contact lens. *CLAO J*, **23**, 226–36. 65, 66

Young, G., Riley, C.M., Chalmers, R.L. & Hunt, C. (2007). Hydrogel lens comfort in challenging environments and the effect of refitting with silicone hydrogel lenses. *Optom Vis Sci*, **84**, 302–8. 65, 193, 336

Young, T. (1805). An essay on the cohesion of fluids. *Philosophical Transactions of the Royal Society of London*, **95**. 86

Zekman, T.N. & Sarnat, L.A. (1972). Clinical evaluation of the silicone corneal contact lens. *Am J Ophthalmol*, **74**, 534–7. 31, 33, 93

Zhang, H. (2006). The permeability characteristics of silicone rubber. Society for the Advancement of Material and Process Engineering, Global Advances in Materials and Process Engineering, Dallas, Tx. 32

Zhang, J. & Herskowitz, R. (1992). Is there more than one angle to the wetting characteristics of contact lenses? *Contact lens spectrum*, **7**, 26–32. 92